Liposomal Drug Delivery of Anticancer Agents

Synthesis, Biophysical Characterization and Biological Studies of Enzyme Sensitive Phospholipid Prodrugs

Pedersen, Palle Jacob

Publication date:
2010

Liposomal Drug Delivery of Anticancer Agents

Synthesis, Biophysical Characterization and Biological Studies of Enzyme Sensitive Phospholipid Prodrugs

Ph.D. Thesis

Palle Jacob Pedersen

May 2010

Department of Chemistry
Technical University of Denmark

Liposomal Drug Delivery of Anticancer Agents

Synthesis, Biophysical Characterization and Biological Studies of Enzyme Sensitive Phospholipid Prodrugs

Palle Jacob Pedersen

Ph.D. Thesis

May 2010

Department of Chemistry
Technical University of Denmark
Kemitorvet
Building 201
DK-2800 Kgs. Lyngby
Denmark

Preface

This thesis describes the work carried out during my three years as a Ph.D. student at Department of Chemistry, Technical University of Denmark (DTU) under supervision of Associate Professor Mads H. Clausen, Senior Scientist Thomas L. Andresen and Professor Robert Madsen. Chapter 1–9 covers the work towards a new generation of liposomal drug delivery systems for anticancer agents, including organic synthesis along with biophysical, biological and computational studies. Chapter 10–11 covers the synthesis of small natural-product-like molecules carried out during a 6 month research stay at School of Chemistry, University of Leeds under supervision of Professor Adam Nelson.

There are numerous people that have contributed and being involved in the projects I have worked on in the last three years and I would like to thank the following persons for help and collaboration.

First of all I would like to thank Associate Professor Mads H. Clausen for your great supervision during the years. You have always motivated and inspired me and during the hard times you remained optimistic and led me in the right directions. Thanks for believing in me. Senior Scientist Thomas L. Andresen and his crew at DTU Nano, Risø are thanked for letting me use their equipment and for sharing their enormous knowledge about phospholipids and liposomes with me. Professor Robert Madsen has been an invaluable resource and a go-to-guy when crucial decision had to be made.

I would like to thank all the collaborators on the project of liposomal drug delivery. Dr. Tristan Ruysschaert, Dr. Ahmad Arouri and Professor Ole G. Mouritsen for their involvement in the biophysical characterization, Dr. Fredrik Melander, Dr. Sidsel K. Adolph and Dr. Mogens W. Madsen for doing all the biological studies and Dr. Arun K. Subramanian and Associate Professor Günther H. Peters are thanked for help and guidance with the computational studies in chapter 4. A special thanks goes to Dr. Mikkel S. Christensen for collaboration with the organic synthesis of phospholipids, you have had a significant impact on the work described in this thesis. I thank Dr. Lars Linderoth for introducing me to the field of phospholipid synthesis in the beginning of my Ph.D.

The Clausen group; Charlotte, Kasper, Mads, Hélène, Alexandra and Mikkel have along with the bachelor and master students that have been in the group during the years created a positive and inspiring atmosphere which I have appreciated and you are thanked for many great days. The lab technicians; Brian, Anne and Janne are acknowledged for help with apparatus, NMR and chemicals – your service is always with a smile.

I would like to thank Professor Adam Nelson for allowing me to come and work in his group at University of Leeds and I am thankful to the entire Nelson group for thanking care

of me both in and outside the lab – and no one take away from me that I reach the highest peak in England in the beautiful Lake District.

The Danish Council for Strategic Research (NABIIT Program) is acknowledged for financial support of the liposomal drug delivery project, while Augustinus Fonden, Oticon Fonden, Knud Højgaards Fond, Vera og Carl Johan Michaelsens Legat, Civilingeniør Frants Allings Legat and Kemisk Forenings Rejsefond are acknowledged for financial support concerning my stay in Leeds.

Finally I would like to thank my family and friends for your support and interest – you are there always for me.

I hope you will enjoy the thesis.

_____

Palle Jacob Pedersen
Kgs. Lyngby, May 2010

Abstract

In the first part of the thesis the work towards a new generation of liposomal drug delivery systems for anticancer agents is described. The drug delivery system takes advantage of the elevated level of secretory phospholipase A_2 ($sPLA_2$) IIA in many tumors and the enhanced permeability and retention (EPR) effect. The liposomes consists of $sPLA_2$ IIA sensitive phospholipids having anticancer drugs covalently attached to the *sn*-2 position of the glycerol backbone in the phospholipids, hence drug leakage is avoided from the carrier system.

Various known anticancer agents, like chlorambucil, all-*trans* retinoic acid, α-tocopheryl succinate and calcitriol were examined for their ability to be incorporated into the investigated drug delivery system and syntheses of the phospholipid prodrugs are described.

The majority of the phospholipid prodrugs were able to form particles with diameters close to 100 nm upon extrusion at 20 °C indicating that unilamellar vesicles are formed. When subjected to $sPLA_2$ the phospholipid prodrugs were converted into cytotoxic lysolipids and along with the released anticancer drug a chemotherapeutic cocktail is formed. Cytotoxicity studies in several cancer lines revealed that upon $sPLA_2$ triggering the formulated phospholipid prodrugs displayed IC_{50} values in range from 3–36 μM and complete cell death was observed when higher drug concentrations were applied. Promising for the drug delivery system the majority of the phospholipid prodrugs remain non-toxic in the absence of the enzyme meaning the prodrugs will not damage healthy tissue during the transport in the body.

In the second part of the thesis the synthetic studies towards a library of small natural-product-like molecules are described. The collection of molecules was synthesized via a diversity oriented synthesis (DOS) based strategy using a limited number of reaction types. Upon coupling of unsaturated building blocks ring closing metathesis cascades were used to “reprogram” the molecular scaffold and highly diverse structures were obtained. In total 20 novel compounds with a broad structural diversity were prepared in 5 or 6 synthetic steps.

Resumé

I den første del af afhandlingen beskrives arbejdet med en ny generation af liposomal drug delivery systemer til brug for cytotoksiske stoffer. Drug delivery systemet udnytter forhøjede koncentrationer af secerneret phospholipase A_2 ($sPLA_2$) IIA i kræft svulster og at cancervæv er mere porøst end raskt væv, hvorved nanopartikler som liposomer kan diffundere ind i kræftvæv men ikke ind i raskt væv. Liposomerne består af $sPLA_2$ IIA sensitive phospholipider hvori det cytotoksiske stof kovalent er bundet til *sn*-2 positionen af glycerol enheden i phospholipiderne således at udsivning fra liposomerne undgås.

Adskillige kendte anticancer stoffer, som chlorambucil, retinsyre, α-tocopheryl succinat og calcitriol blev testet for deres evne til at indgå i det undersøgte drug delivery system og syntesen af phospholipid prodrugsene beskrives.

Hovedparten af de fremstillede phospholipid prodrugs var i stand til efter ekstrudering ved 20 °C at danne partikler med diametere omkring 100 nm, hvilket indikerer dannelsen af liposomer. I stedeværelse af $sPLA_2$ omdannes phospholipid prodrugsene til cytotoksiske lysolipider og sammen med det frigjorte anticancer stof dannes en cocktail af kemoterapeutiske stoffer. Evnen til at frembringe celledød blev undersøgt i forskellige kræftceller og i stedeværelse af $sPLA_2$ viste phospholipid prodrugsene IC_{50} værdier mellem 3–36 μM og fuldstændig celledød blev opnået ved anvendelse af højere koncentrationer. Lovende for drug delivery systemet, så var hovedparten af phosphilipid prodrugsene ikke i stand til at frembringe celledød i fravær af enzymet hvorved prodrugsene ikke vil skade raskt væv under transporten i kroppen.

I den anden del af afhandlingen beskrives de syntetiske studier mod fremstillingen af et bibliotek af naturstof-lignende molekyler. Samlingen af molekyler blev syntetiseret ved en DOS (Diversity Oriented Synthesis) baseret syntesestrategi ved anvendelse af få reaktionstyper. Simple byggeblokke blev sammensat og ved hjælp af ringluknings metatese kaskader blev det molekylære skellet af de kombinerede byggeblokke omstruktureret og strukturer med en høj diversitet blev opnået. I alt blev 20 nye stoffer med en bred struktural forskellighed fremstillet i 5 eller 6 syntese trin.

Publications

At the time for submission of this thesis the research had resulted in the following scientific publications.

Pedersen, P. J.; Christensen, M. S.; Ruysschaert, T.; Linderoth, L.; Andresen, T. L.; Melander, F.; Mouritsen, O. G.; Madsen, R.; Clausen, M. H. Synthesis and Biophysical Characterization of Chlorambucil Anticancer Ether Lipid Prodrugs. *J. Med. Chem.* **2009**, *52*, 3408–3415.

Christensen, M. S.; Pedersen, P. J.; Andresen, T. L.; Madsen, R.; Clausen, M. H. Isomerization of all-(*E*)-Retinoic Acid Mediated by Carbodiimide Activation - Synthesis of ATRA Ether Lipid Conjugates. *Eur. J. Org. Chem.* **2010**, 719-724.

Pedersen, P. J.; Adolph, S. K.; Subramanian, A. K.; Arouri, A.; Andresen, T. L.; Mouritsen, O. G.; Madsen, R.; Madsen, M. W.; Peters, G. H.; Clausen, M. H. Liposomal Formulation of Retinoids Designed for Enzyme Triggered Release. *J. Med. Chem.* **2010**, 53, 3782–3792.

Pedersen, P. J.; Adolph, S. K.; Andresen, T. L.; Madsen, R.; Madsen, M. W.; Clausen, M. H. Prostaglandin Phospholipid Conjugates with Unusual Biophysical and Cytotoxic Properties. *Bioorg. Med. Chem. Lett.* Submitted.

Kumar, S. A.; Pedersen, P. J.; Andresen, T. L.; Madsen, R.; Clausen, M. H.; Peters, G. H. A Unique Water In-take Mechanism Observed in Secretory Phospholipase A_2. *J. Am. Chem. Soc.* Submitted.

O'Leary-Steele, C.; Pedersen, P. J.; James, T.; Lanyon-Hogg, T.; Leach, S.; Hayes, J.; Nelson, A. Synthesis of small molecules with high scaffold diversity: Exploitation of metathesis cascades in combination with inter- and intramolecular Diels–Alder reactions. *Chem. Eur. J.* Accepted.

Contents

1. Introduction to Liposomal Drug Delivery

Cancer remains one of the most frequent and devastating diseases and the number of cases continue to grow. [1,2] As illustrated in Figure 1 for the Nordic countries the numbers of death caused by cancer (the mortality) and the number of new cases of cancer (the incidence) have increased during the last 50 years. Althoug the mortality tends to decline[3] there is continuous need for new and better cancer therapies.

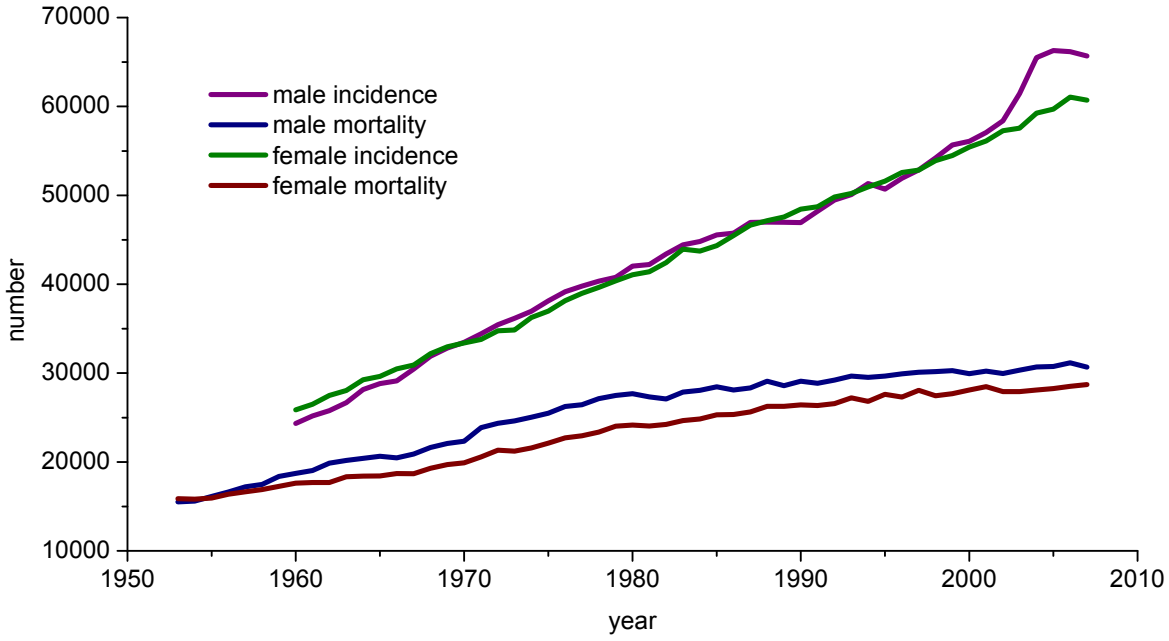

Figure 1. Graphical representation of the number of death (mortality) caused by cancer and the number of new cases of cancer (incidence) in the last 50 years in the Nordic countries, Finland, Sweden, Norway, Denmark, Iceland and the Faroe Islands. Data adapted from Nordcan.[4]

Many potent anticancer drugs have been discovered and developed however their *in vivo* application suffer from inefficient drug delivery to tumors leading to severe side effects on healthy organs. Hence there is a need for drug delivery systems which selectively can deliver chemotherapeutic agents to cancerous tissue thus minimizing side effects and increasing the therapeutic window of the administrated drug affording better antitumor efficiency and patient compliance.

In the beginning of the twentieth century Paul Ehrlich, a German immunologist and a pioneer in medicinal chemistry envisioned the perfect drug as a "magic bullet" that automatically targets and selectively kills the diseased cells without damaging healthy tissue.[5] Liposomes have been proclaimed as a likely candidate to fulfill Paul Ehrlich vision and ever since the discovery of liposomes by Alec Bangham[6,7] in the beginning of the 1960th many efforts have gone into making liposomes applicable as drug carriers.[8]

This thesis describes work towards a new generation of liposomal drug delivery systems with potential in cancer treatment aiming to bring Paul Erhlich vision of a "magic bullet" one step closer. In the following section a brief introduction to phospholipids and liposomes is given followed by an overview of the state of the art in liposomal drug delivery.

1.1 Phospholipids and Liposomes

Phospholipids are among the most abundant biomolecules in nature and the major component in biological membranes. Two main classes of phospholipids exist depending on whether they contain a glycerol or a sphingosyl backbone,[9] for the work described in this thesis only glycerophospholipids have interest and the general skeleton of glycerophospholipids (Figure 2) consists of two chains of fatty acids which via ester bonds are connected to a glycerol backbone with a polar phosphate headgroup, like phosphatidylcholine (PC) (Figure 2). In addition to PC, headgroups like phosphatidylserine (PS), phosphatidylethanolamine (PE) and phosphatidylglycerol (PG) are present in natural occurring phospholipids.[9] Likewise numerous fatty acids have been isolated and identified from natural sources including both fully saturated, like palmitic acid and unsaturated, such as oleic acid.[9]

The dominant nomenclature for phospholipids is the *sn*-nomenclature (stereospecific numbering) proposed by Hirshmann.[10] The *sn*-nomenclature rely on a stereospecific numbering of the the carbon atoms in the glycerol backbone and the atoms are numbered the *sn*-1, *sn*-2 and *sn*-3 position without consideration for the substituents (see Figure 2 and the Abbreviation list for further description of the *sn*-nomenclature).

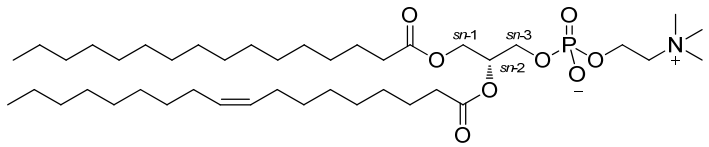

Figure 2. Example of a phospholipid, 1-palmitoyl-2-oleoyl-*sn*-glycero-3-phosphocholine (POPC). The skeleton consists of two chains of fatty acid esters and a glycerol backbone with a polar phosphate headgroup.

In the beginning of the 1960th Bangham and co-workers[6,7] observed that upon dispersion of phospholipids in water a spontaneous aggregation into spherical vesicles occur due to the formation of phospholipid bilayers. Bilayers (Figure 3) are formed because of the amphiphilic character of phospholipids, the hydrophobic tails come together and form an inner layer shielded from water while the polar headgroups hydrated by water provide a thin shell as the outer layers.[11] What Bangham observed was formation of multilamellar vesicles (MLVs), which are lipid bilayers structured in an onion-like fashion (see Figure 3) and with an average diameter above 500 nm.[6,7] MLVs can be converted into unilamellar vesicles (UVs) by e.g. sonication[11,12] or extrusion[11,13] giving particles with diameters close

to 100 nm (see Figure 3). Solutions of MLVs are milky and unclear while UVs provide clear and transparent solutions. By definition liposomes can be seen both as MLVs and UVs but for cancer therapy the smaller UVs are of most interest (*vide infra*).[14]

Aqueous phospholipid solutions display a series of temperature dependent reversible phase transitions, which are important for the properties and behavior of liposomes.[15] The phase transition temperatures can be demonstrated by obtaining a differential scanning calorimetry (DSC) scan. From the DSC scan of MLVs of 1,2-dipalmitoyl-*sn*-glycero-3-phosphocholine (DPPC, Figure 4) it is evident that the bilayers undergo a transformation from an ordered solid phase to a more disordered ripple phase (pre-transition temperature) and then into a fluid phase (main phase transition temperature, T_m). The phase transition temperatures depend on the ability of the to phospholipids to create well ordered and dence bilayers and phospholipids having two saturated fatty acids in the *sn*-1 and *sn*-2 position have high T_m's , (T_m of DPPC is 41 °C)[16] whereas phospholipids having unsaturated fatty acids have lower T_m's , (T_m of POPC is –20 °C).[17] The physical state of the bilayers affect the permeability, stability and flexibility of the liposomes, hence extrusion of MLVs of 1,2-distearoyl-*sn*-glycero-3-phosphocholine (DSPC) through a 100 nm filter needs to be performed above the T_m of DSPC at 55 °C,[17] as it is impossible below the T_m due to the stiffness of the bilayers.

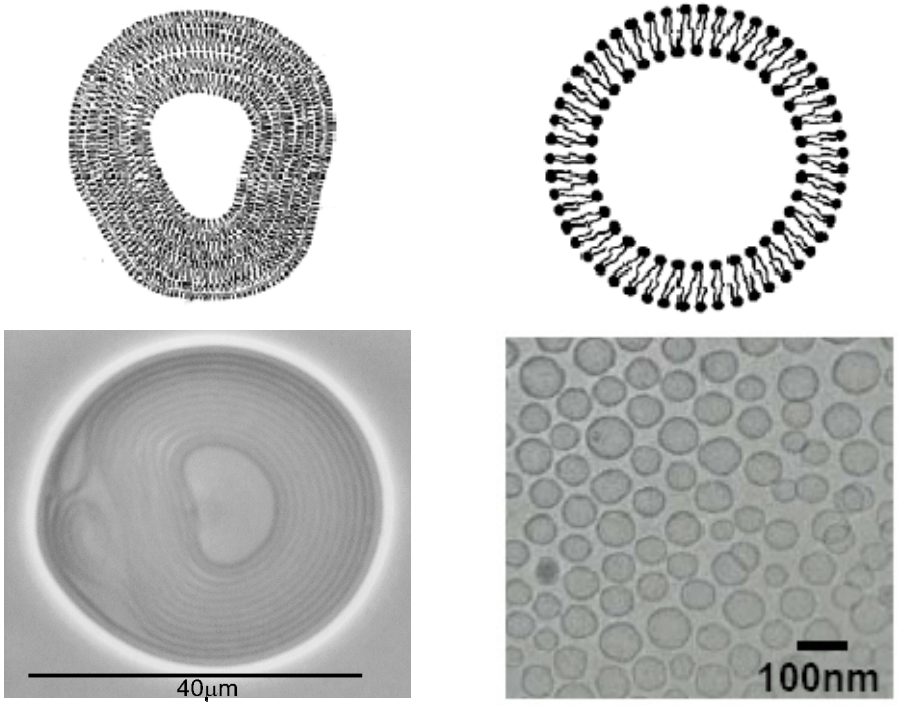

Figure 3. Illustration of phospholipid bilayers in a multilamellar vesicle (top left) and phospholipid bilayer in a unilamellar vesicle (top right). Cryo-electro microscopy pictures of a multilamellar vesicle (bottom left) and unilamellar vesicles (bottom right). Data from Mouritsen.[15]

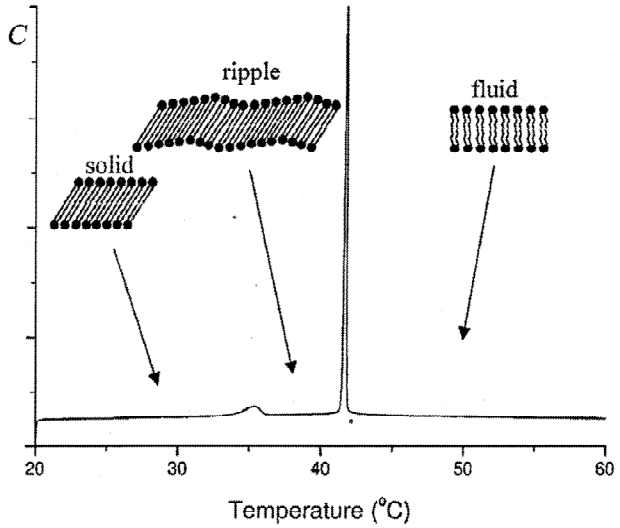

Figure 4. DCS scan of MLVs of DPPC. The small peak separating the solid and the ripples phase corresponds to the pre-transition temperature and the large peak separating the ripple and fluid phase corresponds to T_m. Data from Mouritsen.[15]

1.2 Liposomes in Drug Delivery

A decade after the discovery of liposomes Gregoridis *et al.*[18] suggested that liposomes could have potential as drug carriers due to their ability to encapsulate compounds either in the aqueous interior of the vesicles or in the lipophilic membrane. Initially the use of liposomes was hampered by a poor stability in serum due to interaction with plasma proteins like lipoproteins but that was circumvented by using phospholipids with a high T_m like DPPC in co-formulation with cholesterol (conventional liposomes).[14] However three major obstacles were still to be overcomed in order for liposomes to be a successful drug carrier in cancer therapy, a rapid clearance from the blood stream, a low drug accumulation in the tumors (targeting) and an uncontrolled drug release from the carrier.[8]

For a long time the application of liposomes suffered from a fast clearance from the blood stream, it was observed that when conventional liposomes were injected intravenously they rapidly were recognized and removed by the reticuloendothelial system (RES) hence leading to an accumulation in the liver and spleen followed by a clearance from the body by macrophages.[14,8] Unless you are targeting a disease in these organs, this is not desirable, but a major step forward was the introduction of liposomes coated with the synthetic polymer polyethylene glycol (PEG).[19,20,21] It was shown that pegylated liposomes have a significant longer half-life in the blood stream than conventional liposomes. The reason for this is that the attachment of PEG provides a hydrated environment around the liposomes and together with the steric barrier the recognition and clearance by the RES is reduced. Initial studies by Blume *et al.*[19] revealed that addition of a pegylated conjugate of 1,2-distearoyl-*sn*-glycero-3-phosphoethanolamine (DSPE-PEG) to DSPC increased the half-life in the blood stream in mice from 0.5 h for pure DSPC to 8.5 h for the 9:1 mixture of

DSPC and DSPE-PEG (see Figure 5). For other systems of pegylated liposomes half lives up to 72 h in humans are reported.[22]

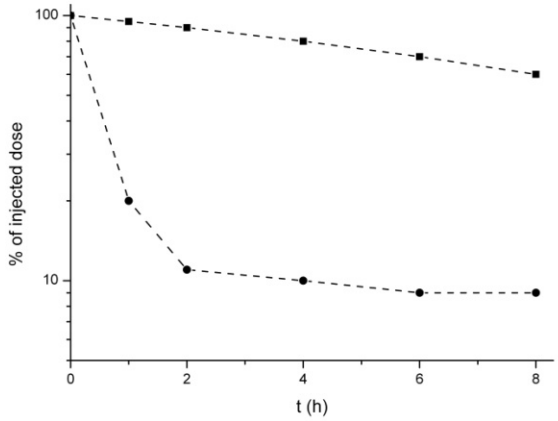

Figure 5. Liposome level in the blood stream as a function of time after intraveneous administration in mice. Tritium-labelled liposomes of DSPC (●) and 9:1 DSPC:DSPE-PEG (■). Figure adapted from Blume *et al.*[19]

Due to the enhanced permeability and retention (EPR) effect long circulating liposomes tend to accumulate in tumors. The EPR effect, first introduced by Maeda and co-workers,[23,24] is a consequence of the leaky vasculature found in tumor tissue and the lack of an effective lymphatic drainage system. The junctions between cells in tumors vary from 100-800 nm which allows penetration of drug carriers like liposomes.[25] In contrast, the gaps between cells in healthy tissue are less than 6 nm meaning liposomes cannot enter here (see Figure 6).[25]

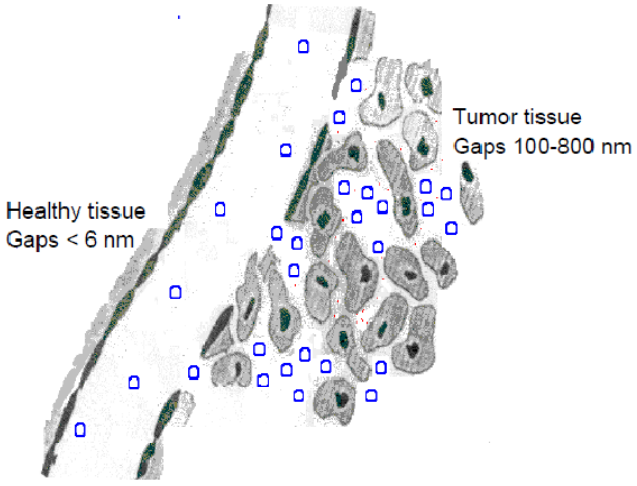

Figure 6. Illustration of passive targeting of long circulating liposomes (o) into tumors. Due to larger junctions between endothelium cells in tumor tissue compared to healthy tissue nanoparticles, such as liposomes, can diffuse into tumors but not into healthy tissue.

However the endothelium gaps in organs like the kidney (40-60 nm), liver and spleen (<150 nm)[25] are bigger by which nanoparticles also penetrate into these organs, but due to the pegylation the clearance of liposomes by macrophages are delayed and thus the liposomes can to some extent pass in and out from the liver and spleen without being cleared from the body while they stay in the tumors due to the unefficient lymphatic drainage system.[22]

Data from Unezaki *et al.*[26] illustrate how pegylated liposomes take advantage of the EPR effect (Table 1). Unezaki *et al.* showed that intravenous administration of doxorubicin encapsulated in pegylated liposomes into tumor-bearing mice provided a significant higher accumulation in tumors than when doxorubicin encapsulated in conventional liposomes or free doxorubicin were administrated (Table 1). Furthermore, as a consequence of the pegylation the circulation time in the blood stream was improved, whereas the degree of accumulation into organs, like the liver and heart was similar to what observed for conventional liposomes.

Table 1. Amount of doxorubicin presented as tissue AUC[a] values after intravenous injection of free doxorubicin and doxorubicin encapsulated in conventional and pegylated liposomes into tumor-bearing mice at a dose of 5 mg doxorubicin per kg. Data adapted from Unezaki *et al.*[26]

	Tissue AUC (h·µg/g)						
Formulation	**Blood**	**Liver**	**Heart**	**Lung**	**Spleen**	**Kidney**	**Tumor**
Doxorubicin	1	169	63	106	178	146	18
Doxorubicin in conventional liposomes[b]	343	341	41	68	366	72	50
Doxorubicin in pegylated liposomes[c]	*810*	309	42	91	320	132	*170*

[a]AUC = area under the concentration-time curve, calculated for 1–24 h after injection and giving as h·µg/g. [b]The conventional liposomes consist of DSPC/cholesterol 1:1. [c]The pegylated liposomes consist of DSPC-PEG/DSPC/cholesterol 6:47:47.

The use of passive targeting and hence the EPR effect is limited and cannot be applied to target all forms of cancers. Thus efforts have been directed towards the development of active approaches for drug targeting. This can be done by specific modification of the drug carrier system with agents or ligands having affinity for recognizing and/or interacting with specific cells, tissues or organs in the body. The approach has been explored targeting various receptors and antigens on cell membranes and an example is targeting of the folate receptor.[27,28,29] The folate receptor is over-expressed in many cancer cells with epithelial origin and the receptor has been targeted with liposomes conjugated to folic acid. Folic acid and thereby also the drug-containing liposomes are taken up by the cells via receptor mediated endocytosis (see Figure 7 for the folic acid phospholipid conjugate studied by Gabizon *et al.*[28]). Another successful approach is conjugation of antibodies to liposomes and hence binding to specific surface proteins[30] and in recent years, several *in vivo* studies have demonstrated the potential of using antibody-coated liposomes to increase drug accumulation in tumors. In a study by Park *et al.*,[31] doxorubicin-loaded liposomes

conjugated to antibodies showed significantly increased antitumor efficacy against breast cancer xenografts in mice as compared with non-coated liposomes of identical composition. Moreover other *in vivo* studies have demonstrated the potential of using antibody-coated liposomes in delivering anticancer drugs to colon and prostate tumors in mice.[32]

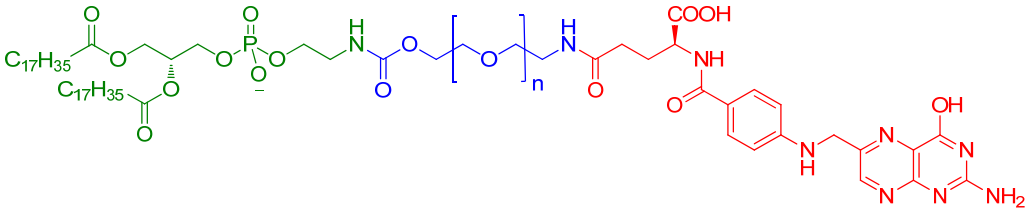

Figure 7. Structure of the folic acid phospholipid conjugate studied by Gabizon *et al.*[28] for active targeting. Folic acid (red) is conjugated via a PEG (blue) chain to DSPE (green).

Having various strategies that can deliver drug-containing liposomes to tumors the next obstacle to overcome is drug release.[i] As discussed above an optimal drug delivery formulation should be able to retain and stabilize the carried drug during blood circulation and effectively deliver the drug to the target tissue. Therefore utilization of site specific release mechanisms are advantageous and several have been investigated,[8] e.g. pH,[33,34] light,[35,36] and heat sensitive liposomes.[37,38] Another appealing type of release mechanism rely on enzymatic triggering. By taking advantage of elevated levels of specific enzymes in diseased tissue site specific triggering is possible.[8, 39, 40] One of the studied release mechanisms takes advantage of elastase and its ubiquitous involvement in inflammatory and tumorigenic conditions. Elastases ability to recognize simple peptide sequences allows for a short peptide attachment to the headgroup of phospholipids. Meers and co-workers have worked with attachments of first *N*-acetyl-Ala-Ala (N-Ac-AA)[41] to the headgroup of 1,2-dioleoyl-*sn*-glycero-3-phosphoethanolamine (DOPE) and later on with the more elastase sensitive sequence of MeO-succinyl-Ala-Ala-Pro-Val (MeO-suc-AAPV).[42] Due to the small headgroup DOPE itself cannot form stable membrane bilayers at physiological pH, however small modifications of the headgroup, like mono-methylation alters the properties and stable liposomes can be formulated.[41,43] Meers and co-workers have shown that conjugation of DOPE to the elestase sensitive peptide chain MeO-suc-AAPV creates phospholipids (MeO-suc-AAPV-DOPE) that can form liposomes but upon subjection to elastase the liposomes collapse as a consequence of formation of fusogenic DOPE lipids and the encapsulated molecules are released (see Figure 8).[42]

[i] A release mechanism is involved in some active targeting strategies.

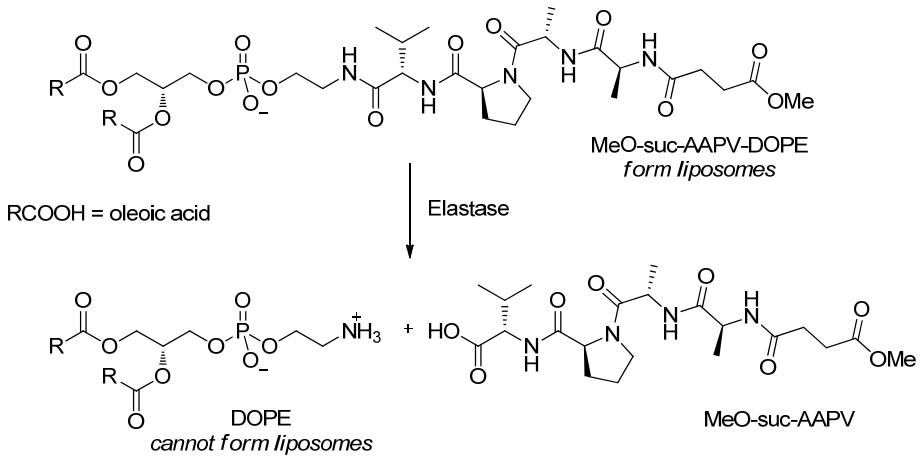

Figure 8. Illustration of the liposome-forming MeO-suc-AAPV-DOPE phospholipid that upon subjection to elastase are hydrolyzed to non-liposome-forming DOPE lipids under release of the peptide chain (MeO-suc-AAPV) resulting in an overall collapse of the drug-containing liposomes.[42]

Another approach described by Davis *et al.*[44] utilize that the membrane-bound form of alkaline phosphatase is over-expressed in some tumor tissue[45] and they have managed to design alkaline phosphatase sensitive liposomes.[44] By mixing DOPE and the cholesterol phosphate derivative shown in Figure 9 stable liposomes were obtained but in the presence of alkaline phosphatase the liposomes collapse as a consequence of the enzyme-mediated cleavage of the phosphate. Furthermore, enzymes like matrix metalloproteinases[46] and secretory phospholipase A_2 ($sPLA_2$)[47,48] have been explored as a site specific trigger in liposomal drug delivery and particular $sPLA_2$ offers an interesting opportunity for enzyme triggered drug release. Therefore, the enzyme and $sPLA_2$ dependent drug delivery systems will be described in further details in the next sections as this form the basis for the work described in the rest of this thesis.

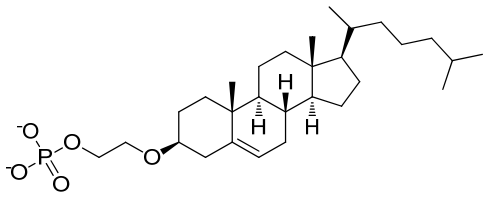

Figure 9. Alkaline phosphatase sensitive cholesterol derivative.[44]

1.3 Secretory Phospholipase A_2 and its Utilization as a Site Specific Trigger

The phospholipase A_2 superfamily consists of a broad range of enzymes defined by their ability to catalyze the hydrolysis of the ester bond at the *sn*-2 position in phospholipids yielding fatty acid and lysolipids (see Figure 10).[49,50] The family of extracelluar $sPLA_2$ enzymes (IB, IIA, IIC, IID, IIE, IIF, III, V, X and XIIA) are small proteins (14-19 kDa) which require Ca^{2+} for enzymatic activity[49,50] and the group I, II V and X $sPLA_2$'s are closely related and share a common mechanism for the hydrolysis.[49]

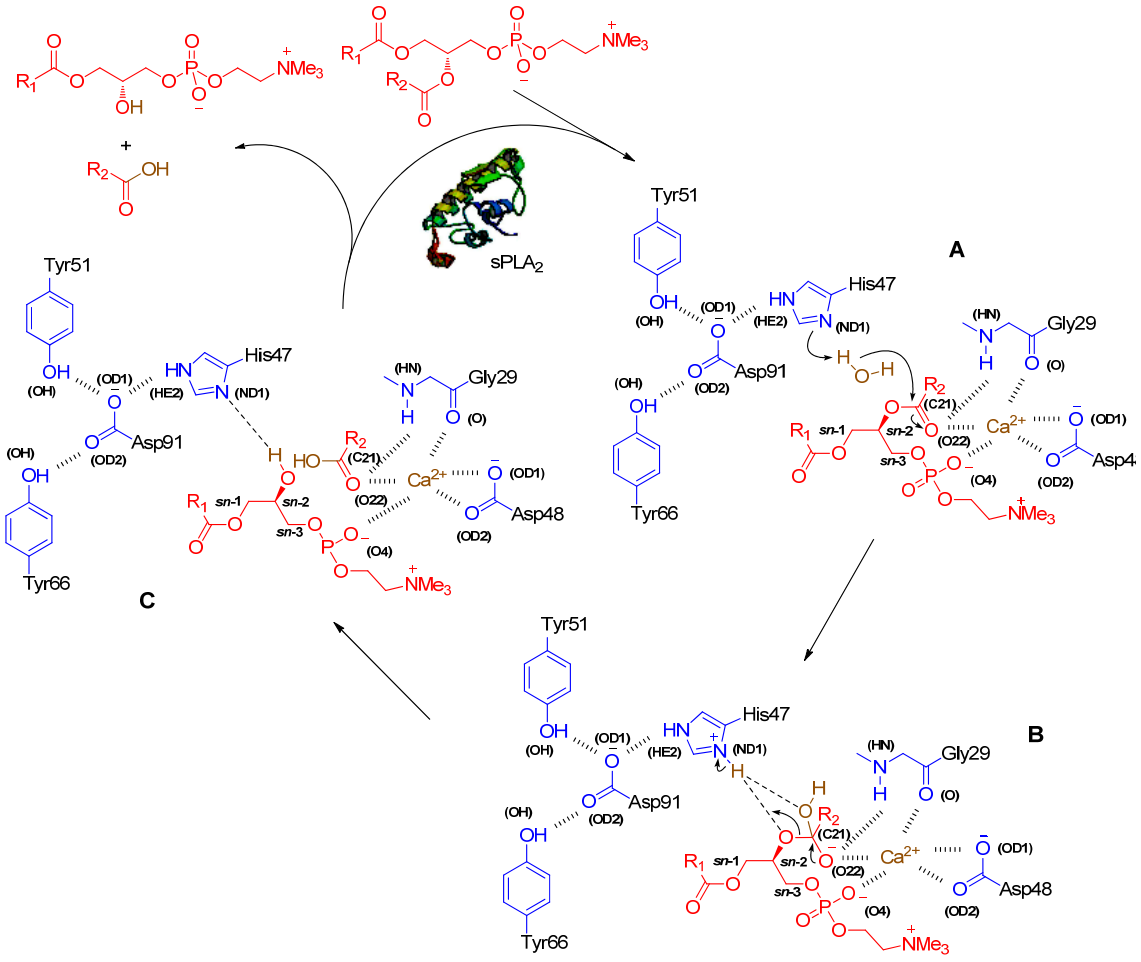

Figure 10. Schematic illustration of the mechanism for the $sPLA_2$ catalyzed hydrolysis of phospholipids yielding fatty acids and lysolipids. Key protein residues are drawn in blue, the substrate in red, the calcium ion and the water molecule both in brown. R_1 and R_2 represents aliphatic chains. Adapted from Scott *et al*.[51]

A prerequisite for hydrolysis is formation of a stable Michaelis-Menten complex between the phospholipid substrate and the enzyme. Coordination from Ca^{2+} to both the phospholipid substrate and the protein residues Gly29 and Asp48 is crucial for the stabilization and keeps the substrate and enzyme together (Figure 10).[51] The ester cleavage proceeds through activation and positioning of a water molecule by hydrogen bonding to

His47 assisted by Asp91 (Figure 10A). After abstraction of a hydrogen from the incoming water molecule a nucleophilic attack on the carbonyl in the *sn*-2 position occurs forming the intermediate (Figure 10B), regeneration of the carbonyl releases the lysolipid and the carboxylic acid by which the catalytic cycle is completed and the enzyme is ready for another substrate (Figure 10).[51]

The subtype of the enzyme family, $sPLA_2$ IIA has been suggested as a therapeutic target for site specific triggering[47,52] due to its over-expression in several human cancer tissues (Table 2)[53,54] including breast, stomach, colorectal, pancreatic, prostate and liver cancer.

Table 2. Concentration of $sPLA_2$ II in effusions from patients with various cancers.[a] Data from Abe *et al*.[53]

	$sPLA_2$ II concentration (ng/mL)	
Cancer	**Mean ± SD**	**Range**
Breast	40 ± 19	12–67
Stomach	51 ± 50	10–188
Pancreas	56 ± 38	31-131
Liver	36[b]	26–45

[a]Healthy tissue <10 ng/mL. [b]Only two measurements.

Interestingly, the catalytic activity of $sPLA_2$ is higher towards aggregated phospholipids such as liposomes and micelles than towards lipid monomers – a phenomenon known as interfacial activation.[55] Also the physical state of the phospholipids alter the activity and whereas it has been demonstrated that snake (*Agkistrodon piscivorus piscivorus*) venom $sPLA_2$ has maximum enzyme activity at the T_m, human $sPLA_2$ IIA increase its activity with the temperature until 50 °C after which the enzyme is completely inactive as a consequence of denaturation.[56] Likewise, the various subtypes of $sPLA_2$ have different substrate affinity and whereas the human $sPLA_2$ IIA subtype acts on negatively charged substrates[57,58,59] subtypes like $sPLA_2$ V and X hydrolyze both negatively charged and zwitterionic lipids.[59] In the design of liposomal drug delivery systems utilizing the elevated levels of $sPLA_2$ IIA in tumors it is therefore important to construct liposomes with a negatively charged surface. However it has been reported that intravenous administration of negatively charged liposomes may induce complement activation[60] but that can be suppressed by mixing with neutral phospholipids. In continuation of this, studies have shown that neutral phospholipids, like PC lipids in mixtures with PG lipids also are hydrolyzed by human $sPLA_2$ IIA.[56,61] Furthermore, enzymatic studies have shown that $sPLA_2$ activity is retained on pegylated liposomes which are important for the construction of liposomal drug carriers having a long circulation time in the blood stream.[47,62]

The natural substrates for $sPLA_2$ are 1,2-diacyl-*sn*-glycerophospholipids like POPC (Figure 2) but the enzyme has a much broader substrate scope and is able to hydrolyze a variety of phospholipids, like phospholipids with a *sn*-1-ether moiety,[63,64] *sn*-2-thioesters[65]

and lipids with alkyl substituents at the *sn*-1 position[66] (see Figure 11). However the enzyme is very sensitive to the stereochemistry of the glycerol backbone and only phospholipids having an L-glycerol backbone are substrates for $sPLA_2$. Indeed D-glycerophospholipids have been exploited as competitive inhibitors.[67]

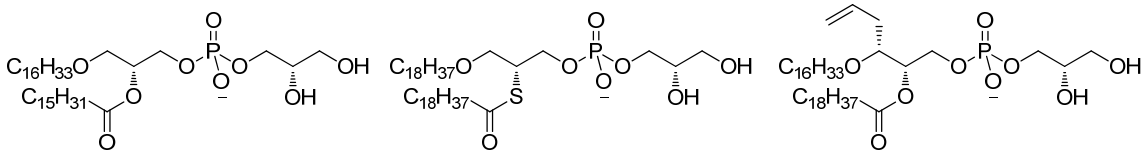

Figure 11. Small selection of the variety of synthetic phospholipids $sPLA_2$ is able to hydrolyze.

By taking advantage of the elevated levels of $sPLA_2$ IIA in tumors and the EPR effect liposomal drug delivery systems consisting of $sPLA_2$ sensitive phospholipids (see Figure 12) have been developed.[48,63] The enzyme sensitive liposomes are constructed of *sn*-1-ether phospholipids having saturated aliphatic chains in the *sn*-1 and *sn*-2 position.[63,64] Upon $sPLA_2$ activation the phospholipids are converted into fatty acids and *sn*-1-ether lysolipids which are highly cytotoxic compounds and also known as anticancer ether lipids.[64,68]

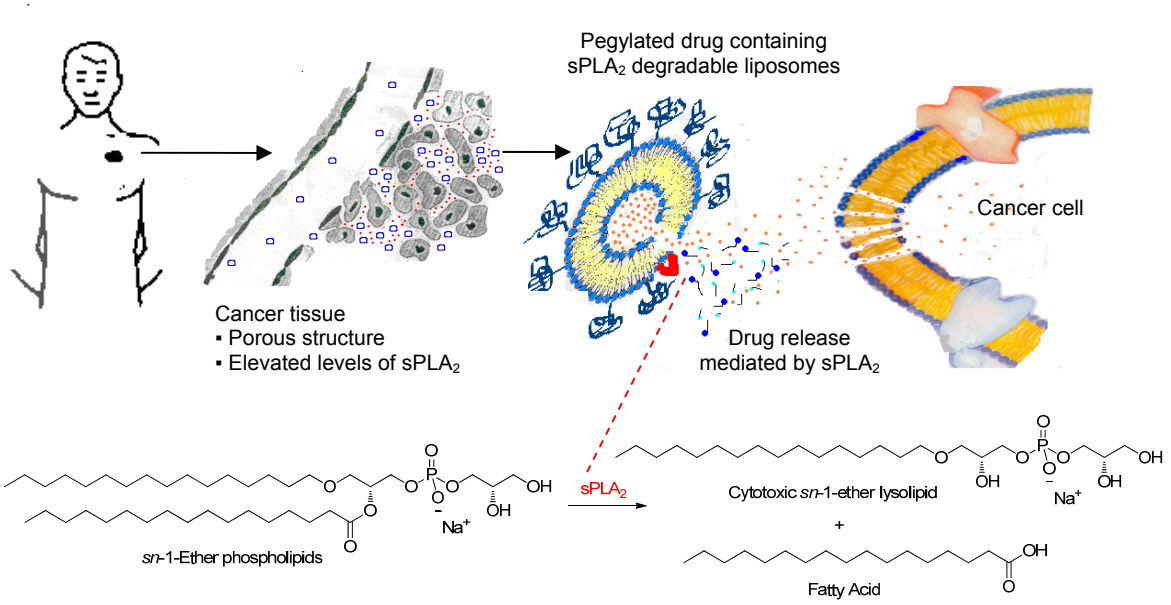

Figure 12. Schematic overview of the strategy for using $sPLA_2$ degradable liposomes in cancer treatment. The *sn*-1-ether phospholipid prodrugs are formulated as liposomes encapsulating anticancer drugs. Because of the EPR effect, the liposomes will accumulate in cancer tissue and $sPLA_2$, which is up-regulated in tumors, will degrade the drug containing liposomes, releasing the encapsulated drugs which together with the cytotoxic lysolipids and the fatty acids attack the cancer cells.

The prodrug strategy masks the anticancer ether lipid and minimizes the hemolytic effect often seen for anticancer ether lipids *in vivo*.[69,70] *In vitro* studies with the $sPLA_2$ sensitive liposomes have shown that the enzyme need to be present in order to induce significant

cell death, showing the potential of the phospholipid prodrug strategy.[63,64] The $sPLA_2$ degradable liposomes are also capable of encapsulating hydrophilic drugs like *cis*-platin and doxorubicin and formulated with pegylated phospholipids long circulating liposomes have been created.[8] Therefore in overall the enzyme activation releases two anticancer drugs selectively in the cancer tissue. *In vivo* studies of the drug delivery system have demonstrated that growth inhibition of $sPLA_2$ expressing tumor cells were significant better when the drug (*cis*-platin or doxorubicin) was encapsulated into the enzyme sensitive liposomes, compared to when the drugs were administrated alone and the formulation was also superior to the commercial available formulation of doxorubicin, Doxil®.[8]

1.4 New Generation of Enzyme Sensitive Phospholipids

Although liposomes are capable of delivering drugs to tumors a major problem in liposomal drug delivery is leakage of the encapsulated drugs. That can be lowered by addition of cholesterol to the liposomal formulation, but for drug delivery strategies relying on site specific drug release via $sPLA_2$ activation it is desirable to avoid or minimize the addition of cholesterol, as cholesterol harms the enzyme activity and studies have revealed that liposomes having >20% cholesterol are non-degradable by $sPLA_2$.[8] An uncontrolled drug leakage can be prevented by covalent attachment of anticancer drugs to phospholipids creating prodrugs that upon triggering, e.g. by $sPLA_2$ release the attached drugs. This strategy makes it possible to use empty liposomes hence avoiding drug leakage from the interior and ideally the liposomes become non-toxic during circulation in the blood stream. An example on such a phospholipid prodrug is empty liposomes of the *sn*-1-ether phospholipids illustrated in Figure 12, which are prodrugs of anticancer ether lipids. More recently incorporation of capsaicin into $sPLA_2$ sensitive phospholipids has been achieved and upon $sPLA_2$ mediated hydrolysis capsaicin was released after cyclization (see Figure 13).[71]

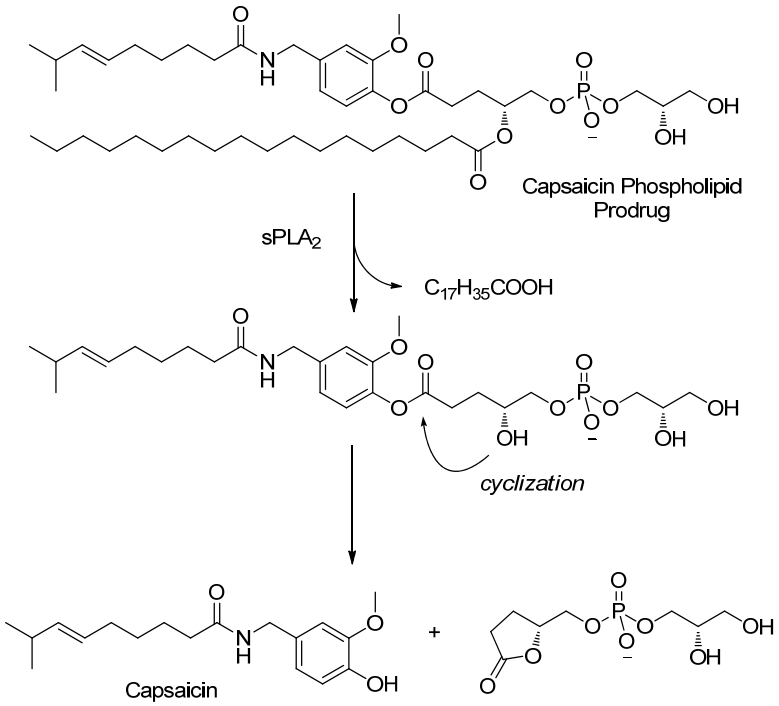

Figure 13. Release of capsaicin from phospholipid prodrug upon cyclization mediated by $sPLA_2$.[71]

The liposomal drug delivery system studied in this work relies on covalent incorporation of anticancer drugs directly to the *sn*-2 position of *sn*-1-ether phospholipids. Hydrolysis of the ester-bond at the *sn*-2 position by $sPLA_2$ will convert the phospholipid prodrugs into two cytotoxic agents, the *sn*-1-ether lysolipid and the anticancer drug (see Figure 14 for an overview of the principle). Lysolipids are known to achieve their cytotoxic activity through

multiple mechanisms,[69] one involves membrane perturbation by which the lysolipids are likely to enhance the cellular uptake of the other anticancer drug causing a synergistic effect between two drugs. Previously, it has been demonstrated that lysolipids and fatty acids enhance membrane permeability.[72]

Interestingly cytotoxicity studies have shown that the stereochemistry of the PG headgroup has an impact on the activity of *sn*-1-ether lysolipids and the (*S*)-isomer displayed significantly higher cytotoxicity than the corresponding (*R*)-isomer which is why the PG lipids are designed to have the (*S*)-configuration.[68]

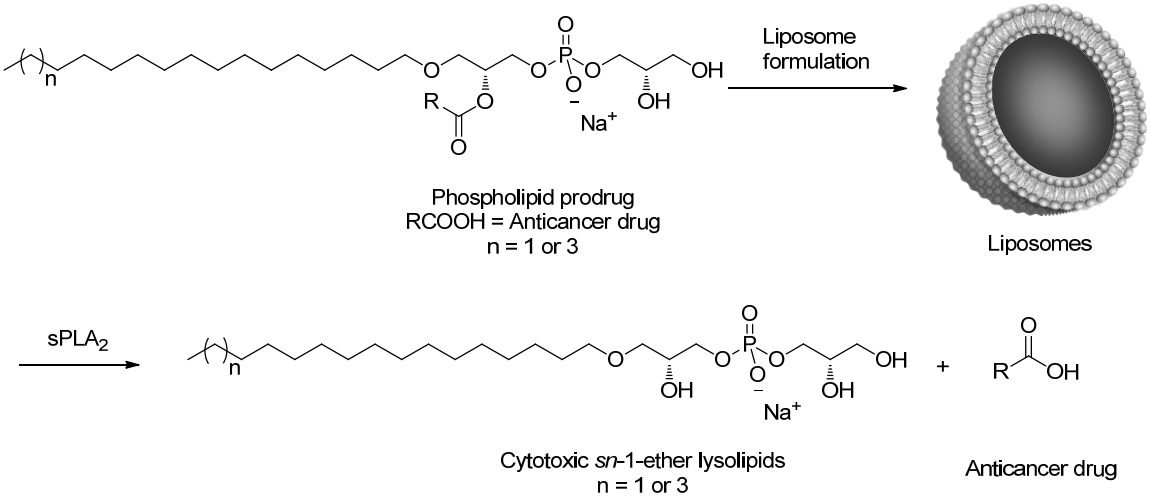

Figure 14. Schematic overview of the investigated drug delivery concept. The phospholipid prodrugs are formulated as liposomes. Because of the EPR effect, the liposomes will accumulate in cancer tissue and $sPLA_2$, which is up-regulated in tumors, will hydrolyze the prodrugs, releasing two anticancer agents.

It is crucial for the prodrug strategy that suitable drug candidates are available. Since the incorporated drug will be part of the lipophilic membrane, a hydrophobic nature is an obvious requirement and, furthermore, a carboxylic acid moiety is needed for the attachment of the drug to the phospholipid backbone. A number of candidates have been identified such as chlorambucil,[73,74] all-*trans* retinoic acid (ATRA),[75,76], α-tocopheryl succinate[77,78] a derivative of vitamin E and prostaglandins like 15-deoxy-$\Delta^{12,14}$-PGJ_2[79] (see Figure 15).

Incorporation of structures like chlorambucil into the phospholipid bilayer contrasts the (predominantly) saturated aliphatic chains in liposome forming phospholipids like in DPPC. In the initial screening for a suitable drug candidate it was therefore interesting to study the ability of the phospholipid prodrugs to form liposomes, furthermore, it was crucial that the ester-bond at the *sn*-2 position was hydrolyzed by $sPLA_2$ hence converting the prodrugs into cytotoxic agents. As a final initial screening parameter it was important that the prodrugs were non-toxic in the absence of $sPLA_2$. The anticancer drugs shown in

Figure 15 have together with calcitriol (Chapter 7) been examined for their ability to be incorporated into the liposomal drug delivery system illustrated in Figure 14.

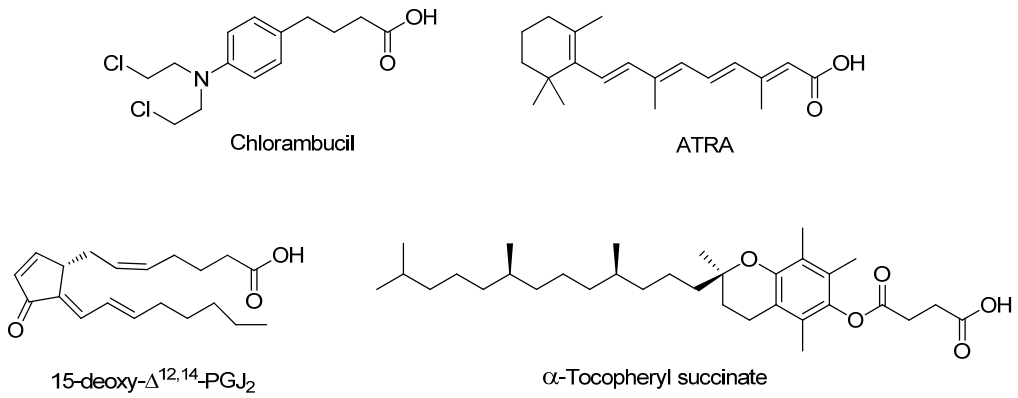

Figure 15. Suitable drug candidates for incorporation into the investigated drug delivery system.

A major part of the work carried out involves synthesis of phospholipids having either a PC or PG headgroup, why the coming section provides a brief overview of the most modern ways of making PC and PG lipids.

2. Phospholipid Synthesis – An Overview

In the following synthesis of phospholipids will be reviewed. Focus will be on mixed-acid 1,2-diacyl-*sn*-glycerophospholipids and 1-*O*-alkyl-2-acyl-*sn*-glycerophospho-lipids having either a PC or PG headgroup. Two general approaches are used for the synthesis of phospholipids having different aliphatic chains at the *sn*-1 and *sn*-2 position (see Figure 16).

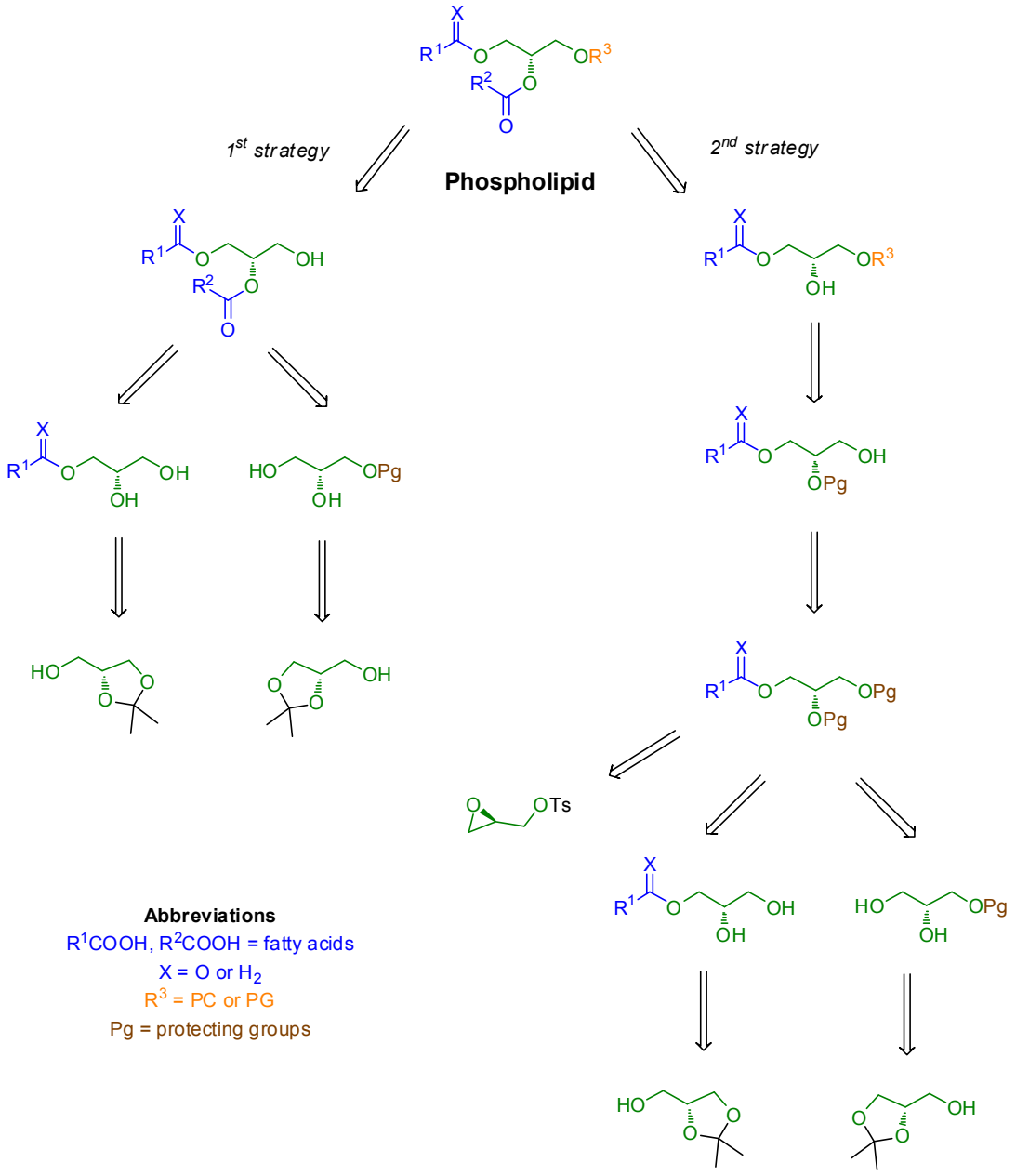

Figure 16. Retrosynthesis of 1,2-diacyl-*sn*-glycerophospholipids and 1-*O*-akyl-2-acyl-*sn*-glycerophospholipids.

One strategy relies on installation of the aliphatic chains and then attachment of the phosphate headgroup (1st strategy in Figure 16) whereas in the second strategy the aliphatic chain at the *sn*-1 position and the phosphate headgroup at the *sn*-3 position are installed first and then acylation of the hydroxyl at the *sn*-2 position is achieved at a later stage (2nd strategy in Figure 16).

Acyl-migration in unprotected glycerol derivatives is a major challenge in synthesizing phospholipids.[80] The migrations are promoted by both base and acid meaning that the synthetic transformations have to be performed under mild conditions. Furthermore, as described in section 1.1 many fatty acids are unsaturated which must be considered when planning the synthesis.

The commercially available compounds 1,2-isopropylidene-*sn*-glycerol and 2,3-isopropylidene-*sn*-glycerol serve as the most applied starting materials for the synthesis of 1,2-*O*-diacyl-glycerophospholipids. 1,2-Isopropylidene-*sn*-glycerol is made from D-mannitol[81,82] whereas 2,3-isopropylidene-*sn*-glycerol can be made from L-erythrulose,[83] L-serine[82] or L-ascorbic acid.[84] In addition to 2,3-isopropylidene-*sn*-glycerol, glycidols like (*R*)-glycidyl tosylate are used in the synthesis of *sn*-1-ether phospholipids. Glycidols can be made in high enantiomeric purity by asymmetric epoxidation of allyl alcohols.[85]

2.1 Synthesis of 1,2-Diacyl-*sn*-glycerophospholipids

Starting from 2,3-isopropylidene-*sn*-glycerol acylation of the *sn*-1 position has been performed using either carbodiimide mediated chemistry or via reaction with acid chlorides (Table 3). The removal of the isopropylidene protecting group without acyl-migration has been achieved under mild acidic conditions using acidic exchange resins, like Amberlyst-H^+ (entry 3 in Table 3), however long reaction times (>24 h) have been necessary in order to obtain good yields. Furthermore, hydroxyl coordinating reagents like $B(OH)_3$ in $MeNO_2$ or trifluoroacetic acid (TFA) in $B(OEt)_3$ has been efficient in the desired deprotection as well (entry 1 and 2 in Table 3).

Table 3. Synthesis of 1-acyl-*sn*-glycerol from 2,3-isopropylidene-*sn*-glycerol.

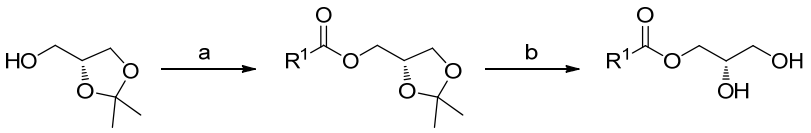

Entry	R^1COOH	Reaction conditions
1[86]	6-heptynoic acid	(a) Ethyl-(3-dimethylaminopropyl)-carbodiimide hydro chloride (EDCI), 4-dimethylaminopyridine (DMAP), CH_2Cl_2 (97%); (b) $B(OH)_3$, $MeNO_2$ (84%).
2[87]	Stearic acid	(a) Stearoyl chloride, Et_3N, DMAP, CH_2Cl_2; (b) TFA, CF_3CH_2OH, $B(OEt)_3$ (74%)
3[88]	Stearic acid	(a) EDCI, DMAP, CH_2Cl_2 (84%); (b) Amberlyst-H^+, MeOH (75%).
4[89]	Linoleic acid	(a) EDCI, DMAP, THF; (b) Dowex 50W, MeOH[a]

[a]Yield not reported.

Starting from 1,2-isopropylidene-*sn*-glycerol, protection of the *sn*-3 position is the first step. Various acid stabile protecting groups have been applied in the synthesis of 3-*O*-protected-*sn*-glycerols (Table 4) and among the used protecting groups are *p*-methoxybenzyl (PMB), *tert*-butyldiphenylsilyl (TBDPS), benzyl (Bn) and tosyl (Ts). The protecting groups are introduced under basic conditions and the following isopropylidene deprotection is achieved using acid catalysis, and having no ester-functionality acyl-migration is not an issue and strong acids are used, giving short reaction times and excellent yields (Table 4). In addition tetrahydropyranyl (THP, entry 3 in Table 4) is also successfully applied in this type of glycerol functionalization.

Table 4. Synthesis of 3-*O*-protected-*sn*-glycerols from 1,2-isopropylidene-*sn*-glycerol.

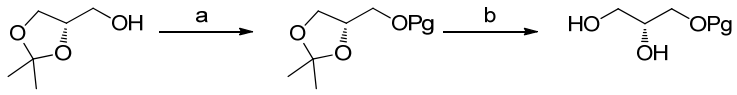

Entry	Pg	Reaction conditions
1[90]	PMB	(a) PMBCl, KH, Bu_4NI, THF; (b) TsOH, MeOH (98%).
2[91,92]	PMB	(a) PMBCl, NaH, DMF (90%); (b) AcOH, MeOH (99%).
3[93]	THP	(a) 3,4-dihydropyran (DHP), pyridine p-toluenesulfonate (PPTS), CH_2Cl_2 (92%); (b) $Bi(OTf)_3$, THF/H_2O 4:1 (76%).
4[94]	TBDPS	(a) TBDPSCl, imidazole, THF; (b) HCl, H_2O, EtOH (97%).
5[95]	Bn	(a) NaH, BnCl, DMSO (55%); (b) AcOH, H_2O (95%).
6[96]	Ts	(a) TsCl, Pyridine (91%); (b) HCl, H_2O, acetone (100%).

The 1-acyl-*sn*-glycerols (from Table 3) are by using appropriate protecting groups converted into 1,2-diacyl-*sn*-glycerols (Table 5). It is crucial that both the protecting of the *sn*-3 position and the final deprotection (step c in Table 5) can be achieved under conditions which avoid racemization. Dimethoxytrityl (DMT) has been used by Neff *et al.*[86] however the group is so acid labile that chromatography through silica must be done with care or with addition of base to the eluent like Neff *et al.*[86] have done. Hence the removal can be done under mild conditions and using $B(OH)_3$ in $MeNO_2$ the desired 1,2-diacyl-*sn*-glycerol is achieved (entry 1 in Table 5). Gaffney *et al.*[87] have used the 9-(9-phenyl)xanthenyl (pixyl or Px) protecting group, prepared by mixing the glycerol derivative and PxOH in AcOH followed by evaporation *in vacuo*. Deprotection was done by treatment with a dilute solution of $Cl_2CHCOOH$ and pyrrole in CH_2Cl_2, which was tolerated by the unsaturated arachidonoyl moiety in the *sn*-2 position (entry 3 in Table 5). Silyl protecting groups like *tert*-butyldimethylsilyl (TBDMS) was ruled out by Dodd *et al.*[97] as an applicable protecting group for glycerols due to acyl-migration upon treatment with fluorine sources like HF or tetrabutylammonium fluoride (TBAF). However Burgos *et al.* [98] have shown that applying the rather unusual deprotection conditions, *N*-bromosuccinimide (NBS) in DMSO and THF[99] migration was avoided and the 1,2-diacyl-*sn*-glycerol was obtained and the enantiomeric purity was verified by Mosher ester analysis[100] (entry 2 in Table 5). Recently Stamatov *et al.*[101] have developed a two step procedure for the deprotection of silyl protected glycerols, in which the silyl ether (such as triisopropylsilyl, TIPS) is converted into the trichloroacetate via treatment with $Et_3N{\cdot}3HF$ and trichloroacetic anhydride at 80 °C, then the trichloroacetate is hydrolyzed by pyridine in MeOH and THF affording the 1,2-diacyl-*sn*-glycerols (entry 5 and 6 in Table 5). A drawback in this method is the reaction temperature at 80 °C required for the trichloroacetate formation which limit the substrate scope, however an oleoyl moiety in both the *sn*-1 and *sn*-2 position has resist the conditions. Examination of other unsaturated fatty acids remains.

Table 5. Synthesis of 1,2-diacyl-*sn*-glycerols from 1-acyl-*sn*-glycerols.

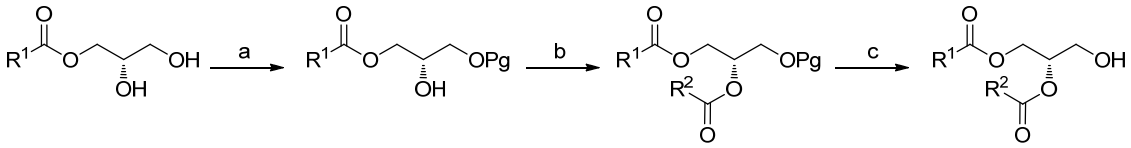

Entry	R^1COOH	Pg	R^2COOH	Reaction conditions
1[86]	6-Heptynoic acid	DMT	Myristic acid	(a) DMTCl, DMAP, pyridine (94%); (b) myristic acid, EDCI, DMAP, CH_2Cl_2 (92%); (c) $B(OH)_3$, $MeNO_2$ (81%).
2[98]	Stearic acid	TBDMS	Stearic acid	(a) TBDMSCl, imidazole, THF; (b) $C_{17}H_{35}COCl$, pyridine (77%); NBS, DMSO, THF.
3[87]	Stearic acid	Px	Arachidonic acid	(a) PxOH, AcOH (72%); (b) arachidonic acid, 2,6-$Cl_2C_6H_3COCl$, 1-methylimidazole, CH_2Cl_2; (c) $Cl_2CHCOOH$, pyrrole, CH_2Cl_2 (90%).
4[88]	Stearic acid	DMT	Arachidonic acid	(a) DMTCl, pyridine (96%); (b) arachidonic acid, DCC, DMAP, CH_2Cl_2 (100%); (c) TFA, pyrrole (72%).
5[101]	Oleic acid	TBDMS	Acetic acid	(a) TBDMSCl, imidazole, THF (85%); (b) AcCl, pyridine (94%); (c) (i) $Et_3N{\cdot}3HF$, $(CCl_3CO)_2O$; (ii) pyridine, MeOH, THF (93%).
6[101]	Oleic acid	TIPS	Oleic acid	(a) TIPSCl, imidazole, THF (80%); (b) oleoyl chloride, pyridine (93%); (c) (i) $Et_3N{\cdot}3HF$, $(CCl_3CO)_2O$ (ii) pyridine, MeOH, THF (92%).

Monoacylation of 3-*O*-protected-glycerols (from Table 4) have been achieved in moderate to good yields using a Steglich esterification[102] (Table 6). Applying the coupling reagents in excess double-acylation has also been obtained (entry 2 in Table 6). Likewise attachment of the second fatty acid to the *sn*-2 position (step b in Table 6) have been achieved using the Steglich coupling or via reaction with acid chlorides. When double bonds are absent the benzyl protected strategy has been used and Martin *et al.*[103] have removed the benzyl ether by hydrogenolysis to obtain pure 1,2-diacyl-*sn*-glycerols (entry 3 in Table 6). The PMB-group has efficiently been removed by 2,3-dichloro-5,6-dicyano-

1,4-benzoquinone (DDQ) in moist CH_2Cl_2 allowing a carboxybenzyl (Cbz) group to be present (entry 4 in Table 6).[92]

Table 6. Synthesis of 1,2-diacyl-*sn*-glycerols from 3-*O*-protected-*sn*-glycerols.

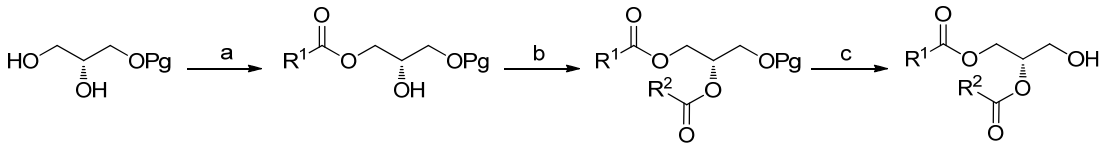

Entry	Pg	R^1COOH	R^2COOH	Reaction conditions
1[104]	PMB	Stearic acid	Eicosanoic acid	(a) Stearic acid, dicyclohexylcarbodiimide (DCC), DMAP, CH_2Cl_2 (63%); (b) Eicosanoic acid, DCC, DMAP, CH_2Cl_2 (82%); (c) DDQ, H_2O, CH_2Cl_2 (88%).
2[93]	THP	Palmitic acid	Palmitic acid	(a+b) Palmitic acid, DCC, DMAP, $CHCl_3$ (79%); (c) 0.15 M HCl, $CHCl_3$, MeOH (93%).
3[103]	Bn	Palmitic acid	Propanoic acid	(a) Palmitic acid, DCC, DMAP, $CHCl_3$ (69%); (b) Propionoic acid, DCC, DMAP, $CHCl_3$ (96%); (c) H_2, Pd/C, EtOH, AcOH (99%).
4[92]	PMB	$CbzNH(CH_2)_{11}CO_2H$	Palmitic acid	(a) $CbzNH(CH_2)_{11}COOH$, DCC, DMAP, CH_2Cl_2 (89%); (b) Palmitoyl chloride, pyridine, DMAP, CH_2Cl_2 (70%); (c) DDQ, H_2O, CH_2Cl_2 (91%).

When it is desirable to install the ester at the *sn*-2 position at a later stage, e.g. after attachments of the phosphate headgroup, 1-acyl-2-*O*-protected-*sn*-glycerols are needed and although this is not the most applied strategy for synthesis of phospholipids examples are reported. Starting from a 1-acyl-*sn*-glycerol Bibak *et al.*[105] (Table 7) have used a protecting group strategy which initiate with a (9-fluorenylmethyl) carbamate (Fmoc) protection of the *sn*-3 position followed by a THP protection of the *sn*-2 position. Subsequent removal of Fmoc with piperidine in CH_2Cl_2 gave the 1-acyl-2-*O*-protected-*sn*-glycerol.

Table 7. Synthesis of 1-acyl-2-*O*-protected-*sn*-glycerols from 1-acyl-*sn*-glycerols.

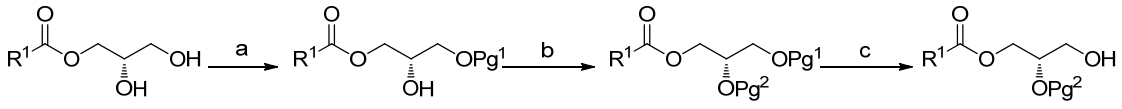

Entry	R^1COOH	Pg^1	Pg^2	Reaction conditions
1[105]	Palmitic acid	Fmoc	THP	(a) FmocCl, DMAP, $CHCl_3$ (58%); (b) DHP, PPTS, CH_2Cl_2 (86%); (c) Piperidine, CH_2Cl_2 (87%).

1-Acyl-2-*O*-protected-*sn*-glycerols have also been obtained from 3-*O*-protected-*sn*-glycerols (Table 8). Like described earlier selective acylations of the *sn*-1 position have been achieved using the Steglich coupling.[102] Having the *sn*-3 position PMB-protected Martin *et al.*[103] were successful with benzyloxy methyl (BOM) protection of the *sn*-2 position and liberation of the *sn*-3 position was mediated by DDQ in moist CH_2Cl_2 (entry 1 in Table 8). Starting from 3-*O*-tosyl-*sn*-glycerol Rosseto *et al.*[106] have used a strategy in which the *sn*-2 position was THP protected and the tosylate was then converted into the corresponding methoxyacetate and after some optimization it was found that *tert*-butylamine in MeOH and $CHCl_3$ was capable to selective hydrolyze the methoxyacetate over the ester at the *sn*-1 position (entry 2 in Table 8).

Table 8. Synthesis of 1-acyl-2-*O*-protected-*sn*-glycerols from 3-*O*-protected-*sn*-glycerols.

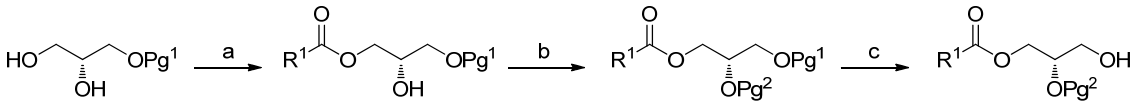

Entry	Pg^1	R^1COOH	Pg^2	Reaction conditions
1[91,103]	PMB	Palmitic acid	BOM	(a) Palmitic acid, DCC, DMAP, CH_2Cl_2 (54%); (b) BOMCl, DIPEA, CH_2Cl_2 (94%); (c) DDQ, H_2O, CH_2Cl_2 (88%).
2[106]	Ts	Palmitic acid	THP	(a) Palmitic acid, DCC, DMAP, CH_2Cl_2 (72%); (b) 3,4-dihydropyran, PPTS, CH_2Cl_2 (95%); (c) (i) $CH_3OCH_2COO^-Et_4N^+$, MeCN (ii) $^tBuNH_2$, MeOH, $CHCl_3$ (80%).

After installation of a phosphate headgroup (see section 2.3 and 2.4) on 1-acyl-2-*O*-protected-*sn*-glycerols (Table 9) removal of the protecting group at the *sn*-2 position has to be done under conditions in which acyl-migration is prevented, and using either a Bn or BOM protection, palladium catalyzed hydrogenolysis has been capable of doing that (entry 1, 3 and 4 in Table 9). Using slightly acidic conditions Hajdu and co-workers[105,106] have been able to remove a THP group without migration (entry 2 in Table 9). Acylation of the liberated *sn*-2 position has been done using various acylation methods, such as the Steglich coupling[102] (entry 1 in Table 9) and various carboxylic acid has been attached like the unsaturated docosahexaenoic acid (entry 1 in Table 9). In general good yields are reported for esterification on PC lysolipids (like in entry 1 and 2 in Table 9 and Table 14) however Shizuka *et al.*[91] report that no conversion was observed when acylation of 1-palmitoyl-2-lyso-*sn*-glycero-3-phosphocholine with *ent*-15-*epi*-F_{2t}-isoprostanoic acid was attempted using various coupling methods. But when the PC headgroup was protected as (2-chloroethyl) methyl phosphate the desired acylation occurred (entry 3 in Table 9).

Table 9. Synthesis of 1,2-diacyl-*sn*-glycerophospholipids from 1-acyl-2-*O*-protected-*sn*-glycerols.

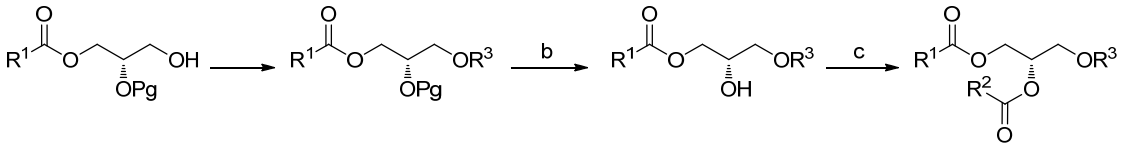

Entry	R^1COOH	Pg	R^3 [a]	R^2COOH	Reaction conditions
1[107]	Stearic acid	Bn	PC	Docosahexaenoic acid[b]	(a) H_2, $Pd(OH)_2/C$, MeOH, H_2O; (b) docosahexaenoic acid, DCC, DMAP, $CHCl_3$ (62%).
2[105,106]	Palmitic acid	THP	PC	Palmitic acid	(a) 0.15 M HCl, dioxane, H_2O; (b) *p*-nitrophenyl palmitate, DMAP, $CHCl_3$ (62%).
3[91]	Palmitic acid	BOM	PC[c]	*ent*-15-*epi*-F_{2t}-isoprostanoic acid	(a) H_2, Pd/C, THF, H_2O (99%); (b) EDCI, DMAP, CH_2Cl_2 (54%).
4[108]	Dodecanoic acid	Bn	PG[d]	Oleic acid	(a) H_2, Pd/C, EtOAc, MeOH (100%); (b) oleic acid, EDCI, DMAP, CH_2Cl_2 (85%).

[a]Phosphate headgroup, see section 2.3 and 2.4 for synthesis. [b]*cis*-4,7,10,13,16,19-docosahexaenoic acid. [c]Protected as (2-chloroethyl) methyl phosphate. [d]Protected, see section 2.4.

2.2 Synthesis of 1-*O*-Alkyl-2-acyl-*sn*-glycerophospholipids

In the following synthesis of 1-*O*-alkyl-2-acyl-*sn*-glycerophospholipids initiated from 2,3-isopropylidene-*sn*-glycerol or (*R*)-glycidyl tosylate are reviewed. Starting from 2,3-isopropylidene-*sn*-glycerol conversion into 1-*O*-alkyl-*sn*-glycerols have been accessed by alkylation of the *sn*-1 position using a Williamson ether synthesis[109] followed by acid catalyzed acetal hydrolysis (Table 10).

Table 10. Synthesis of 1-*O*-alkyl-*sn*-glycerol from 2,3-isopropylidene-*sn*-glycerol.

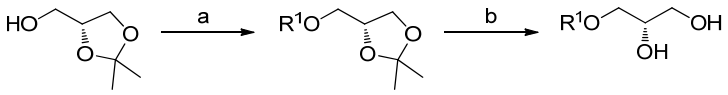

Entry	R^1OH	Reaction conditions
1[110]	Hexadecanol	(a) $C_{16}H_{33}I$, NaH, DMF, THF; (b) TFA/H_2O 9:1 (55%)[a].
2[111]	Hexadecanol	(a) $C_{16}H_{33}OMs$, NaH, benzene (80%); (b) HCl, THF (78%).
3[86]	10-Undecynol	(a) 10-Undecynyl bromide, NaH, DMF (55%); (b) AcOH, H_2O (99%).

[a]Yield over two step

Like for 1,2-diacyl-*sn*-glycerols (see Table 5) synthesis of 1-*O*-alkyl-2-acyl-*sn*-glycerols are achieved by using appropriate protection of the *sn*-3 position (Table 11). However 1-*O*-alkyl-2-acyl-*sn*-glycerols does not have the same tendency to undergo acyl-migration as 1,2-diacyl-*sn*-glycerols and Yashunsky *et al.*[110] have removed a triethylsilyl (TES) group with $Et_3N{\cdot}3HF$ in MeCN and CH_2Cl_2 (entry 1 and 2 in Table 11). While TBDPS have been removed by TBAF in the presence of imidazole (entry 3 in Table 11), in the absence of imidazole substantial acyl-migration took place.[90] The two step procedure developed by Stamatov *et al.*[101] for the deprotection of silyl ethers in 1,2-diacyl-*sn*-glycerols were also capable of removing TBDMS without acyl-migration in 1-*O*-alkyl-2-acyl-*sn*-glycerols (entry 4 in Table 11). Furthermore, DMT protection of the *sn*-3 position has been successful (entry 5 in Table 11).

Table 11. Synthesis of 1-*O*-alkyl-2-acyl-*sn*-glycerols from 1-*O*-alkyl-*sn*-glycerols.

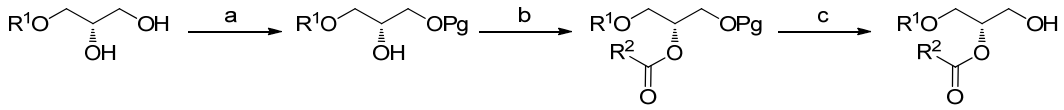

Entry	R^1OH	Pg	R^2COOH	Reaction conditions
1[110]	Hexadecanol	TES	Oleic acid	(a) TESCl, pyridine, CH_2Cl_2; (b) Oleoyl chloride, Et_3N, DMAP, pyridine; (c) $Et_3N{\cdot}3HF$, MeCN, CH_2Cl_2 (58%)[c].
2[110]	Hexadecanol	TES	Linoleic acid	(a) TESCl, pyridine, CH_2Cl_2; (b) Linoleoyl chloride, Et_3N, DMAP, pyridine; (c) $Et_3N{\cdot}3HF$, MeCN, CH_2Cl_2 (58%)[a].
3[90,112]	(*Z*)-1-Octadecenol	TBDPS	Palmitic acid	(a) TBDPSCl, imidazole, DMF (90%); (b) $(C_{15}H_{31}CO)_2O$, DMAP, $CHCl_3$ (98%); (c) TBAF, imidazole, THF (>74%).
4[101]	Hexadecanol	TBDMS	AcOH	(a) TBDMSCl, imidazole, THF (85%); (b) AcCl, pyridine, CH_2Cl_2 (95%); (c) (i) $Et_3N{\cdot}3HF$, $(CCl_3CO)_2O$ (ii) pyridine, MeOH, THF (92%).
5[86]	10-Undecynol	DMT	Myristic acid	(a) DMTCl, DMAP, pyridine (94%); (b) Myristic acid, EDCI, DMAP, CH_2Cl_2 (99%); (c) $B(OH)_3$, $MeNO_2$ (81%).

[a]Yield over three steps.

Another convenient route used for the introduction of the *sn*-1-ether functionality is Lewis acid catalyzed epoxide opening of glycidols like (*R*)-glycidyl tosylate with alcohols (Table 12). Guivisdalsky *et al.*[114] discovered that $BF_3{\cdot}OEt_2$ mediated the desired epoxide opening with excellent regioselectivity and high enantiomeric excess, whereas other Lewis acid like $Ti(O^iPr)_4$ and $SnCl_4$ gave much lower conversion. Furthermore, Guivisdalsky *et al.*[114] demonstrated that while epoxide opening of (*R*)-glycidyl tosylate with hexadecanol exclusively gave the *sn*-1-ether, epoxide opening of the corresponding TBDPS glycidol resulted in a 9:1 ratio between the desired *sn*-1-ether and the undesired *sn*-2-ether. Hence Andresen *et al.*[68] have synthesized a collection of different *sn*-1-ether phsopholipids from (*R*)-glycidyl tosylate. Having the *sn*-1-ether functionality introduced synthesis of 1-*O*-alkyl-2-*O*-protected-*sn*-glycerols has been achieved using either a Bn or THP protection of the *sn*-2 position. Bn protection has been performed under both basic conditions (entry 1 in Table 12) and acidic conditions using benzyl trichloroacetimidate (entry 2 in Table 12). Removal of the tosyl group has been achieved by converting the tosylate into the acetate, which then either has been reduced with $LiAlH_4$ (entry 1 in Table 12) or hydrolyzed (entry 3 in Table 12). Applying $NaNO_2$ Andresen *et al.*[68] have obtained the alcohol in one step

from the tosylate (entry 2 in Table 12) albeit the overall yield was lower than using the two step procedure.

Table 12. Synthesis of 1-*O*-alkyl-2-*O*-protected-*sn*-glycerols from (*R*)-glycidyl tosylate.

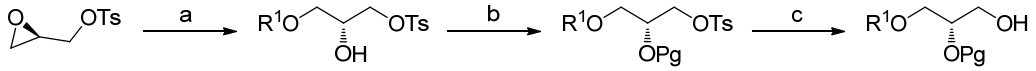

Entry	R^1OH	Pg	Reaction conditions
1[113,114]	Hexadecanol	Bn	(a) $C_{16}H_{33}OH$, $BF_3{\cdot}OEt_2$, $CHCl_3$ (80%); (b) BnOTf, 2,6-di-*tert*-butyl-4-methylpyridine, CH_2Cl_2 (96%); (c) (i) CsOAc, DMF, DMSO (ii) $LiAlH_4$, Et_2O (92%).
2[68]	Octadecanol	Bn	(a) $C_{18}H_{37}OH$, $BF_3{\cdot}OEt_2$, CH_2Cl_2 (91%); (b) $BnOC(NH)CCl_3$, TfOH, dioxane (96%); (c) $NaNO_2$, DMF (72%).
3[115]	$CH_3OCO(CH_2)_4CH_2OH$	THP	(a) $CH_3OCO(CH_2)_4CH_2OH$, $BF_3{\cdot}OEt_2$, CH_2Cl_2 (89%); (b) DHP, PPTS, CH_2Cl_2 (69%); (c) (i) Et_4NOAc, MeCN (ii) K_2CO_3, MeOH (68%).

Ohno *et al.*[111] have also managed to synthesize a 1-*O*-alkyl-2-*O*-protected-*sn*-glycerol from 1-*O*-alkyl-*sn*-glycerol. The *sn*-3 position was selectively protected with a trityl (Tr) group, followed by benzylation of the *sn*-2 position after which the trityl group was removed again via treatment with acid (Table 13).

Table 13. Synthesis of 1-*O*-alkyl-2-*O*-protected-*sn*-glycerols from 1-*O*-alkyl-*sn*-glycerols.

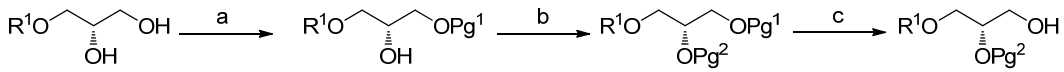

Entry	R^1OH	Pg^1	Pg^2	Reaction conditions
1[111]	Hexadecanol	Tr	Bn	(a) TrCl, DMAP, pyridine (92%); (b) KH, BnCl, benzene (100%); (c) $TsOH{\cdot}H_2O$, MeOH (92%).

Synthesis of 1-*O*-alkyl-2-acyl-*sn*-glycerophospholipids from 1-*O*-alkyl-2-*O*-protected-*sn*-glycerols has been performed in very much the same way as synthesis of 1,2-diacyl-*sn*-glycerophospholipids from 1-acyl-2-*O*-protected-*sn*-glycerols (see Table 9). Benzyl protection of the *sn*-2 position has been used by Guivisdalsky *et al.*[113] and hydrogenolysis under palladium catalysis gave the lysolipids (entry 1-3 in Table 14). Having a vinyl-ether in the *sn*-1 position Shin *et al.*[112] have used a TBDMS protection of the *sn*-2 position and in the presence of imidazole the deprotection was achieved with TBAF in THF (entry 4 in

Table 14). Interestingly, the following acylation of the *sn*-2 position has only been reported via reaction with anhydrides (entry 1,2 and 4 in Table 14) albeit in good yields.

Table 14. Synthesis of 1-*O*-alkyl-2-acyl-*sn*-glycerophospholipids from 1-*O*-alkyl-2-*O*-protected-*sn*-glycerols.

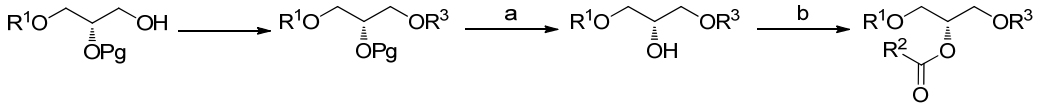

Entry	R^1OH	Pg	R^3 [a]	R^2COOH	Reaction conditions
1[113]	Hexadecanol	Bn	PC	Palmitic acid	(a) H_2, $Pd(OH)_2/C$, MeOH, H_2O (100%); (b) $(C_{15}H_{31}CO)_2O$, DMAP, $CHCl_3$ (98%)
2[68,111]	Octadecanol	Bn	PC	AcOH	(a) H_2, Pd/C, MeOH (>77%); (b) Ac_2O, pyridine (93%).
3[68]	Octadecanol	Bn	PG[b]		(a) H_2, Pd/C, MeOH (>67%).
4[112]	(*Z*)-1-Hexadecenol	TBDMS	PC	Palmitic acid	(a) TBAF, imidazole, THF (98%); (b) $(C_{15}H_{31}CO)_2O$, DMAP, CH_2Cl_2 (53%).

[a]Phosphate headgroup. [b]Protected, see section 2.4.

2.3 Synthesis of Phosphatidylcholine (PC) Headgroup

Installation of the PC headgroup has been done by different procedures[116] however two procedures are mainly used and they are shown in Scheme 1 and further reaction details are giving in Table 15. The first procedure (entry 1 in Table 15 and Scheme 1) is a one pot procedure in which the glycerol are reacted with phosphorus oxychloride, then one equivalent of choline tosylate is added and the *in situ* generated dichlorophosphate undergo substitution with choline and addition of H_2O fulfill the synthesis. The procedure is very sensitive to moisture while inconsistent yields have been reported.[64] In the second procedure (entry 2 in Table 15 and Scheme 1) the glycerol is reacted with ethylene chlorophosphate in the first step and after purification the final step is ring opening of the glycerol-ethylenephosphate-conjugate with Me_3N, which is done at 65 °C in a pressure bottle to avoid evaporation of Me_3N and with reaction times above 24 h. Compared to the first procedure this is rather harsh conditions and furthermore, Me_3N is not convenient to handle due to the low boiling point at 3-4 °C.[117] But this chemistry is less sensitive to moisture and furthermore, the ethylenephosphate-intermidiate can be isolated while deprotection and functionalization of the *sn*-2 position can be done prior to the final conversion into the PC lipid, like reported in entry 3 in Table 9. For further procedures to PC lipids see the review by Paltauf and Hermetter.[116]

Scheme 1. Synthetic routes to the PC headgroup. ROH represent a glycerol-derivative

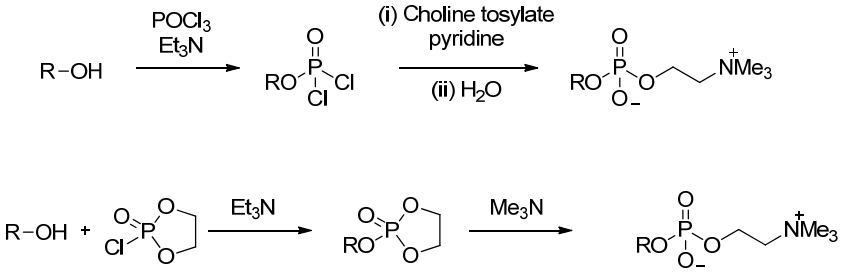

Table 15. Synthesis of the PC headgroup – reaction details (see Scheme 1).

Entry	Reaction conditions	Yield[a]
1[68,113,118]	(i) $POCl_3$, Et_3N, CH_2Cl_2; (ii) choline tosylate, pyridine; (iii) H_2O.	75%
2[68,106,105,112]	(i) ethylene chlorophosphate, Et_3N, benzene; (ii) Me_3N, MeCN, 65 °C (pressure bottle, 24 h).	60%

[a]Representative value

2.4 Synthesis of Phosphatidylglycerol (PG) Headgroup

Although that synthesis of PG lipids are less common than synthesis of PC lipids various procedures have been developed[116] and three of the mainly used are presented in Scheme 2 and Table 16. In the first procedure (entry 1 in Table 16 and Scheme 2) the glycerol is subjected to methyl dichlorophosphate and 2,2,6,6-tetramethyl piperidine (TMP) and followed by addition of 2,3-isopropylidene-*sn*-glycerol the protected PG lipid is obtained and if desirable it can be isolated by column chromatography. Due to the protections of the glycerol and the phosphate, modifications elsewhere in the molecule can be done, like observed in entry 4 in Table 9.[108] Hydrolysis of the methyl phosphate ester has been achieved via treatment with Me_3N in MeCN and ^{i}PrOH while the glycerol has been liberated under slightly acidic conditions, however long reaction times (>14 h) are needed for both conversions.

The two other procedures (entry 2 and 3 in Table 16 and Scheme 2) involve tetrazole mediated phosphoramidite couplings followed by oxidation of the phosphite to the phosphate with peroxides, such as ^{t}BuOOH. All three procedures lead to the formation of the same protected phosphate, and in addition to the Me_3N mediated hydrolysis (entry 2 and 3 in Table 16), the methyl phosphate ester has also been cleaved with NaI in 2-butanone (entry 3 in Table 16). The overall yields for the three routes are comparable.

Scheme 2. Synthetic routes to the PG headgroup. ROH represent a glycerol-derivative.

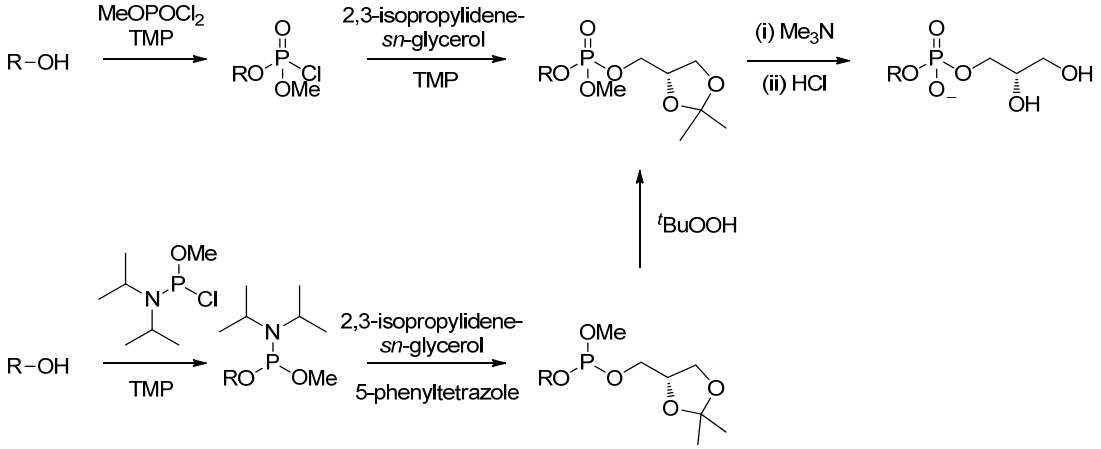

Table 16. Synthesis of the PG headgroup – reaction details (see Scheme 2).

Entry	Reaction conditions	Yield
1[68]	(i) $MeOPOCl_2$, TMP, toluene; (ii) 2,3-isopropylidene-*sn*-glycerol, TMP; (iii) Me_3N, MeCN, ^{i}PrOH; (iv) HCl, MeOH, CH_2Cl_2.	61%
2[68]	(i) $(^{i}Pr)_2NPClOMe$, TMP, CH_2Cl_2; (ii) 5-phenyltetrazole, 2,3-isopropylidene-*sn*-glycerol; (iii) ^{t}BuOOH; (iv) Me_3N, MeCN, ^{i}PrOH; (v) HCl, MeOH, CH_2Cl_2.	67%
3[108]	(i) $((^{i}Pr)_2N)_2POMe$, tetrazole, CH_2Cl_2; (ii) 2,3-isopropylidene-*sn*-glycerol, tetrazole; (iii) *m*CPBA; (iv) NaI, 2-butanone; (v) TFA, MeOH, CH_2Cl_2.	55%

3. Chlorambucil Phospholipid Prodrugs

3.1 Introduction

To demonstrate proof-of-principle chlorambucil was selected for incorporation into the investigated liposomal drug delivery system. Chlorambucil is a chemotherapeutic agent of the mustard gas type[119] and it was originally synthesized by Everett *et al*. in 1953.[73] It is used clinically for the treatment of lymphocytic leukemia[120] typically in combination with other drugs. Chlorambucil is orally administrated (Leukeran®), but undergoes rapid metabolism, and as a result the stability in aqueous environments is low and chlorambucil has an elimination half-life of 1.5 h.[121,122,123] The prodrug formulation could remedy this, since this system will shield chlorambucil from degradation through the incorporation in the lipophilic part of the liposomal membrane and deliver it directly to the tumor, decreasing metabolism compared to the oral administration route. To investigate the effect of *sn*-1 ether chain length and headgroup charge on enzymatic activity, prodrugs **1** and **2** (Figure 17) were prepared with both C_{16} and C_{18} ether chains and a PC and PG headgroup, respectively.

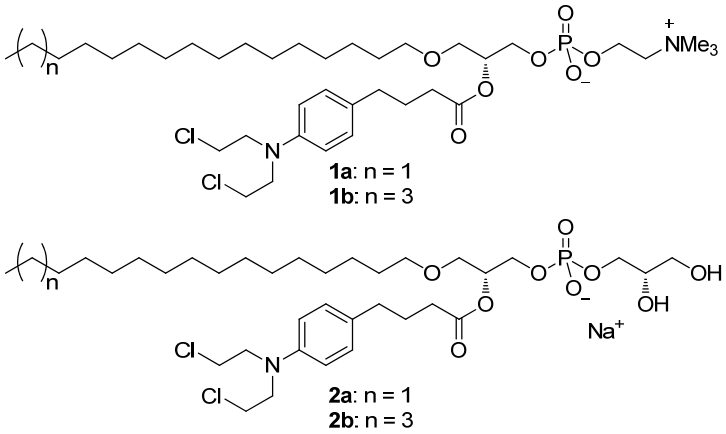

Figure 17. The four target chlorambucil *sn*-1-ether phospholipid prodrugs. Prodrugs **1a** and **1b** have a PC headgroup with a C_{16} and a C_{18} ether chain respectively. Target compounds **2a** and **2b** have the negatively charged PG headgroup.

3.2 Synthesis of Chlorambucil Phospholipid Prodrugs

The synthesis of *sn*-1-ether phospholipids have, as described in section 2.2, been accessed via different routes, starting from 2,3-isopropylidene-*sn*-glycerol (see Table 10) or (*R*)-glycidyl tosylate (see Table 12). (*R*)-Glycidyl tosylate ((–)-**3**) served as the starting material in this work and the aliphatic ether chain was introduced by ring-opening of the epoxide under Lewis acid catalysis,[114] resulting in yields of 89% and 97% for **4a** and **4b**, respectively (Scheme 3). The PMB group was chosen for protection of the secondary alcohol and introduced by using *para*-methoxybenzyl trichloroacetimidate (PMBTCA) with $La(OTf)_3$ catalysis.[124,125] The resulting tosylate was converted into the acetate with CsOAc in a 9:1 mixture of DMSO and DMF and the ester was hydrolyzed with NaOMe in

MeOH at 40 °C yielding the primary alcohols **5a** and **5b** in overall yields of 70% and 78% respectively over 3 steps (Scheme 3). It was essential to carry out the hydrolysis at elevated temperature in order to obtain homogeneous reaction mixtures and achieve full conversion in the transformations. Inspired by Andresen *et al.*[68] a direct conversion of the tosylates to the alcohols **5a** and **5b** using $NaNO_2$ in DMSO was attempted and yields up to 94% over two steps (including the PMB-protection) were achieved, but the result was not reproducible and inconsistent yields from 60% to 94% were obtained. The corresponding carboxylic acid was observed as the major by-product in the experiments giving low yields and since there is precedence for oxidation of alcohols in aqueous environments in the presence of HNO_2 and oxygen[126,127] it is likely that the oxidation occurred during the aqueous workup. It was attempted to circumvent the undesired oxidation by applying a basic workup, but that did not improve the yield of the desired alcohol.

Scheme 3. Synthesis of phospholipid precursor **5a** and **5b**.[a]

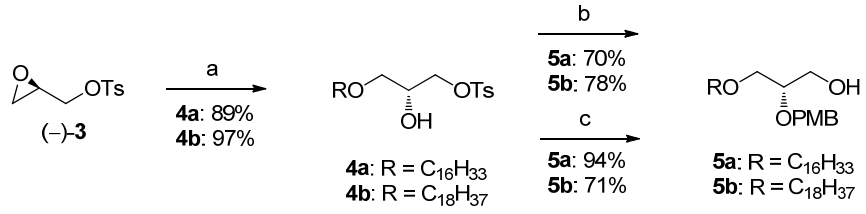

[a]Reagents: (a) $C_{16}H_{33}OH$ or $C_{18}H_{37}OH$, $BF_3{\cdot}OEt_2$, CH_2Cl_2; (b) (i) PMBTCA, $La(OTf)_3$, toluene; (ii) CsOAc, DMSO, DMF; (iii) NaOMe, MeOH; (c) (i) PMBTCA, $La(OTf)_3$, toluene; (ii) $NaNO_2$, DMSO.

The PC headgroup was attached to the primary alcohols **5a** and **5b** by reaction with phosphorus oxychloride and Et_3N, followed by addition of choline tosylate, pyridine and finally H_2O (Scheme 4 and compare with Table 15). Excess choline tosylate was removed on an MB-3 ion-exchange column and after purification by column chromatography the PMB-group was removed by hydrogenolysis mediated by Pd/C in a quantitative yield, but disappointingly upon scaleup a slow conversion was observed. Instead DDQ in an 18:1 mixture of CH_2Cl_2 and H_2O,[128] was attempted and these conditions resulted in full conversion within 3 h and with satisfactory isolated yields of **6** (Scheme 4). The final attachment of chlorambucil to the phospholipid backbone was achieved via a Steglich esterification[102] with DCC and a catalytic amount of DMAP. When the acylation of **6a** was performed in ethanol-free chloroform at 20 °C or CH_2Cl_2 in the temperature range from 0 °C to reflux no incorporation of chlorambucil was observed, but when the conditions were changed to reflux in 1,2-dichloroethane the acylation occurred in a 75% yield, albeit only after adding 5 equivalents of chlorambucil and DCC in portions over 31 h. The acylation of **6b** led to an isolated yield of 76% in refluxing chloroform and that was not improved by using 1,2-dichlorethane as the solvent. Changing the coupling reagents to EDCI and DMAP[129] did not improve the conversion of the **6**. In continuation of this

Shizuka *et al.*[91] report that acylation of compounds like **6** was not achievable in their hands whereas fine yields have been obtained by others (see Table 9 and Table 14).

Scheme 4. Synthesis of chlorambucil phospholipid prodrugs **1**.[a]

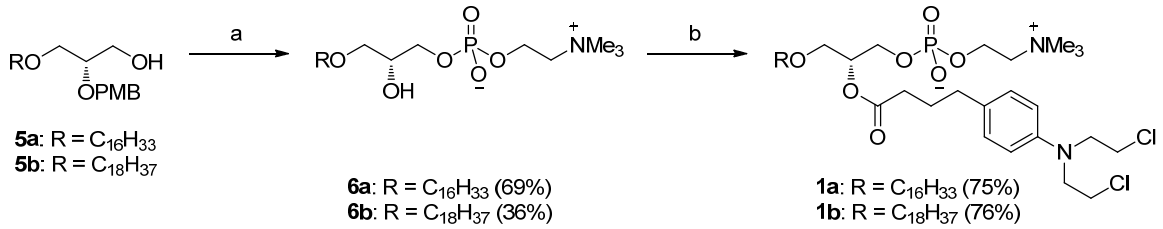

5a: R = $C_{16}H_{33}$
5b: R = $C_{18}H_{37}$

6a: R = $C_{16}H_{33}$ (69%)
6b: R = $C_{18}H_{37}$ (36%)

1a: R = $C_{16}H_{33}$ (75%)
1b: R = $C_{18}H_{37}$ (76%)

[a]Reagents: (a) (i) $POCl_3$, Et_3N, CH_2Cl_2; (ii) choline tosylate, pyridine; (iii) H_2O; (iv) H_2, Pd/C, EtOAc, MeOH or DDQ, CH_2Cl_2, H_2O; (b) chlorambucil, DCC, DMAP, $CHCl_3$ or 1,2-dichloroethane.

3.3 Biophysical Characterization and Enzyme Activity

The chlorambucil phospholipid prodrugs (**1** and **2**[ii]) were formulated as liposomes by extrusion in 4-(2-hydroxyethyl)-piperazine-1-ethanesulfonic acid (HEPES) buffer using the dry lipid film technique.[130] The phospholipid solutions were analyzed by dynamic light scattering (DLS) in order to investigate the particle size and the DLS analysis revealed that **1** and **2** form particles in the liposome size region (Table 17) and with a low polydispersity, indicating formation of unilaminar vesicles. The thermodynamic phase behavior was investigated by DSC but no phase transition was observed in the tested temperature range (20–70 °C) illustrating that the phospholipid bilayers are in a fluid state at 20 °C. Furthermore, the prodrugs were not able to encapsulate calcein. Presumably, these observations are a consequence of the incorporation of chlorambucil which prevents well ordered chain packing.

Table 17. DLS analysis of chlorambucil phospholipid prodrugs.

Compound	Particle size	
	Diameter (nm)	PdI[a]
1a	124	0.12
1b	125	0.22
2a	104	0.08
2b	113	0.05

[a]PdI = polydispersity index

The ability of $sPLA_2$ to degrade the chlorambucil phospholipid prodrugs **1** and **2** were studied by treating the liposome solutions with snake (*Agkistrodon piscivorus piscivorus*) venom $sPLA_2$ at 37 °C. Snake venom $sPLA_2$ is a convenient model enzyme, since it is not

[ii] The synthesis of phospholipid **2** was performed by colleague Dr. Mikkel S. Christensen.[135]

sensitive to the charge of the surface, unlike human $sPLA_2$ IIA, but shows the same substrate specificity.[61,56,131] In order to investigate the enzymatic activity on a molecular level matrix-assisted laser desorption/ionization time of flight mass spectrometry (MALDI-TOF MS) and HPLC were applied. MALDI-TOF MS has recently been exploited as a very fast and sensitive technique for detection of phospholipids[132,133,134] and it was decided to study the enzyme activity with this method in order to verify that the phospholipid prodrugs were consumed and the anticancer drugs released. For the measurements 2,5-dihydroxybenzoic acid (DHB) and CF_3COONa in methanol containing 1,2-dipalmitoyl-*sn*-glycero-3-phosphoglycerol (DPPG) as an internal standard was used as the matrix, which did not interfere with the regions of interest in the MS spectra. The disappearance over time of the prodrugs signals ($M+H^+$ and $M+Na^+$) in the MS spectra in Figure 18 shows that snake (*Agkistrodon piscivorus piscivorus*) venom $sPLA_2$ hydrolyze the prodrugs **1a** and **2a** and the emergence of the lysolipid signals ($M+H^+$ and $M+Na^+$) verify the release of the expected lysolipids. From the spectra it is also possible to get information about the conversion rate, and whereas **2a** is almost fully consumed after 2 h, **1a** needs more than 24 h for full digestion by $sPLA_2$. The MALDI-TOF MS analysis of **1b** and **2b** revealed that full degradation is obtained in 2–6 h (Table 18). These results were verified by HPLC (Figure 19 and Table 18).

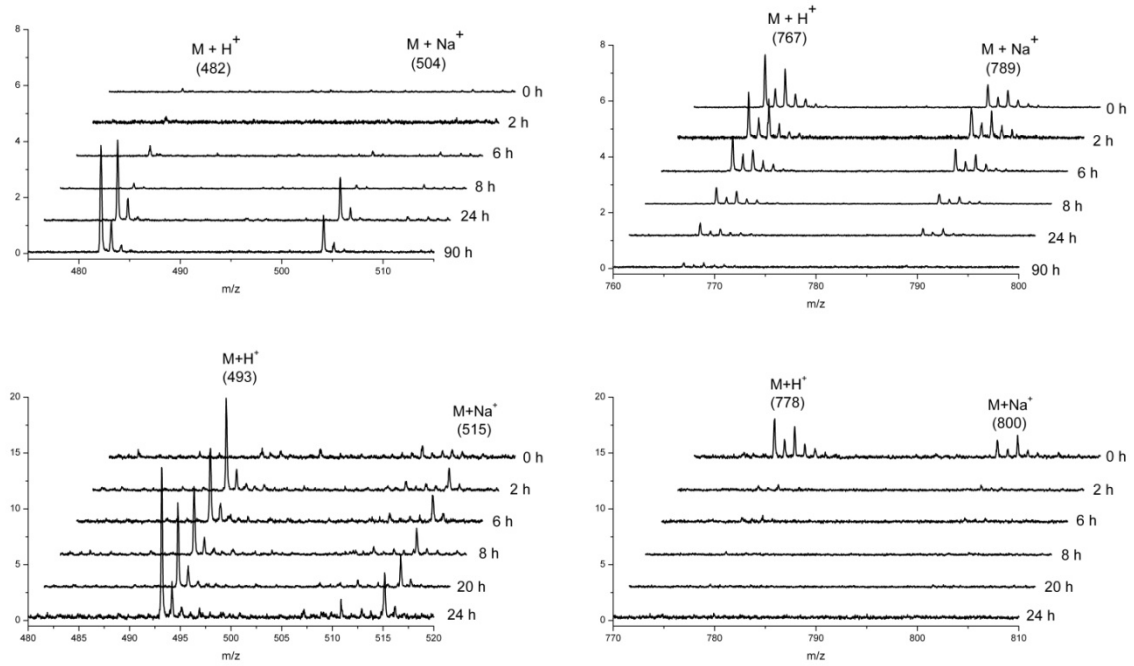

Figure 18. MALDI-TOF MS monitoring of snake (*Agkistrodon piscivorus piscivorus*) venom $sPLA_2$ activity on chlorambucil phospholipid prodrug **1a** (top) and **2a** (bottom). The spectra demonstrate that the prodrugs (right) are consumed and the lysolipids (left) are released.

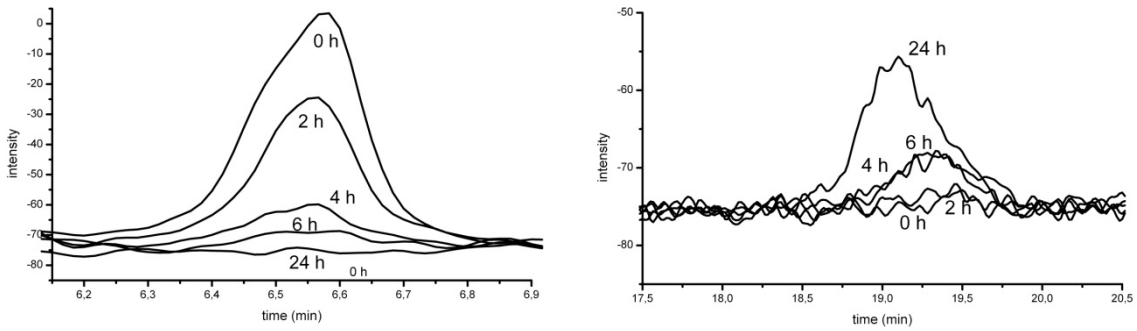

Figure 19. HPLC chromatogram for the snake (*Agkistrodon piscivorus piscivorus*) venom $sPLA_2$ experiment on chlorambucil phospholipid prodrug **1a** showing the amount of prodrug (left) and lysolipid **6a** (right) before the addition of the enzyme and after 2, 4, 6 and 24 h.

Table 18. Activity of snake (*Agkistrodon piscivorus piscivorus*) venom and human $sPLA_2$ IIA on prodrugs **1** and **2**, monitored by MALDI-TOF MS and HPLC.[a]

Substrate	**Full Hydrolysis by $sPLA_2$ within 48 h**		
	Snake venom $sPLA_2$		**Human $sPLA_2$ IIA**
	MALDI-TOF MS	HPLC	MALDI-TOF MS
1a	+	+	–
1b	+	+	*nd*
2a	+	+	*nd*
2b	+	+	+

[a]See Pedersen *et al*.[135] for all MS spectra and HPLC chromatograms. *nd* = not determined.

To further elucidate the scope of the drug delivery system, the activity of human $sPLA_2$ IIA on the liposome solutions of **1a** and **2b** was investigated. As expected and evident from the MS spectra in Figure 20 the human enzyme is sensitive to the surface charged and only **2b** with the negatively charged PG headgroup was hydrolyzed while **1a** having a neutral headgroup was not degraded. Neither HPLC nor MALDI-TOF MS was capable of detecting the released chlorambucil, but that was not surprising given the low stability of free chlorambucil in an aqueous environment.[121] Chatterji *et al*. report 15 min as the half-life of chlorambucil in a buffer like the HEPES buffer at 37 °C.[122] Subjection of the chlorambucil phospholipid prodrugs to the reaction conditions for 48 h but in absence of the enzyme revealed that the prodrugs remain intact. No significant degradation of the prodrugs (Figure 20) or hydrolysis of the chloroethyl groups of chlorambucil was detected by MALDI-TOF MS, proving that the liposomal formulation enhances the stability by having the chlorambucil moiety in the lipophilic membrane and thereby shield it from the aqueous environment. These findings were further supported by the 4-(4-nitrobenzyl)-pyridine alkylating assay (Figure 21),[136,137,138] which showed that alkylation occurred when

liposomes of **1b** and **2b** were subjected to $sPLA_2$, whereas no alkylating activity of **1b** and **2b** was detected in the absence of $sPLA_2$ (Figure 21).[iii]

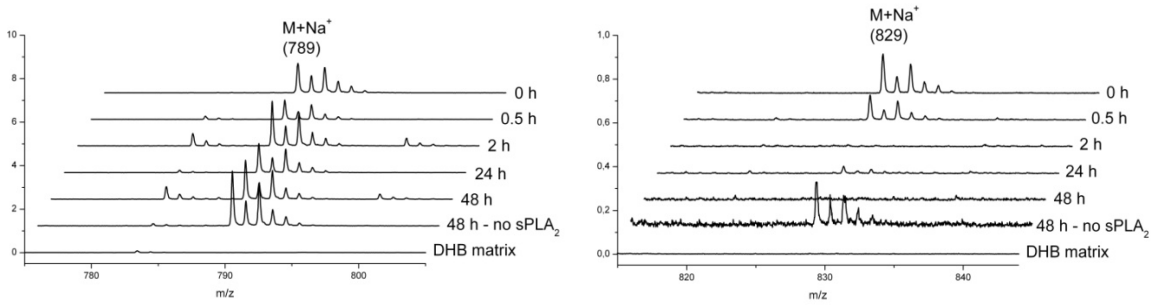

Figure 20. MALDI-TOF MS monitoring of human $sPLA_2$ IIA activity on **1a** (left) and **2b** (right). The spectra demonstrate that the negatively charged phospholipid **2b** is hydrolyzed by the humane enzyme whereas the neutral phospholipid **1a** is not.

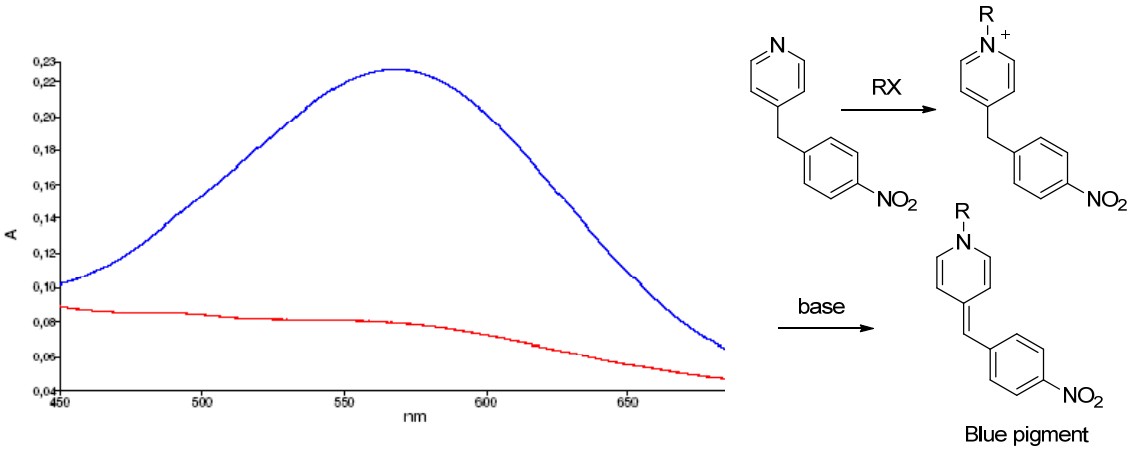

Figure 21. UV spectra (left) from alkylation of prodrug **2b** (red linie) and prodrug **2b** + $sPLA_2$ (blue linie) determined by the 4-(4-nitrobenzyl)-pyridine alkylating assay. A strong absorption at 560 nm illustrates alkylating activity. Concept behind the 4-(4-nitrobenzyl)-pyridine alkylating assay (right). The blue pigment has high UV absorbans at 560 nm. RX = alkylating agent

3.4 Cytotoxicity

To demonstrate the $sPLA_2$ dependent cytotoxicity of the chlorambucil phospholipid prodrugs, the activity of **1b** against HT-29 colon and MT-3 breast cancer cells for 24 h and **2b** against the same two cell lines in addition to ES-2 ovarian cancer cells was investigated (Table 19). None of these cells secrete $sPLA_2$, which is an advantage in these studies as it enables to control the presence or absence of the enzyme in each experiment. Without

[iii] Control experiments demonstrated that no absorption at 560 nm was observed for 4-(4-nitrobenzyl)-pyridine, HEPES buffer, HEPES buffer + $sPLA_2$ or chlorambucil, whereas the combination 4-(4-nitrobenzyl)-pyridine and chlorambucil gave a highly colored solution with a strong absorption at 560 nm. See also Pedersen *et al.*[135]

addition of snake (*Agkistrodon piscivorus piscivorus*) venom $sPLA_2$, **1b** and **2b** were not able to induce significant cell death demonstrating that in absence of the enzyme the prodrugs are not cytotoxic, which is crucial for the prodrug strategy. In the presence of the enzyme, **1b** and **2b** become cytotoxic and IC_{50} values in the range from 8–36 μM were obtained, illustrating that the cytotoxicity arise from a $sPLA_2$ triggered breakdown of the prodrugs into cytotoxic lysolipids and chlorambucil. However the IC_{50} values for lysolipid **6b** and chlorambucil show that the effect of the incorporated chlorambucil is minor than the effect of the lysolipid. It is hard to see the effect of chlorambucil for **1b** in HT-29 and MT-3 cells and for **2b** in MT-3 cells, whereas the IC_{50} values for **2b** in HT-29 and ES-2 cells are below those of chlorambucil and lysolipid **6b** indicating that a co-operative effect of the compounds released may occur here. When the cells were treated only with snake (*Agkistrodon piscivorus piscivorus*) venom $sPLA_2$ no effect on cell viability was observed.

Table 19. IC_{50} values (μM) of chlorambucil, lysolipid (**6b**) and the prodrugs **1b** and **2b** in the presence and absence of $sPLA_2$.[a]

Compound	HT-29 IC_{50} (μM)	MT-3 IC_{50} (μM)	ES-2 IC_{50} (μM)
Chlorambucil	70 ± 10	95 ± 21	34 ± 3
1b	> 200	> 200	*nd*
2b	> 200	> 200	97 ± 2
1b + $sPLA_2$	32 ± 2	36 ± 4	*nd*
2b + $sPLA_2$	10 ± 1	36 ± 4	8 ± 0.5
6b	18 ± 5	35 ± 1	30 ± 1
$sPLA_2$	-[b]	-[b]	-[b]

[a]Cytotoxicity was measured using the MTT assay as cell viability 48 h after incubation with the indicated substances for 24 h and showed by mean ± SD (n = 3); *nd* = not determined; snake (*Agkistrodon piscivorus piscivorus*) venom $sPLA_2$ was added to a final concentration of 5 nM. [b]No change in cell viability was observed after 24 h.

3.5 Conclusion

Synthesis of prodrug **1** was achieved and the synthetic route allows for an easy incorporation of other drugs since the drug is attached in the last synthetic step. Prodrug **1** and **2** were able to form particles in the liposome size region indicating formation of unilamellar vesicles, which demonstrate that incorporation of a bulky and partly hydrophilic substituent, like chlorambucil, to the *sn*-2-position maintain the ability of phospholipids to form bilayers. Gratifyingly, the chlorambucil prodrugs **1** and **2** were consumed by $sPLA_2$, the enzyme activity was investigated with HPLC and MALDI-TOF MS, which proven to be an easy and reliable method for analyzing enzymatic activity. The cytotoxicity studies demonstrated that in the absence of the enzyme no significant cell death occurred but upon $sPLA_2$ activation the prodrugs are converted into cytotoxic components, chlorambucil and lysolipids. Furthermore, it was demonstrated that this liposomal drug delivery system shields the chlorambucil moiety from the aqueous

environment and enhance the stability. Taken together, the results obtained from this work was very promising for the overall scope of the investigated drug delivery system, although the effect from chlorambucil in the tested cell line was not significant compared to the cytotoxicity of the lysolipids.

4. Liposomal Formulation of Retinoids Designed for Enzyme Triggered Release

4.1 Introduction

Retinoids,[139] such as ATRA (Figure 22), are known for their broad and diverse biological functions and various strategies have been explored to make retinoids applicable as drugs.[140] One of the biological functions of ATRA is its anticancer activity towards a broad range of cancer types, like breast, prostate and colon cancer.[75,76] For example, orally administrated ATRA is used clinically in the treatment of leukaemia.[141,142] However, the oral administration route is restricted by a relative low bioavailability[143] and a fast clearance from the blood stream,[144] and thus alternative ways of administrating ATRA would be beneficial. Intravenous administration is hampered by the low water solubility of ATRA but this can be circumvented by formulating ATRA in liposome based drug delivery systems.[145,146,147,148] Unfortunately, the liposomal formulation strategies have often been plagued by problems with leakage, which have led to an uncontrolled release of ATRA from the carrier system. Furthermore, ATRA is sensitive to acid and light[139] thus a liposomal formulation could be beneficial and the presence of a carboxylic acid moiety allows incorporation into the investigated drug delivery system. The target ATRA phospholipid prodrugs are illustrated in Figure 22.

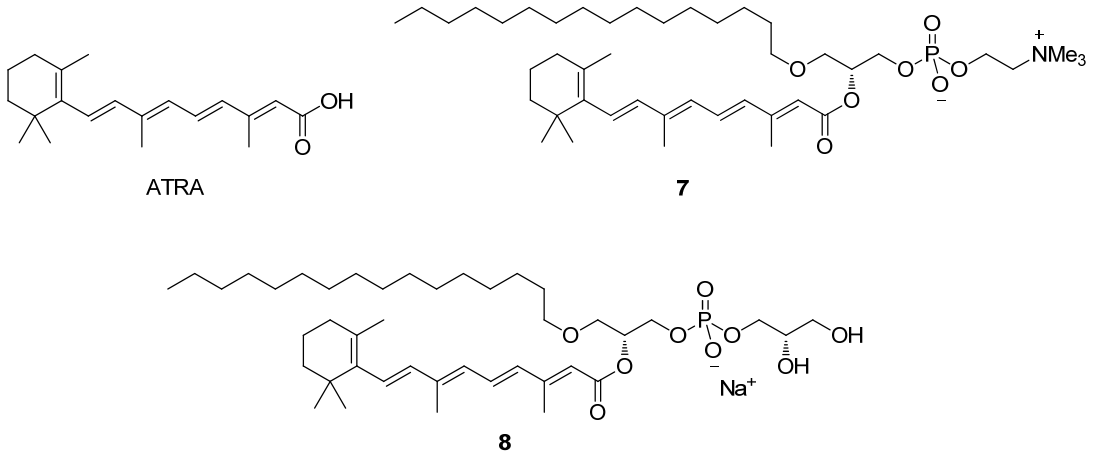

Figure 22. Structure of ATRA and the target ATRA phospholipids prodrug **7** and **8**.

4.2 Synthesis of ATRA Phospholipid Prodrugs

With lysolipid **6a** in hand (from Scheme 4) the synthesis of phospholipid **7** was attempted by acylation of **6a** with ATRA. The reaction was investigated applying the same conditions as used in the synthesis of **1**, and as observed under the incorporation of chlorambucil it was necessary to use an excess of ATRA and the coupling reagents in order to get a decent conversion of **6a** (Scheme 5). However, ^{1}H NMR analysis of the isolated material revealed that two isomers was formed, corresponding to esters of ATRA ((13*E*)-retinoic acid) and (13*Z*)-retinoic acid. The isomers was distinguished in ^{1}H NMR by the signal for the proton alpha to the carbonyl in the retinoids which resonate at 5.8 ppm for the (13*E*)-isomer and at

5.6 ppm for the (13*Z*)-isomer and determined by ^{1}H NMR the (13*E*)/(13*Z*) isomer ratio was 3:1. When Keck acylation conditions[129] in refluxing 1,2-dichloroethane was attempted neither the yield nor the ratio between the two isomers was improved.

Scheme 5. Acylation of lysolipid **6a** with ATRA using DCC and DMAP gave a mixture of two inseparable retinoid isomers. [a]

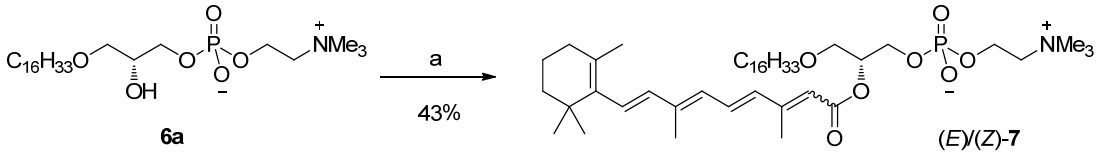

[a] Reagents: (a) ATRA, DCC, DMAP, $CHCl_3$.

The disappointing outcome of the acylation with ATRA motivated an examination of the carbodiimide mediated isomerisation. Extensive studies[iv] of acylation on hexadecanol revealed that the isomerisation only occurs when DMAP and a proton source are present, while a significant lower degree of isomersation was observed when either DMAP or a proton source was absent.[149] The proposed isomerization mechanism[150] is illustrated in Figure 23.

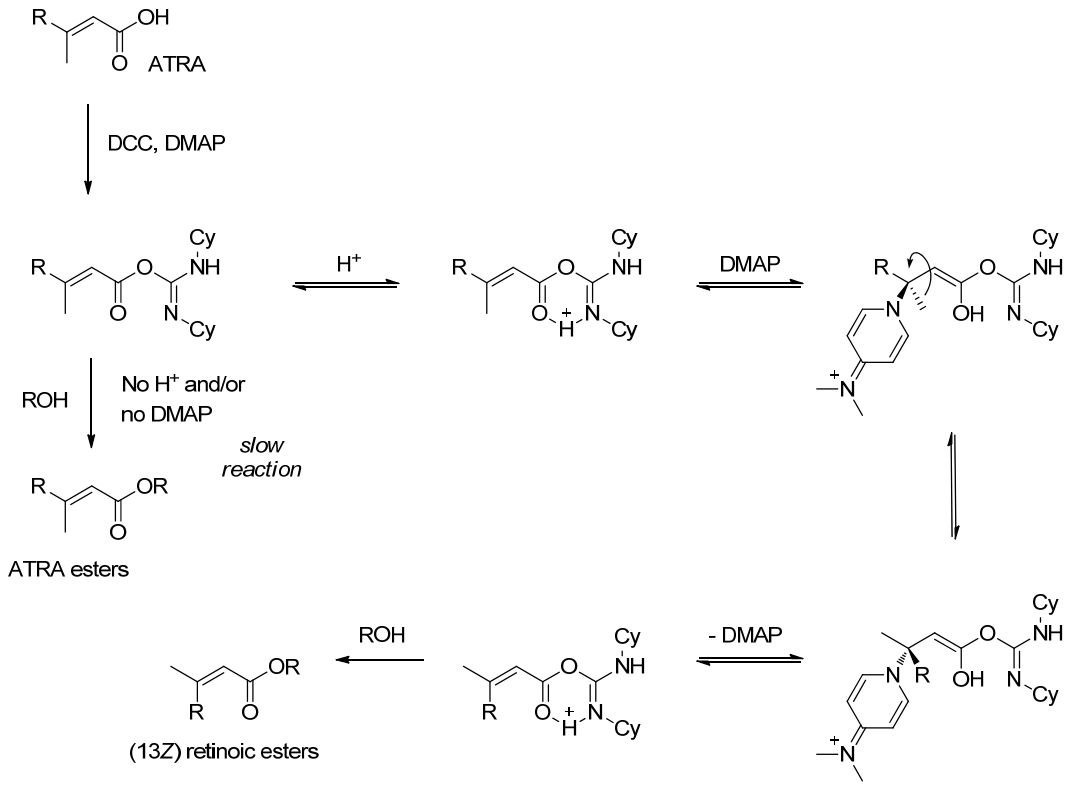

Figure 23. Proposed mechanism for the isomerization of ATRA mediated by carbodiimide activation.

[iv] The studies were carried out by colleague Dr. Mikkel S. Christensen, see Christensen *et al*.[149]

The observed isomerization occurred when the carboxylic acid in ATRA was activated in the carbodiimide mediated esterification. To circumvent this, an acylation method in which the alcohol is activated was examined. Therefore the Mitsunobu reaction[151] was explored and studies on hexadecanol revealed that the acylation occurs without isomerization and the ATRA ester was isolated in a high yield.[149] Applying the Mitsunubu conditions, initial studies on lysolipid **6a** showed a very low conversion into the ATRA ester, wherefore it was decided to incorporate ATRA at an earlier stage in the synthesis and a revised synthetic strategy was initiated from (*S*)-glycidyl tosylate ((+)-**3**). Ring opening of the epoxide (+)-**3** under Lewis acid catalysis with hexadecanol gave the desired ether and removal of the tosylate applying the two-step procedure also used in the synthesis of **5** (Scheme 3) gave the diol **9** (Scheme 6). Selective TBDMS-protection of the primary alcohol to give **10** was achieved in a good yield and **10** was then esterified with ATRA using Mitsunubu conditions applying diisopropyl azodicarboxylate (DIAD) and PPh_3 in THF. Coelution of DIAD and the product precluded isolation hence the ATRA ester was deprotected immediately. Desilylation with TBAF and imidazole in THF[90] led to acyl migration from the *sn*-2 to the *sn*-3 position, but that was circumvented by the use of aqueous HF in MeCN, and the desired alcohol **11** was isolated in 35 % yield over the two steps (Scheme 6). Installation of the PC headgroup was achieved in the same way as under the synthesis of **6** (Scheme 4). The somewhat low yield on 40%, which also was observed during the synthesis of **6**, is presumably related to the use of the water sensitive $POCl_3$ and the hydroscopic choline tosylate.

Scheme 6. Synthesis of ATRA phospholipid prodrug **7** using a revised synthetic strategy. [a]

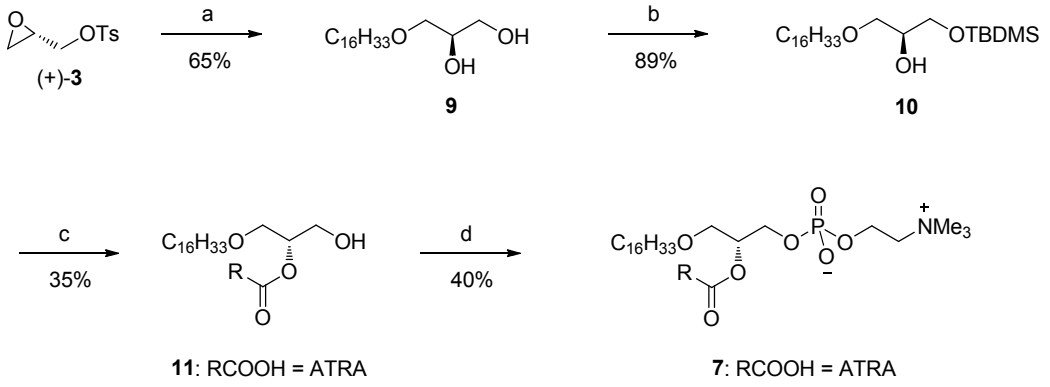

[a] Reagents: (a) (i) $C_{16}H_{33}OH$, $BF_3{\cdot}OEt_2$, CH_2Cl_2; (ii) CsOAc, DMSO, DMF; (iii) NaOMe, MeOH; (b) TBDMSCl, Et_3N, DMAP, DMF, CH_2Cl_2; (c) (i) ATRA, DIAD, PPh_3, THF; (ii) HF, H_2O, MeCN; (d) (i) $POCl_3$, Et_3N, CH_2Cl_2; (ii) choline tosylate, pyridine; (iii) H_2O.

4.3 Enzymatic Activity

In order to study $sPLA_2$ activity the phospholipid prodrugs **7** and **8**[v] were formulated as liposomes in HEPES buffer and particles with an average diameter close to 100 nm was formed. The liposome solutions were incubated with snake (*Agkistrodon piscivorus piscivorus* or *Naja mossambica mossambica*) venom $sPLA_2$ at 37 °C for 48 h however MALDI-TOF MS analysis of the liposome solutions revealed that no hydrolysis had occurred (Figure 24). Fawzy *et al.*[152] and Hope *et al.*[153] have demonstrated two decades ago that ATRA is an inhibitor of $sPLA_2$ and therefore the hydrolysis of DPPG in the presence of ATRA was investigated. Snake (*Naja mossambica mossambica*) venom $sPLA_2$ was subjected to solutions of DPPG and 0, 0.1 or 1 eq. ATRA. Complete hydrolysis of DPPG was observed within 24 h in all three experiments,[vi] by which it can be ruled out that the lack of hydrolysis is a consequence of $sPLA_2$ inhibition. The lack of hydrolysis must therefore be related to the structure of ATRA, the rigidity of the molecule and the presence of a methyl substituent in close vicinity to the carboxylic acid contrast with naturally occurring fatty acids, that are predominantly saturated and flexible molecules without branching. Furthermore, Bonsen *et al*. have demonstrated that compounds like 2-methylhexanoic acid and 3,3-dimethylbutanoic acid are not released from the *sn*-2 position by $sPLA_2$,[67] illustrating that substituents in close proximity to the *sn*-2 position hamper the enzyme activity.

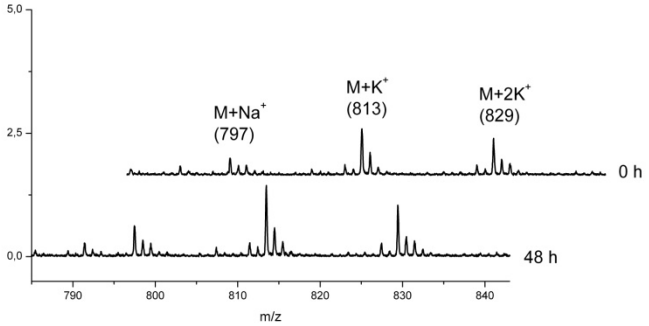

Figure 24. MALDI-TOF MS monitoring of snake (*Naja mossambica mossambica*) venom activity on ATRA phospholipid prodrug **8**.

4.4 Molecular Dynamics Simulations of Enzymatic Activity

To get a better understanding of why substrates like **8** is not hydrolyzed by $sPLA_2$, molecular dynamics (MD) simulations were performed of the Michaelis-Menten complex of **8** in the active site of $sPLA_2$ (denoted as $sPLA_2$–**8**). The enzymatic activity of $sPLA_2$ on phospholipids depends on several factors, including binding of the enzyme to the membrane surface, membrane properties, formation of the Michaelis-Menten complex, etc.[154] In this MD study only the stability of the Michaelis-Menten complex is investigated and it is then assumped that if a stable Michaelis-Menten complex is observed during the

[v] The synthesis of ATRA phospholipid prodrug **8** was performed by colleague Dr. Mikkel S. Christensen.[149]
[vi] See Christensen *et al.*[149] for further details.

simulations and water molecules enter the active site then hydrolysis is expected to occur. Previous work has demonstrated good correlation between experimental results and MD simulations.[66,131] Five simulations of 13 ns of the sPLA$_2$–**8** complex were obtained and the stability of the simulations was checked by computing the time evolution of the root mean square deviation (RMSD) of the Cα atoms with respect to the protein structure obtained after minimization. Stable RMSD data were obtained with a constant value between 1–1.5 Å (Figure 25, left), which is in agreement with earlier obtained results.[66,131]

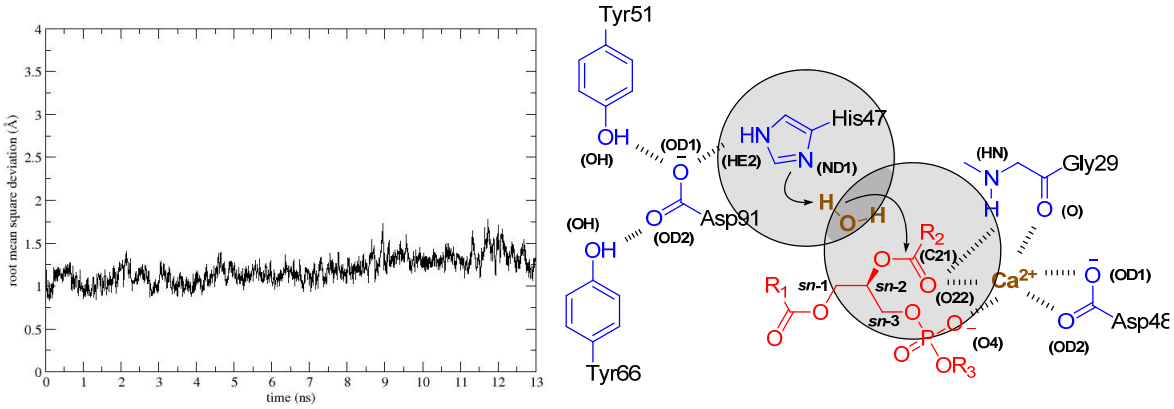

Figure 25. RMSDs of Cα atoms with respect to the initial protein structure of sPLA$_2$ as a function of simulation time (left). Representation of the active site in sPLA$_2$ with hydrogen bonds and ionic interactions indicated with dashed bonds (right). Key protein residues are drawn in blue, the substrate in red, the calcium ion and the water molecule both in brown. The two gray circles indicate the *H–S* region, where the overlap in dark grey represents the water count region. Labels are shown in black and atom types indicated in parentheses refer to the Protein Data Bank nomenclature.

A schematic representation of the catalytic mechanism is shown in Figure 25 indicating that the calcium ion (co-factor) is coordinated to the Asp48 carboxylate groups (atoms: OD1 and OD2), the Gly29 carbonyl (O), the carbonyl (O22) in the substrate (S) and the phosphate (O4) in S. Atom types given in parentheses refer to the Protein Data Bank nomenclature. Furthermore, the catalytic residue, His47, is stabilized by Asp91, which forms hydrogen bonds with Tyr51 and Tyr66. The water molecule acting as the nucleophile enters the region between His47^{ND1} and S^{C21}. This region will be referred to as the *H–S* region (Figure 25). The stability of the Michaelis-Menten complex for sPLA$_2$–**8** was investigated by monitoring the following distances during the simulations: Ca^{2+}–Gly29^{O}, Ca^{2+}–Asp48^{OD1}, Ca^{2+}–Asp48^{OD2}, Ca^{2+}–S^{O4}, Ca^{2+}–S^{O22}, S^{O22}–Gly29^{NH}, His47^{HE2}–Asp91^{OD1}, His47^{ND1}–S^{C21}, Asp91^{OD2}–Tyr66^{OH} and Asp91^{OD1}–Tyr51^{OH}. The time evolution of these distances is given in Table 20.

The key distance analysis revealed that many of distances remain constant for the sPLA$_2$–**8** complex, e.g. the Ca^{2+}–S^{O4} distance (see Figure 26) and with values comparable to sPLA$_2$–DPPG (Table 20). However three of the distances (His47^{ND1}–S^{C21}, S^{O22}–Gly29^{NH} and Ca^{2+}–S^{O22}) were significantly longer than observed in the sPLA$_2$–DPPG complex,

demonstrating that **8** do not fit perfectly into the active site of the enzyme. From the distance versus time plots in Figure 26 it is evident that the carbonyl (S^{O22}) in the ATRA moiety of **8** changes its position constantly and never finds a stable position in the enzyme pocket. This observation is verified by snapshots (Figure 26) from the simulations, which reveal that the ATRA moiety rotates almost 180° during the simulation, causing distortion in the desired Michaelis-Menten complex, by which the conclusion from the key distance analysis is that no hydrolysis is expected to occur.

Table 20. Monitored key distances between selected atoms that are involved in stabilization of the Michaelis-Menten complex, compare with Figure 25. The reported data are the mean distances ± SD in Å.

Distances	**Compound**	
	8	**DPPG**[a]
$Asp91^{OD1}$–$Tyr51^{OH}$	1.8 ± 0.3	3.1 ± 0.3
$Asp91^{OD2}$–$Tyr66^{OH}$	1.7 ± 0.1	2.7 ± 0.1
$His47^{HE2}$–$Asp91^{OD1}$	1.8 ± 0.1	1.9 ± 0.3
$His47^{ND1}$–S^{C21}	6.0 ± 0.4	4.5 ± 0.4
Ca^{2+}–$Asp48^{OD1}$	2.2 ± 0.1	2.2 ± 0.2
Ca^{2+}–$Asp48^{OD2}$	2.2 ± 0.1	2.2 ± 0.1
Ca^{2+}–$Gly29^{O}$	2.4 ± 0.2	2.4 ± 0.2
S^{O22}–$Gly29^{NH}$	3.5 ± 0.6	2.7 ± 0.5
Ca^{2+}–S^{O22}	4.8 ± 0.6	2.4 ± 0.2
Ca^{2+}–S^{O4}	2.1 ± 0.1	2.1 ± 0.1

[a] Data from Linderoth *et al*.[66]

Entrance of water into the active site is another crucial factor for enzyme activity, and previous studies have showed a good correlation between experimentally obtained $sPLA_2$ activity and detection of water molecules in the *H–S* region within 3.5 Å of $His47^{ND1}$ and S^{C21} in MD simulations for phospholipids in which the key distances are constant.[66,131] The number of water molecules in the *H–S* region within 3.5 Å, 4.5 Å and 5.5 Å were counted and normalized to the number of water molecules at 6 Å (Table 21). The relative water count at 3.5 Å for $sPLA_2$–**8** is significantly lower than that of $sPLA_2$–DPPG, contributing to the hypothesis that hydrolysis of **8** by the enzyme is highly disfavoured. But it is also evident from Table 21 that some water molecules enter the active site, and in order to rule out that hydrolysis can occur when that happens the Ca^{2+}–S^{O22} distance were measured, and it was found that every time water was within the *H–S* region the Ca^{2+}–S^{O22} distance never become shorter than 4.4 Å which is 2 Å longer than observed in the $sPLA_2$– DPPG complex. In Figure 27 a snapshot from the simulation is shown in which water is within 3.5 Å of $His47^{ND1}$ and S^{C21} but key distances, like Ca^{2+}–S^{O22} are longer than tolerated in order to obtain hydrolysis. Therefore, the conclusion from the MD simulations is that the key distance analysis showed that **8** has an imperfect positioning in $sPLA_2$ and the water count analysis displayed that the number of water molecules reaching the active site is low

and therefore it is expected that no hydrolysis will occur which is in agreement with the experimental observations.

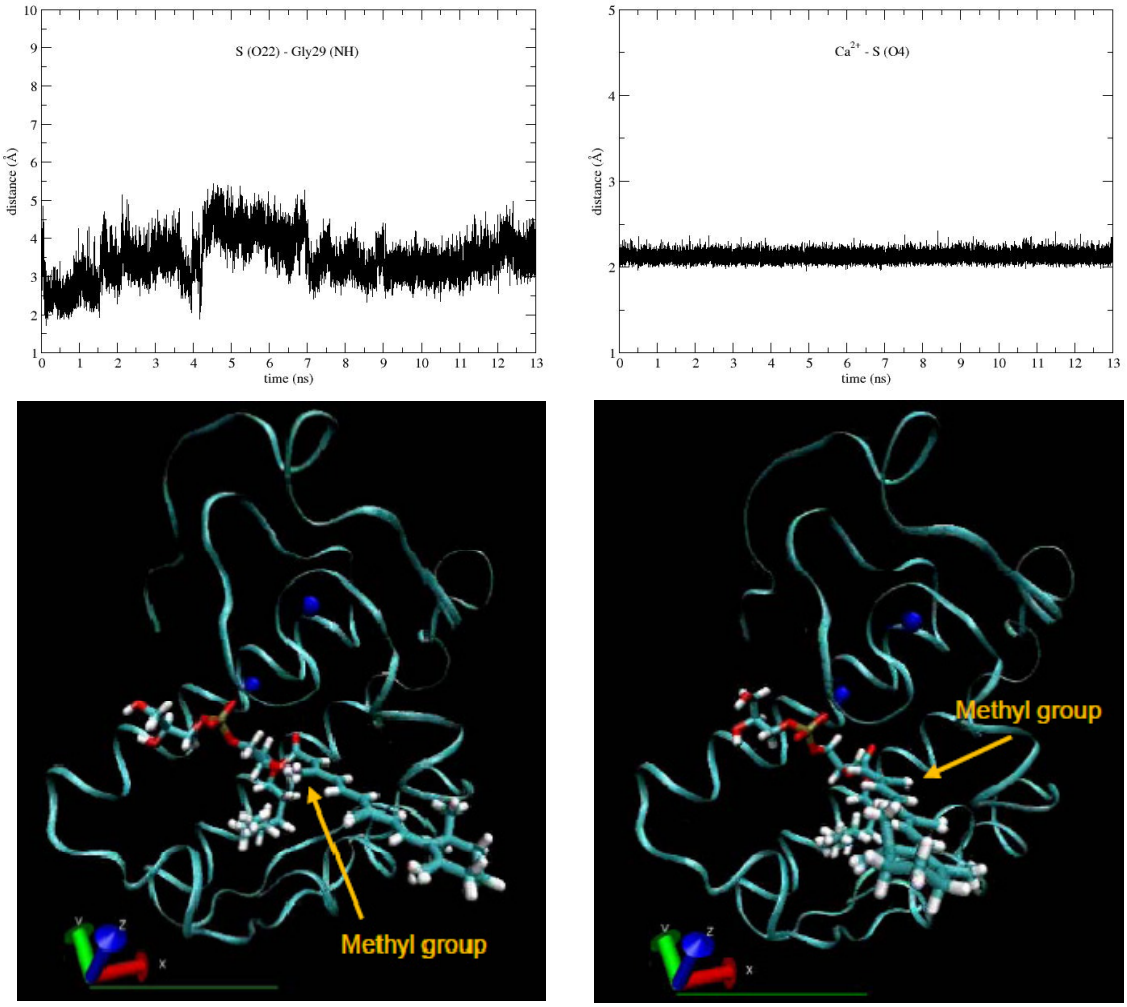

Figure 26. Distance versus time plots for S^{O22}–$Gly29^{NH}$ (top right) and Ca^{2+}–S^{O4} (top left). Snapshot from the beginning of the simulation (bottom left), in which the β-methyl group in the ATRA moiety points "left" and snapshot from the end of the simulation (bottom right) in which the same β-methyl points "right".

Table 21. Relative water counts as a function of the distance from both $His47^{ND1}$ and S^{C21} (the *H–S* region).[a]

Compound	**Relative water count at 3.5 Å**	**Relative water count at 4.5 Å**	**Relative water count at 5.5 Å**
8	0.001	0.3	1.0
$DPPG^{66}$	0.1	0.4	0.7

[a] Normalized to the water count at 6 Å.

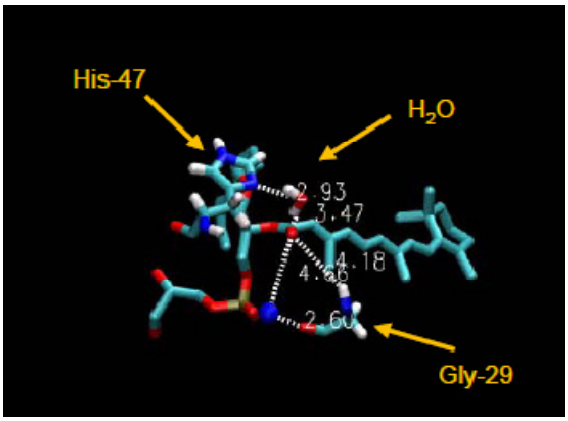

Figure 27. Snapshot from the simulation of $sPLA_2$–**8**, in which H_2O is within 3.5 Å of $His47^{ND1}$ and S^{C21} but the Ca^{2+}–S^{O22} distance is 4.66 Å which is significantly longer than observed in substrates for $sPLA_2$, like DPPG. Furthermore, the distances for $His47^{ND1}$–S^{C21} (4.18 Å) and Ca^{2+}–$Gly29^{O}$ (2.60 Å) are included.

4.5 Revised Prodrug Strategy for Liposomal Delivery of Retinoids

The efforts towards $sPLA_2$ sensitive phospholipids which can release retinoids like ATRA was not successful, however knowing that some esters and amides of ATRA retain their anticancer activity[155,156,157,158] it was decided to incorporate an aliphatic C_6-linker between ATRA and the phospholipid backbone (see Figure 29). MD simulations of **13** in the active site of $sPLA_2$ showed that incorporation of the aliphatic C_6-linker creates sufficient flexibility to obtain a stable Michaelis-Menten complex and the amount of water entering the catalytic site was similar to what was observed for the $sPLA_2$–DPPG complex and thus it is expected that the hydrolysis of **13** will occur.[vii] One major drawback in applying ATRA as a drug is its nonselective activation of retinoic acid receptor (RAR) subtypes (RARs, α, β, γ), retinoic X receptor subtypes (RXRs, α, β, γ) and/or the subtype RAR isoforms, α1, α2, β1–β5, γ1 and γ2.[75, 159] The lack of selectivity is believed to be responsible for the severe side effects that have been observed during chronic administration of ATRA[159] and therefore there is much interest in discovering more selective RAR agonists.[160,161] Targeting of RARβ2 has been found to have a suppressive effect on human tumors,[162] and recently 4-(4-octylphenyl)-benzoic acid (**12**, Figure 28) was identified as a selective RARβ2 agonist.[163,164,165] The lipophilicity of **12** makes it is a good candidate for incorporation into the investigated liposomal drug delivery system. However, since Bonsen *et al*. have demonstrated that benzoic acid is not released from the *sn*-2-position by $sPLA_2$[67] direct attachment of **12** to the phospholipids was ruled out. Instead, it was decided to investigate how attachment of an aliphatic C_6-linker would influence the cytotoxicity of **12** and the $sPLA_2$ activity towards the corresponding prodrug.

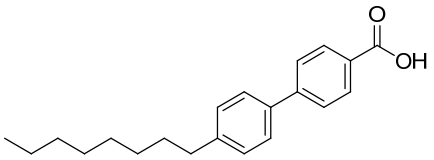

12

Figure 28. Structure of the selective RARβ2 agonist **12**.

At this stage of the project it was decide to focus on PG lipids and furthermore, it became interesting in addition to *sn*-1-ether phospholipids to investigate *sn*-1-ester phospholipids and so the prodrugs was designed to contain either an *sn*-1-ester or an *sn*-1-ether functionality (Figure 29). Upon activation of $sPLA_2$, the prodrugs will be converted into the free drug and lysolipids (Figure 29) and while *sn*-1-ether lysolipids have good metabolic stability and are cytotoxic against many cell lines,[68,69] *sn*-1-ester lysolipids are rapidly metabolized (by e.g. lysophospholipases) and have been dismissed as suitable lysolipid drug candidates.[69] Information about the cytotoxicity of *sn*-1-ester lysolipids is limited and covers only lysophosphatidylcholine lipids,[166,167,168] however these lipids have

[vii] The MD simulations of $sPLA_2$–**14** were performed by collaborator Dr. Arun K. Subramanian, see Pedersen *et al*.[174]

shown to be slightly better substrates for $sPLA_2$ than *sn*-1-ether lipids,[131] and therefore it was decided to synthesize both types of prodrugs in order to study their relative hydrolysis rate and cytotoxicity.

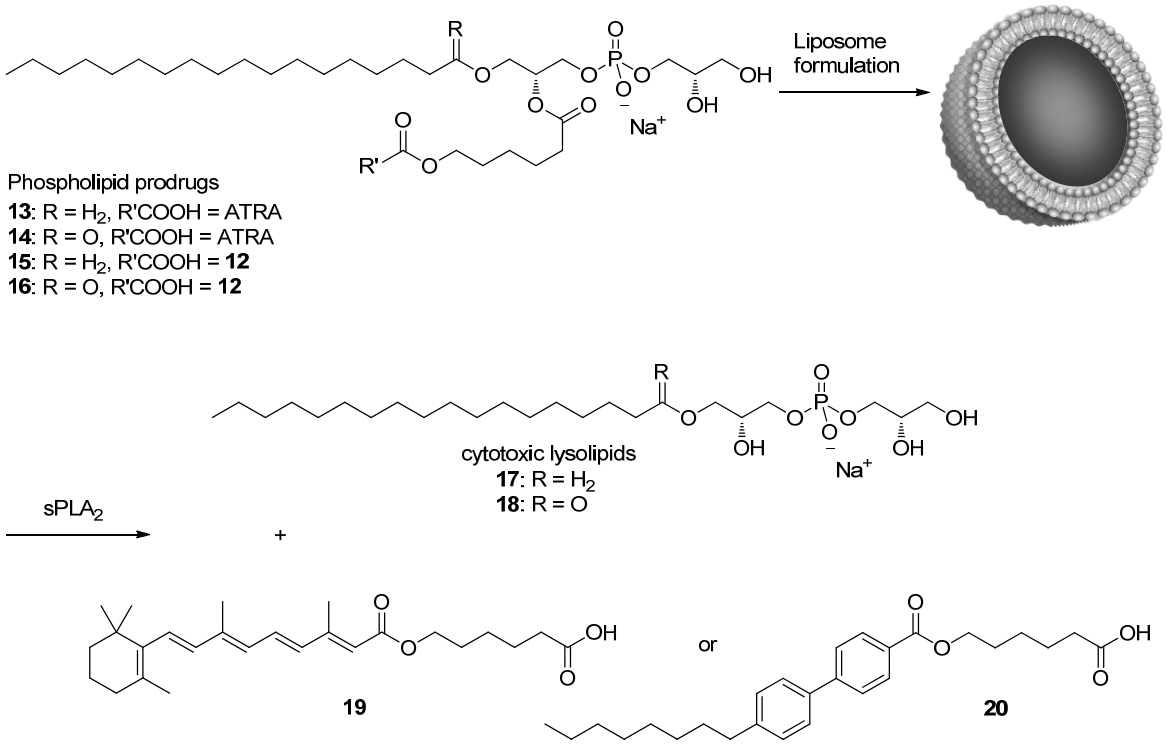

Figure 29. Schematic overview of the revised drug delivery strategy for liposomal delivery of retinoids. The $sPLA_2$ degradable phospholipid prodrugs are designed to have an aliphatic C_6-linker incorporated between the drug, R'COOH (ATRA and **12**) and the phospholipid backbone.

4.6 Synthesis of Retinoid Esters

The linker moiety *tert*-butyl 6-hydroxyhexanoate (**22**), which was synthesized in one step from 6-caprolactone (**21**, Scheme 7), was coupled with ATRA by a Mitsunobu reaction[151] (Scheme 7). The following *tert*-butyl deprotection led to degradation of the ATRA skeleton under acidic conditions (5% TFA or $ZnBr_2$[169] in CH_2Cl_2 or HF in refluxing MeCN), but using 2,6-lutidine and TMSOTf in CH_2Cl_2[170] the carboxylic acid **9** was afforded in a good yield (Scheme 7). The ATRA ester **19** was isolated as yellow crystals and was stable when stored at –20 °C under an inert atmosphere whereas the oily *tert*-butyl ester of **19** decomposes upon less than one month of storage. This highlights the importance of storing ATRA-analogues as solids in order to avoid decomposition. The corresponding linker-molecule of **12**[viii] was synthesized by a Steglich coupling[102] with **22** followed by a deprotection of the *tert*-butyl ester with TFA in CH_2Cl_2 (Scheme 7). In contrast to the ATRA-analogues no decomposition of the synthetic derivatives of **12**

[viii] Compound **12** is commercially available (CAS no. 59662-49-6), but in this work **12** was synthesized in one step from the corresponding nitrile (CAS no. 52709-84-9) by a NaOH mediated hydrolysis in 98% yield.

neither as oils nor solids was observed. The cytotoxicity of ATRA, **12**, **19** and **20** were evaluated in three cancer cell lines and the retinoid esters had activities comparable to the acids (*vide infra*).

Scheme 7. Synthesis of the retinoid esters.[a]

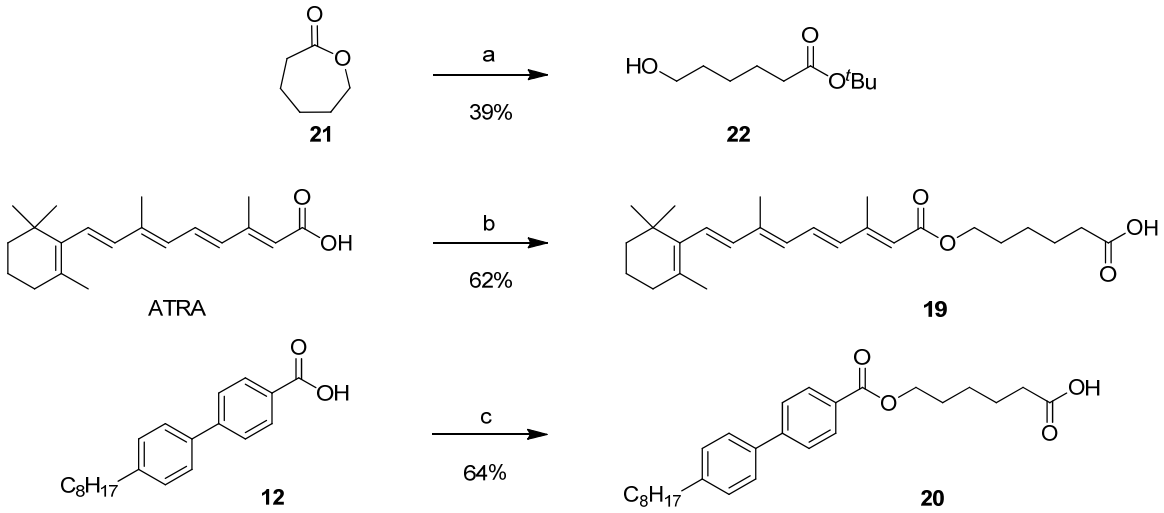

[a] Reagents: (a) KO^{t}Bu, ^{t}BuOH; (b) (i) **22**, DIAD, PPh_3, THF; (ii) TMSOTf, 2,6-lutidine, CH_2Cl_2; (c) (i) **22**, DCC, DMAP, CH_2Cl_2; (ii) TFA, triisopropylsilane, CH_2Cl_2.

4.7 Synthesis of Retinoid Phospholipid Prodrugs

The cytotoxicity of the esters **19** and **20** and the results from the MD simulations prompted to proceed with the synthesis of the corresponding *sn*-1-ether and *sn*-1-ester phospholipid prodrugs. As presented in section 2.4 PG lipids have previously been synthesized via isopropylidene proptection of the glycerol moiety in the headgroup and protection of the phosphate by the methyl ester however both deprotections require long reaction times hence it was desirable to access PG lipids in a more convenient way. Inspired by oligonucleotide synthesis [171] a new synthetic route to PG lipids was initiated with phosphoramidite **27** (Scheme 8) as the key building block.

The synthesis of phosphoramidite **27** was accomplished in 5 steps from allyl alcohol (**23**, Scheme 8). Treatment of allyl alcohol with 4-methoxybenzoyl chloride gave the desired allylic ester **24**. The key step in the synthesis was the asymmetric dihydroxylation[172,173] of **24**, which occurred with excellent enantioselectivity (ee 97%, chiral HPLC) and TBDMS protection of the diol gave **25** in an excellent yield (Scheme 8). Reduction of **25** with diisobutylaluminium hydride (DIBAL-H) at –78 °C afforded the TBDMS-protected glycerol **26**. The coupling between **26** and the commercially available phosphorylating agent $(i\text{-Pr})_2NPClO(CH_2)_2CN$ resulted in the desired phosphoramidite **27** in a very satisfactory yield, isolated as a 1:1 diastereomeric mixture as evident from ^{31}P NMR (Scheme 8). The synthesis of phosphoramidite **27** was achieved on gram scale and when

stored at –20 °C the stability of the compound was found to be at least one year. The glycerol moiety in phosphoramidite **27** was designed to be the (*S*)-stereoisomer because Andresen *et al.*[68] have demonstrated that the (*S*)-stereoisomer of lysolipids, like **17**, are significantly more cytotoxic than the corresponding (*R*)-stereoisomer.

Scheme 8. Synthesis of the phosphoramidite **27**.[a]

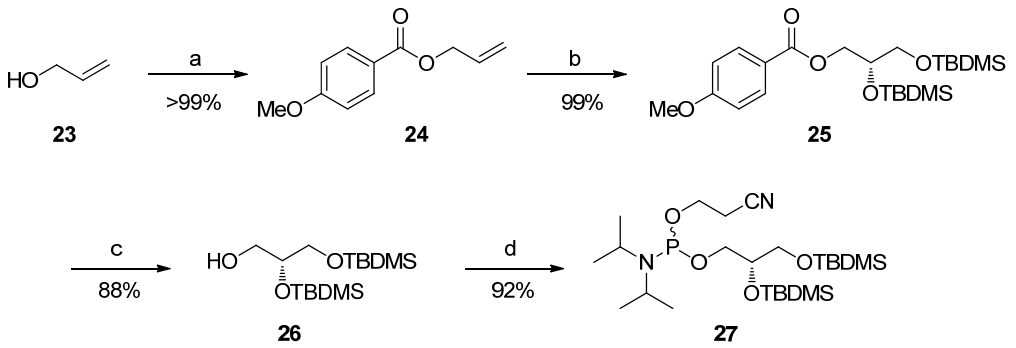

[a]Reagents: (a) 4-Methoxybenzoyl chloride, Et_3N, DMAP, CH_2Cl_2; (b) (i) $K_2OsO_4{\cdot}2H_2O$, $(DHQD)_2PHAL$, $K_3Fe(CN)_6$, K_2CO_3, ^{t}BuOH, H_2O; (ii) TBDMSCl, imidazole, DMF; (c) DIBAL-H, CH_2Cl_2; (d) 2-cyanoethyl *N*,*N*-diisopropylchlorophosphoramidite, DIPEA, CH_2Cl_2.

With the phosphoramidite **27** in hand the backbone of the *sn*-1-ether prodrugs was constructed by a tetrazole mediated coupling of alcohol **5b** and phosphoramidite **27**, followed by an oxidation of the phosphite to the phosphate with ^{t}BuOOH (Scheme 9).

Scheme 9. Synthesis of the *sn*-1-ether phospholipid precursor **30**.[a]

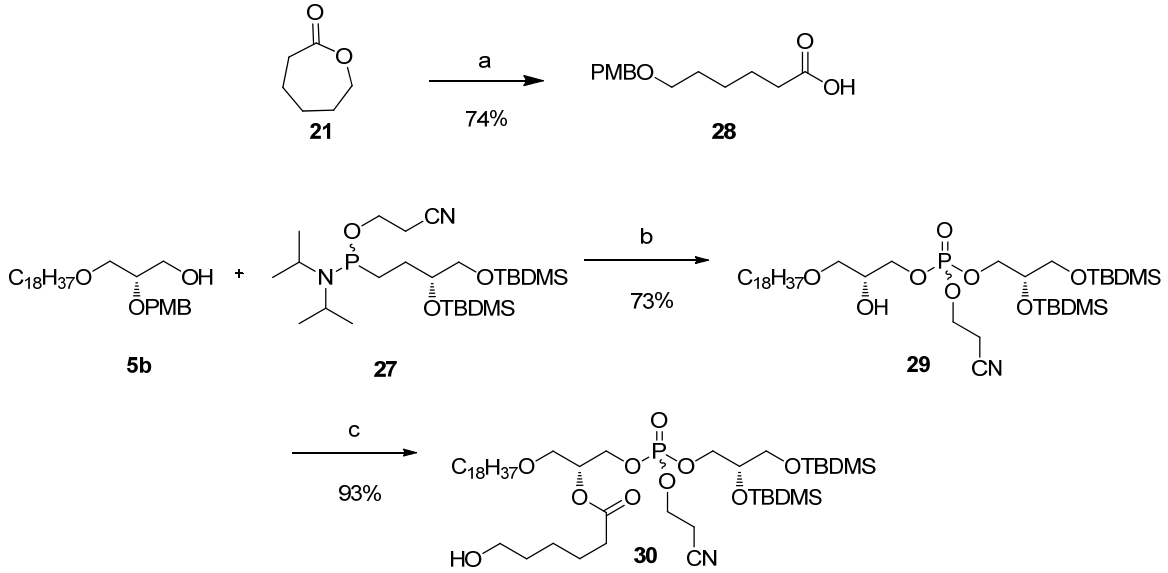

[a] Reagents: (a) 4-Methoxybenzyl chloride, KOH, toluene; (b) (i) tetrazole, CH_2Cl_2, MeCN; (ii) ^{t}BuOOH; (iii) DDQ, H_2O, CH_2Cl_2; (c) (i) **28**, DCC, DMAP, CH_2Cl_2; (ii) DDQ, H_2O, CH_2Cl_2.

Deprotection of the PMB group in moist CH_2Cl_2 with DDQ afforded the secondary alcohol **29** in 73% yield from **5b**. The linker moiety was introduced by coupling of carboxylic acid **28** (Scheme 9) and the secondary alcohol **29** to give an ester and removal of the introduced PMB-group afforded alcohol **30** in an overall yield of 93% (Scheme 9). To avoid migration of the phosphate headgroup from the *sn*-3 position to the *sn*-2 position it was crucial that the secondary alcohol **29** was esterified promptly after isolation. Furthermore, it was observed that subjection of **29** to Keck acylation conditions[129] to some extent caused migration while that was prevented by using Steglich conditions.[102]

The *sn*-1-ester phospholipid precursor **35** was synthesized from 2,3-*O*-isopropylidene-*sn*-glycerol (**31**, Scheme 10). Acylation with stearic acid gave the desired ester and applying the conditions published by Gaffney *et al*.[87] the following isopropylidene deprotection occurred without racemization to give diol **32** (Scheme 10). Selective TBDMS protection of the primary alcohol in **32** was achieved using the procedure from Burgos *et al*.[98] Diester **34** was obtained by coupling of **28** and **33** and the following TBDMS deprotection was best achieved using NBS in a mixture of DMSO, THF and H_2O (Scheme 10),[98,99] while alternative conditions like TBAF and imidazole in THF[90] or HF in MeCN led to a significant degree of acyl migration. Mosher ester analysis[100] of **34** showed that the enantiomeric purity was >95%. The PG headgroup was attached in the same way as for the *sn*-1-ether phospholipids and PMB deprotection gave the primary alcohol **35** (Scheme 10).

Scheme 10. Synthesis of the *sn*-1-ester phospholipid precursor **35**.[a]

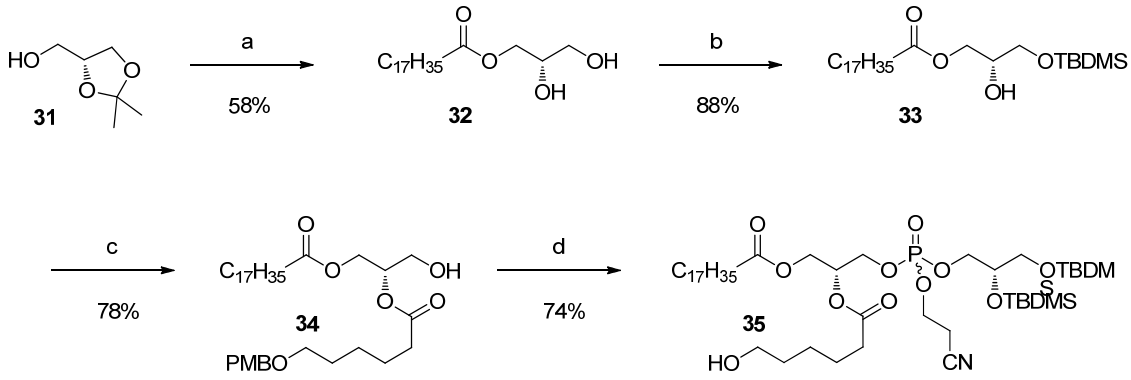

[a] Reagents: (a) (i) $C_{17}H_{35}COOH$, DCC, DMAP, CH_2Cl_2; (ii) TFA, $B(OEt)_3$, CF_3CH_2OH; (b) TBDMSCl, imidazole, THF; (c) (i) **28**, EDCI, DMAP, CH_2Cl_2; (ii) NBS, DMSO, THF, H_2O; (d) (i) phosphoramidite **27**, tetrazole, CH_2Cl_2, MeCN; (ii) ^{t}BuOOH; (iii) DDQ, H_2O, CH_2Cl_2.

The phospholipid precursors **30** and **35** were converted to the desired prodrugs of ATRA and **12** (Scheme 11). The ATRA moiety was introduced either by the Mitsunobu reaction or the Steglich coupling and the final prodrugs **13** and **14** were obtained after removal of the base labile cyanoethyl group with 1,8-diazabicyclo[5.4.0]undec-7-ene (DBU) and TBDMS-deprotection mediated by HF in a mixture of MeCN, CH_2Cl_2 and H_2O (Scheme

11). Thereby the novel route to PG lipids was completed and compared to previous routes (see Table 16) shorter reaction times[ix] are a major improvement making the chemistry convenient and applicable. Prodrugs **15** and **16** were accessed by coupling between **12** and the primary alcohols **30** and **35**, after which the remaining chemistry was similar to the synthesis of **13** and **14** (Scheme 11). ^{31}P NMR of the synthesized prodrugs showed one signal resonating between –1 ppm and 2 ppm, demonstrating high diastereomeric and regioisomeric purity (>95%).

Scheme 11. Synthesis of the *sn*-1-ether and *sn*-1-ester prodrugs **13**, **14**, **15** and **16**.[a]

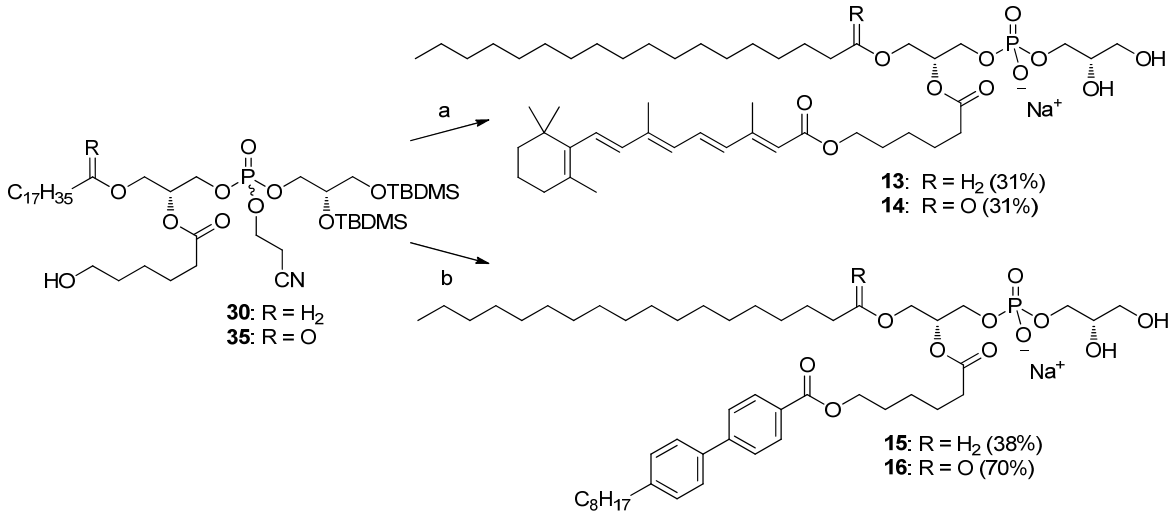

[a] Reagents: (a) (i) **30**, ATRA, DIAD, PPh_3, THF or **35**, ATRA, DCC, DMAP, Et_3N, Et_2O; (ii) DBU, CH_2Cl_2; (iii) HF, H_2O, CH_2Cl_2, MeCN; (b) (i) **12**, DCC, DMAP, CH_2Cl_2; (ii) DBU, CH_2Cl_2; (iii) HF, H_2O, CH_2Cl_2, MeCN.

For the cytotoxicity studies access to lysolipids **17** and **18** are needed as standards for comparison with the tested phospholipid prodrugs and while *sn*-1-ester lysolipid **18** is commercially available lysolipid **17** was synthesized in two steps from alcohol **29** (Scheme 12). Likewise access to phospholipids with stearic acid in the *sn*-2 position instead of the retinoid esters are needed and while 1,2-distearoyl-*sn*-glycero-3-phosphoglycerol (DSPG) is commercially available 1-*O*-stearyl-2-stearoyl-*sn*-glycero-3-phosphoglycerol (1-*O*-DSPG) was synthesized in three steps from alcohol **29** (Scheme 12).

[ix] The last two deprotections in Scheme 11 were achieved within reaction times of 1 h and 3.5 h, respectively.

Scheme 12. Synthesis of lysolipid **17** and 1-*O*-DSPG.[a]

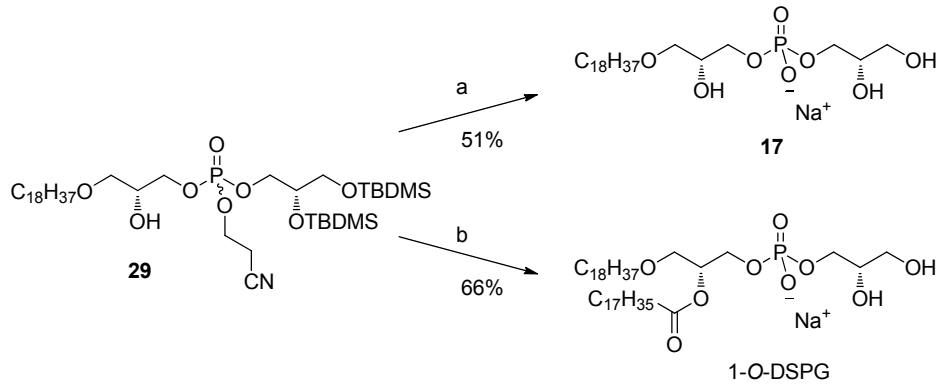

[a] Reagents: (a) (i) DBU, CH_2Cl_2; (iii) HF, H_2O, CH_2Cl_2, MeCN; (b) (i) $C_{17}H_{35}COOH$, DCC, DMAP, CH_2Cl_2, (ii) DBU, CH_2Cl_2; (iii) HF, H_2O, CH_2Cl_2, MeCN.

4.8 Biophysical Characterization and Enzyme Activity

The phospholipid prodrugs (**13**–**16**) were formulated as liposomes by extrusion in HEPES buffer using the dry lipid film technique,[130] yielding clear solutions. The particle size of the formulated phospholipids was measured by DLS. The DLS analysis revealed that all of the phospholipids were able to form particles with a diameter around 100 nm (Table 22) and with a low polydispersity, indicating formation of unilamellar vesicles.

Table 22. Measurement of particle size with DLS

	Particle size	
Prodrug	**Diameter (nm)**	**PdI**
13	94	0.08
14	97	0.13
15	118	0.16
16	118	0.05

DSC scans (15–65 °C) of the phospholipid solutions of **13** and **15** displayed no phase transitions in the tested temperature range indicating that the phospholipid bilayers are in a fluid state. This was not surprising taking into account the bulky and stiff nature of the substituents in the *sn*-2-position, which precludes well-ordered chain packing.

The ability of $sPLA_2$ to hydrolyze the formulated phospholipids at 37 °C was investigated with MALDI-TOF MS. In Figure 30 the obtained MS data for the *sn*-1-ether prodrug **13** subjected to purified $sPLA_2$ from snake (*Agkistrodon piscivorus piscivorus*) venom is shown. Gratifying and as evident from the spectra (Figure 30) the prodrug ($M+H^+$) is consumed by the enzyme and the desired constituents, lysolipid **17** ($M+H^+$) and ATRA ester **19** ($M+Na^+$) are released.

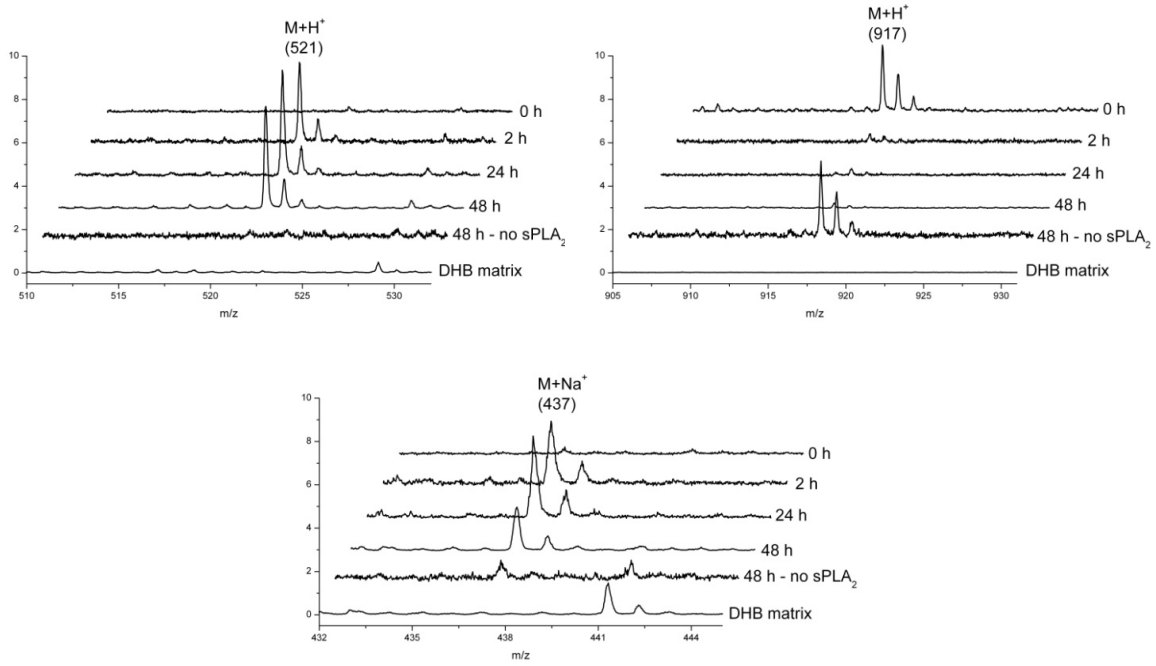

Figure 30. MALDI-TOF MS monitoring of snake (*Agkistrodon piscivorus piscivorus*) venom $sPLA_2$ activity on the *sn*-1-ether prodrug **13**. The spectra demonstrate that the prodrug **13** (top right) is consumed and that the lysolipid **17** (top left) and the ATRA ester **19** (bottom) are released.

The MALDI-TOF MS analysis of the *sn*-1-ether prodrugs **13** and **15** and the *sn*-1-ester prodrugs **14** and **16** revealed that all of the prodrugs were degraded by the enzyme (Table 23) and the desired molecules were released. The observation that the *sn*-1-ether prodrugs were consumed by $sPLA_2$ to the same extent as the *sn*-1-ester prodrugs illustrate and confirm that *sn*-1-ether phospholipids are excellent substrates for $sPLA_2$. Based on the MALDI-TOF MS analysis of the $sPLA_2$ activity for the various prodrugs it can be concluded that the incorporation of an aliphatic C_6-linker between ATRA and the phospholipid backbone resolved the issue of $sPLA_2$ activity on ATRA-phospholipid prodrugs. The experimental observations are in agreement with the outcome from the MD simulations, illustrating the power and potential of using MD simulations in the design of $sPLA_2$ degradable phospholipid prodrugs. In order to rule out that the degradation of the prodrugs was caused by non-enzymatic hydrolysis, a sample of each prodrug was subjected to the reaction conditions in the absence of $sPLA_2$. As evident from the spectra in Figure 30 no degradation of the prodrugs was observed within 48 h and none of the release products were detectable. Finally, the enzyme activity of the purified $sPLA_2$ from snake (*Agkistrodon piscivorus piscivorus*) venom and commercially available $sPLA_2$ from snake (*Naja mossambica mossambica*) venom was compared and as can be seen in Table 23, both enzymes were able to hydrolyze the substrates and no significant differences in hydrolysis rate or extent were observed.

Table 23. Measurement of $sPLA_2$ activity on the prodrugs **13**–**16** by MALDI-TOF MS.

Prodrug	Hydrolysis by snake venom $sPLA_2$[a]	
	Agkistrodon piscivorus piscivorus	*Naja mossambica mossambica*
13	+	*nd*
14	+	+
15	+[b]	+[b]
16	+	+

[a]Determined by MALDI-TOF MS after 48 h incubation at 37 °C with purified $sPLA_2$ from snake (*Agkistrodon piscivorus piscivorus* or *Naja mossambica mossambica*) venom, see Pedersen *et al*.[174] for all MS spectra; [b]After 48 h a small signal for prodrug **15** remains; *nd* = not determined.

As described in section 4.3 ATRA has been reported as an inhibitor for $sPLA_2$, with IC_{50} values of <50 μM[152] and 10 μM.[153] However, it was shown that DPPG is fully hydrolyzed by $sPLA_2$ in the presence of 0.1 eq. and 1.0 eq. ATRA, proving that the lack of hydrolysis for the ATRA-phospholipid prodrug **8** is not a consequence of inhibition by ATRA. These observations were further supported by determination of the IC_{50} value and the inhibition constant (K_i) for ATRA and ATRA ester **19**.[x] It was found that **19** (IC_{50} = 8 μM, K_i = 6 μM) inhibits $sPLA_2$ at the same level as ATRA (IC_{50} = 15 μM, K_i = 11 μM), and whereas the ATRA-phospholipid prodrug **8** is not consumed by the enzyme the prodrugs **13** and **14** are fully degraded. This demonstrates that under the conditions used, the released ATRA ester **19** does not inhibit $sPLA_2$ and the difference in degradation of the prodrugs therefore solely relies on the ability of $sPLA_2$ to hydrolyze the different prodrugs. Additionally, Cunningham *et al*. have reported K_i values <100 nM[175] for potent $sPLA_2$ inhibitors, illustrating that ATRA and **19** are weak inhibitors.

4.9 Cytotoxicity

The cytotoxicity of ATRA, **12**, **19** and **20** were evaluated in MT-3 breast, HT-29 colon and Colo205 colon cancer cell lines (Table 24). Interestingly, the retinoid esters were either more active than ATRA and **12** or equal in potency in the tested cell lines. A possible explanation for the enhanced activity of these molecules is that the derivatization increases the lipophilicity of the drugs, augmenting transport over the cell membrane. RARβ2 agonists **12** and **20** showed very little activity against HT-29 cells, and presumably this is because growth inhibition in this cell line is induced by RARα agonists[176] and **12** has a low affinity for that receptor.[163,164,165] The result is also an indicator that the cytotoxicity of **20** in MT-3 and Colo205 originate from RARβ2 activation.

[x] The work was performed by collaborator Dr. Ahmad Arouri, see Pedersen *et al.* for further details.[174]

Table 24. IC_{50} (μM) values for the retinoids in three cancer cell lines.[a]

Compound	MT-3 IC_{50} (μM)	HT-29 IC_{50} (μM)	Colo205 IC_{50} (μM)
ATRA	30 ± 4	4.3 ± 0.2	37 ± 1
19	17 ± 1	3.6 ± 1.8	17 ± 2
12	51 ± 3	>200	>200
20	14 ± 1	>200	127 ± 18

[a] Cytotoxicity was measured using the MTT assay as cell viability 48 h after incubation with the indicated substances for 24 h and shown by mean ± SD (n = 3).

The cytotoxicity of the prodrugs **13**–**16** was investigated in HT-29 and Colo205 colon cancer cells. HT-29 cells do not secrete $sPLA_2$, which allowed evaluation of the activity in the presence and absence of $sPLA_2$. As evident from Table 25 and the dose-response curve for **13** and **15** (Figure 31) none of the prodrugs were able to induce significant cell death in the absence of $sPLA_2$, whereas upon $sPLA_2$ addition all of the prodrugs displayed IC_{50} values below 10 μM in HT-29 cells (Table 25) and complete cell death was obtained when higher concentrations were applied (see Figure 31). Evidently, the cytotoxicity is induced by $sPLA_2$ triggered breakdown of the prodrugs into **19** or **20** and the lysolipids. Interestingly, it was observed that the *sn*-1-ester prodrug **16** in the presence of $sPLA_2$ displayed almost the same cytotoxicity towards HT-29 cells as the corresponding *sn*-1-ether prodrug **15** and taking the low activity of **20** in HT-29 cells (Table 25) into account these results indicate that *sn*-1-ester lysolipids (**18**) contribute with the same degree of potency as *sn*-1-ether lysolipids (**17**). These findings were verified when the free lysolipids **17** and **18** were tested against HT-29 cells. Both lysolipids displayed IC_{50} values close to 10 μM and similar results were obtained for DSPG and 1-*O*-DSPG in the presence of $sPLA_2$ (Table 25). It is conclude that even though *sn*-1-ester lysolipids generally are rapidly metabolized, under these *in vitro* conditions there is no significant metabolism of the phospholipid backbone and therefore an equal potency of the two lysolipids is observed. With the control experiments in hand it is possible to determine the origin of the cytotoxicity of the prodrugs in HT-29 cells and as evident from Table 24 and Table 25 the majority of the activity arises from the lysolipids in prodrug **15** and **16** while for the prodrugs **13** and **14** there appear to be an equal contribution from the lysolipids (**17** and **18**) and the ATRA ester **19**. Colo205 cells express $sPLA_2$ and encouragingly the four prodrugs induce cell death with IC_{50} values below 20 μM (Table 25) and complete cell death was obtained when higher concentrations were applied (see Figure 31), indicating that the secreted $sPLA_2$ in Colo205 cells provides the desired hydrolysis and release of the anticancer agents. Additionally, the prodrugs **13** and **14** displayed IC_{50} values below the free lysolipids but similar to **19**, indicating that the majority of the cytotoxicity can be ascribed to the released ATRA ester **19**. For prodrugs **15** and **16** the IC_{50} values indicate a cumulative effect, since these prodrugs are more potent than both of the released compounds, demonstrating the advantage of the prodrug formulation.

Table 25. IC_{50} (μM) values for the prodrugs **13–16**, the lysolipids **17** and **18**, DSPG and 1-*O*-DSPG in HT-29 and Colo205 cancer cell lines.[a]

Compound	HT-29 IC_{50} (μM)	HT-29 + $sPLA_2$[b] IC_{50} (μM)	Colo205 IC_{50} (μM)
13	>200	7 ± 2	16 ± 4
14	>200	6 ± 1	12 ± 3
15	>200	3 ± 1	7 ± 6
16	>200	8 ± 1	19 ± 4
17	11 ± 6	*nd*	25 ± 2
18	7 ± 1	*nd*	22 ± 3
DSPG	>200	25 ± 11	54 ± 7
1-*O*-DSPG	>200	9 ± 2	33 ± 4
$C_{17}H_{35}COOH$	>200	*nd*	>200
$sPLA_2$	*c*	*c*	*c*

[a] Cytotoxicity was measured using the MTT assay as cell viability 48 h after incubation with the indicated substances for 24 h and shown by mean ± SD ($n \geq 3$); *nd* = not determined; [b] Snake (*Agkistrodon piscivorus piscivorus*) venom $sPLA_2$ was added to a final concentration of 5 nM; [c] No change in cell viability was observed after 24 h.

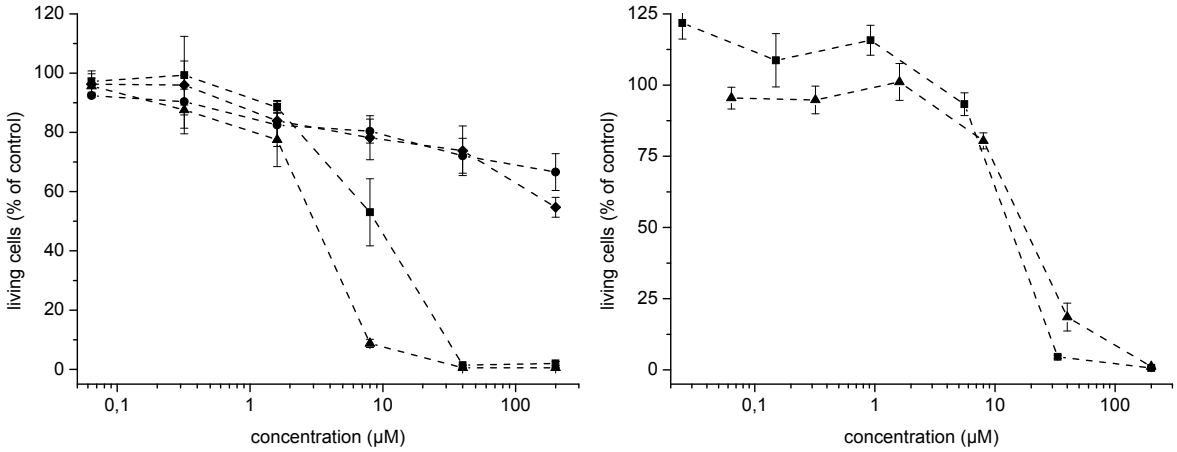

Figure 31. Dose–response curves for the treatment of HT-29 cells (left) with the *sn*-1-ether prodrugs **13** (●), **13** + $sPLA_2$ (■), **15** (♦) and **15** + $sPLA_2$ (▲). Dose–response curves for the treatment of Colo205 cells (right) with *sn*-1-ester prodrugs **14** (■) and **16** (▲).

4.10 Conclusion

The ATRA phospholipid prodrug was synthesized but $sPLA_2$ was not able to hydrolyze the desired ester bond and MD simulations confirmed that **8** has an imperfect positioning in $sPLA_2$. Based on MD simulations, a revised prodrug strategy for enzyme triggered delivery of retinoids was developed in which an aliphatic C_6-linker was incorporated between the glycerol backbone of the phospholipids and the retinoids. The phospholipid prodrugs of retinoids (**13**–**16**) were synthesized and gratifyingly, it was demonstrated that they can be formulated as liposomes that are degraded by $sPLA_2$. The cytotoxicity studies showed that prodrug **13**–**16** require $sPLA_2$ in order to induce significant cell death. It is therefore evident that the revised prodrug strategy presents a solution to liposomal formulation of retinoids.

5. Enzymatic Studies on Vitamin E Succinate Phospholipid Conjugates

5.1 Introduction

Vitamin E's are important antioxidants which protect cell membranes against oxidation by scavenging of lipid peroxidation produced radicals.[177] Vitamin E is a family of α, β, γ, and δ-tocopherol (Figure 32) and the corresponding four tocotrienols[177] and while all vitamin E's are non-toxic and have low cytotoxicty against cancer cells, vitamin E succinates are potent growth inhibitors towards various cancer cells, with α-tocopheryl succinate as the most active member of the family (Figure 32).[77,78] Like the vitamin E compounds, the succinates do not display toxicity towards healthy cells.[77] The skeleton of the family of vitamin E compounds are divided into three domains[178] (Figure 32) and for the functional domain (I in Figure 32) structure activity relationship (SAR) studies have shown that the attachment of short dicarboxylic acids (like malonic acid or succinic acid) provide the most cytotoxic agents, whereas longer dicarboxylic acids provide less potent agents.[78] Furthermore, SAR studies have demonstrated that the carboxylate is crucial for the anticancer activity, since e.g. the methyl ester of α-tocopheryl succinate is completely inactive.[78] It is believed that the role of the carboxylate is to cause destabilization of cell membranes via a detergent-like behavior leading to a higher drug uptake.[179] SAR studies on the other domains, the signaling and the hydrophobic (II and III in Figure 32, respectively) revealed that both domains are needed for maintaining activity, however modifications in the length of the hydrophobic domain are tolerated.[78]

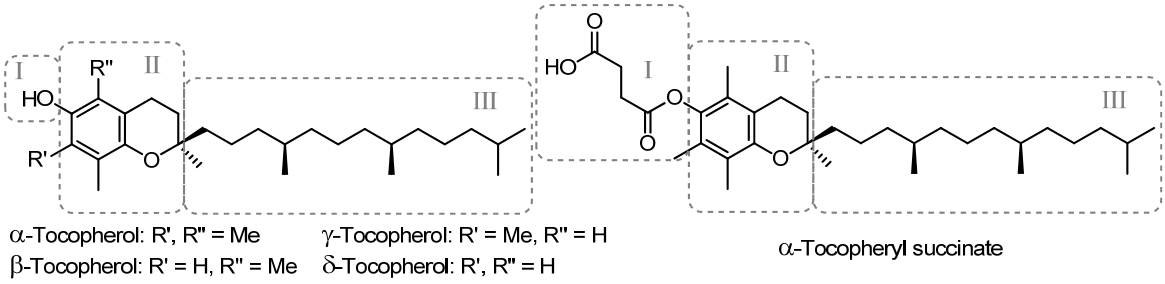

Figure 32. Structure of the four tocopherols from the vitamin E family (left). The three domains (I, II and III) are indicated. Structure of α-tocopheryl succinate (right), which is the most potent vitamin E succinate and selected for incorporation into the investigated drug delivery system.

The use of vitamin E derivatives in cancer treatment is restricted due to their low water solubility hampering an intravenous administration route, and an oral administration route of the vitamin E succinates may not be effective due to hydrolysis of the ester bond by esterases during the transport through the intentinal tract.[178] Therefore incorporation into a liposomal drug delivery system could be beneficial. The carboxylic acid moiety allows direct attachment to the *sn*-2 position of the phospholipid backbone making vitamin E succinates applicable as drug candidate for the investigated drug delivery system. Furthermore, the liposomal formulation will scavenge the biological important carboxylate

moiety by formation of an ester bond hence only tissue with an over expression of $sPLA_2$ will be affected by the injected liposomes. α-Tocopheryl succinate was selected as the vitamin E succinate to study, since this compound is commercially available, cheap and potent. The target phospholipid prodrugs are shown in Figure 33 and in order to examine differences in biophysical and biological properties along with enzyme activity both the *sn*-1-ester and the *sn*-1-ether phospholipid prodrug were synthesized.

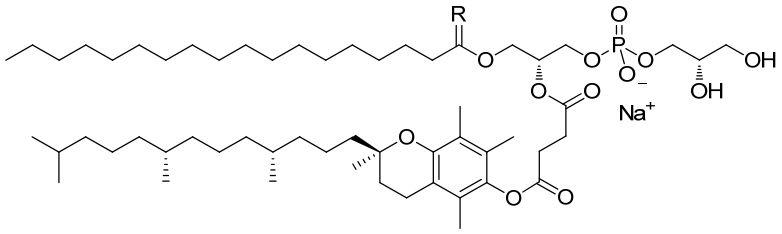

36: R = H_2
37: R = O

Figure 33. Structure of the target α-tocopheryl succinate phospholipid prodrugs.

5.2 Synthesis of α-Tocopheryl Succinate Phospholipid Prodrugs

The *sn*-1-ether phospholipid prodrug **36** was accessible in three synthetic steps from the previously prepared secondary alcohol **29** (Scheme 13). Acylation of **29** with α-tocopheryl succinate gave the desired ester bond and the following deprotections of the cyanoethyl and the TBDMS groups were achieved using the same conditions as in synthesis of **13**–**16** (Scheme 11), giving the *sn*-1-ether phospholipid prodrug **36** in 61% yield over the three steps (Scheme 13).

Scheme 13. Synthesis of the *sn*-1-ether phospholipid prodrug **36**.[a]

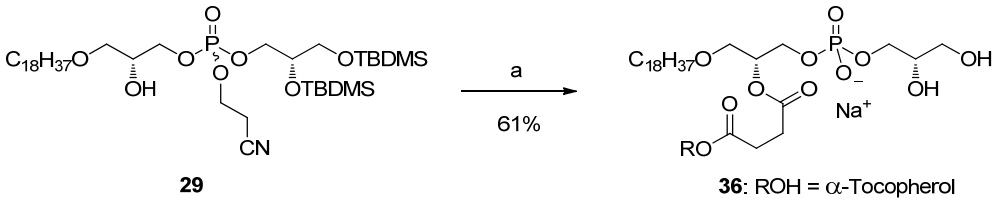

29 **36**: ROH = α-Tocopherol

[a]Reagents: (a) (i) α-Tocopheryl succinate, EDCI, DMAP, EtOAc, CH_2Cl_2; (ii) DBU, CH_2Cl_2; (iii) HF, H_2O, CH_2Cl, MeCN.

The synthesis of the *sn*-1-ester phospholipid prodrug **37** (Scheme 14) was initiated from the previously prepared secondary alcohol **33** (Scheme 10). Alcohol **33** was reacted with α-tocopheryl succinate creating the ester bond and the TBDMS group was removed by the NBS mediated desilylation method, also applied in the synthesis of **34** (Scheme 10), and no migration or degradation of the α-tocopheryl succinyl moiety was observed. The phosphate headgroup was inserted via reaction with the phosphoramidite **27** applying the established

coupling procedure (see e.g. Scheme 9) and after the final deprotections the *sn*-1-ester phospholipid prodrug **37** was accessed in 44% yield from **38** (Scheme 14).

Scheme 14. Synthesis of the *sn*-1-ester phospholipid prodrug **37**.[a]

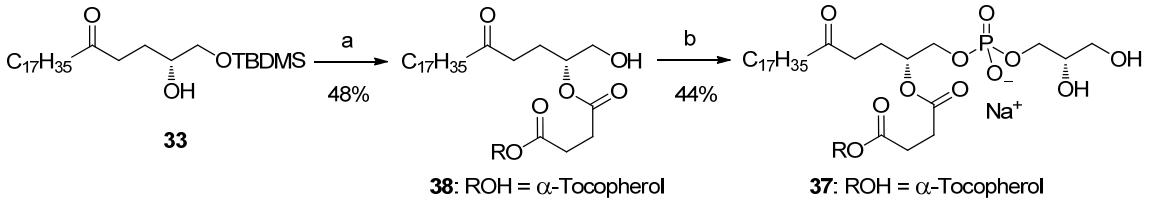

[a]Reagents: (a) (i) α-tocopheryl succinate, EDCI, DMAP, CH_2Cl_2; (ii) NBS, DMSO, THF, H_2O; (b) (i) phosphoramidite **27**, tetrazole, CH_2Cl_2, MeCN; (ii) ^{t}BuOOH; (iii) DBU, CH_2Cl_2; (iv) HF, H_2O, CH_2Cl, MeCN.

5.3 Enzyme Activity and Cytotoxicity

The α-tocopheryl succinate phospholipid prodrugs **36** and **37** were hydrated in HEPES buffer yielding milky solutions and a DSC scan (20–65 °C) was obtained. But no T_m was observed in the tested range, indicating that **36** and **37** are in a fluid state at 20 °C. These findings were further supported during the formulation where it was possible to extrude the solutions of **36** and **37** through a 100 nm filter at 20 °C, yielding clear and transparent solutions. DLS analysis of the formulated phospholipids revealed that particles with an average diameter of 115 nm and a low polydispersity was formed (Table 26), indicating formation of unilamellar vesicles.

Table 26. DLS analysis of phospholipid solutions hydrated in HEPES buffer and extruded through a 100 nm filter.

Compound	Particle size	
	Diameter (nm)	PdI
36	115	0.09
37	115	0.06
40	80	0.14
41[a]	191	0.23
41	115	0.49
42[a]	168	0.33
42	100	0.35

[a]Not extruded

In order to study the enzyme activity snake (*Naja mossambica mossambica*) venom $sPLA_2$ was added to the phospholipid solutions and the mixtures were incubated at 37 °C for 48 h. The activity was monitored by MALDI-TOF MS but disappointingly and as evident from the MS spectra in Figure 34 both phospholipids are poor substrates for the enzyme and

based on the MS spectra no significant degradation has occurred, however small amounts of the lysolipids and α-tocopheryl succinate were detected in the MS spectra (data not shown). The inability of $sPLA_2$ to release α-tocopheryl succinate was verified by evaluation of the cytotoxicity in HT-29 and Colo205 cells. As evident from Figure 35 no significant cell death was obtained when **36** and **37** were subjected to HT-29 cells neither in absence nor presence of $sPLA_2$ and likewise no cell death was observed in the $sPLA_2$ secreting Colo205 cells (Figure 35). In contrast to the phospholipids α-tocopheryl succinate induced significant cell death in both cell lines.

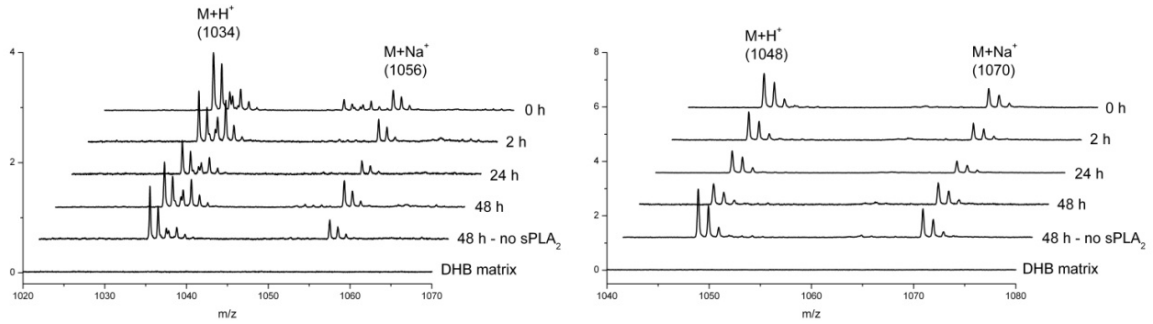

Figure 34. MALDI-TOF MS monitoring of snake (*Naja mossambica mossambica*) venom $sPLA_2$ activity on α-tocopheryl succinate conjugates **36** (left) and **37** (right).

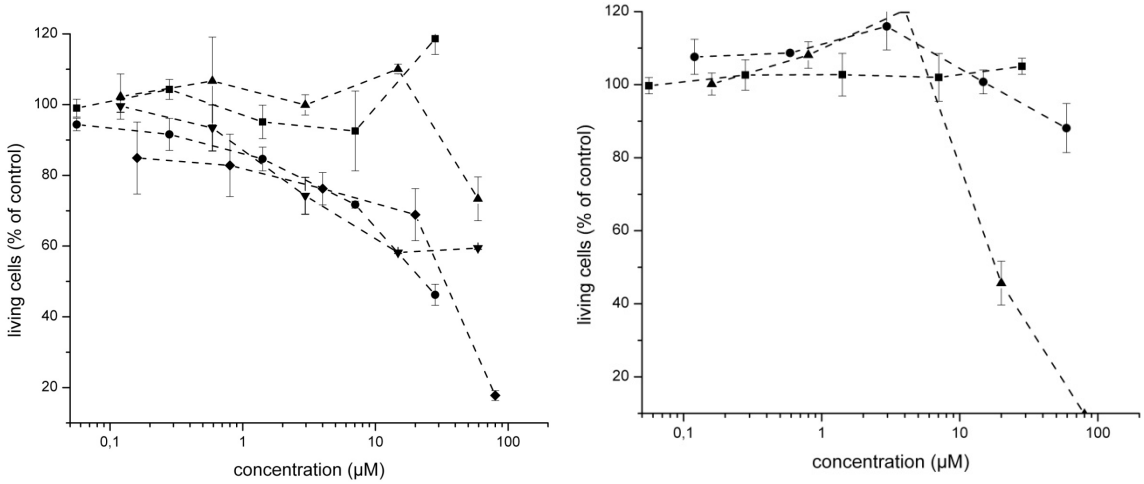

Figure 35. Dose-response curves for the treatment of HT-29 cells (left) with α-tocopheryl succinate (♦) and the phospholipid prodrugs, **36** (■), **36** + $sPLA_2$ (●), **37** (▲), **37** + $sPLA_2$ (▼). Dose-response curves for the treatment of Colo205 cells (right) with α-tocopheryl succinate (▲) and the phospholipid prodrugs, **36** (■) and **37** (●). The cytotoxicity was measured using the MTT assay as cell viability 48 h after incubation with the indicated substances for 24 h and shown by mean + SD (n=3). Snake (*Agkistrodon piscivorus piscivorus*) venom $sPLA_2$ was added to a final concentration of 5 nM in studies of HT-29 cells.

5.4 Synthesis and Enzyme Activity of Alkyl and Phenyl Succinate Phospholipids

The low extent of $sPLA_2$ activity that was observed on prodrug **36** and **37** prompted to an investigation of which structural features of α-tocopheryl succinate that hinders the hydrolysis to occur efficiently. Recent MD studies[180] on the chlorambucil prodrugs (**1** and **2**) and DPPG have indicated that water enter the active site of the enzyme via the hydrophobic channel in the protein[51] following a specific route controlled by the aromatic residues in Phe5 and Tyr51. Interestingly, the studies indicated that the aromatic moiety in the chlorambucil prodrugs increase the diameter of the hydrophobic channel without affecting the orientation of the residues in the active site meaning water molecules more freely can reach the catalytic region in complexes of $sPLA_2$ and the chlorambucil prodrugs than in the $sPLA_2$–DPPG complex. The extensive substitution of the phenyl ring in α-tocopherol may therefore block the hydrophopic channel hampering the flow of water into the active site meaning the hydrolysis rate will be slowed down. In order to study the hypothesis a SAR study was initiated, in which the octyl succinate phospholipid **40**, the phenyl succinate phospholipid **41** and the 2,6-dimethylphenyl succinate phospholipid **42** were synthesized (Scheme 15). The succinate moiety was attached to the phospholipid backbone by coupling of building block **29** and benzyl succinate (**44**, see Scheme 15) and hydrogenolysis of the benzyl ester gave **39** (Scheme 15). The carboxylic acid **39** was diversified into the desired phospholipids **40**, **41** and **42**, by first a Steglich coupling with the corresponding alcohol, followed by deprotections of the cyanoethyl and TBDMS groups (Scheme 15).

Scheme 15. Synthesis of the succinate phospholipids **40**, **41** and **42** and benzyl succinate (**44**).[a]

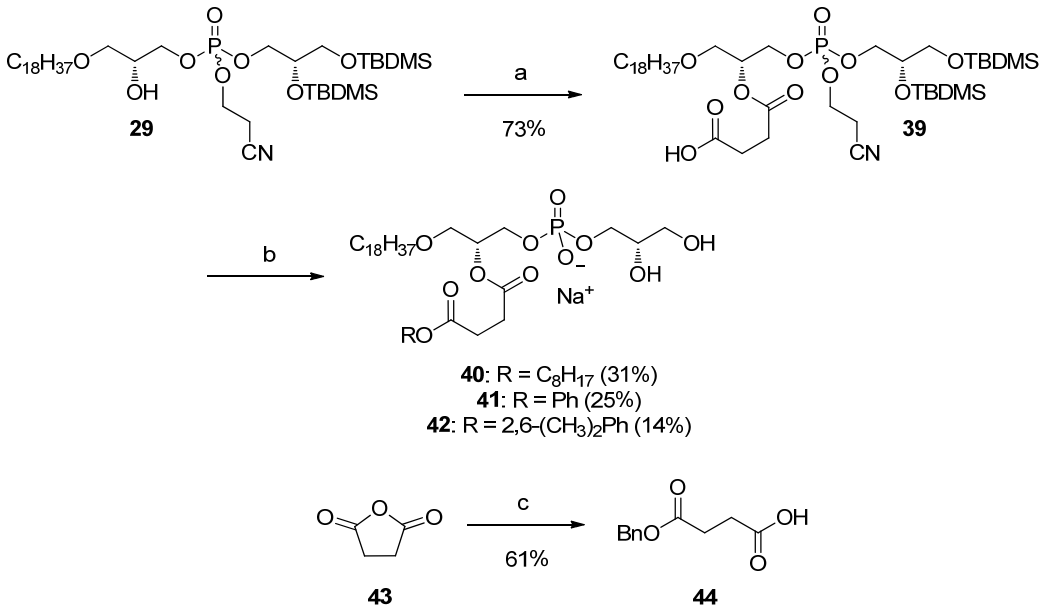

[a]Reagents: (a) (i) **44**, DCC, DMAP, CH_2Cl_2; (ii) H_2, Pd/C, EtOAc, MeOH; (b) (i) $C_8H_{17}OH$, PhOH or 2,6-dimethylphenol, DCC, DMAP, CH_2Cl_2; (ii) DBU, CH_2Cl_2; (iii) HF, H_2O, CH_2Cl, MeCN; (c) BnOH, DMAP, CH_2Cl_2.

Hydration of **41** and **42** in HEPES buffer at 20 °C gave clear solutions and DLS analysis revealed that particles with an average diameter of 190 nm for **41** and 168 nm for **42** (Table 26) were present, indicating that some kind of non-multilamellar vesicles were formed. Surprisingly, it was not possible to extrude the clear phospholipid solutions of **41** and **42** through a 100 nm filter at 20 °C and the extrusion was therefore performed at 65 °C. DLS analysis of the extrude solutions showed that the average diameter was decreased to 115 and 100 nm for the phospholipid solutions of **41** and **42**, respectively whereas the polydispersity was increased (Table 26). The results from the DLS analysis and the extrusions indicate that some form of robust particles with a diameter >100 nm is formed spontaneously upon subjection to HEPES buffer and it is likely this can be associated with the molecular structure of **41** and **42**. The significant shorter chain in the *sn*-2 position than in the *sn*-1 position gives phospholipids with a different curvature and hence packing properties than phospholipids having chains of (almost) the same length, like in DPPG. But as these results were obtained in last part of the Ph.D. study there was not time for further investigations. Hydration of **40** in HEPES buffer at 20 °C gave the same milky solution as observed for the α-tocopheryl succinate phospholipid prodrugs **36** and **37** and the following extrusion through a 100 nm filter at 20 °C gave a clear solution with particles having an average diameter of 80 nm as measured by DLS (Table 26). The extruded solutions of **40**, **41** and **42** were subjected to snake (*Naja mossambica mossambica*) venom $sPLA_2$ and the enzyme activity was monitored by MALDI-TOF MS. As evident from Figure 36 the octyl succinate phospholipid **40** was completely degraded by the enzyme within 24 h, demonstrating that it is not the succinate moiety that hinders $sPLA_2$ in releasing α-tocopheryl succinate. The enzyme activity on the phenyl succinate phospholipids **41** and **42** was almost as good as on **40**, although small peaks for **41** and **42** remain in the MS spectra (Figure 36). Beyond the information that **40**, **41** and **42** were consumed by $sPLA_2$ the MS spectra also revealed that the desired lysolipid **17** was released in the three experiments (Figure 36). The enzymatic studies could indicate that the attachment of a phenyl moiety to the succinate to some extent reduce the enzyme activity, but compared to the α-tocopheryl succinate phospholipids the degree of hydrolysis is significantly higher for **41** and **42** by which the lack of hydrolysis on **36** and **37** cannot directly be associated with either the phenyl ring or the two methyl groups *ortho* to the hydroxyl group in α-tocopherol. It is therefore necessary to extend the SAR study with attachment of further phenols to the succinate moiety and likewise it will be interesting to examine other tocopherols like δ-tocopherol (see Figure 32) in order to get valuable information about the consequence of the methyl groups on the phenyl ring. Furthermore, MD simulations of vitamin E succinate phospholipid conjugates in the active site of $sPLA_2$ would be interesting to obtain in order to study which structural features that hamper the enzyme activity.

Potentially, the low degree of hydrolysis on **36** and **37** could also be related to an inhibition of $sPLA_2$ by α-tocopheryl succinate. α-Tocopherol are reported as an inhibitor of $sPLA_2$ by

Chandra *et al*.,[181] whereas no information is available on esters of α-tocopherol. The ability of α-tocopheryl succinate to inhibit $sPLA_2$ was therefore investigated by the same assay as applied during the inhibitions studies of ATRA and the ATRA ester **19**. Gratifyingly, the studies demonstrated that α-tocopheryl succinate is a weaker inhibitor than ATRA ester **19** meaning that the low enzyme activity is not due to inhibition.

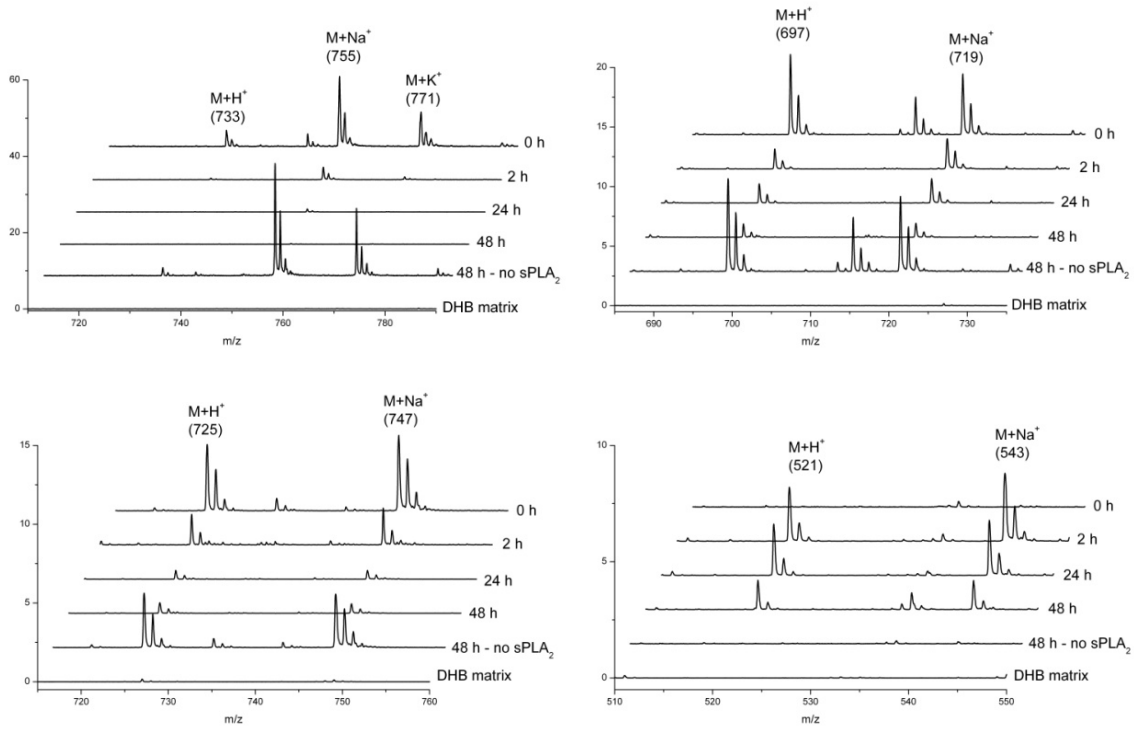

Figure 36. MALDI-TOF MS monitoring of snake (*Naja mossambica mossambica*) venom $sPLA_2$ activity on the succinate phospholipid **40** (top left), **41** (top right) and **42** (bottom left). The lysolipid **17** (bottom right) was detected in all three experiments and shown from the enzyme study on **41**.

5.5 Conclusion

The α-tocopheryl succinate phospholipid prodrugs **36** and **37** were prepared in good yields utilizing previously developed chemistry, however the extent of hydrolysis by $sPLA_2$ was low. Thus an investigation of the structural features preventing hydrolysis from occurring efficiently was initiated and the succinate phospholipids **40**, **41** and **42** were synthesized. The enzymatic studies demonstrated that the succinate moiety is tolerated by the enzyme, whereas the studies indicated that the phenyl ring to some extent hampers the activity, but more phenyl succinate phospholipid analogues are needed in order to localize which structural motifs in α-tocopheryl succinate that reduce the enzyme activity.

6. Prostaglandin Phospholipid Conjugates with Unusual Properties

6.1 Introduction

Since von Euler[182] and Goldblatt[183] independently isolated and studied prostaglandins for the first time these fatty acids have attracted attention due to their involvement in many important biological functions.[184,185,186] The biosynthetic precursor for protaglandins is arachidonic acid, which by a number of enzyme catalyzed reactions is converted into the diverse selections of prostaglandins known today.[184,185,186]

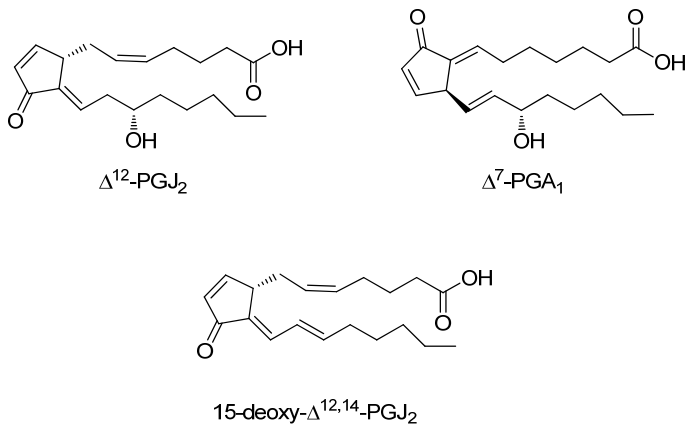

Figure 37. Potent antiproliferative prostaglandins.

Many prostaglandins have shown antiproliferative activity in tumor cells, but among the most studied and active prostaglandins are the dienone prostaglandins like Δ^{12}-PGJ_2 and Δ^{7}-PGA_1 (see Figure 37).[187] Likewise, 15-deoxy-$\Delta^{12,14}$-PGJ_2, a metabolic derivative of Δ^{12}-PGJ_2 (Figure 37) has demonstrated high antitumor activity against L1210 leukemia cells[79] and for incorporation into the investigated drug delivery system that compound is more suitable than the former prostaglandins since 15-deoxy-$\Delta^{12,14}$-PGJ_2 has a higher lipophilicity. The 15-deoxy-$\Delta^{12,14}$-PGJ_2 phospholipid conjugates was designed to have the PG headgroup and C_{18} chains in the *sn*-1-position linked through either an ether-bond or ester-bond (see Figure 38).

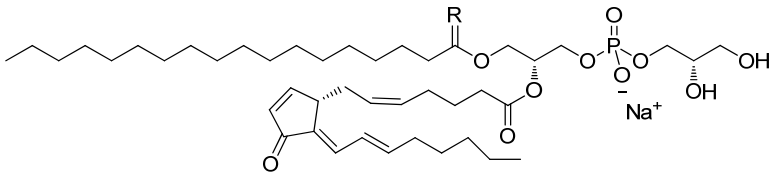

Figure 38. Targeted 15-deoxy-$\Delta^{12,14}$-PGJ_2 phospholipid conjugates.

6.2 Synthesis of Prostaglandin Phospholipid Conjugates

The *sn*-1-ether conjugate **45** (Scheme 16) was prepared by Steglich acylation[102] of the phospholipid precurcor **29** with 15-deoxy-$\Delta^{12,14}$-PGJ_2 after which the PG headgroup was deprotected under the same conditions as in the synthesis of **13**–**16** (Scheme 11). Access to the corresponding *sn*-1-ester conjugate **46** was attempted via the same route as applied in the synthesis of α-tocopheryl succinate prodrug **37** (Scheme 14), but the NBS mediated deprotection of the TBDMS group caused decomposition of the prostaglandin moiety. Therefore an approach similar to the synthesis of the *sn*-1-ether phospholipid prodrugs was initiated from alcohol **32** (Scheme 17). The secondary alcohol was PMB protected via subjection to PMBTCA in an acidic solution of toluene and the TBDMS group was removed with NBS in a moist mixture of DMSO and THF to afford **47** (Scheme 17). Conversion to phospholipid precursor **48** (Scheme 17) was achieved in the same way as **29** was obtained from **5b** (Scheme 9). Then, freshly prepared **48** was acylated with 15-deoxy-$\Delta^{12,14}$-PGJ_2 and deprotection of the PG headgroup led to the desired conjugate **46** (Scheme 16). Urea formation was observed during the carbodiimide mediated acylations with 15-deoxy-$\Delta^{12,14}$-PGJ_2 which resulted in low yields of **45** and **46** (Scheme 16) but since 15-deoxy-$\Delta^{12,14}$-PGJ_2 is expensive the compound was not used in excess and alternative acylation methods was not examined.

Scheme 16 Synthesis of the 15-deoxy-$\Delta^{12,14}$-PGJ_2 phospholipid conjugates **45** and **46**.[a]

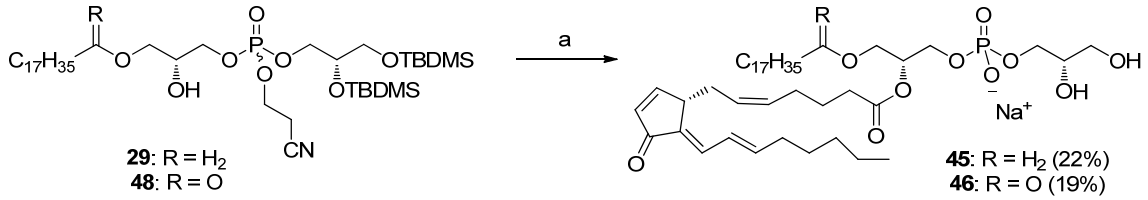

[a]Reagents: (a) (i) 15-deoxy-$\Delta^{12,14}$-PGJ_2, DCC, DMAP, CH_2Cl_2; (ii) DBU, CH_2Cl_2; (iii) HF, H_2O, CH_2Cl_2, MeCN.

Scheme 17. Synthesis of *sn*-1-ester phospholipid precursors.[a]

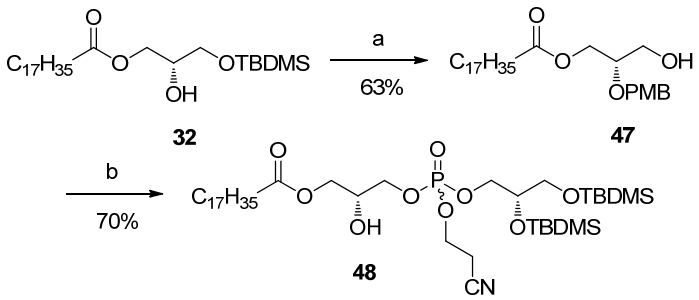

[a]Reagents: (a) (i) PMBTCA, $La(OTf)_3$, toluene; (ii) NBS, DMSO, THF, H_2O; (b) (i) phosphoramidite **27**, tetrazole, CH_2Cl_2, MeCN; (ii) ^{t}BuOOH; (iii) DDQ, H_2O, CH_2Cl_2.

6.3 Biophysical Characterization and Enzymatic Studies

The prostaglandin conjugates **45** and **46** were hydrated in HEPES buffer at 20 °C yielding clear solutions. DLS analysis of the phospholipid suspension of **46** revealed that particles with a average diameter of around 100 nm were formed (Table 27), indicating that the prostaglandin conjugates spontaneously form unilamellar vesicles at 20 °C. Self-aggregation into unilamellar vesicles upon dispersion in a buffer is very rare for phospholipids and has only been reported in the literature once before.[71] Extrusion through a 100 nm filter at 20 °C narrowed the average diameter and the polydispersity of the vesicles (Table 27), presumably because filtration removed the minor population of flocculated particles. Twelve days after formulation, the particle distribution of the phospholipid suspensions was investigated with DLS again. As evident from Table 27, neither the diameter nor the polydispersity changed significantly, showing that the vesicles formed maintain their size and does not aggregate into larger particles.

Table 27. DLS analysis of the 15-deoxy-$\Delta^{12,14}$-PGJ_2 conjugates formulated by extrusion. Data was obtained immediately after the formulation and 12 days later.

	0 days		12 days[b]	
Compound	**Diameter**	**PdI**	**Diameter**	**PdI**
45	51	0.26	61	0.26
46[a]	112	0.45	98	0.39
46	81	0.35	76	0.41

[a]Not extruded. [b]The lipid suspensions were stored at 4 °C for 12 days.

The formulated phospholipid suspensions of **45** and **46** were investigated for their susceptibility to $sPLA_2$ hydrolysis. Purified snake venom $sPLA_2$ from *Agkistrodon piscivorus piscivorus* and *Naja mossambica mossambica* were used and the enzyme activity was investigated with MALDI-TOF MS.

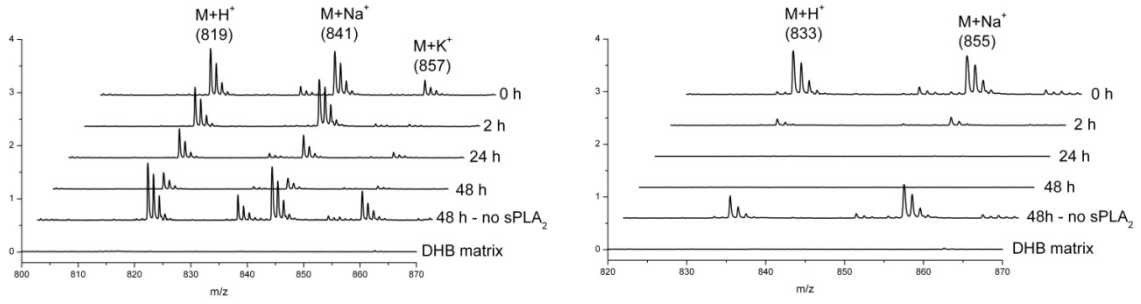

Figure 39. MALDI-TOF MS monitoring of snake (*Naja mossambica mossambica*) venom $sPLA_2$ activity on the 15-deoxy-$\Delta^{12,14}$-PGJ_2 conjugates **45** (left) and **46** (right).

The formulated phospholipids **45** and **46** were subjected to $sPLA_2$ and stirred at 37 °C and samples for MALDI-TOF analysis were taken after 2, 24 and 48 h. As evident from the MS spectra in Figure 39 the *sn*-1-ester conjugate **46** was completely consumed by $sPLA_2$

after 24 h. However, the *sn*-1-ether conjugate **45** was not completely degraded after 48 h and the conversion was estimated to 70%. This difference in hydrolysis rate and extent for the *sn*-1-ester versus the *sn*-1-ether phospholipids is remarkable and to your knowledge has not been observed before, but the observation verifies that *sn*-1-ester phospholipids are better substrates for $sPLA_2$ than *sn*-1-ether phospholipids.[131] For both conjugates 15-deoxy-$\Delta^{12,14}$-PGJ_2 and the lysolipid **17** and **18** were detected as the released products (data not shown). Also evident from Figure 39 is the requirement for $sPLA_2$ for hydrolysis of both **45** and **46**.

6.4 Cytotoxicity

The cytotoxicity of the conjugates was evaluated in two colon cancer cell lines, HT-29 and Colo205 (Table 28). The activity of the conjugates towards HT-29 cells was investigated in the presence and in the absence of $sPLA_2$. Surprisingly, it was observed that the conjugates induced significant cell death (see Table 28 and Figure 40) also in the absence of the enzyme, albeit to a lesser degree than when $sPLA_2$ was present. Despite having studied a number of other phospholipid prodrugs, like **1**, **13** and **15** this is the first time cytotoxicity of the phospholipid conjugates in the absence of $sPLA_2$ has been observed. It can be speculated that this behavior is due to a spontaneous cellular uptake of the 15-deoxy-$\Delta^{12,14}$-PGJ_2 conjugates followed by metabolic breakdown in the cytosol. This facile uptake is likely a consequence of the dynamic behavior of the 15-deoxy-$\Delta^{12,14}$-PGJ_2 conjugates, which also manifests itself during formulation, where self-aggregation into unilamellar vesicles was observed (*vide supra*).

Table 28. IC_{50} values for 15-deoxy-$\Delta^{12,14}$-PGJ_2 and the conjugates **45** and **46** in HT-29 and Colo205 colon cancer cell lines.[a]

Compound	HT-29 IC_{50} (μM)	HT-29 + $sPLA_2$[b] IC_{50} (μM)	Colo205 IC_{50} (μM)
15-deoxy-$\Delta^{12,14}$-PGJ_2	1.6 ± 0.3	*nd*	4 ± 2
45	6 ± 1	2.2 ± 0.2	9 ± 2
46	32 ± 2	6.4 ± 0.4	17 ± 5

[a]Cytotoxicity was measured using the MTT assay as cell viability 48 h after incubation with the indicated substances for 24 h and shown by mean ± SD ($n \geq 3$); nd = not determined; [b]$sPLA_2$ was added to a final concentration of 5 nM.

The cytotoxicity of the released compounds 15-deoxy-$\Delta^{12,14}$-PGJ_2 (Table 28) and the lysolipids **17** and **18** (Table 25) was obtained also. As evident the IC_{50} values for the released compounds are in the same range as for the conjugates **45** and **46** indicating that the activity originate from 15-deoxy-$\Delta^{12,14}$-PGJ_2 and the lysolipids, released either extra- or intracellularly. The conjugates were also able to induce cell death in Colo205 cells, with IC_{50} values below 20 μM (Table 28) and complete cell death was observed when higher concentrations were used (Figure 40). However, since Colo205 cells secrete $sPLA_2$ it is not possible to conclude whether the hydrolysis of the conjugates occurs extra- or

intracellularly, but it is promising that the 15-deoxy-$\Delta^{12,14}$-PGJ_2 conjugates show activity in this cancer cell line as well.

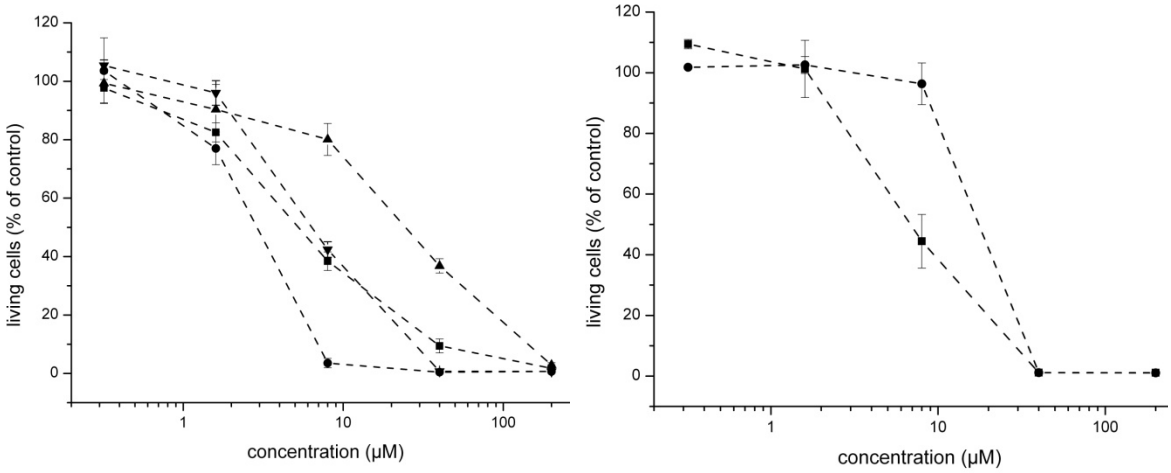

Figure 40. Dose-response curves for the treatment of HT-29 cells (left) with the 15-deoxy-$\Delta^{12,14}$-PGJ_2 conjugates; **45** (■), **45** + $sPLA_2$ (●), **46** (▲) and **46** + $sPLA_2$ (▼). Dose-response curves for the treatment of Colo205 cells (right) with the conjugates **45** (■) and **46** (●).

6.5 Conclusion

The conjugates **45** and **46** form unilamellar vesicles spontaneously, upon dispersion in HEPES buffer, which is rare for phospholipids. Furthermore, a significant difference in rate and extent of $sPLA_2$ hydrolysis between the *sn*-1-ester and the *sn*-1-ether conjugates was observed. In the cytotoxicity studies it was observed that **45** and **46** induce cell death in Colo205 cells and in HT-29 cells both in the presence and absence of $sPLA_2$, however this is not desirable in regard to a prodrug strategy. Therefore based on the observed results incorporation of 15-deoxy-$\Delta^{12,14}$-PGJ_2 into the investigated drug delivery system does not seem the way to go. But this is an exceptional example on how differently phospholipids can behave and further investigations of the ability to self-aggregate into unilamellar vesicles and a better understanding of the compounds permeability and membrane properties will have impact, not only on the design of phospholipid prodrug but also as a platform for designing highly permeable or membrane destabilizing phospholipids.

7. Towards Liposomal Delivery of Calcitriol

7.1 Introduction

At this stage of the project it became evident that the potency of the incorporated drugs was not strong enough to separate the effect from the lysolipids. Therefore it was necessary to come up with a more potent drug and calcitriol, a biological active metabolite of vitamin D_3, was chosen as the new drug candidate (Figure 41). Calcitriol plays a crucial role in calcium and phosphorus homeostatis, but it has also been established that it inhibits proliferation and causes differentiation in various cancer cells.[188,189] Calcitriol mediates its activity through the vitamin D receptor (VDR), and the hydroxyl groups at C-1 (1α-OH) and C-25 are important for binding (see Figure 41).[190]

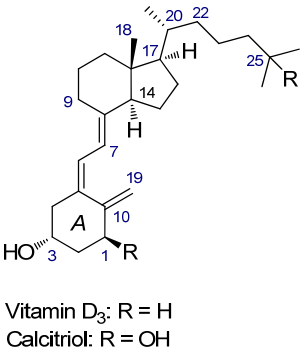

Figure 41. Structure of vitamin D_3 and calcitriol.

The absence of a carboxylic acid moiety in calcitriol obstructs direct attachment to the phospholipid backbone while incorporation of a linker is necessary. The results from the liposomal formulation of retinoids, in which $sPLA_2$ sensitive phospholipids were achieved by incorporation of an aliphatic linker between the retinoid and the phospholipid backbone (section 4.5), inspired an incorporation of a dicarboxylic acid, such as succinic acid or adipic acid (Figure 42). For this prodrug strategy to be successful it is crucial that the calcitriol analogues **51** and **52** retain the affinity for the VDR, either by direct binding or upon hydrolysis (e.g. by esterases) of the ester bond.

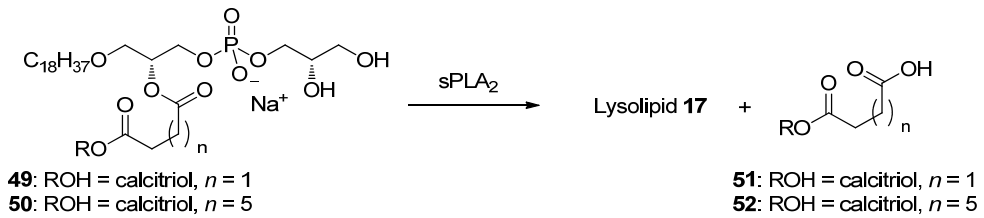

Figure 42. Schematic overview of the "dicarboxylic acid linker" based prodrug strategy for $sPLA_2$ triggered delivery of calcitriol analogues.

Initial studies have revealed that phospholipids with a carbonate in the *sn*-2 position are substrates for $sPLA_2$[191] and with this in hand a second strategy for enzyme triggered

release of calcitriol was investigated (Figure 43). The strategy relies on that upon $sPLA_2$ activation the released carbonate **54** will decompose to CO_2 and alcohol **55**, which then cyclize to δ-valerolactone under release of calcitriol. Drug release upon lactonization has previously been demonstrated by Wang *et al*.[192]

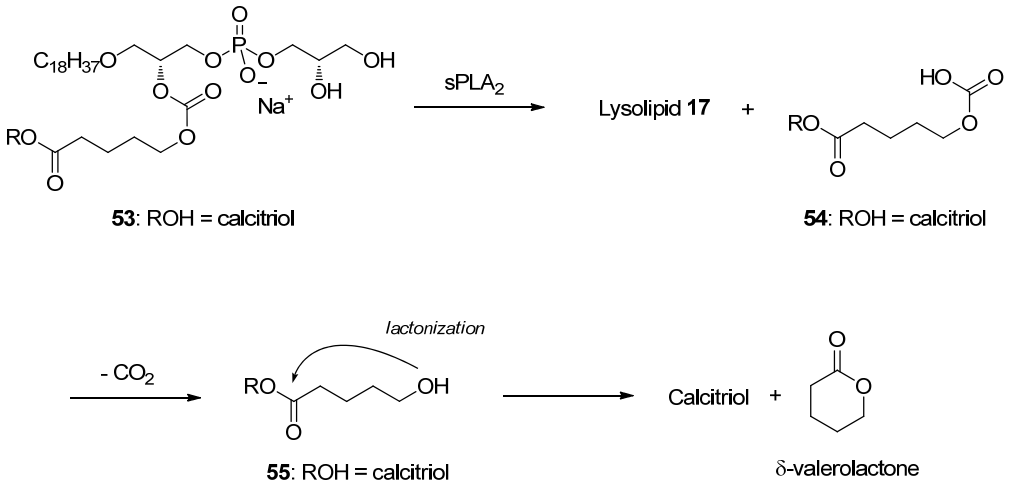

Figure 43. Schematic overview of the carbonate based prodrug strategy for $sPLA_2$ triggered delivery of calcitriol.

7.2 Calcitriol Esters

It is crucial for the prodrug strategy presented in Figure 42 that calcitriol analogues, like **51** and **52** retain their cytotoxicty and ability to bind to the VDR and in order to study that, the synthesis of the calcitriol esters **51** and **52** was initiated. Monoesterification of calcitriol and other 1α-hydroxyvitamin D_3 analogues is challenging due to the presence of two secondary hydroxyl groups at C-1 and C-3, and only low isolated yields have been reported.[193] The hydroxyl group at C-1 is important for the binding to the VDR hence esterification of the hydroxyl group at C-3 is desirable.

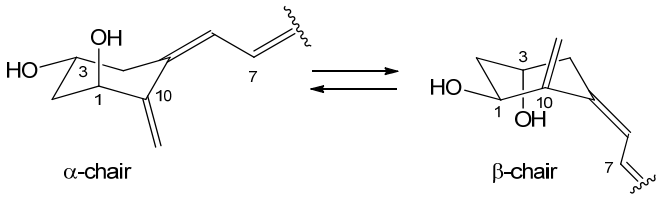

Figure 44. Conformational equilibrium between the α-chair and β-chair in the A-ring of Calcitriol (compare with Figure 41).[195]

Conformational studies of the *A*-ring (see Figure 41) by NMR[194,195,196] have demonstrated that the α-chair and β-chair conformation (see Figure 44) of the *A*-ring exist in a 1:1 ratio by which the two hydroxyl groups cannot be differentiated by their steric surroundings. The similarity in reactivity of the hydroxyl groups was confirmed when calcitriol was

subjected to succinic anhydride and DMAP (Figure 45 and Table 29), since **1-*O*-51** and **3-*O*-51** was formed in a 1:1 ratio as inseparable isomers. Reisolation of calcitriol (56%) compensates for the somewhat low yield, which very likely also can be associated with the low solubility of calcitriol in CH_2Cl_2 that made it necessary to add THF as a co-solvent. When calcitriol was treated with adipic anhydride and DMAP no conversion of calcitriol was observed, despite reaction of vitamin D_2 under identical conditions afforded the desired product in a good yield (data not shown).

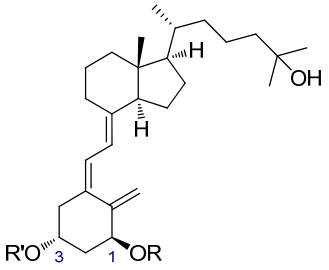

1-*O*-51: R = $CO(CH_2)_2COOH$, R' = H
3-*O*-51: R = H, R' = $CO(CH_2)_2COOH$
1-*O*-52: R = $CO(CH_2)_4COOH$, R' = H
3-*O*-52: R = H, R' = $CO(CH_2)_4COOH$
1-*O*-56: R = $COCF_2CH_2CH_3$, R' = H
3-*O*-56: R = H, R' = $COCF_2CH_2CH_3$

Figure 45. Synthesized calcitriol esters, see also Table 29.

Table 29. Synthesis of calcitriol esters, compare with Figure 45.

Compound	Ratio[a]	Reagents[b]	Yield
1-*O*-51 and **3-*O*-51**	1:1	a	29%
1-*O*-52 and **3-*O*-52**	1:3	b	19%
1-*O*-56 and **3-*O*-56**[c]	0:1	c	8%
1-*O*-56 and **3-*O*-56**[c]	1:1	c	17%

[a]Ratio between the 1-*O*-calcitriol ester and the 3-*O*-calcitriol ester. [b]Reagents: (a) calcitriol, succinic anhydride, DMAP, CH_2Cl_2, THF; (b) (i) calcitriol, carboxylic acid **58**, EDCI, DMAP, CH_2Cl_2, THF; (ii) TBAF, THF; (c) calcitriol, $CH_3CH_2CF_2COOH$, EDCI, DMAP, CH_2Cl_2, THF. [c]Same Experiment.

After idea from Blæhr *et al.*[193] the desired adipate analogue of calcitriol was assessed by a two step synthesis starting with an esterification of calcitriol with carboxylic acid **58** (Table 29). It was found that a Fischer esterification[197,198] of adipic acid (**57**) was the most appropriate method for making carboxylic acid **58** (Scheme 18). Interesting the Keck acylation[129] of calcitriol showed selectivity towards acylation of the hydroxyl group at C-3 and trimethylsilylethyl protected **1-*O*-52** and **3-*O*-52** was isolated in a 1:3 ratio. Furthermore, diacylation was observed to some extent as well. Deprotection of the trimethylsilylethyl protection group was achieved with TBAF in THF affording the mixture of **1-*O*-52** and **3-*O*-52** in 19 % yield over the two steps. The biological studies of the calcitriol analogues **51** and **52** revealed that the cytotoxicity was retained but the ability

to induce transcription of vitamin D-responsive genes was 10 times lower than for calcitriol (*vide infra*) demonstrating a low affinity towards the VDR. Therefore studies of *α*,*α*-difluoro esters of calcitriol was initiated, since *α*,*α*-difluoro esters are more labile towards chemical hydrolysis than aliphatic esters.[199] 2,2-Difluorobutyric acid is commercially available and became the starting point for the investigation. The attachment to calcitriol was achieved using a Keck acylation (Table 29) and gratifying it was possible by column chromatography to isolate **3-*O*-56** in 8% yield (see Figure 46 for the down-field part of the ^{1}H NMR spectrum) whereas a 1:1 mixture of **1-*O*-56** and **3-*O*-56** also was isolated in 17 % yield (Table 29). As evident from the ^{1}H NMR spectra in Figure 46 upon acylation the chemical shifts for H-1 and H-3 increase with ~1.2 ppm making the identification of the 1-*O*-esters and 3-*O*-esters of calcitriol possible. Furthermore, the ^{1}H NMR spectra illustrate that the signals for other protons in the down-field region separate for the two regioisomers which allows the determination of the ratio between them.

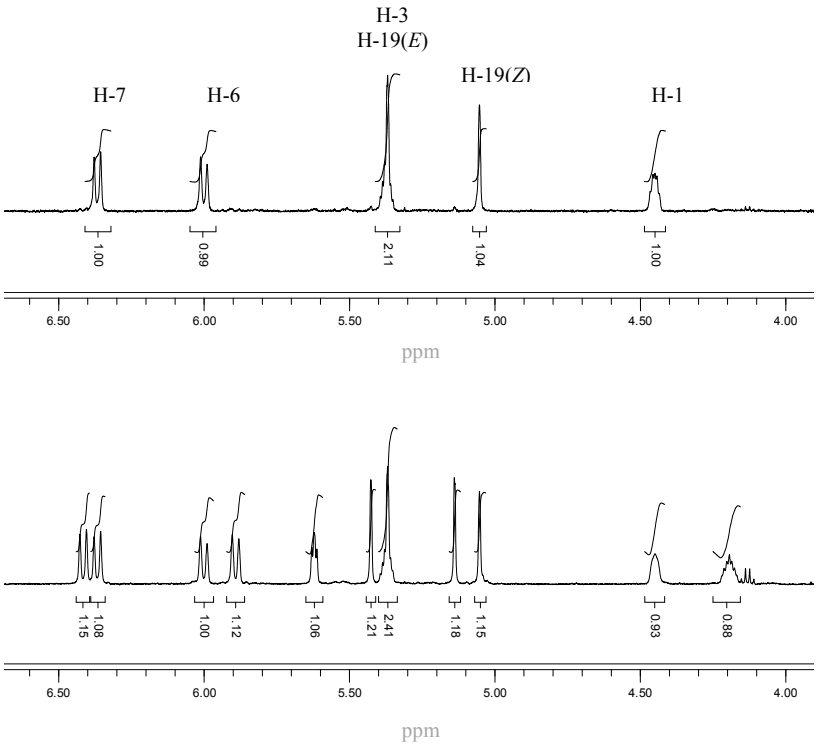

Figure 46. Snapshot from the down-field part of the 500 MHz ^{1}H NMR spectra for pure **3-*O*-56** (top) and the 1:1 mixture of **1-*O*-56** and **3-*O*-56** (bottom).

Scheme 18. Synthesis of carboxylic acid **58**.[a]

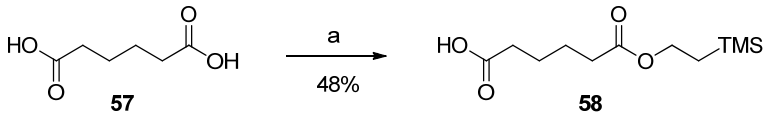

[a] Reagents: (a) $Me_3SiCH_2CH_2OH$, $TsOH{\cdot}H_2O$, toluene.

Encouraging the biological studies demonstrated that **1-*O*-56** and **3-*O*-56** binds to the VDR to the same extent as calcitriol (*vide infra*) hence attachment of a *α*,*α*-difluoro dicarboxylic acid to calcitriol was initiated. In order to get the same linker length as in the carbonate based prodrug strategy (Figure 43) it was decide to attach 2,2-difluoroheptanedioic acid. Applying chemistry developed by Burton and co-workers[200] coupling of the commercially available *α*,*α*-difluoro ester **61** and alkene **60** was successfully achieved and hydrogenolysis of the benzyl ester gave the desired carboxylic acid **62** in 46% yield (Scheme 19). Access to **62** was also achieved in 55% from **61** (Scheme 19) using a three steps procedure involving a dithionite mediated alkylation.[201,202] Elimination of iodide by DBU gave the corresponding alkene which was reduced during hydrogenolysis of the benzyl ester.

Scheme 19. Synthesis of *α*,*α*-difluoro esters.[a]

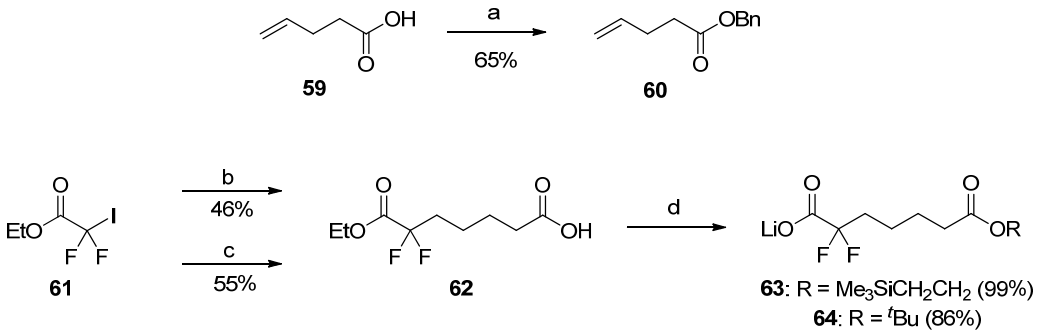

[a] Reagents: (a) BnOH, EDCI, DMAP, CH_2Cl_2; (b) (i) **60**, $NiCl_2{\cdot}6H_2O$, Zn, THF; (ii) H_2, Pd/C, EtOAc; (c) (i) **60**, $Na_2S_2O_4$, $NaHCO_3$, MeCN, H_2O; (ii) DBU, Et_2O; (iii) H_2, Pd/C, EtOAc; (d) (i) $Me_3SiCH_2CH_2OH$ or ^{t}BuOH, 2,4,6-$Cl_3C_6H_2COCl$, DMAP, THF; (ii) LiOH, H_2O, THF.

Trimethylsilylethyl protection of the carboxylic acid was efficient in the synthesis of **52** (Table 29), and building block **63** (Scheme 19) was prepared via a Yamaguchi esterification[203] followed by selective hydrolysis of the *α*,*α*-difluoro ethyl ester with LiOH in a cold mixture of H_2O and THF (Scheme 19). At this stage of the project the Yamaguchi esterification proved to be advantageous for acylations of calcitriol since better conversion and selectivity towards the 3-*O*-ester was observed compared to the previously applied carbodiimide chemistry. Exemplified by the coupling of **63** and calcitriol (Scheme 20)

which in 30 % yield gave the 1-*O*-ester and the 3-*O*-ester in a 1:10 ratio. Disappointingly treatment with TBAF in THF led to hydrolysis of the *α,α*-difluoro ester instead of the trimethylsilylethyl ester and alternatives like HF in MeCN at 20 °C did not give any conversion while heating to 60 °C caused complete decomposition of the calcitriol skeleton. Instead the *tert*-butyl protection group was examined, and building block **64** was made in the same way as **63** (Scheme 19). Acylation of calcitriol applying the Yamaguchi esterification gave almost exclusively the 3-*O*-ester (the ratio between the 3-*O*-ester and the 3-*O*-ester was >10:1), but selective deprotection of the *tert*-butyl ester was not possible (Scheme 20). TMSOTf and 2,6-lutidine in CH_2Cl_2 which was efficient in the synthesis of ATRA ester **19** (Scheme 7), did not give any conversion, whereas TFA or $ZnBr_2$[169] in CH_2Cl_2 led to decomposition of the calcitriol skeleton and that was also observed for SiO_2 in hot (90 °C) toluene.[204] Finally KO^{t}Bu in THF[205] resulted in release of calcitriol instead of the desired *tert*-butyl deprotection. These results were obtained in the end of the Ph.D. study and therefore there was not time for further synthetic studies towards the desired calcitriol ester **65** (Scheme 20). As presented in the next section synthesis of the corresponding phospholipid prodrug **69** was achieved.

Scheme 20. Synthetic studies towards calcitriol ester **65**.[a]

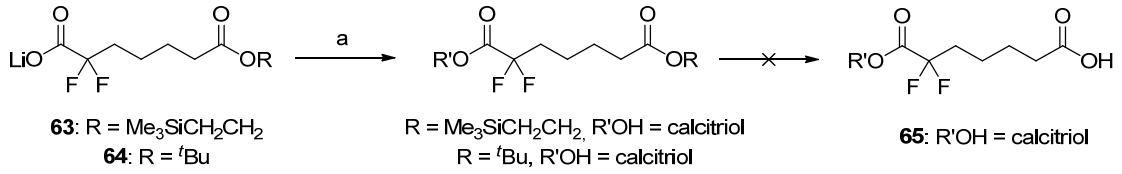

63: R = $Me_3SiCH_2CH_2$
64: R = ^{t}Bu

R = $Me_3SiCH_2CH_2$, R'OH = calcitriol
R = ^{t}Bu, R'OH = calcitriol

65: R'OH = calcitriol

[a] Reagents: (a) Calcitriol, 2,4,6-$Cl_3C_6H_2COCl$, DMAP, THF.

7.3 Synthesis of Phospholipid in Conjugate with *α,α*-Difluoro Calcitriol Ester

To evaluate the stability in aqueous environments of phospholipids having a *α,α*-difluoro ester moiety the simple model phospholipid **66** (Scheme 21) was synthesized prior to phospholipid prodrug **69** (Scheme 22). Phsopholipid **66** was accessed in 67 % yield from precursor **29**. The stability studies demonstrated that no significant degradation of phospholipid **66** occurs during subjection to HEPES buffer (*vide infra*) and the synthesis of **69** was initiated.

The *α,α*-difluoro benzyl ester **67** was synthesized in two steps from **64** (Scheme 22) and with no acid sensitive functionalities in the molecule, the *tert*-butyl deprotection was achieved using TFA in CH_2Cl_2. Attachment of **67** to the phospholipid precursor **29** and hydrogenolysis of the benzyl ester gave carboxylic acid **68** (Scheme 22). Then calcitriol was introduced via the Yamaguchi esterification and the final deprotections of the PG headgroup was achieved using the well known conditions without decomposition of the calcitriol skeleton, emphasizing the substrate scope and applicability of this synthetic route

to PG lipids. As a consequence of the Yamaguchi coupling phospholipid prodrug **69** was isolated as a 6:1 mixture of **3-*O*-69** and **1-*O*-69** confirming the selectivity trend towards the 3-*O*-ester of calcitriol (Scheme 22).

Scheme 21. Synthesis of phospholipid **66**.[a]

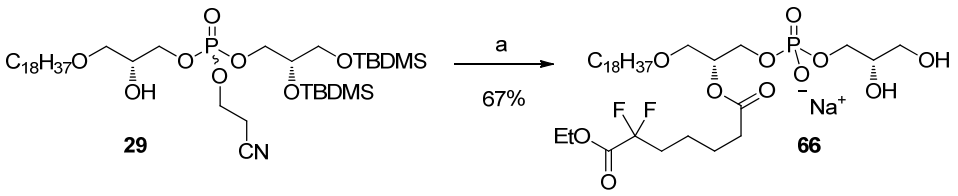

[a] Reagents: (a) (i) Carboxylic acid **62**, 2,4,6-$Cl_3C_6H_2COCl$, DMAP, THF; (ii) DBU, CH_2Cl_2; (iii) HF, H_2O, CH_2Cl_2, MeCN.

Scheme 22. Synthesis of phospholipid prodrug **69**.[a]

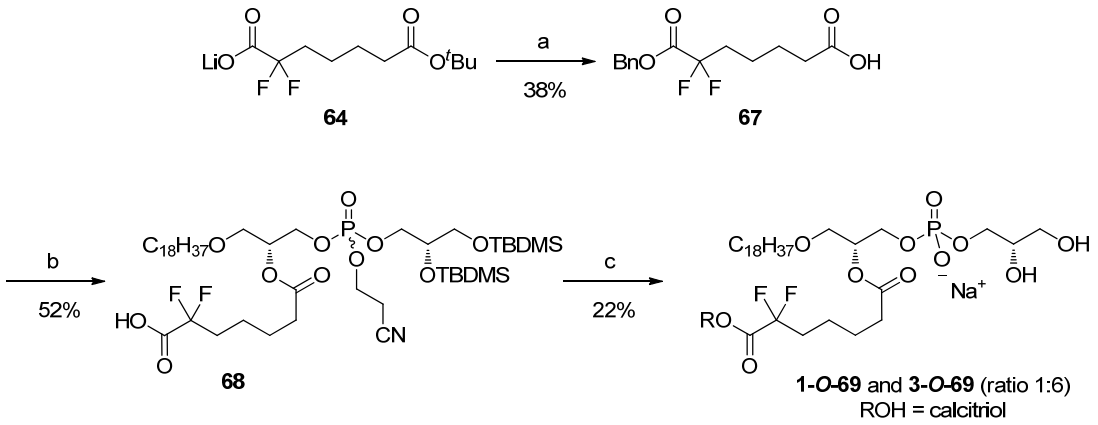

[a] Reagents: (a) (i) BnOH, 2,4,6-$Cl_3C_6H_2COCl$, DMAP, THF; (ii) TFA, triisopropylsilane, CH_2Cl_2; (b) (i) alcohol **29**, 2,4,6-$Cl_3C_6H_2COCl$, DMAP, THF; (ii) H_2, Pd/C, EtOAc, THF; (c) (i) calcitriol, 2,4,6-$Cl_3C_6H_2COCl$, DMAP, THF; (ii) DBU, CH_2Cl_2; (iii) HF, H_2O, CH_2Cl_2, MeCN.

7.4 Synthesis of Phospholipid Carbonate in Conjugate with Calcitriol Ester

The synthesis of phospholipid prodrug **53** was initiated from building block **5b**. TBDMS protection of the primary alcohol followed by removal of the PMP group with DDQ in moist CH_2Cl_2 gave the seconady alcohol **71** in 82% yield (Scheme 23).

Scheme 23. Synthesis of phospholipid prodrug **53**.[a]

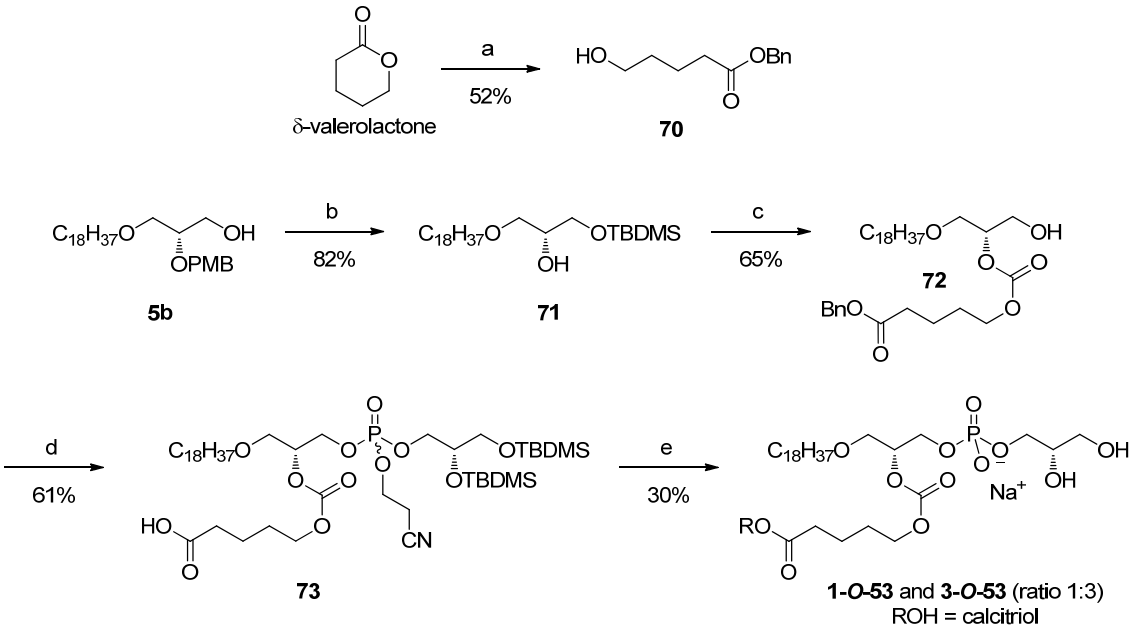

[a] Reagents: (a) (i) NaOH, H_2O; (ii) BnBr, Bu_4NBr, MeCN, acetone; (b) (i) TBDMSCl, imidazole, THF; (ii) DDQ, H_2O, CH_2Cl_2; (c) (i) triphosgene, pyridine, CH_2Cl_2; (ii) alcohol **70**, pyridine; (iii) NBS, DMSO, THF, H_2O; (d) (i) phosphoramidite **27**, tetrazole, CH_2Cl_2, MeCN (ii) ^{t}BuOOH; (iii) H_2, Pd/C, EtOAc, THF; (e) calcitriol, 2,4,6-$Cl_3C_6H_2COCl$, DMAP, THF; (ii) DBU, CH_2Cl_2; (iii) HF, H_2O, CH_2Cl_2, MeCN.

Alcohol **70** required for the carbonate formation was synthesized via a hydroxide mediate ring opening of δ-valerolactone after which the carboxylate was reacted with benzyl bromide (Scheme 23). Installation of the carbonate functionality was achieved via treatment of **71** with triphosgene after which the carbonochloridate was trapped *in situ* with alcohol **70**. The desired alcohol **72** was formed by removal of the TBDMS group applying the NBS mediated desilylation method and no migration of the carbonate moiety was observed. The phosphate headgroup was attached via coupling with phosphoramidite **27** using the established procedure described previously and hydrogenolysis of the benzyl ester gave carboxylic acid **73**. With **73** in hand the next step was incorporation of calcitriol and a significant improvement in conversion of **73** into the calcitriol ester was observed when Yamaguchi conditions were applied in contrast to application of carbodiimide based coupling reagents (e.g. EDCI), where the undesired urea formation was observed to a major extent as well. Determined by ^{1}H NMR the final phospholipid prodrug **53** was isolated as a 3:1 mixture of **3-*O*-53** and **1-*O*-53** (Scheme 23).

7.5 Biophysical Characterization and Enzyme Activity

Interesting upon hydration in HEPES buffer at 20 °C phospholipid **66** behaves in the same way as **41** and **42** (section 5.4) and a clear solution was obtained. DLS analysis showed that particles with an average diameter of 238 nm (PdI = 0.43) was formed and like observed for **41** and **42** extrusion through a 100 nm filter was not possible at 20 °C but at 65 °C it was accomplished and as determined by DLS a phospholipid solution with smaller particles (113 nm in average diameter) but a higher polydispersity (PdI = 0.62) was obtained. These observations contribute to the hypothesis that some kind of robust particles are formed spontaneously upon hydration for phospholipids like **41** and **42**. MALDI-TOF MS analysis of the formulated solution of **66** revealed that the *α*,*α*-difluoro ethyl ester in **66** was stable during the formulation and to incubation at 37 °C in HEPES buffer for 48 h (Figure 47). Subjection of snake (*Naja mossambica mossambica*) venom $sPLA_2$ to the phospholipid solution resulted in a complete digestion of **66** within 0.5 h and release of lysolipid **17** (Figure 47). The other release product carboxylic acid **62** was not visible in the MS spectra.

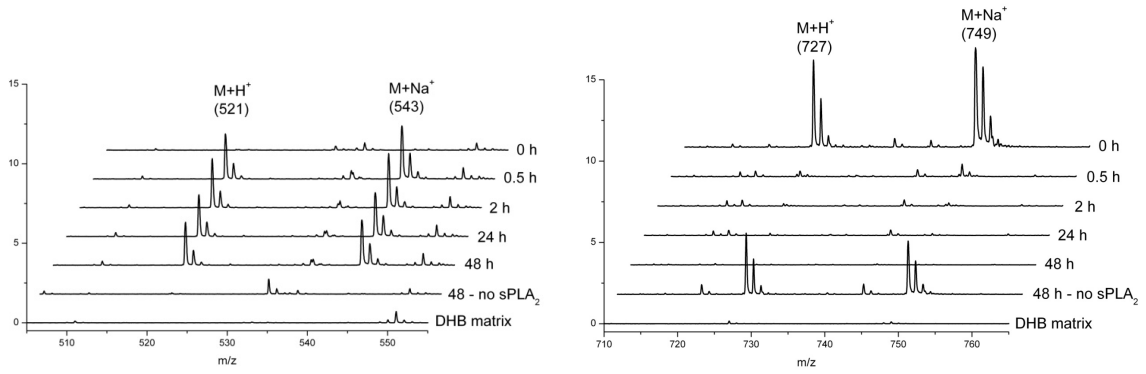

Figure 47. MALDI-TOF MS monitoring of snake (*Naja mossambica mossambica*) venom $sPLA_2$ activity on model phospholipid **66**. The spectra demonstrate that **66** (right) is degraded by the enzyme while no degradation occur in the absence of $sPLA_2$. Furthermore, the desired lysolipid **17** (left) is detected upon $sPLA_2$ addition.

The phospholipid prodrugs **53** and **69** were hydrated in HEPES buffer but extrusion through a 100 nm filter was not possible hence co-formulation with DSPC was investigated. By mixing **53** and **69** with DSPC in a 1:1 ratio extrusion at 65 °C through a 100 nm filter became possible and DLS analysis of the lipid solutions revealed that particles with an average diameter close to 100 nm was formed. DSPC was chosen for the co-formulation as it is an uncharged phospholipid and hence providing a reduction in the negative surface charge, which is necessary in order to avoid complement activation upon *in vivo* administration. However, the overall surface charge of the liposomes remain negative and therefore human $sPLA_2$ will have affinity towards the mixed liposomes of DSPC and **53** or **69**.[56,61]

The enzymatic activity was evaluated both with snake (*Naja mossambica mossambica*) venom and human $sPLA_2$ IIA. MALDI-TOF MS analysis of the phospholipid mixtures of **69** and DSPC showed that $sPLA_2$ from snake venom consume **69** within 0.5 h whereas DSPC was completely degraded within 24 h (Figure 48).[xi] Furthermore, the lysolipid from DSPC (lyso-SPC) was visible in the MS spectra (data not shown) whereas the lysolipid **17** only appear with a small signal and neither calcitriol nor the calcitriol ester **65** was detectable. But in the absence of $sPLA_2$ no degradation occurs meaning the disappearance of the signals for **69** ($M+2K^+$, 1151 m/z) in the MS spectra must be associated with the enzyme. The enzymatic study of human $sPLA_2$ activity showed that **69** is not consume to the same extent as with the enzyme from snake venom (Figure 48) and also the consumption of DSPC is significantly lower (data not shown). Detection of lyso-SPC (Figure 48) demonstrates that the two phospholipids **69** and DSPC mix in the formation of bilayers since pure DSPC is not degrade by human $sPLA_2$ IIA.

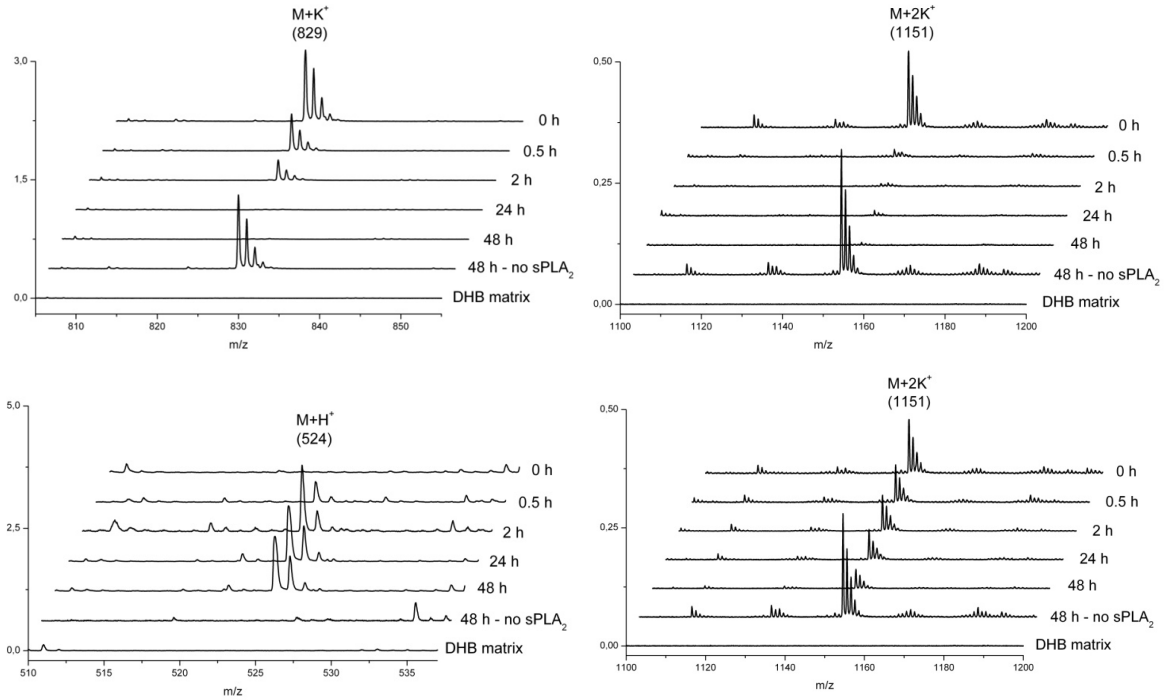

Figure 48. MALDI-TOF MS monitoring of snake (*Naja mossambica mossambica*) venom and human $sPLA_2$ activity on liposomes of phospholipid prodrug **69** and DSPC in a 1:1 mixture. The spectra demonstrate that the lipid mixture of **69** (top right) and DSPC (top left) are degraded by the enzyme from snake venom whereas less consumption of **69** (bottom right) is observed upon subjection to the human enzyme. Lyso-SPC (bottom left) was detected upon subjection to both enzymes, here illustrated for the study with human $sPLA_2$.

The enzymatic studies on carbonate phospholipid prodrug **53** showed that the amount of **53** decreased during the incubation with the enzyme from snake venom but within 48 h complete degradation was not obtained as evident from the MS spectra in Figure 49

[xi] Application of a CF_3COOK based DHB matrix gave a better signal to noisy ratio for **69** than the corresponding CF_3COONa based matrix hence **69** appears as the $2K^+$ adduct.

whereas full consumption of DSPC was seen after 0.5 h. As observed for **69**, lysolipid **17** was only detected to a very low extent by MALDI-TOF MS (data not shown) despite that **17** has been detected multiple times before (see e.g. Figure 47). Furthermore, calcitriol or the calcitriol ester **55** (compare with Figure 43) could not be detected hence it cannot be proven from the MALDI-TOF MS analysis that $sPLA_2$ trigger the release of calcitriol upon lactonization. But it can be concluded that addition of $sPLA_2$ provides a reduction in the prodrug level thus the absent of signals corresponding to calcitriol in the MS spectra can be due to a poor extraction of calcitriol into the organic layer during the MS sample preparation or due to limitations in the detection technique, which was supported by a low signal to noisy ratio when a pure sample of calcitriol was subjected to MALDI-TOF MS analysis (data not shown). Additional stearic acid released from DSPC also could not be detected by MALDI-TOF MS showing that this method has limitations in detection of degradation constituents from enzyme activity studies on phospholipids. When human $sPLA_2$ was used as the enzyme source results similar to those obtained with the enzyme from snake venom were obtained (Figure 49), however the hydrolysis of DSPC occurred significantly slower and less efficiently. Like for the mixture of **69** and DSPC, lyso-SPC was detected demonstrating that mixed bilayers of **53** and DSPC are formed.

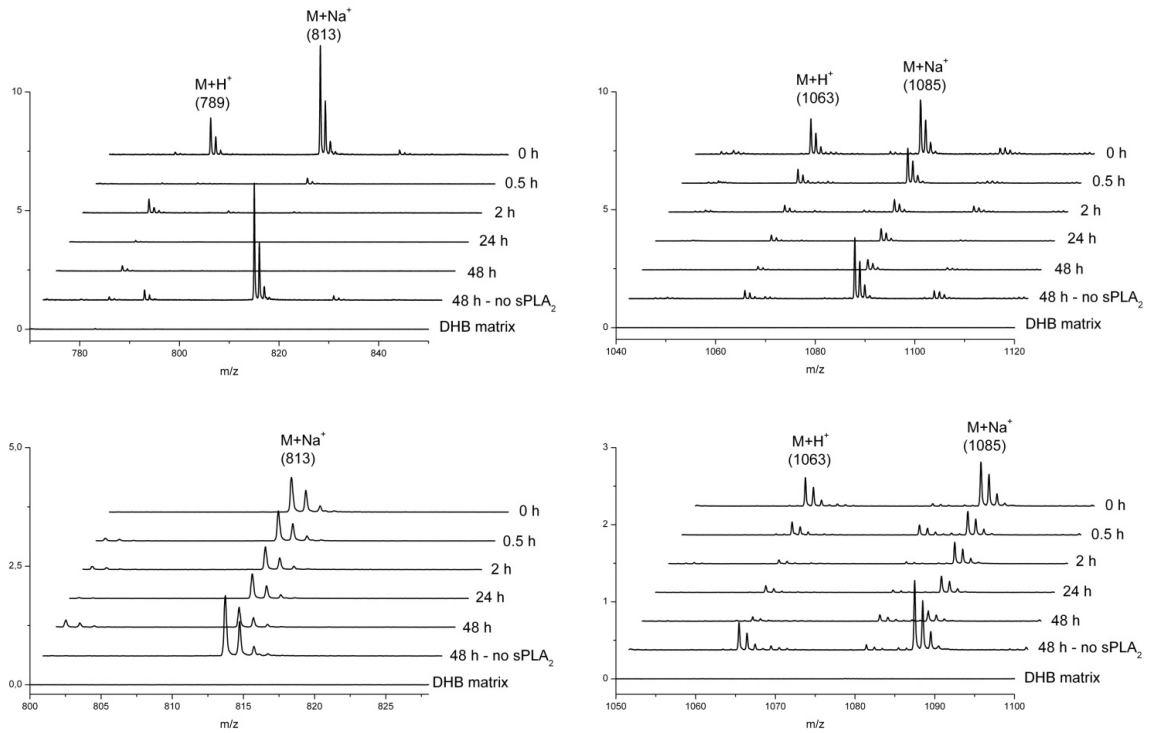

Figure 49. MALDI-TOF MS monitoring of snake (*Naja mossambica mossambica*) venom and human $sPLA_2$ activity on liposomes of phospholipid prodrug **53** and DSPC in a 1:1 mixture. The spectra demonstrate that **53** (top right) is partly degraded whereas DSPC (top left) is fully degraded by the enzyme from snake venom. Likewise partly degradation of **53** (bottom right) and DSPC (bottom left) is observed upon subjection to the human enzyme.

7.6 Biological Studies of the Calcitriol Esters

The cytotoxicity of calcitriol and the calcitriol esters **51** and **52** were evaluated in MCF-7 cancer cells and as evident from the dose-response curves in Figure 50 the esters **51** and **52** displayed potency similar to calcitriol itself. The IC_{50} values <100 nM emphasize the superior potency of calcitriol in contrast to the previously applied drugs, like ATRA. To investigate that the cytotoxicity origins from an activation of the VDR the ability to induce transcription of vitamin D-responsive genes was examined using the 24-hydroxylase luciferase reporter gene assay[206] in MCF-7 cells. It was established that the mixture of **1-*O*-51** and **3-*O*-51** along with the mixture of **1-*O*-52** and **3-*O*-52** had 10 times lower activity with respect to calcitriol (Figure 51) demonstrating that the affinity towards the VDR for **51** and **52** is low and the displayed cytotoxicity must therefore be induced via some unspecific pathways. Gratifying **3-*O*-56** and the mixture of **1-*O*-56** and **3-*O*-56** induce transcription to same extent as calcitriol (Figure 51), and taking into account that the hydroxyl group at C-1 is essential for binding to the VDR the results indicate that hydrolysis of the α,α-difluoroesters occur prior to VDR binding.

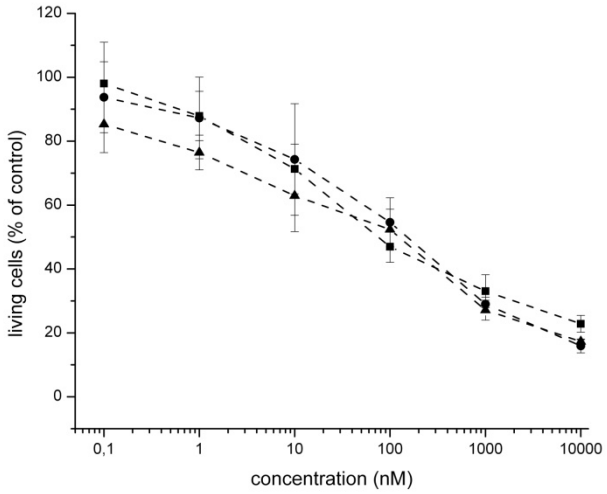

Figure 50. Dose-response curves for the treatment of MCF-7 cells with calcitriol (■), the 1:1 mixture of **1-*O*-51** and **3-*O*-51** (▲) and the 1:3 mixture of **1-*O*-52** and **3-*O*-52** (●). The cytotoxicity was measured using the MTT assay as cell viability 48 h after incubation with the indicated substances for 24 h and shown by mean + SD (n=3).

The biological evaluation of the calcitriol phospholipid prodrugs **53** and **69** was not completed at the end of the Ph.D. study hence these results cannot be presented. The biological evaluation will be important in order to clarify the somewhat inconclusive results obtained in the enzymatic studies, particular the 24-hydroxylase luciferase reporter gene assay will provide some valuable information concerning the degree of calcitriol release from the enzyme triggered breakdown of the calcitriol phospholipid prodrugs.

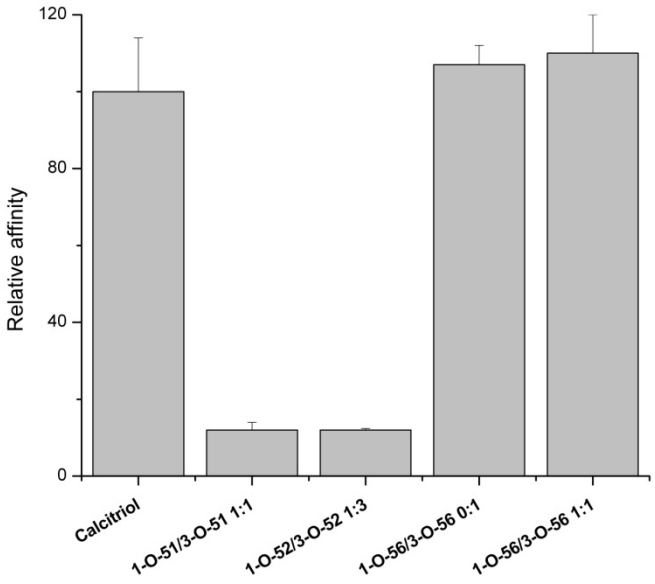

Figure 51: Relative affinity towards the VDR with respect to calcitriol measured by the 24-hydroxylase luciferase reporter gene assay in MCF-7 cells after incubation for 48 h with 100 nM of the investigated compound. Reported as mean ± SD (n = 3).

7.7 Conclusion

As calcitriol does not have a carboxylic acid moiety new ways for incorporation and drug release was necessary and two drug delivery strategies utilizing $sPLA_2$ triggering was investigated. Attachment of a dicarboxylic acid linker was studied and it was found that α,α-difluoroesters induce transcription of vitamin D-responsive genes to the same extent as calcitriol and hence synthesis of calcitriol ester **65** was initiated but not accomplished and further synthetic studies are necessary. However the corresponding phospholipid prodrug **69** was synthesized and when co-formulated with DSPC, particles with a diameter close to 100 nm were obtained after extrusion at 65 °C. Likewise a strategy relying on $sPLA_2$ mediated hydrolysis of a phospholipid carbonate conjugate was investigated and the desired phsopholipid prodrug **53** was synthesized and co-formulated with DSPC. The enzymatic studies with snake venom and human $sPLA_2$ showed that the signals in the MS spectra for the phospholipid prodrug decrease but the released products were not detectable in the MS spectra hence no clear conclusions can be made. The results from the biological studies will be highly interesting in order to evaluate the potential of the investigated strategies for liposomal delivery of calcitriol to tumors.

In addition, it was discovered that acylation of calcitriol using the Yamaguchi coupling displayed selectivity towards the 3-*O*-calcitriol esters and gave better conversion why this coupling procedure will be preferable to use in the future.

8. Conclusion: Liposomal Drug Delivery

During the work towards a new generation of liposomal drug delivery systems for anticancer agents several phospholipid prodrugs have been synthesized. The synthesized phospholipids had either a PC or PG headgroup and they were accessed via short synthetic routes in which derivatization into the various prodrugs was accomplished in the later part of the synthesis.

Various know anticancer drugs, like chlorambucil, ATRA and α-tocopheryl succinate have been examined for their ability to be incorporated into the investigated drug delivery system. Initial screening parameters were investigated including the ability of the phospholipid prodrugs to form liposomes, the ability of $sPLA_2$ to liberate the cytotoxic agents and finally the ability of the prodrugs to remain non-toxic in absence of the enzyme.

Gratisfyingly, the majority of the phospholipid prodrugs were able to form particles with a diameter close to 100 nm upon extrusion at 20 °C indicating formation of unilamellar vesicles. This demonstrate that incorporation of structures like chlorambucil or ATRA which contrast naturally occurring fatty acids do not hamper the ability of the synthetic phospholipids to form bilayers. However it was necessary to co-formulate the calcitriol prodrugs **53** and **69** with DSPC in order to achieve phospholipid suspensions suitable for extrusion.

The ability of $sPLA_2$ to mediate hydrolysis of the ester bond at the *sn*-2 position and release the incorporated anticancer drug was studied and in general it was observed that the enzyme is sensitive to substituents in close vicinity of the *sn*-2 position exemplified by ATRA prodrug **8**, which was not degraded. But for substrates with no branching in proximity to the *sn*-2 position, like the chlorambucil prodrugs, full hydrolysis was observed and when the enzyme activity was analyzed with MALDI-TOF MS, that was reliable and convenient to use, it was possible to verify that the desired constituents, the lysolipids and the anticancer drug were released.

The cytotoxicity studies revealed that the phospholipid prodrugs in the presence of $sPLA_2$ were able to induce cell death towards various cancer cell lines and IC_{50} values below 10 μM was obtained. In the absence of the enzyme the phospholipid prodrugs remain non-toxic and no significant cell death was observed, verifying that the displayed cytotoxicity arise from a $sPLA_2$ triggered breakdown of the prodrugs. The non-toxic behavior of the unactivated prodrugs is crucial for the drug delivery concept meaning that the prodrugs during the transport in the body will not harm healthy tissue. The prostaglandin prodrugs **45** and **46** was in this regard an outlier as significant cell death was displayed also in the absence of the enzyme in HT-29 cells.

The overall conclusion from the studies of the phospholipid prodrugs of chlorambucil, retinoids, prostaglandin and α-tocopheryl succintate (chapter 3–6) is that the cytotoxic effect from the incorporated anticancer drug is hard to separate from the cytotoxicity caused by the lysolipids. Hence the next obstacle to overcome in order to bring this drug delivery concept one step further is to indentify or develop a more potent lipophilic drug having a carboxylic acid moiety but no substituents α, β or γ to the carbonyl, because the results described in thesis clearly demonstrate that the concept has potential in future cancer therapy and many valuable experiences and results have been obtained throughout the described work.

Work towards incorporation of the more potent calcitriol was initiated however the biological studies remains to be done so the potential of this drug in the investigated drug delivery system cannot be evaluated at this stage.

9. Experimental: Liposomal Drug Delivery

9.1 General Experimental

Starting materials, reagents, and solvents were purchased from Sigma-Aldrich Chemical Co. and used without further purification. 15-deoxy-$\Delta^{12,14}$-Prostaglandin J_2 and calcitriol were purchased from Cayman Chemical, USA. The purified snake venom $sPLA_2$ from *Agkistrodon piscivorus piscivorus* was donated by Dr. R. L. Biltonen (University of Virginia) and $sPLA_2$ from *Naja mossambica mossambica* was purchased from Sigma-Aldrich Chemical Co. CH_2Cl_2 was dried over 4 Å molecular sieves and THF was dried over sodium/benzophenone and distilled before use. Evaporation of solvents was done under reduced pressure (*in vacuo*). Thin layer chromatography (TLC) was performed on Merck aluminum sheets precoated with silica gel 60 F254. Compounds were visualized by charring after dipping in a solution of 6.25 g of $(NH_4)_6Mo_7O_{24}$ and 1.5 g of $Ce(SO_4)_2$ in 250 mL of 10% aqueous H_2SO_4, in an ethanolic solution of phosphomolybdenic acid (48 g/L) or in a solution of 10 mL of *p*-anialdehyde, 10 ml of a concentrated aqueous solution of H_2SO_4 and 250 mL EtOH. Column chromatography was performed using Matrex 60 Å silica gel. The purity of the tested compounds was found to be >95% by HPLC. HPLC was performed on a Waters Alliance HPLC equipped with a diode array detector, using a LiChrospher Si 60 column and eluting with water/isopropanol/hexane mixtures.[207,208] NMR spectra were recorded using a Bruker AC 200 MHz spectrometer, a Varian Mercury 300 MHz spectrometer or a Varian Unity Inova 500 MHz spectrometer. Chemical shifts were measured in ppm and coupling constants in Hz, and the field is indicated in each case. IR analysis was carried out on a Bruker Alpha FT-IR spectrometer and optical rotations were measured with a Perkin-Elmer 341 polarimeter, units for $[\alpha]_{589}^{20}$ are 10^{-1} deg cm^2 g^{-1}. HRMS was recorded on an Ionspec Ultima Fourier transform mass spectrometer. Melting points were measured by a Buch & Holm melting point apparatus and given in degrees Celsius (°C) uncorrected. Elemental analyses were obtained from H. Kolbe, Mikroanalytisches Laboratorium, Mülheim/Ruhr, Germany.

9.2 Procedures for Biophysical and Biological Characterization

Liposome Preparation and Particle Size Determination

The phospholipid prodrugs were dissolved in $CHCl_3$ in a test tube and dried under vacuum for 15 h to form a thin film. The phospholipid prodrugs (2 mM) were solubilized by addition of aqueous buffer (0.15 M KCl, 30 µM $CaCl_2$, 10 µM EDTA, 10 mM HEPES, pH 7.5) and vortexed periodically over 1 h at 20 °C. Subsequently, the solutions were extruded through a 100 nm polycarbonate cutoff membrane (20-30 repetitions) using a Hamilton syringe extruder (Avanti Polar Lipids, Birmingham, AL). The particle size distribution of the formulated lipids was measured by DLS. The DLS measurements were obtained using a Zetasizer Nano Particle Analyzer (ZS ZEN3600, Malvern Instrument, Westborough, MA).

$sPLA_2$ Activity Measurements Monitored by MALDI-TOF MS and HPLC

The formulated phospholipid prodrugs (0.40 mL, 2 mM) were diluted in an aqueous buffer (2.1 mL, 0.15 M KCl, 30 μM CaCl2, 10 μM EDTA, 10 mM HEPES, pH 7.5) and the mixture was stirred at 37 °C in a test tube protected from light. The catalytic reaction was initiated by addition of snake (*Agkistrodon piscivorus piscivorus* (20 μL, 42 μM) or *Naja mossambica mossambica* (12 μL, 71 μM)) venom $sPLA_2$ or human $sPLA_2$ IIA (40 μL tear fluid). Sampling was done after 0, 2, 24 and 48 h by collecting 100 μL of the reaction mixture and rapidly mixing it with a solution of $CHCl_3$/MeOH/H_2O/AcOH 4:8:1:1 (0.5 mL) in order to stop the reaction. The mixture was washed with water (0.5 mL) and the organic phase (80 μL) was isolated by extraction and then concentrated *in vacuo*. For the MALDI-TOF MS analysis the extract was mixed with 9 μL of DHB matrix (0.5 M DHB, 2 mM CF_3COONa, 1 mg/mL DPPG in MeOH), and 0.5 μL of this mixture was used for the MS analysis. For HPLC 30-75 μL of the organic phase was injected on a 5 μm diol column and eluted with an isocratic eluent ($CHCl_3$/MeOH/H_2O 730:230:30 for **1a** and **1b**; $CHCl_3$/MeOH/25% aqueous NH_3 800:195:5 for **2a** and **2b**). An evaporative light scattering detector was used for detection. Tear fluid was used as the source for human $sPLA_2$ IIA. Tear fluid was collected from healthy volunteers exposed to tiger balm fumes. Tear fluid has a high concentration of $sPLA_2$ IIA and is the only prevalent $sPLA_2$ species found in tears. The $sPLA_2$ IIA content in tears in healthy subjects (54.5 μg/ml) is one of the highest amounts of $sPLA_2$ IIA content reported in human secretions.[209,210,211]

Alkylating Assay[136,137,138]

The formulated chlorambucil phospholipid prodrugs (0.40 mL, 2 mM) were diluted in an aqueous buffer (2.1 mL, 0.15 M KCl, 30 μM $CaCl_2$, 10 μM EDTA, 10 μM HEPES, pH = 7.5) and 4-nitrobenzyl pyridine (63 mg, 0.29 mmol) was added and the mixture was stirred at 37 °C. When $sPLA_2$ was used to degrade the liposomes, the catalytic reaction was initiated by addition of snake (*Agkistrodon piscivorus piscivorus*) venom $sPLA_2$ (20 μL, 42 μM). After 1.5 h incubation 2-amino-1-propanol in *tert*-butyl alcohol (25% v/v, 3.0 mL) was added and the colaration of the reaction mixture was measured using a UV-visible spectrophometer (PerkinElmer, Lambda 25 UV/Vis Spectrometer) at 450–700 nm with a maximum absorption at 560 nm for the colored pigment. Measurements of pure chlorambucil samples in HEPES buffer with and without 4-nitrobenzyl pyridine, of HEPES buffer with and without $sPLA_2$ and of pure 4-nitrobenzyl pyridine in HEPES buffer were obtained as controls (see Pedersen *et al*.[135]).

Cytotoxicity

Colon cancer HT-29 and ovarian cancer ES-2 cells were cultured in McCoy's 5A medium in the presence of 10% fetal calf serum and 1% Pen-Strep (InVitrogen). Breast cancer MT-3 and colon cancer Colo205 cells were cultured in RPMI 1640 supplemented with 10 % fetal calf serum and 1% Pen-Strep in a humidified atmosphere containing 5 % CO_2. Colo205 cells secrete $sPLA_2$-IIA, however as the cytotoxicity assay was made with low

cell density and for a short incubation period, inadequate concentrations were reached in the medium, and therefore a conditioned medium was used. The conditioned medium was made as follows: Colo205 cells were grown to confluency for 72h, at which point the cells were pelleted and the medium, which contained approximately 100 ng/ml, was collected and used for the assay. Cells were plated in 96-well plates at a density of 1×10^4 cells per well for HT-29 and 2×10^4 cells per well for Colo205 cells, 24 h prior to addition of the tested compound. Chlorambucil, ATRA, ATRA ester **19**, **12**, **20**, 15-deoxy-$\Delta^{12,14}$-PGJ_2 and α-tocopheryl succinate were solubilized in DMSO and water (final DMSO concentration ≤ 0.5%). Liposomes were diluted in PBS, and initial phospholipid concentrations in the liposome solutions were determined by phosphorus analysis.[212] After 24 h of incubation, the substances were removed and the cells were washed and incubated in complete medium for another 48 h. Cytotoxic activity was assessed using a standard 3-(4,5-dimethylthiazolyl)-2,5-diphenyltetrazolium bromide (MTT) assay (Cell Proliferation Kit I, Roche, Germany).[213] Cell viability is expressed as percentage reduction of incorporated MTT.

Molecular Dynamics Simulations

The crystal structures of bee-venom (*Apis Mellifera*) phospholipase A_2 complexed with the transition-state analog, 1-*O*-Octyl-2-heptylphosphonyl-*sn*-glycero-3-phosphoethanolamine (diC8(2Ph)PE),[51] resolved to 2.0 Å and human phospholipase A_2 IIA complexed with 6-phenyl-4-(*R*)-(7-phenyl-heptanoylamino)-hexanoic acid[214] resolved to 2.1 Å were obtained from the Protein Data Bank[215] (entry codes: 1poc and 1kqu, respectively). The initial modeling step involved placing diC8(2Ph)PE into the binding cleft of human phospholipase A_2 IIA, as described previously.[131] A previously assembled $sPLA_2$-substrate complex[131] was used as the template to place phospholipid prodrugs into the active site. The optimized phospholipid prodrugs were manually overlapped with the pre-existing substrate, which was subsequently deleted. NAMD software[216] with the Charmm27 all-atom parameter set and TIP3 water model was used for all simulations.[217] The phospholipid prodrugs were first energy-minimized for 1000 steps before using them in simulations. Missing force field parameters for the prodrug molecules were taken from similar atom types in the CHARMM27 force field. The $sPLA_2$–phospholipid complexes were solvated using the program SOLVATE.[218] Eighteen water molecules were randomly replaced with chloride ions to neutralize the systems. Ultimately, the system contained ~4900 water molecules in a simulation cell of dimensions 52.7 x 51.7 x 67.3 $Å^3$. An initial energy minimization of the complex was carried out for 1000 steps, and the system was further minimized for 100, 200, 300, 400 and 500 steps to generate different starting structures. Periodic boundary conditions were applied in x,y, and z directions. Initial MD simulations were conducted for ~100 ps in which each system was slowly heated to 300 K. Simulations were carried out for 13 ns in the NPT ensemble; i.e. at constant number of atoms (*N*), pressure (*P*) and temperature (*T*). A time step of 1 fs and an isotropic pressure of 1 atm using the Langevin piston method[219] were employed. Electrostatic forces were

calculated using the particle mesh Ewald method with a uniform grid spacing of ~1 Å.[220] A 12 Å cut-off was used for terminating the van der Waals interactions in combination with a switching function starting at 10 Å. Analysis of the trajectories were performed using the Visualization Molecular Dynamics (VMD) software suite.[221]

9.3 Experimental Data for Compounds

4-Methoxybenzyl trichloroacetimidate (PMBTCA)[222]

NaH (60% in mineral oil, 81 mg, 2.03 mmol) was washed with heptane (2 × 3 mL) and THF (11 mL) was added followed by dropwise addition of 4-methoxybenzyl alcohol (2.52 mL, 20.3 mmol). The reaction mixture was stirred at 20 °C for 30 min and then cooled to 0 °C. Cl_3CCN (2.2 mL, 22.3 mmol) was added dropwise and the reaction mixture was stirred at 0 °C for 1 h and then at 20 °C for 45 min. The reaction mixture was concentrated *in vacuo* yielding an orange oil which was treated with a mixture of pentane and MeOH (12 mL, pentane/MeOH 275:1) and stirred for 30 min. Then the mixture was filtered through a pad of celite and the filtrate was evaporated *in vacuo* to afford 5.72 g (99%) of PMBTCA as a yellow oil. ^{1}H NMR (300 MHz, $CDCl_3$): δ 8.37 (s, 1H), 7.39 (d, *J* = 8.8 Hz, 2H), 6.92 (d, *J* = 8.8 Hz, 2H), 5.29 (s, 2H), 3.83 (s, 3H). ^{13}C NMR (75 MHz, $CDCl_3$): δ 162.7, 159.8, 129.8 (2C), 127.6, 114.0 (2C), 91.6, 70.8, 55.4.

1-*O*-Hexadecyl-2-(4-(4-(bis-(2-chloroethyl)-amino)-phenyl)-butanoyl)-*sn*-glycero-3-phosphocholine (1a)

Compound **6a** (67 mg, 0.14 mmol) was dissolved in 1,2-dichloroethane (3.5 mL) and the mixture was heated to reflux. DMAP (10 mg, 0.082 mmol), chlorambucil (64 mg, 0.21 mmol) and DCC (1 M in CH_2Cl_2, 0.2 mL, 0.2 mmol) were added and after 5 h and 19 h additional portions of chlorambucil (64 mg, 0.21 mmol) and DCC (1 M in CH_2Cl_2, 0.2 mL, 0.2 mmol) were added. After 27 h the mixture was concentrated *in vacuo* and purified by column chromatography (CH_2Cl_2/MeOH 4:1 then CH_2Cl_2/MeOH/H_2O 30:20:1) to give 80 mg (75%) of **1a** as a colorless amorphous solid. R_f = 0.18 (CH_2Cl_2/MeOH/H_2O 30:20:1). ^{1}H NMR (500 MHz, $CDCl_3$/CD_3OD 4:1): δ 7.08 (d, *J* = 8.6 Hz, 2H), 6.65 (d, *J* = 8.6 Hz, 2H), 5.16 (p, *J* = 5.9 Hz, 1H), 4.22 (s, 2H), 4.03–3.99 (m, 2H), 3.72 (t, *J* = 7.1 Hz, 4H), 3.64 (t, *J* = 7.1 Hz, 4H), 3.63–3.59 (m, 2H), 3.56 (s, 2H), 3.49–3.39 (m, 2H), 3.19 (s, 9H), 2.56 (t, *J* = 7.6 Hz, 2H), 2.36 (t, *J* = 7.6 Hz, 2H), 1.90 (p, *J* = 7.6 Hz, 2H), 1.54 (p, *J* = 6.8 Hz, 2H), 1.32-1.26 (m, 26H), 0.88 (t, *J* = 6.8 Hz, 3H). ^{13}C NMR (75 MHz, $CDCl_3$/CD_3OD 4:1) δ 174.1, 144.8, 130.8, 130.0 (2C), 112.6 (2C), 72.2 (d, *J* = 8.2 Hz), 72.1, 69.6, 66.8, 64.4 (d, *J* = 5.2 Hz), 59.2 (d, *J* = 5.2 Hz), 54.5, 54.4, 54.4, 53.9 (2C), 40.9 (2C), 34.2, 34.0, 32.3, 30.1 (8C), 29.9, 29.9, 29.7, 27.2, 26.4, 23.0, 14.3. IR (neat) 2923, 2852, 2366, 1734, 1091 cm^{-1} HRMS (ESI+) $C_{38}H_{69}Cl_2N_2O_7P$, m/z [M+H$^+$] 767.4298, found 767.4312.

1-*O*-Octadecyl-2-(4-(4-(bis-(2-chloroethyl)-amino)-phenyl)-butanoyl)-*sn*-glycero-3-phosphocholine (1b)

Compound **6b** (67 mg, 0.13 mmol) was dissolved in $CHCl_3$ (4 mL) and the mixture was heated to reflux. DMAP (10 mg, 0.082 mmol), chlorambucil (40 mg, 0.13 mmol) and DCC (1 M in CH_2Cl_2, 130 µL, 0.13 mmol) were added and after 3, 6.5, 23.5, 26.5 and 31 h additional portions of chlorambucil (40 mg, 0.13 mmol) and DCC (1 M in CH_2Cl_2, 130 µL, 0.13 mmol) were added. After 48 h the mixture was concentrated *in vacuo* and purified by column chromatography (CH_2Cl_2/MeOH 4:1 then CH_2Cl_2/MeOH/H_2O 30:20:1) to give 79 mg (76%) of **1b** as a colorless amorphous solid. R_f = 0.15 (CH_2Cl_2/MeOH/H_2O 30:20:1). ^{1}H NMR (500 MHz, $CDCl_3$/CD_3OD 4:1) δ 7.07 (d, *J* = 8.5 Hz, 2H), 6.65 (d, *J* = 8.5 Hz, 2H), 5.16 (p, *J* = 5.8 Hz, 1H), 4.22 (s, 2H), 4.06–3.94 (m, 2H), 3.72 (t, *J* = 6.8 Hz, 4H), 3.64 (t, *J* = 6.8 Hz, 4H), 3.63–3.59 (m, 2H), 3.56 (s, 2H), 3.48–3.40 (m, 2H), 3.20 (s, 9H), 2.56 (t, *J* = 7.5 Hz, 2H), 2.36 (t, *J* = 7.5 Hz, 2H), 1.90 (p, *J* = 7.5 Hz, 2H), 1.54 (m, 2H), 1.32–1.26 (m, 30H), 0.88 (t, *J* = 6.9 Hz, 3H). ^{13}C NMR (75 MHz, $CDCl_3$/CD_3OD 4:1) δ 174.1, 144.9, 130.8, 130.1 (2C), 112.6 (2C), 72.3 (d, *J* = 8.6 Hz), 72.1, 69.6, 66.9, 64.5 (d, *J* = 5.2 Hz), 59.4 (d, *J* = 5.2 Hz), 54.5, 54.4, 54.4, 53.9 (2C), 40.9 (2C), 34.3, 34.0, 32.3, 30.1 (10C), 29.9, 29.9, 29.8, 27.3, 26.4, 23.1, 14.3. IR (neat) 2923, 2852, 2366, 1734, 1518, 1247, 1088, 750 cm^{-1}. HRMS (ESI+) $C_{40}H_{73}Cl_2N_2O_7P$, m/z [M+Na$^+$] 817.4425, found 817.4430.

1-*O*-Hexadecyl-3-(*p*-toluenesulfonyl)-*sn*-glycerol (4a)[68]

(*R*)-Glycidyl tosylate (2.0 g, 8.76 mmol) and hexadecanol (3.0 g, 12.37 mmol) were dissolved in CH_2Cl_2 (40 mL) and $BF_3{\cdot}OEt_2$ (0.5 mL) was added. The solution was stirred for 24 h at 20 °C and concentrated *in vacuo*. A white solid was formed and recrystallized from hexane (35 mL) to give 2.75 g of **4a**. The filtrate, which contain some product, was concentrated *in vacuo* and purified by column chromatography (CH_2Cl_2/Et_2O 10:1) to give 0.98 g of **4a** (89% overall). R_f = 0.58 (CH_2Cl_2/Et_2O 10:1); mp = 53–55 °C (lit.[223] 53–54 °C). ^{1}H NMR (300 MHz, $CDCl_3$): δ 7.81 (d, *J* = 8.4 Hz, 2H), 7.36 (d, *J* = 8.4 Hz, 2H), 4.12–3.93 (m, 3H), 3.48–3.27 (m, 4H), 2.46 (s, 3H), 2.18 (s, 1H), 1.51 (t, *J* = 6.4 Hz, 2H), 1.32–1.26 (m, 26H), 0.88 (t, *J* = 6.7 Hz, 3H).

1-*O*-Octadecyl-3-(*p*-toluenesulfonyl)-*sn*-glycerol (4b)[68]

Performed as for **4a** using (*R*)-Glycidyl tosylate (5.25 g, 23.0 mmol) and octadecanol (8.7 g, 32.2 mmol) to afford 11.2 g (97 %) of **4b** as white crystals. R_f = 0.65 (CH_2Cl_2/Et_2O 10:1); mp = 66–68 °C (lit.[224] 67–68 °C). ^{1}H NMR (300 MHz, $CDCl_3$): δ 7.80 (d, *J* = 8.1 Hz, 2H), 7.38 (d, *J* = 8.1 Hz, 2H), 4.05-3.95 (m, 3H), 3.45-3.35 (m, 4H), 2.43 (s, 3H), 2.10 (s, 1H), 1.51 (m, 2H), 1.35-1.23 (m, 30H), 0.90 (t, *J* = 6.7 Hz, 3H).

1-*O*-Hexadecyl-2-*O*-(4-methoxybenzyl)-*sn*-glycerol (5a)

Alcohol **4a** (1.19 g, 2.53 mmol) and PMBTCA (1.10 g, 3.89 mmol) were dissolved in toluene (21 mL) and La(OTf)$_3$ (70 mg, 0.12 mmol) was added. The reaction mixture was

stirred at 20 °C for 2.5 h, then concentrated *in vacuo* to give a white solid that was dissolved in DMSO (20 mL) and DMF (5 mL). CsOAc (1.49 g, 7.38 mmol) was added and the mixture was heated to 60 °C and stirred for 14 h, after which the reaction mixture was washed with H_2O (30 mL) and the organic layer was isolated via extraction with Et_2O (3x50 mL). The combined organic phases were dried over $MgSO_4$ and filtration followed by concentration *in vacuo* gave a solid that was dissolved in MeOH (40 mL). NaOMe (140 mg, 2.59 mmol) was added and the mixture was heated to 40 °C and stirred for 16 h. The mixture was neutralized by addition of concentrated aqueous solution of HCl, washed with H_2O (20 mL) and the organic layer was isolated via extraction with CH_2Cl_2 (3x20 mL). The combined organic phases were dried over $MgSO_4$ and after concentration *in vacuo* the residue was purified by column chromatography (heptane/EtOAc 1:1) yielding 772 mg (70%) of **5a** as a greasy solid. R_f = 0.46 (heptane/EtOAc 1:1). ^{1}H NMR (300 MHz, $CDCl_3$): δ 7.29 (d, *J* = 8.6 Hz, 2H), 6.89 (d, *J* = 8.6 Hz, 2H), 4.66 (d, *J* = 11.4 Hz, 1H), 4.56 (d, *J* = 11.4 Hz, 1H), 3.81 (s, 3H), 3.78–3.50 (m, 5H), 3.44 (t, *J* = 6.7 Hz, 2H), 1.61–1.53 (m, 2H), 1.26 (br.s. 26H), 0.88 (t, *J* = 6.7 Hz, 3H). ^{13}C NMR (75 MHz, $CDCl_3$): δ 159.4, 130.5, 129.6 (2C), 114.0 (2C), 77.5, 72.0, 71.9, 71.3, 63.2, 55.4, 32.1, 29.8 (9C), 29.6, 29.5, 26.3, 22.9, 14.3. Anal. Calcd. $C_{27}H_{48}O_4$: C 74.26, H 11.08; Found: C 74.26, H 11.03. IR (neat) 3374, 2923, 1695 1613, 1513, 1466, 1248, 1110, 824 cm^{-1}.

1-*O*-Hexadecyl-2-*O*-(4-methoxybenzyl)-*sn*-glycerol (5a) using $NaNO_2$

Alcohol **4a** (842 mg, 1.79 mmol) and PMBTCA (859 mg, 3.04 mmol) were dissolved in toluene (15 mL) and $La(OTf)_3$ (52 mg, 0.09 mmol) was added. The reaction mixture was stirred at 20 °C for 2.5 h and concentration *in vacuo* gave a white solid, that along with $NaNO_2$ (3.69 g, 53.6 mmol) were dissolved in degassed DMSO (35 mL). The mixture was stirred at 40 °C for 17 h, then a saturated aqueous solution of $NaHCO_3$ (10 mL) was added and the mixture was stirred for 20 min further after which the organic layer was isolated via extraction with Et_2O (3×100 mL). The combined organic phases were dried over $MgSO_4$, filtered, concentrated *in vacuo* and purified by column chromatography (heptane/EtOAc 1:1) to give 731 mg (94%) of **5a** as a greasy solid.

1-*O*-Octadecyl-2-*O*-(4-methoxybenzyl)-*sn*-glycerol (5b)

Performed as for **5a**, starting from alcohol **4b** (2.211 g, 4.433 mmol) and affording 1.60 g (78%) of **5b** as a greasy solid. ^{1}H NMR (300 MHz, $CDCl_3$): δ 7.29 (d, *J* = 8.6Hz, 2H), 6.89 (d, *J* = 8.6Hz, 2H), 4.66 (d, *J* = 11.4Hz, 1H), 4.56 (d, *J* = 11.4 Hz, 1H), 3.81 (s, 3H), 3.78–3.50 (m, 5H), 3.44 (t, *J* = 6.7 Hz, 2H), 1.62–1.53 (m, 2H), 1.26 (br.s. 30H), 0.88 (t, *J* = 6.7 Hz, 3H). ^{13}C NMR (75 MHz, $CDCl_3$): δ 159.4, 130.5, 129.6 (2C), 114.0 (2C), 77.5, 72.0, 71.9, 71.3, 63.2, 55.4, 32.1, 29.8 (11C), 29.6, 29.5, 26.3, 22.8, 14.3. Anal. Calcd. $C_{29}H_{52}O_4$: C 74.95, H 11.28; Found: C 75.08, H 11.24. IR (neat) 3524, 2916, 1709 1612, 1511, 1472, 1253, 1108, 1032, 824 cm^{-1}.

1-*O*-Octadecyl-2-*O*-(4-methoxybenzyl)-*sn*-glycerol using $NaNO_2$ (5b)
Performed as for **5a**, starting from alcohol **4a** (440 mg, 0.882 mmol) and affording 291 mg (71%) of **5b** as a greasy solid.

1-*O*-Hexadecyl-2-lyso-*sn*-glycero-3-phosphocholine (6a)
To a solution of $POCl_3$ (28 µL, 0.30 mmol) in CH_2Cl_2 (1.2 mL) at 0 °C was added a solution of **5a** (104 mg, 0.24 mmol) along with Et_3N (44 µL, 0.31 mmol) in CH_2Cl_2 (1.7 mL) dropwise over 20 min. The reaction was stirred 30 min at 20 °C, after which pyridine (0.15 mL, 1.9 mmol) and choline tosylate (132 mg, 0.48 mmol) were added. The reaction was stirred for 19 h at 20 °C, then H_2O (0.15 mL) was added and stirring was continued for 40 min. Continuous concentration with EtOH/toluene 1:1 (6 mL) gave the crude product as a white foam. The residue was dissolved in THF/H_2O 9:1 and slowly passed through an MB-3 column. The solvent was removed by continuous concentration with EtOH/toluene 1:1 (6 mL). The crude product was purified by column chromatography (CH_2Cl_2/MeOH then CH_2Cl_2/MeOH/H_2O 65:25:4) giving 100 mg that was dissolved in CH_2Cl_2/H_2O 18:1 (10 mL) along with DDQ (76 mg, 0.34 mmol). The mixture was stirred for 2 h after which it was concentrated *in vacuo* and the residue was purified by column chromatography (MeOH until the eluent was colorless, then CH_2Cl_2/MeOH/H_2O 65:25:4) to give 80 mg (69%) of **6a** as a colorless amorphous solid. R_f = 0.10 (CH_2Cl_2/MeOH/H_2O 65:25:4). ^{1}H NMR (500 MHz, $CDCl_3$/CD_3OD 4:1): δ 4.26 (s, 2H), 3.99–3.82 (m, 3H), 3.61–3.60 (m, 2H), 3.48–3.44 (m, 4H), 3.21 (s, 9H), 1.59–1.54 (m, 2H), 1.32–1.26 (m, 26H), 0.88 (t, *J* = 6.9 Hz, 3H).[68]

1-*O*-Octadecyl-2-lyso-*sn*-glycero-3-phosphocholine (6b)
Performed as for **6a** starting from **5b** (127 mg, 0.27 mmol) affording 70 mg (36%) of **6b** as a colorless amorphous solid. R_f = 0.10 (CH_2Cl_2/MeOH/H_2O 30:10:2). ^{1}H NMR (300 MHz, $CDCl_3$/CD_3OD 4:1): δ 4.26 (s, 2H), 3.99–3.82 (m, 3H), 3.61–3.60 (m, 2H), 3.48–3.44 (m, 4H), 3.21 (s, 9H), 1.59–1.54 (m, 2H), 1.32–1.26 (m, 30H), 0.88 (t, *J* = 6.9 Hz, 3H).[68]

1-*O*-Hexadecyl-2-all-*trans*-retinoyl-*sn*-glycero-3-phosphocholine (7)
To a solution of $POCl_3$ (32 µL, 0.35 mmol) in CH_2Cl_2 (1.5 mL) at 0 °C was added a solution of alcohol **11** (166 mg, 0.28 mmol) along with Et_3N (50 µL, 0.36 mmol) in CH_2Cl_2 (4 mL) dropwise over 15 min. The reaction mixture was stirred at 20 °C for 30 min, after which pyridine (180 µL, 2.23 mmol) and choline tosylate (153 mg, 0.55 mmol) were added. The reaction mixture was stirred at 20 °C for 16.5 h, then H_2O (0.2 mL) was added and stirring was continued for 40 min. Continuous concentration with EtOH/toluene 1:1 (20 mL) gave a yellow residue which was redissolved in THF/H_2O 9:1 and slowly passed through a MB-3 column. The solvent was removed by continuous concentration with EtOH/toluene 1:1 (20 mL). The crude product was purified by column chromatography (CH_2Cl_2/MeOH 4:1 then CH_2Cl_2/MeOH/H_2O 15:10:1) giving 84 mg (40%) of **7** as a yellow oil. R_f = 0.30 (CH_2Cl_2/MeOH/H_2O 15:10:1). ^{1}H NMR (500 MHz,

$CDCl_3/CD_3OD$ 4:1): δ 7.03 (dd, *J* = 15.0, 11.5 Hz, 1H), 6.30 (d, *J* = 16.0 Hz, 1H), 6.29 (d, *J* = 15.0 Hz, 1H), 6.15 (d, *J* = 16.0 Hz, 1H), 6.15 (d, *J* = 11.5 Hz, 1H), 5.79 (s, 1H), 5.20–5.16 (m, 1H), 4.23 (br.s, 2H), 4.09–4.02 (m, 2H), 3.67–3.62 (m, 2H), 3.58 (br.s, 2H), 3.49–3.42 (m, 2H), 3.20 (s, 9H), 2.34 (s, 3H), 2.05–2.00 (m, 5H), 1.72 (s, 3H), 1.66–1.60 (m, 2H), 1.57–1.51 (m, 2H), 1.49–1.47 (m, 2H) 1.26 (s, 26H), 1.03 (s, 6H), 0.88 (t, *J* = 6.9 Hz, 3H). ^{13}C NMR (75 MHz, $CDCl_3/CD_3OD$ 4:1): δ 167.2, 154.2, 140.5, 138.0, 137.6, 135.1, 132.0, 130.4, 129.7, 129.3, 118.3, 72.1, 71.6 (d, *J* = 8.6 Hz), 69.6, 66.9, 64.6 (d, *J* = 5.3 Hz), 59.2 (d, *J* = 5.0 Hz), 54.5, 54.5, 54.4, 39.9, 34.6, 33.4, 32.3, 30.0 (9C), 29.8, 29.7, 29.2 (2C), 26.3, 23.0, 21.9, 19.5, 14.3, 14.1, 13.1. $[\alpha]_{589}^{20}$ = –7.7 (*c* = 0.64, $CHCl_3$). IR (neat) 2923, 2853, 2490, 1706, 1458, 1238, 1152, 1085, 967 cm^{-1}. HRMS (ESI+) $C_{44}H_{78}NO_7P$, m/z [M+Na^+] 786.5408, found 786.5422.

3-*O*-Hexadecyl-*sn*-glycerol (9)

(*S*)-Glycidyl tosylate (2.0 g, 8.76 mmol) and hexadecanol (2.97 g, 12.3 mmol) were dissolved in CH_2Cl_2 (40 mL) and $BF_3{\cdot}OEt_2$ (0.5 mL) was added. The reaction mixture was stirred at 20 °C for 19 h and then concentrated *in vacuo* yielding a white solid that was dissolved in DMSO (73 mL) and DMF (18 mL). CsOAc (5.89 g, 30.7 mmol) was added and the reaction mixture was heated to 60 °C and stirred for 14 h, after which the mixture was washed with H_2O (50 mL) and the organic layer was isolated via extraction with Et_2O (3x200 mL). The combined organic phases were dried over Na_2SO_4 and filtration followed by concentration *in vacuo* gave a white solid that was dissolved in MeOH (90 mL) along with NaOMe (482 mg, 8.76 mmol). The reaction mixture was heated to 40 °C and stirred for 12 h, then the mixture was neutralized by addition of concentrated aqueous solution of HCl and concentrated *in vacuo*. The residue was purified by column chromatography (heptane/EtOAc 1:1) yielding 1.80 g (65%) of **9** as white crystals. R_f = 0.18 (heptane/EtOAc 1:1). mp = 61–63°C (hexane) (lit.[225] 63–64 °C). ^{1}H NMR (300 MHz, $CDCl_3$):[226] δ 3.91–3.90 (m, 1H), 3.80–3.63 (m, 2H), 3.53 (t, *J* = 4.8 Hz, 2H), 3.50–3.45 (m, 2H), 2.61 (d, *J* = 5.2 Hz, 1H, *OH*), 2.17 (dd, *J* = 7.0, 5.2 Hz, 1H, *OH*), 1.60–1.56 (m, 2H), 1.26 (s, 26H), 0.89 (t, *J* = 6.7 Hz, 3H). ^{13}C NMR (75 MHz, $CDCl_3$): δ 72.7, 72.0, 70.5, 64.5, 32.1, 29.8 (9C), 29.6, 29.5, 26.2, 22.9, 14.3.

1-*O*-*tert*-Butyldimethylsilyl-3-*O*-hexadecyl-*sn*-glycerol (10)

Alcohol **9** (187 mg, 0.59 mmol), Et_3N (190 µL, 1.36 mmol) and DMAP (58 mg, 0.47 mmol) were dissolved in CH_2Cl_2 (5 mL) and DMF (0.5 mL). *tert*-Butyldimethylsilyl chloride (107 mg, 0.71 mmol) was added and the mixture was stirred at 20 °C for 2 days after which concentration *in vacuo* followed by purification with column chromatography afforded 228 mg (89%) of **10** as clear oil. R_f = 0.48 (heptanes/EtOAc 4:1). ^{1}H NMR (300 MHz, $CDCl_3$):[227] δ 3.84–3.80 (m, 1H), 3.67–3.63 (m, 2H), 3.48–3.40 (m, 4H), 2.49 (d, *J* = 4.5 Hz, *OH*), 1.62–1.53 (m, 2H), 1.26 (s, 26H), 0.91–0.90 (m, 12H), 0.08 (s, 6H). ^{13}C NMR (75 MHz, $CDCl_3$): δ 71.8, 71.5, 70.8, 64.2, 32.1, 29.9 (9C), 29.6, 29.5, 26.3, 26.0 (3C), 22.9, 18.5, 14.3, –5.3 (2C). $[\alpha]_{589}^{20}$ = +1.5 (*c* = 1.05, $CHCl_3$).

1-*O*-Hexadecyl-2-all-*trans*-retinoyl-*sn*-glycerol (11)

Alcohol **10** (300 mg, 0.70 mmol), ATRA (314 mg, 1.05 mmol) and PPh_3 (365 mg, 1.39 mmol) were dissolved in THF (18 mL) and cooled to 0 °C. DIAD (280 μL, 1.42 mmol) was added dropwise and the reaction mixture was allowed to reach 20 °C and stirred for 3 h, then concentrated *in vacuo* and purified by column chromatography (heptane/EtOAc 9:1) to give 207 mg of a yellow oil, that was dissolved in MeCN (15 mL) and cooled to 0 °C. Aqueous HF (40%, 0.6 mL) was added dropwise and the reaction mixture was allowed to reach 20 °C and after stirring for 8 h the reaction was quenched by addition of a saturated aqueous solution of $NaHCO_3$ (40 mL). The organic layer was isolated via extraction with CH_2Cl_2 (3x50 mL) and the combined organic phases were concentrated *in vacuo* and the residue was purified by column chromatography (heptane/EtOAc 1:1) to afford 144 mg (35%) of **11** as a yellow oil. ^{1}H NMR (300 MHz, $CDCl_3$): δ 7.03 (dd, J = 15.0, 11.3 Hz, 1H), 6.31–6.26 (m, 2H), 6.17–6.12 (m, 2H), 5.84 (s, 1H), 5.05 (p, J = 4.7 Hz, 1H), 3.88–3.84 (m, 2H), 3.71–3.61 (m, 2H), 3.51–3.43 (m, 2H), 2.36 (s, 3H), 2.06–2.00 (m, 5H), 1.72 (s, 3H), 1.64–1.45 (m, 4H), 1.26 (s, 26H), 1.03 (s, 6H), 0.88 (t, J = 6.7 Hz, 3H). ^{13}C NMR (75 MHz, $CDCl_3$): δ 166.9, 154.1, 140.1, 137.8, 137.3, 135.0, 131.6, 130.2, 129.6, 129.0, 118.1, 72.4, 72.1, 70.3, 63.4, 39.7, 34.4, 33.3, 32.1, 29.9 (9C), 29.6, 29.5, 29.1 (2C), 26.2, 22.8, 21.9, 19.3, 14.3, 14.1, 13.1. $[\alpha]_{589}^{20}$ = +17.1 (c = 1.55, $CHCl_3$). IR (neat) 3447, 2924, 2855, 1708, 1584, 1458, 1358, 1240, 1152 cm^{-1}. HRMS (ESI+) $C_{39}H_{66}O_4$, m/z [M+Na$^+$] 621.4859, found 621.4848.

4'-octyl-4-phenylbenzoic acid (12)

4'-octyl-4-biphenylcarbonitrile (1.38 g, 4.74 mmol) was dissolved in a mixture of DMSO (200 mL) and H_2O (100 mL). NaOH (44.1 g, 1.10 mol) was added and the reaction mixture was heated to 180 °C for 16 h after which the solution was cooled to 20 °C and neutralized by addition of aqueous HCl (37%). The organic layer was isolated by extraction with EtOAc (4x200 mL) and the combined organic layers were concentrated *in vacuo* and purified by column chromatography (heptane/EtOAc 1:1) to give 1.39 g (95 %) of **12** as a white solid. R_f = 0.11 (heptane/EtOAc 1:1). mp = 148–152 °C (CH_2Cl_2). ^{1}H NMR (300 MHz, $CDCl_3$): δ 8.17 (d, J = 8.2 Hz, 2H), 7.70 (d, J = 8.2 Hz, 2H), 7.58 (d, J = 8.1Hz, 2H), 7.30 (d, J = 8.1 Hz, 2H), 2.67 (t, J = 7.7 Hz, 2H), 1.71–1.61 (m, 2H), 1.40–1.27 (m, 10H), 0.89 (t, J = 6.7 Hz, 3H). ^{13}C NMR (75 MHz, $CDCl_3$): δ 172.0, 146.6, 143.5, 137.2, 130.9 (2C), 129.2 (2C), 127.7, 127.3 (2C), 127.1 (2C), 35.8, 32.0, 31.6, 29.6, 29.5, 29.4, 22.8, 14.3.

1-*O*-Octadecyl-2-(6-(all-*trans*-retinoyloxy)-hexanoyl)-*sn*-glycero-3-phospho-(*S*)-glycerol (13)

Alcohol **30** (13 mg, 0.014 mmol), ATRA (6 mg, 0.019 mmol) and PPh_3 (9 mg, 0.043 mmol) were dissolved in THF (1.0 mL). DIAD (11 μL, 0.043 mmol) was added and the reaction mixture was stirred at 20 °C for 1 h, then concentrated *in vacuo* and purified by column chromatography (heptane/EtOAc 2:1 then heptane/EtOAc 1:2) to give 13 mg that

was dissolved in CH_2Cl_2 (1.0 mL) and DBU (2 µL, 0.012 mmol) was added. The reaction mixture was stirred for 30 min at 20 °C and then purified directly by column chromatography (heptane/EtOAc 1:1 then CH_2Cl_2/MeOH 9:1) to afford 8 mg that was dissolved in MeCN (0.9 mL) and CH_2Cl_2 (0.3 mL) and cooled to 0 °C. Aqueous HF (40%, 30 µL) was added dropwise and the reaction mixture was allowed to reach 20 °C. After 3.5 h the reaction was quenched by dropwise addition of $MeOSiMe_3$ (0.3 mL) and the mixture was stirred for 30 min, after which $NaHCO_3$ (6 mg, 0.07 mmol) was added and the mixture was concentrated *in vacuo* and purified by column chromatography (CH_2Cl_2/MeOH 10:1 then CH_2Cl_2/MeOH 4:1) to afford 4 mg (31%) of **13** as a yellow amorphous solid. R_f = 0.44 (CH_2Cl_2/MeOH 4:1). ^{1}H NMR (500 MHz, $CDCl_3/CD_3OD$ 4:1): δ 7.02 (dd, *J* = 15.0, 11.4 Hz, 1H), 6.32–6.27 (m, 2H), 6.15 (d, *J* = 11.4 Hz, 1H), 6.14 (d, *J* = 16.2 Hz, 1H), 5.77 (s, 1H), 5.18–5.13 (m, 1H), 4.11 (t, *J* = 6.6 Hz, 2H), 4.03–3.94 (m, 2H), 3.94–3.90 (m, 2H), 3.82–3.77 (m, 1H), 3.62 (t, *J* = 5.2 Hz, 2H), 3.60–3.57 (m, 2H), 3.49–3.39 (m, 2H), 2.39–2.33 (m, 5H), 2.05–2.00 (m, 5H), 1.72 (s, 3H), 1.71–1.60 (m, 6H), 1.57–1.51 (m, 2H), 1.50–1.45 (m, 2H), 1.45–1.40 (m, 2H), 1.31–1.23 (m, 30H), 1.03 (s, 6H), 0.88 (t, *J* = 6.9 Hz, 3H). ^{13}C NMR (50 MHz, $CDCl_3/CD_3OD$ 4:1): δ 174.0, 168.0, 153.7, 140.0, 138.0, 137.7, 135.3, 131.7, 130.3, 129.8, 129.2, 118.5, 72.2 (2C), 71.2, 69.4, 66.7, 64.5, 64.1, 62.7, 40.0, 34.5 (2C), 33.4, 32.3, 30.1, 29.7 (12C), 29.2 (2C), 28.7, 26.4, 25.9, 24.9, 23.0, 22.0, 19.6, 14.3, 14.1, 13.3. IR (neat) 3325, 2923, 2853, 1733, 1709, 1609, 1584, 1457, 1259, 1064, 798 cm^{-1}. HRMS (ESI+) $C_{50}H_{86}O_{11}PNa$, m/z [M+H$^+$] 917.5879, found 917.5834.

1-Stearoyl-2-(6-(all-*trans*-retinoyloxy)-hexanoyl)-*sn*-glycero-3-phospho-(*S*)-glycerol (14)

Alcohol **35** (47 mg, 0.052 mmol), ATRA (31 mg, 0.10 mmol), DMAP (13 mg, 0.10 mmol) and Et_3N (72 µL, 0.52 mmol) were dissolved in Et_2O (1.2 mL). DCC (27 mg, 0.13 mmol) was added and the reaction mixture was stirred at 20 °C for 22 h, then concentrated *in vacuo* and purified by column chromatography (toluene then toluene/EtOAc 5:1) to give 32 mg that was dissolved in CH_2Cl_2 (2.2 mL) and DBU (4.2 µL, 0.028 mmol) was added. The reaction mixture was stirred for 30 min at 20 °C and then purified directly by column chromatography (heptane/EtOAc 1:1 then CH_2Cl_2/MeOH 9:1) to afford 21 mg that was dissolved in MeCN (1.5 mL) and CH_2Cl_2 (0.5 mL) and cooled to 0 °C. Aqueous HF (40%, 90 µL) was added dropwise and the reaction mixture was allowed to reach 20 °C. After 3.5 h the reaction was quenched by dropwise addition of $MeOSiMe_3$ (0.3 mL) and the mixture was stirred for 30 min, after which $NaHCO_3$ (6 mg, 0.07 mmol) was added and the mixture was concentrated *in vacuo* and purified by column chromatography (CH_2Cl_2/MeOH 10:1 then CH_2Cl_2/MeOH 4:1 then CH_2Cl_2/MeOH/H_2O 65:25:1) to afford 15 mg (31%) of **14** as a yellow amorphous solid. R_f = 0.56 (CH_2Cl_2/MeOH 5:1). ^{1}H NMR (500 MHz, $CDCl_3/CD_3OD$ 4:1): δ 7.02 (dd, *J* = 15.0, 11.4 Hz, 1H), 6.32–6.27 (m, 2H), 6.15 (d, *J* = 11.4 Hz, 1H), 6.15 (d, *J* = 16.2 Hz, 1H), 5.77 (s, 1H), 5.25–5.20 (m, 1H), 4.39 (dd, *J* = 12.0, 3.3 Hz, 1H), 4.16 (dd, *J* = 12.0, 6.6 Hz, 1H), 4.11 (t, *J* = 6.6 Hz, 2H), 3.99–3.91 (m,

4H), 3.83–3.78 (m, 1H), 3.63 (t, *J* = 5.1 Hz, 2H), 2.36 (t, *J* = 7.5 Hz, 2H), 2.34 (s, 3H), 2.31 (t, *J* = 7.6 Hz, 2H), 2.05–2.00 (m, 5H), 1.71 (s, 3H), 1.71–1.65 (m, 4H), 1.65–1.57 (m, 4H), 1.50–1.45 (m, 2H), 1.45–1.41 (m, 2H), 1.34–1.21 (m, 28H), 1.03 (s, 6H), 0.88 (t, *J* = 7.0 Hz, 3H). ^{13}C NMR (50 MHz, $CDCl_3/CD_3OD$ 4:1): δ 174.2, 173.5, 168.0, 153.6, 140.1, 138.0, 137.6, 135.3, 131.6, 130.3, 129.7, 129.1, 118.5, 71.2, 70.7, 66.8, 64.0 (2C), 62.6 (2C), 39.9, 34.3 (3C), 33.4, 32.2, 29.9 (12C), 29.2 (2C), 28.7, 25.8, 25.1, 24.8, 23.0, 21.9, 19.5, 14.3, 14.1, 13.1. ^{31}P NMR (202 MHz, $CDCl_3/CD_3OD$ 4:1): δ –0.08. IR (neat): 3390, 2924, 2853, 1734, 1709, 1661, 1458, 1260, 1237, 1153, 1050, 805 cm^{-1}. HRMS (ESI+) $C_{50}H_{84}O_{12}PNa$, m/z [M+H$^+$] 931.5676, found 931.5712.

1-*O*-Octadecyl-2-(6-(4'-octyl-4-phenylbenzoyloxy)-hexanoyl)-*sn*-glycero-3-phospho-(*S*)-glycerol (15)

Alcohol **30** (62 mg, 0.068 mmol), carboxylic acid **12** (43 mg, 0.14 mmol) and DMAP (25 mg, 0.20 mmol) were dissolved in CH_2Cl_2 (4.5 mL). DCC (42 mg, 0.20 mmol) was added and the reaction mixture was stirred at 20 °C for 18 h. The mixture was concentrated *in vacuo* and purified by column chromatography (toluene then toluene/EtOAc 5:1) to give 65 mg that was dissolved in CH_2Cl_2 (5.0 mL) and DBU (9 µL, 0.06 mmol) was added. The reaction mixture was stirred for 35 min at 20 °C and then purified directly by column chromatography (heptane/EtOAc 1:1 then CH_2Cl_2/MeOH 10:1) to afford 58 mg that was dissolved in mixture of MeCN (4.2 mL) and CH_2Cl_2 (1.4 mL) and cooled to 0 °C. Aqueous HF (40%, 250 µL) was added dropwise and the reaction mixture was allowed to reach 20 °C. After 3.5 h, the reaction was quenched by dropwise addition of $MeOSiMe_3$ (0.93 mL) and the mixture was stirred for 30 min, after which $NaHCO_3$ (8 mg, 0.095 mmol) was added and the mixture was concentrated *in vacuo* and purified by column chromatography (CH_2Cl_2/MeOH 10:1 then CH_2Cl_2/MeOH 4:1) to afford 24 mg (38%) of **15** as a colorless amorphous solid. R_f = 0.23 (CH_2Cl_2/MeOH 4:1). ^{1}H NMR (500 MHz, $CDCl_3/CD_3OD$ 4:1): δ 8.08 (d, *J* = 8.3 Hz, 2H), 7.67 (d, *J* = 8.3 Hz, 2H), 7.55 (d, *J* = 8.1 Hz, 2H), 7.29 (d, *J* = 8.1 Hz, 2H), 5.19–5.14 (m, 1H), 4.34 (t, *J* = 6.6 Hz, 2H), 4.06–3.93 (m, 4H), 3.85–3.80 (m, 1H), 3.66–3.61 (m, 2H), 3.60–3.56 (m, 2H), 3.48–3.38 (m, 2H), 2.66 (t, *J* = 7.7 Hz, 2H), 2.40 (t, *J* = 7.5 Hz, 2H), 1.86–1.79 (m, 2H), 1.76–1.70 (m, 2H), 1.69–1.62 (m, 2H), 1.56–1.49 (m, 4H), 1.39–1.19 (m, 40H), 0.89 (t, *J* = 6.8 Hz, 3H), 0.88 (t, *J* = 6.9 Hz, 3H). ^{13}C NMR (50 MHz, $CDCl_3/CD_3OD$ 4:1): δ 173.9, 167.3, 146.1, 143.6, 137.5, 130.3 (2C), 129.3 (2C), 128.9, 127.4 (2C), 127.1 (2C), 72.1 (2C), 71.3, 69.3, 66.7, 65.2, 64.6, 62.6, 35.9, 34.5, 32.1 (2C), 31.8, 30.0, 29.7 (15C), 28.8, 26.3, 25.8, 24.9, 23.0 (2C), 14.3 (2C). ^{31}P NMR (202 MHz, $CDCl_3/CD_3OD$ 4:1): δ –1.02. IR (neat): 3320, 2920, 2851, 1717, 1276, 1102, 1069 cm^{-1}. HRMS (ESI+) $C_{51}H_{84}O_{11}PNa$, m/z [M+H$^+$] 927.5727, found 927.5766.

1-Stearoyl-2-(6-(4'-octyl-4-phenylbenzoyloxy)-hexanoyl)-*sn*-glycero-3-phospho-(*S*)-glycerol (16)

The synthesis was performed as for **15**, starting from alcohol **35** (70 mg, 0.077 mmol) and affording 51 mg (70%) of **16** as a colorless amorphous solid. R_f = 0.54 (CH_2Cl_2/MeOH 5:1). ^{1}H NMR (500 MHz, $CDCl_3$/CD_3OD 4:1): δ 8.08 (d, *J* = 8.3 Hz, 2H), 7.67 (d, *J* = 8.3 Hz, 2H), 7.56 (d, *J* = 8.1 Hz, 2H), 7.29 (d, *J* = 8.1 Hz, 2H), 5.27–5.22 (m, 1H), 4.39 (dd, *J* = 12.0, 3.2 Hz, 1H), 4.34 (d, *J* = 6.6 Hz, 2H), 4.17 (dd, *J* = 12.0, 6.6 Hz, 1H), 4.05–4.00 (m, 2H), 3.98–3.91 (m, 2H), 3.85–3.80 (m, 1H), 3.65–3.61 (m, 2H), 2.66 (t, *J* = 7.7 Hz, 2H), 2.40 (t, *J* = 7.5 Hz, 2H), 2.31 (t, *J* = 7.6 Hz, 2H), 1.86–1.78 (m, 2H), 1.76–1.69 (m, 2H), 1.68–1.62 (m, 2H), 1.62-1.56 (m, 2H), 1.55–1.49 (m, 2H), 1.39–1.20 (m, 38H), 0.89 (t, *J* = 6.7 Hz, 3H), 0.88 (t, *J* = 6.8 Hz, 3H). ^{13}C NMR (50 MHz, $CDCl_3$/CD_3OD 4:1): δ 174.4, 173.6, 167.4, 146.3, 143.7, 137.6, 130.4 (2C), 129.4 (2C), 129.0, 127.5 (2C), 127.2 (2C), 71.2, 70.8, 67.1, 65.2, 64.4, 62.7 (2C), 36.0, 34.4 (2C), 32.3 (2C), 31.8, 29.9 (15C), 28.8, 25.9, 25.2, 24.9, 23.0 (2C), 14.3 (2C). ^{31}P NMR (202 MHz, $CDCl_3$/CD_3OD 4:1): δ –1.30. IR (neat): 3314, 2921, 2851, 1737, 1467, 1277, 1103 cm^{-1}. HRMS (ESI+) $C_{51}H_{82}O_{12}PNa$, m/z [$M+H^+$] 941.5520, found 941.5549.

1-*O*-Octadecyl-2-lyso-*sn*-glycero-3-phospho-(*S*)-glycerol (17)

Alcohol **29** (92 mg, 0.12 mmol) was dissolved in CH_2Cl_2 (10.0 mL) and DBU (20 µL, 0.14 mmol) was added. The reaction mixture was stirred for 2 h at 20 °C and then purified directly by column chromatography (heptane/EtOAc 1:1 then CH_2Cl_2/MeOH 9:1) to afford 63 mg, that was dissolved in MeCN (7.0 mL) and CH_2Cl_2 (2.3 mL) and cooled to 0 °C. Aqueous HF (40%, 0.24 mL) was added dropwise and the reaction mixture was allowed to reach 20 °C. After 3.5 h the reaction was quenched by dropwise addition of $MeOSiMe_3$ (1.6 mL) and the mixture was stirred for 30 min, after which $NaHCO_3$ (13 mg, 0.15 mmol) was added and the mixture was concentrated *in vacuo* and purified by column chromatography (CH_2Cl_2/MeOH 20:1 then CH_2Cl_2/MeOH/H_2O 65:25:4) to give 31 mg (69%) of **17** as an amorphous solid. R_f = 0.47 (CH_2Cl_2/MeOH/H_2O 65:25:4). ^{1}H NMR (300 MHz, $CDCl_3$/CD_3OD 4:1):[68] δ 4.01–3.87 (m, 5H), 3.85–3.78 (m, 1H), 3.65–3.42 (m, 6H), 1.62–1.52 (m, 2H), 1.36–1.24 (m, 30H), 0.88 (t, *J* = 6.6 Hz, 3H).

1-*O*-Octadecyl-2-stearoyl-*sn*-glycero-3-phospho-(*S*)-glycerol (1-*O*-DSPG)

Alcohol **29** (70 mg, 0.090 mmol), stearic acid (51 mg, 0.18 mmol) and DMAP (11 mg, 0.090 mmol) were dissolved in CH_2Cl_2 (2.0 mL). DCC (56 mg, 0.27 mmol) was added and the reaction mixture was stirred at 20 °C. After 19 h the mixture was concentrated *in vacuo* and purified by column chromatography (heptane then heptane/EtOAc 3:1) to give 90 mg, that was dissolved in CH_2Cl_2 (5.5 mL) along with DBU (14 µL, 0.095 mmol). The reaction mixture was stirred for 1 h at 20 °C and then purified directly by column chromatography (heptane/EtOAc 1:1 then CH_2Cl_2/MeOH 9:1) to afford 71 mg, that was dissolved in MeCN (5.8 mL) and CH_2Cl_2 (2.0 mL) and cooled to 0 °C. Aqueous HF (40%, 0.35 mL) was added dropwise and the reaction mixture was allowed to reach 20 °C. After 4 h the excess

reagent was quenched by dropwise addition of $MeOSiMe_3$ (1.2 mL) and the mixture was stirred for 30 min, after which $NaHCO_3$ (12 mg, 0.14 mmol) was added and the mixture was concentrated *in vacuo* and purified by column chromatography (CH_2Cl_2/MeOH 9:1 then CH_2Cl_2/MeOH 4:1 then CH_2Cl_2/MeOH/H_2O 65:25:4) to give 47 mg (66%) of **1-*O*-DSPG** as an amorphous colorless solid. R_f = 0.54 (CH_2Cl_2/MeOH 4:1). ^{1}H NMR (300 MHz, $CDCl_3$/CD_3OD 4:1): δ 5.20–5.12 (m, 1H) 4.00–3.87 (m, 4H), 3.83–3.76 (m, 1H), 3.66–3.56 (m, 4H), 3.49–3.39 (m, 2H), 2.33 (t, *J* = 7.7 Hz, 2H), 1.66–1.48 (m, 4H), 1.40–1.18 (m, 58H), 0.91–0.85 (m, 6H). ^{13}C NMR (50 MHz, $CDCl_3$/CD_3OD 4:1): δ 174.4, 72.1, 71.3, 69.5, 66.9, 64.4, 62.8, 34.7, 32.3 (2C), 29.7 (26C), 26.4, 25.3, 23.0 (2C), 14.3 (2C). ^{31}P NMR (202 MHz, $CDCl_3$/CD_3OD 4:1): δ 2.20. IR (neat): 3382, 2917, 2850, 1721, 1468, 1252, 1062 cm^{-1}. MALDI-TOF (ES^+) $C_{42}H_{84}O_9PNa$, m/z [$M+H^+$] 787.58, found 787.33.

6-(all-*trans*-Retinoyloxy)-hexanoic acid (19)

ATRA (67 mg, 0.22 mmol), *tert*-butyl 6-hydroxyhexanoate (**22**, 126 mg, 0.67 mmol) and PPh_3 (226 mg, 1.12 mmol) were dissolved in THF (3.4 mL) and cooled to 0 °C. DIAD (0.29 mL, 1.12 mmol) was added dropwise. The mixture was stirred for 1 h after which the mixture was concentrated *in vacuo* and purified by column chromatography (heptane/EtOAc 4:1) to give 78 mg of a yellow oil that was dissolved in CH_2Cl_2 (12 mL) and cooled to 0 °C. 2,6-Lutidine (58 µL, 0.50 mmol) and TMSOTf (60 µL, 0.33 mmol) were added and the mixture was stirred at 0 °C for 1 h after which an additional portion of 2,6-lutidine (40 µL, 0.34 mmol) and TMSOTf (0.60 µL, 0.33 mmol) were added and 3 h later another portion of 2,6-lutidine (20 µL, 0.17 mmol) and TMSOTf (0.30 µL, 0.16 mmol) were added. After 5.5 h the excess reagent was quenched by addition of a cold saturated aqueous solution of NH_4Cl (10 mL) and the organic layer was isolated by extraction with Et_2O (1x30 mL). The combined organic phases were dried over Na_2SO_4, filtered and concentrated *in vacuo*. The residue was purified by column chromatography (heptane/EtOAc 2:1) to give 58 mg (62%) of **19** as yellow crystals. R_f = 0.27 (heptane/EtOAc 2:1). mp = 97–100 °C (CH_2Cl_2). ^{1}H NMR (300 MHz, $CDCl_3$): δ 7.00 (dd, *J* = 15.0 Hz and 11.4 Hz, 1H), 6.31–6.26 (m, 2H), 6.15 (d, *J* = 11.4 Hz, 1H), 6.14 (d, *J* = 16.0 Hz, 1H), 5.77 (s, 1H), 4.12 (t, *J* = 6.5 Hz, 2H), 2.41–2.36 (m, 5H), 2.05–2.00 (m, 5H), 1.71–1.57 (m, 9H), 1.49–1.45 (m, 4H), 1.03 (s, 6H). ^{13}C NMR (75 MHz, $CDCl_3$): δ 178.1, 167.4, 153.0, 139.8, 137.8, 137.4, 135.3, 131.2, 130.2, 129.6, 128.8, 118.6, 63.6, 39.7, 34.4, 33.7, 33.2, 29.1 (2C), 28.6, 25.7, 24.5, 21.9, 19.4, 14.0, 13.1. IR (neat): 2926, 1706, 1578, 1458, 1356, 1238, 1152, 966 cm^{-1}. HRMS (ESI+) $C_{26}H_{38}O_4$, m/z [$M+Na^+$] 437.2663, found 437.2657.

6-(4'-Octyl-4-phenylbenzoyloxy)-hexanoic acid (20)

4'-octyl-4-phenylbenzoic acid (**12**, 72 mg, 0.23 mmol), *tert*-butyl 6-hydroxyhexanoate (**22**, 131 mg, 0.69 mmol) and DMAP (113 mg, 0.93 mmol) were dissolved in CH_2Cl_2 (7.2 mL). DCC (1M in CH_2Cl_2, 0.94 mL, 0.94 mmol) was added dropwise. The mixture was stirred for 1.5 h after which the mixture was concentrated *in vacuo* and purified by column

chromatography (heptane/toluene 1:1 then heptane/EtOAc 20:1) to give 82 mg of the desired ester that was dissolved in CH_2Cl_2 (5 mL). TFA (0.39 mL, 5.12 mmol) and triisopropylsilane (176 μL, 0.86 mmol) were added and the mixture was stirred at 20 °C. Additional portions of TFA (0.20 mL, 2.61 mmol) were added after 7.5 and 23.5 h. After 27.5 h toluene (10 mL) was added and the mixture was concentrated *in vacuo* and purified by column chromatography (heptane/EtOAc 1:1) to give 63 mg (64%) of **20** as white crystals. R_f = 0.24 (heptane/EtOAc 1:1). mp = 90–92 °C (CH_2Cl_2). ^{1}H NMR (300 MHz, $CDCl_3$): δ 8.09 (d, *J* = 8.4 Hz, 2H), 7.66 (d, *J* = 8.4 Hz, 2H), 7.55 (d, *J* = 8.1 Hz, 2H), 7.29 (d, *J* = 8.1 Hz, 2H), 4.35 (t, *J* = 6.5 Hz, 2H), 2.66 (t, *J* = 7.7 Hz, 2H), 2.42 (t, *J* = 7.4 Hz, 2H), 1.88–1.50 (m, 8H), 1.41–1.27 (m, 10H), 0.89 (t, *J* = 6.6 Hz, 3H). ^{13}C NMR (75 MHz, $CDCl_3$): δ 179.1, 166.7, 145.7, 143.3, 137.4, 130.2 (2C), 129.1 (2C), 128.9, 127.2 (2C), 126.9 (2C), 64.8, 35.8, 33.9, 32.0, 31.6, 29.6, 29.5, 29.4, 28.6, 25.7, 24.5, 22.8, 14.3. IR (neat): 2921, 1711, 1275, 1123, 766 cm^{-1}. HRMS (ESI+) $C_{27}H_{36}O_4$, m/z [M+Na$^+$] 447.2512, found 447.2501.

tert-Butyl 6-hydroxyhexanoate (22)[228]

6-Caprolactone (**21**, 2.00 g, 17.5 mmol) and KO^{t}Bu (2.16 g, 19.3 mmol) were dissolved in ^{t}BuOH (55 mL) and heated to reflux. After 24 h H_2O (20 mL) was added and the organic layer was isolated by extraction with Et_2O (2x75 mL). The combined organic phases were concentrated *in vacuo* and purification by column chromatography (heptane/EtOAc 1:1) gave 1.29 g (39%) of **22** as a colorless oil. R_f = 0.38 (heptane/EtOAc 1:1). ^{1}H NMR (300 MHz, $CDCl_3$): δ 3.64 (t, *J* = 6.5 Hz, 2H), 2.23 (t, *J* = 7.4 Hz, 2H), 1.68–1.54 (m, 4H), 1.44 (s, 9H), 1.41–1.38 (m, 2H). ^{13}C NMR (75 MHz, $CDCl_3$): δ 173.3, 80.2, 62.8, 35.6, 32.5, 28.3 (3C), 25.3, 24.9.

Allyl 4-Methoxybenzoate (24)

Allyl alcohol (**23**, 5.0 mL, 73.5 mmol), Et_3N (15.4 mL, 110.3 mmol) and DMAP (0.45 g, 3.7 mmol) were dissolved in CH_2Cl_2 (250 mL). 4-Methoxybenzoyl chloride (11.9 mL, 88.2 mmol) was added dropwise and the reaction mixture was stirred at 20 °C for 2 h after which H_2O (200 mL) was added and the organic layer was isolated via extraction with CH_2Cl_2 (3x300 mL). The combined organic phases were dried over $MgSO_4$ and then concentrated *in vacuo* yielding 14.1 g (100%) of **24** as colorless oil. R_f = 0.77 (heptane/EtOAc 1:1). ^{1}H NMR (300 MHz, $CDCl_3$):[173] δ 8.03 (d, *J* = 9.0 Hz, 2H), 6.93 (d, *J* = 9.0 Hz, 2H), 6.05 (ddt, *J* = 17.2, 10.5, 5.6 Hz, 1H), 5.41 (dd, *J* = 17.2, 1.6 Hz, 1H), 5.31–5.26 (m, 1H), 4.81 (dt, *J* = 5.6, 1.4 Hz, 2H), 3.78 (s, 3H).

1-(4-Methoxybenzoyl)-2,3-*O*-di-*tert*-butyldimethylsilyl-*sn*-glycerol (25)

$K_2OsO_4 \cdot 2H_2O$ (271 mg, 0.74 mmol), $(DHQD)_2PHAL$ (687 mg, 0.88 mmol), $K_3Fe(CN)_6$ (72.6 g, 220.6 mmol) and K_2CO_3 (30.5 g, 220.6 mmol) were dissolved in a mixture of ^{t}BuOH (370 mL) and H_2O (370 mL) and stirred at 20 °C for 15 min after which **24** (14.1 g, 73.5 mmol) was added. After 2 h excess reagent was quenched by addition of Na_2SO_3 (111

g, 0.88 mol) and the organic layer was isolated by extraction with EtOAc (3x500 mL). Toluene (200 mL) was added to the combined organic phases and concentration *in vacuo* afforded (*S*)-1-*O*-(4-methoxybenzoyl)-glycerol as a white solid, ^{1}H NMR was similar to the data reported.[173] 300 MHz ^{1}H NMR of the crude product indicates that further purification was not necessary and the enantiomeric excess (>97%) was determined from chiral HPLC. HPLC (chiral) Chiralpak AS-H at at 20 °C, λ= 254 nm, hexane/2-propanol 75:25, retention times 17.8 min (S), 23.4 min *(R)* at 0.4 mL/min flow rate. The crude product of (*S*)-1-*O*-(4-methoxybenzoyl)-glycerol and imidazole (16.0 g, 235.3 mmol) were dissolved in DMF (78 mL) and heated to 60 °C after which TBDMSCl (33.2 g, 220.6 mmol) was added. After 4 h an extra portion of TBDMSCl (5.5 g, 36.5 mmol) and imidazole (2.5 g, 36.7 mmol) were added. After 6 h H_2O (50 mL) and Et_2O (150 mL) were added and the organic layer was isolated by extraction with Et_2O (3x150 mL mL). The combined organic phases were washed with a saturated aqueous solution of $NaHCO_3$ (100 mL). Toluene (200 mL) was added to the combined organic phases and concentration *in vacuo* gave a colorless oil which was purified by column chromatography (heptane/EtOAc 8:1) to give 32.6 g (99%) of **25** as clear oil. R_f = 0.28 (heptane/EtOAc 10:1). ^{1}H NMR (300 MHz, $CDCl_3$): δ 8.01 (d, *J* = 9.0 Hz, 2H), 6.93 (d, *J* = 8.6 Hz, 2H), 4.41 (dd, *J* = 11.3, 4.0 Hz, 1H), 4.25 (dd, *J* = 11.2, 6.1 Hz), 4.06–4.00 (m, 1H), 3.89 (s, 3H), 3.65–3.63 (m, 2H), 0.90 (s, 9H), 0.88 (s, 9H), 0.10–0.07 (m, 12H). ^{13}C NMR (75 MHz, $CDCl_3$): δ 166.4, 163.4, 131.8 (2C), 122.9, 113.7 (2C), 71.5, 66.5, 65.0, 55.5, 26.1 (3C), 25.9 (3C), 18.5, 18.2, –4.4, –4.6, –5.2, –5.3. Anal. Calcd. $C_{23}H_{42}O_5Si_2$: C 60.75, H 9.31; Found C 60.83, H 9.38. IR (neat) 2955, 2857, 1718, 1607, 1512, 1472, 1256, 1102, 840, 774 cm^{-1}.

2,3-*O*-Di-*tert*-butyldimethylsilyl-*sn*-glycerol (26)

Ester **25** (9.80 g, 21.6 mmol) was dissolved in CH_2Cl_2 (75 mL) and cooled to –78 °C under atmosphere of N_2. DIBAL-H (1 M in hexane, 41.0 mL) was added dropwise and the reaction mixture was kept at –78 °C. After 2.5 h an additional portion of DIBAL-H (1 M in hexane, 6.5 mL) was added dropwise. After 3 h MeOH (2.0 mL) was added and 1 h later Rochelle's salt (2.0 mL) was added and the mixture was allowed to reach 20 °C. H_2O (100 mL) was added and the organic layer was isolated via extraction with EtOAc (3x200 mL). The combined organic phases were concentrated *in vacuo* and purified by column chromatography (CH_2Cl_2) to give 6.05 g (88%) of **26** as a clear oil. R_f = 0.45 (CH_2Cl_2). ^{1}H NMR (300 MHz, $CDCl_3$): δ 3.81–3.71 (m, 1H), 3.69–3.56 (m, 4H), 2.17 (dd, *J* = 7.5, 5.1 Hz, 1H, *OH*), 0.89 (br. s, 18H), 0.09 (s, 6H), 0.06 (s, 6H). ^{13}C NMR (75 MHz, $CDCl_3$): δ 72.7, 65.0, 64.9, 26.0 (3C), 25.9 (3C), 18.4, 18.2, –4.4, –4.7, –5.3, –5.4. $[\alpha]_{589}^{20}$ = +18.5° (*c* 0.6, $CHCl_3$). HRMS (ESI+) $C_{15}H_{36}O_3Si_2$, m/z [M+Na$^+$] 343.2101, found 343.2110.

(2,3-*O*-Di-*tert*-butyldimethylsilyl)-*sn*-glycero-2-cyanoethyl-*N*,*N*-diisopropylphosphoramidite (27)

Alcohol **26** (904 mg, 2.82 mmol) and diisopropylethylamine (1.0 mL, 5.92 mmol) were dissolved in CH_2Cl_2 (10 mL). 2-Cyanoethyl-*N*,*N*-diisopropylchlorophosphoramidite (1.0 g,

4.22 mmol) was added dropwise and the reaction mixture was stirred at 20 °C for 1.5 h after which EtOAc (20 mL) and a saturated aqueous solution of $NaHCO_3$ (50 mL) were added and the organic layer was isolated by extraction with EtOAc (2x50 mL). The combined organic phases were concentrated *in vacuo* and the residue was purified by column chromatography (EtOAc) to give 1.35 g (92%) of **27** (two diastereoisomers 1:1) as a clear oil. R_f = 1.0 (EtOAc). ^{1}H NMR (300 MHz, $CDCl_3$, two diastereoisomers): δ 3.87–3.46 (m, 5H), 2.67–2.61 (m, 2H), 1.20–1.17 (m, 12H), 0.90 (s, 9H), 0.89 (s, 9H), 0.09–0.06 (m, 12H). ^{13}C NMR (75 MHz, $CDCl_3$, two diastereoisomers); δ 117.8 (0.5C), 117.7 (0.5C), 73.3 (d, *J* = 7.3 Hz, 0.5C), 73.2 (d, *J* = 8.3 Hz, 0.5C), 65.1 (d, *J* = 15.2 Hz, 0.5C), 65.0 (0.5C), 64.9 (0.5C), 64.8 (d, *J* = 15.7 Hz, 0.5C), 58.7 (d, *J* = 11.9 Hz, 0.5C), 58.4 (d, *J* = 12.5 Hz, 0.5C), 43.2 (d, *J* = 4.7 Hz), 43.1 (d, *J* = 4.6 Hz), 26.1 (3C), 26.0 (3C), 24.8, 24.7 (2C), 24.6, 20.6 (0.5C), 20.5 (0.5C), 18.5, 18.3, –4.3 (0.5C), –4.4 (0.5C), –4.5, –5.2, –5.3. ^{31}P NMR (202 MHz, $CDCl_3$): δ 149.0, 148.4. HRMS (ESI+) $C_{24}H_{53}N_2O_4PSi_2$, m/z [M+Na^+] 543.3179, found 543.3186. IR (neat): 2958, 2929, 2883, 2857 cm^{-1}.

6-(4-Methoxybenzyloxy)-hexanoic acid (28)

6-Caprolactone (**21**, 1.0 g, 8.76 mmol), KOH (2.46 g, 43.8 mmol) and 4-methoxybenzyl chloride (3.6 mL, 26.3 mmol) were dissolved in toluene (15 mL) and heated to reflux. After 18 h H_2O (50 mL) was added and the solution was acidified until pH 2 with aqueous HCl (37%). The organic layer was isolated by extraction with Et_2O (2×100 mL) and the combined organic phases were concentrated *in vacuo* and purified by column chromatography (heptane/EtOAc 3:2) to give 1.6 mg (74%) of **28** as a colorless clear oil. R_f = 0.15 (heptane/EtOAc 3:2). ^{1}H NMR (300 MHz, $CDCl_3$):[229] δ 7.27 (d, *J* = 8.7 Hz, 2H), 6.89 (d, *J* = 8.7 Hz, 2H), 4.39 (s, 2H), 3.81 (s, 3H), 3.45 (t, *J* = 6.5 Hz, 2H), 2.37 (t, *J* = 7.5 Hz, 2H), 1.71–1.59 (m, 4H), 1.48–1.39 (m, 2H). ^{13}C NMR (75 MHz, $CDCl_3$): δ 179.7, 159.2, 130.7, 129.4 (2C), 113.9 (2C), 72.7, 69.9, 55.4, 34.1, 29.5, 25.8, 24.6.

1-*O*-Octadecyl-*sn*-glycero-3-(2-cyanoethylphospho)-(*S*)-2,3-*O*-di-*tert*-butyldimethylsilyl-glycerol (29)

Alcohol **5b** (268 mg, 0.58 mmol) and phosphoramidite **27** (405 mg, 0.77 mmol) were dissolved in CH_2Cl_2 (4.3 mL), tetrazole (0.45 M in MeCN, 1.7 mL, 0.77 mmol) was added and the mixture was stirred for 30 min at 20 °C after which ^{t}BuOOH (5.5 M in nonane, 0.14 mL, 0.77 mmol) was added. After 70 min the mixture was concentrated *in vacuo* and purified by column chromatography (heptane/EtOAc 3:1) to afford 452 mg that was dissolved in CH_2Cl_2 (10 mL) and H_2O (0.6 mL). DDQ (171 mg, 0.75 mmol) was added and the mixture was stirred at 20 °C for 1.5 h after which Na_2SO_4 (15 g) was added and the mixture was purified directly by column chromatography (CH_2Cl_2 then heptane/EtOAc 1:1) to give 328 mg (73%) of **29** (two distereoisomers 1:1) as a colorless oil. R_f = 0.21 (heptane/EtOAc 1:1). ^{1}H NMR (300 MHz, $CDCl_3$, two diastereoisomers): δ 4.32–3.97 (m, 8H), 3.92–3.84 (m, 1H), 3.59–3.43 (m, 6H), 2.78 (t, *J* = 6.3 Hz, 2H), 1.59–1.52 (m, 2H), 1.33–1.24 (m, 30H), 0.92–0.86 (m, 21H), 0.10 (s, 3H), 0.09 (s, 3H), 0.06 (s, 6H). ^{13}C NMR

(75 MHz, $CDCl_3$, two diastereoisomers): δ 116.5, 77.4, 72.0, 70.8, 70.8, 69.7 (0.5C), 69.6 (0.5C), 69.5 (0.5C), 69.5 (0.5C), 64.0, 62.1 (0.5C), 62.0 (0.5C), 32.1, 29.9 (12C), 29.6, 29.5, 26.2, 26.0 (3C), 25.9 (3C), 22.9, 19.8 (0.5C), 19.7 (0.5C), 18.4 (0.5C), 18.2 (0.5C), 14.3, –4.5, –4.6, –5.3, –5.3. ^{31}P NMR (202 MHz, $CDCl_3$): δ –0.10 and –0.19. HRMS (ESI+) $C_{39}H_{82}NO_8PSi_2$, m/z [M+Na^+] 802.5209, found 802.5205.

1-*O*-Octadecyl-2-(6-hydroxyhexanoyl)-*sn*-glycero-3-(2-cyanoethylphospho)-(*S*)-2,3-O-di-*tert*-butyldimethylsilyl-glycerol (30)

Alcohol **29** (65 mg, 0.083 mmol), carboxylic acid **28** (42 mg, 0.17 mmol) and DMAP (0.5 mg, 0.004 mmol) were dissolved in CH_2Cl_2 (4.0 mL) and EtOAc (1.4 mL). DCC (0.25 mL, 1 M in CH_2Cl_2, 0.25 mmol) was added and the reaction mixture was stirred at 20 °C. After 70 min **28** (42 mg, 0.17 mmol) and DCC (0.25 mL, 1 M in CH_2Cl_2, 0.25 mmol) were added and the reaction mixture was stirred for additional 21 h after which the mixture was concentrated *in vacuo* and purified by column chromatography (toluene/EtOAc 5:1) to give a residue that was dissolved in CH_2Cl_2 (6 mL) and H_2O (0.3 mL) along with DDQ (28 mg, 0.12 mmol). The reaction mixture was stirred at 20 °C for 1 h after which Na_2SO_4 was added and the mixture was purified directly by column chromatography (heptane/EtOAc 2:1 then EtOAc/heptane 1:2) to give 70 mg (93%) of **30** as a colorless oil. R_f = 0.50 (heptane/EtOAc 1:2). ^{1}H NMR (300 MHz, $CDCl_3$, two diastereoisomers): δ 5.23–5.16 (m, 1H), 4.31–4.14 (m, 5H), 4.04–3.96 (m, 1H), 3.92–3.84 (m, 1H), 3.65 (t, *J* = 6.3 Hz, 2H), 3.59–3.54 (m, 4H), 3.47–3.40 (m, 2H), 2.77 (td, *J* = 6.3 and 2.0 Hz, 2H), 2.39 (t, *J* = 7.3 Hz, 2H), 1.74–1.63 (m, 2H), 1.63–1.51 (m, 4H), 1.49–1.39 (m, 2H), 1.33–1.23 (m, 30H), 0.92–0.86 (m, 21H), 0.11 (s, 3H), 0.10 (s, 3H), 0.07 (s, 6H). ^{31}P NMR (202 MHz, $CDCl_3$): δ –0.87 and –1.08. IR (neat): 3443, 2925, 2854, 1741, 1463, 1255, 1101, 1035, 836 cm^{-1}. HRMS (ESI+) $C_{45}H_{92}NO_{10}PSi_2$, m/z [M+Na^+] 893.5890, found 893.5878.

1-Stearoyl-*sn*-glycerol (32)

2,3-*O*-Isopropylidene-*sn*-glycerol (**31**, 1.12 g, 8.47 mmol), octadecanol (3.13 g, 11.0 mmol) and DMAP (259 mg, 2.12 mmol) were dissolved in CH_2Cl_2 (75 mL) and DCC (3.49 g, 16.9 mmol) was added. The mixture was stirred at 20 °C for 2 h, then concentrated *in vacuo* and purified by column chromatography (CH_2Cl_2) to give a white solid that was dissolved in $B(OEt)_3$ (45 mL) and CF_3CH_2OH (5.6 mL). CF_3COOH (5.6 mL) was added and the reaction mixture was stirred at 20 °C for 5 h, then toluene (2×50 mL) was added and the resulting solution was concentrated *in vacuo*. The residue was dissolved in MeOH (120 mL) and carefully H_2O (120 mL) was added. A colorless precipitate was formed and collected by filtration, washed with H_2O, then dissolved in Et_2O (200 mL) and dried over Na_2SO_4. After filtration the mixture was concentrated *in vacuo* and the residue was crystallized from first hexane and then CH_2Cl_2 to give 1.77 g (58%) of **32** as white crystals. R_f = 0.24 (heptane/EtOAc 1:1). mp = 78–80 °C (lit.[87] 69 °C). ^{1}H NMR (300 MHz, $CDCl_3$): δ 4.25–4.13 (m, 2H), 3.99–3.91 (m, 1H), 3.75–3.66 (m, 1H), 3.65–3.56 (m, 1H), 2.51 (d, *J* = 5.1 Hz, 1H, *OH*), 2.36 (t, *J* = 7.5 Hz, 2H), 2.06 (d, *J* = 6.2 Hz, 1H, *OH*), 1.69–1.59 (m,

2H), 1.39–1.20 (m, 28H), 0.89 (t, *J* = 6.2 Hz, 3H). $[\alpha]_{589}^{20}$ = +3.47 (*c* = 3.0, pyridine) (lit.[98] $[\alpha]_{D}^{25}$ =+3.55 (*c* = 5.24, pyridine).

1-Stearoyl-3-O-*tert*-butyldimethylsilyl-*sn*-glycerol (33)

Alcohol **32** (300 mg, 0.84 mmol) and imidazole (142 mg, 2.09 mmol) were dissolved in THF (8.5 mL) and *tert*-butyldimethylsilyl chloride (202 mg, 1.34 mmol) was added. The reaction mixture was stirred at 20 °C for 2 h, then concentrated *in vacuo* and purified by column chromatography (heptane/EtOAc 3:1) to give 350 mg (88%) of **33** as a colorless oil. R_f = 0.75 (heptane/EtOAc 1:1). ^{1}H NMR (300 MHz, $CDCl_3$):[98] δ 4.17 (dd, *J* = 10.7, 4.2 Hz, 1H), 4.11 (dd, *J* = 10.7, 5.1 Hz, 1H), 3.93–3.84 (m, 1H), 3.69 (dd, *J* = 10.1, 4.6 Hz, 1H), 3.61 (dd, *J* = 10.1, 5.6 Hz, 1H), 2.51 (d, *J* = 5.4 Hz, 1H, *OH*), 2.35 (t, *J* = 7.5 Hz, 2H), 1.69–1.59 (m, 2H), 1.37–1.22 (m, 28H), 0.92–0.86 (m, 12H), 0.09 (s, 6H). ^{13}C NMR (50 MHz, $CDCl_3$): δ 174.1, 70.2, 65.1, 63.9, 34.4, 32.1, 29.8 (8C), 29.6, 29.5, 29.4, 29.3, 26.0 (3C), 25.1, 22.8, 18.4, 14.3, –5.3 (2C). $[\alpha]_{589}^{20}$ = +1.79 (*c* = 5.2, $CHCl_3$) (lit.[98] $[\alpha]_{D}^{20}$ =+1.70 (*c* = 6.0, $CHCl_3$).

1-Stearoyl-2-(6-(4-methoxybenzyloxy)hexanoyl)-*sn*-glycerol (34)

Alcohol **33** (89 mg, 0.19 mmol), carboxylic acid **28** (95 mg, 0.38 mmol) and DMAP (53 mg, 0.44 mmol) were dissolved in CH_2Cl_2 (2.7 mL) and EDCI (79 mg, 0.41 mmol) was added. The reaction mixture was stirred at 20 °C for 20 h, then concentrated *in vacuo* and purified by column chromatography (heptane/EtOAc 7:1) to give 126 mg of the desired ester, that was dissolved in a mixture of DMSO (3.4 mL), THF (2.8 mL) and H_2O (0.34 mL) in a flask protected from light. NBS (149 mg, 0.84 mmol) was added and the reaction mixture was stirred at 20 °C for 21 h, after which excess reagent was quenched by addition of a aqueous solution of $Na_2S_2O_3$ (1%, 7.7 mL). The mixture was stirred at 20 °C for 10 min, then the organic layer was isolated by extraction with Et_2O (3x20 mL). The combined organic phases were dried over Na_2SO_4, filtrated, concentrated *in vacuo* and purified by column chromatography (heptane/EtOAc 1:1) to give 87 mg (78%) of **34** as a colorless oil. R_f = 0.44 (heptane/EtOAc 1:1). ^{1}H NMR (300 MHz, $CDCl_3$): δ 7.26 (d, *J* = 8.3 Hz, 2H), 6.88 (d, *J* = 8.3 Hz, 2H), 5.12–5.05 (m, 1H), 4.43 (s, 2H), 4.32 (dd, *J* = 11.9 and 4.6 Hz, 1H), 4.23 (dd, *J* = 11.9 and 5.7 Hz, 1H), 3.81 (s, 3H), 3.73–3.71 (m, 2H), 3.45 (dt, *J* = 6.3 and 1.1 Hz, 2H), 2.36 (t, *J* = 7.4 Hz, 2H), 2.32 (t, *J* = 7.5 Hz, 2H), 1.71–1.58 (m, 6H), 1.48–1.38 (m, 2H), 1.33-1.24 (m, 28H), 0.88 (t, *J* = 6.7 Hz, 3H). ^{13}C NMR (75 MHz, $CDCl_3$): δ 174.0, 173.5, 159.4, 130.8, 129.5 (2C), 114.0 (2C), 72.8, 72.4, 70.0, 62.2, 61.7, 55.5, 34.4, 32.2, 29.9 (10C), 29.7, 29.6, 29.5, 29.4, 25.9, 25.1, 25.0, 23.0, 14.4. $[\alpha]_{589}^{20}$ = –2.58 (*c* = 2.4, $CHCl_3$). IR (neat): 3466, 2923, 2853, 1739, 1513, 1247, 1171, 1098 cm^{-1}. HRMS (ESI+) $C_{35}H_{60}O_7$, m/z [M+Na^+] 615.4231, found 615.4256.

Mosher ester analysis of compound 34

1-Stearoyl-2-(6-(4-methoxybenzyloxy)hexanoyl)-3-((*R*)-methoxytrifluoromethylphenylacetoyl)-*sn*-glycerol (Mosher (*R*)-ester)

Alcohol **34** (21 mg, 0.035 mmol) was dissolved in pyridine (0.35 mL) and (*R*)-methoxytrifluoromethylphenylacetyl chloride (27 mg, 0.11 mmol) was added and the mixture was stirred at 20 °C. After 45 min a saturated aqueous solution of $NaHCO_3$ (4 mL) was added and the organic layer was isolated by extraction with CH_2Cl_2 (3×4 mL). The combined organic layers were dried over Na_2SO_4, filtered and concentrated *in vacuo* to give 26 mg of the crude ester which was subjected to NMR analysis. ^{1}H NMR (300 MHz, $CDCl_3$): δ 7.53–7.39 (m, 5H), 7.26 (d, *J* = 8.3 Hz, 2H), 6.88 (d, *J* = 8.3 Hz, 2H), 5.34–5.27 (m, 1H), 4.60 (dd, *J* = 11.9 and 3.9 Hz, 1H), 4.43 (s, 2H), 4.37 (dd, *J* = 11.9 and 5.6 Hz, 1H), 4.27 (dd, *J* = 11.9 and 4.8 Hz, 1H), 4.12 (dd, *J* = 11.9 and 5.7 Hz, 1H), 3.81 (s, 3H), 3.54 (s, 3H), 3.43 (t, *J* = 6.5 Hz, 2H), 2.33–2.23 (m, 4H), 1.65–1.54 (m, 6H), 1.43–1.34 (m, 2H), 1.33–1.21 (m, 28H), 0.88 (t, *J* = 6.7 Hz, 3H). ^{19}F NMR (282 MHz, $CDCl_3$): δ –72.05.

1-Stearoyl-2-(6-(4-methoxybenzyloxy)hexanoyl)-3-((*S*)-methoxytrifluoromethylphenylacetoyl)-*sn*-glycerol (Mosher (*S*)-ester)

Alcohol **34** (21 mg, 0.035 mmol) was dissolved in pyridine (0.35 mL) and (*S*)-methoxytrifluoromethylphenylacetyl chloride (27 mg, 0.11 mmol) was added and the mixture was stirred at 20 °C. After 45 min a saturated aqueous solution of $NaHCO_3$ (4 mL) was added and the organic layer was isolated by extraction with CH_2Cl_2 (3×4 mL). The combined organic layers were dried over Na_2SO_4, filtered and concentrated *in vacuo* to give 23 mg of the crude ester which was subjected to NMR analysis. ^{1}H NMR (300 MHz, $CDCl_3$): δ 7.53–7.40 (m, 5H), 7.26 (d, *J* = 8.3 Hz, 2H), 6.88 (d, *J* = 8.3 Hz, 2H), 5.33–5.26 (m, 1H), 4.60 (dd, *J* = 11.9 and 3.9 Hz, 1H), 4.43 (s, 2H), 4.37 (dd, *J* = 11.9 and 5.8 Hz, 1H), 4.28 (dd, *J* = 11.9 and 4.7 Hz, 1H), 4.08 (dd, *J* = 11.9 and 5.6 Hz, 1H), 3.81 (s, 3H), 3.53 (s, 3H), 3.43 (t, *J* = 6.5 Hz, 2H), 2.33–2.24 (m, 4H), 1.65–1.55 (m, 6H), 1.43–1.34 (m, 2H), 1.33–1.23 (m, 28H), 0.88 (t, *J* = 6.7 Hz, 3H). ^{19}F NMR (282 MHz, $CDCl_3$): δ –72.06.

1-Stearoyl-2-(6-hydroxyhexanoyl)-*sn*-glycero-3-(2-cyanoethylphospho)-(*S*)-2,3-O-di-*tert*-butyldimethylsilyl-glycerol (35)

Alcohol **34** (75 mg, 0.13 mmol) and phosphoramidite **27** (88 mg, 0.17 mmol) were dissolved in CH_2Cl_2 (0.90 mL) and tetrazole (0.45 M in MeCN, 193 µL, 0.17 mmol) was added and the mixture was stirred 20 °C for 30 min after which ^{t}BuOOH (5.5 M in nonane, 31 µL, 0.17 mmol) was added. After 90 min the reaction mixture was concentrated *in vacuo* and purified by column chromatography (heptane/EtOAc 1:1) to give 118 mg that was dissolved in CH_2Cl_2 (2.3 mL) and H_2O (0.13 mL). DDQ (39 mg, 0.17 mmol) was added and the reaction mixture was stirred for 1.5 h at 20 °C. Na_2SO_4 was added and the mixture was purified directly by column chromatography (heptane/EtOAc 3:1 then heptane/EtOAc 1:1) to give 85 mg (74%) of **35** (two diastereoisomers 1:1) as a colorless oil. R_f = 0.12 (heptane/EtOAc 1:1). ^{1}H NMR (300 MHz, $CDCl_3$, two diastereoisomers): δ

5.30–5.22 (m, 1H), 4.38–4.11 (m, 7H), 4.05–3.96 (m, 1H), 3.90–3.83 (m, 1H), 3.63 (t, *J* = 6.3 Hz, 2H), 3.59–3.52 (m, 2H), 2.77 (t, *J* = 6.3 Hz, 2H), 2.37 (t, *J* = 7.3 Hz, 2H), 2.32 (t, *J* = 7.6 Hz, 2H), 1.74–1.53 (m, 6H), 1.48–1.38 (m, 2H), 1.33–1.23 (m, 28H), 0.92–0.86 (m, 21H), 0.10 (s, 3H), 0.09 (s, 3H), 0.06 (s, 6H). IR (neat) 3507, 2925, 2855, 1743, 1463, 1255, 1147, 1102, 1037, 836 cm^{-1}. HRMS (ESI+) $C_{45}H_{90}NO_{11}PSi_2$, m/z [M+Na^+] 930.5688, found 930.5649.

1-*O*-Octadecyl-2-(4-(α-tocopheroxy)-4-oxobutanoyl)-*sn*-glycero-3-phospho-(*S*)-glycerol (36)

Alcohol **29** (48 mg, 0.062 mmol), α-tocopheryl succinate (0.032 M in EtOAc, 1.5 mL, 0.048 mmol) and DMAP (18 mg, 0.14 mmol) were dissolved in CH_2Cl_2 (4 mL). EDCI (28 mg, 0.14 mmol) was added and the reaction mixture was stirred for 1 h at 20 °C, then concentrated *in vacuo* and purified by column chromatography (heptane/EtOAc 2:1 then heptane/EtOAc 1:2) to give 61 mg of the desired ester, that was dissolved in CH_2Cl_2 (1.3 mL) along with DBU (8 µL, 0.050 mmol). The reaction mixture was stirred at 20 °C for 40 min and then purified directly by column chromatography (CH_2Cl_2/MeOH 10:1) to afford 41 mg that was dissolved in MeCN (2.3 mL) and CH_2Cl_2 (0.8 mL) and cooled to 0 °C. Aqueous HF (40%, 0.14 mL) was added dropwise and the reaction mixture was allowed to reach 20 °C. After 3 h the reaction was quenched by dropwise addition of $MeOSiMe_3$ (0.6 mL) and the mixture was stirred for 30 min, after which $NaHCO_3$ (5 mg, 0.059 mmol) was added and the mixture was concentrated *in vacuo* and purified by column chromatography (CH_2Cl_2/MeOH 20:1 then CH_2Cl_2/MeOH 4:1) to give 30 mg (61%) of **36** as a colorless amorphous solid. R_f = 0.09 (CH_2Cl_2/MeOH 9:1). ^{1}H NMR (300 MHz, $CDCl_3$/CD_3OD 4:1): δ 5.22–5.14 (m, 1H), 4.05–3.98 (m, 2H), 3.98–3.90 (m, 2H), 3.86–3.79 (m, 1H), 3.67–3.56 (m, 4H), 3.47–3.40 (m, 2H), 2.98–2.90 (m, 2H), 2.83–2.76 (m, 2H), 2.60 (t, *J* = 6.4 Hz), 2.09 (s, 3H), 2.01 (s, 3H), 1.97 (s, 3H), 1.84–1.74 (m, 2H), 1.59–1.48 (m, 7H), 1.47–1.01 (m, 49H), 0.91–0.83 (m, 15H). ^{13}C NMR (75 MHz, $CDCl_3$/CD_3OD 4:1): δ 172.4, 171.8, 149.7, 140.7, 126.9, 125.2, 123.3, 117.8, 75.4, 72.6, 72.1, 71.1, 69.1, 66.7, 64.4, 62.4, 39.7 (2C), 37.7 (3C), 37.6, 33.1, 33.0, 32.2, 31.4, 30.0 (13C), 29.3, 29.0, 28.2, 26.3, 25.1, 24.7, ~24, 23.0, 22.9, 22.8, 21.3, 20.9, 20.0, 19.9, 14.3, 13.1, 12.2, 12.0. ^{31}P NMR (202 MHz, $CDCl_3$/CD_3OD 4:1): δ 3.43. IR (neat) 3423, 2923, 2853, 1722, 1696, 1660, 1397, 1264, 1062, 804 cm^{-1}. HRMS (ESI+) $C_{57}H_{102}O_{12}PNa$, m/z [M+H^+] 1033.7085, found 1033.7094.

1-Stearoyl-2-(4-(α-tocopheroxy)-4-oxobutanoyl)-*sn*-glycero-3-phospho-(*S*)-glycerol (37)

Alcohol **38** (56 mg, 0.064 mmol) and phosphoramidite **27** (45 mg, 0.087 mmol) were dissolved in CH_2Cl_2 (0.45 mL) and the mixture was stirred for 15 min at 20 °C before tetrazole (0.45 M in MeCN, 193 µL, 0.087 mmol) was added. 30 min later ^{t}BuOOH (5.5 M in nonane, 15 µL, 0.087 mmol) was added and the reaction mixture was stirred for 70 min after which the mixture was concentrated *in vacuo* and purified by column chromatography

(heptane/EtOAc 2:1) to give 76 mg that was dissolved in CH_2Cl_2 (4.5 mL) and DBU (10 µL, 0.064 mmol) was added. The reaction mixture was stirred for 1 h at 20 °C and then purified directly by column chromatography (heptane/EtOAc 1:1 then CH_2Cl_2/MeOH 9:1) to afford 58 mg that was dissolved in MeCN (3.8 mL) and CH_2Cl_2 (1.3 mL) and cooled to 0 °C. Aqueous HF (40%, 125 µL) was added dropwise and the reaction mixture was allowed to reach 20 °C. After 4 h the reaction was quenched by dropwise addition of $MeOSiMe_3$ (0.84 mL) and the mixture was stirred for 30 min, after which $NaHCO_3$ (7 mg, 0.083 mmol) was added and the mixture was concentrated *in vacuo* and purified by column chromatography (CH_2Cl_2/MeOH 20:1 then CH_2Cl_2/MeOH 4:1) to give 30 mg (44%) of **37** as a colorless amorphous solid. R_f = 0.26 (CH_2Cl_2/MeOH 4:1). ^{1}H NMR (500 MHz, $CDCl_3$/CD_3OD 4:1): δ 5.29–5.24 (m, 1H), 4.37 (dd, *J* = 12.0, 3.4 Hz, 1H), 4.20 (dd, *J* = 12.0, 6.5 Hz, 1H), 4.08–4.04 (m, 2H), 4.00–3.91 (m, 2H), 3.83–3.78 (m, 1H), 3.65–3.58 (m, 2H), 2.97–2.92 (m, 2H), 2.80 (t, *J* = 6.7 Hz, 2H), 2.60 (t, *J* = 6.6 Hz, 2H), 2.28 (t, *J* = 7.6 Hz, 2H), 2.09 (s, 3H), 2.01 (s, 3H), 1.97 (s, 3H), 1.85–1.74 (m, 2H), 1.60–1.03 (m, 54H), 0.90–0.85 (m, 15H). ^{13}C NMR (50 MHz, $CDCl_3$/CD_3OD 4:1): δ 174.3, 172.2, 171.6, 149.8, 140.8, 126.9, 125.2, 123.3, 117.8, 75.5, 71.1 (2C), 67.2, 64.3, 62.6 (2C), 40 (br), 39.7, 37.8 (4C), 34.3, 33.1 (2C), 32.2, 31.5, 30.0 (12C), 29.4, 29.0, 28.3, 25.1 (2C), 24.7, ~24, 22.9 (3C), 21.3, 20.9, 20.0 (2C), 14.3, 13.1, 12.2, 12.0. ^{31}P NMR (202 MHz, $CDCl_3$/CD_3OD 4:1): δ –0.88. IR (neat) 3406, 2924, 2853, 1728, 1518, 1449, 1247, 1144, 1105, 740 cm^{-1}. HRMS (ESI+) $C_{57}H_{100}O_{13}PNa$, m/z [M+H$^+$] 1047.6879, found 1047.6858.

1-Stearoyl-2-(4-(α-tocopheroxy)-4-oxobutanoyl)-*sn*-glycerol (38)

Alcohol **33** (63 mg, 0.13 mmol), α-tocopheryl succinate (84 mg, 0.16 mmol) and DMAP (26 mg, 0.21 mmol) were dissolved in CH_2Cl_2 (1.9 mL). EDCI (38 mg, 0.20 mmol) was added and the reaction mixture was stirred at 20 °C for 2 h, then concentrated *in vacuo* and purified by column chromatography (heptane/EtOAc 7:1) to give 122 mg of the desired ester, that was dissolved in a mixture of DMSO (2.4 mL), THF (2.0 mL) and H_2O (0.24 mL) in a flask protected from light. NBS (104 mg, 0.58 mmol) was added and the reaction mixture was stirred at 20 °C for 70 h, after which the reaction was quench by addition of aqueous $Na_2S_2O_3$ (1%, 5.4 mL). The mixture was stirred at 20 °C for 10 min, then the organic layer was isolated via extraction with Et_2O (3x14 mL). The combined organic phases were dried over Na_2SO_4, filtrated, concentrated *in vacuo* and purified by column chromatography (heptane/EtOAc 1:1) to give 56 mg (48%) of **38** as a colorless oil. R_f = 0.45 (heptane/EtOAc 1:1). ^{1}H NMR (300 MHz, $CDCl_3$): δ 5.16–5.09 (m, 1H), 4.33 (dd, *J* = 12.0, 4.7 Hz, 1H), 4.26 (dd, *J* = 12.0, 5.6 Hz, 1H), 3.77 (dd, *J* = 12.3, 4.4 Hz, 1H), 3.71 (dd, *J* = 12.3, 5.1 Hz, 1H), 3.01–2.94 (m, 2H), 2.83–2.76 (m, 2H), 2.59 (t, *J* = 6.4 Hz. 2H), 2.32 (t, *J* = 7.5 Hz, 2H), 2.09 (s, 3H), 2.02 (s, 3H), 1.97 (s, 3H), 1.85–1.72 (m, 2H), 1.66–1.02 (m, 54H), 0.92–0.84 (m, 15H). ^{13}C NMR (50 MHz, $CDCl_3$): δ 173.9, 171.9, 171.2, 149.6, 140.6, 126.7, 125.0, 123.2, 117.6, 75.2, 73.1, 62.0, 61.5, 40.3, 39.5, 37.6 (3C), 37.4, 34.2, 32.9 (2C), 32.1, 31.2, 29.8 (12C), 29.3, 29.1, 28.1, 25.0 (2C), 24.6, 24, 22.8 (3C),

21.2, 20.7, 19.8 (2C), 14.3, 13.1, 12.2, 12.0. IR (neat) 3493, 2923, 2853, 1741, 1462, 1377, 1146 cm^{-1}. HRMS (ESI+) $C_{54}H_{94}O_8$, m/z [M+Na^+] 893.6847, found 893.6817.

1-*O*-Octadecyl-2-(4-hydroxy-4-oxobutanoyl)-*sn*-glycero-3-(2-cyanoethylphospho)-(*S*)-2,3-di-*O*-*tert*-butyldimethylsilyl-glycerol (39)

Alcohol **29** (96 mg, 0.12 mmol) and carboxylic acid **44** (51 mg, 0.25 mmol) were dissolved in CH_2Cl_2 (2.5 mL). DCC (76 mg, 0.37 mmol) and DMAP (15 mg, 0.12 mmol) were added and the reaction mixture was stirred at 20 °C for 1 h, then concentrated *in vacuo* and purified by column chromatography (heptane then heptane/EtOAc 2:1) to afford 81 mg of the desired ester, that was dissolved in a mixture of EtOAc (0.7 mL) and MeOH (0.7 mL). Pd/C (10 wt%, 12 mg, 0.012 mmol) was added and the mixture was stirred under an atmosphere of H_2 for 2 h at 20 °C, after which filtration through celite gave 74 mg (73%) of **39** (two diastereoisomers 1:1) as a colorless oil. ^{1}H NMR (300 MHz, $CDCl_3$, two diastereoisomers): δ δ 5.23–5.16 (m, 1H), 4.32–4.13 (m, 5H), 4.06–3.97 (m, 1H), 3.92–3.84 (m, 1H), 3.62–3.53 (m, 4H), 3.48–3.39 (m, 2H), 2.77 (t, *J* = 6.3 Hz, 2H), 2.70–2.64 (m, 4H), 1.59–1.49 (m, 2H), 1.32–1.23 (m, 30H), 0.92–0.86 (m, 21H), 0.10 (s, 3H), 0.09 (s, 3H), 0.07 (s, 6H). ^{13}C NMR (50 MHz, $CDCl_3$, two diastereoisomers): δ 175.1, 171.5, 116.5, 72.1 (2C), 71.2, 69.7, 68.2, 66.7, 64.1, 62.2, 32.1, 29.8 (13C), 29.0 (2C), 26.0 (7C), 22.8, 19.6, 18.4 (2C), 14.2, -4.6 (2C), -5.3 (2C). IR (neat): 2924, 2854, 1737, 1463, 1252, 1152, 1102. HRMS (ESI+) $C_{43}H_{86}NO_{11}PSi_2$, m/z [M+Na^+] 902.5370, found 902.5415.

1-*O*-Octadecyl-2-(4-octanoxy-4-oxobutanoyl)-*sn*-glycero-3-phospho-(*S*)-glycerol (40)

Carboxylic acid **39** (26 mg, 0.031 mmol) and octanol (7.2 µL, 0.045 mmol) were dissolved in CH_2Cl_2 (0.5 mL). DCC (8 mg, 0.04 mmol) and DMAP (2 mg, 0.016 mmol) were added and the reaction mixture was stirred at 20 °C for 1 h, after which the mixture was purified directly by column chromatography (heptane/EtOAc 4:1 then heptane/EtOAc 2:1) to give 12 mg of the desired ester, that was dissolved in CH_2Cl_2 (1.1 mL) along with DBU (1.9 µL, 0.013 mmol). The reaction mixture was stirred for 1 h and then purified directly by column chromatography (heptane/EtOAc 1:1 then CH_2Cl_2/MeOH 9:1) to give 11 mg of a colorless oil, that was dissolved in a mixture of MeCN (1.0 mL) and CH_2Cl_2 (0.33 mL) and cooled to 0 °C. Aqueous HF (40%, 60 µL) was added dropwise and the reaction mixture was allowed to reach 20 °C. After 3.5 h excess reagent was quenched by dropwise addition of $MeOSiMe_3$ (225 µL) and the mixture was stirred for 30 min, after which $NaHCO_3$ (3 mg, 0.035 mmol) was added and the mixture was concentrated *in vacuo* and purified by column chromatography (CH_2Cl_2/MeOH 10:1 then CH_2Cl_2/MeOH 4:1) to give 7 mg (31%) of **40** as a colorless amorphous solid. R_f = 0.38 (CH_2Cl_2/MeOH 4:1). ^{1}H NMR (300 MHz, $CDCl_3$/CD_3OD 4:1): δ 5.18–5.11 (m, 1H), 4.08 (t, *J* = 6.8 Hz, 2H), 3.97–3.90 (m, 4H), 3.85–3.79 (m, 1H), 3.66–3.62 (m, 2H), 3.60–3.55 (m, 2H), 3.47–3.40 (m, 2H), 2.68–2.61 (m, 4H), 1.67–1.58 (m, 2H), 1.58–1.50 (m, 2H), 1.35–1.23 (m, 40H), 0.89 (t, *J* = 6.0 Hz, 3H), 0.88 (t, *J* = 5.8 Hz, 3H). ^{13}C NMR (50 MHz, $CDCl_3$/CD_3OD 4:1): δ 172.3, 172.0, 71.8 (2C), 70.4, 68.1, 67.3, 65.1 (2C), 62.2, 31.7 (2C), 29.6 (18C), 25.8, 24.0, 22.5 (2C),

13.8 (2C). IR (neat): 3352, 2922, 2853, 1736, 1220, 1162, 1118, 1053. HRMS (ESI-) $C_{36}H_{70}O_{11}P$, m/z [M^-] 709.4660, found 709.4687.

1-*O*-Octadecyl-2-(4-phenoxy-4-oxobutanoyl)-*sn*-glycero-3-phospho-(*S*)-glycerol (41)

The synthesis was performed as for **40**, starting from carboxylic acid **39** (30 mg, 0.034 mmol) and phenol (10 mg, 0.10 mmol) and affording 6 mg (25 %) of **41** as a colorless amorphous solid. R_f = 0.14 (CH_2Cl_2/MeOH 4:1). ^{1}H NMR (500 MHz, $CDCl_3$/CD_3OD 4:1): δ 7.38 (t, 2H, *J* = 7.8 Hz), 7.24 (t, *J* = 7.8 Hz, 1H), 7.09 (d, *J* = 7.8 Hz, 2H), 5.22–5.17 (m, 1H), 4.05–3.96 (m, 2H), 3.93–3.89 (m, 2H), 3.79–3.76 (m, 1H), 3.63–3.57 (m, 4H), 3.47–3.38 (m, 2H), 2.90 (t, *J* = 6.7 Hz, 2H), 2.79 (t, *J* = 6.7 Hz, 2H), 1.55–1.49 (m, 2H), 1.31–1.22 (m, 30H), 0.88 (t, *J* = 6.9 Hz, 3H). ^{13}C NMR (50 MHz, $CDCl_3$/CD_3OD 4:1): δ 172.5, 171.7, 150.9, 129.8 (2C), 126.3, 121.8 (2C), 72.6, 72.2, 71.2, 69.2, 66.8, 64.5, 62.5, 32.2, 30.0 (15C), 26.3, 23.0, 14.3. ^{31}P NMR (202 MHz, $CDCl_3$/CD_3OD 4:1): δ –0.64. IR (neat): 3333, 2922, 2852, 1763, 1737, 1251, 1198, 1131, 1068. HRMS (ESI+) $C_{34}H_{58}O_{11}P$, m/z [M^-] 673.3721, found 673.3702.

1-*O*-Octadecyl-2-(2,6-dimethylphenoxy-4-oxobutanoyl)-*sn*-glycero-3-phospho-(*S*)-glycerol (42)

The synthesis was performed as for **40**, starting from carboxylic acid **39** (71 mg, 0.086 mmol) and 2,6-dimethylphenol (32 mg, 0.26 mmol) and affording 9 mg (14 %) of **42** as a colorless amorphous solid. R_f = 0.09 (CH_2Cl_2/MeOH 4:1). ^{1}H NMR (500 MHz, $CDCl_3$/CD_3OD 4:1): δ 7.06–7.05 (m, 3H), 5.20–5.15 (m, 1H), 4.05–3.97 (m, 2H), 3.95–3.89 (m, 2H), 3.82–3.77 (m, 1H), 3.63–3.56 (m, 4H), 3.47–3.38 (m, 2H), 2.95 (t, *J* = 6.7 Hz, 2H), 2.80 (t, *J* = 6.7 Hz, 2H), 2.14 (s, 6H), 1.55–1.49 (m, 2H), 1.30–1.22 (m, 30H), 0.88 (t, *J* = 6.9 Hz, 3H). ^{13}C NMR (50 MHz, $CDCl_3$/CD_3OD 4:1): δ 172.4, 171.1, 148.3, 130.4 (2C), 129.0 (2C), 126.3, 72.6, 72.2, 71.2, 69.2, 66.8, 64.5, 62.5, 32.2, 30.0, 29.3 (13C), 28.9, 26.3, 23.0, 16.4 (2C), 14.3. ^{31}P NMR (202 MHz, $CDCl_3$/CD_3OD 4:1): δ –2.62. IR (neat): 3331, 2922, 2853, 1753, 1738, 1233, 1139, 1058. HRMS (ESI-) $C_{36}H_{62}O_{11}P$, m/z [M^-] 701.7034, found 701.4017.

Benzyl succinate (44)[230]

Succinic anhydride (**43**, 1.0 g, 9.93 mmol), benzyl alcohol (1.12 mL, 10.9 mmol) and DMAP (1.22 g, 10.0 mmol) were dissolved in CH_2Cl_2 (10 mL). The reaction mixture was stirred at 20 °C for 20.5 h, after which CH_2Cl_2 (50 mL) and a saturated aqueous solution of NH_4Cl (50 mL) were added and the organic layer was isolated by extraction with CH_2Cl_2 (2×50 mL). The combined organic phases were dried over Na_2SO_4 and concentration *in vacuo* gave 1.27 g (61%) of **44** as a colorless oil. ^{1}H NMR (300 MHz, $CDCl_3$): δ 7.31–7.22 (m, 5H), 5.07 (s, 2H), 2.68–2.57 (m, 4H). ^{13}C NMR (75 MHz, $CDCl_3$): δ 176.9, 173.2, 136.2, 128.5 (2C), 128.0 (3C), 66.1, 30.8, 30.3.

1-*O*-Octadecyl-2-(11-oxo-(5*Z*,9*Z*,12*E*,14*E*)-prostatetraenoyl)-*sn*-glycero-3-phospho-(*S*)-glycerol (45)

Alcohol **29** (16 mg, 0.021 mmol), DMAP (0.4 mg, 0.003 mmol) and 15-deoxy-$\Delta^{12,14}$-prostaglandin J_2 (0.5 mL, 0.032 M in MeOAc, 0.016 mmol) were dissolved in CH_2Cl_2 (1.5 mL) and DCC (40 µL, 1.0 M in CH_2Cl_2, 0.04 mmol) was added. The reaction mixture was stirred for 4.5 h at 20 °C after which the mixture was concentrated *in vacuo* and purified by column chromatography (heptane/EtOAc 2:1 then heptane/EtOAc 1:2) to give 11 mg of the desired ester that was dissolved in CH_2Cl_2 (0.8 mL). DBU (2 µL, 0.011 mmol) was added and the reaction mixture was stirred for 1 h at 20 °C and then purified directly by column chromatography (CH_2Cl_2/MeOH 10:1) to give 8 mg, that was dissolved in MeCN (0.9 mL) and CH_2Cl_2 (0.3 mL) and cooled to 0 °C. Aqueous HF (40%, 30 µL) was added dropwise and the reaction mixture was allowed to reach 20 °C. After 2.5 h the reaction was quenched by dropwise addition of $MeOSiMe_3$ (0.2 mL) and the mixture was stirred for 30 min, after which $NaHCO_3$ (5 mg, 0.06 mmol) was added and the mixture was concentrated *in vacuo* and purified by column chromatography (CH_2Cl_2/MeOH 10:1 then CH_2Cl_2/MeOH 4:1 then CH_2Cl_2/MeOH/H_2O 65:25:1) to give 4 mg (22%) of **45** as a colorless amorphous solid. R_f = 0.22 (CH_2Cl_2/MeOH 4:1). ^{1}H NMR (500 MHz, $CDCl_3$/CD_3OD 4:1): δ 7.55 (dd, *J* = 5.8, 1.8 Hz, 1H), 6.96 (d, *J* = 11.0 Hz, 1H), 6.39–6.32 (m, 2H), 6.30 (dt, *J* = 15.0, 6.6 Hz, 1H), 5.47 (dt, *J* = 10.4, 7.2 Hz, 1H), 5.36 (dt, *J* = 10.4, 7.2 Hz, 1H), 5.16–5.12 (m, 1H), 3.99–3.91 (m, 4H), 3.81–3.79 (m, 1H), 3.66–3.61 (m, 3H), 3.59–3.56 (m, 2H), 3.49–3.40 (m, 2H), 2.64–2.59 (m, 1H), 2.35–2.30 (m, 3H), 2.28–2.24 (m, 2H), 2.04 (q, *J* = 7.2 Hz, 2H), 1.68–1.62 (m, 2H), 1.54–1.52 (m, 2H), 1.49–1.45 (m, 2H), 1.34–1.31 (m, 4H), 1.30–1.23 (m, 30H), 0.92–0.87 (m, 6H). ^{13}C NMR (50 MHz, $CDCl_3$/CD_3OD 4:1): δ 198.9, 173.9, 162.5, 148.3, 135.3 (2C), 133.1, 131.9, 126.0(2C), 72.1 (2C), 71.3, 69.5, 66.7, 64.5, 62.6, 44.0, 34.1, 33.9, 32.3, 31.8, 30.9, 30.1 (12C), 29.7, 28.2, 27.0, 26.4, 25.1, 23.0, 22.9, 14.3 (2C). ^{31}P NMR (202 MHz, $CDCl_3$/CD_3OD 4:1): δ 3.60. IR (neat) 3364, 2923, 2853, 1733, 1695, 1632, 1464, 1259, 1207, 1097, 1058, 800 cm^{-1}. HRMS (ESI+) $C_{44}H_{76}O_{10}PNa$, m/z [M+H^+] 819.5147, found 819.5166.

1-Stearoyl-2-(11-oxo-(5*Z*,9*Z*,12*E*,14*E*)-prostatetraenoyl)-*sn*-glycero-3-phospho-(*S*)-glycerol (46)

Alcohol **47** (18 mg, 0.037 mmol) and phosphoamidite **27** (26 mg, 0.050 mmol) were dissolved in CH_2Cl_2 (260 µL) and the mixture was stirred for 15 min at 20 °C before tetrazole (0.45 M in MeCN, 111 µL, 0.050 mmol) was added. 30 min later ^{t}BuOOH (5.5 M in nonane, 9 µL, 0.050 mmol) was added and the reaction mixture was stirred for 30 min after which the mixture was concentrated *in vacuo* and purified by column chromatography (heptane/EtOAc 3:1) to give 30 mg that was dissolved in CH_2Cl_2 (0.70 mL) and H_2O (40 µL). DDQ (12 mg, 0.052 mmol) was added and the reaction mixture was stirred for 3 h at 20 °C. Na_2SO_4 was added and the mixture was purified directly by column chromatography (CH_2Cl_2 then heptane/EtOAc 1:1) to afford 21 mg of **48**, which was dissolved in CH_2Cl_2 (0.40 mL) along with 15-deoxy-$\Delta^{12,14}$-prostaglandin J_2 (10 mg, 0.32

mmol) and DMAP. DCC (13 mg, 0.065 mmol) was added and the reaction mixture was stirred for 2.5 h at 20 °C, then purified directly by column chromatography (toluene then toluene/EtOAc 5:1) to afford 15 mg that was dissolved in CH_2Cl_2 (1.2 mL) and treated with DBU (2.2 µL, 0.015 mmol). The reaction mixture was stirred for 30 min at 20 °C and then purified directly by column chromatography (heptane/EtOAc 1:1 then CH_2Cl_2/MeOH 9:1) to afford 7 mg, that was dissolved in MeCN (560 µL), CH_2Cl_2 (352 µL) and H_2O (34 µL) and cooled to 0 °C. Aqueous HF (40%, 34 µL) was added dropwise and the reaction mixture was allowed to reach 20 °C. After 3.5 h the reaction was quenched by dropwise addition of $MeOSiMe_3$ (120 µL) and the mixture was stirred for 30 min, after which $NaHCO_3$ (1 mg, 0.012 mmol) was added and the mixture was concentrated *in vacuo* and purified by column chromatography (CH_2Cl_2/MeOH 20:1 then CH_2Cl_2/MeOH 5:1 then CH_2Cl_2/MeOH/H_2O 65:25:1) to give 4 mg (13%) of **46** as a colorless amorphous solid. R_f = 0.63 (CH_2Cl_2/MeOH 5:1). ^{1}H NMR (300 MHz, $CDCl_3$/CD_3OD 4:1): δ 7.54 (dd, *J* = 6.5, 2.5 Hz, 1H), 6.96 (d, *J* = 10.5 Hz, 1H), 6.40–6.28 (m, 3H), 5.51–5.35 (m, 2H), 5.25–5.18 (m, 1H), 4.39 (dd, *J* = 12.1, 3.4 Hz, 1H), 4.16 (dd, *J* = 12.1, 6.4 Hz, 1H), 3.99–3.85 (m, 4H), 3.82–3.77 (m, 1H), 3.66–3.60 (m, 3H), 2.67–2.56 (m, 1H), 2.41–2.21 (m, 7H), 2.05 (q, *J* = 7.0 Hz, 2H), 1.70–1.55 (m, 4H), 1.51–1.40 (m, 2H), 1.38–1.22 (m, 32H), 0.91 (t, *J* = 7.0 Hz, 3H), 0.88 (t, *J* = 6.2 Hz, 3H). ^{13}C NMR (50 MHz, $CDCl_3$/CD_3OD 4:1): δ 197.2, 174.3, 173.4, 162.3, 148.2, 135.3 (2C), 132.8, 131.7, 126.1, 126.0, 71.2, 70.9, 66.8, 64.0, 62.8, 62.6, 43.9, 34.4, 33.8, 32.4, 31.7, 30.0 (14C), 28.8, 26.9, 25.2, 25.0, 23.0, 22.8, 14.3 (2C). IR (neat) 3391, 2924, 2854, 1737, 1697, 1633, 1459, 1377, 1227, 1103, 1066, 816 cm^{-1}. HRMS (ESI+) $C_{44}H_{74}O_{11}PNa$, m/z [M+H$^+$] 833.4939, found 833.4958.

1-Stearoyl-2-*O*-(4-methoxybenzyl)-*sn*-glycerol (47)

Alcohol **32** (189 mg, 0.091 mmol) and PMBTCA (193 mg, 0.70 mmol) were dissolved in toluene (4.0 mL) and $La(OTf)_3$ (12 mg, 0.02 mmol) was added. The reaction mixture was stirred at 20 °C for 3.5 h, then concentrated *in vacuo* and purified by column chromatography (heptane then heptane/EtOAc 7:1) to give 194 mg that subsequently was dissolved in a mixture of DMSO (6.5 mL), THF (5.4 mL) and H_2O (0.65 mL) in a flask protected from light. NBS (274 mg, 1.54 mmol) was added and the reaction mixture was stirred at 20 °C for 17 h, after which the reaction was quenched by addition of an aqueous solution of $Na_2S_2O_3$ (1%, 15 mL). The mixture was stirred at 20 °C for 10 min, then the organic layer was isolated by extraction with Et_2O (3x40 mL). The combined organic phases were dried over Na_2SO_4, filtered, concentrated *in vacuo* and purified by column chromatography (heptane/EtOAc 2:1) to give 120 mg (63%) of **47** as a colorless oil. R_f = 0.51 (heptane/EtOAc 1:1). ^{1}H NMR (300 MHz, $CDCl_3$): δ 7.27 (d, *J* = 8.7 Hz, 2H), 6.89 (d, *J* = 8.7 Hz, 2H), 4.65 (d, *J* = 11.3 Hz, 1H), 4.52 (d, *J* = 11.3 Hz, 1H), 4.23-4.20 (m, 2H), 3.81 (s, 3H), 3.71–3.56 (m, 3H), 2.32 (t, *J* = 7.5 Hz, 2H), 1.67–1.55 (m, 2H), 1.33–1.21 (m, 28H), 0.88 (t, *J* = 6.3 Hz, 3H). ^{13}C NMR (50 MHz, $CDCl_3$): δ 174.0, 159.6, 130.1, 129.7 (2C), 114.1 (2C), 77.3, 72.0, 62.9, 62.2, 55.4, 38.2, 34.4, 29.6 (12C), 25.1, 22.8,

14.3. IR (neat) 2926, 2855, 1740, 1514, 1464, 1251, 1106, 1036, 836 cm^{-1}. HRMS (ESI+) $C_{29}H_{50}O_5$, m/z [M+Na^+] 501.3550, found 501.3560.

1-*O*-(4-hydroxy-4-oxobutanoyl) 1α,25-dihydroxyvitamin D_3 (1-*O*-51) and 3-*O*-(4-hydroxy-4-oxobutanoyl) 1α,25-dihydroxyvitamin D_3 (3-*O*-51)

Calcitriol (10 mg, 024 mmol), succinic anhydride (2.4 mg, 0.024 mmol) and DMAP (2.9 mg, 0.024 mmol) were dissolved in a mixture of CH_2Cl_2 (0.66 mL) and THF (80 µL). The reaction mixture was stirred at 20 °C for 40 h and then purified directly by column chromatography (heptane/EtOAc 1:3 then CH_2Cl_2/MeOH 4:1) to afford 3.6 mg (29%) as a 1:1 mixture of **1-*O*-51** and **3-*O*-51** (deterimed by 300 MHz ^{1}H NMR). Also, 5.6 mg (56%) of Calcitriol was reisolated. ^{1}H NMR (300 MHz, $CDCl_3$, for **1-*O*-51**): δ 6.37 (d, *J* = 11.2 Hz, 1H), 5.91 (d, *J* = 11.2 Hz, 1H), 5.53–5.46 (m, 1H), 5.30 (s, 1H), 5.03 (s, 1H), 4.18–4.09 (m, 1H), 2.87–2.24 (m, 7H), 2.20-0.80 (m, 20H), 1.21 (s, 6H), 0.93 (d, *J* = 5.5 Hz, 3H), 0.51 (s, 3H). ^{1}H NMR (300 MHz, $CDCl_3$, for **3-*O*-51**): δ 6.32 (d, *J* = 11.2 Hz, 1H), 6.02 (d, *J* = 11.2 Hz, 1H), 5.36 (s, 1H), 5.27–5.20 (m, 1H), 5.03 (s, 1H), 4.42–4.35 (m, 1H), 2.87–2.24 (m, 7H), 2.20–0.80 (m, 20H), 1.21 (s, 6H), 0.93 (d, *J* = 5.5 Hz, 3H), 0.54 (s, 3H). MALDI-TOF (ES^+) Calcd. for $C_{31}H_{48}O_6$ (M+Na^+) 539.33. Found: 539.20.

1-*O*-(6-hydroxy-6-oxohexanoyl) 1α,25-dihydroxyvitamin D_3 (1-*O*-52) and 3-*O*-(6-hydroxy-6-oxohexanoyl) 1α,25-dihydroxyvitamin D_3 (3-*O*-52)

Calcitriol (10 mg, 0.024 mmol) and carboxylic acid **58** (7 mg, 0.03 mmol) were dissolved in CH_2Cl_2 (0.66 mL) and THF (80 µL). EDCI (6 mg, 0.03 mmol) and DMAP (4 mg, 0.03 mmol) were added and the reaction mixture was stirred at 20 °C. After 2 h further amounts of the carboxylic acid **58** (2 mg, 0.008 mmol), EDCI (2 mg, 0.01 mmol) and DMAP (2 mg, 0.016 mmol) were added and the mixture was stirred for 3 h more, then concnetrated *in vacuo* and purified by column chromatography (heptane/EtOAc 3:1 then heptane/EtOAc 1:1) to afford 4.1 mg, that was dissolved in THF (0.5 mL) and TBAF (1.0 M in THF, 20 µL, 0.019 mmol) was added and the reaction mixture was stirred at 20 °C. After 2 h an additional amount of TBAF (1.0 M in THF, 20 µL, 0.019 mmol) was added and the mixture was stirred for 1 h more, then EtOAc (1.5 mL) and heptane (1.5 mL) were added and the mixture was purified directly by column chromatography (heptane/EtOAc 1:1 then CH_2Cl_2/MeOH 10:1) to afford 2.5 mg (19%) as a 1:3 mixture of **1-*O*-52** and **3-*O*-52** (determined by 500 MHz ^{1}H NMR). ^{1}H NMR (500 MHz, $CDCl_3$, for **1-*O*-52**): δ 6.38 (d, *J* = 11.2 Hz, 1H), 5.89 (d, *J* = 11.2 Hz, 1H), 5.52–5.50 (m, 1H), 5.34 (s, 1H), 5.05 (s, 1H), 4.18–4.13 (m, 1H), 2.85–2.79 (m, 1H), 2.65 (dd, *J* = 13.0, 3.7 Hz, 1H), 2.44–0.80 (m, 29H), 1.23 (s, 6H), 0.93 (d, *J* = 6.5 Hz, 3H), 0.52 (s, 3H). ^{1}H NMR (500 MHz, $CDCl_3$, for **3-*O*-52**): δ 6.33 (d, *J* = 11.4 Hz, 1H), 6.03 (d, *J* = 11.4 Hz, 1H), 5.36 (s, 1H), 5.26–5.22 (m, 1H), 5.03 (s, 1H), 4.44–4.40 (m, 1H), 2.85–2.79 (m, 1H), 2.59 (dd, *J* = 13.4, 2.7 Hz, 1H), 2.44–0.80 (m, 29H), 1.23 (s, 6H), 0.95 (d, *J* = 6.5 Hz, 3H), 0.55 (s, 3H). IR (neat): 3399, 2930, 2871, 1732, 1457, 1376, 1260, 1064. MALDI-TOF (ES^+) Calcd. for $C_{33}H_{52}O_6$ (M+Na^+) 567.37. Found: 567.19.

1-*O*-Octadecyl-2-((5-((5*Z*,7*E*)-(1*S*,3*R*)-9,10-seco-5,7,10(19)-cholestatriene-3,25-diol-1-oxy)-5-oxopentyloxy)-carbonyl)-*sn*-glycero-3-phospho-(S)-glycerol (1-*O*-53) and 1-*O*-Octadecyl-2-((5-((5*Z*,7*E*)-(1*S*,3*R*)-9,10-seco-5,7,10(19)-cholestatriene-1,25-diol-3-oxy)-5-oxopentyloxy)-carbonyl)-*sn*-glycero-3-phospho-(*S*)-glycerol (3-*O*-53)

Carboxylic acid **72** (20 mg, 0.022 mmol) and calcitriol (9 mg, 0.022 mmol) were dissolved in THF (1.3 mL). 2,4,6-Trichlorobenzoyl chloride (4.4 µL, 0.029 mmol) and then DMAP (5 mg, 0.044 mmol) were added and the mixture was stirred at 20 °C for 1.5 h, then concentrated *in vacuo* and purified by column chromatography (CH_2Cl_2 then CH_2Cl_2/EtOAc 1:1) to give 15 mg of a colorless oil, that was dissolved in CH_2Cl_2 (1.0 mL) along with DBU (1.8 µL, 0.012 mmol). The reaction mixture was stirred at 20 °C for 1 h and then purified directly by column chromatography (heptane/EtOAc 1:3 then CH_2Cl_2/MeOH 9:1) to give 13 mg of a colorless oil, that was dissolved in a mixture of MeCN (1.0 mL), CH_2Cl_2 (0.33 mL) and H_2O (0.16 mL) and cooled to 0 °C. Aqueous HF (40%, 60 µL) was added and the reaction mixture was allowed to reach 20 °C. After 3 h excess reagent was quenched by dropwise addition of $MeOSiMe_3$ (0.20 mL) and the mixture was stirred for 30 min, after which $NaHCO_3$ (3 mg, 0.036 mmol) was added and the mixture was concentrated *in vacuo* and purified by column chromatography (CH_2Cl_2/MeOH 9:1 then CH_2Cl_2/MeOH 4:1) to give 7 mg (30%) as a 1:4 mixture of **1-*O*-53** and **3-*O*-53** (determined by 500 MHz ^{1}H NMR) as a colorless amorphous solid. R_f = 0.10 (CH_2Cl_2/MeOH 4:1). ^{1}H NMR (500 MHz, $CDCl_3$/CD_3OD 4:1, for **1-*O*-53**): δ 6.37 (d, *J* = 11.1 Hz, 1H), 5.90 (d, *J* = 11.1 Hz, 1H), 5.48–5.45 (m, 1H), 5.33 (s, 1H), 5.05 (s, 1H), 5.00–4.95 (m, 1H), 4.16–4.07 (m, 3H), 4.06–3.99 (m, 2H), 3.96–3.89 (m, 2H), 3.83–3.77 (m, 1H), 3.66–3.59 (m, 4H), 3.49–3.40 (m, 2H), 2.63–2.59 (m, 1H), 2.47–2.40 (m, 1H), 2.40–2.30 (m, 3H), 2.16–0.93 (m, 56H), 1.20 (s, 6H), 0.94 (d, *J* = 6.4 Hz, 3H), 0.88 (t, *J* = 6.9 Hz, 3H), 0.51 (s, 3H). ^{1}H NMR (500 MHz, $CDCl_3$/CD_3OD 4:1, for **3-*O*-53**): δ 6.29 (d, *J* = 11.1 Hz, 1H), 6.05 (d, *J* = 11.1 Hz, 1H), 5.38 (s, 1H), 5.23–5.19 (m, 1H), 5.01 (s, 1H), 5.00–4.95 (m, 1H), 4.38–4.34 (m, 1H), 4.16–4.07 (m, 2H), 4.06–3.99 (m, 2H), 3.96–3.89 (m, 2H), 3.83–3.77 (m, 1H), 3.66–3.59 (m, 4H), 3.49–3.40 (m, 2H), 2.87–2.77 (m, 1H), 2.58–2.53 (m, 1H), 2.40–2.30 (m, 3H), 2.16–0.93 (m, 56H), 1.20 (s, 6H), 0.94 (d, *J* = 6.4 Hz, 3H), 0.88 (t, *J* = 6.9 Hz, 3H), 0.55 (s, 3H). ^{13}C NMR (50 MHz, $CDCl_3$/CD_3OD 4:1, for **3-*O*-53**): δ 173.5, 155.2, 147.9, 143.2, 133.2, 124.7, 117.5, 111.6, 75.6, 72.3 (2C), 71.2, 71.0, 70.7, 69.8, 68.8, 68.2, 65.4, 62.7, 57.0, 56.7, 46.3, 44.6, 41.6, 40.9, 40.0, 36.8, 36.5, 34.3, 32.3, 30.0 (16C), 28.0, 26.3 (2C), 24.0, 23.0, 22.5, 21.5, 21.2, 19.0, 14.3, 12.2. IR (neat): 3371, 2923, 2853, 1737, 1641, 1464, 1377, 1261, 1104, 1065. HRMS (ESI-) $C_{57}H_{100}O_{14}P$, m/z [M^-] 1039.6856, found 1039.6833.

1-*O*-(2,2-difluorobutanoyl) 1α,25-dihydroxyvitamin D_3 (1-*O*-56) and 3-*O*-(2,2-difluorobutanoyl) 1α,25-dihydroxyvitamin D_3 (3-*O*-56)

Calcitriol (5.0 mg, 0.012 mmol) and 2,2-difluorobutanoic acid (1.5 µL, 0.014 mmol) were dissolved in CH_2Cl_2 (0.33 mL) and THF (40 µL). EDCI (3 mg, 0.016 mmol) and DMAP (2 mg, 0.016 mmol) were added and the reaction mixture was stirred at 20 °C. After 2 h

further amounts of 2,2-difluorobutanoic acid (1.5 μL, 0.014 mmol), EDCI (3 mg, 0.016 mmol) and DMAP (2 mg, 0.016 mmol) were added and the mixture was stirred for 18 h more, then concnetrated *in vacuo* and purified by column chromatography (heptane/EtOAc 3:1 then heptane/EtOAc 1:1) to afford 0.5 mg (8%) of pure **3-*O*-56** and 1.1 mg (17%) as a 1:1 mixture of **1-*O*-56** and **3-*O*-56** (determined by 500 MHz ^{1}H NMR). Also, 2.0 mg (40%) of calcitriol was reisolated. ^{1}H NMR (500 MHz, $CDCl_3$, for **1-*O*-56**): δ 6.42 (d, *J* = 11.2 Hz, 1H), 5.89 (d, *J* = 11.2 Hz, 1H), 5.64–5.61 (m, 1H), 5.43 (s, 1H), 5.14 (s, 1H), 4.22–4.17 (m, 1H), 2.83 (dd, *J* = 10.6, 3.5 Hz, 1H), 2.67 (dd, *J* = 12.2, 4.2 Hz, 1H), 2.32 (dd, *J* = 12.2, 9.5 Hz, 1H), 2.24–0.80 (m, 22H), 1.23 (s, 6H), 1.01 (t, *J* = 7.5 Hz, 3H), 0.94 (d, *J* = 6.2 Hz, 3H), 0.50 (s, 3H). ^{1}H NMR (500 MHz, $CDCl_3$, for **3-*O*-56**): δ 6.37 (d, *J* = 11.2 Hz, 1H), 6.00 (d, *J* = 11.2 Hz, 1H), 5.40–5.35 (m, 2H), 5.05 (s, 1H), 4.47–4.43 (m, 1H), 2.80 (dd, *J* = 12.1, 4.1 Hz, 1H), 2.68 (dd, *J* = 13.4, 3.0 Hz, 1H), 2.49 (dd, *J* = 13.4, 6.8 Hz, 1H), 2.16–0.80 (m, 22H), 1.23 (s, 6H), 1.02 (t, *J* = 7.5 Hz, 3H), 0.95 (d, *J* = 6.4 Hz, 3H), 0.55 (s, 3H). MALDI-TOF (ES^+) Calcd. for $C_{31}H_{48}F_2O_4$ ($M+Na^+$) 545.34. Found: 545.05.

2-Trimethylsilylethyl adipate (58)[198]

Adipic acid (**57**, 730 mg, 5.0 mmol), 2-trimethylsilylethanol (1.01 mL, 7.1 mmol) and $TsOH{\cdot}H_2O$ (5 mg, 0.025 mmol) were dissolved in toluene (5.0 mL). A Dean Stark distilling trap was attached to the reaction flask and the reaction mixture was heated to reflux. After 2.5 h the mixture was purified directly by column chromatography (heptane then heptane/EtOAc 3:1) to afford 587 mg (48%) of **58** as a colorless oil. ^{1}H NMR (300 MHz, $CDCl_3$): δ 11.6 (s, 1H, *OH*), 4.17–4.11 (m, 2H), 2.39–2.26 (m, 4H), 1.69–1.61 (m, 4H), 1.00–0.92 (m, 2H), 0.01 (s, 9H). ^{13}C NMR (75 MHz, $CDCl_3$): δ 179.7, 173.6, 62.7, 34.1, 33.8, 24.4, 24.2, 17.4, –1.4 (3C).

Benzyl 4-pentenoate (60)

4-Pentenoic acid (**59**, 2.0 g, 20.0 mmol), BnOH (3.1 mL, 30.0 mmol) and DMAP (1.2 g, 10.0 mmol) were dissolved in CH_2Cl_2 (50 mL). EDCI (5.0 g, 26.0 mmol) was added and the reaction mixture was stirred at 20 °C for 1.5 h, then the mixture was concentrated *in vacuo* and purified by column chromatography (heptane then heptane/EtOAc 5:1) to afford 2.46 g (65%) of **60** as a colorless oil. R_f = 0.77 (heptane/EtOAc 1:1). ^{1}H NMR (300 MHz, $CDCl_3$):[231] δ 7.30–7.24 (m, 5H), 6.05 (tdd, *J* = 5.8, 10.3, 16.5 Hz, 1H), 5.04 (s, 2H), 5.01–4.89 (m, 2H), 2.41–2.30 (m, 4H). ^{13}C NMR (75 MHz, $CDCl_3$): δ 172.9, 136.7, 136.1, 128.6 (2C), 128.3 (3C), 115.7, 66.3, 33.6, 28.9.

7-Ethoxy-6,6-difluoro-7-oxoheptanoic acid (62) using $NiCl_2$ and Zn

$NiCl_2{\cdot}6H_2O$ (110 mg, 0.46 mmol) and Zn (312 mg, 4.80 mmol) were dissolved in THF (4.8 mL), one drop of H_2O was added and the mixture was stirred at 20 °C for 10 min under N_2 atmosphere. Then alkene **60** (913 mg, 4.80 mmol) in THF (0.9 ml) and ethyl 2,2-difluoro-2-iodo-acetate (**61**, 600 mg, 2.40 mmol) in THF (0.9 mL) were added. The

reaction mixture was stirred at 20 °C for 16 h and then transferred to a flask with a saturated aqueous solution of NH_4Cl (15 mL) and Et_2O (30 mL). The black solid was removed by filtration and the organic layer was isolated by extraction with Et_2O (2×20 mL), the combined organic layers were dried over Na_2SO_4 and concentrated *in vacuo*. The residue was purified by column chromatography (heptane/EtOAc 10:1) to afford 344 mg of a colorless oil, that was dissolved in EtOAc (12 mL) and Pd/C (10 wt%, 51 mg, 0.058 mmol) was added. The mixture was stirred at 20 °C for 1 h under an atmosphere of H_2, after which filtration through celite gave 245 mg (46%) of **62** as a colorless oil. ^{1}H NMR (300 MHz, $CDCl_3$): δ 11.4 (s, 1H, *OH*), 4.33 (q, *J* = 7.1 Hz, 2H), 2.39 (t, *J* = 7.3 Hz, 2H), 2.17–2.01 (m, 2H), 1.71 (p, *J* = 7.3 Hz, 2H), 1.61–1.50 (m, 2H), 1.36 (t, *J* = 7.1 Hz, 3H). ^{13}C NMR (75 MHz, $CDCl_3$): δ 179.7, 164,4 (t, *J* = 33 Hz), 116,2 (t, *J* = 250 Hz), 63.0, 34.2 (t, *J* = 23.4 Hz), 33.8, 24.1, 21.1 (t, *J* = 4.4 Hz), 14.1. ^{19}F NMR (282 MHz, $CDCl_3$): δ –106.5 (t, *J* = 16.8 Hz). IR (neat): 2944, 2878, 1760, 1706, 1181, 1095, 1020. HRMS (ESI+) $C_9H_{14}O_4F_2$, m/z [M+NH_4^+] 224.1204, found 224.1200.

7-Ethoxy-6,6-difluoro-7-oxoheptanoic acid (62) using $Na_2S_2O_4$

Alkene **60** (456 mg, 2.40 mmol) and ethyl 2,2-difluoro-2-iodo-acetate (**61**, 600 mg, 2.40 mmol) were dissolved in a mixture of MeCN (7.2 mL) and H_2O (2.4 mL) and cooled to 0 °C. A mixture of $Na_2S_2O_4$ (692 mg, 3.60 mmol) and $NaHCO_3$ (302 mg) was added and the reaction mixture was allowed to reach 20 °C. After 15.5 h H_2O (10 mL) was added and the organic layer was isolated by extraction with Et_2O (2×40 mL), the combined organic layers were dried over Na_2SO_4, filtered and concentrated *in vacuo*. The residue was dissolved in Et_2O (4.3 mL) and DBU (0.32 mL, 2.12 mmol) was added and the mixture was stirred at 20 °C. After 3.5 h a saturated aqueous solution of NH_4Cl (40 mL) was added and the organic layer was isolated by extraction with Et_2O (2×60 mL). The combined organic layers were dried over Na_2SO_4 and concentrated *in vacuo*. The residue was purified by column chromatography (heptane/EtOAc 6:1 then heptane/EtOAc 3:1) to afford 415 mg of a colorless oil that was dissolved in EtOAc (18.3 mL) along with Pd/C (10 wt%, 79 mg, 0.065 mmol). The mixture was stirred at 20 °C for 3 h under an atmosphere of H_2, after which filtration through celite gave 298 mg (55%) of **62** as a colorless oil.

Lithium 2,2-difluoro-7-oxo-7-(2-(trimethylsilyl)-ethoxy)-heptanoate (63)

Carboxylic acid **62** (81 mg, 0.36 mmol) and 2-trimethylsilyl ethanol (67 µL, 0.47 mmol) were dissolved in THF (3.6 mL). 2,4,6-Trichlorobenzoyl chloride (61 µL, 0.40 mmol) and then DMAP (88 mg, 0.72 mmol) were added. The mixture was stirred at 20 °C for 50 min, then concentrated *in vacuo* and purified by column chromatography (heptane/EtOAc 8:1) to give 117 mg of a colorless oil, that was dissolved in THF (5.5 mL) and H_2O (1.4 mL) and cooled to 0 °C. To the cold solution LiOH (2.9 mg, 0.12 mmol) was added and after 20 min and 40 min the same amount of LiOH (2.9 mg, 0.12 mmol) was added. After 1 h toluene (40 mL) was added and the mixture was concentrated *in vacuo* to afford 108 mg (99%) of **63** as a colorless amorphous solid. ^{1}H NMR (300 MHz, $CDCl_3$): δ 4.19–4.12 (m,

2H), 2.26 (t, *J* = 7.2 Hz, 2H), 2.06–1.85 (m, 2H), 1.65–1.51 (m, 2H), 1.50–1.36 (m, 2H), 1.02–0.92 (m, 2H), 0,03 (s, 9H). ^{13}C NMR (50 MHz, $CDCl_3$): δ 175.0, 171.1 (t, *J* = 33 Hz), 118.3 (t, *J* = 244 Hz), 63.1, 34.2, 33.6 (t, *J* = 23 Hz), 24.4, 21.4, 17.2, –1.4. ^{19}F NMR (282 MHz, $CDCl_3$): δ –106.1. IR (neat): 2954, 2899, 1731, 1639, 1452, 1249, 1099 cm^{-1}. HRMS (ESI+) $C_{12}H_{22}O_4F_2Si$, m/z [M+NH_4^+] 314.1599, found 314.1598.

Lithium 7-(*tert*-butoxy)-2,2-difluoro-7-oxoheptanoate (64)

The synthesis was performed as for **63**, starting from carboxylic acid **62** (64 mg, 0.29 mmol) and *tert*-butanol (53 μL, 0.57 mmol) and affording 74 mg (86 %) of **64** as a colorless amorphous solid. ^{1}H NMR (300 MHz, $CDCl_3$): δ 2.26–2.12 (m, 2H), 2.05–1.83 (m, 2H), 1.63–1.48 (m, 2H), 1.48–1.35 (m, 11H). ^{13}C NMR (75 MHz, $CDCl_3$): δ 174.4, 171.2 (t, *J* = 29.0 Hz), 118.2 (t, *J* = 249 Hz), 81.0, 35.4, 33.9 (t, *J* = 24.7 Hz), 28.1 (3C), 24.6, 21.1. ^{19}F NMR (282 MHz, $CDCl_3$): δ –106.2 (t, *J* = 17.2 Hz). IR (neat): 3468, 2978, 2936, 1727, 1637, 1451, 1368, 1152, 1100. HRMS (ESI+) $C_{11}H_{18}O_4F_2$, m/z [M+NH_4^+] 270.1517, found 270.1517.

1-*O*-Octadecyl-2-(7-ethoxy-6,6-difluoro-7-oxoheptanoyl)-*sn*-glycero-3-phospho-(*S*)-glycerol (66)

Alcohol **29** (40 mg, 0.051 mmol) and carboxylic acid **62** (17 mg, 0.077 mmol) were dissolved in THF (1.0 mL). 2,4,6-Trichlorobenzoyl chloride (12 μL, 0.077 mmol) and then DMAP (13 mg, 0.10 mmol) were added and the reaction mixture was stirred at 20 °C for 1 h, then concentrated *in vacuo* and purified by column chromatography (heptane/EtOAc 5:1 then hepatne/EtOAc 3:1) to afford 43 mg of a colorless oil, that was dissolved in CH_2Cl_2 (4.0 mL) along with DBU (6.0 μL, 0.040 mmol). The reaction mixture was stirred at 20 °C for 1 h and then purified directly by column chromatography (heptane/EtOAc 1:1 then CH_2Cl_2/MeOH 9:1) to give 38 mg of a colorless oil, that was dissolved in a mixture of MeCN (3.3 mL) and CH_2Cl_2 (1.1 mL) and cooled to 0 °C. Aqueous HF (40%, 0.20 mL) was added and the reaction mixture was allowed to reach 20 °C. After 3.5 h excess reagent was quenched by dropwise addition of $MeOSiMe_3$ (0.75 mL) and the mixture was stirred for 30 min, after which $NaHCO_3$ (10 mg, 0.12 mmol) was added and the mixture was concentrated *in vacuo* and purified by column chromatography (CH_2Cl_2/MeOH 10:1 then CH_2Cl_2/MeOH 4:1) to give 25 mg (67%) of **66** as a colorless amorphous solid. R_f = 0.11 (CH_2Cl_2/MeOH 4:1). ^{1}H NMR (500 MHz, $CDCl_3$/CD_3OD 4:1): δ 5.19–5.14 (m, 1H), 4.33 (q, *J* = 7.1 Hz, 2H), 4.12–4.03 (m, 2H), 4.01–3.95 (m, 2H), 3.80–3.85 (m, 1H), 3.64–3.61 (m, 2H), 3.59–3.57 (m, 2H), 3.49–3.39 (m, 2H), 2.39 (t, *J* = 7.4 Hz, 2H), 2.14–2.04 (m, 2H), 1.73–1.67 (m, 2H), 1.57–1.51 (m, 4H), 1.36 (t, *J* = 7.1 Hz, 3H), 1.32–1.23 (m, 30H), 0.88 (t, *J* = 6.9 Hz, 3H). ^{13}C NMR (50 MHz, $CDCl_3$/CD_3OD 4:1): δ 173.4, 164.8, 116.5 (t, *J* = 250 Hz), 72.2, 71.7, 71.0, 69.0, 67.7, 65.4, 63.4, 62.2, 34.1 (t, *J* = 23 Hz), 33.9, 32.3, 29.8 (13C), 26.3, 24.6, 23.0, 21.3, 14.3, 14.1. ^{31}P NMR (202 MHz, $CDCl_3$/CD_3OD 4:1): δ –0.47. IR (neat): 3406, 2924, 2853, 1765, 1738, 1452, 1241, 1098, 1065, 1044 cm^{-1}. HRMS (ESI-) $C_{33}H_{62}O_{11}F_2P$, m/z [M^-] 703.4002, found 703.3981.

7-Benzyloxy- 6,6-difluoro-7-oxoheptanoic acid (67)

Lithium salt **64** (31 mg, 0.12 mmol) and benzyl alcohol (19 µL, 0.18 mmol) were dissolved in THF (1.1 mL). 2,4,6-Trichlorobenzoyl chloride (21 µL, 0.14 mmol) and then DMAP (29 mg, 0.24 mmol) were added and the mixture was stirred at 20 °C for 3 h, then concentrated *in vacuo* and purified by column chromatography (heptane/EtOAc 10:1) to give 27 mg of a colorless oil, that was dissolved in CH_2Cl_2 (2.0 mL). Triisopropylsilane (79 µL, 0.40 mmol) and TFA (0.36 mL, 4.74 mmol) were added and after stirring for 1 h at 20 °C toluene (5 mL) was added and the mixture was concentrated *in vacuo*. The residue was purified by column chromatography (heptane/EtOAc 10:1 then heptane/EtOAc 2:1) to give 13 mg (38%) of **67** as a colorless oil. ^{1}H NMR (300 MHz, $CDCl_3$): δ 7.40–7.38 (m, 5H), 5.29 (s, 2H), 2.34 (t, *J* = 7.3 Hz, 2H), 2.17–2.00 (m, 2H), 1.67 (p, *J* = 7.3 Hz, 2H), 1.55–1.44 (m, 2H). ^{13}C NMR (75 MHz, $CDCl_3$): δ 179.2, 164.2 (t, *J* = 33 Hz), 134.4, 129.0, 128.9, 128.6, 116.2 (t, *J* = 250 Hz), 68.4, 34.3 (s, *J* = 23 Hz), 33.6, 24.1, 21.1 (t, *J* = 4.4 Hz). ^{19}F NMR (282 MHz, $CDCl_3$): δ –106.2 (t, *J* = 16.8 Hz). IR (neat): 3036, 2949, 1763, 1706, 1456, 1293, 1172, 1098. HRMS (ESI+) $C_{14}H_{16}O_4F_2$, m/z [M+NH_4^+] 304.1361, found 304.1358.

1-*O*-Octadecyl-2-(7-hydroxy-6,6-difluoro-7-oxoheptanoyl)-*sn*-glycero-3-(2-cyanoethylphospho)-(*S*)-2,3-di-*O*-*tert*-butyldimethylsilyl-glycerol (68)

Alcohol **29** (25 mg, 0.032 mmol) and carboxylic acid **67** (13 mg, 0.045 mmol) were dissolved in THF (1.0 mL). 2,4,6-Trichlorobenzoyl chloride (6.9 µL, 0.045 mmoL) and then DMAP (8 mg, 0.064 mmol) were added and the reaction mixture was stirred at 20 °C for 21 h, then concentrated *in vacuo* and purified by column chromatography (heptane/EtOAc 10:1 then hepatane/EtOAc 3:1) to afford 20 mg of the desired ester, that was dissolved in a mixture of EtOAc (2.0 mL) and THF (1.0 mL). Pd/C (10 wt%, 10 mg, 0.01 mmol) was added and the mixture was stirred under an atmosphere of H_2 for 4 h at 20 °C, after which filtration through celite gave 16 mg (52%) of **68** (two diastereoisomers 1:1) as a colorless oil. ^{1}H NMR (300 MHz, $CDCl_3$, two diastereoisomers): δ 5.21–5.12 (m, 1H), 4.32–4.11 (m, 5H), 4.03–3.95 (m, 1H), 3.90–3.83 (m, 1H), 3.60–3.50 (m, 4H), 3.46–3.38 (m, 2H), 2.78 (t, *J* = 5.7 Hz, 2H), 2.37 (t, *J* = 6.8 Hz, 2H), 2.10–1.92 (m, 2H), 1.72–1.60 (m, 2H), 1.60–1.42 (m, 4H), 1.35–1.17 (m, 30H), 0.93–0.81 (m, 21H), 0.10 (s, 3H), 0.09 (s, 3H), 0.07 (s, 6H). ^{31}P NMR (202 MHz, $CDCl_3$/CD_3OD 4:1): δ –1.27, –1.47. IR (neat): 2924, 2854, 1737, 1655, 1463, 1251, 1099, 1036. HRMS (ESI+) $C_{46}H_{90}O_{11}F_2NPSi_2$, m/z [M+$Na^+$] 980.5651, found 980.5623.

1-*O*-Octadecyl-2-(7-((5*Z*,7*E*)-(1*S*,3*R*)-9,10-seco-5,7,10(19)-cholestatriene-1,25-diol-3-oxy)-6,6-difluoro-7-oxoheptanoyl)-*sn*-glycero-3-phospho-(*S*)-glycerol (3-*O*-69)

Carboxylic acid **68** (31 mg, 0.033 mmol) and calcitriol (14 mg, 0.033 mmol) were dissolved in THF (2.0 mL). 2,4,6-Trichlorobenzoyl chloride (5.0 µL, 0.033 mmol) and then DMAP (8 mg, 0.066 mmol) were added and the mixture was stirred at 20 °C for 4 h, then concentrated *in vacuo* and purified by column chromatography (CH_2Cl_2 then

CH_2Cl_2/EtOAc 2:1) to give 14 mg of a colorless oil, that was dissolved in CH_2Cl_2 (2.0 mL) along with DBU (1.6 µL, 0.010 mmol). The reaction mixture was stirred at 20 °C for 1 h and then purified directly by column chromatography (heptane/EtOAc 1:3 then CH_2Cl_2/MeOH 9:1) to give 9 mg of a colorless oil, that was dissolved in a mixture of MeCN (1.0 mL) and CH_2Cl_2 (0.33 mL) and cooled to 0 °C. Aqueous HF (40%, 60 µL) was added and the reaction mixture was stirred at 0 °C. After 3 h excess reagent was quenched by dropwise addition of $MeOSiMe_3$ (0.25 mL) and the mixture was stirred for 30 min, after which $NaHCO_3$ (4 mg, 0.048 mmol) was added and the mixture was concentrated *in vacuo* and purified by column chromatography (CH_2Cl_2/MeOH 9:1 then CH_2Cl_2/MeOH 4:1) to give 8 mg (22%) of 1:6 mixture of **1-*O*-69** and **3-*O*-69** (determined by 500 MHz ^{1}H NMR) as a colorless amorphous solid. R_f = 0.14 (CH_2Cl_2/MeOH 4:1). ^{1}H NMR (500 MHz, $CDCl_3$/CD_3OD 4:1 for **3-*O*-69**): δ 6.31 (d, *J* = 11.1 Hz, 1H), 6.05 (dd, *J* = 11.1 Hz, 1H), 5.40 (s, 1H), 5.37–5.33 (m, 1H), 5.19–5.13 (m, 1H), 5.04 (s, 1H), 4.39–4.34 (m, 1H), 4.18–4.06 (m, 2H), 4.06–3.96 (m, 2H), 3.85–3.81 (m, 1H), 3.65–3.56 (m, 4H), 3.49–3.41 (m, 2H), 2.81 (dd, *J* = 11.8, 3.4 Hz, 1H), 2.66–2.61 (m, 1H), 2.52 (dd, *J* = 14.1, 5.8 Hz, 1H), 2.41–2.35 (m, 2H), 2.19–0.98 (m, 58H), 1.20 (s, 6H), 0.94 (d, *J* = 6.4 Hz, 3H), 0.88 (t, *J* = 6.9 Hz, 3H), 0.55 (s, 3H). ^{13}C NMR (50 MHz, $CDCl_3$/CD_3OD 4:1 for **3-*O*-69**): δ 173.2, 164 (missing), 147.2, 143.7, 131.9, 125.2, 117.3, 116.0, 112.2, 73.6, 72.2 (2C), 71.2, 70.8, 69.7, 68.8, 68.0, 65.7, 62.6, 56.9, 56.6, 46.2, 44.5, 44.0, 41.3, 40.8, 36.7, 36.4, 34.4, 34.0, 32.2, 30.0 (15C), 27.9, 26.3 (2C), 24.5, 23.8, 23.0, 22.5, 21.2 (2C), 19.0, 14.3, 12.1. IR (neat): 3337, 2925, 2854, 1737, 1717, 1658, 1585, 1479, 1259, 1198, 1146, 1073, 1045. HRMS (ESI+) $C_{58}H_{100}O_{13}F_2PNa$, m/z [M+H$^+$] 1097.6840, found 1097.6872.

Benzyl 5-hydroxypentanoate (70)

δ-Valerolactone (5.90 g, 59.2 mmol) and NaOH (2.37 g, 59.2 mmol) were dissolved in H_2O (59 mL) and the mixture was stirred at 70 °C for 5.5 h. Concentration *in vacuo* gave a white solid, which was concentrated with toluene (2×20 mL) to remove traces of H_2O. The white solid was dissolved in a mixture of MeCN (60 mL) and acetone (60 mL) along with benzyl bromide (8.46 mL, 71.1 mmol) and Bu_4NBr (955 mg, 2.96 mmol). The reaction mixture was stirred at 55 °C for 22 h, then concentrated *in vacuo* and purified by column chromatography (heptane/EtOAc 1:1) to afford 6.20 g (54%) of **70** as a colorless oil. ^{1}H NMR (300 MHz, $CDCl_3$):[232] δ 7.33–7.29 (m, 5H), 5.08 (s, 2H), 3.57 (t, *J* = 6.2 Hz, 2H), 2.69 (s, 1H, *OH*), 2.36 (t, *J* = 7.3 Hz, 2H), 1.74–1.64 (m, 2H), 1.59–1.49 (m, 2H). ^{13}C NMR (75 MHz, $CDCl_3$): δ 173.5, 135.9, 128.4 (2C), 128.1, 128.0 (2C), 66.1, 61.8, 33.8, 31.9, 21.1.

1-*O*-Octadecyl-3-*O*-(*tert*-butyldimethylsilyl)-*sn*-glycerol (71)

Alcohol **5b** (500 mg, 1.08 mmol) was dissolved in THF (3 mL), TBDMSCl (206 mg, 1.37 mmol) and imidazole (138 mg, 2.03 mmol) were added and the reaction mixture was stirred at 20 °C for 1 h and then concentrated *in vacuo*. The residue was purified by column chromatography (heptane then heptane/EtOAc 5:1) to afford 642 mg of a white solid, that

was dissolved in CH_2Cl_2 (8 mL) followed by addition of DDQ (277 mg, 1.22 mmol) and H_2O (0.44 mL). The reaction mixture was stirred at 20 °C for 1 h, then Na_2SO_4 was added and the mixture was purified directly by column chromatography (heptane then heptane/EtOAc 10:1) to give 407 mg (82%) of **71** as a colorless oil. ^{1}H NMR (300 MHz, $CDCl_3$):[233] δ 3.87–3.85 (m, 1H), 3.70–3.60 (m, 2H), 3.50–3.41 (m, 4H), 2.48 (d, *J* = 4.5 Hz, *OH*), 1.67–1.53 (m, 2H), 1.26 (s, 30H), 0.91–0.88 (m, 12H), 0.08 (s, 6H). ^{13}C NMR (75 MHz, $CDCl_3$): δ 71.8, 71.5, 70.8, 64.2, 32.1, 29.9 (11C) 29.6, 29.5, 26.3, 26.0 (3C), 22.9, 18.4, 14.3, –5.3 (2C). $[\alpha]_{589}^{20}$ = + 0.7 (*c* = 2.0, $CHCl_3$).

1-*O*-Octadecyl-2-((5-benzyloxy-5-oxopentyloxy)-carbonyl)-*sn*-glycerol (72)

Alcohol **71** (100 mg, 0.22 mmol) was dissolved in CH_2Cl_2 (1.1 mL) and cooled to 0 °C. Triphosgene (33 mg, 0.11 mmol) and pyridine (30 µL, 0.35 mmol) were added and the reaction mixture was stirred at 0 °C for 1.5 h after which alcohol **70** (124 mg, 0.65 mmol) and pyridine (30 µL, 0.35 mmol) were added. The reaction mixture was allowed to reach 20 °C and after 19.5 h the mixture was purified directly by column chromatography (toluene then toluene/EtOAc 10:1) to afford 117 mg of a colorless oil that was dissolved in a mixture of DMSO (4.3 mL), THF (3.5 mL) and H_2O (0.43 mL) in a flask protected from light. NBS (184 mg, 1.03 mmol) was added and the reaction mixture was stirred at 20 °C for 18 h after which excess reagents were quenched by addition of an aqueous solution of $Na_2S_2O_3$ (1%, 9.5 mL). The mixture was stirred for 10 min at 20 °C, then the organic layer was isolated by extraction with Et_2O (3×25 mL). The combined organic phases were dried over Na_2SO_4, concentrated *in vacuo* and purified by column chromatography (heptane/EtOAC 5:1 then heptane/EtOAc 3:1) to give 82 mg (65%) of **72** as a colorless oil. ^{1}H NMR (300 MHz, $CDCl_3$): δ 7.39–7.33 (m, 5H), 5.12 (s, 2H), 4.89–4.82 (m, 1H), 4.19–4.14 (m, 2H), 3.88–3.83 (m, 2H), 3.67 (dd, *J* = 10.5 and 5.1 Hz, 1H), 3.63 (dd, *J* = 10.5 and 5.2 Hz, 1H), 3.52–3.40 (m, 2H), 2.41 (t, *J* = 7.1 Hz, 2H), 2.25 (t, *J* = 6.4 Hz, 1H), 1.77–1.71 (m, 4H), 1.59–1.52 (m, 2H), 1.33–1.22 (m, 30H), 0.89 (t, *J* = 6.7 Hz, 3H). ^{13}C NMR (50 MHz, $CDCl_3$): δ 173.2, 155.1, 136.1, 128.7 (2C), 128.4 (3C), 77.0, 72.1, 69.8, 67.8, 66.4, 62.8, 33.8, 32.1, 29.8 (13C), 28.2, 26.2, 22.8, 21.4, 14.3. $[\alpha]_{589}^{20}$ = – 3.3 (*c* = 1.4, $CHCl_3$). IR (neat): 3479, 2917, 2805, 1737, 1466, 1257, 1162, 1030. HRMS (ESI+) $C_{34}H_{58}O_7$, m/z [M+Na^+] 601.4075, found 601.4048.

1-*O*-Octadecyl-2-((5-hydroxy-5-oxopentyloxy)-carbonyl)-*sn*-glycero-3-(2-cyanoethylphospho)-(*S*)-2,3-di-*O*-*tert*-butyldimethylsilyl-glycerol (73)

Alcohol **72** (80 mg, 0.14 mmol) and phosphoramidite **27** (99 mg, 0.19 mmol) were dissolved in CH_2Cl_2 (1.0 mL) and tetrazole (0.45 M in MeCN, 0.42 mL, 0.19 mmol) was added and the mixture was stirred for 30 min at 20 °C after which ^{t}BuOOH (5.5 M in nonane, 35 µL, 0.19 mmol) was added. After 80 min the mixture was concentrated *in vacuo* and purified by column chromatography (heptane/EtOAc 3:1 then heptane/EtOAc 1:1) to afford 108 mg of colorless oil, that was dissolved in mixture of EtOAc (0.8 mL) and THF (0.8 mL). Pd/C (10 wt%, 5 mg, 0.005 mmol) was added and the mixture was

stirred under an atmosphere of H_2 for 5 h at 20 °C, then concentrated *in vacuo* and purified by column chromatography (heptane/EtOAc 1:1 then CH_2Cl_2/MeOH 9:1) to afford 77 mg (61%) of **73** (two diastereoisomers 1:1) as a colorless oil. ^{1}H NMR (300 MHz, $CDCl_3$, two diastereoisomers): δ 5.05–4.97 (m, 1H), 4.41–4.12 (m, 7H), 4.07–3.96 (m, 1H), 3.92–3.83 (m, 1H), 3.66–3.52 (m, 4H), 3.49–3.40 (m, 2H), 2.78 (t, *J* = 6.3 Hz, 2H), 2.43–2.37 (m, 2H), 1.81–1.72 (m, 4H), 1.60–1.50 (m, 2H), 1.38–1.22 (m, 30H), 0.91–0.88 (m, 21H), 0.10 (s, 3H), 0.09 (s, 3H), 0.06 (s, 6H). ^{13}C NMR (50 MHz, $CDCl_3$, two diastereoisomers): δ 177.5, 154.6, 116.5, 74.6, 72.1 (2C), 69.7, 68.1 (2C), 66.6, 64.0, 62.2, 33.8, 32.1, 29.8 (13C), 28.0, 25.9 (7C), 22.8, 21.4, 19.6, 18.2 (2C), 14.2, –4.7 (2C), –5.3 (2C). ^{31}P NMR (202 MHz, $CDCl_3$): δ –1.05, –1.27. HRMS (ESI+) $C_{45}H_{90}NO_{12}PSi_2$, m/z [M+Na^+] 946.5641, found 946.5649.

10. Synthesis of Small Natural-Product-Like Molecules

10.1 Introduction

This part of the thesis describes the synthesis of small natural-product-like molecules using a diversity-oriented synthesis (DOS) based strategy. The work was carried out during a six month research stay at University of Leeds under supervision of Professor Adam Nelson. This chapter constitutes an independent part of the thesis and have no relation with the investigation of liposomal drug delivery presented in the first part.

In the aspiration to discover novel small molecules with biological activity the exploration of unknown chemical space has been suggested as a reasonable way to go.[234,235] The introduction of combinatorial chemistry and DOS[234,236,237,238] have liberated libraries of small molecules with high substitutional, stereochemical and/or scaffold diversity,[239,240,241,242,243] but a lot of the chemical space remain unexplored. Recent studies by Lipkus *et al.* of the scaffold for known cyclic organic molecules[244] have revealed that 50% of the compounds are described by 0.25% of the known hetero frameworks (Table 30) and the similarity in molecular skeletons for known organic molecules is even more significant when the scaffold analysis is made on graph frameworks (Table 30). Lipkus *et al.*[244] conclude that the uneven distribution of frameworks amongst known organic compounds can reflects the way in which chemical space is usually explored, whereas Schreiber and co-workers see the lack of structural diversity as a potential bottleneck in the discovery of new drugs.[234,244]

Table 30. Scaffold analysis for known cyclic organic molecules, registred in the CAS registry[244] – examples of the terms hetero framework and graph framework is illustrated in the bottom of the Table.

Hetero frameworks	Graph frameworks
● 2 594 176 frameworks in total.	● 836 708 frameworks in total.
● 50% of the compounds are described by 0.25% of the frameworks.	● 70% of the compounds are described by 0.20% of the frameworks.
● 17% of the compounds have one of the 30 most common frameworks.	● 36% of the compounds have one of the 30 most common frameworks.
● 51% of the frameworks were found in just one compound.	● 47% of the frameworks were found in just one compound.

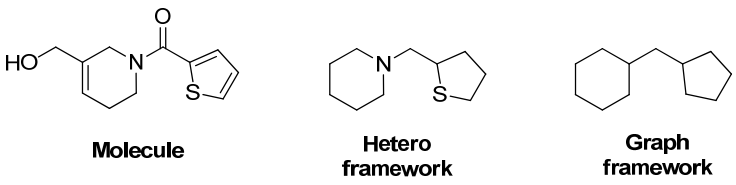

Thus there is a need for new synthetic strategies for making diverse molecules and recently, Nelson and co-workers[245] have prepared a DOS library using a "double branching

then folding"[xii] strategy by which the synthesis of over 80 distinct scaffolds were achieved in 4 or 5 steps from simple building blocks using not more than six different reaction types (see Figure 53). The powerful strategy involved the attachment of pairs of unsaturated building blocks to a fluorous-tagged linker[246] to give compounds like **81** and **82** (Figure 53). The fluorous tag allowed removal of excess reagents at each stage by fluorous-solid phase extraction (F-SPE) only.[247] Metathesis cascades were used, as the "folding" pathway, to "reprogram" the scaffolds of the metathesis substrates and the design of the fluorous-tagged linker[246] allowed only cyclised products to be released from the linker. Desilylation of the cyclic silaketals afforded the final products (like **85** and **86**), and applying this strategy Nelson and co-workers synthesized more than 90 natural-product-like molecules with an unprecedented structural diversity.[248, 249, 250] The synthesized molecules have many of the structural features that are present in natural products, including isolated, fused and spirocyclic ring systems, hydrogen bonding moieties, unsaturated carbon atoms and chiral centers, by which the molecules can be classified as natural-product-like. Known alkaloids like morphine, piperine and anabasine (
Figure **52**) are examples on natural products having the mentioned features.

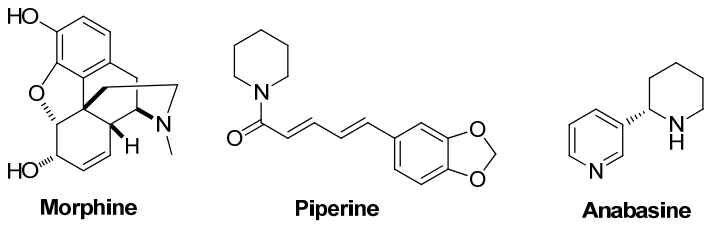

Figure 52. Biological active alkaloids – which have some of the same structural features as in the natural-product-like molecules prepared by Nelson and co-workers.[245]

Many of the natural-product-like molecules prepared by Nelson and co-workers have, due to the 2-nitrophenylsulfonyl (nosyl or Ns) protected amine, a scope for further derivatisation and the aim of this work was to prepare in a similar and elegant way a small library of natural-product-like molecules which after nosyl deprotection can be functionalized with various electrophiles.

[xii] In DOS terminology a "branching pathway"[238,243] is when the same substrate is exposed to different reactions conditions (e.g. attachment of various building blocks using different reaction types) and a "folding pathway"[238,242] is when different substrates are exposed to the same reaction conditions (e.g. a metathesis cascade).

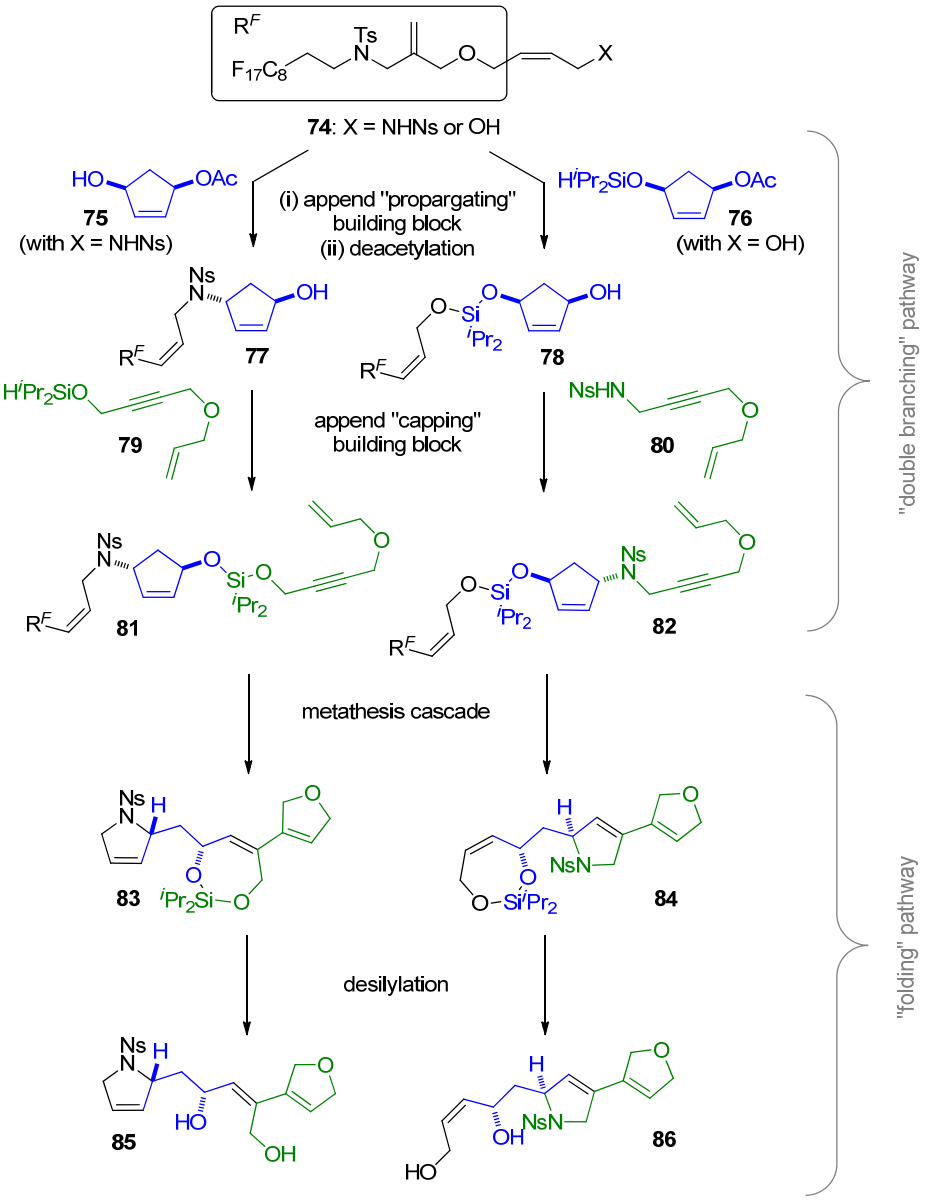

Figure 53. Outline of the "double branching then folding" strategy used by Nelson and co-workers[245] in the preparation of over 90 natural-product-like molecules with an unprecedented scaffold diversity.[248,249,250]

10.2 Project Outline

The DOS approach to synthesis of natural-product-like molecules in this work is outlined in Figure 54 and using DOS terminology the approach can be seen as a "branching-then-folding-then-branching" strategy. The coupling between the fluorous-tagged building blocks and the non-fluorous-tagged building blocks using the Fukuyama-Mitsunobu reaction[251] represents the first branching pathway. The fluorous tag can be seen as an anchor, which allows removal of excess reagents at each stage by F-SPE only.[247] Subjection of the coupling products (**90** and **91** in Figure 54) to a metathesis catalyst provide a metathesis cascade, the folding pathway, in which the catalyst "zips up" and

recombines the skeleton of the unsaturated substrates yielding a different molecular scaffold in the products (**92** and **93** in Figure 54). Removal of the nosyl group[252,253] allows derivatisation of the amines with various electrophiles and with the fluorous tag remained in the molecules the second branching pathway can be done in parallel and with F-SPE[254,255,256] purification. Removal of the fluorous tag completes the approach to prepare diverse molecules with natural-product-like features.

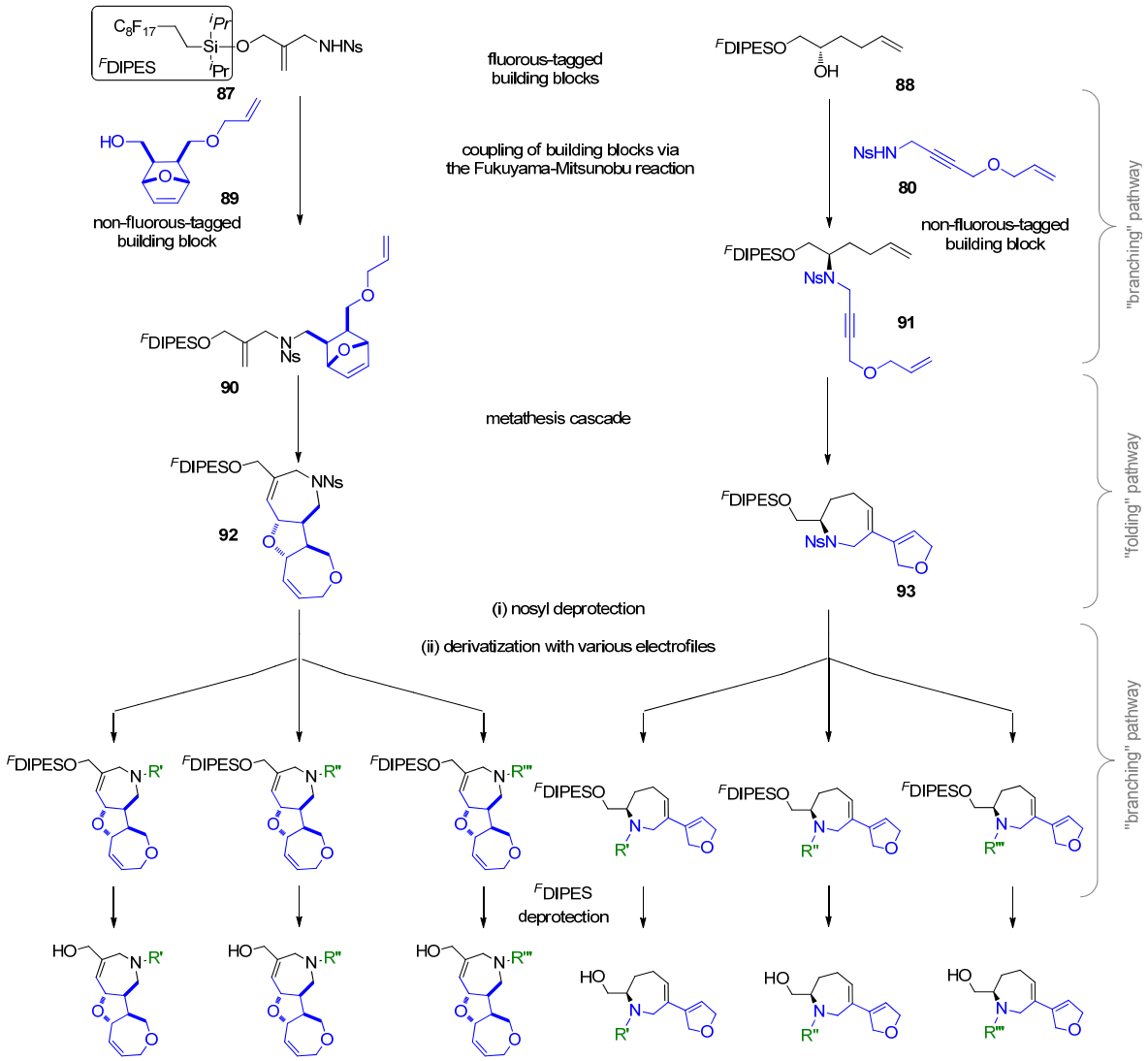

Figure 54. Outline of the approach to prepare natural-product-like molecules using a DOS based strategy.

10.3 Synthesis of Fluorous-Tagged Building Blocks

The fluorous tagged version (^{F}DIPES) of diisopropylethylsilyl (DIPES) was introduced from the corresponding hydrosilane **96** through a NBS activation, yielding the silyl bromide **97** which *in situ* was reacted with primary alcohols yielding the desired attachment (Scheme 25 and Scheme 28). The hydrosilane **96** was purchased from commercial suppliers, Fluorous Technoligies Inc. or Sigma Aldrich, or synthesized from alcohol **94** that was converted into the iodide **95** and then into the desired silane **96** in excellent yields (Scheme 24), applying the conditions given by Carrel *et al.*[257]

Scheme 24: Synthesis of the fluorous-tagged silane **24**.[a]

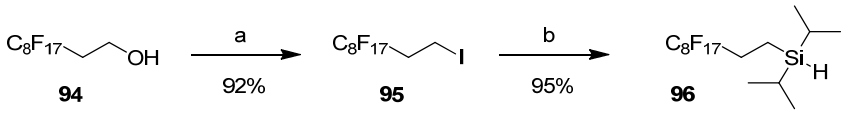

[a]Reagents: (a) I_2, PPh_3, imidazole, Et_2O, MeCN; (b) (i) ^{t}BuLi, Et_2O; (ii) chlorodiisoproylsilane, Et_2O.

The fluorous-tagged building block **99** was made in one step from 2-methylene-1,3-propanediol (**98**) and the hydrosilane **24** (Scheme 25) via the NBS activation, using the procedure used within the Nelson group to form silaketals.[245,258] However the isolated yield never became higher than 39%.[xiii] The silianol was the major by-product indicating some moisture in the reaction mixture, whereas none of the starting hydrosilane **96** was re-isolated demonstrating a good conversion into the silyl bromide **97**.

Scheme 25: Synthesis of the fluorous-tagged building block **99** via NBS activation of silane **96**.[a]

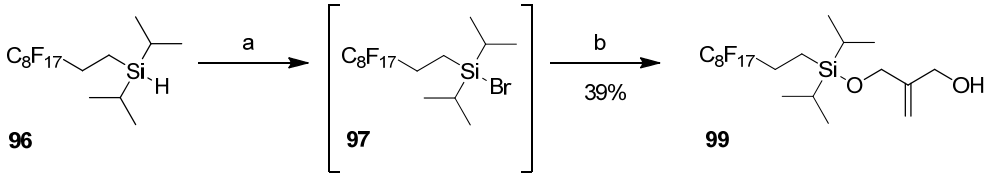

[a]Reagents: (a) NBS, CH_2Cl_2; (b) 2-methylene-1,3-propanediol (**98**), DMAP; CH_2Cl_2.

Conversion of the fluorous-tagged building block **99** into the corresponding sulfonamide **87** was achieved via the Fukuyama-Mitsunobu reaction[253] in a moderate yield on 45% (Scheme 26) applying the reagents 2-nitrophenylsulfonamide, PPh_3 and DEAD in excess. Unfortunately, the reaction gave a couple of unindentified by-products hence it was necessary after the F-SPE purification to purify the compound by column chromatography. To increase the overall yield a two step procedure, starting with a Fukuyama-Mitsunobu

[xiii] Recent studies in the Nelson group have revealed that imidazole provides significantly better yields for these kinds of reactions than DMAP.

reaction between the alcohol **99** and the Boc-protected sulfonamide **100**[xiv] followed by a Boc-deprotection, was attempted. Fukuyama *et al.*[259] and Leach *et al.*[246] have in almost quantitatively yield applied this strategy for the conversions of alcohols into sulfonamides. The Fukuyama-Mitsunobu reaction between **99** and sulfonamide **100** (Scheme 26) proceeded smoothly using F-SPE purification only to give the sulfonamide **101** in an excellent yield and good purity.[xv]

Scheme 26: Conversion of the fluorous-tagged alcohol **99** into sulfonamides using the Fukuyama-Mitsunobu reaction. **101** was isolated using F-SPE only with a mass recovery on 94% and a purity >95%.[a]

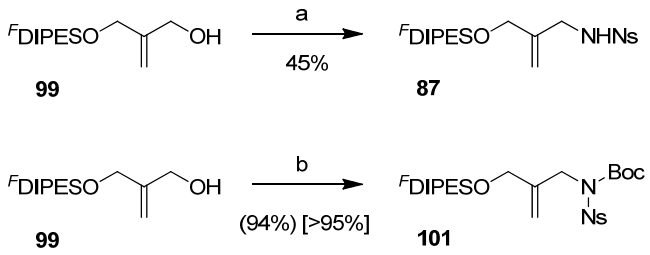

[a]Reagents: (a) $NsNH_2$, PPh_3, DEAD, THF; (b) NHNsBoc (**100**), PPh_3, DEAD, THF.

Unfortunately, the following Boc-deprotecting of **101** was not achievable (Scheme 27). Under standard Boc-deprotecting conditions, 5% TFA in CH_2Cl_2, the fluorous-tagged silyl ether was cleaved much faster (1 h) than the Boc-group, showing that the stability of ^{F}DIPES in an acid environment is limited and compared to the traditionally TIPS protecting group the stability is considerably lower. Application of TMSOTf and 2,6-lutidine[170] in CH_2Cl_2 did not gave any conversion of **101**, and the starting material was re-isolated with F-SPE. Finally, treatment of **101** in refluxing DMSO[260] was attempted, but that resulted in deprotection of both the Boc-group and the ^{F}DIPES-group to give alcohol **102**.

Scheme 27: Attempted Boc-deprotection of **101** using three different reactions conditions.[a]

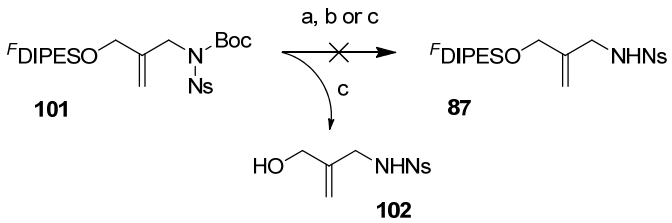

[a]Reagents: (a) 5% TFA, CH_2Cl_2; (b) TMSOTf, 2,6-lutidine, CH_2Cl_2; (c) DMSO, 180 °C.

[xiv] Sulfonamide **100** was donated by Dr. Catherine O´Leary-Steele from the Nelson group, and was synthesised in one step from $(Boc)_2O$, 2-nitrophenylsulfonamide, Et_3N and DMAP in CH_2Cl_2 in 85% yield.
[xv] The purity of the products purified by F-SPE only was determined by 500 MHz ^{1}H NMR using signals from the fluorous tag as an internal standard.

The synthesis of the fluorous-tagged building block **88** was initiated from (*R*)-glycidol (**103**). The fluorous tag was introduced through the same NBS activation procedure as applied in the synthesis of **99** to give the desired silyl ether **104** (Scheme 28) in a similar yield as obtained for **99**. The following expoxide opening was achieved with allyl magnesium bromide and Li_2CuCl_4, (Kochi's Catalyst)[261,262] to afford the fluorous-tagged alcohol **88** (Scheme 28).

Scheme 28. Preparation of the fluorous-tagged building block **88**.[a]

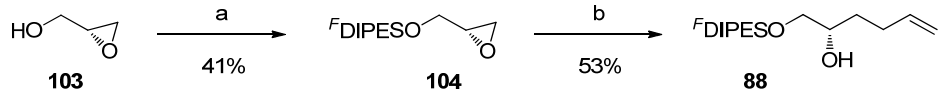

[a]Reagents: (a) Silyl bromide **97**, DMAP, CH_2Cl_2; (b) allyl magnesium bromide, Li_2CuCl_4, Et_2O.

As for **99** it was desirable to convert the fluorous-tagged alcohol **88** into the corresponding sulfonamide (Scheme 29). The conditions applied for the conversion of **99** to **87** (Scheme 26) were attempted, but none of the desired product was isolated, instead NMR of the isolated material revealed that a 1,2-silyl-migration had occurred to give alcohol **106**.

Scheme 29: Attempted conversion of the alcohol **16** into the corresponding sulfonamide **34**, which instead resulted in a 1,2-silyl-migration.[a]

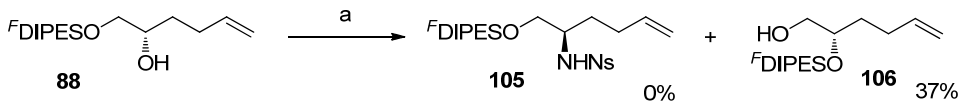

[a]Reagents: (a) $NsNH_2$, PPh_3, DEAD, THF.

Since the transformation of **88** into the corresponding sulfonamide **105** was not feasible in our hands a sulfonamide functionality was introduced by a Steglich coupling[102] between the alcohol **88** and the amino acid derivate **108** to give the sulfonamide **109** (Scheme 30). **108** was synthesized in one step from L-alanine (**107**) and 2-nitrophenylsulfonyl chloride (Scheme 30) via a procedure published by Ciolli *et al*.[263]

Scheme 30. Synthesis of amino acid derivate **108** and the fluorous-tagged building block **109**.[a]

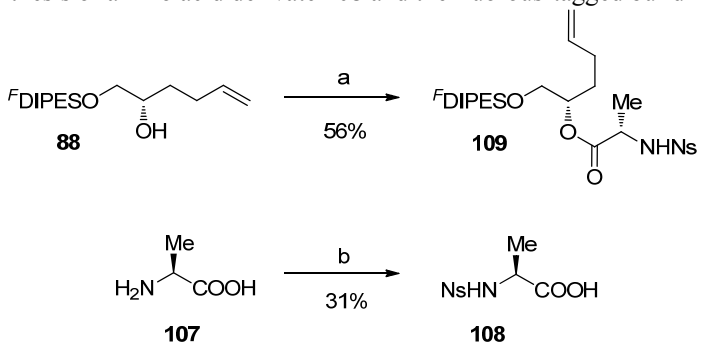

[a]Reagents: (a) Carboxylic acid **108**, DCC, DMAP, CH_2Cl_2; (b) NsCl, NaOH, H_2O, THF.

10.4 Synthesis of Non-Fluorous-Tagged Building Blocks

The building blocks applied in this work are shown in Figure 55. Sulfonamide **80**[xvi] and alcohol **111**[xvii] were donated from members of the Nelson group.

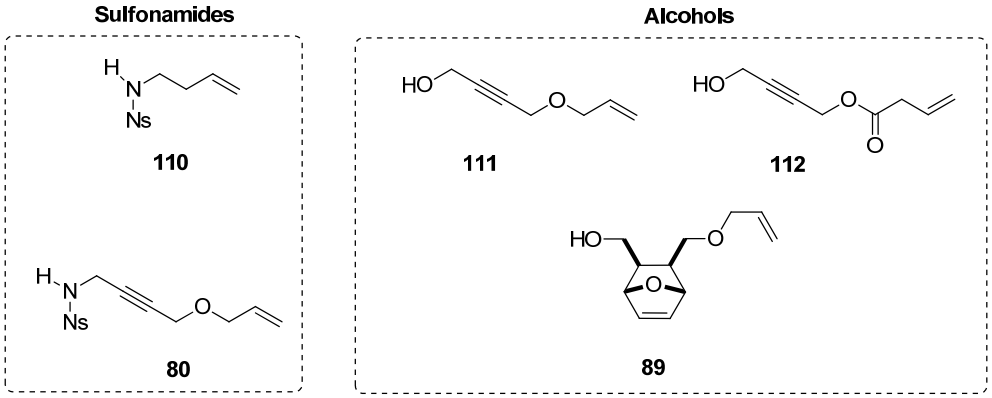

Figure 55. The applied non-fluorous-tagged building blocks – two kinds of building blocks were used; sulfonamides and alcohols.

The sulfonamide **110** was synthesized from the commercial available amine **113** and 2-nitrophenylsulfonyl chloride (Scheme 31) in a 71% yield as white needles. It was crucial that the recrystallisation from 1:1 toluene–hexane removed all traces of 2-nitrophenylsulfonyl derivates; otherwise it was observed that the Fukuyama-Mitsunobu reaction between **110** and various alcohols did not occur.

The vinylacetate **112** was synthesized by a Steglich coupling[102] between the diol **114** and vinylacetic acid (**115**, Scheme 31) in a poor yield on 31%. Although the reaction was carried out under dilute conditions (0.01 M) the diester **116** was also isolated in 11% yield.

Scheme 31. Synthesis of the sulfonamide **110** and the ester **112**.[a]

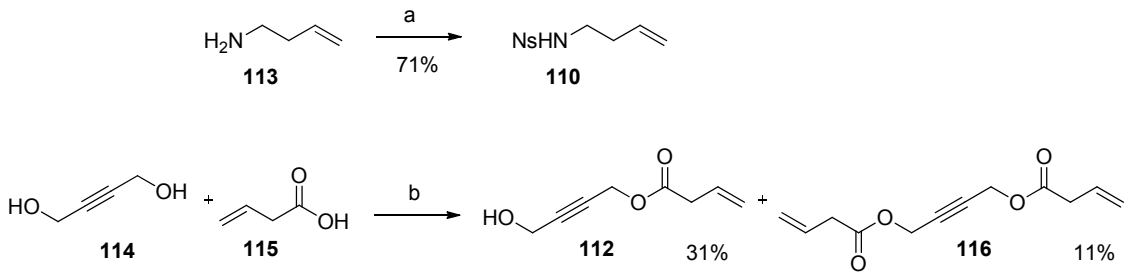

[a]Reagents: (a) NsCl, K_2CO_3, CH_2Cl_2; (b) DCC, DMAP, CH_2Cl_2.

[xvi] Alcohol **111** was donated by Dr. Stuart Leach, former member of the Nelson group, and was synthesised from 1,4-butyndiol, allyl bromide and NaH in DMF in 63% yield.
[xvii] Sulfonamide **80** was donated by Dr. Catherine O´Leary-Steele from the Nelson group and was synthesised over two step in 72%. The first step was a Fukuyama-Mitsunobu coupling between the alcohol **111** and the sulfonamide **100** activated by PPh_3 and DEAD in THF, followed by a Boc-deprotection with 10% TFA in CH_2Cl_2.

The last building block **89** was prepared in an excellent yield (Scheme 32) from the enantiomerically pure acetate **117**[xviii] using a four step TBDMS-protection, deacetylation, allylation, desilylation sequence in which no purification of the intermediates was necessary.[258]

Scheme 32. Four step synthesis of alcohol **89**.[a]

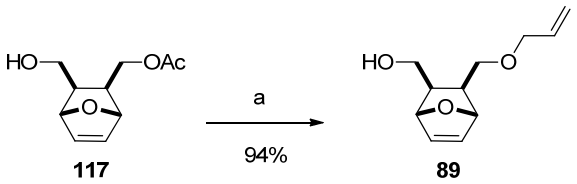

[a]Reagents: (a) (i) TBDMSCl, imidazole, CH_2Cl_2; (ii) saturated solution of NH_3 in MeOH; (iii) allyl bromide, NaH, DMF; (iv) TBAF, THF.

[xviii] Acetate **117** was donated by Dr. Thomas Woodhall, former member of the Nelson group.

10.5 Coupling of Building Blocks

The coupling between the various fluorous-tagged building blocks and the non-fluorous-tagged building blocks was achieved under mild conditions using the Fukuyama-Mitsunobu reaction,[251] and the fluorous tag allowed the use of reagents in excess due to the following F-SPE purification. The results are summarised in Table 31 and sulfonamide **118** (entry 1) and **119** (entry 2) were obtained in good yields and purities after F-SPE purification only. To illustrate the potential of the F-SPE purification the 500 MHz ^{1}H NMR spectrum for **119** is shown in Figure 56, emphasizing the good purity the fast and simple F-SPE purification delivers. In the preparation of sulfonamide **90** (entry 3), **91** (entry 4) and **121** (entry 6) it was necessary after the F-SPE to purify the products by column chromatography, since a significant amount of other fluorous-tagged compounds also were formed. But the removal of excess reagents by F-SPE was still very valuable making the following purification by column chromatography much simpler than it would have been without the F-SPE step. The product formed from the coupling between **109** and **112** (entry 6) was not the desired, the terminal double bond in the vinylacetate moiety was migrated forming 3-methylacryloate **121** instead.

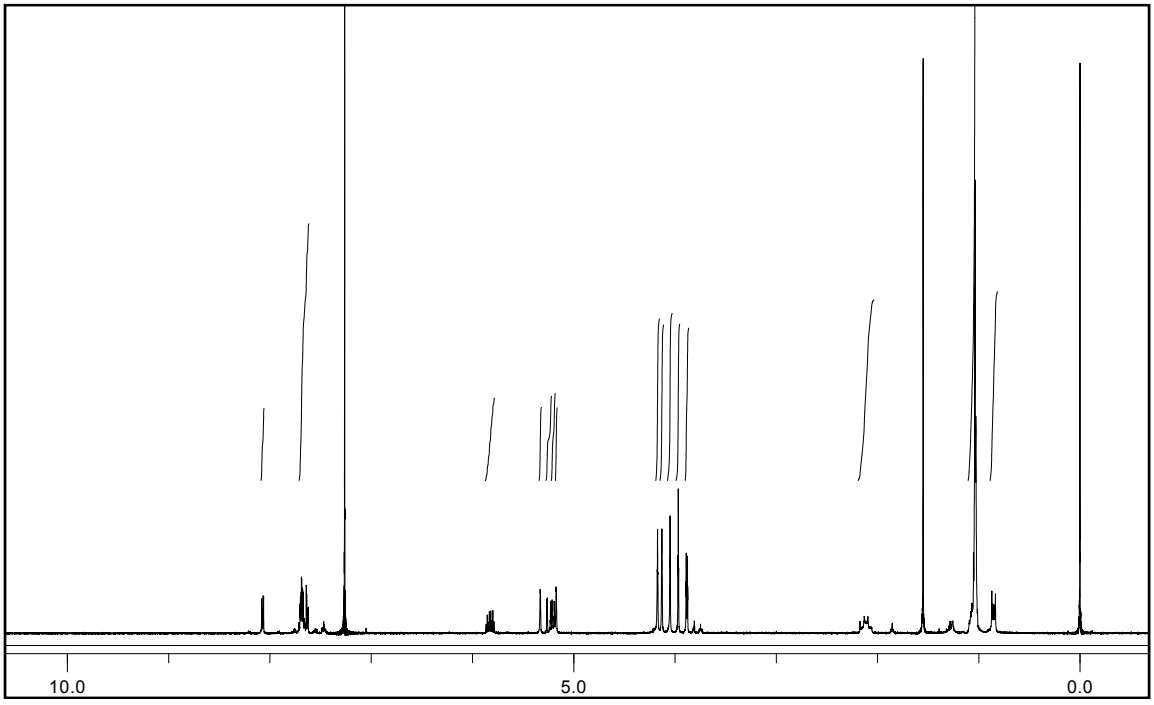

Figure 56. The 500 MHz ^{1}H NMR spectrum for the Fukuyma-Mitsunobu coupling product **119** purified by F-SPE only.

Table 31: Attachment of non-fluorous-tagged building blocks to the fluorous tagged building blocks using the Fukuyama-Mitsunobu alkylation reaction.

Entry	Fluorous-tagged building block	Non-fluorous-tagged building block	Method[a]	Product (mass recovery) [purity] [b]
1	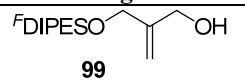 **99**	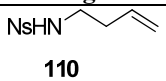 **110**	A	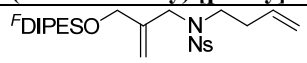 **118** (95%) [>85%]
2	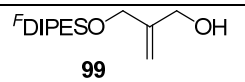 **99**	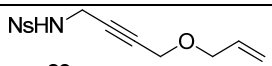 **80**	A	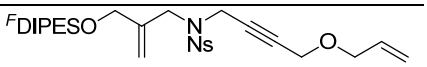 **119** (96%) [>85%]
3	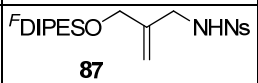 **87**	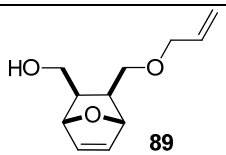 **89**	B	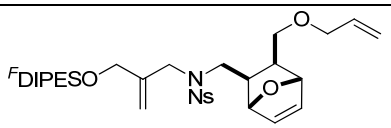 **90** (48%)[c]
4	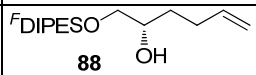 **88**	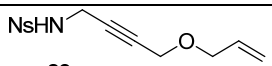 **80**	A	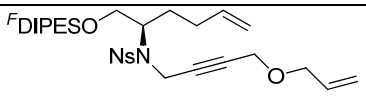 **91** (55%)[c]
5	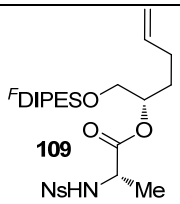 **109**	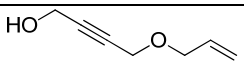 **111**	B	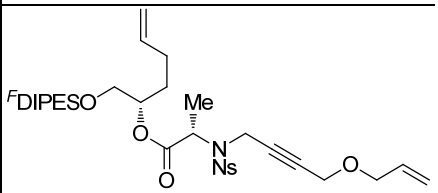 **120** (68%) [>75%]
6	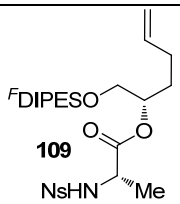 **109**	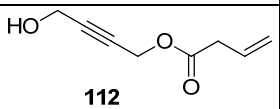 **112**	B	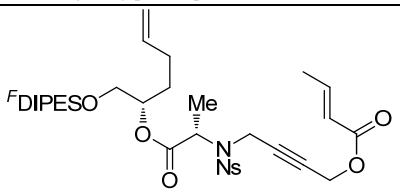 **121** (50%)[c]

[a]Methods: A: (i) fluorous-tagged alcohol (1 eq.), sulfonamide (4 eq.), PPh_3 (4 eq.), DEAD (4 eq.), THF. (ii) F–SPE; B: fluorous-tagged sulfonamide (1 eq.), alcohol (4 eq.), PPh_3 (4 eq.), DEAD (4 eq.), THF, when necessary additional amounts of alcohol, PPh_3 and DEAD were used – see experimental section for details. (ii) F–SPE. [b]The purity, determined by 500 MHz ^{1}H-NMR spectroscopy, after F–SPE purification only. [c]Yield after F–SPE and column chromatography purification.

10.6 Metathesis Cascade Reactions

The key step in the approach to prepare natural product-like molecules was the ring-closing metathesis cascade which was used to "reprogram" the scaffold of the metathesis substrates (**90**, **91**, **118**, **119** and **120**) into diverse molecules, having a rare but also natural product-like scaffold. Various ruthenium and molybdenum based catalysts have been developed for ring-closing metathesis,[264,265,266] and particularly the stable and functional group tolerant ruthenium based catalysts, like **G I**[267] and **HG II**[268] (Figure 57) have been widely used in organic chemistry to formation of cyclic molecules, including numerous of natural products like callystatin,[269] migrastatin,[270] and cyclophellitol.[271]

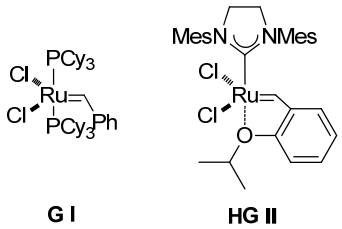

Figure 57. The applied metathesis catalysts; Grubbs Catalyst, 1st generation (**G I**) and Hoveyda-Grubbs Catalyst, 2nd generation (**HG II**)

In this work **HG II** in refluxing CH_2Cl_2 (0.5 mM) was used in the metathesis cascades. Previous results from the Nelson group has demonstrated that **HG II** works well in metathesis cascades on similar substrates.[245,246] In the ring-closing metathesis forming the six-membered ring in compound **112** (Table 32, entry 1) **G I** was applied. To prevent further metathesis reactions to occur during the work-up the catalyst was quenched by addition of $P(CH_2OH)_3$, Et_3N and silica followed by filtration through celite.[272] This changed the color of the reaction mixture from green (for **HG II**) or purple (for **G I**) to almost colorless.

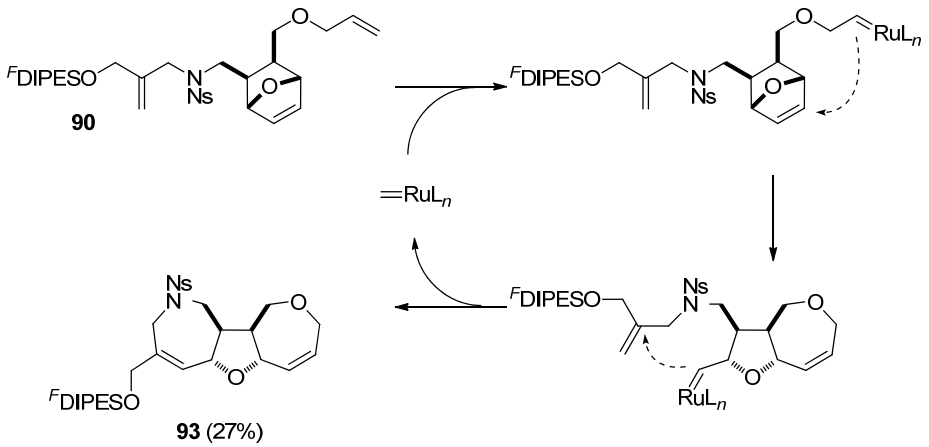

Figure 58. Illustration of the supposed reaction pathway for the metathesis cascade in formation of the fused tricyclic **93**.

The results for the metathesis cascades are summarised in Table 32, and gratifying the desired cascades occurred yielding the products in low to good yields. The “reprogram” of **90** led to the formation of the fused tricyclic **92** (entry 3) and making the assumption that the metathesis cascade initiate at the terminal alkene[273] the cascade proceed as illustrated in Figure 58. For some of the cascades (entry 2, 5 and 6) having an enyne ring-closing metathesis as part of the cascade more than more product was isolated and identified. In the literature it is an on-going discussion whether the mechanism for the enyne ring-closing metathesis proceed by a ”yne-then-ene” pathway or by a "ene-then-yne" pathway. Recent studies indicate that the "ene-then-yne" pathway seems to be the most predominant,[274,275] but it depends on the substrate and the catalyst.[274,275] Making the assumption that the transformation occurs by the “ene-then-yne” pathway the formation of the observed products (in entry 2, 5 and 6) can be explained by first an enyne ring-closing metathesis (step a in Figure 59) and then either a cycloaddition with the next double bond in the molecule (step b in Figure 59) forming the desired cascade product **123** or a cycloaddition with a terminal double bond in another molecule (step c in Figure 59) forming the pure enyne ring-closing metathesis product **124**. In the metathesis cascade of substrate **120** (entry 5) the desired 10-membered ring in **125** was formed but in a much lower yield than the pure enyne ring-closing metathesis product **126**. Presumably the explanation for this is that the intramolecular cycloaddition between the terminal alkene in the hexenyl moiety and the ruthenium carbene complex is less feasible in **120** than in substrates like **91** and **119**, due to an increased flexibility and mobility. To increase the formation of the desired product the metathesis cascade was attempted in refluxing benzene (entry 6), but the yield of **125** was not improved and in addition to **125** and **126** these conditions also forced the cross-metathesis product of **126** to be formed giving **127**.

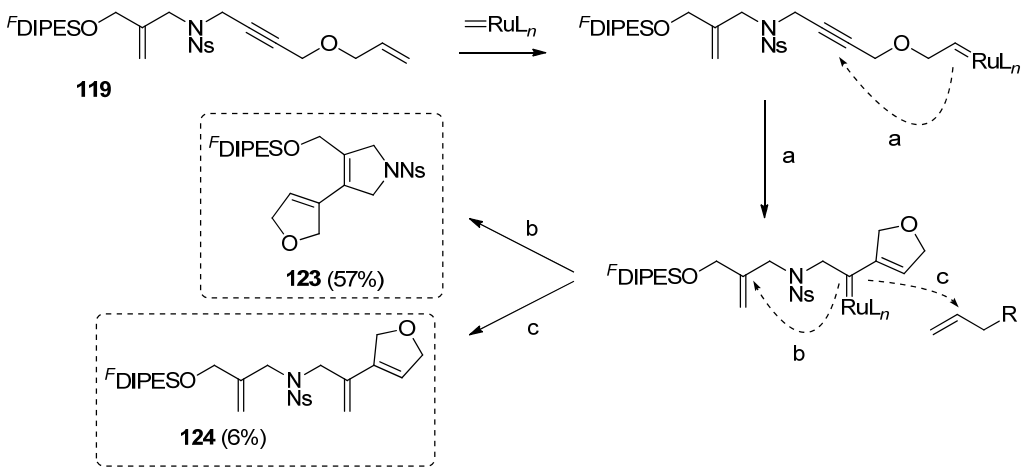

Figure 59. The proposed reaction pathways to the metathesis cascade product **123** and to the pure enyne ring-closing metathesis product **124**.

Table 32: *Metathesis cascade reactions.*

Entry	Metathesis substrate [purity]	Catalyst[a] (loading)	Time	Product(s) (yield)
1	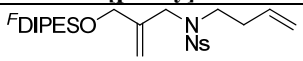 **118** [>85%]	**G-I** (5 mol%)	2 h	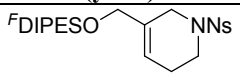 **122** (95%)[c]
2	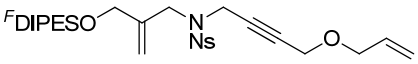 **119** [>85%]	**HG-II** (5 mol%)	22 h	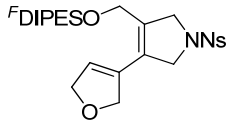 **123** (57%) 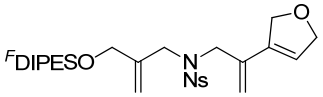 **124** (6%)
3	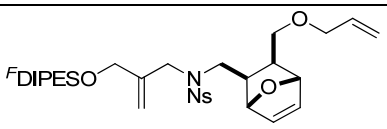 **90** [>95%]	**HG-II** (5+10 mol%)	47 h	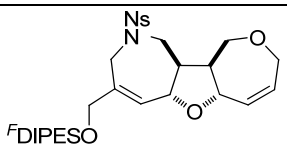 **92** (27%)
4	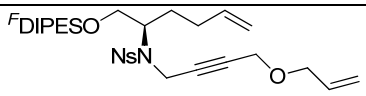 **91** [>95%]	**HG-II** (5 mol%)	22 h	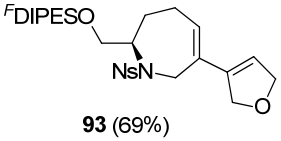 **93** (69%)
5	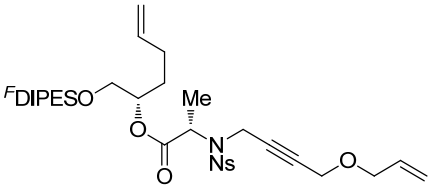 **120** [>75%]	**HG-II** (5+15 mol%)	19 h	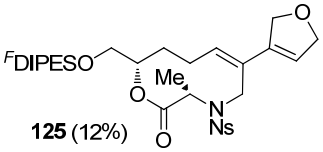 **125** (12%) 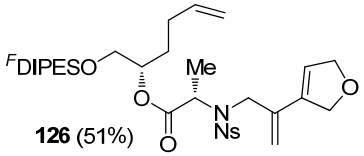 **126** (51%)
6	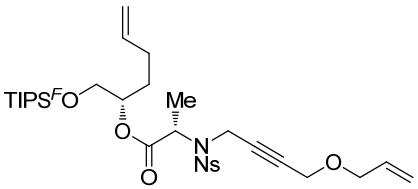 **120** [>75%]	**HG-II**[b] (10 mol%)	14.5 h	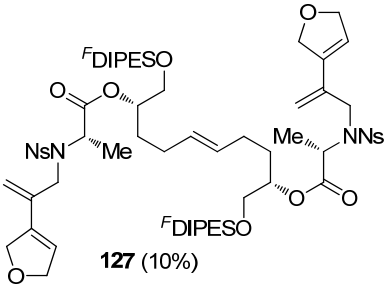 **127** (10%) also obtained was **125** (9%) and **126** (27%)

[a]Reaction conditions: (i) Metathesis substrate, metathesis catalyst (**G-I** or **HG-II**), CH_2Cl_2 (0.5 mM), 45 °C; (ii) Et_3N (86 eq.), $P(CH_2OH)_3$ (86 eq.) then silica then filter through celite; (iii) purification by column chromatography unless otherwise stated. [b]Reaction conditions: (i) Metathesis substrate, **HG-II**, benzene (0.5 mM), 80 °C; (ii) Et_3N (86 eq.), $P(CH_2OH)_3$ (86 eq.) then silica then filter through celite; (iii) purification by column chromatography. [c]Purification by F-SPE only, mass recovery 95% and purity >90% purity (determined by 500 MHz ^1H NMR).

10.7 Diels Alder Reaction with Cookson's Reagent

To increase the complexity of the dihydropyrrole **123** a Diels Alder reaction with the dienophile **128**, called Cookson's reagent,[240,276,277] was attempted and achieved in a good yield (Scheme 33).

Scheme 33: Diels-Alder reaction between the diene **123** and Cookson's reagent **128**.

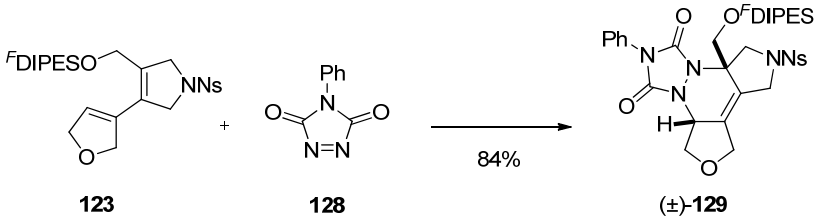

10.8 Nosyl Deprotection

Nosyl became applicable as protecting group for amines when Fukuyama *et al.*[251] discovered that nosyl groups can be removed under mild conditions using thiolate nucleophiles. In general upon treatment with PhSH and K_2CO_3 in DMF[251,252] at room temperature the nosyl group is cleaved off in good yields. But reaction conditions like PhSH and DBU in MeCN[278] and the odourless decanethiol and NaH in DMF[279] are also reported. The mechanism for the deprotection is believed to go through a Meisenheimer complex (Figure 60).[251,252]

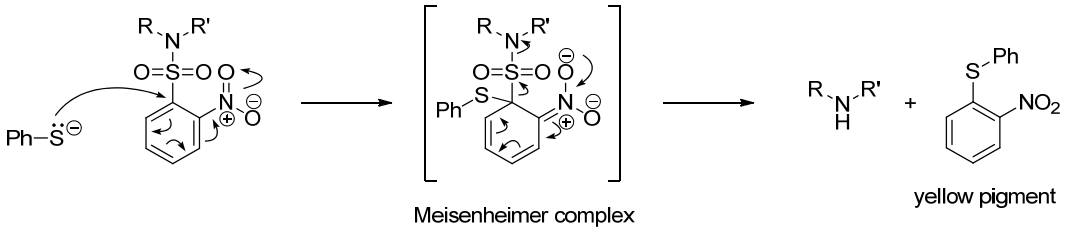

Figure 60. Mechanism for nosyl deprotection.[251,252]

In this work the standard conditions, PhSH and K_2CO_3 in DMF was used and the nosyl deprotections were achieved in good yields (Table 33) within short reaction times (1 h) and the amines were isolated by F-SPE in good purity. In the F-SPE purification it was crucial to add 0.5% Et_3N to the eluent systems otherwise it was observed that the amine stuck to the silica in the F-SPE cartridges. In the deprotection of **123** (entry 2 in Table 33) NMR analysis of the isolated material revealed that an aromatisation had occurred giving the pyrrole **131**. The aromatisation was observed for the dihydropyrrole **123** only.

Table 33: Nosyl deprotection using PhSH and K_2CO_3 in DMF.[a]

Entry	Nosyl substrate[a]	Product (mass recovery) [purity] [b]
1	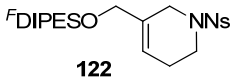 **122**	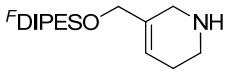 **130** (106%) [>80%]
2	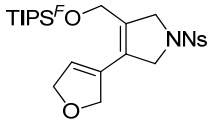 **123**	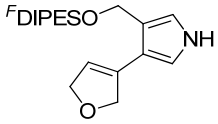 **131** (43%)[c]
3	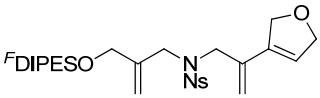 **124**	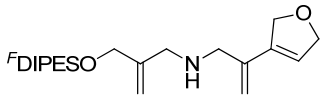 **132** (95%) [>75%]
4	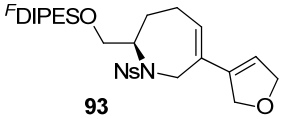 **93**	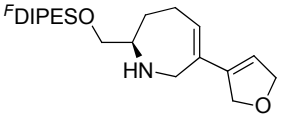 **133** (107%, [>80%]
5	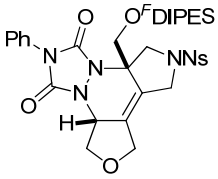 (±)-**129**	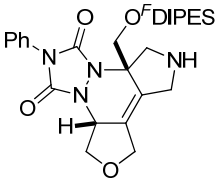 (±)-**134** (99%) [>95%]

[a]Reaction conditions: (i) nosyl substrate (1 eq.), K_2CO_3 (4 eq), PhSH (3 eq.), DMF; (ii) purification by F-SPE only unless otherwise stated. [b]The purity, determined by 500 MHz ^{1}H-NMR spectroscopy, after F–SPE purification only. [c]Yield after purification by F-SPE and column chromatography.

10.9 Synthesis of the Final Products

With the secondary amines in hand the next target was the functionalization with various electrophiles followed by removal of the fluorous-tag to give the final products. Four kinds of elctrophiles (acid chlorides, isocyanates, isothiocyanates and sulfonyl chlorides) were included in the preliminary screening for suitable candidates and the candidates were tested on amine **130** (Scheme 34 and Table 34). Benzoyl chloride (entry 1 in Table 34), phenyl isocyanate (entry 4), benzyl isothiocyanante (entry 6) and benzene sulfonyl chloride (entry 7) were selected as representative for each type of electrophile. The electrophiles were reacted with the amine and the desired products were isolated in good yields and purities (Table 34) after F-SPE purification only. To make F-SPE applicable in purification of multiple reaction mixtures at the same time the F-SPE cartridges were placed in a 10 port SPE vacuum manifold (Figure 61).

Scheme 34. Example on functionalization of fluorous-tagged amine with electrophile followed by removal of the fluorous tag on the silylated product in order to give the final product. For the silylated product the number in brackets and square brackets refers to the mass recovery and the purity, respectively.[a]

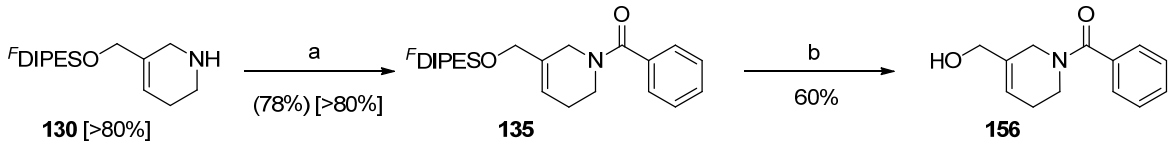

[a]Reagents: (a) (i) Benzoyl chloride, DMAP, CH_2Cl_2; (ii) F-SPE; (b) (i) HF, H_2O, MeCN, CH_2Cl_2; (ii) column chromatography.

The preliminary results revealed that acid chlorides, isocyanates, isothiocyanates and sulfonyl chlorides all were suitable electrophiles and further electrophiles, 2-thiophenecarbonyl chloride (entry 2 in Table 34), 5-carbonylisoxazole chloride (entry 3), furfuryl isocyanate (entry 5) and methanesulfonyl chloride (entry 8) were selected and derivatization of amine **130** with these electrophiles was performed in parallel and purified by F-SPE only applying the "10 port SPE vacuum manifold" (Figure 61) and the desired products were obtained in good yields and purities. The electrophiles was selected with the aim that they should contribute with heteroatoms, which often are crucial for biological activity, and/or (different) ring-systems, which would diversify the molecular skeleton in the final products. The removal of the fluorous-tag was achieved with HF in a moist mixture of MeCN and CH_2Cl_2 and the desired products were isolated in moderate to good yields (Table 34, entry 1-4 and 6-8). It was attempted to isolate the final products by F-SPE purification, but that purification technique was not capable to deliver the required purity thus the reaction mixtures were purified by column chromatography. For the furfuryl urea **76** (entry 5) none of the desired product was isolated after the HF-mediated deprotection, presumably as a consequence of decomposition of the acid sensitive furfuryl moiety. With

the promising results from the functionalization of amine **130** in hand the same transformations were performed on the other amines **132**, **133** and (±)-**134** (Table 34). When limited amounts of the amine (like for **132** and (±)-**134**) was produced fewer derivatives were made. As evident from Table 34 the derivatization of the amines **132**, **133** and (±)-**134** with various electrophiles was achieved with good isolated yields and purities and in general also the removal of the fluorous tag was obtained in good yields. For the nosyl protected amine **92** (entry 21) a one-pot procedure was applied for the nosyl deprotection and the functionalization with phenyl isocyanate. The nosyl was deprotected using PhSH and DBU in MeCN and when TLC deduced full conversion (1.5 h) phenyl isocyanate was added and after 2 h the product **155** was isolated by F-SPE like the other silylated products. In total 20 final and novel products were synthesized.

Figure 61. Pictures of 10 port SPE vacuum manifold with F-SPE cartridges.

Table 34. Functionalization of the amines (**130**, **132**, **133** and (±)-**134**) with various electrophiles followed by removal of the fluorous-tag to give the final products.

Entry	Fluorous-tagged Amine [purity]	Electrophile	Method[a]	Silylated product (mass recovery) [purity][b]	Final product[c] (yield)
1	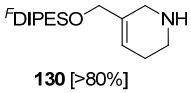 **130** [>80%]	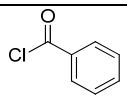	A	**135** (78%) [>80%]	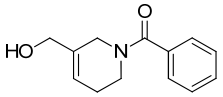 **156** (60%)
2		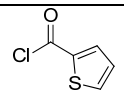	A	**136** (88%) [>85%]	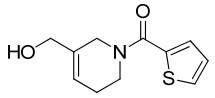 **157** (83%)
3		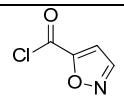	A	**137** (83%) [>80%]	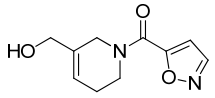 **158** (80%)
4		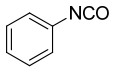	B	**138** (73%) [>90%]	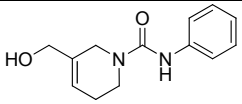 **159** (89%)
5		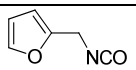	B	**139** (88%) [>80%]	none
6		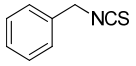	C	**140** (60%) [>90%]	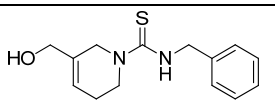 **160** (60%)
7		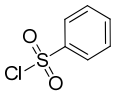	D	**141** (83%) [>95%]	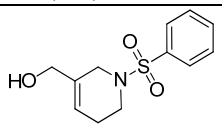 **161** (95%)
8		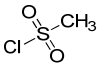	D	**142** (77%) [>80%]	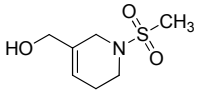 **162** (75%)
9	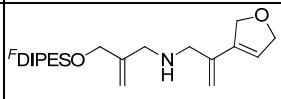 **132** [>75%]	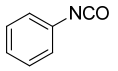	B	**143** (95%) [>75%]	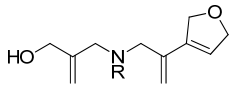 **163**, R = CONHPh (60%)
10	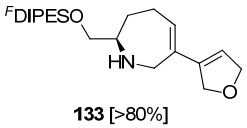 **133** [>80%]	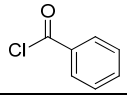	A	**144** (98%) [>85%]	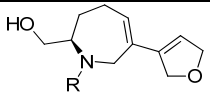 **164**, R = COPh (77%)
11		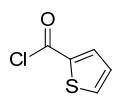	A	**145** (98%) [>90%]	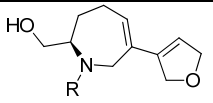 **165**, R = 2-thiophenecarbonyl (90%)

12	 **133** [>80%]		A	**146** (91%) [>70%]	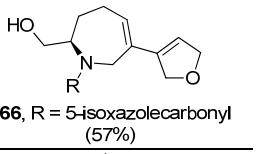 **166**, R = 5-isoxazolecarbonyl (57%)
13		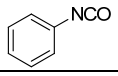	B	**147** (98%) [>85%]	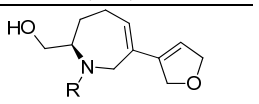 **167**, R = CONHPh (25%)
14		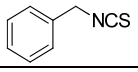	C	**148** (77%) [>80%]	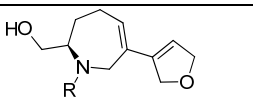 **168**, R = CSNHBn (22%)[f]
15		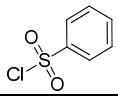	D	**149** (86%) [>80%]	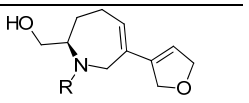 **169**, R = SO_2Ph (81%)
16		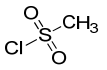	D	**150** (92%) [>80%]	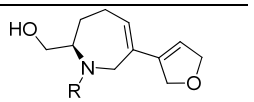 **170**, R = SO_2Me (61%)
17	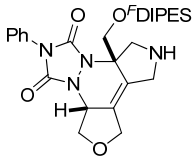 (±)-**134** [>95%]	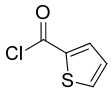	A	(±)-**151** (86%) [>95%]	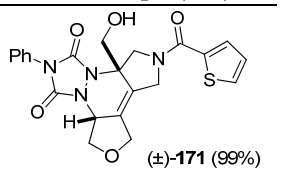 (±)-**171** (99%)
18		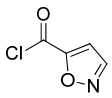	A	(±)-**152** (68%) [>80%]	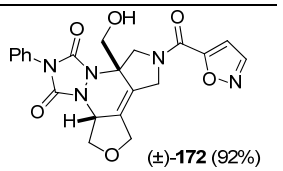 (±)-**172** (92%)
19		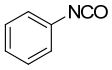	B	(±)-**153** (84%) [>95%]	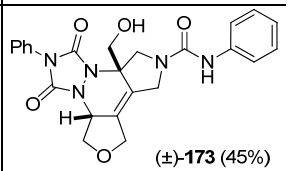 (±)-**173** (45%)
20		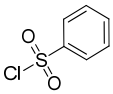	D	(±)-**154** (91%) [>95%]	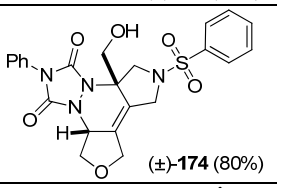 (±)-**174** (80%)
21	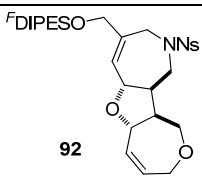 **92**	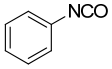	E	**155** (100%) [>75%]	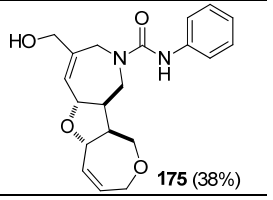 **175** (38%)

[a]Methods: A: (i) fluorous-tagged amine (1 eq.), acid chloride (4 eq.), DMAP (5 eq.), CH_2Cl_2; (ii) parallel F-SPE; B: (i) fluorous-tagged amine (1 eq.), isocyanate (4 eq.), CH_2Cl_2; (ii) parallel F-SPE; C: fluorous-tagged amine (1 eq.), isothiocyanate (4 eq.), CH_2Cl_2; (ii) parallel F-SPE; D: (i) fluorous-tagged amine (1 eq.), sulfonyl chloride (4 eq.), DMAP (5 eq.), CH_2Cl_2; (ii) parallel F-SPE; E: One-pot procedure – (i) nosyl protected amine (1 eq.), PhSH (3 eq.), K_2CO_3 (4 eq.), MeCN; (ii) isocyanate (8 eq.); (iii) parallel F-SPE. [b]The purity, determined by 500 MHz ^{1}H NMR spectroscopy, after F-SPE purification only. [c]Reagents: (i) HF, H_2O, MeCN, CH_2Cl_2; (ii) purification by column chromatography.

10.10 Scaffold Analysis

The molecular scaffold of the prepared library of natural-product-like molecules was analyzed using the framework concept proposed by Bemis *et al.*[280] and introduced in the beginning of this chapter (Table 30). The analysis revealed that 15 different graph frameworks were prepared (Figure 62) and no graph framework was prepared more than two times. Gratifying, all 20 molecules have their own hetero framework (Figure 62), illustrating that the developed chemistry afford molecules with a broad diversity and that the functionalization of the secondary amines with various electrophiles contribute with a valuable increase in the complexity of the molecular scaffolds. Beyond the tetrahydropyridine compounds (**156-162**) none of the prepared molecules have a graph or hetero framework that there are amongst the 30 most common in the investigation done by Lipkus *et al.*[244] (highlighted in Table 30) confirming the rarity and diversity of the prepared molecules.

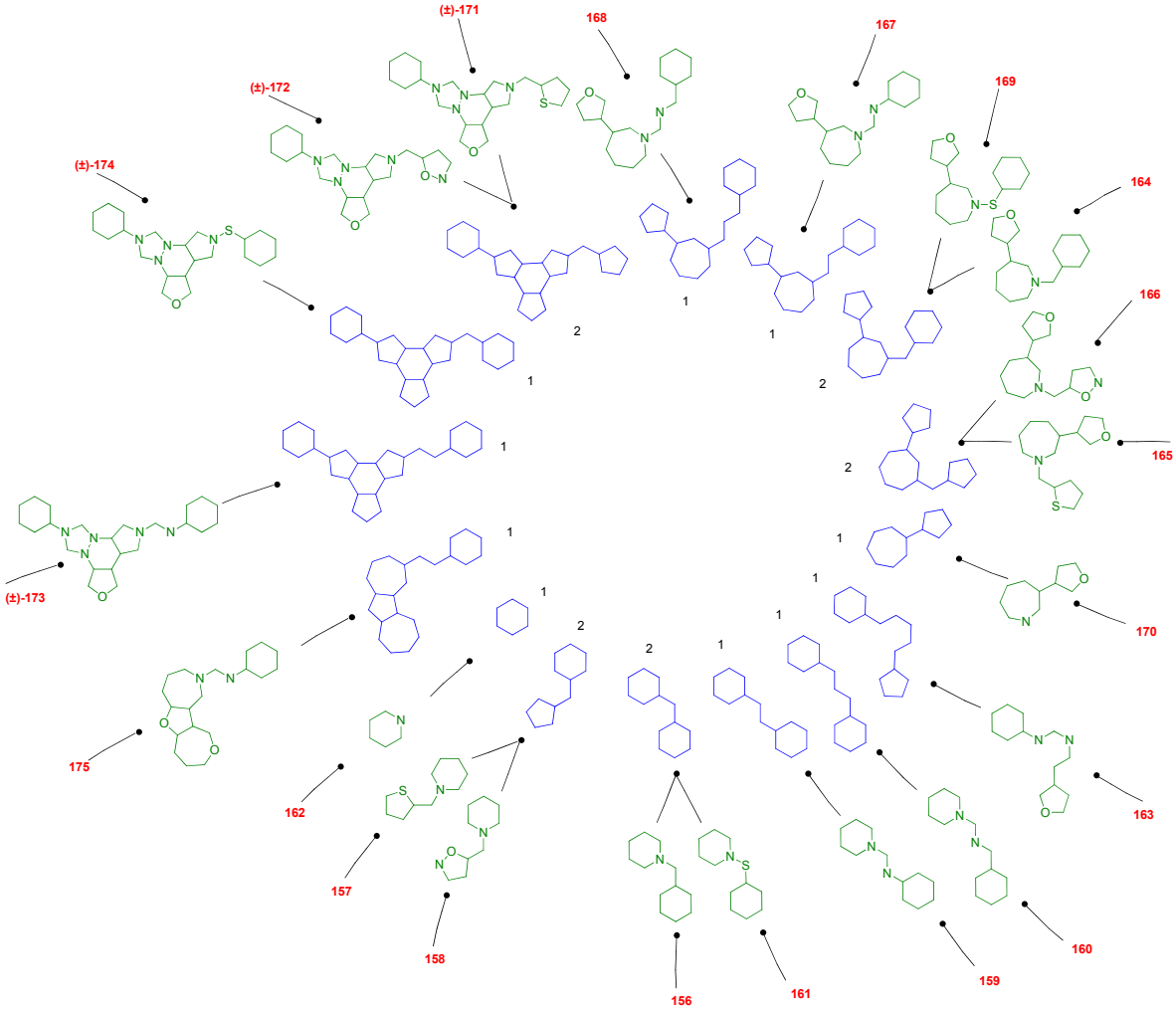

Figure 62: Scaffold analysis on the synthesized molecules, showing that the 20 different molecules (red numbers) have 15 different graph frameworks (blue structures) and 20 different hetero frameworks (green structures).

10.11 Conclusion

In total 20 novel compounds with a broad structural diversity were prepared using a short 5 or 6 steps "branching-then-folding-then-branching" strategy in overall yields from 75% to 5% (36% in average). A limited number of reaction types were applied, including the Fukuyama-Mitsunobu reaction and the ring closing metathesis cascade as the key reactions. Furthermore, in average the rapid F-SPE purification was sufficient in 3 out of 5 steps limiting the use of column chromatography. The prepared natural-product-like molecules are subjected to biological testing and it will be interesting to see whether some of the molecules will provide a biological response and potentially be a novel lead compound in the development of a new drug.

11. Experimental: Natural-Prodruct-Like Molecules

11.1 General Experimental

Starting materials, reagents and solvents were purchased from Sigma–Aldrich, Alfa Aesar or Fluorous Technologies and used without further purification unless otherwise stated. DMF, MeCN and CH_2Cl_2 were dried over 4 Å molecular sieves. THF was freshly distilled from Na, using benzophenone as a self-indicator. Saturated NH_3 in MeOH (*ca.* 0.025 M) was prepared by bubbling NH_3 gas through MeOH for a minimum of 30 min. NBS was recrystallised from water and dried under vacuum prior to use. Solvents were removed under reduced pressure using a Büchi rotary evaporator and a Vacuubrand diaphragm pump or a Genevac HT-4 evaporation system. Petrol refers to petroleum spirit (bp 40–60 °C). Column chromatography was carried out using silica (35-70 μm particles). TLC was carried out on commercially available pre-coated plates (Merck silica Kieselgel 60F254). ^{1}H and ^{13}C NMR spectra were recorded on a Bruker Avance 500, Avance DPX300 or DRX500 spectrophotometer with an internal deuterium lock. Chemical shifts are quoted in ppm downfield of tetramethylsilane and values of coupling constants are given in Hz. ^{13}C NMR spectra were recorded with broad band proton decoupling. Melting points were determined on a Reichert hot stage apparatus and are uncorrected. Infrared spectra were recorded on a Perkin Elmer spectrum one FT-IR infrared spectrophotometer. Mass spectra were recorded using a Micromass LCT-KA111 electrospray mass spectrometer (for ES+ mode) or a Quatro II triple quadrupole instrument (for EI mode). Optical activity measurements were recorded at room temperature (20 °C) on an AA-1000 polarimeter; units for $[\alpha]_D^{20}$ are 10^{-1} deg cm^2 g^{-1}.

11.2 General Procedures

General Procedure for F-SPE Purification

Fluorous–Solid Phase Extraction (F–SPE) was carried out using pre-packed Fluoro*Flash*® cartridges purchased from Fluorous Technologies Inc. The F–SPE cartridges were washed extensively with acetone and were pre-conditioned with 8:2 MeOH–H_2O. Crude reaction mixtures were loaded onto cartridges using CH_2Cl_2 or 8:2 MeOH–H_2O, and eluted using 8:2 MeOH–H_2O as the fluorophobic eluent, and then MeOH as the fluorophilic eluent; compressed air was used in a manner similar to that described by Curran *et al*.[247]

Procedure for Parallel F-SPE Purification

The F–SPE cartridges (2 g) were placed in the ports of a 10 port SPE vacuum manifold and washed extensively with acetone and pre-conditioned with 160:40:1 MeOH–H_2O–Et_3N. The crude reaction mixtures were loaded onto the F–SPE cartridge by CH_2Cl_2 (0.2 mL), and the reaction flasks were rinsed with 160:40:1 MeOH–H_2O–Et_3N (1 mL) which was added to F–SPE cartridge as well. Elution under vacuum (*ca.* 100 mmHg) with 160:40:1 MeOH–H_2O–Et_3N (3×3 mL) gave the fluorofrobic fraction which were collected in 17.5

mL vials after which elution under vacuum (*ca.* 100 mmHg) with 200:1 MeOH–Et_3N (3×3 mL) gave the fluorophilic fraction which were collected in 17.5 mL vials. The vials containing the fluorophilic fractions were concentrated on a Genevac EZ-2 vacuum centrifuge to give the purified products. The purity of the products purified by F-SPE only was determined by 500 MHz ^1H NMR using signals from the fluorous tag as an internal standard.

General Procedure A: Method for Fukuyama–Mitsunobu Reactions of Fluorous-tagged Alcohols with a non-Fluorous-tagged Sulfonamide.
The fluorous-tagged alcohol (1 eq.), the sulfonamide (4 eq.) and PPh_3 (4 eq.) were dissolved in THF (0.022 M in alcohol) and cooled to 0 °C. DEAD (4 eq.) was added dropwise and the reaction mixture was allowed to reach room temperature and stirred for 1 h after which the mixture was concentrated under reduced pressure and purified by F–SPE.

General Procedure B: Method for Ring-closing Metathesis Reactions of Fluorous-tagged Substrates.
The metathesis substrate (1 eq.) was dissolved in CH_2Cl_2 (0.5 mM) and heated to reflux. Grubbs Catalyst, 1st generation (5 mol%) or Hoveyda-Grubbs Catalyst, 2nd generation (5 mol%) was added and the reaction mixture was stirred until completion was indicated by TLC. The reaction mixture was cooled to room temperature, Et_3N (86 eq.) and tris(hydroxymethyl)phosphine (86 eq.) were added and the mixture was stirred for 15 min after which silica (*ca.* 10 g per mmol of substrate) was added and the mixture was stirred for another 15 min. The suspension was filtrated through a pad of celite, washed with EtOAc, concentrated under reduced pressure and purified by F-SPE or column chromatography.

General Procedure C: Method for 2-Nitrophenylsulfonyl Deprotection of Fluorous-tagged Sulfonamides.
The fluorous-tagged sulfonamide (1 eq.) and K_2CO_3 (4 eq.) were dissolved in DMF (0.05 M). PhSH (3 eq.) was added dropwise and the reaction mixture was stirred at room temperature for 1 h. A solution of 160:40:1 MeOH–H_2O–Et_3N (5 mL per mL DMF) was added and the mixture was purified directly by F–SPE, eluting with 160:40:1 MeOH–H_2O–Et_3N then 200:1 MeOH–Et_3N.

General Procedure D: Method for Amide Formation from Fluorous-tagged Amines.
The fluorous-tagged amine (0.030 mmol) and DMAP (18 mg, 0.15 mmol) were dissolved in CH_2Cl_2 (0.5 mL) and the acid chloride (0.12 mmol) was added. The reaction mixture was stirred for 2 h at room temperature, concentrated under a flow of N_2 and purified by F–SPE.

General Procedure E: Method for Urea Formation from Fluorous-tagged Amines.
The fluorous-tagged amine (0.030 mmol) was dissolved in CH_2Cl_2 (0.5 mL) and the isocyanate (0.12 mmol) was added. The reaction mixture was stirred for 2 h at room temperature, concentrated under a flow of N_2 and purified by F–SPE.

General Procedure F: Method for Thiourea Formation from Fluorous-tagged Amines.
The fluorous-tagged amine (0.030 mmol) was dissolved in CH_2Cl_2 (0.5 mL) and the isothiocyanate (0.12 mmol) was added. The reaction mixture was stirred for 2 h at room temperature, concentrated under a flow of N_2 and purified by F–SPE.

General Procedure G: Method for Sulfonamide Formation from Fluorous-tagged Amines.
The fluorous-tagged amine (0.030 mmol) and DMAP (18 mg, 0.15 mmol) were dissolved in CH_2Cl_2 (0.5 mL) and the sulfonyl chloride (0.12 mmol) was added. The reaction mixture was stirred for 2 h at room temperature, concentrated under a flow of N_2 and purified by F–SPE.

General Procedure H: Method for the ^{F}DIPES-deprotection
The fluorous-tagged silyl ether (0.030 mmol) was dissolved in MeCN (0.5 mL) and CH_2Cl_2 (0.4 mL) and HF (50% aq, 0.1 mL) was added. The reaction mixture was stirred for 1.5 h at room temperature after which $MeOSiMe_3$ (0.36 mL) was added and the mixture was stirred for another 1.5 h, concentrated under a flow a of N_2 and purified by column chromatography, eluting with either 20:1 CH_2Cl_2–MeOH or 25:1 CH_2Cl_2–MeOH.

11.3 Experimental Data for Compounds

***N*-(3-((3',3',4',4',5',5',6',6',7',7',8',8',9',9',10',10',10'-Heptadecafluorodecyl)-diisopropyl-silyloxy)-2-methylene-propyl) 2-nitrobenzenesulfonamide (87)**
By general procedure A, the alcohol **99** (600 mg, 0.93 mmol), 2-nitrophenylsulfonamide (726 mg, 3.59 mmol), PPh_3 (942 mg, 3.59 mmol) and DEAD (0.57 mL, 3.59 mmol) in THF (55 mL) gave a crude product which was purified by column chromatography, eluting with CH_2Cl_2, to give the *sulfonamide* **87** (349 mg, 45%) as a colorless oil, R_f 0.10 (10:1 petrol–EtOAc); ν_{max}/cm^{-1} (neat) 3348, 2948, 2869, 1542, 1359, 1208; δ_H (500 MHz, $CDCl_3$) 8.12–8.10 (1H, m, nosyl 3-H), 7.87–7.85 (1H, m, nosyl 5-H), 7.74–7.72 (2H, m, nosyl 4-H and 6-H), 5.53 (1H, t, *J* 5.8, *NH*), 5.10–5.09 (1H, m, 2-CH_{2a}), 5.05–5.04 (1H, m, 2-CH_{2b}), 4.17–4.16 (2H, m, 3-H_2), 3.79–3.77 (2H, m, 1-H_2), 2.14–2.02 (2H, m, 2'-H_2), 1.08-1.00 (14H, m, ^{i}Pr), 0.87–0.83 (2H, m, 1'-H_2); δ_C (75 MHz, $CDCl_3$) 143.0, 133.7, 132.8, 131.2, 125.4, 113.3, 64.7, 46.2, 17.6 (2C), 17.5 (2C), 12.5 (2C) (the signals for nosyl 1-C, 2-C, 1'-C, 2'-C and C_8F_{17} are missing); *m/z* (ES+) (Found: MNa^+ 855.1177, $C_{26}H_{29}F_{17}N_2O_5SSi$ requires *MNa* 855.1187).

(*S*)-(3',3',4',4',5',5',6',6',7',7',8',8',9',9',10',10',10'-Heptadecafluorodecyl)-diisopropylsilyl 2-hydroxy-5-hexenyl ether (88)

The epoxide **104** (658 mg, 1.04 mmol) was dissolved in Et_2O (15 mL) and the mixture was cooled to –30 °C. Li_2CuCl_4 (0.1 M in THF, 0.26 mL, 0.025 mmol) and then allyl magnesium bromide (1 M in Et_2O, 1.50 mL, 1.50 mmol) were added dropwise and the reaction mixture was stirred for 2 h at -30 °C, after which a saturated aqueous solution of NH_4Cl (6 mL) was added and the mixture was allowed to reach room temperature and H_2O (60 mL) was added. The organic layer was isolated by extraction with Et_2O (3×60 mL) and the combined organic phases were concentrated under reduced pressure and purified by column chromatography, eluting with 97:3 petrol–EtOAc, to give the *alcohol* **88** (374 mg, 53%) as a clear colorless oil, R_f 0.60 (9:1 petrol–EtOAc); $[\alpha]_D^{20}$ –3.0 (*c* 0.009 in $CHCl_3$); δ_H (500 MHz, $CDCl_3$) 5.83 (1H, ddt, *J* 17.0, 10.2 and 6.7, 5-H), 5.05 (1H, ddd, *J* 17.0, 3.4 and 1.2, 6-H_a), 4.98 (1H, ddt, *J* 10.2, 2.1 and 1.2, 6-H_b), 3.70–3.67 (2H, m, 1-H_a and 2-H), 3.49 (1H, dd, *J* 10.6 and 8.2, 1-H_b), 2.31 (1H, d, *J* 3.5, *OH*), 2.28–2.07 (4H, m, 4-H_2 and 2'-H_2), 1.58–1.47 (2H, m, 3-H_2), 1.08–1.03 (14H, m, ^{i}Pr), 0.91–0.87 (2H, m, 1'-H_2).

Allyl (((1*S*,2*S*,3*R*,4*R*)-3-hydroxymethyl-7-oxa-bicyclo[2.2.1]-5-hepten-2-yl)-methyl) ether (89)[258]

The alcohol **117** (1.35 g, 7.25 mmol) and imidazole (0.98 g, 14.5 mmol) were dissolved in CH_2Cl_2 (73 mL) and TBDMSCl (1.64 g, 10.9 mmol) was added. The reaction mixture was stirred at room temperature for 1.5 h after which the reaction mixture was concentrated under reduced pressure to give the crude *((1S,2S,3R,4R)-3-((tert-butyldimethylsilyloxy)-methyl)-7-oxa-bicyclo[2.2.1]-hept-5-en-2-yl)-methyl acetate*, R_f 0.82 (1:1 Petrol–EtOAc). The crude product was redissolved in a saturated solution of NH_3 in MeOH (150 mL, 0.025 M) and stirred at room temperature for 3 days after which the reaction mixture was concentrated under reduced pressure to give a colorless amorphous solid, which was treated with a saturated aqueous solution of NH_4Cl (10 mL), H_2O (150 mL) and Et_2O (150 mL). The organic layer was isolated by extraction with Et_2O (2×150 mL) and the combined organic phases were concentrated under reduced pressure to give the crude *((1S,2S,3R,4R)-3-((tert-butyldimethylsilyloxy)-methyl)-7-oxa-bicyclo[2.2.1]-hept-5-en-2-yl)-methanol*, R_f 0.10 (3:1 petrol–EtOAc). The crude product and allyl bromide (2.50 mL, 29.0 mmol) were dissolved in DMF (30 mL) and cooled to 0 °C. NaH (700 mg, 60% suspension) was added and the reaction mixture was stirred at room temperature for 16 h after which the reaction was quenched by addition of a saturated aqueous solution of NH_4Cl (10 mL) and H_2O (150 ml). The organic layer was isolated by extraction with Et_2O (3×150 mL). The combined organic phases were concentrated under reduced pressure to give the crude *allyl ((1S,2S,3R,4R)-3-((tert-butyldimethylsilyloxy)-methyl)-7-oxa-bicyclo[2.2.1]-hept-5-en-2-yl)-methyl ether*, R_f 0.68 (3:1 petrol–EtOAc). The crude product was dissolved in THF and TBAF (29 mL, 1.0 M in THF) was added. The reaction mixture was stirred at room temperature for 3 h after which the mixture was concentrated under reduced pressure and purified by column chromatography, eluting with 1:1 Petrol–EtOAc,

to give the alcohol **89** (1.34 g, 94%) as a yellow oil, R_f 0.19 (1:1 Petrol–EtOAc); δ_H (500 MHz, $CDCl_3$) 6.41 (1H, dd, *J* 5.8 and 1.6, 5-H or 6-H), 6.38 (1H, dd, *J* 5.8 and 1.6, 5-H or 6-H), 5.92 (1H, ddt, *J* 17.2, 10.4 and 5.8, allyl 2-H), 5.30 (1H, ddd, *J* 17.2, 2.9 and 1.4, allyl 3-H_{trans}), 5.22 (1H, ddd, *J* 10.4, 2.4 and 1.1, allyl 3-H_{cis}), 4.74–4.72 (1H, m, 1-H or 4-H), 4.71–4.69 (1H, m, 1-H or 4-H), 4.06–3.99 (2H, m, allyl 1-H_2), 3.83 (1H, dd, *J* 11.1 and 8.1, 3-CH_{2a}), 3.71–3.65 (1H, m, 3-CH_{2b}), 3.67 (1H, t, *J* 9.1, 3-CH_{2a}), 3.60 (1H, dd, *J* 9.1 and 6.6, 3-CH_{2b}), 3.12–3.07 (1H, m, *OH*), 2.04 (1H, ddd, *J* 9.1, 8.1 and 6.6, 2-H), 1.94 (1H, td, *J* 8.1 and 5.8, 3-H).

_N_-(((1_R_,2_R_,3_S_,4_S_)-3-(Allyloxymethyl)-7-oxa-bicyclo[2.2.1]-5-hepten-2-yl)-methyl) _N_-((3-(3',3',4',4',5',5',6',6',7',7',8',8',9',9',10',10',10'-heptadecafluorodecyl)-diisopropyl-silyloxy)-2-methylene-propyl) 2-nitrobenzenesulfonamide (90)

The sulfonamide **87** (20 mg, 0.024 mmol), the alcohol **89** (19 mg, 0.096 mmol) and PPh_3 (25 mg, 0.096 mmol) were dissolved in THF (1.1 mL) and cooled to 0 °C. DEAD (0.15 μL, 0.096 mmol) was added dropwise and the reaction mixture was allowed to reach room temperature. After 1 h PPh_3 (25 mg, 0.096 mmol) and DEAD ((0.15 μL, 0.096 mmol) were added and after 4 h the mixture was concentrated under reduced pressure and purified by F–SPE, eluting with 8:2 MeOH–H_2O then MeOH, and by column chromatography, eluting with CH_2Cl_2, to give the *sulfonamide* **90** (11 mg, 46%) as a colorless oil, R_f 0.45 (3:1 petrol–EtOAc); $[\alpha]_D^{20}$ –24.4 (*c* 0.0095 in $CHCl_3$); ν_{max}/cm^{-1} (neat) 3088, 2948, 2869, 1547, 1371, 1241; δ_H (500 MHz, $CDCl_3$) 8.07 (1H, dd, *J* 7.7 and 1.6, nosyl 3-H), 7.73–7.64 (3H, m, nosyl 4-H, 5-H and 6-H), 6.32 (1H, dd, *J* 5.8 and 1.7, 5-H or 6-H), 6.19 (1H, dd, *J* 5.8 and 1.7, 5-H or 6-H), 5.89 (1H, ddt, *J* 17.0, 10.4 and 5.7, allyl 2-H), 5.29–5.23 (2H, m, propyl 2-CH_{2a} and allyl 3-H_a), 5.18 (1H, ddd, *J* 10.4, 2.7 and 1.3, allyl 3-H_b), 5.12–5.09 (1H, m, propyl 2-CH_{2b}), 4.76–4.74 (1H, m, 1-H or 4-H), 4.62–4.60 (1H, m, 1-H or 4-H), 4.15–3.94 (6H, m, propyl 1-H_2, propyl 3-H_2 and allyl 1-H_2), 3.46–3.33 (4H, m, 2-CH_2 and 3-CH_2), 2.16–2.05 (2H, m, 2'-H_2), 1.96–1.85 (2H, m, 2-H and 3-H), 1.09–1.00 (14H, m, ^{i}Pr), 0.87–0.82 (2H, m, 1'-H_2); δ_C (75 MHz, $CDCl_3$) 148.1, 142.6, 136.3, 135.1, 134.7, 133.8, 133.4, 131.8, 131.7, 124.4, 117.3, 113.8, 80.9, 80.4, 72.3, 69.7, 64.2, 50.3, 47.2, 40.7, 38.0, 17.7 (2C), 17.6 (2C), 12.5, 12.5 (the signals for 1'-C, 2'-C and C_8F_{17} are missing); *m/z* (ES+) (Found: MNa^+ 1033.2155, $C_{37}H_{43}F_{17}N_2O_7SSi$ requires *MNa* 1033.2181).

(_R_)-_N_-(4-Allyloxy-2-butynyl) _N_-1-((3',3',4',4',5',5',6',6',7',7',8',8',9',9',10',10',10'-heptadecafluorodecyl)-diisopropyl-silyloxy)-5-hexen-2-yl 2-nitrobenzenesulfonamide (91)

By general procedure A, the alcohol **88** (195 mg, 0.29 mmol), the sulfonamide **80** (357 mg, 1.15 mmol), PPh_3 (300 mg, 1.15 mmol) and DEAD (0.18 mL, 1.15 mmol) in THF (13 mL) gave a crude product which was purified by column chromatography, eluting with 9:1 petrol–EtOAc, to give the *sulfonamide* **91** (155 mg, 55%) as a clear colorless oil, R_f 0.38 (9:1 petrol–EtOAc); $[\alpha]_D^{20}$ –6.9 (*c* 0.011 in $CHCl_3$); ν_{max}/cm^{-1} (neat) 2951, 2870, 1548,

1372, 1244, 1209; δ_H (500 MHz, $CDCl_3$) 8.16 (1H, dd, *J* 7.4 and 2.0, nosyl 3-H), 7.70–7.61 (3H, m, nosyl 4-H, 5-H and 6-H), 5.85 (1H, ddt, *J* 17.2, 10.3 and 5.7, allyl 2-H), 5.71 (1H, ddt, *J* 17.1 10.1 and 6.5, 5-H), 5.27 (1H, ddd, *J* 17.2, 3.0 and 1.2, allyl 3-H_{trans}), 5.20 (1H, ddd, *J* 10.4, 3.0 and 1.2, allyl 3-H_{cis}), 4.96–4.91 (2H, m, 6-H_2), 4.36 (1H, dt, *J* 18.6 and 1.7, 1-H_a), 4.26 (1H, dt, *J* 18.6 and 1.9, 1-H_b), 4.00 (2H, t, *J* 1.6, butynyl 1-H_2 or 4-H_2), 3.95–3.89 (1H, m, 2-H), 3.94 (2H, dt, *J* 5.7 and 1.2, allyl 1-H_2), 3.88–3.85 (2H, m, butynyl 1-H_2 or 4-H_2), 2.14–2.03 (2H, m, 2'-H_2), 1.99–1.80 (2H, m, 4-H_2), 1.06–1.00 (14H, m, ^{i}Pr), 0.89–0.80 (4H, m, 3-H_2 and 1'-H_2); δ_C (75 MHz, $CDCl_3$) 148.2, 137.4, 134.1, 134.0, 133.6, 131.8, 131.6, 124.2, 117.8, 115.2, 82.3, 80.6, 70.7, 65.4, 59.4, 57.3, 34.1, 29.8, 28.6, 17.6 (2C), 17.5 (2C), 12.3 (2C) (the signals for 1'-C, 2'-C and C_8F_{17} are missing); *m/z* (ES+) (Found: MNa^+ 991.2035, $C_{35}H_{41}F_{17}N_2O_6SSi$ requires *MNa* 991.2075).

(1*S*,3*R*,9*R*,10*S*)-5-(((3',3',4',4',5',5',6',6',7',7',8',8',9',9',10',10',10'-Heptadecafluorodecyl)-diisopropyl-silyloxy)-methyl) 7-(2-nitrobenzenesulfonyl)-2,12-dioxa-7-azatricyclo[8.5.0.0^{3,9}]4,14-pentadecadiene (92)

By general procedure B, after 47 h the metathesis substrate **90** (11 mg, 0.011 mmol) and Hoveyda-Grubbs Catalyst, 2nd generation (0.3 mg, 0.5 μmol and 0.6 mg, 0.001 mmol) in CH_2Cl_2 (22 mL) gave the crude product, which was purified by column chromatography, eluting with a gradient 5:1→1:1 petrol–EtOAc, to give the *tricycle* **92** (3 mg, 27%) as a colorless oil, R_f 0.62 (1:1 petrol–EtOAc); $[\alpha]_D^{20}$ –48.0 (*c* 0.0040 in $CHCl_3$); ν_{max}/cm^{-1} (neat) 2946, 2868, 1546, 1371, 1240, 1205; δ_H (500 MHz, $CDCl_3$) 7.99 (1H, dd, *J* 7.6 and 1.5, nosyl 3-H), 7.71 (1H, td, *J* 7.6 and 1.5, nosyl 5-H), 7.66 (1H, td, *J* 7.6 and 1.5, nosyl 4-H), 7.62 (1H, dd, *J* 7.6 and 1.5, nosyl 6-H), 6.06–6.04 (2H, m, 4-H and 15-H), 5.69 (1H, ddt, *J* 10.8, 5.2 and 2.8, 14-H), 4.61 (1H, d, *J* 9.8, 1-H), 4.39 (1H, d, *J* 9.8, 3-H), 4.26–4.10 (4H, m, 5-CH_2 and 13-H_2), 4.02 (1H, d, *J* 17.3, 6-H_a), 3.88 (1H, dd, *J* 10.8 and 6.6, 11-H_a), 3.80 (1H, d, *J* 17.3, 6-H_b), 3.76 (1H, dd, *J* 12.4 and 10.8, 11-H_b), 3.56 (1H, dd, *J* 12.4 and 5.3, 8-H_a), 3.50 (1H, *t*, J 12.4, 8-H_b), 2.67 (1H, tdd, *J* 12.4, 9.8 and 6.6, 10-H), 2.46 (1H, tdd, *J* 12.4, 9.8 and 5.3, 9-H), 2.19–2.06 (2H, m, 2'-H_2), 1.11–0.99 (14H, m, ^{i}Pr), 0.90–0.85 (2H, m, 1'-H_2); δ_C (75 MHz, $CDCl_3$) 147.7 (HMBC), 137.6, 133.8, 133.1, 132.4, 131.8, 131.0, 129.5, 128.5, 124.3, 82.8, 82.2, 67.6, 67.4, 65.7, 47.5, 46.7, 46.5, 44.9, 17.7 (2C), 17.6 (2C), 12.5 (2C) (the signals for 1'-C, 2'-C and C_8F_{17} are missing); *m/z* (ES+) (Found: MNa^+ 1005.1826, $C_{35}H_{39}F_{17}N_2O_7SSi$ requires *MNa* 1005.1868).

(*R*,*Z*)-6-(2,5-Dihydrofuran-3-yl)-2-(((3',3',4',4',5',5',6',6',7',7',8',8',9',9',10',10',10'-heptadecafluorodecyl)-diisopropyl-silyloxy)-methyl)-1-(2-nitrophenylsulfonyl)-2,3,4,7-tetrahydro-1*H*-azepine (93)

By general procedure B, after 22 h the metathesis substrate **91** (245 mg, 0.25 mmol) and Hoveyda-Grubbs Catalyst, 2nd generation (8 mg, 0.013 mmol) in CH_2Cl_2 (500 mL) gave the crude product, which was purified by column chromatography, eluting with CH_2Cl_2, to give the *tetrahydro-1H-azepine* **93** (162 mg, 69%) as a colorless oil, R_f 0.44 (CH_2Cl_2); $[\alpha]_D^{20}$ +22.9 (*c* 0.003 in $CHCl_3$); ν_{max}/cm^{-1} (neat) 2928, 2866, 1546, 1371, 1245, 1204; δ_H

(500 MHz, $CDCl_3$) 7.91 (1H, dd, *J* 7.8 and 1.3, nosyl 3-H), 7.64 (1H, td, *J* 7.8 and 1.3, nosyl 5-H), 7.55 (1H, td, *J* 7.8 and 1.3, nosyl 4-H), 7.52 (1H, dd, *J* 7.8 and 1.3, nosyl 6-H), 5.86–5.84 (1H, m, dihydrofuran 4-H), 5.25-5.22 (1H, m, 5-H), 4.83–4.71 (2H, m, dihydrofuran 2-H_2), 4.69 (1H, d, *J* 18.1, 7-H_a), 4.64–4.58 (1H, m, dihydrofuran 5-H_a), 4.56–4.50 (1H, m, dihydrofuran 5-H_b), 4.33–4.27 (1H, m, 7-H_b), 4.20–4.14 (1H, m, 2-H), 3.76 (1H, dd, *J* 10.0 and 5.5, 2-CH_{2a}), 3.71 (1H, dd, *J* 10.0 and 3.8, 2-CH_{2a}), 2.35–2.00 (6H, m, 3-H_2, 4-H_2 and 2'-H_2), 1.05–0.97 (14H, m, ^{i}Pr), 0.84–0.81 (2H, m, 1'-H_2); δ_C (75 MHz, $CDCl_3$) 138.6, 133.4, 131.2, 130.4, 123.7, 120.0, 76.9, 75.1, 66.7, 59.0, 44.1, 29.8, 26.4, 17.5 (2C), 17.5 (2C), 12.3, 12.3 (the signals for 4 unsaturated C, 1'-C, 2'-C and C_8F_{17} are missing); *m/z* (ES+) (Found: MNa^+ 963.1758, $C_{33}H_{37}F_{17}N_2O_6SSi$ requires *MNa* 963.1762).

3,3,4,4,5,5,6,6,7,7,8,8,9,9,10,10,10-Heptadecafluorodecane iodide (95)[257]

3,3,4,4,5,5,6,6,7,7,8,8,9,9,10,10,10-heptadecafluorodecanol (8.60 g, 18.5 mmol), imidazole (3.80 g, 55.6 mmol) and PPh_3 (7.29 g, 27.8 mmol) were dissolved in Et_2O (46 mL) and MeCN (15 mL) and the mixture was cooled to 0 °C. I_2 (7.06 g, 27.8 mmol) was added over 15 min and the reaction mixture was stirred at 0 °C for 15 min and then at room temperature for 15 h. Et_2O (200 mL) was added and the mixture was lead through a pad of celite and the celite was washed with Et_2O (4×50 mL). The colorless organic mixture was concentrated under reduced pressure and purified by column chromatography, eluting with hexane, to give the *iodide* **95** (9.83 g, 92%) as a colorless amorphous solid, mp = 51.5–52.0 °C (hexane), (lit.[281] 54.0–55.5 °C); R_f 0.76 (hexane); δ_H (500 MHz, $CDCl_3$) 3.27–3.23 (2H, m, 1-H_2), 2.73–2.66 (2H, m, 2-H_2).

(3,3,4,4,5,5,6,6,7,7,8,8,9,9,10,10,10-Heptadecafluorodecyl)-diisopropylsilane (96)[257]

To a stirred solution of ^{t}BuLi (1.7 M in pentane, 20.1 mL, 34.2 mmol) ín Et_2O (58 mL) at –78 °C was added a solution of the iodide **95** (9.80 g, 17.1 mmol) in Et_2O (80 mL) over 15 min. The reaction mixture was stirred for 1 h at -78°C after which chlorodiisopropylsilane (2.06 g, 13.7 mmol) was added and the mixture was allowed to reach room temperature. After 2 h the reaction was quenched by carefully addition of a saturated aqueous solution of NH_4Cl (50 mL). H_2O (*ca.* 20 mL) was added until the aqueous phase was clear and the organic layer was isolated by extraction. The aqueous phase was washed with Et_2O (2×100 mL) and the combined organic phases were concentrated under reduced pressure and purified by column chromatography, eluting with hexane, to the give *silane* **96** (7.29 g, 95%) as colorless oil, R_f 0.89 (hexane); δ_H (500 MHz, $CDCl_3$) 3.49 (1H, s, Si-H), 2.18–2.06 (2H, m, 2-H_2), 1.08–1.00 (14H, m, ^{i}Pr), 0.87–0.82 (2H, m, 1-H_2).

3-((3',3',4',4',5',5',6',6',7',7',8',8',9',9',10',10',10'-Heptadecafluorodecyl)-diisopropyl-silyloxy) 2-methylene-propanol (99)

NBS (1.19 g, 6.68 mmol) was added to a stirred solution of silane **96** (3.76 g 6.68 mmol) along with 4 Å molecular sieves in CH_2Cl_2 (60 mL) at 0 °C. The reaction mixture was

allowed to reach room temperature and stirred for 20 min, after which the mixture was added to a solution of 2-methylene-1,3-propanediol (491 mg, 5.57 mmol), DMAP (1.70 g, 13.9 mmol) and 4 Å molecular sieves in CH_2Cl_2 (500 mL). The reaction mixture was stirred at room temperature for 1.5 h, then the molecular sieves were removed by filtration and the filtrate was concentrated under reduced pressure and purified by column chromatography, eluting with 10:1 petrol–EtOAc, to give the *silyl ether* **99** (1.42 mg, 39%) as a clear colorless oil, R_f 0.40 (10:1 petrol–EtOAc); ν_{max}/cm^{-1} (neat) 3338, 2927, 2870, 1708, 1463, 1368, 1243, 1206; δ_H (500 MHz, $CDCl_3$) 5.14–5.11 (2H, m, 2-CH_2), 4.30 (2H, s, 1-H_2), 4.18 (2H, d, *J* 6.0, 3-H_2), 2.19–2.08 (2H, m, 2'-H_2), 1.07–1.04 (14H, m, ^{i}Pr) and 0.91–0.83 (2H, m, 1'-H_2); δ_C (75 MHz, $CDCl_3$) 147.4, 111.3, 65.1, 64.5, 17.7, 17.6, 12.6 (the signals for 1'-C, 2'-C and C_8F_{17} are missing); *m/z* (ES+) (Found: MH^+ 649.1398, $C_{20}H_{25}F_{17}O_2Si$ requires *MH* 649.1425).

N-tert-Butoxycarbonyl *N*-(3-((3',3',4',4',5',5',6',6',7',7',8',8',9',9',10',10',10'-heptadecafluorodecyl)-diisopropyl-silyloxy)-2-methylene-propyl) 2-nitrobenzenesulfonamide (101)

By general procedure A, the alcohol **99** (300 mg, 0.46 mmol), the sulfonamide **100** (559 mg, 1.85 mmol), PPh_3 (485 mg, 1.85 mmol) and DEAD (0.29 mL, 1.85 mmol) in THF (21 mL) gave the *sulfonamide* **101** (404 mg, 94%, >95% purity by 500 MHz ^{1}H NMR spectroscopy) as a colorless oil, R_f 0.15 (10:1 petrol–EtOAc); ν_{max}/cm^{-1} (neat) 2946, 2869, 1737, 1547, 1369, 1206; δ_H (500 MHz, $CDCl_3$) (1H, m, nosyl 3-H), 7.77–7.74 (3H, m, nosyl 4-H, 5-H and 6-H), 5.27–5.25 (1H, m, 2-CH_{2a}), 5.21–5.19 (1H, m, 2-CH_{2b}), 4.39–4.37 (2H, m, 1-H_2 or 3-H_2), 4.29–4.27 (2H, m, 1-H_2 or 3-H_2), 2.23–2.11 (2H, m, 2'-H_2), 1.35 (9H, s, ^{t}Bu), 1.09–1.05 (14H, m, ^{i}Pr), 0.92–0.88 (2H, m, 1'-H_2); δ_C (75 MHz, $CDCl_3$) 143.6, 134.3, 133.9, 131.8, 124.5, 111.0, 85.2, 64.6, 49.6, 27.9, 17.7 (2C), 17.6 (2C), 12.6 (2C) (the signals for nosyl 1-C, 2-C, C=O, 1'-C, 2'-C and C_8F_{17} are missing); *m/z* (ES+) (Found: MNa^+ 955.1724, $C_{31}H_{37}F_{17}N_2O_7SSi$ requires *MNa* 955.1711).

(*S*)-(3',3',4',4',5',5',6',6',7',7',8',8',9',9',10',10',10'-Heptadecafluorodecyl)-diisopropylsilyl oxiranylmethyl ether (104)

NBS (548 mg, 3.08 mmol) was added to a stirred solution of silane **96** (1.73 g, 3.08 mmol) and 4 Å molecular sieves in CH_2Cl_2 (27 mL) at 0 °C. The reaction mixture was allowed to reach room temperature and stirred for 25 min, after which the mixture was added to a solution of (*R*)-glycidol (190 mg, 2.57 mmol), DMAP (786 mg, 6.43 mmol) and 4 Å molecular sieves in CH_2Cl_2 (225 mL). The reaction mixture was stirred at room temperature for 1.5 h, then the molecular sieves were removed by filtration and the filtrate was concentrated under reduced pressure and purified by column chromatography, eluting with 45:1 petrol–EtOAc, to give the *silyl ether* **104** (660 mg, 40%) as a clear colorless oil, R_f 0.28 (45:1 petrol–EtOAc); $[\alpha]_D^{20}$ –8.5 (*c* 0.016 in $CHCl_3$); δ_H (300 MHz, $CDCl_3$) 3.95 (1H, dd, *J* 11.8 and 2.9, 3-H_a), 3.68 (1H, dd, *J* 11.8 and 5.0, 3-H_b), 3.13–3.07 (1H, dddd, *J* 5.0, 4.1, 2.9 and 2.7, 2-H), 2.78 (1H, dd, *J* 5.1 and 4.1, 1-H_a), 2.63 (1H, dd, *J* 5.1 and 2.7,

1-H_b), 2.25–2.06 (2H, m, 2'-H_2), 1.08–1.02 (14H, m, ^{i}Pr), 0.91–0.84 (2H, m, 1'-H_2); δ_C (75 MHz, $CDCl_3$) 64.3, 52.5, 44.5, 24.6 (t, *J* 24), 17.7, 17.6, 12.6 (the signals for 1'-C and C_8F_{17} are missing).

L-*N*-(2-Nitrophenylsulfonyl) alanine (108)

L-Alanine (1.50 g, 16.8 mmol) was dissolved in mixture of THF (18 mL) and aqueous NaOH (1M, 20 mL, 20 mmol) and cooled to 0 °C. A solution of 2-nitrobenzenesulfonyl chloride (4.48 g, 20.2 mmol) in aqueous NaOH (1M, 24 mL, 24 mmol) was added in small portions over 1 h and the reaction mixture was stirred at 0 °C for an additional 30 min after which THF was removed by concentration under reduced pressure. The remaining aqueous solution was washed with Et_2O (2×15 mL) then the pH was adjusted to 1 via addition of concentrated HCl yielding a colorless amorphous solid in the aqueous solution. The solid was isolated by filtration and recrystallation from H_2O gave the *sulfonamide* **108** (1.44 g, 31%) as white needles, mp = 166.8–168.1 °C (H_2O); $[\alpha]_D^{20}$ –137.6 (*c* 0.017 in acetone); ν_{max}/cm^{-1} (neat) 3299, 3099, 1723, 1543, 1351, 1171; δ_H (500 MHz, acetone-d_6) 8.15-8.13 (1H, m, nosyl 3-H), 7.98–7.96 (1H, m, nosyl 5-H), 7.93–7.86 (2H, m, nosyl 4-H and 6-H), 7.01–6.96 (1H, m, *NH*), 4.27–4.20 (1H, m, 2-H), 1.48 (3H, d, *J* 7.2, CH_3); δ_C (75 MHz, acetone-d_6) 173.1, 134.9, 133.6, 131.3, 125.9, 52.8, 29.8, 19.6 (the signal for nosyl 2-C is missing); *m/z* (ES+) (Found: MNa^+ 297.0153, $C_9H_{10}O_6S$ requires *MNa* 297.0152).

(*S*)-((*S*)-1-((3',3',4',4',5',5',6',6',7',7',8',8',9',9',10',10',10'-Heptadecafluorodecyl)-diisopropyl-silyloxy)-5-hexen-2-yl) 2-(2-nitrophenylsulfonamido)-propanoate (109)

The alcohol **88** (200 mg, 0.30 mmol), the carboxylic acid **108** (325 mg, 1.19 mmol) and DMAP (18 mg, 0.15 mmol) were dissolved in THF (22 mL) and cooled to 0 °C. A solution of DCC (246 mg, 1.19 mmol) in THF (8 mL) was added dropwise over 5 min. The reaction mixture was stirred at 0 °C for 1.5 h after which the mixture was concentrated under reduced pressure and purified by F–SPE, eluting with 8:2 MeOH–H_2O then MeOH, and column chromatography, eluting with a gradient 9:1→6:1 Petrol–EtOAc, to give the *ester* **109** (155 mg, 56%) as a slightly yellow oil, R_f 0.10 (9:1 Petrol–EtOAc); $[\alpha]_D^{20}$ –53.0 (*c* 0.014 in $CHCl_3$); ν_{max}/cm^{-1} (neat) 2949, 2871, 1743, 1546, 1360, 1244, 1208; δ_H (500 MHz, $CDCl_3$) 8.10–8.07 (1H, m, nosyl 3-H), 7.94–7.92 (1H, m, nosyl 6-H), 7.73–7.67 (2H, m, nosyl 4-H and 5-H), 6.16 (1H, d, *J* 7.3, *NH*), 5.68 (1H, ddt, *J* 16.9, 10.4 and 6.6, hexenyl 5-H), 4.96–4.90 (2H, m, hexenyl 6-H_2), 4.78 (1H, dt, *J* 10.1 and 5.1, hexenyl 2-H), 4.25 (1H, p, *J* 7.3, 2-H), 3.60 (2H, d, *J* 5.1, hexenyl 1-H_2), 2.11–1.99 (2H, m, 2'-H_2), 1.95–1.81 (2H, m, hexenyl 4-H_2), 1.61–1.49 (2H, m, hexenyl 3-H_2), 1.48 (3H, d, *J* 7.3, 3-H_3), 1.03–0.98 (14H, m, ^{i}Pr), 0.84–0.79 (2H, m, 1'-H_2); δ_C (75 MHz, $CDCl_3$) 171.6, 147.9, 137.2, 134.7, 133.6, 133.0, 130.5, 125.8, 115.6, 75.8, 64.4, 52.7, 29.7, 29.4, 25.5 (t, *J* 23), 20.0, 17.6, 17.5, 17.5 (2C), 12.4, 12.4 (the signals for 1'-C and C_8F_{17} are missing); *m/z* (ES+) (Found: MNa^+ 955.1691, $C_{31}H_{37}N_2O_7SSi$ requires *MNa* 955.1711).

_N_-3-Butenyl 2-nitrobenzenesulfonamide (110)[245]

3-Butenyl amine hydrochloride (790 mg, 7.34 mmol), 2-nitrobenzenesulfonyl chloride (1.63 g, 7.34 mmol) and K_2CO_3 (2.23 g, 16.1 mmol) were dissolved in CH_2Cl_2 (13 mL) and the reaction mixture was stirred for 64 h at room temperature. Carefully, H_2O (1.3 mL) and an aqueous solution of HCl (10%, 13 mL) were added and the organic layer was isolated by extraction, washed with a saturated aqueous solution of Na_2SO_4 (12 mL) and dried over $MgSO_4$. Concentration under reduced pressure and recrystallisation (1:1 toluene–hexane) gave the *sulfonamide* **110** (1.33 mg, 71%) as white needles, mp = 53.0–53.5 °C (1:1 toluene–hexane); R_f 0.55 (3:1 toluene–EtOAc); δ_H (300 MHz, $CDCl_3$) 8.18–8.13 (1H, m, nosyl 3-H), 7.90–7.86 (1H, m, nosyl 6-H), 7.78–7.73 (2H, m, nosyl 4-H and 5-H), 5.73–5.59 (1H, m, 3-H), 5.33 (1H, br s, NH), 5.10–5.02 (2H, m, 4-H_2), 3.19 (2H, dd, *J* 12.8 and 6.6, 1-H_2) and 2.32–2.25 (2H, m, 2-H_2).

4-Hydroxy-2-butynyl vinylacetate (112)

4-hydroxy-2-butynol (1.00 g, 11.6 mmol), vinylacetic acid (1.10 g, 12.8 mmol) and DMAP (280 mg, 2.3 mmol) were dissolved in CH_2Cl_2 (1160 mL). DCC (4.78 g, 23.2 mmol) in CH_2Cl_2 (20 mL) was added and the reaction mixture was stirred for 3 h, then concentrated under reduced pressure and purified by column chromatography, eluting with 4:1 CH_2Cl_2–MeOH, to give the *monoester* **112**, contaminated with DCC, hence the mixture was purified by column chromatography, eluting with 1:1 petrol–EtOAc, to give the pure *monoester* **112** (559 mg, 31%) as a colorless oil, R_f 0.70 (2:1 petrol–EtOAc); ν_{max}/cm^{-1} (neat) 3434, 1743, 1167, 1144, 1023, 986; δ_H (500 MHz, $CDCl_3$) 5.92 (1H, ddt, *J* 16.7, 9.8 and 6.9, 3-H), 5.22–5.17 (2H, m, 4-H_2), 4.74 (2H, t, *J* 1.8, butynyl 1-H_2), 4.31 (2H, dt, *J* 6.1 and 1.8, butynyl 4-H_2), 3.15 (2H, dt, *J* 6.9 and 1.4, 2-H_2), 2.23 (1H, t, *J* 6.1, *OH*); δ_C (75 MHz, $CDCl_3$) 171.0, 129.7, 119.1, 85.4, 79.6, 52.6, 51.0, 38.9; *m/z* (ES+) (Found: MNa^+ 177.0516, $C_8H_{10}O_3$ requires *MNa* 177.0522).

_N_-3-Butenyl _N_-(3-((3',3',4',4',5',5',6',6',7',7',8',8',9',9',10',10',10'-heptadecafluorodecyl)-diisopropyl-silyloxy))-2-methylene-propyl 2-nitrobenzenesulfonamide (118)

By general procedure A, the alcohol **99** (260 mg, 0.40 mmol), the sulfonamide **110** (410 mg, 1.60 mg), PPh_3 (420 mg, 1.60 mmol) and DEAD (0.25 mL, 1.60 mmol) in THF (18 mL) gave the *sulfonamide* **118** (338 mg, 95%, >85% purity by 500 MHz ^{1}H NMR spectroscopy) as a colorless oil, R_f 0.37 (10:1 petrol–EtOAc); ν_{max}/cm^{-1} (neat) 2926, 2869, 1729, 1548, 1463, 1372, 1242, 1206; δ_H (500 MHz, $CDCl_3$) 8.05 (1H, dd, *J* 7.4 and 1.8, nosyl 3-H), 7.71–7.62 (3H, m, nosyl 4-H, 5-H, 6-H), 5.66–5.57 (1H, m, butenyl 3-H), 5.27–5.26 (1H, m, 2-CH_{2a}), 5.10 (1H, d, *J* 1.0, 2-CH_{2b}), 5.00 (1H, ddd, *J* 17.2, 3.0 and 1.4, butenyl 4-H_{trans}), 4.98–4.95 (1H, m, butenyl 4-H_{cis}), 4.08 (2H, s, 3-H_2), 4.04 (2H, s, 1-H), 3.36–3.33 (2H, m, butenyl 1-H_2), 2.26–2.21 (2H, m, butenyl 2-H_2), 2.15–2.05 (2H, m, 2'-H_2), 1.09–1.01 (14H, m, ^{i}Pr), 0.86–0.82 (2H, m, 1'-H_2); δ_C (75 MHz, $CDCl_3$) 148.3, 142.7, 134.5, 133.8, 131.9, 131.5, 124.6, 117.7, 114.0, 64.1, 50.0, 46.6, 32.5, 17.9 (2C), 17.8

(2C), 12.7 (2C) (the signals for 1''-C, 2''-C, C_8F_{17} and nosyl 1-C are missing); *m/z* (ES+) (Found: MNa^+ 909.1677, $C_{30}H_{35}F_{17}N_2O_5SSi$ requires *MNa* 909.1657).

_N_-(4-Allyloxy-2-butynyl) _N_-3-((3',3',4',4',5',5',6',6',7',7',8',8',9',9',10',10',10'-heptadecafluorodecyl)-diisopropyl-silyloxy)-2-methylene-propyl 2-nitrobenzenesulfonamide (119)

By general procedure A, the alcohol **99** (200 mg, 0.31 mmol), the sulfonamide **80** (382 mg, 1.23 mmol), PPh_3 (322 mg, 1.23 mmol) and DEAD (0.19 mL, 1.23 mmol) in THF (14 mL) gave the *sulfonamide* **119** (280 mg, 96%, >85% purity by 500 MHz ^{1}H NMR spectroscopy) as a colorless oil, R_f 0.10 (10:1 petrol–EtOAc); ν_{max}/cm^{-1} (neat) 2947, 2868, 1548, 1371, 1205; δ_H (500 MHz, $CDCl_3$) 8.08–8.06 (1H, m, nosyl 3-H), 7.70–7.62 (3H, m, nosyl 4-H, 5-H and 6-H), 5.83 (1H, ddt, *J* 17.2, 10.4 and 5.7, allyl 2-H), 5.34–5.32 (1H, d, *J* 1.4, 2-CH_{2a}), 5.24 (1H, ddd, *J* 17.2, 3.0 and 1.3, allyl 3-H_{trans}), 5.20 (1H, ddd, *J* 10.4, 3.0 and 1.3, alllyl 3-H_{cis}), 5.18–5.17 (1H, m, 2-CH_{2b}), 4.17 (2H, t, *J* 1.7, 1-H_2 or 3-H_2), 4.13 (2H, s, butynyl 1-H_2 or 3-H_2), 4.05 (2H, s, butynyl 1-H_2 or 3-H_2), 3.97 (2H, t, *J* 1.8, 1-H_2 or 3-H_2), 3.88 (2H, dt, *J* 5.7 and 1.3, allyl 1-H_2), 2.17–2.06 (2H, m, 2'-H_2), 1.05–1.02 (14H, m, ^{i}Pr), 0.87–0.83 (2H, m, 1'-H_2); δ_C (75 MHz, $CDCl_3$) 161.0, 150.5, 141.6, 133.8, 131.7, 131.3, 124-3, 118.0, 114.8, 112.8, 77.4, 70.7, 63.7, 61.1, 57.2, 49.4, 36.3, 17.7 (2C), 17.6 (2C), 12.5 (2C) (the signals for 1'-C, 2'-C and C_8F_{17} are missing); *m/z* (ES+) (Found: MNa^+ 963.1718, $C_{33}H_{37}F_{17}N_2O_6SSi$ requires *MNa* 963.1762).

(_S_)-((_S_)-1-((3',3',4',4',5',5',6',6',7',7',8',8',9',9',10',10',10'-Heptadecafluorodecyl)-diisopropyl-silyloxy)-5-hexen-2-yl) 2-_N_-(4-allyloxy-2-butynyl) 2-(2-nitrophenylsulfonamido)-propanoate (120)

The sulfonamide **109** (155 mg, 0.17 mmol), the alcohol **111** (105 mg, 0.83 mmol) and PPh_3 (218 mg, 0.83 mmol) were dissolved in THF (7.5 mL) and cooled to 0 °C. DEAD (0.13 mL, 0.83 mmol) was added dropwise and the reaction mixture was stirred at room temperature. After 1 h PPh_3 (109 mg, 0.41 mmol) and DEAD (0.07 mL, 0.41 mmol) were added and the reaction mixture was stirred for another 1.5 h after which the mixture was concentrated under reduced pressure and purified by F–SPE, eluting with 8:2 MeOH–H_2O then MeOH, to give the *sulfonamide* **120** (120 mg, 68%, >75% purity by 500 MHz ^{1}H NMR spectroscopy) as a colorless oil, R_f 0.64 (3:1 petrol–EtOAc); δ_H (500 MHz, $CDCl_3$) 8.19–8.16 (1H, m, nosyl 3-H), 7.70–7.64 (3H, m, nosyl 4-H, 5-H and 6-H), 5.88–5.79 (1H, m, allyl 2-H), 5.75 (1H, ddd, *J* 16.9, 10.1 and 6.6, hexenyl 5-H), 5.25 (1H, ddd, *J* 17.1, 3.0 and 1.4, allyl 3-H_{trans}), 5.21–5.18 (1H, m, allyl 3-H_{cis}), 5.02–4.95 (2H, m, hexenyl 6-H_2), 4.93–4.88 (1H, m, hexenyl 2-H), 4.84 (1H, q, *J* 7.4, 2-H), 4.51 (1H, dt, *J* 18.8 and 1.8, butynyl 1-H_a), 4.11 (1H, dt, *J* 18.8 and 1.8, butynyl 1-H_b), 3.99–3.97 (2H, m, butynyl 3-H_2), 3.91 (2H, dt, *J* 5.8 and 1.4, allyl 1-H_2), 3.67–3.65 (2H, m, hexenyl 1-H_2), 2.15–1.99 (4H, m, hexenyl 4-H_2 and 2'-H_2), 1.68–1.63 (2H, m, hexenyl 3-H_2), 1.63 (3H, d, *J* 7.4, 3-H_3), 1.06–0.99 (14H, m, ^{i}Pr), 0.86–0.81 (2H, m, 1'-H_2); *m/z* (ES+) (Found: MNa^+ 1063.2240, $C_{38}H_{45}F_{17}N_2O_8SSi$ requires *MNa* 1063.2287).

3-((3',3',4',4',5',5',6',6',7',7',8',8',9',9',10',10',10'-Heptadecafluorodecyl)-diisopropyl-silyloxy)-methyl-1-(2-nitrophenylsulfonyl)-1,2,5,6-tetrahydropyridine (122)

By general procedure B, after 2 h the metathesis substrate **118** (330 mg, 0.37 mmol) and Grubbs Catalyst, 1st generation (15 mg, 0.019 mmol) in CH_2Cl_2 (370 mL) gave the crude product, which was purified by F–SPE, eluting with 8:2 MeOH–H_2O then MeOH, to give the *tetrahydropyridine* **122** (300 mg, 95%, >90% purity by 500 MHz ^{1}H NMR spectroscopy) as a brown amorphous solid, R_f 0.33 (10:1 petrol–EtOAc); ν_{max}/cm^{-1} (neat) 2924, 2853, 1548, 1462, 1374, 1242, 1207; δ_H (500 MHz, $CDCl_3$) 8.00 (1H, dd, *J* 7.7 and 1.6, nosyl 3-H), 7.71–7.60 (3H, m, nosyl 4-H, 5-H and 6-H), 5.77–5.74 (1H, m, 4-H), 4.13 (2H, s, 3-CH_2), 3.81 (2H, d, *J* 1.8, 2-H_2), 3.44 (2H, t, *J* 5.8, 6-H_2), 2.26–2.22 (2H, m, 5-H_2), 2.15–2.04 (2H, m, 2'-H_2), 1.09–1.00 (14H, m, ^{i}Pr) and 0.88–0.83 (2H, m, 1'-H_2); δ_C (75 MHz, $CDCl_3$) 148.0, 132.7, 132.5, 131.1, 130.4, 129.8, 123.1, 119.3, 64.2, 43.8, 41.6, 23.7, 16.5 (2C), 16.4 (2C), 11.4 (2C) (the signals for 1'-C', 2'-C and C_8F_{17} are missing); *m/z* (ES+) (Found: MNa$^+$ 881.1373, $C_{28}H_{31}F_{17}N_2O_5SSi$ requires *MNa* 881.1344).

3-(2,5-Dihydro-3-furanyl)-4-(((3',3',4',4',5',5',6',6',7',7',8',8',9',9',10',10',10'-heptadecafluorodecyl)-diisopropyl-silyloxy)-methyl)-1-(2-nitrophenylsulfonyl)-2,5-dihydro-pyrrole (123)

By general procedure B, after 22 h the metathesis substrate **119** (246 mg, 0.26 mmol) and Hoveyda-Grubbs Catalyst, 2nd generation (8 mg, 0.013 mmol) in CH_2Cl_2 (500 mL) gave the crude product, which was purified by column chromatography, eluting with CH_2Cl_2, to give the *dihydropyrrole* **123** (136 mg, 57%) as a colorless amorphous solid, R_f 0.45 (CH_2Cl_2); ν_{max}/cm^{-1} (neat) 2949, 2868, 1548, 1372, 1206; δ_H (500 MHz, $CDCl_3$) 8.01 (1H, dd, *J* 7.6 and 1.6, nosyl 3-H), 7.72–7.66 (2H, m, nosyl 4-H and 5-H), 7.63 (1H, dd, *J* 7.3 and 1.8, nosyl 6-H), 5.80–5.78 (1H, m, dihydrofuran 4-H), 4.79–4.76 (2H, m, dihydrofuran 2-H_2 or 5-H_2), 4.71–4.68 (2H, m, dihydrofuran 2-H_2 or 5-H_2), 4.50–4.45 (4H, m, 2-H_2 and 5-H_2), 4.36–4.35 (2H, m, 3-CH_2), 2.12–2.01 (2H, m, 2'-H_2), 1.07–0.99 (14H, m, ^{i}Pr), 0.87–0.82 (2H, m, 1'-H_2); δ_C (75 MHz, $CDCl_3$) 133.9, 133.8, 132.1, 132.0, 131.7, 130.7, 126.6, 124.3, 123.9; 75.4, 75.2, 59.1, 57.0, 56.9, 17.6 (2C), 17.5 (2C), 12.4 (2C) (the signals for nosyl 1-C, 1'-C, 2'-C and C_8F_{17} are missing); *m/z* (ES+) (Found: MNa$^+$ 935.1443, $C_{31}H_{33}F_{17}N_2O_6SSi$ requires *MNa* 935.1449).

Also obtained was *N-(2-(2,5-dihydrofuran-3-yl)-allyl)-N-(3-(((3',3',4',4',5',5',6',6',7',7',8',8',9',9', 10',10',10'-heptadecafluorodecyl)-diisopropyl)-silyloxy)-2-methylene-propyl)-2-nitrobenzenesulfonamide* **124** (14 mg, 6 %) as a clear colorless oil; R_f 0.59 (CH_2Cl_2); δ_H (500 MHz, $CDCl_3$) 8.05–8.03 (1H, m, nosyl 3-H), 7.70–7.63 (3H, m, nosyl 4-H, 5-H and 6-H), 5.81–5.79 (1H, m, dihydrofuran 4-H), 5.21–5.19 (1H, m, 2-CH_2 or allyl 3-H), 5.01–4.99 (2H, m, 2-CH_2 or allyl 3-H), 4.84–4.82 (1H, m, 2-CH_2 or allyl 3-H), 4.21–4.19 (2H, m, 1-H_2, 3-H_2 or allyl 1-H_2), 4.15–4.12 (4H, m, dihydrofuran 2-H_2 and 5-H_2), 4.04–4.02 (2H, m, 1-H_2, 3-H_2 or allyl 1-H_2), 4.02–4.00 (2H, m, 1-H_2, 3-H_2 or allyl 1-H_2), 2.14–2.02 (2H, m, 2'-H_2), 1.05–0.99 (14H, m, ^{i}Pr), 0.84–0.81 (2H, m, 1'-H_2); δ_C (75 MHz, $CDCl_3$) 147.9, 142.3, 138.1, 134.1, 133.7, 131.8, 131.5, 128.5,

127.2, 124.3, 113.4, 108.2, 69.7, 66.2, 64.0, 50.0, 47.6, 17.6 (2C), 17.5 (2C), 12.5 (2C) (the signals for 1'-C', 2'-C and C_8F_{17} are missing); *m/z* (ES+) (Found: MNa^+ 963.1742, $C_{33}H_{37}F_{17}N_2O_6SSi$ requires *MNa* 963.1762).

(3*S*,10*S*,*Z*)-6-(2,5-Dihydrofuran-3-yl)-10-(((3',3',4',4',5',5',6',6',7',7',8',8',9',9',10',10',10'-heptadecafluorodecyl)-diisopropyl)-silyloxy)-methyl)-3-methyl-4-(2-nitrophenylsulfonyl)-4,5,9,10-tetrahydro-3*H*-1,4-oxazecin-2(8*H*)-one (125)

By general procedure B, after 19 h the metathesis substrate **120** (71 mg, 0.068 mmol) and Hoveyda-Grubbs catalyst, 2nd generation (2.3 mg, 0.004 mmol and 6.0 mg, 0.010 mmol) in CH_2Cl_2 (150 mL) gave the crude product, which was purified by column chromatography, eluting with 3:1 petrol–EtOAc, to give the *tetrahydro-3H-1,4-oxazecin-2(8H)-one* **125** (8 mg, 12%) as a colorless oil, R_f 0.26 (3:1 petrol–EtOAc); $[\alpha]_D^{20}$ –10.0 (*c* 0.004 in $CHCl_3$); ν_{max}/cm^{-1} (neat) 2947, 2868, 1738, 1546, 1371, 1205; δ_H (500 MHz, $CDCl_3$) 8.06 (1H, dd, *J* 7.6 and 1.4, nosyl 3-H), 7.73 (1H, td, *J* 7.6 and 1.4, nosyl 5-H), 7.69 (1H, td, *J* 7.6 and 1.4, nosyl 4-H), 7.65 (1H, dd, *J* 7.6 and 1.4, nosyl 6-H), 5.99–5.94 (1H, m, 7-H), 5.79–5.77 (1H, m, dihydrofuran 4-H), 4.95–4.89 (1H, m, 10-H), 4.85–4.64 (5H, m, 3-H, dihydrofuran 2-H_2 and 5-H_2), 4.61–4.55 (1H, m, 5-H_a), 3.70–3.65 (2H, m, 10-CH_{2a} and 5-H_b), 3.61 (1H, dd, *J* 10.4 and 5.6, 10-CH_{2b}), 2.42–2.28 (2H, m, 8-H_2), 2.14–2.03 (2H, m, 2'-H_2), 1.86–1.74 (2H, m, 9-H_2), 1.11 (3H, d, *J* 7.0, 3-CH_3), 1.06–0.98 (14H, m, ^{i}Pr), 0.86–0.80 (2H, m, 1'-H_2); δ_C (75 MHz, $CDCl_3$) 170.2, 137.2, 134.6, 133.9, 131.8, 131.0, 124.9, 124.4, 124.1, 77.0, 76.1, 75.6, 65.4, 53.7, 47.1, 29.9, 28.0, 17.5, 17.5, 17.5 (2C), 13.3, 12.4, 12.4 (the signals for 5-C, nosyl 2-C, 1'-C, 2'-C and C_8F_{17} are missing); *m/z* (ES+) (Found: MNa^+ 1035.1988, $C_{36}H_{41}N_2O_8SSi$ requires *MNa* 1035.1974).

Also obtained was *(S)-((S)-1-((3',3',4',4',5',5',6',6',7',7',8',8',9',9',10',10',10'-heptadecafluorodecyl)-diisopropyl-silyloxy)-5-hexen-2-yl) 2-N-(2-(2,5-dihydro-3-furanyl)-allyl) 2-(2-nitrophenylsulfonamido)-propanoate* **126** (36 mg, 51%) as a colorless oil, R_f 0.52 (3:1 petrol–EtOAc); $[\alpha]_D^{20}$ –14.6 (*c* 0.015 in $CHCl_3$); ν_{max}/cm^{-1} (neat) 2947, 2867, 1741, 1546, 1243, 1206, 1152; δ_H (500 MHz, $CDCl_3$) 8.03 (1H, dd, *J* 7.6 and 1.6, nosyl 3-H), 7.68 (1H, tt, *J* 7.6 and 1.6, nosyl 5-H), 7.64 (1H, tt, *J* 7.6 and 1.6, nosyl 4-H), 7.60 (1H, dd, *J* 7.6 and 1.6, nosyl 6-H), 5.96–5.94 (1H, m, dihydrofuran 4-H), 5.74 (1H, ddt, *J* 17.0, 10.3 and 6.6, hexenyl 5-H), 5.27–5.25 (1H, m, allyl 3-H_a), 5.02–4.98 (1H, m, hexenyl 6-H_a), 4.98–4.96 (1H, m, hexenyl 6-H_b), 4.90 (1H, t, *J* 7.4, 2-H), 4.86–4.81 (2H, hexenyl 2-H and allyl 3-H_b), 4.77–4.72 (2H, hexenyl 1-H_2), 4.71–4.64 (3H, dihydrofuran 2-H_a and 5-H_2), 4.01 (1H, d, *J* 17.9, dihydrofuran 2-H_b), 3.64–3.61 (2H, m, allyl 1-H_2), 2.13–1.96 (4H, hexenyl 4-H_2 and 2'-H_2), 1.68–1.57 (2H, hexenyl 3-H_2), 1.48 (3H, d, *J* 7.4, 3-H_3), 1.05–0.98 (14H, m, ^{i}Pr), 0.85–0.80 (2H, m, 1'-H_2); δ_C (75 MHz, $CDCl_3$) 171.1, 148.1, 137.4, 137.1, 136.2, 133.7, 131.6, 131.5, 129.2, 124.1, 122.3, 115.5, 115.2, 76.9, 75.5, 75.3, 64.3, 56.6, 48.2, 29.7, 29.3, 17.5 (2C), 17.5 (2C), 17.0, 12.4 (2C) (the signals for 1'-C, 2'-C and C_8F_{17} are missing); *m/z* (ES+) (Found: MNa^+ 1063.2278, $C_{38}H_{45}F_{17}N_2O_8SSi$ requires *MNa* 1063.2287).

(2*S*,2'*S*)-((14*S*,21*S*,*E*)-1,1,1,2,2,3,3,4,4,5,5,6,6,7,7,8,8,27,27,28,28,29,29,30,30,31,31,32,32,33,33,34,34,34-Tetratriacontafluoro-11,11,24,24-tetraisopropyl-12,23-dioxa-11,24-disilatetratriacont-17-ene-14,21-diyl) bis(2-(*N*-(2-(2,5-dihydrofuran-3-yl)-allyl)-2-nitrophenylsulfonamido)-propanoate) (127)

The metathesis substrate **120** (120 mg, 0.12 mmol) was dissolved in benzene (230 mL) and heated to reflux. Hoveyda-Grubbs Catalyst, 2nd generation (7.2 mg, 0.011 mmol) was added and the reaction mixture was stirred for 14.5 h. The reaction mixture was cooled to room temperature, Et_3N (1.5 mL, 10.3 mmol) and tris(hydroxymethyl)phosphine (500 mg, 4.03 mmol) were added and the mixture was stirred for 15 min after which silica (1.5 g) was added and the mixture was stirred for another 15 min. The suspension was filtrated through a pad of celite, washed with EtOAc, concentrated under reduced pressure and purified by column chromatography, eluting with 3:1 petrol–EtOAc, to give the *11,24-disilatetratriacont-17-ene* **127** (24 mg, 10%) as a colorless oil, R_f 0.08 (3:1 petrol–EtOAc); $[\alpha]_D^{20}$ –16.0 (*c* 0.012 in $CHCl_3$); ν_{max}/cm^{-1} (neat) 2947, 2869, 1739, 1547, 1372, 1206, 1152; δ_H (500 MHz, $CDCl_3$) 8.02 (2H, dd, *J* 7.8 and 1.4, nosyl 3-H), 7.71–7.60 (6H, m, nosyl 4-H, 5-H and 6-H), 5.96–5.93 (2H, dihydrofuran 4-H), 5.34–5.31 (2H, 17-H and 18-H), 5.23–5.21 (2H, allyl 3-H_a), 4.90 (2H, q, *J* 7.4, propanoate 2-H), 4.87–4.82 (2H, 14-H and 21-H), 4.82–4.80 (2H, allyl 3-H_b), 4.76–4.65 (10H, allyl 1-H_a, dihydrofuran 2-H_2 and 5-H_2), 4.03 (2H, d, *J* 18.1, allyl 1-H_b), 3.65–3.61 (4H, 13-H_2 and 22-H_2), 2.14–1.88 (8H, 9-H_2, 16-H_2, 19-H_2 and 26-H_2), 1.59–1.53 (4H, 15-H_2 and 20-H_2), 1.48 (6H, d, *J* 7.4, propanoate 3-H_3), 1.04–0.97 (28H, ^{i}Pr), 0.85–0.80 (4H, 10-H_2 and 25-H_2); δ_C (75 MHz, $CDCl_3$) 171.2 (2C), 148.0 (2C), 137.1 (2C), 136.2 (2C), 133.8 (2C), 133.7 (2C), 131.7 (2C), 131.4 (2C), 129.9 (2C), 124.1 (2C), 122.3 (2C), 115.1 (2C), 76.9 (2C), 75.5 (2C), 75.3 (2C), 64.5 (2C), 56.6 (2C), 48.1 (2C), 30.3 (2C), 28.1 (2C), 17.5 (2C), 17.5 (2C), 17.4 (4C), 16.9 (2C), 12.4 (4C) (the signals for 9-C, 10-C, 24-C, 25-C and C_8F_{17} are missing); *m/z* (ES+) (Found: MNa^+ 2075.4348, $C_{74}H_{86}F_{34}N_4O_{16}S_2Si_2$ requires *MNa* 2075.4368).
Also obtained was **125** (11 mg, 9%) and **126** (32 mg, 27%).

(3a*R*,8a*S*)-8a-(((3',3',4',4',5',5',6',6',7',7',8',8',9',9',10',10'-Heptadecafluorodecyl)-diisopropyl-silyloxy)-methyl)-10-(2-nitrophenylsulfonyl)-6-phenyl-3,3a,8a,9,10,11-hexahydrofuro[3,4-*e*]pyrrolo[3,4-*c*][1,2,4]triazolo[1,2-*a*]pyridazine-5,7(1*H*,6*H*)-dione ((±)-129)

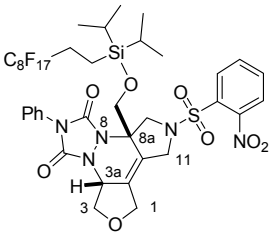

The diene **60** (97 mg, (0.089 mmol) was dissolved in CH_2Cl_2 (3 mL) and 4-phenyl-[1,2,4]-triazole-3,5-dione (**128**, 156 mg, 0.89 mmol) was added. The reaction mixture was stirred at room temperature for 1.5 h after which the mixture was concentrated under reduced pressure and purified by F–SPE, eluting with 8:2 MeOH–H_2O then MeOH, and column chromatography, eluting with 3:1 Petrol–EtOAc, to give the *tetracycle* (±)-**129** (93 mg, 84%) as a colorless amorphous solid, R_f 0.10 (3:1 Petrol–

EtOAc); ν_{max}/cm^{-1} (neat) 2947, 2869, 1767, 1708, 1547, 1242, 1206; δ_H (500 MHz, $CDCl_3$) 8.09 (1H, dd, *J* 7.6 and 1.7, nosyl 3-H), 7.78–7.72 (2H, m, nosyl 4-H and 5-H), 7.67 (1H, dd, *J* 7.6 and 1.7, nosyl 6-H), 7.48–7.42 (4H, m, phenyl 2-H and 3-H), 7.39–7.34 (1H, m, phenyl 4-H), 4.75 (1H, dd, *J* 8.7 and 7.3, 9-H_a), 4.53–4.47 (2H, m, 3a-H and 1-H_a), 4.45–4.41 (1H, m, 1-H_b), 4.33 (1H, d, *J* 10.4, 8a-CH_{2a}), 4.27–4.24 (2H, m, 11-H_2), 4.22 (1H, d, *J* 10.7, 9-H_a), 3.76 (1H, d, *J* 10.4, 8a-CH_{2b}), 3.62 (1H, dd, *J* 9.4 and 8.7, 3-H_b), 3.56 (1H, d, *J* 10.7, 9-H_b), 2.08–1.95 (2H, m, 1'-H_2), 1.02–0.94 (14H, m, ^{i}Pr), 0.83–0.78 (2H, m, 2'-H_2); δ_C (75 MHz, $CDCl_3$) 150.1, 149.6, 148.2, 134.4, 133.0, 132.1, 131.6, 131.5, 131.2, 129.3 (2C), 128.4, 125.2 (2C), 125.0, 124.5, 71.3, 67.3, 64.9, 63.7, 54.4, 53.9, 47.8, 17.4 (2C), 17.4 (2C), 12.3, 12.2 (the signals for 1'-C, 2'-C and C_8F_{17} are missing); *m/z* (ES+) (Found: MNa^+ 1110.1800, $C_{39}H_{38}F_{17}N_5O_8SSi$ requires *MNa* 1110.1831).

3-((3',3',4',4',5',5',6',6',7',7',8',8',9',9',10',10',10'-Heptadecafluorodecyl)-diisopropyl-silyloxy)-methyl-1,2,5,6-tetrahydropyridine (130)

By general procedure C, the sulfonamide **122** (100 mg, 0.12 mmol), K_2CO_3 (64 mg, 0.46 mmol) and PhSH (35 μL, 0.35 mmol) in DMF (2 mL) gave the *tetrahydropyridine* **130** (83 mg, 106%, >80% purity by 500 MHz ^{1}H NMR spectroscopy) as a colorless oil, ν_{max}/cm^{-1} (neat) 2926, 2868, 1463, 1368, 1241, 1206; δ_H (500 MHz, $CDCl_3$) 5.75–5.72 (1H, m, 4-H), 4.07 (2H, d, *J* 0.5, 3-CH_2), 3.30 (2H, d, *J* 1.7, 2-H_2), 2.92 (2H, t, *J* 5.7, 6-H_2), 2.18–2.05 (4H, m, 5-H_2 and 2'-H_2), 1.07–1.03 (14H, m, ^{i}Pr) and 0.89–0.82 (2H, m, 1'-H_2); δ_C (75 MHz, $CDCl_3$) 137.3, 120.8, 66.1, 45.6, 43.2, 29.9, 25.6, 17.7 (2C), 17.6 (2C) 12.6 (2C) (the signals for 1'-C and C_8F_{17} are missing); *m/z* (EI+) (Found: M^+ 673.1664, $C_{22}H_{28}F_{17}NOSi$ requires *M* 673.1669).

(*R,Z*)-6-(2,5-Dihydrofuran-3-yl)-2-(((3',3',4',4',5',5',6',6',7',7',8',8',9',9',10',10',10'-heptadecafluorodecyl)-diisopropyl-silyloxy)-methyl)-2,3,4,7-tetrahydro-1*H*-azepine (133)

By general procedure C, the sulfonamide **93** (155mg, 0.16 mmol), K_2CO_3 (88 mg, 0.64 mmol) and PhSH (50 μL, 0.49 mmol) in DMF (3 mL) gave the *tetrahydro-1H-azepine* **133** (129 mg, 107%, >80% purity by 500 MHz ^{1}H NMR spectroscopy) as a colorless oil, R_f 0.12 (2:1 petrol–EtOAc); ν_{max}/cm^{-1} (neat) 2922, 2852, 1461, 1375, 1240, 1205; δ_H (500 MHz, $CDCl_3$) 5.73–5.71 (1H, m, dihydrofuran 4-H), 5.66–5.62 (1H, m, 5-H), 4.76–4.69 (4H, m, dihydrofuran 2-H_2 and 5-H_2), 3.79 (1H, d, *J* 15.4, 7-H_a), 3.59–3.55 (2H, m, 2-CH_2), 3.51–3.47 (1H, m, 7-H_b), 2.99–2.94 (1H, m, 2-H), 2.44–2.37 (1H, m, 3-H_a), 2.33–2.25 (1H, m, 3-H_b), 2.18–2.06 (2H, m, 2'-H_2), 1.79–1.66 (1H, m, 4-H_a), 1.42–1.23 (1H, m, 4-H_b), 1.10–0.98 (14H, m, ^{i}Pr), 0.90–0.82 (2H, m, 1'-H_2); *m/z* (ES+) (Found: MH^+ 756.2128, $C_{27}H_{35}F_{17}NO_2Si$ requires *MH* 756.2160).

(3a*R*,8a*S*)-8a-(((3',3',4',4',5',5',6',6',7',7',8',8',9',9',10',10'-Heptadecafluorodecyl)-diisopropyl-silyloxy)-methyl)-6-phenyl-3,3a,8a,9,10,11-hexahydrofuro[3,4-*e*]pyrrolo[3,4-*c*][1,2,4]triazolo[1,2-*a*]pyridazine-5,7(1*H*,6*H*)-dione ((±)-134)

By general procedure C, the sulfonamide (±)-**129** (113 mg, 0.10 mmol), K_2CO_3 (55 mg, 0.40 mmol) and PhSH (31 μL, 0.30 mmol) in DMF (2.5 mL) gave the *amine* (±)-**134** (89 mg, 99%, >95% purity by 500 MHz ^{1}H NMR spectroscopy) as a colorless amorphous solid, ν_{max}/cm^{-1} (neat) 3335, 2949, 2870, 1755, 1693, 1426, 1203; δ_H (500 MHz, $CDCl_3$) 7.52–7.49 (2H, m, phenyl 2-H), 7.47–7.43 (2H, m, phenyl 3-H), 7.37–7.33 (1H, m, phenyl 4-H), 4.76 (1H, dd, *J* 8.4 and 7.2, 3-H$_a$), 4.59–4.53 (1H, m, 3a-H), 4.47 (1H, ddd, *J* 13.6, 3.5 and 2.0, 1-H$_a$), 4.39 (1H, ddd, *J* 13.6, 3.0 and 1.7, 1-H$_b$), 4.27 (1H, d, *J* 10.1, 8a-CH$_{2a}$), 3.81 (1H, d, *J* 10.1, 8a-CH$_{2b}$), 3.74 (1H, d, *J* 11.8, 9-H$_a$), 3.69–3.66 (2H, m, 11-H$_2$), 3.59 (1H, dd, *J* 9.1 and 8.4, 3-H$_b$), 3.25 (1H, d, *J* 11.8, 9-H$_b$), 2.10–1.98 (2H, m, 2'-H$_2$), 1.05–0.98 (14H, ^{i}Pr), 0.89–0.82 (2H, m, 1'-H$_2$); δ_C (75 MHz, $CDCl_3$) 149.8, 149.7, 131.6, 131.4, 129.7 (2C), 128.1, 125.3 (2C), 71.6, 67.4, 66.1, 64.7, 54.9, 53.9, 47.4, 17.5 (2C), 17.5 (2C), 12.4, 12.4, (the signals for 11a-C, 1'-C, 2'-C and C_8F_{17} are missing); *m/z* (ES+) (Found: MH$^+$ 903.2208, $C_{33}H_{35}F_{17}N_4O_4Si$ requires *MH* 903.2234).

3-((3',3',4',4',5',5',6',6',7',7',8',8',9',9',10',10',10'-Heptadecafluorodecyl)-diisopropyl-silyloxy)-methyl-1-(furfuryl aminecarbonyl)-1,2,5,6-tetrahydropyridine (139)

By general procedure E, the amine **130** (20 mg, 0.030 mmol) and furfuryl isocyanate (13 μL, 0.12 mmol) gave *3-((3',3',4',4',5',5',6',6',7',7',8',8',9',9',10',10',10'-heptadecafluorodecyl)-diisopropyl-silyloxy)-methyl-1-(furfuryl aminecarbonyl)-1,2,5,6-tetrahydropyridine* **139** (21 mg, 88%, >80% purity by 500 MHz ^{1}H NMR spectroscopy) as a colorless oil, δ_H (500 MHz, $CDCl_3$) 7.34 (1H, dd, *J* 1.9 and 0.8, furfuryl 5-H), 6.31 (1H, dd, *J* 3.1 and 1.9, furfuryl 4-H), 6.23 (1H, dd, *J* 3.1 and 0.8, furfuryl 3-H), 5.83–5.80 (1H, m, 4-H), 4.71 (1H, t, *J* 5.4, NH), 4.44 (2H, d, *J* 5.4, furfuryl 3-CH$_2$), 4.14–4.12 (2H, m, 3-CH$_2$), 3.82–3.80 (2H, m, 2-H$_2$), 3.47 (2H, t, *J* 5.7, 6-H$_2$), 2.19–2.05 (4H, m, 5-H$_2$ and 2'-H$_2$), 1.09–1.00 (14H, m, ^{i}Pr), 0.89–0.85 (2H, m, 1'-H$_2$).

3-hydroxymethyl-1-benzenecarbonyl-1,2,5,6-tetrahydropyridine (156)

By general procedure D, the amine **130** (20 mg, 0.030 mmol), DMAP (18 mg, 0.12 mmol) and benzyl chloride (14 μL, 0.12 mmol) gave *3-((3',3',4',4',5',5',6',6',7',7',8',8',9',9',10',10',10'-heptadecafluorodecyl)-diisopropyl-silyloxy)-methyl-1-benzenecarbonyl-1,2,5,6-tetrahydropyridine* **135** (18 mg, 78%, 55:45 mixture of rotamers, >80% purity by 500 MHz ^{1}H NMR spectroscopy) as a colorless oil, δ_H (500 MHz, $CDCl_3$) 7.43–7.37 (5H, m, phenyl 2-H, 3-H and 4-H), 5.85–5.78 (1H, m, 4-H), 4.22–4.15 (2H, 3-CH$_2$), 4.04–3.99 (2H, 2-H$_2^{maj}$), 3.93–3.89 (2H, m, 2-H$_2^{min}$), 3.86–3.80 (2H, m, 6-H$_2^{min}$), 3.49–3.42 (2H, m, 6-H$_2^{maj}$), 2.31–2.07 (4H, m, 5-H$_2$ and 2'-H$_2$), 1.13–0.73 (16H, m, 1'-H$_2$ and ^{i}Pr).

By general procedure H, the silyl ether **135** (18 mg, 0.023 mmol) gave the *amide* **156** (3 mg, 60%, 10:7 mixture of rotamers) as a colorless oil, R_f 0.46 (20:1 CH_2Cl_2–MeOH);

ν_{max}/cm^{-1} (neat) 3396, 2926, 2854, 1614, 1447, 1255, 1137; δ_H (500 MHz, $CDCl_3$) 7.45–7.38 (5H, m, phenyl 2-H, 3-H and 4-H), 5.90–5.86 (1H, m, 4-H), 4.28–4.22 (2H, m, 2-H_2^{maj}), 4.17–4.12 (4H, m, 2-H_2^{min} and 3-CH_2^{min}), 4.00–3.93 (2H, m, 3-CH_2^{maj}), 3.86–3.80 (2H, m, 6-H_2^{min}), 3.49–3.43 (2H, m, 6-H_2^{maj}), 2.33–2.25 (2H, m, 5-H_2^{min}), 2.23–2.15 (2H, m, 5-H_2^{maj}); *m/z* (EI+) (Found: M^+ 217.1107, $C_{13}H_{15}NO_2$ requires *M* 217.1103).

3-Hydroxymethyl-1-(2-thiophenecarbonyl)-1,2,5,6-tetrahydropyridine (157)

By general procedure D, the amine **130** (20 mg, 0.030 mmol), DMAP (18 mg, 0.12 mmol) and 2-thiophenecarbonyl chloride (13 μL, 0.12 mmol) gave *3-((3',3',4',4',5',5',6',6',7',7',8',8',9',9',10',10',10'-heptadecafluorodecyl)-diisopropyl-silyloxy)-methyl-1-(2-thiophenecarbonyl)-1,2,5,6-tetrahydropyridine* **136** (21 mg, 88%, >85% purity by 500 MHz ^{1}H NMR spectroscopy) as a colorless oil, δ_H (500 MHz, $CDCl_3$) 7.44 (1H, dd, *J* 5.0 and 1.1, thiophene 5-H), 7.32 (1H, dd, *J* 3.6 and 1.1, thiophene 3-H), 7.04 (1H, dd, *J* 5.0 and 3.6, thiophene 4-H), 5.84–5.82 (1H, m, 4-H), 4.22–4.12 (4H, m, 2-H_2 and 3-CH_2), 3.77 (2H, t, *J* 5.6, 6-H_2), 2.29–2.25 (2H, m, 5-H_2), 2.16–2.03 (2H, m, 2'-H_2), 1.08–0.95 (14H, m, ^{i}Pr), 0.90–0.83 (2H, m, 1'-H_2).

By general procedure H, the silyl ether **136** (21 mg, 0.027 mmol) gave the *amide* **157** (5 mg, 83%) as a colorless oil, R_f 0.27 (20:1 CH_2Cl_2–MeOH); ν_{max}/cm^{-1} (neat) 3400, 2528, 1601, 1443, 1084; δ_H (500 MHz, CD_3OD) 7.65 (1H, dd, *J* 5.0 and 1.1, thiophene 5-H), 7.46–7.44 (1H, m, thiophene 3-H), 7.13 (1H, dd, *J* 5.0 and 3.7, thiophene 4-H), 5.90–5.87 (1H, m, 4-H), 4.31–4.22 (2H, m, 2-H_2), 4.03–3.97 (2H, m, 3-CH_2), 3.79 (2H, t, *J* 5.8, 6-H_2), 2.31–2.26 (2H, m, 5-H_2); *m/z* (ES+) (Found: MNa^+ 246.0553, $C_{11}H_{13}NO_2S$ requires *MNa* 246.0559).

3-Hydroxymethyl-1-(5-isoxazolecarbonyl)-1,2,5,6-tetrahydropyridine (158)

By general procedure D, the amine **130** (20 mg, 0.030 mmol), DMAP (18 mg, 0.12 mmol) and 5-isoxazolecarbonyl chloride (15 μL, 0.12 mmol) gave *3-((3',3',4',4',5',5',6',6',7',7',8',8',9',9',10',10',10'-heptadecafluorodecyl)-diisopropyl-silyloxy)-methyl-1-(5-isoxazolecarbonyl)-1,2,5,6-tetrahydropyridine* **137** (19 mg, 83%, 55:45 mixture of rotamers, >80% purity by 500 MHz ^{1}H NMR spectroscopy) as a colorless oil, δ_H (500 MHz, $CDCl_3$) 8.32 (1H, d, *J* 1.7, isoxazole 3-H^{maj}) and 8.29 (1H, d, *J* 1.7, isoxazole 3-H^{min}), 6.78–6.77 (1H, m, isoxazole 4-H), 5.86–5.82 (1H, m, 4-H_2), 4.22–4.10 (4H, m, 2-H_2 and 3-CH_2), 3.82 (2H, t, *J* 5.7, 6-H^{min}) and 3.73 (2H, t, *J* 5.7, 6-H^{maj}), 2.34–2.26 (2H, m, 5-H_2), 2.18–2.02 (2H, m, 2'-H_2), 1.09–0.99 (14H, m, ^{i}Pr), 0.91–0.83 (2H, m, 1'-H_2).

By general procedure H, the silyl ether **137** (19 mg, 0.025 mmol) gave the *amide* **158** (4 mg, 80%, 60:40 mixture of rotamers) as a colorless oil, R_f 0.21 (20:1 CH_2Cl_2–MeOH); ν_{max}/cm^{-1} (neat) 3407, 2923, 2853, 1633, 1428; δ_H (500 MHz, CD_3OD) 8.52 (1H, d, *J* 1.8, isoxazole 3-H), 6.86 (1H, d, *J* 1.8, isoxazole 4-H^{min}) and 6.83 (1H, d, *J* 1.8, isoxazole 4-H^{maj}), 5.90–5.87 (1H, m, 4-H), 4.23–4.20 (2H, m, 3-CH_2), 4.06–3.96 (2H, m, 2-H_2), 3.82

(2H, t, *J* 5.8, 6-H_2^{min}) and 3.67 (2H, t, *J* 5.8, 6-H_2^{maj}), 2.34–2.26 (2H, m, 5-H_2); *m/z* (ES+) (Found: MNa^+ 231.0740, $C_{10}H_{12}N_2O_3$ requires *MNa* 231.0740).

3-Hydroxymethyl-1-(phenyl-aminecarbonyl)-1,2,5,6-tetrahydropyridine (159)

By general procedure E, the amine **130** (35 mg, 0.052 mmol) and phenyl isocyanate (23 μL, 0.21 mmol) gave *3-((3',3',4',4',5',5',6',6',7',7',8',8',9',9',10',10',10'-heptadecafluorodecyl)-diisopropyl-silyloxy)-methyl-1-(phenyl-aminecarbonyl)-1,2,5,6-tetrahydropyridine* **138** (30 mg, 73%, >90% purity by 500 MHz ^{1}H NMR spectroscopy) as a colorless oil, δ_H (500 MHz, $CDCl_3$) 7.36 (2H, d, *J* 8.5, phenyl 2-H), 7.28 (2H, dd, *J* 8.5 and 7.4, phenyl 3-H), 7.03 (1H, t, *J* 7.4, phenyl 4-H), 6.33 (1H, s, *NH*), 5.88–5.85 (1H, m, 4-H), 4.18–4.16 (2H, m, 3-CH_2), 3.96–3.94 (2H, m, 2-H_2), 3.57 (2H, t, *J* 5.7, 6-H_2), 2.26–2.21 (2H, m, 5-H_2), 2.18–2.07 (2H, m, 2'-H_2), 1.08–1.03 (14H, m, ^{i}Pr), 0.91–0.87 (2H, m, 1'-H_2).

By general procedure H, the silyl ether **138** (30 mg, 0.038 mmol) gave the *urea* **159** (8 mg, 89%) as a colorless oil, R_f 0.35 (20:1 CH_2Cl_2–MeOH); ν_{max}/cm^{-1} (neat) 3318, 2916, 2854, 1630, 1441; δ_H (500 MHz, CD_3OD) 7.35 (2H, d, *J* 8.5, phenyl 2-H), 7.26 (2H, dd, *J* 8.5 and 7.5, phenyl 3-H), 7.01 (1H, t, *J* 7.5, phenyl 4-H), 5.90–5.86 (1H, m, 4-H), 4.04–4.00 (4H, m, 2-H_2 and 3-CH_2), 3.59 (2H, t, *J* 5.7, 6-H_2), 2.26–2.21 (2H, m, 5-H_2); δ_C (75 MHz, CD_3OD) 158.1, 140.9, 136.9, 129.5 (2C), 124.1, 122.7, 122.3 (2C), 65.2, 45.5, 41.8, 25.9; *m/z* (ES+) (Found: MH^+ 233.1280, $C_{13}H_{16}N_2O_2$ requires *MH* 233.1285).

3-Hydroxymethyl-1-(benzyl-aminethiocarbonyl)-1,2,5,6-tetrahydropyridine (160)

By general procedure F, the amine **130** (20 mg, 0.030 mmol) and benzyl isothiocyanate (16 μL, 0.12 mmol) gave *3-((3',3',4',4',5',5',6',6',7',7',8',8',9',9',10',10',10'-heptadecafluorodecyl)-diisopropyl-silyloxy)-methyl-1-(benzyl-aminethiocarbonyl)-1,2,5,6-tetrahydropyridine* **140** (15 mg, 60%, >90% purity by 500 MHz ^{1}H NMR spectroscopy) as a colorless oil, δ_H (500 MHz, $CDCl_3$) 7.36–7.30 (5H, m, benzyl 3-H, 4-H and 5-H), 5.89–5.87 (1H, m, 4-H), 5.56 (1H, t, *J* 4.7, *NH*), 4.89 (2H, d, *J* 4.7, benzyl 1-H_2), 4.15–4.13 (2H, m, 3-CH_2), 4.11 (2H, d, *J* 1.3, 2-H_2), 4.00 (2H, t, *J* 5.7, 6-H_2), 2.29–2.25 (2H, m, 5-H_2), 2.15–2.03 (2H, m, 2'-H_2), 1.06–1.00 (14H, m, ^{i}Pr), 0.90–0.82 (2H, m, 1'-H_2).

By general procedure H, the silyl ether **140** (15 mg, 0.018 mmol) gave the *thiourea* **160** (3 mg, 60%) as a colorless oil, R_f 0.42 (20:1 CH_2Cl_2–MeOH); ν_{max}/cm^{-1} (neat) 3304, 2920, 2855, 1538, 1325; δ_H (500 MHz, $CDCl_3$) 7.37–7.30 (5H, m, benzyl 3-H, 4-H and 5-H), 5.96–5.93 (1H, m, 4-H), 5.66–5.63 (1H, m, NH), 4.90 (2H, d, *J* 4.8, benzyl 1-H_2), 4.16–4.14 (2H, m, 2-H_2), 4.11–4.08 (2H, m, 3-CH_2), 4.04 (2H, t, *J* 5.7, 6-H_2), 2.30–2.26 (2H, m, 5-H_2), 1.43 (1H, t, *J* 5.6, *OH*); δ_C (75 MHz, $CDCl_3$) 138.1, 134.4, 129.0 (2C), 128.4 (2C), 128.0, 123.4, 65.2, 50.6, 47.2, 45.2, 24.8 (the signal for C=S is missing); *m/z* (ES+) (Found: MH^+ 263.1207, $C_{14}H_{18}OS$ requires *MH* 263.1213).

3-Hydroxymethyl-1-phenylsulfonyl-1,2,5,6-tetrahydropyridine (161)

By general procedure G, the amine **130** (20 mg, 0.030 mmol), DMAP (18 mg, 0.12 mmol) and benzenesulfonyl chloride (15 μL, 0.12 mmol) gave *3-((3',3',4',4',5',5',6',6',7',7',8',8',9',9',10',10',10'-heptadecafluorodecyl)-diisopropyl-silyloxy)-methyl-1-phenylsulfonyl-1,2,5,6-tetrahydropyridine* **141** (20 mg, 83%, >95% purity by 500 MHz ^{1}H NMR spectroscopy) as a colorless oil, δ_H (500 MHz, $CDCl_3$) 7.80 (2H, d, *J* 7.4, phenyl 2-H), 7.59 (1H, t, *J* 7.4, phenyl 4-H), 7.52 (2H, t, *J* 7.4, phenyl 3-H), 5.70–5.67 (1H, m, 4-H), 4.09–4.07 (2H, m, 3-CH_2), 3.57–3.55 (2H, m, 2-H_2), 3.17 (2H, t, *J* 5.7, 6-H_2), 2.24–2.19 (2H, m, 5-H_2), 2.12–2.01 (2H, m, 2'-H_2), 1.07–0.99 (14H, m, ^{i}Pr), 0.87–0.81 (2H, m, 1'-H_2).

By general procedure H, The silyl ether **141** (20 mg, 0.025 mmol) gave the *sulfonamide* **161** (6 mg, 95%) as a colorless oil, R_f 0.38 (20:1 CH_2Cl_2–MeOH); ν_{max}/cm^{-1} (neat) 3405, 2924, 2854, 1446, 1335, 1158; δ_H (500 MHz, $CDCl_3$) 7.81 (2H, d, *J* 7.3, phenyl 2-H), 7.60 (1H, t, *J* 7.3, phenyl 4-H), 7.54 (2H, t, *J* 7.3, phenyl 3-H), 5.76–5.74 (1H, m, 4-H), 4.04–4.02 (2H, m, 3-CH_2), 3.64–3.61 (2H, m, 2-H_2), 3.18 (2H, t, *J* 5.7, 6-H_2), 2.27–2.22 (2H, m, 5-H_2), 1.37 (1H, br s, *OH*); δ_C (75 MHz, $CDCl_3$) 136.7, 134.3, 132.9, 129.2 (2C), 127.9 (2C), 121.8, 65.3, 45.5, 42.9, 25.2; *m/z* (ES+) (Found: MNa^+ 276.0657, $C_{12}H_{15}NO_3S$ requires *MNa* 276.0665).

3-Hydroxymethyl-1-methylsulfonyl-1,2,5,6-tetrahydropyridine (162)

By general procedure G, the amine **130** (20 mg, 0.030 mmol), DMAP (18 mg, 0.12 mmol) and methanesulfonyl chloride (9 μL, 0.12 mmol) gave *3-((3',3',4',4',5',5',6',6',7',7',8',8',9',9',10',10',10'-heptadecafluorodecyl)-diisopropyl-silyloxy)-methyl-1-methylsulfonyl-1,2,5,6-tetrahydropyridine* **142** (17 mg, 77%, >80% purity by 500 MHz ^{1}H NMR spectroscopy) as a colorless oil, δ_H (500 MHz, $CDCl_3$) 5.82–5.79 (1H, m, 4-H), 4.15–4.13 (2H, m, 3-CH_2), 3.77–3.75 (2H, m, 2-H_2), 3.36 (2H, t, *J* 5.8, 6-H_2), 2.81 (3H, s, CH_3), 2.30–2.25 (2H, m, 5-H_2), 2.17–2.06 (2H, m, 2'-H_2), 1.09–1.01 (14H, m, ^{i}Pr) and 0.90–0.82 (2H, m, 1'-H_2).

By general procedure H, the silyl ether **142** (17 mg, 0.023 mmol) gave *sulfonamide* **162** (3 mg, 75%) as a colorless oil, R_f 0.25 (20:1 CH_2Cl_2–MeOH); ν_{max}/cm^{-1} (neat) 3363, 2926, 2855, 1323, 1147; δ_H (500 MHz, CD_3OD) 5.84–5.81 (1H, m, 4-H), 4.01–3.99 (2H, m, 3-CH_2), 3.79–3.77 (2H, m, 2-H_2), 3.33 (2H, t, *J* 5.8, 6-H_2), 2.86 (3H, s, CH_3) and 2.30–2.25 (2H, m, 5-H_2); δ_C (75 MHz, CD_3OD) 136.1, 122.2, 65.0, 46.1, 43.6, 35.2, 25.9; *m/z* (ES+) (Found: MNa^+ 214.0499, $C_7H_{13}NO_3S$ requires *MNa* 214.0508).

1-*N*-(2-(2,5-Dihydrofuran-3-yl)-allyl)-1-*N*-(3-hydroxy-2-methylene-propyl)-3-*N*-phenylurea (163)

By general procedure C, the sulfonamide **124** (17 mg, 0.018 mmol), K_2CO_3 (8 mg, 0.054 mmol) and PhSH (2.3 μL, 0.022 mmol) in DMF (1 mL) gave *1-N-(2-(2,5-dihydrofuran-3-yl)-allyl)-(3-(((3',3',4',4',5',5',6',6',7',7',8',8',9',9', 10',10',10'-heptadecafluorodecyl)-diisopropyl)-silyloxy)-2-methylene-propyl)-1-amine* **132** (13 mg, 96%, >80% purity by 500

MHz ^{1}H NMR spectroscopy) as a colorless oil, δ_H (500 MHz, $CDCl_3$) 5.90–5.87 (1H, m, dihydrofuran 4-H), 5.15–5.14 (1H, m, 2-CH_2 or allyl 3-H), 5.05–5.03 (2H, m, 2-CH_2 or allyl 3-H), 4.85–4.83 (1H, m, 2-CH_2 or allyl 3-H), 4.29–4.27 (2H, m, 1-H_2, 3-H_2 or allyl 1-H_2), 4.25–4.22 (4H, m, dihydrofuran 2-H_2 and 5-H_2), 3.40–3.38 (2H, m, 1-H_2, 3-H_2 or allyl 1-H_2), 3.28–3.26 (2H, m, 1-H_2, 3-H_2 or allyl 1-H_2), 2.20–2.06 (2H, m, 2'-H_2), 1.08–1.02 (14H, m, ^{i}Pr), 0.90–0.86 (2H, m, 1'-H_2).

By general procedure E, the amine **132** (13 mg, 0.017 mmol) and phenylisocyanate (7.5 μL, 0.069 mmol) gave *1-N-(2-(2,5-dihydrofuran-3-yl)-allyl)-1-N-(3-(((3',3',4',4',5',5',6',6',7',7',8',8',9',9', 10',10',10'-heptadecafluorodecyl)-diisopropyl)-silyloxy)-2-methylene-propyl)-3-N-phenylurea* **143** (14 mg, 95%, >75% purity by 500 MHz ^{1}H NMR spectroscopy) as a colorless oil, R_f 0.47 (5:1 petrol–EtOAc); δ_H (500 MHz, $CDCl_3$) 7.33–7.30 (2H, m, phenyl 2-H), 7.28–7.25 (2H, m, phenyl 3-H), 7.02 (1H, tt, *J* 7.3 and 1.2, phenyl 4-H), 6.71 (1H, s, *NH*), 5.85–5.82 (1H, m, dihydrofuran 4-H), 5.30–5.28 (1H, m, 2-CH_2 or allyl 3-H), 5.15–5.12 (2H, m, 2-CH_2 or allyl 3-H), 4.91–4.88 (1H, m, 2-CH_2 or allyl 3-H), 4.33–4.29 (2H, m, 1-H_2, 3-H_2 or allyl 1-H_2), 4.26–4.23 (4H, m, dihydrofuran 2-H_2 and 5-H_2), 4.23–4.21 (2H, m, 1-H_2, 3-H_2 or allyl 1-H_2), 3.98–3.95 (2H, m, 1-H_2, 3-H_2 or allyl 1-H_2), 2.19–2.05 (2H, m, 2'-H_2), 1.08–1.03 (14H, m, ^{i}Pr), 0.86–0.82 (2H, m, 1'-H_2).

By general procedure H, the silyl ether **143** (14 mg, 0.016 mmol) gave the *urea* **163** (3 mg, 60%) as a colorless amorphous solid, R_f 0.31 (20:1 CH_2Cl_2–MeOH); ν_{max}/cm^{-1} (neat) 3418, 2528, 1641, 1470, 1445, 1116, 1082; δ_H (500 MHz, CD_3OD) 7.34–7.32 (2H, m, phenyl 2-H), 7.27–7.23 (2H, m, phenyl 3-H), 7.03–6.99 (1H, m, phenyl 4-H), 5.83–5.82 (1H, m, dihydrofuran 4-H), 5.23–5.22 (1H, m, 2-CH_{2a} or allyl 3-H_a), 5.12–5.11 (1H, m, 2-CH_{2a} or allyl 3-H_a), 5.03–5.02 (1H, m, 2-CH_{2b} or allyl 3-H_b), 4.92–4.91 (1H, m, 2-CH_{2b} or allyl 3-H_b), 4.29–4.27 (2H, m, 1-H_2, 3-H_2 or allyl 1-H_2), 4.24–4.23 (4H, m, dihydrofuran 2-H_2 and 5-H_2), 4.11–4.09 (2H, m, 1-H_2, 3-H_2 or allyl 1-H_2), 4.04–4.03 (2H, m, 1-H_2, 3-H_2 or allyl 1-H_2); δ_C (75 MHz, CD_3OD) 146.0, 140.2, 129.6 (2C), 127.4, 124.2, 122.1 (2C), 113.1, 108.1, 70.6, 67.1, 64.2, 47.8 (the signals for four carbon atoms are missing); *m/z* (ES+) (Found: MH^+ 315.1698, $C_{18}H_{23}O_3N_2$ requires *MH* 315.1703).

(*R,Z*)-6-(2,5-Dihydrofuran-3-yl)-2-hydroxymethyl-1-phenylcarbonyl-2,3,4,7-tetrahydro-1*H*-azepine (164)

By general procedure D, the amine **133** (20 mg, 0.026 mmol), DMAP (16 mg, 0.13 mmol) and benzoyl chloride (12 μL, 0.10 mmol) gave *(R,Z)-6-(2,5-dihydrofuran-3-yl)-2-(((3',3',4',4',5',5',6',6',7',7',8',8',9',9', 10',10',10'-heptadecafluorodecyl)-diisopropyl-silyloxy)-methyl)-1-phenylcarbonyl-2,3,4,7-tetrahydro-1H-azepine* **144** (22 mg, 98%, 70:30 mixture of rotamers, >85% purity by 500 MHz ^{1}H NMR spectroscopy) as a colorless oil, δ_H (500 MHz, $CDCl_3$) 7.46–7.27 (5H, m, phenyl 2-H, 3-H and 4-H), 6.00–5.98 (1H, m, dihydrofuran 4-H^{min}), 5.63–5.59 (1H, m, 5-H^{maj}), 5.52–5.49 (1H, m, 5-H^{min}), 5.09–3.65 (9H, m, 2-H, 2-CH_2, 7-H_2, dihydrofuran 2-H_2 and 5-H_2), 4.95–4.92 (1H, m, dihydrofuran

4-H^{maj}), 2.54–1.99 (6H, m, 3-H$_2$, 4-H$_2$ and 2'-H$_2$), 1.17–1.00 (14H, m, ^{i}Pr), 0.93–0.81 (2H, m, 1'-H$_2$).

By general procedure H, the silyl ether **144** (22 mg, 0.026 mmol) gave the *amide* **164** (6 mg, 77%, 60:40 mixture of rotamers) as a colorless oil, R_f 0.10 (25:1 CH_2Cl_2–MeOH); ν_{max}/cm^{-1} (neat) 3400, 2922, 2842, 1612, 1446, 1425, 1077; δ_H (500 MHz, CD_3OD) 7.47–7.30 (5H, m, phenyl 2-H, 3-H and 4-H), 6.03–6.01 (1H, m, dihydrofuran 4-H^{min}), 5.69–5.66 (1H, m, 5-H^{maj}), 5.60–5.57 (1H, m, 5-H^{min}), 5.05–5.02 (1H, m, dihydrofuran 4-H^{maj}), 4.98–3.53 (9H, m, 2-H, 2-CH$_2$, 7-H$_2$, dihydrofuran 2-H$_2$ and 5-H$_2$), 2.55–1.70 (5H, m, 3-H$_2$, 4-H$_2$ and *OH*); *m/z* (ES+) (Found: MNa$^+$ 322.1412, $C_{18}H_{21}NO_3$ requires *MNa* 322.1414).

(*R,Z*)-6-(2,5-Dihydrofuran-3-yl)-2-hydroxymethyl-1-(2-thiophenecarbonyl)-2,3,4,7-tetrahydro-1*H*-azepine (165)

By general procedure D, the amine **133** (20 mg, 0.026 mmol), DMAP (16 mg, 0.13 mmol) and 2-thiophenecarbonyl chloride (11 μL, 0.10 mmol) gave *(R,Z)-6-(2,5-dihydrofuran-3-yl)-2-(((3',3',4',4',5',5',6',6',7',7',8',8',9',9',10',10',10'-heptadecafluorodecyl)-diisopropyl-silyloxy)-methyl)-1-(2-thiophenecarbonyl)-2,3,4,7-tetrahydro-1H-azepine* **145** (22 mg, 98%, 60:40 mixture of rotamers, >90% purity by 500 MHz ^{1}H NMR spectroscopy) as a colorless oil, δ_H (500 MHz, $CDCl_3$) 7.58–7.08 (2H, m, thiophene 5-H and 3-H), 7.03–6.99 (1H, m, thiophene 4-H^{min}), 6.97–6.93 (1H, m, thiophene 4-H^{maj}), 5.98–5.94 (1H, m, dihydrofuran 4-H^{min}), 5.72–5.66(1H, m, 5-H^{maj}), 5.51–5.45 (1H, m, 5-H^{min}), 5.44–5.40 (1H, m, dihydrofuran 4-H^{maj}), 4.92–3.79 (9H, m, 2-H, 2-CH$_2$, 7-H$_2$, dihydrofuran 2-H$_2$ and 4-H$_2$), 2.50–1.91 (6H, m, 3-H$_2$, 4-H$_2$ and 2'-H$_2$), 1.15–0.97 (14H, m, ^{i}Pr), 0.95–0.81 (2H, m, 1'-H$_2$).

By general procedure H, the silyl ether **145** (22 mg, 0.025 mmol) gave the *amide* **165** (7 mg, 90%, 55:45 mixture of rotamers) as a colorless oil, R_f 0.09 (25:1 CH_2Cl_2–MeOH); ν_{max}/cm^{-1} (neat) 3398, 2921, 2845, 1600, 1431, 1079; δ_H (500 MHz, CD_3OD) 7.68–7.18 (2H, m, thiophene 5-H and 3-H), 7.10 (1H, t, *J* 4.1, thiophene 4-H^{maj}), 7.03 (1H, t, *J* 4.1, thiophene 4-H^{min}), 6.00–5.52 (2H, m, 5-H and dihydrofuran 4-H), 4.82–3.67 (9H, m, 2-H, 2-CH$_2$, 7-H$_2$, dihydrofuran 2-H$_2$ and 5-H$_2$), 2.54–1.71 (5H, m, 3-H$_2$, 4-H$_2$ and *OH*); *m/z* (ES+) (Found: MH$^+$ 306.1147, $C_{16}H_{20}O_3S$ requires *MH* 306.1158).

(*R,Z*)-6-(2,5-Dihydrofuran-3-yl)-2-hydroxymethyl-1-(5-isoxazolecarbonyl)-2,3,4,7-tetrahydro-1*H*-azepine (166)

By general procedure D, the amine **133** (20 mg, 0.026 mmol), DMAP (16 mg, 0.13 mmol) and 5-isoxazolecarbonyl chloride (13 μL, 0.10 mmol) gave *(R,Z)-6-(2,5-dihydrofuran-3-yl)-2-(((3',3',4',4',5',5',6',6',7',7',8',8',9',9',10',10',10'-heptadecafluorodecyl)-diisopropyl-silyloxy)-methyl)-1-(5-isoxazolecarbonyl)-2,3,4,7-tetrahydro-1H-azepine* **146** (20 mg, 91%, 55:45 mixture of rotamers, >70% purity by 500 MHz ^{1}H NMR spectroscopy) as a colorless oil, δ_H (500 MHz, $CDCl_3$) 8.29 (1H, d, *J* 1.8, isoxazole 3-H^{maj}), 8.25 (1H, d, *J* 1.8, isoxazole 3-H^{min}), 6.82 (1H, d, *J* 1.8, isoxazole 4-H^{maj}), 6.58 (1H, d, *J* 1.8, isoxazole 4-

H^{min}), 5.97–5.95 (1H, m, dihydrofuran 4-H^{maj}), 5.56 (1H, d, *J* 7.5, 5-H^{maj}), 5.52–5.50 (1H, m, dihydrofuran 4-H^{min}), 5.49 (1H, d, *J* 7.5, 5-H^{min}), 4.91–3.81 (9H, m, 2-H, 2-CH_2, 7-H_2, dihydrofuran 2-H_2 and 5-H_2), 2.51–1.97 (6H, m, 3-H_2, 4-H_2 and 2'-H_2), 1.09–1.00 (14H, m, ^{i}Pr), 0.91–0.83 (2H, m, 1'-H_2).

By general procedure H, the silyl ether **146** (20 mg, 0.024 mmol) gave the *amide* **166** (4 mg, 57%, 55:45 mixture of rotamers) as a colorless oil, R_f 0.22 (20:1 CH_2Cl_2–MeOH); ν_{max}/cm^{-1} (neat) 3418, 2919, 2853, 1633, 1424, 1076; δ_H (500 MHz, CD_3OD) 8.49(1H, d, *J* 1.9, isoxazole 3-H^{maj}), 8.45 (1H, d, *J* 1.9, isoxazole 3-H^{min}), 6.88 (1H, d, *J* 1.9, isoxazole 4-H^{maj}), 6.64 (1H, d, *J* 1.9, isoxazole 4-H^{min}), 6.02–6.00 (1H, m, dihydrofuran 4-H^{maj}), 5.68–5.65 (1H, m, 5-H^{maj}), 5.61–5.59 (1H, m, dihydrofuran 4-H^{min}), 5.58–5.55 (1H, m, 5-H^{min}), 4.90 (1H, d, *J* 16.1, 7-H_a), 4.78–4.63 (4H, m, dihydrofuran 2-H_2 and 5-H_2), 4.43–4.40 (1H, m, 2-H), 4.11–4.06 (1H, m, 7-H_b), 3.78–3.65 (2H, m, 2-CH_2), 2.51–1.81 (5H, m, 3-H_2, 4-H_2 and *OH*); *m/z* (ES+) (Found: MNa^+ 313.1158, $C_{15}H_{18}N_2O_4$ requires *MNa* 313.1159).

(*R,Z*)-6-(2,5-Dihydrofuran-3-yl)-2-hydroxymethyl-1-(phenyl-aminecarbonyl)-2,3,4,7-tetrahydro-1*H*-azepine (167)

By general procedure E, the amine **133** (10 mg, 0.014 mmol) and phenyl isocyanate (6 μL, 0.056 mmol) gave *(R,Z)-6-(2,5-dihydrofuran-3-yl)-2-(((3',3',4',4',5',5',6',6',7',7',8',8',9',9',10',10',10'-heptadecafluoro-decyl)-diisopropyl-silyloxy)-methyl)-1-(phenyl-aminecarbonyl)-2,3,4,7-tetrahydro-1H-azepine* **147** (11 mg, 92%, >50% purity by 500 MHz ^{1}H NMR spectroscopy) as a colorless oil, δ_H (500 MHz, $CDCl_3$) 7.33–7.29 (2H, m, phenyl 2-H), 7.26–7.22 (2H, m, phenyl 3-H), 6.98 (1H, t, *J* 7.3, phenyl 4-H), 5.94 (1H, m, dihydrofuran 4-H), 5.53–5.48 (1H, m, 5-H), 4.86–4.67 (5H, m, 7-H_a, dihydrofuran 2-H_2 and 5-H_2), 4.26–4.14 (1H, m, 2-H), 3.87–3.82 (2H, m, 2-CH_{2a}, 7-H_b), 3.77–3.71 (1H, m, 2-CH_{2b}), 2.49–2.32 (2H, m, 4-H_2), 2.19–2.06 (3H, m, 3-H_a and 2'-H_2), 1.94–1.89 (1H, m, 3-H_b), 1.17–0.94 (14H, m, ^{i}Pr), 0.90–0.82 (2H, m, 1'-H_2).

By general procedure H, the silyl ether **147** (11 mg, 0.013 mmol) gave the *urea* **167** (1 mg, 25%) as a colorless amorphous solid, R_f 0.21 (20:1 CH_2Cl_2–MeOH); ν_{max}/cm^{-1} (neat) 3308, 2851, 1651, 1535, 1445, 1178, 1079; δ_H (500 MHz, CD_3OD) 7.25–7.23 (4H, m, phenyl 2-H and 3-H), 7.00–6.96 (1H, m, phenyl 3-H), 6.00–5.97 (1H, m, dihydrofuran 4-H), 5.57–5.53 (1H, m, 5-H), 4.79–4.67 (4H, m, dihydrofuran 2-H_2 and 5-H_2), 4.54 (1H, d, *J* 16.8, 7-H_a), 4.25–4.16 (1H, m, 2-H), 4.00–3.93 (1H, m, 7-H_b), 3.73–3.66 (2H, m, 2-CH_2), 2.49–2.41 (1H, m, 4-H_a), 2.37–2.29 (1H, m, 4-H_b), 1.97–1.92 (1H, m, 3-H_a), 1.91–1.87 (1H, m, 3-H_b); *m/z* (ES+) (Found: MNa^+ 337.1520, $C_{18}H_{22}N_2O_3$ requires *MNa* 337.1523).

(*R,Z*)-6-(2,5-Dihydrofuran-3-yl)-2-hydroxymethyl-1-(benzyl-aminethiocarbonyl)-2,3,4,7-tetrahydro-1*H*-azepine (168)

By general procedure F, the amine **133** (20 mg, 0.026 mmol) and benzyl thioisocyanate (14 μL, 0.10 mmol) gave *(R,Z)-6-(2,5-dihydrofuran-3-yl)-2-(((3',3',4',4',5',5',6',6',7',7',8',8',9',9', 10',10',10'-heptadecafluorodecyl)-diisopropyl-silyloxy)-methyl)-1-(benzyl-aminethiocarbonyl)-2,3,4,7-tetrahydro-1H-azepine* **148** (23

mg, 98%, >60% purity by 500 MHz ^{1}H NMR spectroscopy) as a colorless oil, δ_H (500 MHz, $CDCl_3$) 7.34–7.26 (5H, m, benzyl 3-H, 4-H and 5-H), 5.56–5.48 (1H, m, dihydrofuran 4-H), 5.39–5.22 (1H, m, 5-H), 4.78–3.63 (11H, m, 2-H, 2-CH_2, 7-H_2, dihydrofuran 2-H_2, 5-H_2 and benzyl 1-H_2), 2.54–2.22 (2H, m, 4-H_2), 2.21–1.89 (4H, m, 3-H_2 and 2'-H_2), 1.15–1.75 (16H, m, 1'-H_2 and ^{i}Pr).

By general procedure H, the silyl ether **148** (23 mg, 0.025 mmol) gave the *thiourea* **168** (2 mg, 22%) as a colorless oil, R_f 0.21 (25:1 CH_2Cl_2–MeOH); ν_{max}/cm^{-1} (neat) 3337, 2853, 1542, 1335, 1164, 1074; δ_H (500 MHz, $CDCl_3$) 7.36–7.29 (4H, m, benzyl 3-H and 4-H), 7.25–7.23 (1H, m, benzyl 5-H), 5.90–5.88 (1H, m, *NH*), 5.64–5.57 (1H, m, dihydrofuran 4-H), 5.55–5.52 (1H, m, 5-H), 4.81–4.57 (7H, m, 7-H_a, dihydrofuran 2-H_2, 5-H_2 and benzyl 1-H_2), 4.23–4.17 (1H, m, 2-H), 4.14 (1H, d, *J* 18.8, 7-H_b), 3.63–3.59 (2H, m, 2-CH_{2a}), 2.51–2.43 (1H, m, 4-H_a), 2.39–2.33 (1H, m, 4-H_b), 2.02–1.94 (1H, m, 3-H_a), 1.81–1.76 (1H, m, 3-H_b); *m/z* (ES+) (Found: MH^+ 345.1628, $C_{19}H_{25}N_2O_2S$ requires *MH* 345.1631).

(*R,Z*)-6-(2,5-Dihydrofuran-3-yl)-2-hydroxymethyl-1-phenylsulfonyl-2,3,4,7-tetrahydro-1*H*-azepine (169)

By general procedure G, the amine **70** (20 mg, 0.026 mmol), DMAP (16 mg, 0.13 mmol) and benzenesulfonyl chloride (13 μL, 0.10 mmol) gave *(R,Z)-6-(2,5-dihydrofuran-3-yl)-2-(((3',3',4',4',5',5',6',6',7',7',8',8',9',9',10',10',10'-heptadecafluorodecyl)-diisopropyl-silyloxy)-methyl)-1-phenylsulfonyl-2,3,4,7-tetrahydro-1H-azepine* **149** (20 mg, 86%, >80% purity by 500 MHz ^{1}H NMR spectroscopy) as a colorless oil, δ_H (500 MHz, $CDCl_3$) 7.74 (2H, d, *J* 7.5, phenyl 2-H), 7.51 (1H, t, *J* 7.5, phenyl 4-H), 7.40 (2H, d, *J* 7.5, phenyl 3-H), 5.87–5.84 (1H, m, dihydrofuran 4-H), 5.04–5.00 (1H, m, 5-H), 4.84–4.72 (4H, m, dihydrofuran 2-H_2 and 5-H_2), 4.69 (1H, d, *J* 17.7, 7-H_a), 4.19–4.13 (1H, m, 7-H_b), 3.88–3.83 (2H, m, 2-H and 2-CH_{2a}), 3.79–3.74 (1H, m, 2-CH_{2b}), 2.19–2.06 (3H, m, 4-H_a and 2'-H_2), 1.95–1.89 (2H, m, 3-H_2), 1.49–1.40 (1H, m, 4-H_b), 1.10–1.01 (14H, m, ^{i}Pr), 0.90–0.85 (2H, m, 1'-H_2).

By general procedure H, the silyl ether **149** (20 mg, 0.022 mmol) gave the *sulfonamide* **169** (6 mg, 81%) as a colorless oil, R_f 0.21 (20:1 CH_2Cl_2–MeOH); ν_{max}/cm^{-1} (neat) 3424, 2924, 2848, 1446, 1329, 1155; δ_H (500 MHz, CD_3OD) 7.78–7.76 (2H, m, phenyl 2-H), 7.61–7.55 (1H, m, phenyl 4-H), 7.50–7.46 (2H, m, phenyl 3-H), 5.94–5.92 (1H, m, dihydrofuran 4-H), 5.10–5.07 (1H, m, 5-H), 4.81–4.68 (2H, m, dihydrofuran 2-H_2), 4.64 (1H, dt, *J* 18.0 and 1.0, 7-H_a), 4.59–4.49 (2H, m, dihydrofuran 5-H_2), 4.21 (1H, dt, *J* 18.0 and 3.3, 7-H_b), 3.94–3.88 (1H, m, 2-H), 3.68 (1H, dd, *J* 11.1 and 4.6, 2-CH_{2a}), 3.62 (1H, dd, *J* 11.1 and 6.3, 2-CH_{2b}), 2.21–2.13 (1H, m, 4-H_a), 1.93–1.87 (2H, m, 3-H_2), 1.56–1.48 (1H, m, 4-H_b); δ_C (75 MHz, CD_3OD) 142.0, 140.1, 133.7, 131.5, 129.7 (2C), 128.4 (2C), 120.7, 77.6, 75.8, 66.1, 61.2, 43.8, 28.9, 27.9 (the signal for one carbon atom is missing); *m/z* (ES+) (Found: MH^+ 336.1257, $C_{17}H_{22}NO_4S$ requires *MH* 336.1264).

(*R*,*Z*)-6-(2,5-Dihydrofuran-3-yl)-2-hydroxymethyl-1-methylsulfonyl-2,3,4,7-tetrahydro-1*H*-azepine (170)

By general procedure G, the amine **133** (20 mg, 0.026 mmol), DMAP (16 mg, 0.013 mmol) and methanesulfonyl chloride (8 μL, 0.10 mmol) gave *(R,Z)-6-(2,5-dihydrofuran-3-yl)-2-(((3',3',4',4',5',5',6',6',7',7',8',8',9',9',10',10',10'-heptadecafluorodecyl)-diisopropyl-silyloxy)-methyl)-1-methylsulfonyl-2,3,4,7-tetrahydro-1H-azepine* **150** (20 mg, 92%, >80% purity by 500 MHz ^{1}H NMR spectroscopy) as a colorless oil, δ_H (500 MHz, $CDCl_3$) 5.85–5.83 (1H, m, dihydrofuran 4-H), 5.55–5.51 (1H, m, 5-H), 4.76–4.65 (4H, m, dihydrofuran 2-H_2 and 5-H_2), 4.49 (1H, d, *J* 17.9, 7-H_a), 4.15–4.09 (1H, m, 7-H_b), 3.94–3.87 (1H, m, 2-H), 3.81 (1H, dd, *J* 10.0 and 4.6, 2-CH_{2a}), 3.73 (1H, dd, *J* 10.0 and 5.9, 2-CH_{2b}), 2.84 (3H, s, CH_3), 2.57–2.49 (1H, 4-H_a), 2.39–2.30 (1H, 4-H_b), 2.18–1.94 (4H, 3-H_2 and 2'-H_2), 1.10–1.01 (14H, ^{i}Pr), 0.90–0.85 (2H, 1'-H_2).

By general procedure H, the silyl ether **149** (20 mg, 0.024 mmol) gave the *sulfonamide* **170** (4 mg, 61%) as a colorless oil, R_f 0.11 (25:1 CH_2Cl_2–MeOH); ν_{max}/cm^{-1} (neat) 3412, 2927, 2848, 1319, 1143; δ_H (500 MHz, CD_3OD) 5.91–5.89 (1H, m, dihydrofuran 4-H), 5.61–5.58 (1H, m, 5-H), 4.76–4.64 (4H, m, dihydrofuran 2-H_2 and 4-H_2), 4.43 (1H, d, *J* 17.8, 7-H_a), 4.15–4.10 (1H, m, 7-H_b), 3.98–3.92 (1H, m, 2-H), 3.63 (1H, dd, *J* 11.4 and 6.2, 2-CH_{2a}), 3.59 (1H, dd, *J* 11.4 and 5.5, 2-CH_{2b}), 2.95 (3H, s, CH_3), 2.47–2.41 (2H, m, 4-H_2), 2.04–1.98 (1H, m, 3-H_a), 1.90–1.81 (1H, m, 3-H_b); δ_C (75 MHz, CD_3OD) 139.7, 133.2, 131.2, 120.8, 77.6, 75.9, 65.1, 61.1, 43.4, 40.2, 29.4, 27.5; *m/z* (ES+) (Found: MH^+ 274.1097, $C_{12}H_{19}NO_4S$ requires *MH* 274.1108).

(3a*R*,8a*S*)-8a-(Hydroxymethyl)-10-(2-thiophenecarbonyl)-6-phenyl-3,3a,8a,9,10,11-hexahydrofuro[3,4-*e*]pyrrolo[3,4-*c*][1,2,4]triazolo[1,2-*a*]pyridazine-5,7(1*H*,6*H*)-dione ((±)-171)

By general procedure D including a elution with CH_2Cl_2 (3×3 mL) as part of the fluorophilic wash in the F-SPE, the amine (±)-**134** (20 mg, 0.022 mmol), DMAP (13 mg, 0.11 mmol) and 2-thiophenecarbonyl chloride (10 μL, 0.09 mmol) gave *(3aR,8aS)-8a-(((3',3',4',4',5',5',6',6',7',7',8',8',9',9',10',10'-heptadecafluorodecyl)-diisopropyl-silyloxy)-methyl)-10-(2-thiophenecarbonyl)-6-phenyl-3,3a,8a,9,10,11-hexahydrofuro[3,4-e]pyrrolo[3,4-c][1,2,4]triazolo[1,2-a]pyridazine-5,7(1H,6H)-dione* (±)-**151** (19 mg, 86%, >95% purity by 500 MHz ^{1}H NMR spectroscopy) as a colorless amorphous solid, δ_H (500 MHz, $CDCl_3$) 7.56–7.45 (6H, m, phenyl 2-H, 3-H, 4-H and thiophene 5-H), 7.40–7.36 (1H, m, thiophene 3-H), 7.11–7.09 (1H, m, thiophene 4-H), 4.79 (1H, dd, *J* 9.0 and 7.2, 3-H_a), 4.65–4.61 (1H, m, 9-H_a), 4.58–4.46 (4H, m, 1-H_2, 3a-H and 11-H_a), 4.39–4.29 (2H, m, 8a-CH_{2a} and 11-H_b), 4.11–4.04 (1H, m, 9-H_b), 3.79 (1H, d, *J* 10.3, 8a-CH_{2b}), 3.68 (1H, t, *J* 9.0, 3-H_b), 2.08–1.96 (2H, m, 2'-H_2), 1.03–0.95 (14H, m, ^{i}Pr), 0.87–0,82 (2H, m, 1'-H_2).

By general procedure H, the silyl ether (±)-**151** (19 mg, 0.019 mmol) gave the *amide* (±)-**171** (8 mg, 99%) as a colorless amorphous solid, R_f 0.21 (20:1 CH_2Cl_2–MeOH); ν_{max}/cm^{-1} (neat) 3417, 2936, 2869, 1764, 1704, 1598, 1429; δ_H (500 MHz, $CDCl_3$) 7.55–7.45 (6H, m, phenyl 2-H, 3-H, 4-H and thiophene 5-H), 7.41–7.37 (1H, m, thiophene 3-H), 7.12–7.08

(1H, m, thiophene 4-H), 4.81–4.77 (1H, m, 3-H_a), 4.74 (1H, d, *J* 10.8, 9-H_a), 4.59–4.54 (2H, m, 1-H_a and 3a-H), 4.52–4.44 (2H, m, 1-H_b and 11-H_a), 4.31–4.23 (1H, m, 11-H_b), 4.19–4.14 (1H, m, 8a-CH_{2a}), 3.93–3.88 (1H, m, 9-H_b), 3.78–3.70 (2H, m, 8a-CH_{2b} and 3-H_b), 3.20–3.13 (1H, m, *OH*); *m/z* (ES+) (Found: MH^+ 453.1226, $C_{22}H_{21}N_4O_5S$ requires *MH* 453.1227).

(3a*R*,8a*S*)-8a-(Hydroxymethyl)-10-(5-isoxazolecarbonyl)-6-phenyl-3,3a,8a,9,10,11-hexahydrofuro[3,4-*e*]pyrrolo[3,4-*c*][1,2,4]triazolo[1,2-*a*]pyridazine-5,7(1*H*,6*H*)-dione ((±)-172)

By general procedure D including a elution with CH_2Cl_2 (3×3 mL) as part of the fluorophilic wash in the F-SPE, the amine (±)-**134** (20 mg, 0.022 mmol), DMAP (13 mg, 0.11 mmol) and 5-isoxazolecarbonyl chloride (12 μL, 0.09 mmol) gave *(3aR,8aS)-8a-(((3',3',4',4',5',5',6',6',7',7',8',8',9',9',10',10'-heptadecafluorodecyl)-diisopropyl-silyloxy)-methyl)-10-(5-isoxazolecarbonyl)-6-phenyl-3,3a,8a,9,10,11-hexahydrofuro[3,4-e]pyrrolo[3,4-c][1,2,4]triazolo[1,2-a]pyridazine-5,7(1H,6H)-dione* (±)-**152** (15 mg, 68%, 55:45 mixture of rotamers, >80% purity by 500 MHz ^{1}H NMR spectroscopy) as a colorless amorphous solid, δ_H (500 MHz, $CDCl_3$) 8.38 (1H, d, *J* 1.8, isoxazole 3-H^{min}), 8.35 (1H, d, *J* 1.8, isoxazole 3-H^{maj}), 7.52–7.45 (4H, m, phneyl 2-H and 3-H), 7.40–7.36 (1H, m, phenyl 4-H), 7.04 (1H, d, *J* 1.8, isoxazole 4-H^{min}), 6.96 (1H, d, *J* 1.8, isoxazole 4-H^{maj}), 4.82–3.63 (11H, m, 1-H_2, 3-H_2, 3a-H, 8a-CH_2, 9-H_2 and 11-H_2), 2.08–1.96 (2H, m, 2'-H_2), 1.03–0.97 (14H, m, ^{i}Pr), 0.88–0.83 (2H, m, 1'-H_2).

By general procedure H, the silyl ether (±)-**152** (15 mg, 0.015 mmol) gave the *amide* (±)-**172** (6 mg, 92%, 60:40 mixture of rotamers) as a colorless amorphous solid, R_f 0.17 (20:1 CH_2Cl_2–MeOH); ν_{max}/cm^{-1} (neat) 3418, 2868, 1766, 1699, 1634, 1411, 1052; δ_H (500 MHz, $CDCl_3$) 8.38 (1H, d, *J* 1.8, isoxazole 3-H^{min}), 8.34 (1H, d, *J* 1.8, isoxazole 3-H^{maj}), 7.53–7.46 (4H, m, phenyl 2-H and 3-H), 7.42–7.39 (1H, m, phenyl 4-H), 7.03 (1H, d, *J* 1.8, isoxazole 4-H^{min}), 6.96 (1H, d, J 1.8, isoxazole 4-H^{maj}), 4.96–3.66 (11H, m, 1-H_2, 3-H_2, 3a-H, 8a-CH_2, 9-H_2 and 11-H_2), 3.26–3.20 (1H, m, OH^{maj}), 3.02–2.97 (1H, m, OH^{min}); *m/z* (ES+) (Found: MH^+ 438.1409, $C_{20}H_{20}N_5O_6$ requires *MH* 438.1408).

(3a*R*,8a*S*)-8a-(Hydroxymethyl)-10-(phenyl-aminecarbonyl)-6-phenyl-3,3a,8a,9,10,11-hexahydrofuro[3,4-*e*]pyrrolo[3,4-*c*][1,2,4]triazolo[1,2-*a*]pyridazine-5,7(1*H*,6*H*)-dione ((±)-173)

By general procedure E, the amine (±)-**134** (20 mg, 0.022 mmol) and phenyl isocyanate (10 μL, 0.09 mmol) gave *(3aR,8aS)-8a-(((3',3',4',4',5',5',6',6',7',7',8',8',9',9',10',10'-heptadecafluorodecyl)-diisopropyl-silyloxy)-methyl)-10-(phenyl-aminecarbonyl)-6-phenyl-3,3a,8a,9,10,11-hexahydrofuro[3,4-e]pyrrolo[3,4-c][1,2,4]triazolo[1,2-a]pyridazine-5,7(1H,6H)-dione* (±)-**153** (19 mg, 84%, >95% purity by 500 MHz ^{1}H NMR spectroscopy) as a colorless amorphous solid, δ_H (500 MHz, $CDCl_3$) 7.51–7.44 (4H, m, 6-phenyl 2-H and 3-H), 7.42–7.38 (3H, m, 6-phenyl 4-H and 10-phenyl 2-H), 7.33–7.29 (2H, m, 10-phenyl 3-H), 7.07 (1H, t, *J* 7.4, 10-phenyl 4-H), 6.26 (1H, s, *NH*), 4.80–4.76 (1H, m, 3-H_a), 4.56–

4.50 (2H, m, 1-H_a and 3a-H), 4.49–4.44 (1H, m, 1-H_b), 4.40 (1H, d, *J* 10.2, 9-H_a), 4.29–4.24 (1H, m, 11-H_a), 4.24–4.22 (1H, m, 11-H_b), 4.21 (1H, d, *J* 10.1, 8a-CH_{2a}), 3.84 (1H, d, *J* 10.2, 9-H_b), 3.76–3.73 (1H, m, 8a-CH_{2b}), 3.66 (1H, t, *J* 9.1, 3-H_b), 2.10–1.98 (2H, m, 2'-H_2), 1.07–0.98 (14H, m, ^{i}Pr), 0.89–0.84 (2H, m, 1'-H_2).

By general procedure H, the silyl ether (±)-**153** (19 mg, 0.019 mmol) gave the *urea* (±)-**173** (4 mg, 45%) as a colorless amorphous solid, R_f 0.14 (20:1 CH_2Cl_2–MeOH); ν_{max}/cm^{-1} (neat) 3348, 2969, 1739, 1696, 1443, 1365; δ_H (500 MHz, $CDCl_3$) 7.52–7.46 (4H, m, 6-phenyl 2-H and 3-H), 7.42–7.37 (3H, m, 6-phenyl 4-H and 10-phenyl 2-H), 7.32–7.28 (2H, m, 10-phenyl 3-H), 7.07 (1H, t, *J* 7.3, 10-phenyl 4-H), 6.39 (1H, s, *NH*), 4.77 (1H, dd, *J* 8.9 and 7.3, 3-H_a), 4.56–4.51 (2H, m, 1-H_a and 3a-H), 4.45–4.41 (1H, m, 1-H_b), 4.35 (1H, d, *J* 9.8, 9-H_a), 4.25–4.16 (2H, m, 11-H_2), 4.13 (1H, dd, *J* 11.6 and 7.1, 8a-CH_{2a}), 3.75 (1H, dd, *J* 11.6 and 4.6, 8a-CH_{2b}), 3.69 (1H, t, *J* 8.9, 3-H_b), 3.57 (1H, d, *J* 9.8, 9-H_b), 3.12–3.08 (1H, m, *OH*); *m/z* (ES+) (Found: MH^+ 462.1753, $C_{24}H_{24}N_5O_5$ requires *MH* 462.1772).

(3a*R*,8a*S*)-8a-(hydroxymethyl)-10-benzenesulfonyl-6-phenyl-3,3a,8a,9,10,11-hexahydrofuro[3,4-*e*]pyrrolo[3,4-*c*][1,2,4]triazolo[1,2-*a*]pyridazine-5,7(1*H*,6*H*)-dione ((±)-174)

By general procedure G, the amine (±)-**134** (20 mg, 0.022 mmol), DMAP (13 mg, 0.11 mmol) and benzenesulfonyl chloride (12 μL, 0.09 mmol) gave *(3aR,8aS)-8a-(((3',3',4',4',5',5',6',6',7',7',8',8',9',9',10',10'-heptadecafluorodecyl)-diisopropyl-silyloxy)-methyl)-10-benzenesulfonyl-6-phenyl-3,3a,8a,9,10,11-hexahydrofuro[3,4-e]pyrrolo[3,4-c][1,2,4]triazolo[1,2-a]pyridazine-5,7(1H,6H)-dione* (±)-**154** (21 mg, 91%, >95% purity by 500 MHz ^{1}H NMR spectroscopy) as a colorless amorphous solid, δ_H (500 MHz, $CDCl_3$) 7.88–7.86 (2H, m, benzene 2-H), 7.69–7.65 (1H, m, benzene 4-H), 7.61–7.57 (2H, m, benzene 3-H), 7.46–7.44 (4H, m, phenyl 2-H and 3-H), 7.39–7.34 (1H, m, phenyl 4-H), 4.70 (1H, dd, *J* 9.0 and 7.2, 3-H_a), 4.48–4.41 (2H, m, 1-H_a and 3a-H), 4.43 (1H, d, *J* 14.5, 1-H_b), 4.24 (1H, d, *J* 10.4, 9-H_a), 4.16 (1H, d, *J* 10.8, 8a-CH_{2a}), 4.08–4.03 (1H, m, 11-H_a), 3.88 (1H, d, *J* 14.5, 11-H_b), 3.54 (1H, t, *J* 9.0, 3-H_b), 3.43 (1H, d, *J* 10.4, 9-H_a), 3.35 (1H, d, *J* 10.8, 8a-CH_{2b}), 2.05–1.91 (2H, m, 2'-H_2), 0.98–0.93 (14H, m, ^{i}Pr), 0.79–0.74 (2H, m, 1'-H_2).

By general procedure H, the silyl ether (±)-**154** (21 mg, 0.020 mmol) gave the *sulfonamide* (±)-**174** (8 mg, 80%) as a colorless amorphous solid, R_f 0.23 (20:1 CH_2Cl_2–MeOH); ν_{max}/cm^{-1} (neat) 3446, 2940, 2869, 1764, 1699, 1428, 1165; δ_H (500 MHz, $CDCl_3$) 7.88–7.85 (2H, m, benzene 2-H), 7.67 (1H, t, *J* 7.5, benzene 4-H), 7.59 (2H, t, *J* 7.5, benzene 3-H), 7.48–7.44 (4H, m, phenyl 2-H and 3-H), 7.40–7.36 (1H, m, phenyl 4-H), 4.72–4.68 (1H, m, 3-H_a), 4.52–4.45 (2H, m, 1-H_a and 3a-H), 4.30 (1H, d, *J* 13.9, 1-H_b), 4.28 (1H, d, *J* 10.4, 9-H_a), 4.11–4.06 (1H, m, 11-H_a), 4.01 (1H, dd, *J* 11.6 and 6.2, 8a-CH_{2a}), 3.84 (1H, d, *J* 13.8, 11-H_b), 3.59 (1H, t, *J* 9.0, 3-H_b), 3.59–3.55 (1H, m, 8a-CH_{2b}), 3.27 (1H, d, *J* 10.4, 9-H_b), 2.54 (1H, t, *J* 4.8, *OH*); δ_C (75 MHz, $CDCl_3$) 150.3, 150.1, 136.3, 133.6, 133.2, 131.0, 129.6 (2C), 129.3 (2C), 128.5, 127.7 (2C), 125.5 (2C), 125.2, 71.3, 67.4, 65.1, 63.8, 54.5, 53.3, 47.4; *m/z* (ES+) (Found: MH^+ 483.1344, $C_{23}H_{23}N_4O_6S$ requires *MH* 483.1333).

(1*S*,3*R*,9*R*,10*S*) 5-Hydroxymethyl-7-(phenyl-aminecarbonyl)-2,12-dioxa-7-azatricyclo[8.5.0.0^{3,9}]4,14-pentadecadiene (175)

The sulfonamide **92** (11 mg, 0.011 mmol) and DBU (7 μL, 0.044 mmol) were dissolved in MeCN (0.5 mL) and PhSH (3 μL, 0.033 mmol) was added dropwise. The reaction mixture was stirred for 1.5 h at room temperature after which phenyl isocyanate (10 μL, 0.088 mmol) was added and the reaction mixture was stirred for another 2 h, concentrated under a flow of N_2 and purified by F–SPE, eluting with 160:40:1 MeOH–H_2O–Et_3N then 200:1 MeOH–Et_3N, to give *(1S,3R,9R,10S)-5-(((3',3',4',4',5',5',6',6',7',7',8',8',9',9',10',10',10'-heptadecafluorodecyl)-diisopropyl-silyloxy)-methyl) 7-(phenyl-aminecarbonyl)-2,12-dioxa-7-azatricyclo[8.5.0.0^{3,9}]4,14-pentadecadiene* **155** (10 mg, 100%, >75% purity by 500 MHz ^{1}H NMR spectroscopy) as a colorless oil, δ_H (500 MHz, $CDCl_3$) 7.28–7.22 (4H, m, phenyl 2-H and 3-H), 7.07–7.03 (1H, m, phenyl 4-H), 6.85 (1H, m, *NH*), 6.08–6.04 (2H, m, 4-H and 15-H), 5.72–5.67 (1H, m, 14-H), 4.62–4.58 (1H, m, 1-H), 4.35 (1H, d, *J* 7.8, 3-H), 4.23–4.11 (5H, m, 5-CH_2, 6-H_a and 13-H_2), 4.03 (1H, t, *J* 12.5, 8-H_a), 3.95–3.80 (3H, m, 6-H_b and 11-H_2), 3.40 (1H, dd, *J* 12.5 and 5.2, 8-H_b), 2.67–2.59 (2H, m, 9-H and 10-H), 2.14–2.00 (2H, m, 2'-H_2), 1.12–0.98 (14H, m, ^{i}Pr), 0.93–0.87 (2H, m, 1'-H_2).

By general procedure H, the silyl ether **155** (10 mg, 0.011 mmol) gave the *urea* **175** (1.5 mg, 38%) as a colorless oil, R_f 0.17 (20:1 CH_2Cl_2–MeOH); ν_{max}/cm^{-1} (neat) 3306, 2928, 2854, 1738, 1643, 1546, 1217; δ_H (500 MHz, $CDCl_3$) 7.96 (1H, s, *NH*), 7.40 (2H, dd, *J* 8.6 and 1.0, phenyl 2-H), 7.27–7.24 (2H, m, phenyl 3-H), 6.99 (1H, tt, *J* 7.5 and 1.0, phenyl 4-H), 6.14–6.12 (1H, m, 4-H), 6.05 (1H, d, *J* 11.5, 15-H), 5.71–5.67 (1H, m, 14-H), 4.64–4.60 (1H, m, 1-H), 4.34 (1H, d, *J* 9.8, 3-H), 4.26–4.11 (4H, m, 5-CH_2 and 13-H_2), 4.05 (1H, d, *J* 17.1, 6-H_a), 3.98 (1H, d, *J* 17.1, 6-H_b), 3.93–3.86 (1H, m, 8-H_a), 3.88 (1H, dd, *J* 11.0 and 6.7, 11-H_a), 3.80 (1H, dd, *J* 11.9 and 11.0, 11-H_b), 3.67–3.58 (1H, m, 8-H_b), 2.72–2.63 (1H, m, 10-H), 2.53–2.48 (1H, m, *OH*), 2.48–2.40 (1H, m, 9-H); *m/z* (ES+) (Found: MH^+ 357.1796, $C_{20}H_{25}N_2O_4$ requires *MH* 357.1809).

Abbreviations

ABD	7-amino-2-1,3-benzoxadiazol-4-yl
ATRA	all-*trans* retinoic acid
AUC	area under the concentration-time curve
Boc	*tert*-butoxycarbonyl
BOM	benzyloxy methyl
Cbz	carboxybenzyl
DBU	1,8-diazabicyclo[5.4.0]undec-7-ene
DCC	dicyclohexylcarbodiimide
DEAD	diethylazodicarboxylate
DDQ	2,3-dichloro-5,6-dicyano-1,4-benzoquinone
DHB	2,5-dihydroxybenzoic acid
DHP	3,4-dihydropyran
DIAD	diisopropyl azodicarboxylate;
DIBAL-H	diisobutylaluminium hydride
DIPEA	diisopropylethylamine
DIPES	diisopropylethylsily
DLS	dynamic light scattering
DMAP	4-(*N*,*N*-dimethylamino)pyridine
DMT	dimethoxytrityl
DOPE	1-palmitoyl-2-oleoyl-*sn*-glycero-3-phosphoethanolamine
DOS	diversity oriented synthesis
DPPC	1,2-dipalmitoyl-*sn*-glycero-3-phosphocholine
DPPG	1,2-dipalmitoyl-*sn*-glycero-3-phosphoglycerol
DSC	differential scanning calorimetry
DSPG	1,2-distearoyl-*sn*-glycero-3-phosphoglycerol
1-*O*-DSPG	1-*O*-stearyl-2-stearoyl-*sn*-glycero-3-phosphoglycerol
EDCI	1-ethyl-3-(3-dimethylaminopropyl)carbodiimide hydrochloride
EPR	enhanced permeability and retention
ESI	electrospray ionization
Fmoc	9-fluorenylmethyl carbamate
F-SPE	fluorous-solid phase extraction
G I	Grubbs Catalyst, 1st generation
HEPES	4-(2-hydroxyethyl)piperazine-1-ethanesulfonic acid
HG II	Hoveyda-Grubbs Catalyst, 2nd generation
HPLC	high pressure liquid chromatography
IC_{50}	half maximal inhibitory concentration
K_i	inhibition constant
Lyso-SPC	1-stearoyl-2-lyso-*sn*-glycero-3-phosphocholine
MALDI-TOF	matrix-assisted laser desorption/ionization time of flight
mCPBA	*m*-chloroperoxybenzoic acid

MD	molecular dynamics;
MLV	multilamellar vesicle
MTT	3-(4,5-dimethylthiazolyl)-2,5-diphenyltetrazolium bromide
NBS	*N*-bromosuccinimide
NBD-DPPE	1,2-dipalmitoyl-*sn*-glycero-3-phosphoethanolamine-*N*-[7-nitro-2-1,3-benzoxadiazol-4-yl];
NMR	nuclear magnetic resonance
Ns	nosyl
PC	phosphatidylcholine
PdI	polydispersity index
PE	phosphatidylethanolamine
PEG	polyethyleneglycol
Pg	protecting group
PG	phosphatidylglycerol
PMB	*p*-methoxybenzyl
PMBTCA	*p*-methoxybenzyl trichloroacetimidate
POPC	1-palmitoyl-2-oleoyl-*sn*-glycero-3-phosphocholine
POPG	1-palmitoyl-2-oleoyl-*sn*-glycero-3-phosphoglycerol
PPTS	pyridine *p*-toluenesulfonate
PS	phosphatidylserine
Px	9-(9-phenyl)xanthenyl, pixyl
RAR	retinoic acid receptor
RES	reticuloendothelial system
RMSD	root mean square deviation
RXR	retinoic X receptor
S	substrate
SAR	structure activity relationship
SD	standard derivation
$sPLA_2$	secretory phospholipase A_2
TBAF	tetrabutylammonium fluoride
TBDMS	*tert*-butyldimethylsilyl
TBDPS	*tert*-butyldiphenylsilyl
TES	triethylsilyl
Tf	trifluoromethanesulfonyl
TFA	trifluoroacetic acid
THP	tetrahydropyranyl
TIPS	triisopropylsilyl
TLC	thin layer chromatography
T_m	main phase transition temperature
TMP	2,2,6,6-tetramethyl piperidine
Tr	trityl

Ts	tosyl
VDR	vitamin D receptor
UV	unilamellar vesicle or ultraviolet

Lipid nomenclature of phospholipids

The phospholipids in this thesis have been named in accordance with the IUPAC-IUB Commission on Biochemical Nomenclature (Marsh, D. *Handbook of Lipid Bilayers*, 1990, CRC Press Inc, Florida). The system is based upon a semisystematic nomenclature, which allows trivial names and employs a fixed glycerol numbering, without considerations about the substituents. The carbon atoms of glycerol are numbered stereospecifically in order to assign the configuration of glycerol derivatives. The carbon atom at the top of a Fisher projection with the hydroxyl group in the C-2 position to the left is nominated C-1. The prefix “sn” (stereospecific numbering) is used to differentiate this numbering from conventional numbering without any steric information.

References

[1] Stewart, B. W. & Kleihues, P. *World Cancer Report* (World Health Organization Press, Geneva, 2003).

[2] Ferlay, J.; Parkin, D. M.; Steliarova-Foucher, E. Estimates of cancer incidence and mortality in Europe in 2008. *Eur. J. Cancer* **2010**, *46*, 765–781.

[3] Bray, F.; Richiardi, L.; Ekbom, A.; Pukkala, E.; Cuninkova, M.; Møller, H. Trends in testicular cancer incidence and mortality in 22 European countries: Continuing increases in incidence and declines in mortality. *Int. J. Cancer* **2006**, *118*, 3099–3111.

[4] Engholm, G.; Ferlay, J.; Christensen, N.; Bray, F.; Gjerstorff, M. L.; Klint, Å.; Køtlum, J. E.; Ólafsdóttir, E.; Pukkala, E.; Storm, H. H. NORDCAN: Cancer Incidence, Mortality, Prevalence and Prediction in the Nordic Countries, Version 3.6. Association of the Nordic Cancer Registries. Danish Cancer Society (http://www.ancr.nu) **2010**. Accessed 18th May 2010.

[5] Strebhardt, K.; Ullrich, A. Paul Ehrlich's magic bullet concept: 100 years of progress. *Nat. Rev. Cancer* **2008**, *8*, 473–480.

[6] Bangham, A. D.;. Standish, M. M.; Watkins, J.C. Diffusion of Univalent Ions across the Lamellae of Swollen Phospholipids. *J. Mol. Biol.* **1965**, *13*, 238–252.

[7] Bangham,A. D. Surrogate cells or Trojan horses. The discovery of liposomes. *Bioessays* **1995**, *17*, 1081–1088.

[8] Andresen, T. L.; Jensen, S. S.; Jørgensen, K. Advanced strategies in liposomal cancer therapy: Problems and prospects of active and tumor specific drug release. *Prog. Lipid Res.* **2005**, *44*, 68–97.

[9] Akoh, C. C.; Min, D. B. Food Lipids: Chemistry, Nutrition and Biotechnology. 3rd edition, CRC Press, USA, **2008**. p. 7–11 and 39–41.

[10] Hirshmann H. The Nature of Substrate Asymmetry in Stereoselective Reactions. *J. Biol. Chem.* **1960**, *235*, 2762–2767.

[11] Weiner, N.; Martin, F.; Riaz, M. Liposomes as a Drug Delivery System. *Drug Dev. Ind. Pharm.* **1989**, *15*, 1523–1554.

[12] Papahadjopoulos, A.; Miller, N. Phospholipid Model Membranes. I Structural Characteristics of Hydrated Liquid Crystals. *Biochim. Biophys. Acta* **1967**, *135*, 624–638

[13] Barenholz,Y.; Amselem,S.; Lichtenberg, D. A New Method for Preparation of Phospholipid Vesicles (Liposomes) –French Press. *FEBS Lett*. **1979**, *99*, 210–214.

[14] Storm, G.; Crommelin, D. J. A. Liposomes: quo vadis? *Pharm. Sci. Technol. Today* **1998**, *1*, 19–31.

[15] Mouritsen, O. G. Life – As a Matter of Fat. Springer, Berlin, **2005**, p.33–51 and 91–100.

[16] Andresen, T. L.; Jørgensen, K. Synthesis and membrane behavior of a new class of unnatural phospholipid analogs useful as phospholipase A_2 degradable liposomal drug carriers. *Biochim. et Biophys. Acta* **2005**, *1669*, 1–7.

[17] Terrell, J.; Yadava, P.; Castro, C.; Hughes, J.; Liposome Fluidity Alters Interactions Between the Ganglioside GM1 and Cholera Toxin B Subunit. *J. Liposome Res.* **2008**, *18*, 21–29.

[18] Gregoriadis, G.; Wills, E. J.; Swain, C. P.; Tavill, A. S. Drug-carrier potential of liposomes in Cancer chemotherapy. *Lancet* **1974**, *1*, 1313–1316.
[19] Blume,G.; Cevc, G. Liposomes for the sustained drug release in vivo. *Biochim. Biophys. Acta* **1990**, *1029*, 91–97.
[20] Klibanovl, A.L.; Maruyamal, K.; Torchilin,V.P.; Huangl, L. Amphipathic polyethyleneglycols effectively prolong the circulation time of liposomes. *FEBS Lett.* **1990**, *268*, 235–237.
[21] Senior, J.; Delgado, C.; Fisher, D.; Tilcock, C.; Gregoriadis, G. Influence of surface hydrophilicity of liposomes on their interaction with plasma protein and clearance from the circulation: studies with poly(ethylene glycol)-coated vesicles. *Biochim. Biophys. Acta* **1991**, *1062*, 77–82.
[22] Drummond, D. C.; Meyer, O.; Hong, K.; Kirpotin, D.B.; Papahadjopoulos, D. Optimizing Liposomes for Delivery of Chemotherapeutic Agents to Solid Tumors. *Pharmacol. Rev.* **1999**, *51*, 691–743.
[23] Matsumura, Y.; Maeda, H. A New Conceps for Macromolecular Therapeutics in Cancer Chemotherapy: Mechanism of tumoritropic Accumulation of Proteins and the Antitumor Agent Smancs. *Cancer Res.* **1986**, *46*, 6387–6392.
[24] Maeda, H.; Wu, J.; Sawa, T.; Matsumura, Y.; Hori, K. Tumor vascular permeability and the EPR effect in macromolecular therapeutics: a review. *J. Controlled Release* **2000**, *65*, 271–284.
[25] Seymour,L. W. Passive tumor targeting of soluble macromolecules and drug conjugates. *Crit. Rev. Ther. Drug Carrier Syst.* **1992**, *9*,135–187.
[26] Unezaki, S.; Maruyama, K.; Ishida, O.; Suginaka, A.; Hosoda, J.; Iwatsuru, M. Enhanced tumor targeting and improved antitumor activity doxorubicin by long-circulating liposomes containing amphipathic poly(ethylene glycol). *Int. J. Pharm*. **1995**, *126*, 41–48.
[27] Lee, R. J.; Lows, P. S. Delivery of Liposomes into Cultured KB Cells via Folate Receptor-mediated Endocytosis. *J. Biol. Chem*. **1994**, *269*, 3198–3204.
[28] Gabizon, A.; Horowitz, A. T.; Goren, D.; Tzemach, D.; Mandelbaum-Shavit, F.; Qazen, M. M.; Zalipsky, S. Targeting Folate Receptor with Folate Linked to Extremities of Poly(ethylene glycol)-Grafted Liposomes: *In Vitro* Studies. *Bioconjugate Chem*. **1999**, *10*, 289–298.
[29] Rui, Y.; Wang, S.; Low, P. S.; Thompson, D. H. Diplasmenylcholine-Folate Liposomes: An Efficient Vehicle for Intracellular Drug Delivery. *J. Am. Chem. Soc*. **1998**, *120*, 11213–11218.
[30] Torchilin, V. Antibody-modified liposomes for cancer chemotherapy. *Expert Opin. Drug Deliv*. **2008**, *5*, 1003–1025.
[31] Park, J. W.; Hong, K.; Kirpotin, D. B.; Colbern, G.; Shalaby, R.; Baselga, J.; Shao, Y.; Nielsen, U. B.; Marks, J. D.; Moore, D.; Papahadjopoulos, D.; Benz, C. C. Anti-HER2 Immunoliposomes: Enhanced Efficacy Attributable to Targeted Delivery. *Clin. Cancer Res.* **2002**, *8*, 1172–1181.

[32] Kaasgaard, T.; Andresen, T. L. Liposomal cancer therapy: exploiting tumor characteristics. *Expert Opin. Drug Deliv.* **2010**, *7*, 225–243.
[33] Connor, J.; Yatvin, M. B.; Huang, L. pH-sensitive liposomes: acid-induced liposome fusion. *Proc. Natl. Acad. Sci. U.S.A.* **1984**, *81*, 1715–1718.
[34] Shin, J.; Shum, P.; Thompson, D. H. Acid-triggered release via dePEGylation of DOPE liposomes containing acid-labile vinyl ether PEG-lipids. *J. Controlled Release* **2003**, *91*, 187–200.
[35] Miller, C. R.; Bennett, D. E.; Chang, D. Y.; O'Brien, D. F. Effect of liposomal composition on photoactivated liposome fusion. *Biochemistry* **1996**, *35*, 11782–11790.
[36] Shum, P.; Kim, J. M.; Thompson, D. H. Phototriggering of liposomal drug delivery systems. *Adv. Drug Delivery Rev.* **2001**, *53*, 273–284.
[37] Yatvin, M. B.; Weinstein, J. N.; Dennis, W. H.; Blumenthal, R. Design of liposomes for enhanced local release of drugs by hyperthermia. *Science* **1978**, *202*, 1290–1293.
[38] Needham, D.; Anyarambhatla, G.; Kong, G.; Dewhirst, M. W. A new temperature-sensitive liposome for use with mild hyperthermia: characterization and testing in a human tumor xenograft model. *Cancer Res.* **2000**, *60*, 1197–1201.
[39] Meers, P. Enzyme-activated targeting of liposomes. *Adv. Drug Delivery Rev.* **2001**, *53*, 265–272.
[40] Drummond, D. C.; Noble, C. O.; Hayes, M. E.; Park, J. W.; Kirpotin, D. B. Pharmacokinetics and In Vivo Drug Release Rates in Liposomal Nanocarrier Development. *J. Pharm. Sci.* **2008**, *97*, 4696–4740.
[41] Pak, C. C.; Ali, S.; Janoff, A. S.; Meers, P. Triggerable liposomal fusion by enzyme cleavage of a novel peptide–lipid conjugate. *Biochim. Biophys. Acta* **1998**, *1372*, 13–27.
[42] Pak, C. C.; Erukulla, R. K.; Ahl, P. L.; Janoff, A. S.; Meers, P. Elastase activated liposomal delivery to nucleated cells. *Biochim. Biophys. Acta* **1999**, *1419*, 111–126.
[43] Gagne, J.; Stamatatos, L.; Diacovo, T.; Hui, S.W.; Yeagle, P. L.; Silvius, J. R. Physical Properties and Surface Interactions of Bilayer Membranes Containing N-Methylated Phosphatidylethanolamines. *Biochemistry* **1985**, *24,* 4400–4408.
[44] Davis, S. C.; Szoka Jr., F. C. Cholesterol Phosphate Derivatives: Synthesis and Incorporation into a Phosphatase and Calsium-Sensitive Triggered Release Liposome. *Bioconjugate Chem.* **1998**, *9*, 783–792.
[45] Millan, J. L.; Fishman, W. H. Biology of Human Alkaline Phosphatases with Special Reference to Cancer. *Crit. Rev. Clin. Lab. Sci.* **1995**, *32*, 1–39.
[46] Sarkar, N. R.; Rosendahl, T.; Krueger, A. B.; Banerjee, A. L.; Benton, K.; Mallik, S.; Srivastava, D. K. ''Uncorking'' of liposomes by matrix metalloproteinase-9. *Chem. Commun*. **2005**, *8*, 999–1001.
[47] Davidsen, J.; Vermehren, C.; Frokjaer, S.; Mouritsen, O. G.; Jørgensen, K. Drug delivery by phospholipase A_2 degradable liposomes. *Int. J. Pharm.* **2001**, *214*, 67–69.
[48] Davidsen, J.; Jørgensen, K.; Andresen, T. L.; Mouritsen, O. G. Secreted phospholipase A_2 as a new enzymatic trigger mechanism for localised liposomal drug release and absorption in diseased tissue. *Biochim. Biophys. Acta* **2003**, *1609*, 95–101.

[49] Six, D. A.; Dennis, E. A. The expanding superfanily of phospholipase A_2 enzymes: classification and characterization. *Biochim. Biophys. Acta* **2000**, *1488*, 1–19.
[50] Murakami, M.; Kudo, I. PhospholipaseA_2. *J. Biochem.* **2002**, *131*, 285–292.
[51] Scott, D. L.; White, S.; Otwinowski, Z.; Yuan, W.; Gelb, M. H.; Sigler, P. B. Interfacial Catalysis;The Mechanism of Phospholipase-A_2. Science **1990**, *250*, 1541–1546.
[52] Laye, J. P.; Gill, J. H. Phospholipase A_2 expression in tumours: a target for therapeutic intervention? *Drug Discovery Today* **2003**, *8*, 710–716.
[53] Abe, T.; Sakamoto, K.; Kamohara, H.; Hirano, Y.; Kuwahara, N.; Ogawa, M. Group II phospholipase A_2 is increased in peritoneal and pleural effusions in patients with various types of cancer. *Int. J. Cancer* **1997**, *74*, 245–250.
[54] Graff, J. R.; Konicek, B. W.; Deddens, J. A.; Chedid, M.; Hurst, B. M.; Colligan, B.; Neubauer, B. L.; Carter, H. W.; Carter, J. H. Expression of group IIa secretory phospholipase A_2 increases with prostate tumor grade. *Clin. Cancer Res.* **2001**, *7*, 3857–3861.
[55] Tatulian, S. A. Toward Understanding Interfacial Activation of Secretory Phospholipase A_2 (PLA_2): Membrane Surface Properties and Membrane-Induced Structural Changes in the Enzyme Contribute Synergistically to PLA_2 Activation. *Biophysical J.* **2001**, *80*, 789–800.
[56] Leidy, C.; Linderoth, L.; Andresen, T. L.; Mouritsen, O. G.; Jørgensen, K.; Peters, G. H. Domain-Induced Activation of Human Phospholipase A_2 Type IIA: Local versus Global Lipid Composition. *Biophysical J.* **2006**, *90*, *3165–3175*.
[57] Buckland, A. G.; Wilton, D. C. Anionic phospholipids, interfacial binding and the regulation of cell functions. *Biochim. Biophys. Acta* **2000**, *1483*, 199–216.
[58] Canaan, S.; Nielsen, R.; Ghomashchi, F.; Robinson, B. H.; Gelb, M. H. Unusual mode of binding of human group IIA secreted phospholipase A_2 to anionic interfaces as studied by continuous wave and time domain electron paramagnetic resonance spectroscopy. *J. Biol. Chem*. **2002**, *277*, 30984–30990.
[59] Singer, A. G.; Ghomashchi, F.; Le Calvez, C.; Bollinger, J.; Bezzine, S.; Rouault, M.; Sadilek, M.; Nguyen, E.; Lazdunski, M.; Lambeau, G.; Gelb, M. H. Interfacial kinetic and binding properties of the complete set of human and mouse groups I, II, V, X, and XII secreted phospholipases A_2. *J. Biol. Chem.* **2002**, *277*, 48535–48549.
[60] Savay, S.; Szebeni, J.; Baranyi, L.; Alving, C.R. Potentiation of liposome-induced complement activation by surface-bound albumin. *Biochim. Biophys. Acta* **2002**, *1559*, 79–86.
[61] Gadd, M. E.; Biltonen, R. L. Characterization of the interaction of phospholipase A_2 with phosphatidylcholine-phosphatidylglycerol mixed lipids. *Biochemistry* **2000**, *39*, 12312–12323.
[62] Jørgensen, K.; Vermehren, C.; Mouritsen, O. G. Enhancement of phospholipase A_2 catalyzed degradation of polymer grafted PEG liposomes: Effects of lipopolymer-concentration and chain length. *Pharm. Res.* **1999**, *16*, 1491–1493.

[63] Jensen, S. S.; Andresen, T. L.; Davidsen, J.; Høyrup, P.; Shnyder, S. D.; Bibby, M. C.; Gill, J. H.; Jørgensen, K. Secretory phospholipase A_2 as a tumor-specific trigger for targeted delivery of a novel class of liposomal prodrug anticancer etherlipids. *Mol. Cancer Ther*. **2004**, *11*, 1451–1458.

[64] Andresen,T. L.; Davidsen, J; Begtrup, M.; Mouritsen, O. G.; Jørgensen, K. Enzymatic Release of Antitumor Ether Lipids by Specific Phospholipase A_2 Activation of Liposome-Forming Prodrugs. *J. Med. Chem*. **2004**, *47,* 1694–1703.

[65] Linderoth, L.; Fristrup, P.; Hansen, M.; Melander, F.; Madsen, R.; Andresen, T. L.; Peters, G. H. Mechanistic Study of the $sPLA_2$-Mediated Hydrolysis of a Thio-ester Pro Anticancer Ether Lipid. *J. Am. Chem. Soc.* **2009**, *131*, 12193–12200.

[66] Linderoth, L.; Andresen, T. L.; Jørgensen, K.; Madsen, R.; Peters, G. H. Molecular Basis of Phospholipase A_2 Activity toward Phospholipids with *sn*-1 Substitutions. *Biophysical J.* **2008**, *94*, 14–26.

[67] Bonsen, P. P. M.; de Haas, G. H.; Pieterson, W. A.; van Deenen, L. L. Studies on Phospholipase A and its Zymogen from Porcine Pancreas. IV. The Influence of Chemical Modification of the Lecithin Structure on Substrate Properties. *Biochim. Biophys. Acta* **1972**, *270*, 364–382.

[68] Andresen, T. L.; Jensen, S. S.; Madsen, R.; Jørgensen, K. Synthesis and Biological Activity of Anticancer Ether Lipids That Are Specifically Released by Phospholipase A_2 in Tumor Tissue. *J. Med. Chem.* **2005**, *48,* 7305–7314.

[69] Houlihan, W. J.; Lohmeyer, M.; Workman, P.; Cheon, S. H. Phospholipid antitumor agents. *Med. Res. Rev.* **1995**, *15*, 157–223.

[70] Ahmad, I.; Filep, J. J.; Franklin, J. C.; Janoff, A. S.; Masters, G. R.; Pattassery, J.; Peters, A.; Schupsky, J. J.; Zha, Y.; Mayhew, E. Enhanced therapeutic effects of liposome-associated 1-*O*-octadecyl-2-*O*-methyl-*sn*-glycero-3-phosphocholine. *Cancer Res.* **1997**, *57*, 1915–1921.

[71] Linderoth, L.; Peters, G. H.; Madsen, R.; Andresen,T. L. Drug Delivery by an Enzyme-Mediated Cyclization of a Lipid Prodrug with Unique Bilayer-Formation Properties. *Angew. Chem. Int. Ed.* **2009**, *48*, 1–5.

[72] Davidsen, J.; Mouritsen, O. G.; Jørgensen, K. Synergistic permeability enhancing effect of lysophospholipids and fatty acids on lipid membranes. *Biochim. Biophys. Acta* **2002**, *1564*, 256–262.

[73] Everett, J. L.; Roberts, J. J.; Ross, W. C. J. Aryl-2-halogenoalkylamines. XII: Some carboxylic derivatives of *N*,*N*-di-2-chloroethylaniline. *J. Chem. Soc.* **1953**, 2386–2392.

[74] Urbaniak, M. D.; Bingham, J. P.; Hartley, J. A.; Woolfson, D. N.; Caddick, S. Design and synthesis of a nitrogen mustard derivative stabilized by apo-neocarzinostatin. *J. Med. Chem.* **2004**, *47*, 4710–4715.

[75] Okuno, M.; Kojima, S.; Matsushima-Nishiwaki, R.; Tsurumi, H.; Muto, Y.; Friedman, S. L.; Moriwaki, H. Retinoids in Cancer Chemoprevention. *Curr. Cancer Drug Targets* **2004**, *4*, 285–298.

[76] Freementle, S. J.; Spinella, M. J.; Dmitrovsky, E. Retinoids in cancer therapy and chemoprevention: promise meets resistance. *Oncogene* **2003**, *22*, 7305–7315.
[77] Neuzil, J.; Weber, T.; Gellert, N.; Weber, C. Selective cancer killing by α-tocopheryl succinate. *Br. J. Cancer* **2000**, *84*, 87–89.
[78] Birringer, M.; EyTina, J. H.; Salvatore, B. A.; Neuzil, J. Vitamin E analogues as inducers of apoptosis: structure-function relation. *Br. J. Cancer* **2003**, *88*, 1948–1955.
[79] Kato, T.; Fukushima, M.; Kurozumi, S.; Noyori, R. Antitumor Activity of Δ^7-Prostaglandin A_1 and Δ^{12}-Prostaglandin J_2 *in Vitro* and *in Vivo*. *Cancer Res.* **1986**, *46*, 3538–3542.
[80] Kodali, D. R.; Tercyak, A.; Fahey, D. A.; Small, D. H. Acyl migration in 1,2-dipalmitoyl-*sn*-glycerol. *Chem. Phys. Lipids.* **1990**, *52*, 163–170.
[81] Eibl, H. An Improved Method for the Preparation of 1,2- Isopropylidene-*sn*-glycerol. *Chem. Phys. Lipids* **1981**, *28* 1–5.
[82] Hirth, G.; Walther, W. Synth'ese des (*R*)- et (*S*)-O-isopropylidéne-1,2-glycérols. Détermination de la pureté optique. *Helv. Chim. Acta.* **1985**, *68*, 1863–1871.
[83] De Wilde, H.; De Clercq, P.; Vandewalle, M.; Röper, H. L-(*S*)-Erythrulose. A Novel Precursor to L-2,3-*O*-isopropylidene-C_3 Chirons. *Tetrahedron Lett.* **1987**, *28*, 4757–4758.
[84] Hubschwerlen, C. A Convenient Synthesis of L-(S)-Glyceraldehyde Acetonide from L-Ascorbic acid. *Synthesis* **1986**, 962–964.
[85] Gao, Y.; Hanson, R. M.; Klunder, J. M.; Ko, S. Y.; Masamune, H.; Sharpless, K. B. Catalytic Asymmetric Epoxidation and Kinetic Resolution: Modified Procedures Including in Situ Derivatization. *J. Am. Chem. Soc.* **1987**, *109*, 5765–5780.
[86] Neff, A. B.; Schultz, C. Selective fluorescent labeling of lipids in living cells. *Angew. Chem. Int. Ed.* **2009**, *48*, 1498–1500.
[87] Gaffney, P. R. J.; Reese, C. B. Synthesis of naturally occurring phosphatidylinositol 3,4,5-triphosphate [PtdIns(3,4,5)P3] and its diastereoisomers. *J. Chem. Soc., Perkin Trans 1*, **2001**, 192–205.
[88] Kubiak, R. J.; Bruzik, K. S. Comprehensive and Uniform Synthesis of All Naturally Occurring Phosphorylated Phosphatidylinositols. *J. Org. Chem.* **2003**, *68*, 960–968.
[89] Lee, W. S.; Kim, M. J.; Beck, Y.; Park, Y. D.; Jeong, T. S. Lp-PLA_2 inhibitory activities of fatty acid glycerols isolated from *Saururus chinensis* roots. *Bioorg. Med. Chem. Lett.* **2005**, *15*, 3573–3575.
[90] Qin, D., Byun, H. S.; Bittman, R. Synthesis of Plasmalogen via 2,3-Bis-*O*-(4'-methoxybenzyl)-*sn*-glycerol. *J. Am. Chem. Soc.* **1999**, *121*, 662–668.
[91] Shizuka, M.; Schrader, T. O.; Snapper. M. L. Synthesis of Isoprostanyl Phosphatidylcholine and Isoprostanyl Phosphatidylethanolamine. *J. Org. Chem.* **2006**, *71*, 1330–1334.
[92] Lim, Z. Y.; Thuring, J. W.; Holmes, A. B.; Manifava, M.; Ktistakis, N. T. Synthesis and biological evaluation of PtdIns(4,5)P_2 and a phosphatidic acid affinity matrix. *J. Chem. Soc., Perkin Trans 1*, **2002**, 1067–1075.

[93] Rosseto, R.; Bibak, N.; Hajdu, J. A new approach to phospholipid synthesis using tetrahydropyranyl glycerol: rapid access to phosphatidic acid and phosphatidylcholine, including mixed-chain glycerophospholipid derivatives. *Org. Biomol. Chem.* **2006**, *4*, 2358–2360.
[94] Boomer, J. A.; Thompson, D. H. Synthesis of acid-labile diplasmenyl lipids for drug and gene delivery applications. *Chem. Phys. Lipids* **1999**, *99*, 145–153.
[95] Ashton, W. T.; Canning, L. F.; Reynolds, G. F.; Tolman, R. L.; Karkas, J. D.; Liou, R.; Davies, M. M.; DeWitt, C. M.; Perry, H. C.; Fjeld, A. K. Synthesis and Antiherpetic Activity of (*S*)-, (*R*)- and (±)-9-[(2,3-Dihydroxy-l-propoxy)methyl]guanine, Linear Isomers of 2'-Nor-2'-deoxyguanosin. *J. Med. Chem.* **1985**, *28*, 926–933.
[96] Baldwin, J. J.; Raab, A. W.; Mender, K.; Arison, B. H.; McClure, D. E. Synthesis of (*R*)- and (*S*)-Epichlorohydrin. *J. Org. Chem.* **1978**, *43*, 4876–4878.
[97] Dodd, G. H.; Golding, B. T.; Ioannou, P. V. Limitations of *t*-Butyldimethylsilyl as a Protecting Group for Hydroxy-functions. *J. Chem. Soc., Chem. Comm.* **1975**, *249–250*.
[98] Burgos, C. E.; Ayer, D. E.; Johnson, R. A. A new, asymmetric synthesis of lipids and phospholipids. *J. Org. Chem.* **1987**, *52*, 4973–4977.
[99] Batten, R. J.; Dixon, A. J.; Taylor, R. J. K. A New Method for Removing the *t*-Butyldimethylsilyl Protecting Group. *Synthesis* **1980**, 234–236.
[100] Dale, J. A.; Mosher, H. S. Nuclear Magnetic Resonance Enantiomer Reagents. Configurational Correlations via Nuclear Magnetic Resonance Chemical Shifts of Diastereomeric Mandelate, O-Methylmandelate, and α-Methoxy-α-trifluoromethylphenylacetate (MTPA) Esters. *J. Am. Chem. Soc.* **1973**, *95*, 512–519.
[101] Stamatov, S. D.; Stawinski, J. Regioselective and stereospecific acylation across oxirane- and silyloxy systems as a novel strategy to the synthesis of enantiomerically pure mono-, di- and triglycerides. *Org. Biomol. Chem.* **2007**, *5*, 3787–3800.
[102] Neises, B.; Steglich, W. Simple Method for the Esterification of Carboxylic Acids. *Angew. Chem. Int. Ed. Engl.* **1978**, *17*, 522–524.
[103] Martin, S. F.; Josey, J. A.; Wong, Y. L.; Dean, D. W. General Method for the Synthesis of Phospholipid Derivatives of 1,2-*O*-Diacyl-*sn*-glycerols. *J. Org. Chem.* **1994**, *59*, 4805–4820.
[104] Greimel, P.; Lapeyre, M.; Nagatsuka, Y.; Hirabayashi, Y.; Ito, Y. Syntheses of phosphatidyl-β-D-glucoside analogues to probe antigen selectivity of monoclonal antibody 'DIM21'. *Bioorg. Med. Chem.* **2008**, *16*, 7210–7217.
[105] Bibak, N.; Hajdu, J. A new approach to the synthesis of lysophosphatidylcholines and related derivatives. *Tetrahedron Lett.* **2003**, *44*, 5875–5877.
[106] Rosseto, R.; Bibak, N.; DeOcampo, R.; Shah, T.; Gabrilian, A.; Hajdu, J. A New Synthesis of Lysophosphatidylcholines and Related Derivatives. Use of *p*-Toluenesulfonate for Hydroxyl Group Protection. *J. Org. Chem.* **2007**, *72*, 1691–1698.
[107] Baba, N.; Kosugi, T.; Daido, H.; Umino, H.; Kishida, Y.; Nakajima, S.; Shimizu, S. Enzymatic Synthesis of Phosphatidylinositol Bearing Polysaturated Acyl Group. *Biosci. Biotech. Biochem.* **1996**, *60*, 1916–1918.

[108] Murakami, K.; Molitor, E. J.; Liu, H. An Efficient Synthesis of Unsymmetrical Optically Active Phosphatidyl Glycerol. *J. Org. Chem.* **1999**, *64*, 648–651.
[109] Williamson, A. *Justus Liebigs Ann. Chem*. **1851**, *77*, 37–49.
[110] Yashunsky, D. V.; Borodkin, V. S.; Ferguson, M. A. J.; Nikolaev, A. V. The Chemical Synthesis of Bioactive Glycosylphosphatidylinositols from *Trypanosoma cruzi* Containing an Unsaturated Fatty Acid in the Lipid. *Angew. Chem. Int. Ed.* **2006**, *45*, 468–474.
[111] Ohno, M.; Fujita, K.; Nakai, H.; Kobayashi, S.; Inoue, K.; Nojima, S. An Enantioselective Synthesis of Platelet-Activating Factors, Their Enantiomers, and Their Analogues from D- and L-Tartaric Acids. *Chem. Pharm. Bull.* **1985**, *33*, 572–582.
[112] Shin, J.; Gerasimov, O.; Thompson, D. H. Facile Synthesis of Plasmalogens via Barbier-Type Reactions of Vinyl Dioxanes and Vinyl Dioxolanes with Alkyl Halides in LiDBB Solution. *J. Org. Chem.* **2002**, *67*, 6503–6508.
[113] Guivisdalsky, P. N.; Bittman, R. An Efficient Stereocontrolled Route to Both Enantiomers of Platelet Activating Factor and Analogues with Long-chain Esters at C_2: Saturated and Unsaturated Ether Glycerolipids by Opening of Glycidyl Arenesulfonates. *J. Org. Chem.* **1989**, *54*, 4643–4648.
[114] Guivisdalsky, P. N.; Bittman, R. Regiospecific Opening of Glycidyl Derivatives Mediated by Boron Trifluoride. Asymmetric Synthesis of Ether-Linked Phospholipids. *J. Org. Chem.* **1989**, *54*, 4637–4642.
[115] Kazi, A. B.; Shidmand, S.; Hajdu, J. Stereospecific Synthesis of Functionalized Ether Phospholipids. *J. Org. Chem.* **1999**, *64*, 9337–9347.
[116] Paltauf, F.; Hermetter, A. Strategies for the Synthesis of Glycerophospholipids. *Prog. Lipid Res.* **1994**, *33*, 239–328.
[117] Safari, H.; Blaschette, A. Darstellung und Eigenschaften yon Trimethyl-dialkylamidosulfonyl)-ammoniumhalogeniden. *Monatsh. Chem.* **1970**, *101*, 1373–1387.
[118] Baer, E.; Kindler, A. L-α-(Dioleoyl)lecithin. An Alternate Route to Its Synthesis. *Biochemistry* **1962**, 1, 518–521.
[119] Kundu, G. C.; Schullek, J. R.; Wilson, I. B. The alkylating properties of chlorambucil. *Pharmacol. Biochem. Behav.* **1993**, *49*, 621–624.
[120] Montserrat, E.; Rozman, C. Chronic lymphocytic leukaemia treatment. *Blood Revs.* **1993**, *7*, 164–175.
[121] Ehrsson, H.; Eksborg, S.; Wallin, I.; Nilsson, S. O. Degradation of Chlorambucil in Aqueous Solution. *J. Pharm. Sci.* **1980**, *69*, 1091–1094.
[122] Chatterji, D. C.; Yeager, R. L.; Gallelli, J. F. Kinetics of Chlorambucil Hydrolysis Using High-Pressure Liquid Chromatography. *J. Pharm. Sci.* **1982**, *71*, 50–54.
[123] Löf, K.; Hovinen, J.; Reinikainen, P.; Vilpo, L. M.; Seppälä, E.; Vilpo, J. A. Kinetics of chlorambucil in vitro: effects of fluid matrix, human gastric juice, plasma proteins and red cells. *Chem. Biol. Interact.* **1997**, *103*, 187–198.
[124] Nakajima, N.; Horita, K.; Abe, R.; Yonemitsu, O. MPM (4-methoxybenzyl) protection of hydroxyl functions under mild acidic conditions. *Tetrahedron Lett.* **1988**, *29*, 4139–4142.

[125] Rai, A. N.; Basu, A. An efficient method for *para*-methoxybenzyl ether formation with lanthanum triflate. *Tetrahedron Lett.* **2003**, *44*, 2267–2269.
[126] Levina, A. B.; Chernaya, S. S.; Trusov, S. R.; Stelmakh, T. V. Rate and Mechanism of Oxidation of Benzyl Alcohol with Oxygen in Aqueous-solutions of Perchloric-acid in the Presence of Sodium-nitrite. *Kinet. Katal.* **1991**, *32*, 1336–1342.
[127] Grigor'eva, I. A.; Chernaya, S. S.; Trusov, S. R.; Oxidation of D-Glucose to D-Gluconic and D-Glucaric Acids Catalyzed by Sodium Nitrite. *Russ. J. Appl. Chem*. **2001**, *74*, 2021–2026.
[128] Horita, K.; Yoshioka, T.; Tanaka, T.; Oikawa, Y.; Yonemitsu, O. On the selectivity of deprotection of benzyl, MPM (4-methoxybenzyl) and DMPM (3,4-dimethoxybenzyl) protecting groups for hydroxyl functions. *Tetrahedron* **1986**, *42,* 3021–3028.
[129] Boden, E. P.; Keck, G. E. Proton-Transfer Steps in Steglich Esterification: A Very Practical new Method for Macrolactonization. *J. Org. Chem.* **1985**, *50*, 2394–2395.
[130] Lichtenberg, D.; Barenholz, Y. Liposomes – Preparation, Characterization and Preservation. *Methods Biochem. Anal.* **1988**, *33*, 337–462.
[131] Peters G. H.; Møller M. S.; Jørgensen K.; Rönnhölm P.; Mikkelsen M.; Andresen T. L. Secretory phospholipase A_2 hydrolysis of phospholipid analogues is dependent on water accessibility to the active site. *J. Am. Chem. Soc.* **2007**, *129*, 5451–5461.
[132] Harvey, D. J. Matrix-assisted Laser Desorption/Ionization Mass Spectrometry of Phospholipids. *J. Mass Spectrom.* **1995**, *30*, 1333–1346.
[133] Schiller, J.; Arnhold, J.; Benard, S.; Müller, M.; Reichl, S.; Arnold, K. Lipid Analysis by Matrix-Assisted Laser Desorption and Ionization Mass Spectrometry: A Methodological Approach. *Anal. Biochem.* **1999**, *267*, 46–56.
[134] Petković, M.; Muller, J.; Muller, M.; Schiller, J.; Arnold, K.; Arnhold, J. Application of matrix-assisted laser desorption/ionization time-of-flight mass spectrometry for monitoring the digestion of phosphatidylcholine by pancreatic phospholipase A_2. *Anal. Biochem.* **2002**, *308*, 61–70.
[135] Pedersen, P. J.; Christensen, M. S.; Ruysschaert, T.; Linderoth, L.; Andresen, T. L.; Melander, F.; Mouritsen, O. G.; Madsen, R.; Clausen, M. H. Synthesis and Biophysical Characterization of Chlorambucil Anticancer Ether Lipid Prodrugs. *J. Med. Chem.* **2009**, *52*, 3408–3415.
[136] Epstein, J.; Rosenthal, R.W., Ess, R.J. Use of p-(4-nitrobenzyl)pyridine as analytical reagent for ethylenimines and alkylating agents. *Anal. Chem.* **1955**, *27*, 1435–1439.
[137] Freidman, O. M.; Boger, E.; Chlorimetric estimation of nitrogen mustard in aqueous media. *Anal. Chem.* **1961***, 33*, 906–910.
[138] Genka, S.; Deutsch, J.; Shetty, U. H.; Stahle, P. L.; John, V.; Lieberburg, I. M.; Ali-Osmant, F.; Rapoport, S. I.; Greig, N. H. Development of lipophilic anticancer agents for the treatment of brain tumors by the esterification of water-soluble chlorambucil. *Clin. Exp. Metastasis,* **1993**, *11*, 131–140.
[139] Barua, A. B.; Furr, H. C. Properties of Retinoids. *Mol. Biotechnol.* **1998**, *10*, 167–182.

[140] Rolewski, S. L. Clinical Review: Topical Retinoids. *Dermatol. Nurs.* **2003**, *15*, 447–465.
[141] Huang, M. E.; Ye, Y. C.; Chen, S. R.; Chai, J.; Lu, J. X.; Zhoa, L.; Gu, L. J.; Wang, Z. Y. Use of all-*trans* retinoic acid in the treatment of acute promyelocytic leukemia. *Blood* **1988**, *72*, 567–572.
[142] Castaigne, S.; Chomienne, C.; Daniel, M. T.; Ballerini, P.; Berger, R.; Fenaux, P.; Degos, L. All-*trans* retinoic acid as a differentiation therapy for acute promyelocytic leukemia. I. Clinical results. *Blood* **1990**, *76*, 1704–1709.
[143] Regazzi, M. B.; Iacona, I.; Gervasutti, C.; Lazzarino, M.; Toma, S. Clinical Pharmacokinetics of Tritinoin. *Clin. Pharmacokinet.* **1997**, *32*, 382–402.
[144] Muindi, J. R. F.; Frankel, S. R.; Huselton, C.; DeGrazia, F.; Garland, W. A.; Young, C. W.; Warrell, R. P. Clinical pharmacology of oral all-*trans*-retinoic acid in patients with acute promyelocytic leukemia. *Cancer Res.* **1992**, *52*, 2138–2142.
[145] Shimizu, K.; Tamagawa, K.; Takahashi, N.; Takayama, K.; Maitani, Y. Stability and antitumor effects of all-*trans* retinoic acid-loaded liposomes contained sterylglucoside mixture. *Int. J. Pharm.* **2003**, *258*, 45–53.
[146] Kawakami, S.; Opanasopit, P.; Yokoyama, M.; Chansri, N.; Yamamoto, T.; Okano, T.; Yamashita, F.; Hasdida, M. Biodistribution Characteristics of All-*trans* Retinoic Acid Incorporated in Liposomes and Polymeric Micelles Following Intravenous Administration. *J. Pharm. Sci.* **2005**, *94*, 2606–2615.
[147] Díaz, C.; Vargas, E.; Gätjens-Boniche, O. Cytotoxic effect induced by retionoic acid loaded into galatosyl-sphingosine containing liposomes on human hepatoma cell lines. *Int. J. Pharm.* **2006**, *325*, 208–115.
[148] Suzuki, S.; Kawakami, S.; Chansri, N.; Yamashita, F.; Hasdida, M. Inhibition of pulmonary metastasis in mice by all-*trans* retinoic acid incorporated in cationic liposomes. *J. Control. Release* **2006**, *116*, 58–63.
[149] Christensen, M. S.; Pedersen, P. J.; Andresen, T. L.; Madsen, R.; Clausen, M. H. Isomerization of all-(*E*)-Retinoic Acid Mediated by Carbodiimide Activation;Synthesis of ATRA Ether Lipid Conjugates. *Eur. J. Org. Chem*. **2009**, 719–724.
[150] Holmberg, K.; Hansen, B. Ester Synthesis with Dicyclohexylcarbodiimide Improved by Acid Catalyst. *Acta Chem. Scand. B* **1979**, *33*, 410–412.
[151] Mitsunobu, O.; The Use of Diethyl Azodicarboxylate and Triphenylphosphine in Synthesis and Transformation of Natural Products. *Synthesis* **1981**, 1–28.
[152] Fawzy, A. A.; Wishwanath, B. S.; Franson, R. C. Inhibition of human nonpancreatic phospholipases A_2 by retinoids and flavonoids. Mechanism of action. *Agents Actions* **1988**, *25*, 394–400.
[153] Hope, W. C.; Patel, B. J.; Fiedler-Nagy, C.; Wittreich, B. H. Retinoids inhibit Phospholipase A_2 in human synovial fluid and arachidonic acid release from rat peritoneal macrophages. *Inflammation* **1990**, *14*, 543–559.

[154] Peters, G. H.; Dahmen-Levison, U.; de Meijere, K.; Brezesinski, G.; Toxvaerd, S.; Svendsen, A.; Kinnunen, P. K. J. Influence of surface properties of mixed monolayers on lipolytic hydrolysis. *Langmuir* **2000**, *16*, 2779–2788.
[155] Newton, D. L.; Henderson, W. R.; Sporn, M. B. Structure-Activity Relationships of Retinoids in Hamster Tracheal Organ Culture. *Cancer Res.* **1980**, *40*, 3413–3425.
[156] Um, S. J.; Kwon, Y. J.; Han, H. S.; Park, S. H.; Park, M. S.; Rho, Y. S.; Sin, H. S. Synthesis and Biological Activity of Novel Retinamide and Retinoate Derivatives. *Chem. Pharm. Bull.* **2004**, *52*, 501–506.
[157] Gediya, L. K.; Khandelwal, A.; Patel, J.; Belosay, A.; Sabnis, G.; Mehta, J.; Purushottamachar, P.; Njar, V. C. O. Design, Synthesis, and Evaluation of Novel Mutual Prodrugs (Hybrid Drugs) of All-*trans*-Retinoic Acid and Histone Deacetylase Inhibitors with Enhanced Anticancer Activities in Breast and Prostate Cancer Cells in Vitro. *J. Med. Chem.* **2008**, *51*, 3895–3904.
[158] Ulukaya, E.; Wood, E. J. Fenretinide and its relation to cancer. *Cancer Treat. Rev.* **1999**, *25*, 229–235.
[159] Camacho, L. H. Clinical applications of retinoids in cancer medicine. *J. Biol. Regul. Homeost Agents* **2003**, *17*, 98–114.
[160] Maden, M. Retinoic Acid in the Development, Regeneration and Maintenance of the Nervous System. *Nat. Rev. Neurosci* **2007**, *8*, 755–765.
[161] Swift, C. B.; Hays, J. L.; Petty, J. W. Distinct Functions of Retinoic Acid Receptor Beta Isoforms: Implications for Targeted Therapy. *Endocr., Metab. Immune Disord.: Drug Targets* **2008**, *8*, 47–50.
[162] Zhuang, Y.; Faria, T. N.; Chambon, P.; Gudas, L. J. Identification and characterization of retinoic acid receptor beta2 target genes in F9 teratocarcinoma cells. *Mol. Cancer Res.* **2003**, *1*, 619–630.
[163] Piu, F.; Gauthier, N. K.; Olsson, R.; Currier, E. A.; Lund, B. W.; Croston, G. E.; Hacksell, U.; Brann, M. R. Identification of novel subtype selective RAR agonists. *Biochem. Pharmacol.* **2005**, *71*, 156–162.
[164] Lund, B. W.; Piu, F.; Gauthier, N. K.; Eeg, A.; Currier, E.; Sherbukhin, V.; Brann, M. R.; Hacksell, U.; Olsson, R. Discovery of a Potent, Orally Available and Isoform-Selective Retinoic Acid β2 Receptor Agonist. *J. Med. Chem.* **2005**, *48*, 7517–7519.
[165] Lund, B. W.; Knapp, A. E.; Piu, F.; Gauthier, N. K.; Begtrup, M.; Hacksell, U.; Olsson, R. Design, Synthesis, and Structure-Activity Analysis of Isoform-Selective Retinoic Acid Receptor β Ligands. *J. Med. Chem.* **2009**, *52*, 1540–1545.
[166] Hsieh, C. C.; Yen, M. H.; Liu, H. W.; Lau, Y. T. Lysophosphatidylcholine induces apoptotic and non-apoptotic death in vascular smooth muscle cells: in comparison with oxidized LDL. *Atherosclerosis* **2000**, *151*, 481–491.
[167] Masamune, A.; Sakai, Y.; Satoh, A.; Fujita, M.; Yoshida, M.; Shimosegawa, T. Lysophosphatidylcholine induces apoptosis in AR42J cells. *Pancreas* **2001**, *22*, 75–83.
[168] Kogure, K.; Nakashima, S.; Tsuchie, A.; Tokumura, A.; Fukuzawa, K. Temporary membrane distortion of vascular smooth muscle cells is responsible for their apoptosis

induced by platelet-activating factor-like oxidized phospholipids and their degradation product, lysophosphatidylcholine. *Chem. Phys. Lipids* **2003**, *126*, 29–38.
[169] Kaul, R.; Brouillette, Y.; Sajjadi, Z.; Hansford, K. A.; Lubell, W. D. Selective *tert*-Butyl Ester Deprotection in the Presence of Acid Labile Protection Groups with $ZnBr_2$. *J. Org. Chem.* **2004**, *69*, 6131–6133.
[170] Borgulya, J.; Bernauer, K. Transformation of Carboxylic Acid *t*-Butyl Esters into the Corresponding Trimethylsilyl Esters or Free Acids under Non-Acidic Conditions. *Synthesis* **1980**, 545–547.
[171] Sinha, N. D.; Biernat, J.; McManus, J.; Koster, H. Polymer support oligonucleotide synthesis: 18: Use of (β-cyanoethyl-*N*,*N*-dialkylamino-/*N*-morpholino phosphoramidite of deoxynucleosides for the synthesis of DNA fragments simplifying deprotection and isolation of the final product. *Nucleic Acids Res.* **1984**, *12*, 4539–4557.
[172] Kolb, H. C.; VanNieuwenhze, M. S.; Sharpless, K. B. Catalytic Asymmetric Dihydroxylation. *Chem. Rev.* **1994**, *94*, 2483–2547.
[173] Corey, E. J.; Guzman-Perez, A.; Noe, M. C. The Application of a Mechanistic Model Leads to the Extension of the Sharpless Asymmetric Dihydroxylation to Allylic 4-Methoxybenzoates and Conformationally Related Amine and Homoallylic Alcohol Derivatives. *J. Am. Chem. Soc.* **1995**, *117*, 10805–10816.
[174] Pedersen, P. J.; Adolph, S. K.; Subramanian, A. K.; Arouri, A.; Andresen, T. L.; Mouritsen, O. G.; Madsen, R.; Madsen, M. W.; Peters, G. H.; Clausen, M. H. Liposomal Formulation of Retinoids Designed for Enzyme Triggered Release. *J. Med. Chem.* **2010**, *53*, 3782–3792.
[175] Cunningham, T. J.; Maciejewski, J.; Yao, L. Inhibition of secreted phospholipase A_2 by neuron survival and anti-inflammatory peptide CHEC-9. *J Neuroinflammation* **2006**, *3*, 25.
[176] Nicke, B.; Kaiser, A.; Wiedernmann, B.; Riecken, E. O.; Rosewicz, S. Retinoic Acid Receptor α Mediates Growth Inhibition by Retinoids in Human Colon Carcinoma HT29 Cells. *Biochem. Biophys. Res. Commun.* **1999**, *261*, 572–577.
[177] KamaI-Eldin, A.; Appelqvist, L. The Chemistry and Antioxidant Properties of Tocopherols and Tocotrienols. *Lipids* **1996**, *31*, 671–701.
[178] Constantinou, C.; Papas, A.; Constantinou, A. I. Vitamin E and cancer: An insight into the anticancer activities of vitamin E isomers and analogs. *Int. J. Cancer* **2008**, *123*, 739–752.
[179] Neuzil, J.; Zhao, M.; Ostermann, G.; Sticha, M.; Gellert, N.; Weber, C.; Eaton, J. W.; Brunk, U. T. α-Tocopheryl succinate, an agent with *in vivo* anti-tumour activity, induces apoptosis by causing lysosomal instability. *Biochem. J.* **2002**, *362*, 709–715.
[180] Kumar, S. A.; Pedersen, P. J.; Andresen, T. L.; Madsen, R.; Clausen, M. H.; Peters, G. H. A Unique Water In-take Mechanism Observed in Secretory Phospholipase A_2. *J. Am. Chem. Soc*. submitted.
[181] Chandra, V.; Jasto, J.; Kaur, P.; Betzel, C.; Srinivasan, A.; Singh, T. P. First Structural Evidence of a Specific Inhibition of Phospholipase A_2 by α-Tocopherol (Vitamin E) and its

Implications in Inflammation: Crystal Structure of the Complex Formed Between Phospholipase A_2 and α-Tocopherol at 1.8 Å Resolution. *J. Mol. Biol.* **2002**, *320*, 215–222.
[182] von Euler, U. S. Über die spezifishe blutdrucksenkende Substanz des menschlichen Prostata- und Samenblased sekrets. *Wien. Klin. Wochenschr.* **1935**, *14*, 1182–1183.
[183] Goldblatt, M. W. Properties of Human Seminal Plasma. *J. Physiol.* **1935**, *84*, 208–218.
[184] Smith, W. L.; Marnett, L. J.; DeWitt, D. L. Prostaglandin and Thromboxane Biosynthesis. *Pharmac. Ther.* **1991**, *49*, 153–179.
[185] Straus, D. S.; Glass, C. K. Cyclopentenone Prostaglandins: New Insights on Biological Activities and Cellular Targets. *Med. Res. Rev.* **2001**, *21*, 185–210.
[186] Miller, S. B. Prostaglandins in Health and Disease: An Overview. *Semin. Arthritis Rheu.* **2006**, *36*, 37–49.
[187] Sasaki, H.; Fukushima, M. Prostaglandins in the treatment of cancer. *Anti-Cancer Drugs* **1994**, *5*, 131–138.
[188] Deeb, K. K.; Trump, D. L.; Johnson, C. S. Vitamin D signalling pathways in cancer: potential for anticancer therapeutics. *Nat. Rev. Cancer* **2007**, *7*, 684–700.
[189] Eisman, J. A.; Barkla, D. H.; Tutton, P. J. M. Suppression of *in Vivo* Growth of Human Cancer Solid Tumor Xenografts by 1,25-Dihydroxyvitamin D_3. *Cancer Res.* **1987**, *47*, 21–25.
[190] Yamada, S.; Shimizu, M.; Yamamoto, K. Structure-Function Relationships of Vitamin D Including Ligand Recognition by the Vitamin D receptor. *Med. Res. Rev.* **2003**, *23*, 89–115.
[191] Initial studies in Associate Professor M. H. Clausen's group have shown that carbonates are hydrolyzed by $sPLA_2$. Unpublished results.
[192] Wang, B.; Zhang, H.; Zheng, A.; Wang, W. Coumarin-based Prodrugs. Part 3: Structural Effects on the Release Kinetics of Esterase-sensitive Prodrugs of Amines. *Bioorg. Med. Chem.* **1998**, *6*, 417–426.
[193] Blæhr, L. K. A.; Björkling, F.; Binderupa, E.; Calverley, M. J.; Kaastrup, P. Polyclonal antibodies to EB1089 (seocalcitol), an analog of 1α,25-dihydroxyvitamin D_3. *Steroids* 2001, *66*, 539–548.
[194] Wing, R. M.; Okamura, W. H.; Rego, A.; Pirio, M. R.; Norman, A. W. Studies on Vitamin D and Its Analogs. VII. Solution Conformations of Vitamin D_3 and 1α,25-Dihydroxyvitamin D_3 by High-Resolution Proton Magnetic Resonance Spectroscopy. *J. Am. Chem. Soc.* **1975**, *97*, 4980–4985.
[195] Helmer, B.; Schnoes, H.; DeLuca, H. K. ^{1}H Nuclear Magnetic Resonance Studies of the Conformations of Vitamin D Compounds in Various Solvents. *Arch. Biochem. Biophys.* **1985**, *241*, 608–615.
[196] Okamura, W. H.; Zhu, G.; Hill, D. K.; Thomas, R. J.; Ringe, K.; Borchardt, D. B.; Norman, A. W.; Mueller, L. J. Synthesis and NMR Studies on ^{13}C-Labeled Vitamin D Metabolites. *J. Org. Chem.* **2002**, *67*, 1637–1650.
[197] Fischer, E.; Speier, A. Darstellung der Ester. *Chemische Berichte* **1895**, *28*, 3252–3258.

[198] Fleming, I.; Leslie, C. P. Stereocontrol of stereogenic centres *para* on a benzene ring using the S_E2" reaction of a pentadienylsilane. *J. Chem. Soc., Perkin Trans. 1*, **1996**, 1197–1204.
[199] Moffat, A.; Hunt, H. The Effect of Substituents upon the Rates of Hydrolysis of Fluorinated Esters. *J. Am. Chem. Soc.* **1957**, *79*, 54–56.
[200] Yang, Z.; Burton, D. J. Nickel-Catalyzed Reaction of Iododifluoroacetates with Alkenes and Zinc: A Novel and Practical Route to α,α-Difluoro-Functionalized Esters and α,α,ω,ω-Tetrafluoro Diesters. *J. Org. Chem.* **1992**, *57*, 5144–5149.
[201] Zou, X.; Wu, F.; Shen, Y.; Xu, S.; Huang, W. Synthesis of polyfluoroalkyl-γ-lactones from polyfluoroalkyl halides and 4-pentenoic acids. *Tetrahedron* **2003**, *59*, 2555–2560.
[202] Yang, X.; Wang, Z.; Zhu, Y.; Fang, X.; Yang, X.; Wu, F.; Shen, Y. Fluoroalkylation of pent-4-en-1-ols initiated by sodium dithionite to synthesize fluorine-containing tetrahydrofuran derivatives. *J. Fluorine Chem.* **2007**, *128*, 1046–1051.
[203] Inanaga, J.; Hirata, K.; Saeki, H.; Katsuki, T.; Yamaguchi, M. A Rapid Esterification by Means of Mixed Anhydride and Its Application to Large-ring Lactonization. *Bull. Chem. Soc. Jpn.* **1979**, *52*, 1989–1993.
[204] Jackson, R. W. A mild and selective method for the cleavage of tert-butyl esters. *Tetrahedron Lett.* **2001**, *42*, 5163–5165.
[205] Alezra, V.; Bouchet, C.; Micouin, L.; Bonin, M.; Husson, H. Fast ester cleavage of sterically hindered α- and β-aminoesters under non-aqueous conditions. Application to the kinetic resolution of aziridine. *Tetrahedron Lett.* **2000**, *41*, 655–658.
[206] Arbour, N. C.; Ross, T. K.; Zierold, C.; Prahl, J. M.; DeLuca, H. F. Highly Sensitive Method for Large-Scale Measurements of 1,25-Dihydroxyvitamin D. *Anal. Biochem.* **1998**, *255*, 148–154.
[207] Geurts van Kassel, W. S. M.; Hax, W. M. A.; Demel, R. A.; de Gier, J. High Performance Liquid Chromatographic Separation and Direct Ultraviolet Detection of Phospholipids. *Biochim. Biophys. Acta* **1977**, *486*, 524–530.
[208] Rivnay, B. Combined Analysis of Phospholipids by High-Performance Liquid Chromatography and Thin-Layer Chromatography. *J. Chromatogr.* **1984**, *294*, 303–315.
[209] Aho, V. V.; Holopainen, J. M.; Tervo, T.; Moilanen, J. A. O.; Nevalainen, T.; Saari, K. M. Group IIA phospholipase A_2 content in tears of patients having photorefractive keratectomy. *J. Cataract Refract. Surg.* **2003**, *29*, 2163–2167.
[210] Aho, V. V.; Nevalainen, T. J.; Saari, K. M. Group IIA phospholipase A_2 content of basal, nonstimulated and reflex tears. *Curr. Eye Res.* **2002**, *24*, 224–227.
[211] Saari, K. M.; Aho, V. V.; Paavilainen, V.; Nevalainen, T. J. Group II PLA_2 content of tears in normal subjects. *Invest. Ophthalmol. Vis. Sci.* **2001**, *42*, 318–320.
[212] Chen, P. S.; Toribara, T. Y.; Warner, H. Microdetermination of phosphorus. *Anal. Chem.* **1956**, *28*, 1756–1758.
[213] Carmichael, J.; DeGraff, W. G.; Gazdar, A. F.; Minna, J. D.; Mitchell, J. B. Evaluation of a tetrazolium-based semiautomated colorimetric assay: assessment of chemosensitivity testing. *Cancer Res.* **1987**, *47*, 936–942.

[214] Hansford, K. A.; Reid, R. C.; Clark, C. I.; Tyndall, J. D. A.; Whitehouse, M. W.; Guthrie, T.; McGeary, R. P.; Schafer, K.; Martin, J. L.; Fairlie, D. P. D-Tyrosine as a chiral precusor to potent inhibitors of human nonpancreatic secretory phospholipase A_2 IIa with antiinflammatory activity. *ChemBioChem* **2003**, *4*, 181–185.
[215] Bernstein, F. C.; Koetzle, T. F.; Williams, G. J.; Meyer, E. E.; Brice, M. D.; Rodgers, J. R.; Kennard, O.; Shimanouchi, T.; Tasumi, M. Protein Data Bank - Computer-Based Archival File for Macromolecular Structures. *J. Mol. Biol.* **1977**, *112*, 535–542.
[216] Phillips, J. C.; Braun, R.; Wang, W.; Gumbart, J.; Tajkhorshid, E.; Villa, E.; Chipot, C.; Skeel, R. D.; Kale, L.; Schulten, K. Scalable molecular dynamics with NAMD. *J. Comp. Chem.* **2005**, *26*, 1781–1802.
[217] Jorgensen, W. L.; Chandrasekhar, J.; Medura, J. D.; Impey, R. W.; Klein, M. L. Comparison of simple potential models for simulating liquid water. *J. Chem. Phys.* **1983**, *79*, 926–935.
[218] Grubmüller, H., Solvate: a program to create atomic solvent models. Electronic publication: http://www.mpibpc.mpg.de/home/grubmueller/downloads/solvate/index.html; accessed 20th of May, 2010
[219] Feller, S. E.; Zhang, Y.; Pastor, R. W.; Brooks. B. R. Constant pressure molecular dynamics simulation: the Langevin piston method. *J. Chem. Phys.* **1995**, *103*, 4613–4621.
[220] Darden, T.; York, D.; Pedersen, L. Particle mesh Ewald an Nlog(n) method for Ewald sums in large systems. *J. Chem. Phys.* **1993**, *98*, 10089–10092.
[221] Humphrey, W.; Dalke, A.; Schulten, K. VMD – Visual Molecular Dynamics. *J. Molec. Graphics* **1996,** *14*, 33–38.
[222] Adams, E.; Hiegemann, M.; Duddeck, H.; Welzel, P. Five membered ring formation of 2-hydroxyalkyl malonate and acetoacetate derivatives the problem of O- versus C-alkylation. *Tetrahedron* **1990**, *46*, 5975–5992.
[223] Baylis, R. L.; Bevan, T. H.; Malkin, T. The synthesis of cephalin (phosphatidylethanolamine) and batyl, chimyl, glycol and alkyl analogues. *J. Chem. Soc.* **1958**, 2962–2966.
[224] Hirth, G.; Barner, R. Synthesis of glyceryl etherphosphatides. 1. Preparation of 1-*O*-octadecyl-2-*O*-acetyl-*sn*-glyceryl-3-phosphorylcholine (Platelet Activating Factor), of its enantiomer and of some analogous compounds. *Helv. Chim. Acta* **1982**, *65*, 1059–1084.
[225] Dumoulin, F.; Lafont, D.; Boullanger, P.; Mackenzie, G.; Mehl, G. H.; Goodby, J. W. Self-Organizing Properties of Natural and Related Synthetic Glycolipids. *J. Am. Chem. Soc.* **2002**, *124*, 13737–13748.
[226] North, E. J.; Osborne, D. A.; Bridson, P. K.; Baker, D. L.; Parrill, A. L. Autotaxin structure–activity relationships revealed through lysophosphatidylcholine analogs. *Bioorg. Med. Chem.* **2009**, *17*, 3433–3442.
[227] Xia, J.; Hui, Y. Z. The chemical synthesis of a series of ether phospholipids from D-mannitol and their properties. *Tetrahedron Asymmetry* **1997**, *8*, 3131–3142.

[228] Larock, R. C.; Leach, D. R. Organopalladium Approaches to Prostaglandins. 3. Synthesis of Bicyclic and Tricyclic 7-Oxaprostaglandin Endoperoxide Analoguesnvia Oxypalladation of Norbornadiene. *J. Org. Chem.* **1984**, *49*, 2144–2148.
[229] Dias, L. C.; de Oliveira, L. G.; Vilcachagua, J. D.; Nigsch, F. Total Synthesis of (+)-Crocacin D. *J. Org. Chem.* **2005**, *70*, 2225–2234.
[230] Isomura, S.; Wirsching, P.; Janda, K. D. An Immunotherapeutic Program for the Treatment of Nicotine Addiction: Hapten Design and Synthesis. *J. Org. Chem.* **2001,** *66,* 4115–4121.
[231] Hogg, J. H.; Ollmann, I. R.; Wetterholm, A.; Andberg, M. B.; Haeggström, J.; Samuelsson, B.; Wong, C. Probing the Activities and Mechanisms of Leukotriene A_4 Hydrolase with Synthetic Inhibitors. *Chem. Eur. J.* **1998**, *4*, 1698–1713.
[232] Gourlaouën, N.; Florentin, D.; Marquet, A. Synthesis of Protein Conjugates of 2-Carboxy-L-Arabinitol 5-Phosphate and 2-Carboxy-L-Ribitol 5-Phosphate. *J.Carbohydr. Chem.* **1998**, *17*, 1219–1238.
[233] Bartolmäs, T.; Heyn, T.; Mickeleit, M.; Fischer, A.; Reutter, W.; Danker, K. Glucosamine-glycerophospholipids That Activate Cell-Matrix Adhesion and Migration. *J. Med. Chem.* **2005**, *48*, 6750–6755.
[234] Burke, M. D.; Berger, E. M.; Schreiber, S. L. Generating Diverse Skeletons of Small Molecules Combinatorially. *Science* **2003**, *302*, 613–618.
[235] Koch, M. A.; Schuffenhauer, A.; Scheck, M.; Wetzel, S.; Casaulta, M.; Odermatt, A.; Ertl, P.; Waldmann, H. Charting biologically relevant chemical space: A structural classification of natural products (SCONP). *Proc. Natl. Acad. Sci., USA* **2005**, *102*, 17272–17277.
[236] Cordier, C.; Morton, D.; Murrison, S.; Nelson, A.; O´'Leary-Steele, C. Natural products as an inspiration in the diversity-oriented synthesis of bioactive compound libraries**.** *Nat. Prod. Rep.* **2008**, *25*, 719–737.
[237] Nielsen, T. E.; Schreiber, S. L. Towards the Optimal Screening Collection: A Synthesis Strategy. *Angew. Chem. Int. Ed.* **2008**, *47*, 48–56.
[238] Burke, M. D.; Schreiber, S. L. A Planning Strategy for Diversity-Oriented Synthesis. *Angew. Chem. Int. Ed.* **2004**, *43*, 46–58.
[239] Burke, M. D.; Berger, E. M.; Schreiber, S. L. A Synthesis Strategy Yielding Skeletally Diverse Small Molecules Combinatorially. *J. Am. Chem. Soc.* **2004**, *126*, 14095–14104.
[240] Spiegel, D. A.; Schroeder, F. C.; Duvall, J. R.; Schreiber, S. L. An Oligomer-Based Approach to Skeletal Diversity in Small-Molecule Synthesis. *J. Am. Chem. Soc.* **2006**, *128*, 14766–14767.
[241] Thomas, G. L.; Spandl, R. J.; Glansdorp, F. G.; Welch, M.; Bender, A.; Cockfield, J.; Lindsay, J. A.; Bryant, C.; Brown, D. F. J.; Loiseleur, D.; Rudyk, H.; Ladlow, M.; Spring, D. R. Anti-MRSA Agent Discovery Using Diversity-Oriented Synthesis. *Angew. Chem. Int. Ed.* **2008**, *47*, 2808–2812.
[242] Oguri, H.; Schreiber, S. L. Skeletal Diversity via a Folding Pathway: Synthesis of Indole Alkaloid-Like Skeletons. *Org. Lett.* **2005**, *7*, 47–50.

[243] Kumagai, N.; Muncipinto, G.; Schreiber, S. L. Short Synthesis of Skeletally and Stereochemically Diverse Small Molecules by Coupling Petasis Condensation Reactions to Cyclization Reactions. *Angew. Chem., Int. Ed.* **2006**, *45*, 3635–3638.
[244] Lipkus, A. H.; Yuan, Q.; Lucas, K. A.; Funk, S. A.; Bartelt III, W. F.; Schenck, R. J.; Trippe, A. J. Structural Diversity of Organic Chemistry. A Scaffold Analysis of the CAS Registry. *J. Org. Chem.* **2008**, *73*, 4443–4451.
[245] Morton, D.; Leach, S.; Cordier, C.; Warriner, S.; Nelson, A. Synthesis of Natural-Product-Like Molecules with Over Eighty Distinct Scaffolds. *Angew. Chem. Int. Ed.* **2009**, *48*, 104–109.
[246] Leach, S. G.; Cordier, C. J.; Morton, D.; McKierman, G. J.; Warriner, S.; Nelson, A. A Fluorous-Tagged Linker from Which Small Molecules Are Released by Ring-Closing Metathesis. *J. Org. Chem.* **2008**, *73*, 2753–2759.
[247] Curran, D. P.; Luo, Z. Fluorous Synthesis with Fewer Fluorines (Light Fluorous Synthesis): Separation of Tagged from Untagged Products by Solid-Phase Extraction with Fluorous Reverse-Phase Silica Gel. *J. Am. Chem. Soc.* **1999**. *121*, 9069–9072.
[248] Schreiber, S. L. Molecular diversity by design. *Nature* **2009**, *457*, 153–154.
[249] Waldman, H. Killing 84 birds with one stone. *Nat. Chem. Biol.* **2009**, *5*, 76–77.
[250] Galloway, W. R. J. D.; Diáz-Gavilán, M.; Isidro-Llobet, A.; Spring, D. R. Synthesis of Unpresedented Scaffold Diversity. *Angew. Chem. Int. Ed.* **2009**, *48*, 2–5.
[251] Fukuyama, T.; Jow, C.-H.; Cheung, M. 2- and 2-Nitrobenzenesulfonamides: Exceptionally Versatile Means for Preparation of Secondary Amines and Protection of Amines. *Tetrahedron Lett.* **1995**, *36*, 6373–6374.
[252] Kan, T.; Fukuyama, T. Ns Strategies: a highly versatile synthetic method for amines. *Chem. Commun.* **2004**, 353–359.
[253] Guisado, C.; Waterhouse, J. E.; Price, W. S.; Jorgensen, M. R.; Miller, A. D. The facile preparation of primary and secondary amines via an improved Fukuyama-Mitsunobu procedure. Application to the synthesis of a lung-targeted gene delivery agent. *Org. Biomol. Chem.* **2005**, *3*, 1049–1057.
[254] Zhang, W.; Lu, Y.; Nagashima, T. Plate-to-Plate Fluorous Solid-Phase Extraction for Solution-Phase Parallel Synthesis. *J. Comb. Chem.* **2005**, *7*, 893–897.
[255] Zhang, W.; Lu, Y. 96 Well Plate-to-Plate Gravity Fluorous Solid-Phase Extraction (F-SPE) for Solution-Phase Library Purification. *J. Comb. Chem.* **2007**, *9*, 836–843.
[256] Zhang, W.; Lu, Y. Automation of Fluorous Solid-Phase Extraction for Parallel Synthesis. *J. Comb. Chem.* **2006**, *8*, 890–896.
[257] Carrel, F. R.; Seeberger, P. H. Cap-and-Tag Solid Phase Oligosaccharide Synthesis. *J. Org. Chem.* **2008**, *73*, 2058–2065.
[258] Cordier, C.; Morton, D.; Leach, S.; Woodhall, T.; O'Leary-Steele, C.; Warriner, S.; Nelson, A. An efficient method for synthesising unsymmetrical silaketals: substrates for ring-closing, including macrocycle-closing, metathesis. *Org. Biomol. Chem.* **2008**, *6*, 1734–1737.

[259] Fukuyama, T.; Cheung, M.; Kan, T. *N*-Carboalkoxy-2-Nitrobenzenesulfonamides: A Pratical Preparation of *N*-Boc, *N*-Alloc, and *N*-Cbz-Protected Primary Amines. *Synlett* **1999**, *8*, 1301–1303.

[260] Rawal, V. H.; Jones, R. J.; Cava, M. P. Photocyclization Strategy for the Synthesis of Antitumor Agent CC-1065: Synthesis of Dideoxy PDE-I and PDE-11. Synthesis of Thiophene and Furan Analogues of Dideoxy PDE-I and PDE-II. *J. Org. Chem.* **1987**, *52*, 19–28.

[261] Tamura, M.; Kochi, J. Coupling of Grinard Reagents with Organic Halides. *Synthesis* **1971**, *93*, 303–305.

[262] Tamura, M.; Kochi, J. Coupling of Grinard Reagents and Alkyl Halides in THF. *J. Organometal. Chem.* **1972**, *42*, 205–228.

[263] Ciolli,C. J.; Kalagher, S.; Belshaw, P. J. TRAM Linker: A Safety-Catch Linker for the Traceless Release of Acrylamides. *Org. Lett.* **2004**, *12*, 1891–1894.

[264] Fürstner, A. Recent advancements in ring closing olefin metathesis. *Top. Catal.* **1997**, *4*, 285–299.

[265] Madsen, R. Synthetic Strategies for Converting Carbohydrates into Carbocycles by the Use of Olefin Metathesis. *Eur. J. Org. Chem.* **2007**, 399–415.

[266] Schrock, R. R. Multiple Metal-Carbon Bonds for Catalytic Metathesis Reactions (Nobel Lecture 2005). *Adv. Synth. Catal.* **2007**, *349*, 41–53.

[267] Schwab, P.; France, M. B.; Ziller, J. W.; Grubbs, R. H. A Series of Well-Defined Metathesis Catalysts - Synthesis of ($RuCl_2$(=CHR')-(PR_3)$_2$) and Its Reactions. *Angew. Chem. Int. Ed.* **1995**, *34*, 2039–2041.

[268] Garber, S. B.; Kingsbury, J. S.; Gray, B. L.; Hoveyda, A. H. Efficient and Recyclable Monomeric and Dendritic Ru-Based Metathesis Catalysts. *J. Am. Chem. Soc.* **2000**, *122*, 8168–8179.

[269] Crimmins, M. T.; King, B. W. Asymmetric Total Synthesis of Callystatin A: Asymmetric Aldol Additions with Titanium Enolates of Acyloxazolidinethiones. *J. Am. Chem. Soc.* **1998**, *120*, 9084–9085.

[270] Gaul, C.; Njardarson, J. T.; Danishefsky, S. J. The Total Synthesis of (+)-Migrastatin. *J. Am. Chem. Soc.* **2003**, *125*, 6042–6043.

[271] Hansen, F. G.; Madsen, R. A Short Synthesis of (+)-Cyclophellitol. *J. Org. Chem.* **2005**, *70*, 10139–10142.

[272] Maynard, H. D.; Grubbs. R. H. Purification Technique for the Removal of Ruthenium from Olefin Metathesis Reaction Products. *Tetrahedron Lett.* **1999**, *40*, 4137–4140.

[273] Ulman, M.; Grubbs, R. H. Relative Reaction Rates of Olefin Substrates with Ruthenium(II) Carbene Metathesis Initiators. *Organometallics* **1998**, *17*, 2484–2489.

[274] Lloyd-Jones, G. C.; Margue, R. G., de Vries, J. G Rate Enhancement by Ethylene in the Ru-Catalyzed Ring-Closing Metathesis of Enynes: Evidence for an “Ene-then-Yne” Pathway that Diverts through a Second Catalytic Cycle. *Angew. Chem. Int. Ed.* **2005**, *44*, 7442 –7447.

[275] Sashuk, V.; Grela, K. Synthetic and mechanistic studies on enyne metathesis: A catalyst influence. *J. Mol. Catal. A-Chem* **2006**, *257*, 59–66.
[276] Cookson, R. C.; Gilani, S. S. H.; Stevens, I. D. R. 4-Phenyl-1,2,4-triazolin-3,5-dione: a powerful dienophile. *Tetrahedron Lett.* **1962**, *3*, 615–618.
[277] Virolleaud, M. A.; Piva, O. Tandem Sequential Ring-Closing Metathesis/Diels–Alder/Cross-Metathesis: Formation of Polycyclic Compounds by a New Three-Component Reaction. *Eur. J. Org. Chem.* **2007**, 1606–1612.
[278] O'Leary-Steele, C.; Cordier, C.; Hayes, J.; Warriner, S.; Nelson, A. A Fluorous-Tagged "Safety Catch" Linker for Preparing Heterocycles by Ring-Closing Metathesis. *Org. Lett.* **2009**, *11*, 915–918.
[279] Hakoki, T.; Taichi, M.; Katsumura, S. Synthesis of a Nitrogen Analogue of Sphingomyelin as a Sphingomyelinase Inhibitor. *Org. Lett.* **2003**, *5*, 2801–2804.
[280] Bemis, G. W.; Murcko, M. A. The Properties of Known Drugs. 1. Molecular Frameworks. *J. Med. Chem.* **1996**, 39*,* 2887–2893.
[281] Firestone, R. A.; Pisano, J. M.; Bailey, P. J.; Sturm, A.; Bonney, R. J.; Wightman, P.; Devlin, R.; Lin, C. S.; Keller, D. L.; Tway, P. C. Lysosomotropic agents. 4. Carbobenzoxyglycylphenylalanyl, a new protease-sensitive masking group for introduction into cells. *J. Med. Chem.* **1982**, *25*, 539–544.

Appendix

Pedersen, P. J.; Christensen, M. S.; Ruysschaert, T.; Linderoth, L.; Andresen, T. L.; Melander, F.; Mouritsen, O. G.; Madsen, R.; Clausen, M. H. Synthesis and Biophysical Characterization of Chlorambucil Anticancer Ether Lipid Prodrugs. *J. Med. Chem.* **2009**, *52*, 3408–3415.

Pedersen, P. J.; Adolph, S. K.; Subramanian, A. K.; Arouri, A.; Andresen, T. L.; Mouritsen, O. G.; Madsen, R.; Madsen, M. W.; Peters, G. H.; Clausen, M. H. Liposomal Formulation of Retinoids Designed for Enzyme Triggered Release. *J. Med. Chem.* **2010**, 53, 3782–3792.

Synthesis and Biophysical Characterization of Chlorambucil Anticancer Ether Lipid Prodrugs

Palle J. Pedersen,[†] Mikkel S. Christensen,[†] Tristan Ruysschaert,[‡] Lars Linderoth,[†] Thomas L. Andresen,[§] Fredrik Melander,[||] Ole G. Mouritsen,[‡] Robert Madsen,[†] and Mads H. Clausen*,[†]

Department of Chemistry, Technical University of Denmark, Kemitorvet, Building 201, DK-2800 Kgs. Lyngby, Denmark, Department of Physics and Chemistry, MEMPHYS—Center for Biomembrane Physics, University of Southern Denmark, Campusvej 55, DK-5230 Odense M, Denmark, Department of Micro- and Nanotechnology, Technical University of Denmark, DK-4000 Roskilde, Denmark, and LiPlasome Pharma A/S, Technical University of Denmark, Kemitorvet, Building 207, DK-2800 Kgs. Lyngby, Denmark

Received September 11, 2008

The synthesis and biophysical characterization of four prodrug ether phospholipid conjugates are described. The lipids are prepared from the anticancer drug chlorambucil and have C16 and C18 ether chains with phosphatidylcholine or phosphatidylglycerol headgroups. All four prodrugs have the ability to form unilamellar liposomes (86−125 nm) and are hydrolyzed by phospholipase A_2, resulting in chlorambucil release. Liposomal formulations of prodrug lipids displayed cytotoxicity toward HT-29, MT-3, and ES-2 cancer cell lines in the presence of phospholipase A_2, with IC_{50} values in the 8−36 μM range.

Introduction

Ever since Gregoriadis et al.[1] suggested liposomes as drug carriers in 1974, serious efforts have been put into the development of liposomes as efficient drug delivery systems for the treatment of cancer. The discovery that liposomes accumulate to a high degree in tumor tissue[2] if their surface is covered with poly(ethylene glycol) was a major improvement over earlier formulations and made these nanoparticles applicable as drug carriers of chemotherapeutics to tumor tissue. Such liposomal drug delivery systems based on the enhanced permeation and retention (EPR[a]) effect were utilized in the commercially successful liposomal formulation of doxorubicin. However, it is now apparent that this formulation is not generally useful for the majority of potentially interesting drug candidates because of the lack of a controlled drug release.[3] An optimal drug delivery formulation should be able to retain and stabilize the carried drug during blood circulation and effectively release the drug in the target tissue.[3] This calls for the utilization of site specific release mechanisms, and several have been investigated, e.g., enzymatic release[4] and pH,[5] light,[6] and heat sensitive liposomes.[7]

Liposomal drug delivery has mainly relied on the encapsulation of hydrophilic drugs in the aqueous core[3,8] or on trapping hydrophobic molecules in the lipid bilayer.[9] Although this approach is successful, it does suffer from some limitations such as the potential for leakage and the fact that the release of the active drug is not directly coupled to the mechanism activating the carrier. One strategy that addresses both these issues is the formulation of a lipid−prodrug conjugate that is susceptible to selective degradation by endogenous enzymes in the target tissue, serving to simultaneously degrade the carrier and release the drug.[3] By covalent incorporation of the active chemotherapeutic agent in the delivery system, the problem with premature leakage is effectively circumvented. Herein, we describe the synthesis and characterization of prodrugs (**1** and **2**, Figure 1) that are suitable for liposomal delivery to cancerous tissue and susceptible to secretory phospholipase A_2 activation.

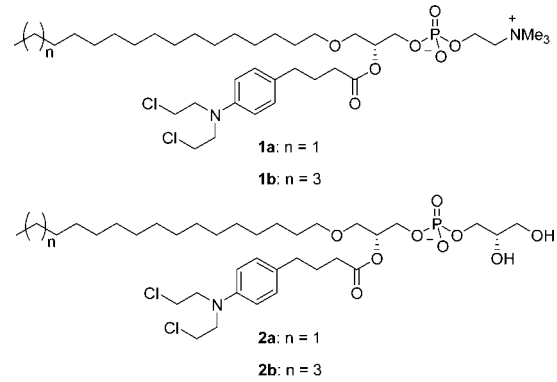

Figure 1. Four target chlorambucil prodrug ether lipids. Prodrugs **1a** and **1b** have a phosphatidylcholine headgroup with a C16 and a C18 ether chain, respectively. Target compounds **2a** and **2b** have the negatively charged phosphatidylglycerol headgroup.

Secretory phospholipase A_2 ($sPLA_2$) is overexpressed in cancer tissue,[10] and has previously been exploited in liposomal drug delivery.[11] Subtype $sPLA_2$ IIA has been identified in several human tumors including breast,[12] stomach,[13] colorectal,[14] pancreatic,[15] prostate,[10a,16] and liver cancer.[17] The prodrugs are based on covalently attaching an anticancer drug in the *sn*-2 position of *sn*-1 ether phospholipids. The principle is illustrated in Figure 2: $sPLA_2$ will hydrolyze the *sn*-2 ester bond, releasing both the anticancer drug bound to the *sn*-2 position and an anticancer ether lipid (AEL). Ether lipids were chosen because of their higher stability and because of the cytotoxicity of the lyso-lipids released upon $sPLA_2$ hydrolysis.[11] Furthermore, the lyso-ether lipids have potential to attenuate the toxicity of chlorambucil by increasing the cellular uptake of the drug,[3] and thus, the two molecules released by $sPLA_2$ hydrolysis will work in unison against cancer cells.

It is crucial for the prodrug strategy that suitable drug candidates are available. Since the incorporated drug will be part of the lipophilic membrane, a hydrophobic nature is an

* To whom correspondence should be addressed. Phone: +45 45252131. Fax: +45 45933968. E-mail: mhc@kemi.dtu.dk.
[†] Department of Chemistry, Technical University of Denmark.
[‡] University of Southern Denmark.
[§] Department of Micro- and Nanotechnology, Technical University of Denmark.
[||] LiPlasome Pharma A/S, Technical University of Denmark.

[a] Abbrevations: EPR, enhanced permeation and retention; $sPLA_2$, secretory phospholipase A_2; AEL, anticancer ether lipid; PMB, *p*-methoxybenzyl; DDQ, 2,3-dichloro-5,6-dicyano-1,4-benzoquinone; DBU, 1,8-diazabicyclo-[5.4.0]undec-7-ene; DLS, dynamic light scattering; SUV, small unilaminar vesicles.

10.1021/jm900091h CCC: $40.75
Published on Web 04/29/2009

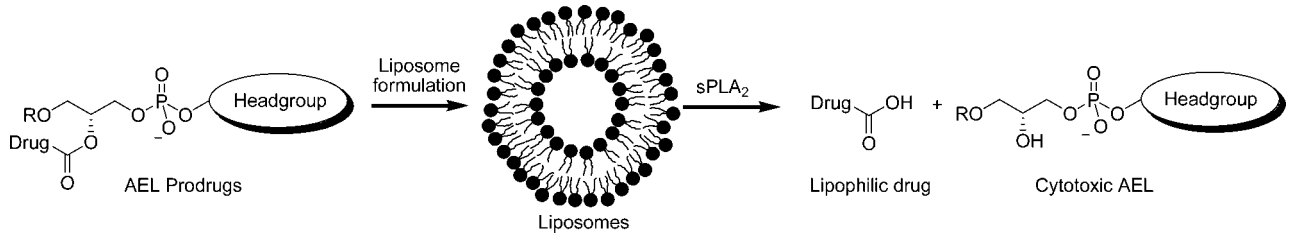

Figure 2. Schematic overview of the drug delivery concept. The AEL prodrugs are formulated as liposomes. Because of the EPR effect, the liposomes will accumulate in cancer tissues and sPLA2, which is up-regulated in cancer tissue, will hydrolyze the AEL prodrug lipids, releasing two anticancer drugs.

Scheme 1. Synthesis of Lipid Precursors **6a** and **6b**[a]

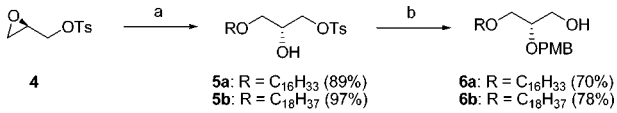

4 **5a**: R = $C_{16}H_{33}$ (89%) **5b**: R = $C_{18}H_{37}$ (97%) **6a**: R = $C_{16}H_{33}$ (70%) **6b**: R = $C_{18}H_{37}$ (78%)

[a] Reagents: (a) $C_{16}H_{33}OH$ or $C_{18}H_{37}OH$, $BF_3 \cdot OEt_2$, CH_2Cl_2; (b) (i) PMBTCA, $La(OTf)_3$, toluene; (ii) CsOAc, DMSO, DMF; (iii) NaOMe, MeOH.

obvious requirement and, furthermore, a carboxylic acid moiety is needed for the attachment of the drug to the AEL backbone. We have identified a number of candidates such as chlorambucil (**3**),[18] all-*trans* retinoic acid,[19] and prostaglandins.[20] In the present study prodrugs made from chlorambucil are investigated. Chlorambucil (**3**) is a chemotherapeutic agent of the mustard gas type,[21] and it was originally synthesized by Everett et al. in 1953.[18a] It is used clinically for the treatment of lymphocytic leukemia[22] typically in combination with other drugs. Chlorambucil is orally administrated but undergoes rapid metabolism, and as a result, the stability in aqueous environments is low and **3** has an elimination half-life of 1.5 h.[23] The prodrug formulation could remedy this, since this system will shield chlorambucil from degradation through the incorporation in the lipophilic part of the liposomal membrane and deliver it directly to the tumor, decreasing metabolism compared to the oral administration route. To investigate the effect of *sn*-1 ether chain length and headgroup charge on enzymatic activity, prodrugs **1** and **2** were prepared with both C16 and C18 ether chains and a choline and a glycerol phosphate headgroup, respectively. Biophysical and biological characterization of the synthesized chlorambucil prodrugs (**1**, **2**) is included, with focus on liposome formulation, particle size determination, and in particular $sPLA_2$ activity. Proof-of-principle of the strategy is demonstrated in three cancer cell lines, providing the first successful example of this prodrug approach to liposomal drug delivery.

Synthesis of Chlorambucil AEL Prodrugs

Anticancer ether lipids have previously been synthesized via different routes, e.g., starting from D-mannitol[24] or glycidols.[25] Commercially available (*R*)-glycidyl tosylate (**4**) served as our starting material, and the aliphatic ether chain was introduced by ring-opening of the epoxide under Lewis acid catalysis,[26] resulting in yields of 89% and 97% for **5a** and **5b**, respectively (Scheme 1). The *p*-methoxybenzyl (PMB) group was chosen for protection of the secondary alcohol[27] and introduced by using *p*-methoxybenzyl trichloroacetimidate with $La(OTf)_3$ catalysis.[28] The resulting tosylate was converted to the acetate with CsOAc in a 9:1 mixture of DMSO and DMF and the ester hydrolyzed with NaOMe in MeOH at 40 °C, yielding the primary alcohols **6a** and **6b** in overall yields of 70% and 78%, respectively, over three steps. It was essential to carry out the hydrolysis at elevated temperature in order to obtain homogeneous reaction mixtures and achieve full conversion in the transformations.

The choline headgroup was attached to the primary alcohols **6a** and **6b** by reaction with phosphorus oxychloride and NEt_3, followed by addition of choline tosylate, pyridine, and finally H_2O (Scheme 2).[11a,29] Excess choline tosylate was removed on an MB-3 ion-exchange column, and after purification by flash column chromatography the PMB-group was removed with 2,3-dichloro-5,6-dicyano-1,4-benzoquinone (DDQ) in an 18:1 mixture of CH_2Cl_2 and H_2O,[30] which resulted in full conversion within 3 h with isolated yields of 99% and 79%. The final attachment of chlorambucil to the lipid was achieved via a Steglich esterification with DCC and a catalytic amount of DMAP.[31] When the acylation of **7a** was performed in ethanol-free chloroform at 20 °C or CH_2Cl_2 in the temperature range from 0 °C to reflux, we did not observe any incorporation of chlorambucil, but when the conditions were changed to reflux in 1,2-dichloroethane, the acylation occurred in a 75% yield, albeit only after adding 5 equiv of chlorambucil and DCC in portions over 31 h. The acylation of **7b** led to an isolated yield of 76% in refluxing chloroform, and that was not improved by using 1,2-dichlorethane as the solvent. Changing the coupling reagents to EDCI and DMAP[32] did not improve the conversion of the AELs.

The phosphoramidite **11** needed for the installment of the glycerol headgroup was synthesized in four steps from allyl *p*-methoxybenzoate (**8**) (Scheme 3). The key step was a Sharpless asymmetric dihydroxylation[33] of **8**, which occurred with excellent enantioselectivity (97% ee, chiral HPLC, and Mosher ester analysis; see Supporting Information). TBDMS protection and reduction of the *p*-methoxybenzoate with DIBAL-H at −78 °C afforded the TBDMS-protected glycerol **10**. The coupling between **10** and the commercially available phosphorylating agent $(i\text{-Pr})_2NPClO(CH_2)_2CN$ resulted in the desired phosphoramidite **11** in a very satisfactory yield, isolated as a 1:1 diastereomeric mixture as evident from ^{31}P NMR.

The glycerol headgroup was attached to the lipid backbone (**6a** and **6b**) via reaction with **11** under activation of tetrazole and successive oxidation with ^{t}BuOOH (Scheme 4). Deprotection of the PMB-group was achieved with DDQ in moist CH_2Cl_2. Acylation with chlorambucil in CH_2Cl_2 followed by 1,8-diazabicyclo[5.4.0]undec-7-ene (DBU) mediated deprotection of the cyanoethylene group[34] afforded the lipids **12a** and **12b** in good yields over five steps. Finally, removal of the TBDMS protection groups was achieved by treatment with HF in $MeCN/H_2O$, providing **2a** and **2b**.

Biophysical and Biological Data

The chlorambucil AEL prodrugs (**1**, **2**) were formulated as liposomes by extrusion in HEPES buffer using the dry lipid film technique.[35] The lipid solutions were analyzed by dynamic

Scheme 2. Synthesis of Chlorambucil AEL Prodrugs **1**[a]

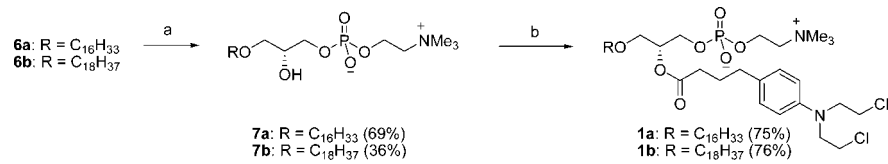

[a] Reagents: (a) (i) $POCl_3$, Et_3N, CH_2Cl_2; (ii) choline tosylate, pyridine; (iii) H_2O; (iv) DDQ, CH_2Cl_2, H_2O; (b) **3**, DCC, DMAP, $CHCl_3$ or 1,2-dichloroethane.

Scheme 3. Synthesis of the Phosphoramidite **11**[a]

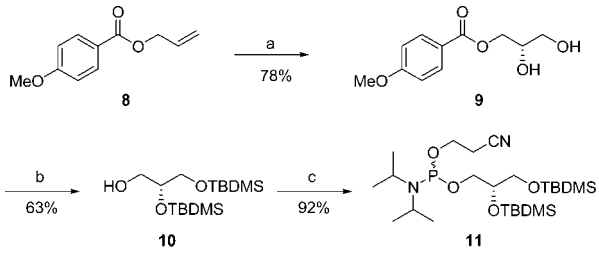

[a] Reagents: (a) $K_2OsO_4 \cdot 2H_2O$, $(DHQD)_2PHAL$, $K_3Fe(CN)_6$, K_2CO_3, ^{t}BuOH, H_2O; (b) (i) TBDMSOTf, DIPEA, CH_2Cl_2; (ii) DIBAL-H, CH_2Cl_2; (c) 2-cyanoethyl *N*,*N*-diisopropylchlorophosphoramidite, DIPEA, CH_2Cl_2.

light scattering (DLS) in order to investigate the particle size, and DLS analysis revealed that **1** and **2** form particles in the liposome size region (Table 1) and with a low polydispersity, indicating formation of small unilaminar vesicles (SUVs). Initial confirmation of enzymatic hydrolysis was obtained by treating the liposome solutions with snake (*Naja mossambica mossambica*) venom $sPLA_2$ for 24 h at 37 °C. Snake venom $sPLA_2$ is a convenient model enzyme, since it is not sensitive to the charge of the interfacial region, unlike human $sPLA_2$, but shows the same substrate specificity.[10d,36] DLS measurements of the resulting solutions confirmed that the liposomes had been degraded, as only particles with a diameter of less than 5 nm were present. Incubation of the liposomes for 24 h without enzyme did not result in a change in particle size as measured by DLS (data not shown).

In order to investigate the hydrolysis on a molecular level, we applied MALDI-TOF MS and HPLC. MALDI-TOF MS has recently been exploited as a very fast and sensitive technique for detection of lipids,[37] and we decided to study the enzyme activity with this method in order to verify that the lipids were consumed and the anticancer drugs released. Figure 3 shows the digestion of the chlorambucil AEL prodrugs **1a** and **2a** and the release of AELs catalyzed by snake (*Agkistrodon piscivorus piscivorus*) venom $sPLA_2$. The spectra show the disappearance over time of the prodrugs signals ($M + H^+$ and $M + Na^+$) and the emergence of the expected AEL signals ($M + H^+$ and $M + Na^+$). From the spectra it is also possible to get information about the conversion rate, and whereas **2a** is almost fully consumed after 2 h, **1a** needs more than 24 h for full digestion by $sPLA_2$. The MALDI-TOF MS analysis of **1b** and **2b** (see Supporting Information) revealed that full degradation is obtained in 2−6 h. These results were verified by HPLC (Figure 4 and Supporting Information). Neither HPLC nor MALDI-TOF MS was capable of detecting the released chlorambucil, but that was not surprising given the low stability of free chlorambucil in an aqueous environment.[23] Chatterji et al. report 15 min as the half-life of chlorambucil in a buffer like the HEPES buffer at 37 °C.[23b] MALDI-TOF analysis (see Supporting Information) of liposome solutions of **1b** and **2b** stored for 6 weeks at 20 °C showed that the prodrug lipids were intact. No significant hydrolysis of the chloroethyl groups of chlorambucil was detected, proving that the liposomal formulation enhances chlorambucil stability significantly. These findings were further supported by the 4-nitrobenzylpyridine alkylating assay,[38] which showed that alkylation by chlorambucil occurred when liposomes of **1b** and **2b** were subjected to $sPLA_2$, whereas no alkylation of **1b** and **2b** was detected in the absence of $sPLA_2$ (see Supporting Information).

To demonstrate the $sPLA_2$-dependent cytotoxicity of the chlorambucil AEL prodrugs, we investigated the activity of **1b** against HT-29 and MT-3 cancer cells for 24 h and **2b** against the same two cell lines in addition to ES-2 cells (Table 2). None of these cells secrete $sPLA_2$, which is an advantage in these studies because it enables us to control the presence or absence of the enzyme in each experiment. Before addition of snake (*Agkistrodon piscivorus piscivorus*) venom $sPLA_2$, all liposome formulations have IC_{50} values significantly higher than that of free chlorambucil (entries 1−3), demonstrating that cytotoxicity is associated with the prodrug activation by $sPLA_2$. Upon addition of the enzyme, both prodrugs display IC_{50} values below that of chlorambucil itself for all three tested cell lines (entries 4 and 5), suggesting a cooperative effect of the two cytotoxic compounds released, chlorambucil and AELs. The lyso-ether lipid **7b** has activity in the same range as the prodrugs with added $sPLA_2$ (compare entries 4−5 and entry 6). Earlier studies of *sn*-1 ether lipids with a fatty acid in the *sn*-2 position have shown that AEL alone is more cytotoxic than the liposome formulation,[11a] lending further support to our belief that the two active components work in unison to kill the cancer cells. Phospholipase A_2 alone has no effect on cell viability (entry 7). Taken together, the data in Table 2 clearly show the potential of this prodrug strategy for $sPLA_2$ mediated degradation of liposomes consisting of *sn*-1 ether lipids with an anticancer drug covalently bound in the *sn*-2 position.

Conclusion

In the present study we have synthesized a series of novel prodrugs and shown that they form small unilamellar vesicles that are stable in size over time. It was found that $sPLA_2$ can hydrolyze all the prodrugs of this type, showing how diverse $sPLA_2$ substrates can be, which makes $sPLA_2$ an excellent target for future prodrug strategies. The approach described here is a new application of prodrugs in liposomal formulations, and we believe it has significant advantages over conventional liposomal drug delivery system, where hydrophilic drugs are encapsulated. Problems with leakage during circulation are circumvented because of the covalent attachment of the active compound to the phospholipids. Furthermore, since the drugs are contained in the liposome membrane until activated by the enzyme, our strategy opens up for the use of lipophilic compounds that would otherwise be too toxic if employed systemically because of their affinity for biological membranes. Lastly, the use of prodrug strategies where the drug is protected in the membrane may open new possibilities with respect to drugs with low stability

Scheme 4. Synthesis of Chlorambucil AEL Prodrugs **2**[a]

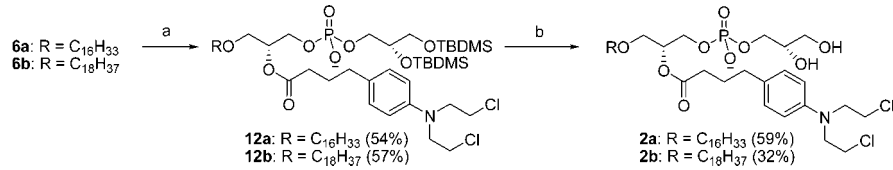

[a] Reagents: (a) (i) **11**, tetrazole, CH_2Cl_2, MeCN; (ii) ^{t}BuOOH; (iii) DDQ, CH_2Cl_2, H_2O; (iv) **3**, EDCI, DMAP, CH_2Cl_2; (v) DBU, CH_2Cl_2; (b) HF, MeCN, H_2O.

Table 1. DLS Analysis of Chlorambucil AEL Prodrugs[a]

	before $sPLA_2$ addition		after $sPLA_2$ addition, diameter (nm)
prodrug	diameter (nm)	polydispersity	
1a	124	0.12	<5
1b	125	0.22	<5
2a	104	0.08	<5
2b	113	0.05	<5

[a] Determined before and after addition of snake venom (*Naja mossambica mossambica*) $sPLA_2$.

in a biological environment, as evident from the stability of chlorambucil in the liposomal formulation.

Experimental Section

General. Starting materials, reagents, and solvents were purchased from Sigma-Aldrich Chemical Co. and used without further purification. Reactions involving air or moisture sensitive reagents were carried out under N_2, and flasks were dried by flame heating under reduced pressure. DMF, DMSO, MeCN, CH_2Cl_2, $CHCl_3$, 1,2-dichloroethane, and toluene were dried over 4 Å molecular sieves. Pyridine and NEt_3 were dried over KOH. Evaporation of solvents was done under reduced pressure (in vacuo). TLC was performed on Merck aluminum sheets precoated with silica gel 60 F_{254} plates. Compounds were visualized by charring after dipping in a solution of *p*-anisaldehyde (10 mL of H_2SO_4 and 10 mL of *p*-anisaldehyde in 200 mL of 95% EtOH), $KMnO_4$ (1.5 g of $KMnO_4$, 10 g of K_2CO_3, and 2.5 mL of 5% NaOH in 150 mL of H_2O), or Cemol (6.25 g of $(NH_4)_6Mo_7O_{24}$ and 1.5 g of $Ce(SO_4)_2$ in 250 mL of 10% aqueous H_2SO_4). Flash column chromatography was performed using Matrex 60 Å silica gel. Purity of all compounds was found to be equal to or greater than 95% by elemental analysis or HPLC (see below).

NMR spectra were recorded using a Varian Mercury 300 MHz spectrometer or a Varian Unity Inova 500 MHz spectrometer. Chemical shifts were measured in ppm and coupling constants in Hz, and the field is indicated in each case. The solvent peaks from $CDCl_3$ (7.26 ppm in ^{1}H NMR and 77.16 ppm in ^{13}C NMR) or acetone-d_6 (2.05 ppm in ^{1}H NMR) were used as standards.[39] HPLC was performed on a Waters Alliance HPLC equipped with a DAD, using a LiChrospher Si 60 column and eluting with water/isopropanol/heptane mixtures. Elemental analyses were obtained from H. Kolbe, Mikroanalytisches Laboratorium, Mülheim/Ruhr, Germany. IR analysis was carried out on a Perkin-Elmer 1600 series FTIR spectrometer, as KBr pills or neat between AgCl plates. Melting points were measured by a Buch & Holm melting point apparatus and given in degrees Celsius (°C) uncorrected. HRMS was recorded on an Ionspec Ultima Fourier transform mass spectrometer.

Liposome Preparation and Particle Size Determination. The chlorambucil AEL prodrugs were dissolved in $CHCl_3$ in a glass tube, dried under a stream of N_2, and then placed under vacuum for 3−15 h to form a thin film. The film was solubilized by addition of aqueous buffer (0.15 M NaCl, 2.5 mM HEPES, pH 7.4) and vortexed periodically over 1 h at 20 °C. Subsequently, the solutions were extruded through a 100 nm polycarbonate cutoff membrane using a Hamilton syringe extruder (Avanti Polar Lipids, Birmingham, AL), yielding unilamellar vesicles with a diameter ranging from 86 to 125 nm and with a low polydispersity as measured by DLS. The DLS measurements were obtained using a BI-200SM goniometer from Brookhaven Instruments (New York), applying a fixed scattering angle of 90° with a 632.8 nm HeNe laser.

$sPLA_2$ Activity Measurements Monitored by DLS. The chlorambucil AEL prodrugs (2 mL, 0.05 mM), formulated in an aqueous buffer (0.15 M NaCl, 5 mM $CaCl_2$, 2.5 mM HEPES, pH 7.4), were incubated at 37 °C with snake venom $sPLA_2$ from *Naja mossambica mossambica* (1.93 nmol) for 24 h. The $sPLA_2$ from *Naja mossambica mossambica* was purchased from Sigma-Aldrich Chemical Co. The resulting solutions were analyzed by DLS as described above.

$sPLA_2$ Activity Measurements Monitored by HPLC and MALDI-TOF MS. The chlorambucil AEL prodrugs (2 mM) were hydrated in an aqueous buffer (0.15 M KCl, 30 μM $CaCl_2$, 10 μM EDTA, 10 mM HEPES, pH 7.5) for 1 h at 60 °C and then sonicated for 1 h at 60 °C, providing a clear solution. The formulated chlorambucil AEL prodrugs (0.40 mL, 2 mM) were diluted in an aqueous buffer (2.1 mL, 0.15 M KCl, 30 μM $CaCl_2$, 10 μM EDTA, 10 μM HEPES, pH 7.5), and the mixture was stirred at 37 °C in a container protected from light. The catalytic reaction was initiated by addition of snake (*Agkistrodon piscivorus piscivorus*) venom $sPLA_2$ (20 μL, 42 μM). The purified snake venom $sPLA_2$ was donated by Dr. R. L. Biltonen (University of Virginia). Sampling was done after 0, 2, 6, 8, 20, 24, and 90 h by collecting 100 μL of the reaction mixture and rapidly mixing it with a solution of $CHCl_3$/MeOH/H_2O/AcOH 4:8:1:1 (0.5 mL) in order to stop the reaction. The mixture was washed with water (0.5 mL), and the organic phase was isolated by extraction. For HPLC 30−75 μL of the organic phase was injected on a 5 μm diol column and eluted with an isocratic eluent ($CHCl_3$/MeOH/H_2O 730:230:30 for **1a** and **2a**; $CHCl_3$/MeOH/25% aqueous NH_3 800:195:5 for **2a** and **2b**). An evaporative light scattering detector was used for detection. For the MALDI-TOF MS measurements 9 μL of the organic phase was mixed with 3 μL of 2,5-dihydroxybenzoic acid (DHB) matrix (0.5 M DHB, 2 mM CF_3COONa in MeOH), and 0.5 μL of this mixture was used for the MS analysis.

Cytotoxicity. Colon cancer HT-29 and ovarian cancer ES-2 cells were cultured in McCoy's 5A medium in the presence of 10% FCS and 1% Pen-Strep (InVitrogen). Breast cancer MT-3 cells were cultured in RPMI medium. Cells were plated in 96-well plates at a density of 1×10^4 cells per well 24 h prior to addition of the tested compound. Chlorambucil (**3**) was solubilized in DMSO and water (final DMSO concentration max of 0.5%). Liposomes were diluted in PBS, and initial lipid concentration in the liposome solutions was determined by phosphorus analysis.[40] After 24 h of incubation, the substances were removed and the cells were washed and incubated in complete medium for another 48 h. Cytotoxic activity was assessed using a standard 3-(4,5-dimethylthiazolyl)-2,5-diphenyltetrazolium bromide (MTT) assay (Cell Proliferation Kit I, Roche, Germany).[41] Cell viability is expressed as percentage reduction of incorporated MTT.

1-*O*-Hexadecyl-2-(4-(4-(bis-(2-chloroethyl)amino)phenyl)butanoyl)-*sn*-glycero-3-phosphocholine (1a). Compound **7a** (67 mg, 0.139 mmol) was dissolved in anhydrous 1,2-dichloroethane (3.5 mL), and the mixture was heated to reflux under an atmosphere of N_2. DMAP (10 mg, 0.082 mmol), chlorambucil (**3**) (64 mg, 0.209 mmol), and DCC (1 M in CH_2Cl_2, 0.2 mL, 0.2 mmol) were added, and after 5 and 19 h additional portions of chlorambucil (**3**) (64 mg, 0.209 mmol) and DCC (1 M in CH_2Cl_2, 0.2 mL, 0.2 mmol)

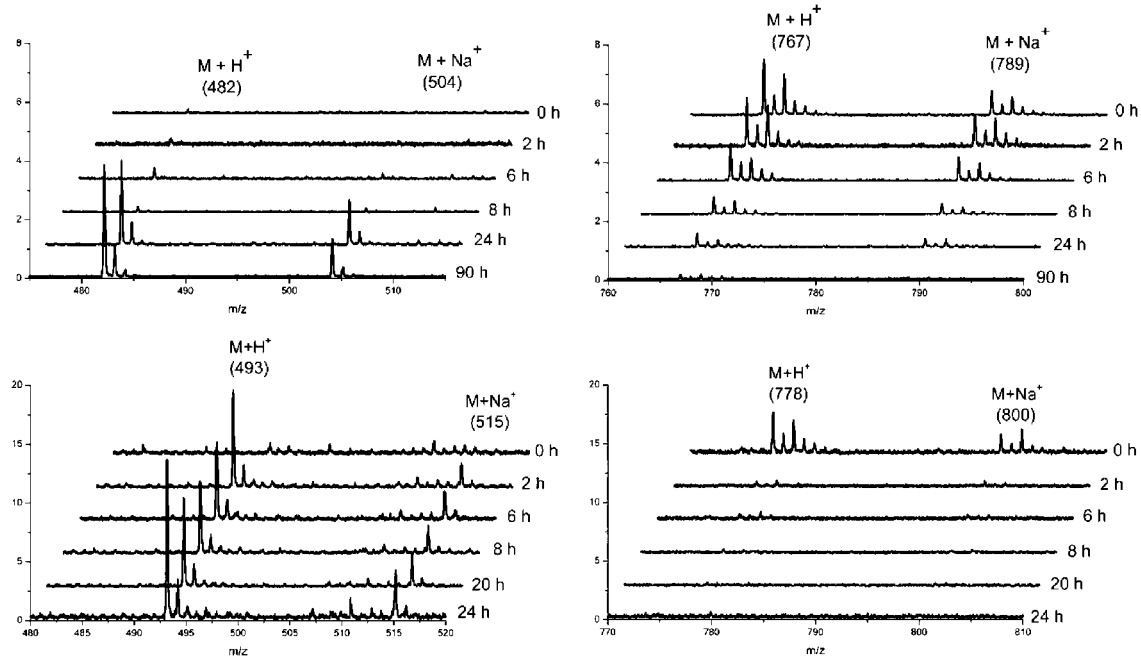

Figure 3. MALDI-TOF MS monitoring of snake (*Agkistrodon piscivorus piscivorus*) venom $sPLA_2$ activity on chlorambucil AEL prodrug **1a** (top) and **2a** (bottom). The spectra demonstrate that the prodrugs (right) are consumed and the AELs (left) are released.

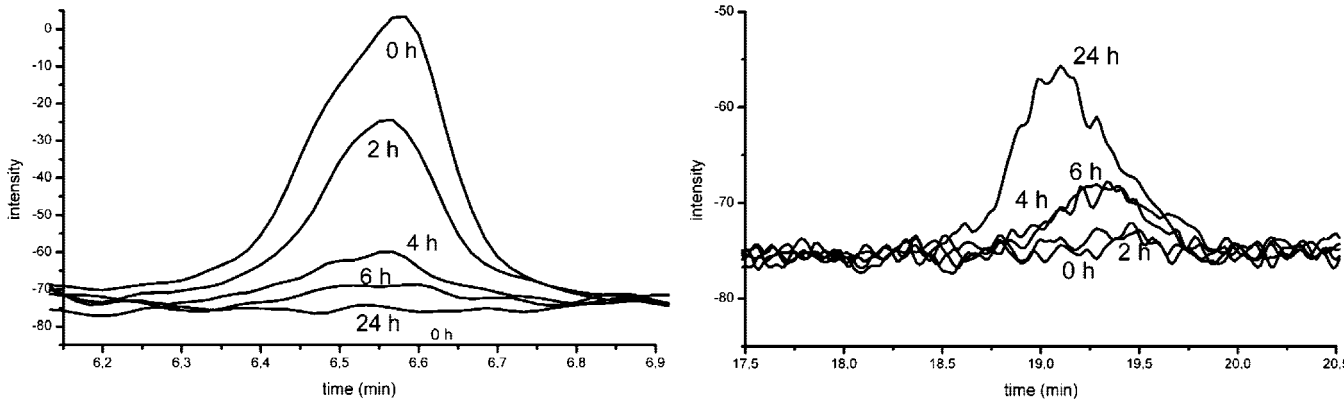

Figure 4. HPLC chromatogram for the snake (*Agkistrodon piscivorus piscivorus*) venom $sPLA_2$ hydrolysis experiment on chlorambucil AEL prodrug **1a** showing the amount of prodrug (left) and AEL (right) before the addition of the enzyme and after 2, 4, 6, and 24 h.

Table 2. IC_{50} Values (μM) of Chlorambucil (**3**), a Lyso-Ether Lipid (**7b**), and the Prodrugs **1b** and **2b** in the Presence and Absence of $sPLA_2$[a]

entry	compd	IC_{50} HT-29	IC_{50} MT-3	IC_{50} ES-2
1	**3**	70 ± 10	95 ± 21	34 ± 3
2	**1b**	>200	>200	nd
3	**2b**	>200	>200	97 ± 2
4	**1b** + $sPLA_2$	32 ± 2	36 ± 4	nd
5	**2b** + $sPLA_2$	10 ± 1	36 ± 4	8 ± 0,5
6	**7b**	18 ± 5	35 ± 1	30 ± 1
7	$sPLA_2$	*b*	*b*	*b*

[a] Cytotoxicity was measured using the MTT assay as cell viability 48 h after incubation with the indicated substances for 24 h and shown by mean ± SD (n = 3); nd = not determined. Snake (*Agkistrodon piscivorus piscivorus*) venom $sPLA_2$ was added to a final concentration of 5 nM. [b] No change in cell viability was observed after 24 h.

were added. After 27 h the mixture was concentrated in vacuo and purified by column chromatography (CH_2Cl_2/MeOH 4:1; then CH_2Cl_2/MeOH/H_2O 30:20:1) to give 80 mg (75%) of **1a** as an oil. R_f = 0.18 (CH_2Cl_2/MeOH/H_2O 30:20:1). ^{1}H NMR (500 MHz, 4:1 $CDCl_3$/CD_3OD) δ 7.08 (d, J = 8.6 Hz, 2H), 6.65 (d, J = 8.6 Hz, 2H), 5.16 (p, J = 5.9 Hz, 1H), 4.22 (s, 2H), 4.03−3.99 (m, 2H), 3.72 (t, J = 7.1 Hz, 4H), 3.64 (t, J = 7.1 Hz, 4H), 3.63−3.59 (m, 2H), 3.56 (s, 2H), 3.49−3.39 (m, 2H), 3.19 (s, 9H), 2.56 (t, J = 7.6 Hz, 2H), 2.36 (t, J = 7.6 Hz, 2H), 1.90 (p, J = 7.6 Hz, 2H), 1.54 (p, J = 6.8 Hz, 2H), 1.32−1.26 (m, 26H), 0.88 (t, J = 6.8 Hz, 3H). ^{13}C NMR (75 MHz, 4:1 $CDCl_3$/CD_3OD) δ 174.1, 144.8, 130.8, 130.0 (2C), 112.6 (2C), 72.2 (d, J = 8.2 Hz), 72.1, 69.6, 66.8, 64.4 (d, J = 5.2 Hz), 59.2 (d, J = 5.2 Hz), 54.5, 54.4, 54.4, 53.9 (2C), 40.9 (2C), 34.2, 34.0, 32.3, 30.1, 30.0, 29.9, 29.9, 29.7, 27.2, 26.4, 23.0, 14.3. IR (neat) 2923, 2852, 2366, 1734, 1091 cm^{-1}. m/z (M + H$^+$) 767.43.

1-*O*-Octadecyl-2-(4-(4-(bis(2-chloroethyl)amino)phenyl)butanoyl)-*sn*-glycero-3-phosphocholine (1b). Compound **7b** (67 mg, 0.131 mmol) was dissolved in anhydrous $CHCl_3$ (4 mL), and the mixture was heated to reflux under an atmosphere of N_2. DMAP (10 mg, 0.082 mmol), chlorambucil (**3**) (40 mg, 0.131 mmol), and DCC (1 M in CH_2Cl_2, 130 μL, 0.130 mmol) were added, and after 3, 6.5, 23.5, 26.5, and 31 h additional portions of chlorambucil (**3**) (40 mg, 0.131 mmol) and DCC (1 M in CH_2Cl_2, 130 μL, 0.130 mmol) were added. After 48 h the mixture was concentrated in vacuo and purified by column chromatography (CH_2Cl_2/MeOH 4:1, then CH_2Cl_2/MeOH/H_2O 30:20:1) to give 79 mg (76%) of **1b** as an oil. R_f = 0.15 (CH_2Cl_2/MeOH/H_2O 30:20:1). ^{1}H NMR (500 MHz, 4:1 $CDCl_3$/CD_3OD) δ 7.07 (d, J = 8.5 Hz, 2H), 6.65 (d, J = 8.5 Hz, 2H), 5.16 (p, J = 5.8 Hz, 1H), 4.22 (s, 2H), 4.06−3.94 (m, 2H), 3.72 (t, J = 6.8 Hz, 4H), 3.64 (t, J = 6.8 Hz, 4H), 3.63−3.59 (m, 2H), 3.56 (s, 2H), 3.48−3.40 (m, 2H), 3.20 (s, 9H), 2.56 (t, J =

7.5 Hz, 2H), 2.36 (t, $J = 7.5$ Hz, 2H), 1.90 (p, $J = 7.5$ Hz, 2H), 1.54 (m, 2H), 1.32−1.26 (m, 30H), 0.88 (t, $J = 6.9$ Hz, 3H). ^{13}C NMR (75 MHz, 4:1 $CDCl_3/CD_3OD$) δ 174.1, 144.9, 130.8, 130.1 (2C), 112.6 (2C), 72.3 (d, $J = 8.6$ Hz), 72.1, 69.6, 66.9, 64.5 (d, $J = 5.2$ Hz), 59.4 (d, $J = 5.2$ Hz), 54.5, 54.4, 54.4, 53.9 (2C), 40.9 (2C), 34.3, 34.0, 32.3, 30.1, 30.0, 29.9, 29.9, 29.8, 27.3, 26.4, 23.1, 14.3. IR (neat) 2923, 2852, 2366, 1734, 1518, 1247, 1088, 750 cm^{-1}. *m/z* (M + Na^+) 817.44.

(*S*)-(2,3-Di-*O*-*tert*-butyldimethylsilyl)glyceryl 2-Cyanoethyl-*N*,*N*-diisopropylphosphoramidite (11). Alcohol **10** (904 mg, 2.82 mmol) and diisopropylethylamine (1.0 mL, 5.92 mmol) were dissolved in anhydrous CH_2Cl_2 (10 mL) under an atmosphere of N_2. 2-Cyanoethyl-*N*,*N*-diisopropylchlorophosphoramidite (1.0 g, 4.22 mmol) was added dropwise, and the mixture was stirred at 20 °C for 1.5 h, after which EtOAc (20 mL) and saturated $NaHCO_3$ (50 mL) were added and the organic layer was isolated by extraction with EtOAc (2 × 50 mL). The combined organic phases were concentrated in vacuo, and the residue was purified by column chromatography (EtOAc) to give 1352 mg (92%) of **11** (two diastereoisomers, 1:1) as a colorless oil. $R_f = 1.0$ (EtOAc). ^{1}H NMR (300 MHz, $CDCl_3$): δ 3.87−3.46 (m, 5H), 2.67−2.61 (m, 2H), 1.20−1.17 (m, 12H), 0.90 (s, 9H), 0.89 (s, 9H), 0.09−0.06 (m, 12H). ^{13}C NMR (75 MHz, $CDCl_3$): δ 117.7, 73.3, 65.0, 58.6, 43.1 (2C), 26.1 (3C), 26.0 (3C), 24.7 (4C), 20.5, 18.5, 18.3, −4.4, −4.5, −5.2, −5.3. ^{31}P NMR (202 MHz, $CDCl_3$): δ 149.0, 148.5. IR (neat): 2958, 2929, 2883, 2857 cm^{-1}. *m/z* (M + Na^+) 543.32.

1-*O*-Hexadecyl-2-(4-(4-(bis-(2-chloroethyl)amino)phenyl)butanoyl)-*sn*-glycero-3-(2-cyanoethylphospho)-(*S*)-2,3-di-*O*-*tert*-butyldimethylsilylglycerol (12a). To a solution of **6a** (0.79 g, 1.8 mmol) and **11** (1.3 g, 2.5 mmol) in CH_2Cl_2 (10 mL) was added molecular sieves (3 Å). After the mixture was stirred for 30 min, 1*H*-tetrazole in acetonitrile (5.5 mL, 0.45 M, 2.5 mmol) was added and the mixture stirred for another 30 min before 5.5 M *tert*-butyl hydroperoxide in decane (0.50 mL, 2.8 mmol) was added and the mixture stirred for 1 h before being concentrated in vacuo. The residue was purified by column chromatography (EtOAc/heptane 1:1) to yield 1.63 g of an oil. ^{31}P NMR showed two signals at −0.66 and −0.82 in the 1:1 ratio set by the amidite. The product was subsequently treated with DDQ (0.45 g, 2.2 mmol) in CH_2Cl_2 (10 mL) and water (0.6 mL) for 2 h before Na_2SO_3 was added and the mixture diluted with CH_2Cl_2. The mixture was filtered and concentrated in vacuo before purification by column chromatography (CH_2Cl_2, then EtOAc/heptane 1:1) afforded 1.16 g. ^{31}P NMR showed two signals at −0.10 and −0.18 ppm. The deprotected compound was dissolved in CH_2Cl_2 (12 mL) together with chlorambucil (0.70 g, 2.3 mmol), and EDCI (0.59 g, 3.1 mmol) and DMAP (0.38 g, 3.1 mmol) were added. After being stirred for 2 h, the mixture was concentrated in vacuo and purified by column chromatography (EtOAc/heptane 1:1) and the resulting 1.36 g product dissolved in CH_2Cl_2 (10 mL) and treated with DBU (0.20 mL, 1.3 mmol) for 30 min. The reaction mixture was concentrated in vacuo and the residue was purified by column chromatography (CH_2Cl_2/MeOH 9:1) to give the phospholipid (0.96 g, 54%). $R_f = 0.73$ (CH_2Cl_2/MeOH/H_2O 65:25:4). ^{1}H NMR (500 MHz, $CDCl_3/CD_3OD$ 3:1): δ 6.90 (d, $J = 8.5$ Hz, 2H), 6.47 (d, $J = 8.5$ Hz, 2H), 5.00 (q, $J = 5$ Hz, 1H), 4.08 (m, 1H), 3.83−3.76 (m, 2H), 3.71−3.59 (m, 3H), 3.55−3.53 (m, 4H), 3.47−3.38 (m, 8H), 3.30−3.21(m, 2H), 2.38 (t, $J = 7.5$ Hz, 2H), 2.19 (t, $J = 7.5$ Hz, 2H), 1.73 (q, $J = 7.3$ Hz, 2H), 1.36 (m, 2H), 1.09 (s, 26 H), 0.72 (s, 18H), −0.06 (s, 6H), −0.11 (s, 6H). ^{13}C NMR (75 MHz, $CDCl_3/CD_3OD$ 3:1): δ 173.1, 144.0, 130.0, 129.3, 111.8, 72.4 (d, $J = 9.5$ Hz), 71.5, 71.4 (d, $J = 6.3$ Hz), 68.8, 66.5 (d, $J = 5.6$ Hz), 64.6, 63.5 (d, $J = 5.2$ Hz), 53.2, 40.1, 33.5, 33.3, 31.5, 29.3, 29.3, 29.2, 29.1, 29.0, 26.4, 25.6, 25.5, 25.4, 22.3, 17.9, 17.7, 13.6, −5.1, −5.1, −5.8, −5.8. ^{31}P NMR (202 MHz, $CDCl_3/CD_3OD$ 3:1): δ −1.82. IR (neat): 3450, 2922, 1732, 1616, 1519, 1463, 1360, 1252, 1102 cm^{-1}. *m/z* (M + Na^+) 1006.53.

1-*O*-Octadecyl-2-(4-(4-(bis-(2-chloroethyl)amino)phenyl)butanoyl)-*sn*-glycero-3-(2-cyanoethylphospho)-(*S*)-2,3-di-*O*-*tert*-butyldimethylsilylglycerol (12b). The synthesis was performed as for **12a**, starting from **6b** (650 mg, 1.40 mmol) and **11** (1.0 g, 1.9 mmol), affording 810 mg (57%) of **12b** as a colorless oil. $R_f = 0.73$ (CH_2Cl_2/MeOH/H_2O 65:25:4. ^{1}H NMR (500 MHz, $CDCl_3/CD_3OD$ 3:1): δ 6.96 (d, $J = 8.7$ Hz, 2H), 6.53 (d, $J = 8.7$ Hz, 2H), 5.08 (q, $J = 5.4$ Hz, 1H), 3.82−3.75 (m, 2H), 3.70−3.58 (m, 3H), 3.54−3.51 (m, 4H), 3.46−3.36 (m, 8H), 3.29−3.22 (m, 2H), 2.45 (t, $J = 7.7$ Hz, 2H), 2.24 ($J = 7.7$ Hz, 2H), 1.77 (q, $J = 7.4$ Hz, 2H), 1.42 (m, 2H), 1.15 (s, 30H), 0.78 (s, 18H), −0.01 (s, 6H), −0.05 (s, 6H). ^{13}C NMR (75 MHz, $CDCl_3/CD_3OD$ 3:1): δ 173.2, 144.1, 130.2, 129.4, 111.8, 72.4 (d, $J = 9.6$ Hz), 71.5, 71.5 (d, $J = 7.8$ Hz), 68.8, 66.6 (d, $J = 5.5$ Hz), 64.6, 63.6 (d, $J = 5.4$ Hz), 53.3, 40.2, 33.6, 33.3, 31.6, 29.4, 29.4, 29.3, 29.2, 29.1, 26.5, 25.7, 25.6, 25.5, 22.4, 18.0, 17.8, 13.8, −4.9, −5.0, −5.7, −5.7. ^{31}P NMR (202 MHz, $CDCl_3/CD_3OD$ 3:1): δ −2.00. IR (neat): 3448, 2926, 2854, 1735, 1617, 1519, 1464, 1360, 1252, 1108 cm^{-1}. *m/z* (M + Na^+) 1034.57.

1-*O*-Hexadecyl-2-(4-(4-(bis(2-chloroethyl)amino)phenyl)butanoyl)-*sn*-glycero-3-phospho-(*S*)-glycerol (2a). Compound **12a** (0.42 g, 0.43 mmol) was dissolved in MeCN (9 mL) and cooled to 0 °C. Then 40% aqueous HF (1 mL) was added, and the mixture was allowed to reach 20 °C while being stirred vigorously for 2 h. The reaction mixture was then poured into saturated aqueous $NaHCO_3$ (20 mL) and extracted with CH_2Cl_2 (3 × 10 mL) and EtOAc (10 mL). The combined organic extracts were dried over Na_2SO_4 and concentrated in vacuo and the residue was purified by column chromatography (CH_2Cl_2/MeOH/H_2O 65:25:4) to afford **2a** (0.19 g, 59%). $R_f = 0.56$ (CH_2Cl_2/MeOH/H_2O 65:25:4). ^{1}H NMR (500 MHz, $CDCl_3$:CD_3OD 3:1): δ 6.88 (d, $J = 8.6$ Hz, 2H), 6.45 (d, $J = 8.6$ Hz, 2H), 4.98 (q, $J = 5$ Hz, 1H), 3.84−3.71 (m, 3H), 3.60 (q, $J = 5$ Hz, 1H), 3.54−3.51 (m, 4H), 3.46−3.39 (m, 8H), 3.30−3.20 (m, 2H), 2.37 (t, $J = 7.5$ Hz, 2H), 2.17 (t, $J = 7.6$ Hz, 2H), 1.71 (q, $J = 7.3$ Hz, 2H), 1.35 (t, $J = 6.6$ Hz, 2H), 1.07 (s, 26H), 0.69 (t, $J = 6.8$ Hz, 3H). ^{13}C NMR (75 MHz, $CDCl_3/CD_3OD$ 3:1): δ 173.2, 144.0, 129.9, 129.2, 111.7, 71.4 (d, $J = 5.4$ Hz), 71.3, 70.4 (d, $J = 4.8$ Hz), 68.7, 66.1 (d, $J = 4.9$ Hz), 63.8 (d, $J = 4.8$), 61.8, 53.1, 40.1, 33.5, 33.4, 33.2, 33.0, 31.5, 29.3, 29.2, 29.1, 29.1, 28.9, 26.4, 25.6, 22.2, 13.5. ^{31}P NMR (202 MHz, $CDCl_3/CD_3OD$ 3:1): δ −0.99. IR (neat): 3345, 2923, 2853, 1732, 1616, 1519, 1466, 1356, 1248, 1115, 1002 cm^{-1}. *m/z* (M + H^+) 778.36.

1-*O*-Octadecyl-2-(4-(4-(bis(2-chloroethyl)amino)phenyl)butanoyl)-*sn*-glycero-3-phospho-(*S*)-glycerol (2b). The synthesis was performed as for **2a**, starting from **12b** (334 mg, 0.33 mmol) and affording **2b** (83 mg, 32%). $R_f = 0.56$ (CH_2Cl_2/MeOH/H_2O 65:25:4). ^{1}H NMR (500 MHz, $CDCl_3/CD_3OD$ 3:1): δ 6.89 (d, $J = 8.5$ Hz, 2H), 6.46 (d, $J = 8.2$ Hz, 2H), 4.99 (q, $J = 5$ Hz, 1H), 3.84−3.72 (m, 3H), 3.60 (q, $J = 5$ Hz, 1H), 3.53 (m, 4H), 3.47−3.41 (m, 8H), 3.30−3.20 (m, 2H), 2.37 (t, $J = 7.5$ Hz, 2H), 2.17 (t, $J = 7.5$ Hz, 2H), 1.71 (q, $J = 7.5$ Hz, 2H), 1.35 (t, $J = 6.5$ Hz, 2H), 1.07 (s, 30H), 0.70 (t, $J = 6.8$ Hz, 3H). ^{13}C NMR (75 MHz, $CDCl_3/CD_3OD$ 3:1): δ 173.3, 144.0, 130.0, 129.2, 111.8, 71.5, 71.4 (d, $J = 6.3$ Hz), 70.5 (d, $J = 4.8$ Hz), 68.7, 66.1, 63.8 (d, $J = 5.6$ Hz), 61.9, 53.2, 40.1, 33.5, 33.2, 31.5, 29.3, 29.3, 29.2, 29.1, 29.0, 26.4, 25.6, 22.3, 13.6. ^{31}P NMR (202 MHz, $CDCl_3/CD_3OD$ 3:1): δ −0.31. IR (neat): 3332, 2923, 2853, 1733, 1616, 1519, 1466, 1355, 1236, 1115, 1002 cm^{-1}. *m/z* (M + Na^+) 828.37.

Acknowledgment. We thank the Danish Council for Strategic Research (NABIIT Program) for financial support. MEMPHYS—Center for Biomembrane Physics is supported by the Danish National Research Foundation.

Supporting Information Available: Analytical and spectral data for all synthesized compounds, experimental procedures for the synthesis of **5a**, **5b**, **6a**, **6b**, **7a**, **7b**, **9**, and **10**, prodrugs stability data, Mosher ester analysis data of **10**, further MALDI-TOF MS and HPLC data for $sPLA_2$ degradation experiments, and alkylating assay data. This material is available free of charge via the Internet at http://pubs.acs.org.

References

(1) Gregoriadis, G.; Wills, E. J.; Swain, C. P.; Tavill, A. S. Drug-carrier potential of liposomes in cancer chemotherapy. *Lancet* **1974**, *1*, 1313–1316.

(2) (a) Maeda, H.; Matsumura, Y. Tumoritropic and lymphotropic principles of macromolecular drugs. *Crit. Rev. Ther. Drug Carrier Syst.* **1989**, *6*, 193–210. (b) Seymour, L. W. Passive tumor targeting of soluble macromolecules and drug conjugates. *Crit. Rev. Ther. Drug Carrier Syst.* **1992**, *9*, 135–187. (c) Yuan, F.; Leunig, M.; Huang, S. K.; Berk, D. A.; Papahadjopoulos, D.; Jain, R. K. Microvascular permeability and interstitial penetration of sterically stabilized (stealth) liposomes in a human tumor xenograft. *Cancer Res.* **1994**, *54*, 3352–3356. (d) Jain, R. K. Delivery of molecular and cellular medicine to solid tumors. *J. Controlled Release* **1998**, *53*, 49–67.

(3) Andresen, T. L.; Jensen, S. S.; Jørgensen, K. Advanced strategies in liposomal cancer therapy: problems and prospects of active and tumor specific drug release. *Prog. Lipid Res.* **2005**, *44*, 68–97.

(4) (a) Pak, C. C.; Ali, S.; Janoff, A. S.; Meers, P. Triggerable liposomal fusion by enzyme cleavage of a novel peptide−lipid conjugate. *Biochim. Biophys. Acta* **1998**, *1372*, 13–27. (b) Meers, P. Enzyme-activated targeting of liposomes. *Adv. Drug Delivery Rev.* **2001**, *53*, 265–272. (c) Davidsen, J.; Jørgensen, K.; Andresen, T. L.; Mouritsen, O. G. Secreted phospholipase A2 as a new enzymatic trigger mechanism for localised liposomal drug release and absorption in diseased tissue. *Biochim. Biophys. Acta* **2003**, *1609*, 95−101.

(5) (a) Connor, J.; Yatvin, M. B.; Huang, L. pH-sensitive liposomes: acid-induced liposome fusion. *Proc. Natl. Acad. Sci. U.S.A.* **1984**, *81*, 1715–1718. (b) Ellens, H.; Bentz, J.; Szoka, F. C. pH-induced destabilization of phosphatidylethanolamine-containing liposomes: role of bilayer contact. *Biochemistry* **1984**, *23*, 1532–1538. (c) Collins, D.; Litzinger, D. C.; Huang, L. Structural and functional comparisons of pH-sensitive liposomes composed of phosphatidylethanolamine and three different diacylsuccinylglycerols. *Biochim. Biophys. Acta* **1990**, *1025*, 234–242. (d) Shin, J.; Shum, P.; Thompson, D. H. Acid-triggered release via dePEGylation of DOPE liposomes containing acid-labile vinyl ether PEG-lipids. *J. Controlled Release* **2003**, *91*, 187–200.

(6) (a) Miller, C. R.; Bennett, D. E.; Chang, D. Y.; O'Brien, D. F. Effect of liposomal composition on photoactivated liposome fusion. *Biochemistry* **1996**, *35*, 11782–11790. (b) Bondurant, B.; Mueller, A.; O'Brien, D. F. Photoinitiated destabilization of sterically stabilized liposomes. *Biochim. Biophys. Acta* **2001**, *1511*, 113–122. (c) Shum, P.; Kim, J. M.; Thompson, D. H. Phototriggering of liposomal drug delivery systems. *Adv. Drug Delivery Rev.* **2001**, *53*, 273–284.

(7) (a) Yatvin, M. B.; Weinstein, J. N.; Dennis, W. H.; Blumenthal, R. Design of liposomes for enhanced local release of drugs by hyperthermia. *Science* **1978**, *202*, 1290–1293. (b) Gaber, M. H.; Hong, K.; Huang, S. K.; Papahadjopoulos, D. Thermosensitive sterically stabilized liposomes: formulation and in vitro studies on mechanism of doxorubicin release by bovine serum and human plasma. *Pharm. Res.* **1995**, *12*, 1407–1416. (c) Kono, K.; Nakai, R.; Morimoto, K.; Takagishi, T. Temperature-dependent interaction of thermo-sensitive polymer-modified liposomes with CV1 cells. *FEBS Lett.* **1999**, *456*, 306–310. (d) Needham, D.; Anyarambhatla, G.; Kong, G.; Dewhirst, M. W. A new temperature-sensitive liposome for use with mild hyperthermia: characterization and testing in a human tumor xenograft model. *Cancer Res.* **2000**, *60*, 1197–1201.

(8) (a) Gabizon, A.; Catane, R.; Uziely, B.; Kaufman, B.; Safra, T.; Cohen, R.; Martin, F.; Huang, A.; Barenholz, Y. Prolonged circulation time and enhanced accumulation in malignant exudates of doxorubicin encapsulated in polyethylene-glycol coated liposomes. *Cancer Res.* **1994**, *54*, 987–992. (b) Gabizon, A.; Shmeeda, H.; Barenholz, Y. Pharmacokinetics of pegylated liposomal doxorubicin. Review of animal and human studies. *Clin. Pharmacokinet.* **2003**, *42*, 419–436.

(9) Graybill, J. R.; Craven, P. C.; Taylor, R. L.; Williams, D. M.; Magee, W. E. Treatment of murine cryptococcosis with liposome-associated amphotericin-B. *J. Infect. Dis.* **1982**, *145*, 748–752.

(10) (a) Abe, T.; Sakamoto, K.; Kamohara, H.; Hirano, Y.; Kuwahara, N.; Ogawa, M. Group II phospholipase A2 is increased in peritoneal and pleural effusions in patients with various types of cancer. *Int. J. Cancer* **1997**, *74*, 245–250. (b) Graff, J. R.; Konicek, B. W.; Deddens, J. A.; Chedid, M.; Hurst, B. M.; Colligan, B.; Neubauer, B. L.; Carter, H. W.; Carter, J. H. Expression of group IIa secretory phospholipase A2 increases with prostate tumor grade. *Clin. Cancer Res.* **2001**, *7*, 3857–3861. (c) Laye, J.; Gill, J. H. Phospholipase A_2 expression in tumours: a target for therapeuticintervention. *Drug Discovery Today* **2003**, *8*, 710–716. (d) Murakami, M.; Kudo, I. Phospholipase A_2. *J. Biochem.* **2002**, *131*, 285–292.

(11) (a) Andresen, T. L.; Jensen, S. S.; Madsen, R.; Jørgensen, K. Synthesis and biological activity of anticancer ether lipids that are specifically released by phospholipase A_2 in tumor tissue. *J. Med. Chem.* **2005**, *48*, 7305–7314. (b) Andresen, T. L.; Davidsen, J.; Begtrup, M.; Mouritsen, O. G.; Jørgensen, K. Enzymatic release of antitumor ether lipids by specific phospholipase A_2 activation of liposome-forming prodrugs. *J. Med. Chem.* **2004**, *47*, 1694–1703.

(12) Yamashita, S.; Yamashita, J.; Sakamoto, K.; Inada, K.; Nakashima, Y.; Murata, K.; Saishoji, T.; Nomura, K.; Ogawa, M. Increased expression of membrane-associated phospholipase-A2 shows malignant potential of human breast-cancer cells. *Cancer* **1993**, *71*, 3058–3064.

(13) (a) Murata, K.; Egami, H.; Kiyohara, H.; Oshima, S.; Kurizaki, T.; Ogawa, M. Expression of group-II phospholipase-A2 in malignant and nonmalignant human gastric-mucosa. *Br. J. Cancer* **1993**, *68*, 103–111. (b) Leung, S. Y.; Chen, X.; Chu, K. M.; Yuen, S. T.; Mathy, J.; Ji, J. F.; Chan, A. S. Y.; Li, R.; Law, S.; Troyanskaya, O. G.; Tu, I. P.; Wong, J.; So, S.; Botstein, D.; Brown, P. O. Phospholipase A2 group IIA expression in gastric adenocarcinoma is associated with prolonged survival and less frequent metastasis. *Proc. Natl. Acad. Sci. U.S.A.* **2002**, *99*, 16203–16208.

(14) (a) Kennedy, B. P.; Soravia, C.; Moffat, J.; Xia, L.; Hiruki, T.; Collins, S.; Gallinger, S.; Bapat, B. Overexpression of the nonpancreatic secretory group II PLA(2) messenger RNA and protein in colorectal adenomas from familial adenomatous polyposis patients. *Cancer Res.* **1998**, *58*, 500–503. (b) Edhemovic, I.; Snoj, M.; Kljun, A.; Golouh, R. Immunohistochemical localization of group II phospholipase A2 in the tumours and mucosa of the colon and rectum. *Eur. J. Surg. Oncol.* **2001**, *27*, 545–548. (c) Praml, C.; Amler, L. C.; Dihlmann, S.; Finke, L. H.; Schlag, P.; Schwab, M. Secretory type II phospholipase A(2) (PLA2G2A) expression status in colorectal carcinoma derived cell lines and in normal colonic mucosa. *Oncogene* **1998**, *17*, 2009–2012.

(15) Kashiwagi, M.; Friess, H.; Uhl, W.; Berberat, P.; Abou-Shady, M.; Martignoni, M.; Anghelacopoulos, S. E.; Zimmermann, A.; Buchler, M. W. Group II and IV phospholipase A(2) are produced in human pancreatic cancer cells and influence prognosis. *Gut* **1999**, *45*, 605–612.

(16) Jiang, J.; Neubauer, B. L.; Graff, J. R.; Chedid, M.; Thomas, J. E.; Roehm, N. W.; Zhang, S.; Eckert, G. J.; Koch, M. O.; Eble, J. N.; Cheng, L. Expression of group IIA secretory phospholipase A2 is elevated in prostatic intraepithelial neoplasia and adenocarcinoma. *Am. J. Pathol.* **2002**, *160*, 667–671.

(17) Ying, Z.; Tojo, H.; Komatsubara, T.; Nakagawa, M.; Inada, M.; Kawata, S.; Matsuzawa, Y.; Okamoto, M. Enhanced expression of group-II phospholipase A(2) in human hepatocellular-carcinoma. *Biochim. Biophys. Acta* **1994**, *1226*, 201–205.

(18) (a) Everett, J. L.; Roberts, J. J.; Ross, W. C. J. Aryl-2-halogenoalkylamines. XII: Some carboxylic derivatives of *N*,*N*-di-2-chloroethylaniline. *J. Chem. Soc.* **1953**, 2386–2392. (b) Urbaniak, M. D.; Bingham, J. P.; Hartley, J. A.; Woolfson, D. N.; Caddick, S. Design and synthesis of a nitrogen mustard derivative stabilized by apo-neocarzinostatin. *J. Med. Chem.* **2004**, *47*, 4710–4715. (c) Sienkiewicz, P.; Bielawski, K.; Bielawska, A.; Palka, J. Amidine analogue of chlorambucil is a stronger inhibitor of protein and DNA synthesis in breast cancer MCF-7 cells than is the parent drug. *Eur. J. Pharmacol.* **2004**, *494*, 95–101.

(19) Altucci, L.; Gronemeyer, H. The promise of retinoids to fight against cancer. *Nat. Rev. Cancer* **2001**, *1*, 181–193.

(20) (a) Forman, B. M.; Tontonoz, P.; Chen, J.; Brun, R. P.; Spiegelman, B. M.; Evans, R. M. 15-Deoxy-$\Delta^{12,14}$-prostaglandin J_2 is a ligand for the adipocyte determination factor PPARγ. *Cell* **1995**, *83*, 803–812. (b) Naitoh, T.; Kitahara, M.; Tsuruzoe, N. The effect of activation of peroxisome proliferator-activated receptor gamma (PPARγ) on human monocyte function: PPARγ ligands do not inhibit tumor necrosis factor-α release in human monocytic cell line THP-1. *Cell Biol. Toxicol.* **2000**, *16*, 131–135.

(21) Kundu, G. C.; Schullek, J. R.; Wilson, I. B. The alkylating properties of chlorambucil. *Pharmacol., Biochem. Behav.* **1993**, *49*, 621−624.

(22) Montserrat, E.; Rozman, C. Chronic lymphocytic leukaemia treatment. *Blood Rev.* **1993**, *7*, 164–175.

(23) (a) Ehrsson, H.; Eksborg, S.; Wallin, I.; Nilsson, S. O. Degradation of chlorambucil in aqueous solution. *J. Pharm. Sci.* **1980**, *69*, 1091–1094. (b) Chatterji, D. C.; Yeager, R. L.; Gallelli, J. F. Kinetics of chlorambucil hydrolysis using high-pressure liquid chromatography. *J. Pharm. Sci.* **1982**, *71*, 50–54. (c) Pettersson-Fernholm, T.; Vilpo, J.; Kosonen, M.; Hakala, K.; Hovinen, J. Reactions of 4-bis(2-chloroethyl)aminophenylacetic acid (phenylacetic acid mustard) in physiological solutions. *J. Chem. Soc., Perkin Trans. 2* **1992**, *2*, 2183–2187. (d) Löf, K.; Hovinen, J.; Reinikainen, P.; Vilpo, L. M.; Seppälä, E.; Vilpo, J. A. Kinetics of chlorambucil in vitro: effects of fluid matrix, human gastric juice, plasma proteins and red cells. *Chem.-Biol. Interact.* **1997**, *103*, 187–198. (e) Balboa, M. A. H.; Arévalo, V. V.; Reyes, V. H. A.; Velázquez, A. M.; Ganem-Quintanar, A.; Quintanar, D.; Camacho, B.; Arzaluz, G. N.; Rosales-Hoz, M.; Leyva, M. A.; Angeles, E. Study of chlorambucil and chlorambucil-trimethyl-*b*-cyclodextrin inclusion complex by CE. *Chromatographia* **2008**, *67*, 193–196.

(24) (a) Peters, U.; Bankova, W.; Welzel, P. Platelet-activating-factor synthetic studies. *Tetrahedron* **1987**, *43*, 3803–3816. (b) Massing, U.; Eibl, H. Synthesis of enantiomerically pure 1-*O*-phosphocholine-2-*O*-acyl-octadecane and 1-*O*-phosphocholine-2-*N*-acyl-octadecane. *Chem. Phys. Lipids* **1994**, *69*, 105–120. (c) Massing, U.; Eibl, H. New optically pure dimethylacetals of glyceraldehydes and their application for lipid and phospholipid synthesis. *Chem. Phys. Lipids* **1995**, *76*, 211–224.

(25) (a) Hirth, G.; Barner, R. Synthesis of glyceryl etherphosphatides. 1. Preparation of 1-*O*-octadecyl-2-*O*-acetyl-*sn*-glyceryl-3-phosphorylcholine (platelet activating factor), of its enantiomer and of some analogous compounds. *Helv. Chim. Acta* **1982**, *65*, 1059–1084. (b) Guivisdalsky, P. N.; Bittman, R. Novel enantioselective synthesis of platelet activating factor and its enantiomer via ring-opening of glycidyl tosylate with 1-hexadecanol. *Tetrahedron Lett.* **1988**, *29*, 4393–4396. (c) Guivisdalsky, P. N.; Bittman, R. An efficient stereocontrolled route to both enantiomers of platelet activating factor and analogues with long chain esters at C2. Saturated and unsaturated ether glycerolipids by opening of glycidyl arenesulfonates. *J. Org. Chem.* **1989**, *54*, 4643–4648. (d) Lindberg, J.; Ekeroth, J.; Konradsson, P. Efficient synthesis of phospholipids from glycidyl phosphates. *J. Org. Chem.* **2002**, *67*, 194–199.

(26) Guivisdalsky, P. N.; Bittman, R. Regiospecific opening of glycidyl derivatives mediated by boron trifluoride. Asymmetric synthesis of ether-linked phospholipids. *J. Org. Chem.* **1989**, *54*, 4637–4642.

(27) Wang, P.; Blank, D. H.; Spencer, T. A. Synthesis of benzophenone-containing analogues of phosphatidylcholine. *J. Org. Chem.* **2004**, *69*, 2693–2703.

(28) (a) Nakajima, N.; Horita, K.; Abe, R.; Yonemitsu, O. MPM (4-methoxybenzyl) protection of hydroxyl functions under mild acidic conditions. *Tetrahedron Lett.* **1988**, *29*, 4139–4142. (b) Rai, A. N.; Basu, A. An efficient method for *para*-methoxybenzyl ether formation with lanthanum triflate. *Tetrahedron Lett.* **2003**, *44*, 2267–2269.

(29) (a) Hirth, G.; Barner, R. Synthesis of glyceryl etherphosphatides. 1. Preparation of 1-*O*-octadecyl-2-*O*-acetyl-*sn*-glyceryl-3-phosphorylcholine (platelet activating factor), of its enantiomer and of some analogous compounds. *Helv. Chim. Acta* **1982**, *65*, 1059–1084. (b) Chupin, V. V.; Ostapenko, O. V.; Klykov, V. N.; Anikin, M. V.; Serebrennikova, G. A. Formation of a structural isomer of platelet-activing-factor during 1-alkyl-*sn*-glycero-3-phosphocholine acetylation. *Bioorg. Khim.* **1993**, *19*, 1111–1121.

(30) Horita, K.; Yoshioka, T.; Tanaka, T.; Oikawa, Y.; Yonemitsu, O. On the selectivity of deprotection of benzyl, MPM (4-methoxybenzyl) and DMPM (3,4-dimethoxybenzyl) protecting groups for hydroxyl functions. *Tetrahedron* **1986**, *42*, 3021–3028.

(31) Neises, B.; Steglich, W. Simple method for the esterification of carboxylic acids. *Angew. Chem., Int. Ed. Engl.* **1978**, *17*, 522−524.

(32) Boden, E. P.; Keck, G. E. Proton-transfer steps in steglich esterification: A very practical new method for macrolactonization. *J. Org. Chem.* **1985**, *50*, 2394–2395.

(33) (a) Kolb, H. C.; VanNieuwenhze, M. S.; Sharpless, K. B. Catalytic asymmetric dihydroxylation. *Chem. Rev.* **1994**, *94*, 2483–2547. (b) Corey, E. J.; Guzman-Perez, A.; Noe, M. C. The application of a mechanistic model leads to the extension of the sharpless asymmetric dihydroxylation to allylic 4-methoxybenzoates and conformationally related amine and homoallylic alcohol derivatives. *J. Am. Chem. Soc.* **1995**, *117*, 10805–10816.

(34) Evans, D. A.; Gage, J. R.; Leighton, J. L. Asymmetric synthesis of calyculin A. 3. Assemblage of the calyculin skeleton and the introduction of a new phosphate monoester synthesis. *J. Org. Chem.* **1992**, *57*1964–1966.

(35) (a) Lichtenberg, D.; Barenholz, Y. Liposomes. Preparation, Characterization and Preservation. *Methods Biochem. Anal.* **1988**, *33*, 337–462. (b) Tirrell, D. A.; Takigawa, D. Y.; Seki, K. Interactions of synthetic polymers with cell-membranes and model membrane systems. 7. pH sensitization of phospholipid-vesicles via complexation with synthetic poly(carboxylic acid)s. *Ann. N.Y. Acad. Sci.* **1985**, *446*, 237–248.

(36) (a) Singer, A. G.; Ghomashchi, F.; Le Calvez, C.; Bollinger, J.; Bezzine, S.; Rouault, M.; Sadilek, M.; Nguyen, E.; Lazdunski, M.; Lambeau, G.; Gelb, M. H. Interfacial kinetic and binding properties of the complete set of human and mouse groups I, II, V, X, and XII secreted phospholipases A(2). *J. Biol. Chem.* **2002**, *277*, 48535–48549. (b) Bahnson, B. J. Structure, function and interfacial allosterism in phospholipase A2: insight from the anion-assisted dimer. *Arch. Biochem. Biophys.* **2005**, *433*, 96–106. (c) Gadd, M. E.; Biltonen, R. L. Characterization of the interaction of phospholipase A(2) with phosphatidylcholine−phosphatidylglycerol mixed lipids. *Biochemistry* **2000**, *39*, 12312–12323. (d) Leidy, C.; Linderoth, L.; Andresen, T. L.; Mouritsen, O. G.; Jørgensen, K.; Peters, G. H. Domain-induced activation of human phospholipase A_2 type IIA: local versus global lipid composition. *Biophys. J.* **2006**, *90*, 3165–3175. (e) Peters, G. H.; Møller, M. S.; Jørgensen, K.; Rönnhölm, P.; Mikkelsen, M.; Andresen, T. L. Secretory phospholipase A(2) hydrolysis of phospholipid analogues is dependent on water accessibility to the active site. *J. Am. Chem. Soc.* **2007**, *129*, 5451–5461.

(37) (a) Harvey, D. J. Matrix-assisted laser desorption/ionization mass spectrometry of phospholipids. *J. Mass Spectrom.* **1995**, *30*, 1333–1346. (b) Schiller, J.; Arnhold, J.; Benard, S.; Müller, M.; Reichl, S.; Arnold, K. Lipid analysis by matrix-assisted laser desorption and ionization mass spectrometry: a methodological approach. *Anal. Biochem.* **1999**, *267*, 46–56. (c) Petković, M.; Muller, J.; Muller, M.; Schiller, J.; Arnold, K.; Arnhold, J. Application of matrix-assisted laser desorption/ionization time-of-flight mass spectrometry for monitoring the digestion of phosphatidylcholine by pancreatic phospholipase A_2. *Anal. Biochem.* **2002**, *308*, 61–70.

(38) (a) Epstein, J.; Rosenthal, R. W.; Ess, R. J. Use of *p*-(4-nitrobenzyl)pyridine as analytical reagent for ethylenimines and alkylating agents. *Anal. Chem.* **1955**, *27*, 1435–1439. (b) Friedman, O. M.; Boger, E. Chlorimetric estimation of nitrogen mustard in aqueous media. *Anal. Chem.* **1961**, *33*, 906–910. (c) Genka, S.; Deutsch, J.; Shetty, U. H.; Stahle, P. L.; John, V.; Lieberburg, I. M.; Ali-Osmant, F.; Rapoport, S. I.; Greig, N. H. Development of lipophilic anticancer agents for the treatment of brain tumors by the esterification of water-soluble chlorambucil. *Clin. Exp. Metastasis* **1993**, *11*, 131–140.

(39) Gottlieb, H. E.; Kotlyar, V.; Nudelman, A. NMR chemical shifts of common laboratory solvents as trace impurities. *J. Org. Chem.* **1997**, *62*, 7512–7515.

(40) Chen, P. S.; Toribara, T. Y.; Warner, H. Microdetermination of phosphorus. *Anal. Chem.* **1956**, *28*, 1756–1758.

(41) Carmichael, J.; DeGraff, W. G.; Gazdar, A. F.; Minna, J. D.; Mitchell, J. B. Evaluation of a tetrazolium-based semiautomated colorimetric assay: assessment of chemosensitivity testing. *Cancer Res.* **1987**, *47*, 936–942.

JM900091H

3782 *J. Med. Chem.* **2010,** *53,* 3782–3792
DOI: 10.1021/jm100190c

Journal of
Medicinal
Chemistry
Article

Liposomal Formulation of Retinoids Designed for Enzyme Triggered Release

Palle J. Pedersen,[†] Sidsel K. Adolph,[|] Arun K. Subramanian,[†] Ahmad Arouri,[‡] Thomas L. Andresen,[§] Ole G. Mouritsen,[‡] Robert Madsen,[†] Mogens W. Madsen,[|] Günther H. Peters,[†] and Mads H. Clausen*,[†]

[†]*Department of Chemistry, Technical University of Denmark, Kemitorvet, Building 201 and 207, DK-2800 Kgs. Lyngby, Denmark,* [‡]*Department of Physics and Chemistry, MEMPHYS−Center for Biomembrane Physics, University of Southern Denmark, Campusvej 55, DK-5230 Odense M, Denmark,* [§]*Department of Micro- and Nanotechnology, Technical University of Denmark, DK-4000 Roskilde, Denmark, and* [|]*LiPlasome Pharma A/S, Technical University of Denmark, Diplomvej 378, DK-2800 Kgs. Lyngby, Denmark*

Received February 12, 2010

The design of retinoid phospholipid prodrugs is described based on molecular dynamics simulations and cytotoxicity studies of synthetic retinoid esters. The prodrugs are degradable by secretory phospholipase A_2 IIA and have potential in liposomal drug delivery targeting tumors. We have synthesized four different retinoid phospholipid prodrugs and shown that they form particles in the liposome size region with average diameters of 94−118 nm. Upon subjection to phospholipase A_2, the lipid prodrugs were hydrolyzed, releasing cytotoxic retinoids and lysolipids. The formulated lipid prodrugs displayed IC_{50} values in the range of 3−19 μM toward HT-29 and Colo205 colon cancer cells in the presence of phospholipase A_2, while no significant cell death was observed in the absence of the enzyme.

Introduction

Retinoids,[1] such as all-*trans* retinoic acid (ATRA,[a] Figure 1), are known for their broad and diverse biological functions, and various strategies have been explored to make retinoids applicable as drugs in the treatment of diseases.[2] One of the biological functions of ATRA is its anticancer activity toward a broad range of cancer types, like breast, prostate, and colon cancer.[3] For example, orally administrated ATRA is used clinically in the treatment of leukemia.[4] However, the oral administration route is restricted by a relative low bioavailability[4c] and a fast clearance from the bloodstream,[5] and thus alternative ways of administrating ATRA would be beneficial. Intravenous administration is hampered by the low water solubility of ATRA, but this can be circumvented by formulating ATRA in liposome based drug delivery systems.[6] Unfortunately, the liposomal formulation strategies have often been plagued by problems with leakage, which have led to an uncontrolled release of ATRA from the carrier system. Recently, we have introduced new liposomal drug delivery systems[7] that address the formulation challenges of relatively hydrophobic drugs. The drug delivery systems consist of secretory phospholipase A_2 ($sPLA_2$) IIA sensitive phospholipids and are constructed of drug−lipid prodrugs, in which the lipophilic anticancer drugs are covalently attached to the phospholipids. Despite successful incorporation of the well-known anticancer drug chlorambucil in the *sn*-2 position,[7a] it was later experienced that the desired delivery of free ATRA was not feasible due to lack of $sPLA_2$ activity on substrates like **1** (Figure 1).[7b] ATRA is a rigid molecule and contains a methyl substituent in close proximity to the carboxylic acid moiety. These features contrast with naturally occurring fatty acids, which are predominantly saturated and flexible molecules without branching. Knowing that some esters and amides of ATRA retain their activity,[8] we decided to incorporate an aliphatic C_6-linker between ATRA and the lipid backbone (Figure 2). To gain further insight into the substrate specificity of the $sPLA_2$ enzyme, hydrolysis of the lipid prodrugs was investigated by molecular dynamics (MD) simulation, which has earlier been demonstrated as a valuable tool for assessing $sPLA_2$ activity toward a range of substrates.[9]

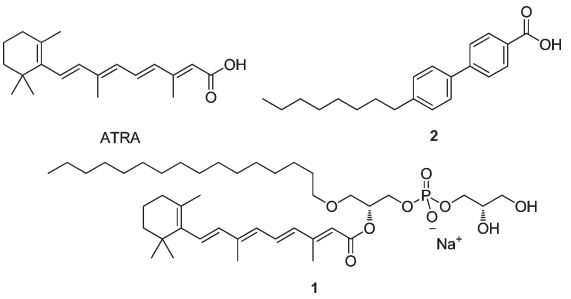

Figure 1. Structure of the cytotoxic compounds ATRA and **2** and the ATRA phospholipid prodrug (**1**) that is not hydrolyzed by $sPLA_2$.[7b]

One major drawback in applying ATRA as a drug is its nonselective activation of retinoic acid receptor (RAR) subtypes (RARs, α, β, γ), retinoic X receptor subtypes (RXRs, α,

*To whom correspondence should be addressed. Phone: +45 45252131. Fax: +45 45933968. E-mail: mhc@kemi.dtu.dk.

[a] Abbrevations: ATRA, all-*trans* retinoic acid; $sPLA_2$, secretory phospholipase A_2; MD, molecular dynamics; RAR, retinoic acid receptor; RXR, retinoic X receptor; rmsd, root-mean-square deviation; S, substrate; PMB, *p*-methoxybenzyl; DDQ, 2,3-dichloro-5,6-dicyano-1,4-benzoquinone; DBU, 1,8-diazabicyclo[5.4.0]undec-7-ene; DIAD, diisopropyl azodicarboxylate; NBS, *N*-bromosuccinimide; DLS, dynamic light scattering; DPPG, 1,2-dipalmitoyl-*sn*-glycero-3-phosphoglycerol; DSPG, 1,2-distearoyl-*sn*-glycero-3-phosphoglycerol; 1-*O*-DSPG, 1-*O*-stearyl-2-stearoyl-*sn*-glycero-3-phosphoglycerol; POPG, 1-palmitoyl-2-oleoyl-*sn*-glycero-3-phosphoglycerol; NBD-DPPE, 1,2-dipalmitoyl-*sn*-glycero-3-phosphoethanolamine-*N*-[7-nitro-2-1,3-benzoxadiazol-4-yl]; MALDI-TOF, matrix-assisted laser desorption/ionization time-of-flight; DHB, 2,5-dihydroxybenzoic acid; MTT, 3-(4,5-dimethylthiazolyl)-2,5-diphenyltetrazolium bromide.

 Published on Web 04/20/2010

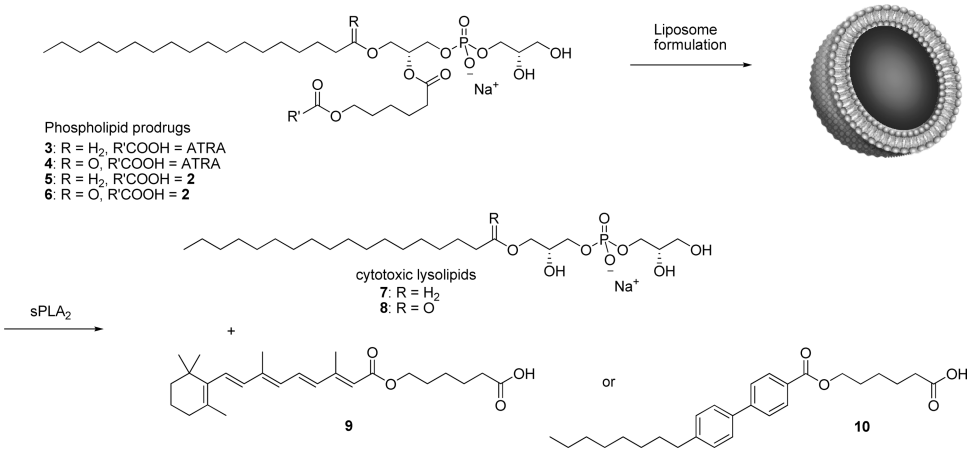

Figure 2. The $sPLA_2$ degradable phospholipid prodrugs **3**−**6**, with an aliphatic C_6-linker incorporated between the drug, R′COOH (ATRA or **2**), and the lipid backbone.

β, γ), and/or the subtype RAR isoforms, α1, α2, β1−β5, γ1, and γ2.[3a,10] The lack of selectivity is believed to be responsible for the severe side effects that have been observed during chronic administration of ATRA,[10] and therefore there is much interest in discovering more selective RAR agonists.[11] Targeting of RARβ2 has been found to have a suppressive effect on human tumors,[12] and recently 4-(4-octylphenyl)-benzoic acid (**2**, Figure 1) was identified as a selective RARβ2 agonist.[13] The lipophilicity of **2** makes it is a good candidate for incorporation into a liposomal drug delivery system through covalent attachment to the lipid backbone. However, since Bonsen et al. have demonstrated that benzoic acid is not released from the *sn*-2-position by $sPLA_2$,[14] direct attachment of **2** to the phospholipids was ruled out. Instead, we decided to investigate how attachment of an aliphatic C_6-linker would influence the cytotoxicity of **2** and the $sPLA_2$ activity toward the corresponding prodrug.

The retinoid−lipid prodrugs are designed to include the phosphatidylglycerol headgroup because human $sPLA_2$ IIA has strong affinity for negatively charged phospholipids.[15] The lipid backbone of the prodrugs contains either an *sn*-1-ester or an *sn*-1-ether functionality. Upon activation of $sPLA_2$, the prodrugs will be converted into the free drug and lysolipids (Figure 2) and while *sn*-1-ether lysolipids have good metabolic stability and are cytotoxic against many cell lines,[16] *sn*-1-ester lysolipids are rapidly metabolized (by e.g., lysophospholipases) and have been dismissed as suitable lysolipid drug candidates.[16a] Information about the cytotoxicity of *sn*-1-ester lysolipids is limited and covers only lysophosphatidylcholine lipids,[17] but these lipids have shown to be slightly better substrates for $sPLA_2$ than *sn*-1-ether lipids.[18] Therefore, we found it interesting to synthesize both types of prodrugs in order to study their relative hydrolysis rate and cytotoxicity.

Molecular Dynamics Simulations

Molecular dynamics (MD) simulations were performed to understand why **1** is not hydrolyzed by $sPLA_2$[7b] and which structural modification(s) of the prodrug would regain enzymatic hydrolysis. Simulations were carried out for $sPLA_2$−DPPG, $sPLA_2$−**1**, and as discussed below also for $sPLA_2$−**3** and $sPLA_2$−**5**. Simulations for each complex were repeated five times to estimate the statistical uncertainties in the calculated quantities. The stability of the simulations of the different $sPLA_2$ complexes were checked by computing the

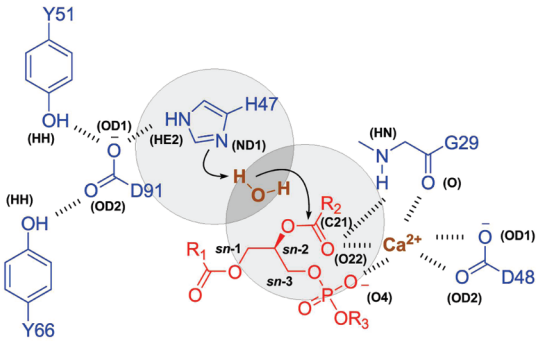

Figure 3. Representation of the active site in $sPLA_2$ with hydrogen bonds and ionic interactions indicated with dashed bonds. Key protein residues are drawn in blue, the substrate in red, and the calcium ion and the water molecule both in brown. The two gray circles indicate the *H*−*S* region, where the overlap in dark gray represents the water count region. Labels are shown in black, and atom types indicated in parentheses refer to the Protein Data Bank nomenclature.

time evolution of the root-mean-square deviation (rmsd) of the Cα atoms with respect to the protein structure obtained after minimization. Stable rmsd data were obtained after 1−2 ns for the $sPLA_2$−DPPG, $sPLA_2$−**3** and $sPLA_2$−**5** complexes reaching a plateau of ∼1.4 Å (Supporting Information). rmsd data for the $sPLA_2$−**1** complex were not stable, increasing to ∼2.5 Å after ∼6.5 ns (Supporting Information).

A prerequisite for successful hydrolysis is that a stable Michaelis−Menten complex is obtained and that a water molecule acting as a nucleophile can enter the catalytic cleft. To monitor the stability of the Michaelis−Menten complex, we have chosen distances according to their importance in the calcium-dependent enzymatic reaction.[19] The catalytic mechanism has been identified by X-ray crystallography, revealing that the catalytic device of $sPLA_2$ is essentially characterized by an aspartic acid−histidine dyad, a calcium-binding site, and a water molecule acting as the nucleophile. A schematic representation of the catalytic mechanism is shown in Figure 3, indicating that the calcium ion (cofactor) is coordinated to the D48 carboxylate groups (atoms: OD1 and OD2), the G29 carbonyl (O), the carbonyl (O22) in the substrate (S), and the phosphate (O4) in S. Atom types given in parentheses refer to the Protein Data Bank nomenclature. Furthermore, the catalytic residue, H47, is stabilized by D91,

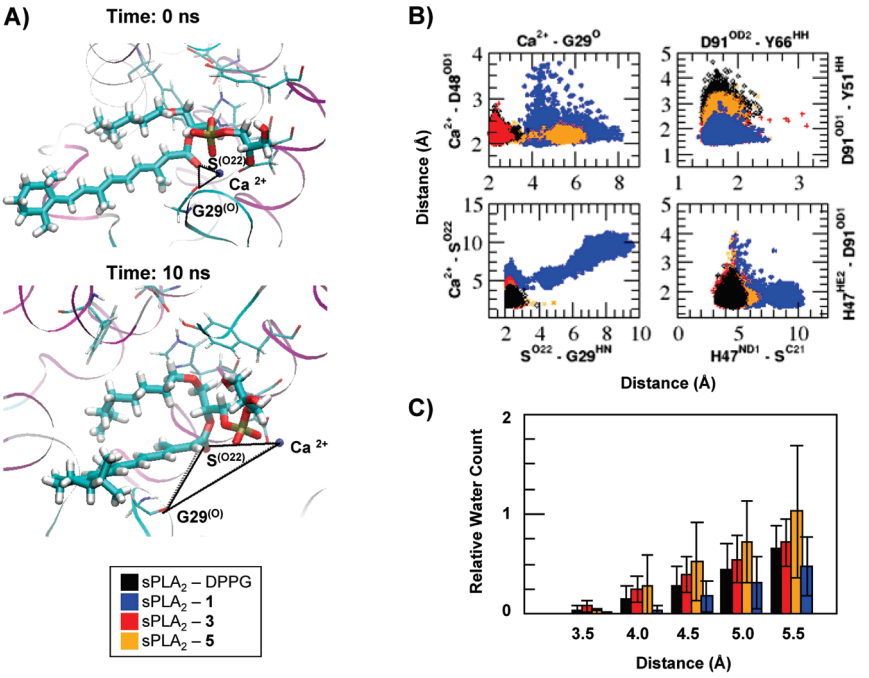

Figure 4. (A) ATRA induced structural perturbation of the Michaelis−Menten complex. Images taken at the beginning (top) and at the end (bottom) of an sPLA$_2$−**1** simulation revealed that ATRA induced conformational changes (as evident from the G29$^{(O)}$−Ca^{2+}−S$^{(O22)}$ distances indicated by the triangles) leading to the distortion of the Michaelis−Menten complex. (B) 2D scatter plots of distances between selected residue pairs important for stabilizing the Michaelis−Menten complex. (C) Histograms of relative water counts as a function of distance from both H47^{ND1} and S^{C21} (*H*−*S* region; Figure 3).

which forms hydrogen bonds with Y51 and Y66. The water molecule acting as the nucleophile enters the region between H47^{ND1} and S^{C21}. This region will be referred to as the *H*−*S* region (Figure 3).

We have checked the stability of the Michaelis−Menten complexes by monitoring the following distances during the simulations: Ca^{2+}−G29^{O}, Ca^{2+}−D48^{OD1}, Ca^{2+}−S^{O22}, S^{O22}−G29^{HN}, H47^{HE2}−D91^{OD1}, H47^{ND1}−S^{C21}, D91^{OD2}−Y66^{HH}, and D91^{OD1}−Y51^{HH}. The time evolution of these distances is provided in the Supporting Information, and 2D scatter plots are shown in Figure 4.

For prodrug **1**, no stable Michaelis−Menten complex could be observed, and hence in accordance with experimental data, no hydrolysis can occur. The rigid nature of the ATRA ester at the *sn*-2-position of the prodrug causes distortion of several distances involved in the Michaelis−Menten complex (Figure 4). For instance, distances Ca^{2+}−S^{O22} and G29^{HN}−S^{O22} are significantly larger for sPLA$_2$−**1** than sPLA$_2$−DPPG (Figure 4). The distortion is also highlighted by the images taken at the beginning and upon completion of an sPLA$_2$−**1** simulation, respectively (Figure 4). Introduction of a C$_6$-linker between the phospholipid backbone and **1** was sufficient to confer stability of the Michaelis−Menten complex in sPLA$_2$−**3** and sPLA$_2$−**5**.

Although a stable Michaelis−Menten complex could be obtained by introducing a C$_6$-linker, the question remained if water can reach the *H*−*S* region (Figure 3) in sPLA$_2$ complexed with **3** or **5**. To quantify the probability that water molecules enter the *H*−*S* region, we counted the number of water molecules within certain distances (d = 3 Å − 6 Å; Δd = 0.5 Å) from both H47^{ND1} and S^{C21}, and the counts were normalized by dividing the respective water counts by the water count determined at 6 Å (Figure 4). Averages and standard deviations of normalized water counts were calculated from the five simulations of each complex. The relative water counts extracted from sPLA$_2$−**3** and −**5** simulations were similar to those extracted from sPLA$_2$−DPPG simulations (Figure 4). Contrarily, the relative water counts extracted from sPLA$_2$−**1** were very low when compared to the other complexes. Because complexes of DPPG, **3**, and **5** show similar relative water counts and their Michaelis−Menten complexes are stable, these results predict that **3** and **5** will be hydrolyzed by sPLA$_2$.

Synthesis of Retinoid Esters

The linker moiety *tert*-butyl 6-hydroxyhexanoate (**11**)[20] was coupled with ATRA by a Mitsunobu reaction (Scheme 1),[21] which we previously have demonstrated as a reliable method for forming esters of ATRA.[7b] The following *tert*-butyl deprotection led to degradation of the ATRA skeleton under acidic conditions (5% TFA or $ZnBr_2$[22] in CH_2Cl_2 or HF in MeCN), but using 2,6-lutidine and TMSOTf in CH_2Cl_2[23] afforded the carboxylic acid **9** in a good yield (Scheme 1). The ATRA ester **9** was isolated as yellow crystals and was stable when stored at −20 °C under an inert atmosphere, whereas the oily *tert*-butyl ester of **9** decomposes upon less than one month of storage. This highlights the importance of storing ATRA-analogues as solids in order to avoid decomposition. The corresponding linker-molecule of **2**[24] was synthesized by a Steglich coupling[25] with **11** followed by a deprotection of the *tert*-butyl ester with TFA in CH_2Cl_2 (Scheme 1). In contrast to the ATRA-analogues, we never observed any decomposition of the synthetic derivatives of **2** neither as oils nor solids. The cytotoxicity of ATRA, **2**, **9**, and **10** were evaluated in three cell lines, and the retinoid esters had activities comparable to the acids (vide infra).

Synthesis of Lipid Prodrugs

The cytotoxicity of the esters **9** and **10** and the results from the MD simulations prompted us to proceed with the synthesis

Scheme 1. Synthesis of the Retinoid Esters[a]

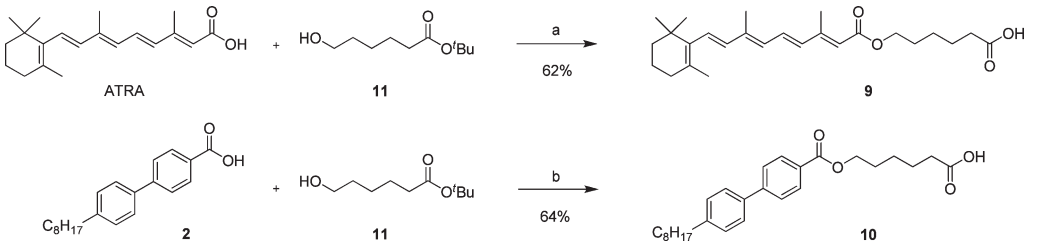

[a] Reagents: (a) (i) diisopropyl azodicarboxylate (DIAD), PPh_3, THF; (ii) TMSOTf, 2,6-lutidine, CH_2Cl_2; (b) (i) dicyclohexylcarbodiimide (DCC), DMAP, CH_2Cl_2; (ii) TFA, triisopropylsilane, CH_2Cl_2.

Scheme 2. Synthesis of the Lipid Precursors **15** and **18**[a]

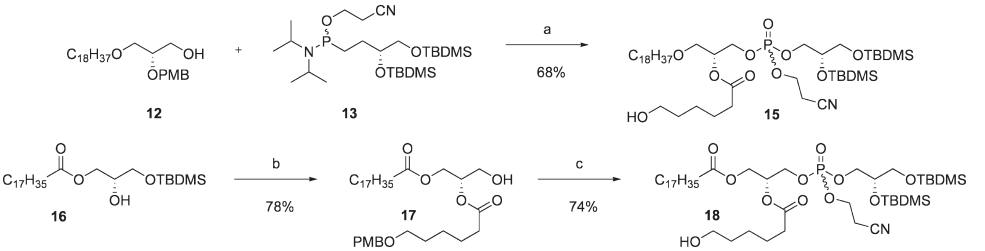

[a] Reagents: (a) (i) tetrazole, CH_2Cl_2, MeCN; (ii) ^{t}BuOOH; (iii) DDQ, H_2O, CH_2Cl_2; (iv) **14**, DCC, DMAP, CH_2Cl_2; (v) DDQ, H_2O, CH_2Cl_2; (b) (i) **14**, EDCI, DMAP, CH_2Cl_2; (ii) NBS, DMSO, THF, H_2O; (c) (i) **13**, tetrazole, CH_2Cl_2, MeCN; (ii) ^{t}BuOOH; (iii) DDQ, H_2O, CH_2Cl_2.

Scheme 3. Synthesis of the *sn*-1-Ether and *sn*-1-Ester prodrugs **3**, **4**, **5**, and **6**[a]

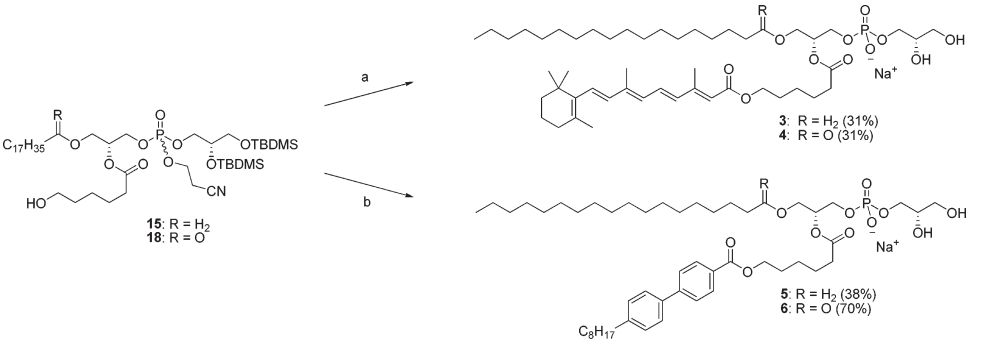

[a] Reagents: (a) (i) **15**, ATRA, DIAD, PPh_3, THF or **18**, ATRA, DCC, DMAP, Et_3N, Et_2O; (ii) DBU, CH_2Cl_2; (iii) HF, H_2O, CH_2Cl_2, MeCN; (b) (i) **2**, DCC, DMAP, CH_2Cl_2; (ii) DBU, CH_2Cl_2; (iii) HF, H_2O, CH_2Cl_2, MeCN.

of the corresponding *sn*-1-ether and *sn*-1-ester lipid prodrugs **3**−**6**. The backbone of the *sn*-1-ether prodrugs was constructed by a tetrazole mediated coupling of alcohol **12** and phosphoramidite **13**, followed by an oxidation of the phosphite to the phosphate with ^{t}BuOOH (Scheme 2).[7a] Deprotection of the *p*-methoxybenzyl (PMB) group in moist CH_2Cl_2 with 2,3-dichloro-5,6-dicyano-1,4-benzoquinone (DDQ) afforded the secondary alcohol, which was reacted with 6-(4-methoxybenzyloxy)-1-hexanoic acid (**14**) to give an ester. The newly introduced PMB-group was then removed, affording alcohol **15** in an overall yield of 51% (Scheme 2). Secondary alcohol **16**, synthesized from 2,3-*O*-isopropylidene-*sn*-glycerol according to the procedures by Gaffney et al[26] and Burgos et al.,[27] served as the starting material for the *sn*-1-ester prodrugs (Scheme 2). Diester **17** was obtained by coupling of **14** and **16**, and the following TBDMS deprotection was best achieved using *N*-bromosuccinimide (NBS) in a mixture of DMSO, THF, and H_2O (Scheme 2),[27,28] while alternative conditions like Bu_4NF and imidazole in THF[29] or HF in MeCN led to a significant degree of acyl migration. Mosher ester analysis[30] of **17** showed that the enantiomeric purity was >95%. The phosphate headgroup was attached in the same way as for the *sn*-1-ether lipids, and PMB deprotection gave the primary alcohol **18** (Scheme 2). Phospholipids **15** and **18** were converted to the desired prodrugs of ATRA and **2** (Scheme 3). The ATRA moiety was introduced either by the Mitsunobu reaction or the Steglich coupling, and the final prodrugs **3** and **4** were obtained after removal of the cyanoethyl group with 1,8-diazabicyclo[5.4.0]undec-7-ene (DBU) and TBDMS-deprotection mediated by HF in MeCN/CH_2Cl_2/H_2O. Prodrugs **5** and **6** were accessed by coupling between **2** and the primary alcohols **15** and **18**, after which the remaining chemistry was similar to the synthesis of **3** and **4** (Scheme 3). ^{31}P NMR of the synthesized prodrugs showed one signal resonating between −1 ppm and 2 ppm, demonstrating high diastereomeric and regioisomeric purity (>95%).

Biophysical Characterization

The lipid prodrugs (**3**−**6**) were formulated as liposomes by extrusion in HEPES buffer using the dry lipid film technique,[31] yielding clear solutions. The particle size of the formulated

Table 1. Measurement of Particle Size with DLS

	particle size	
prodrug	diameter (nm)	polydispersity index
3	94	0.08
4	97	0.13
5	118	0.16
6	118	0.05

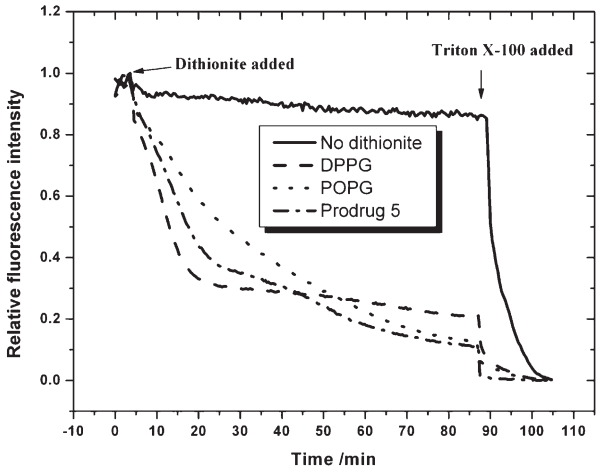

Figure 5. Time-dependent fluorescence from NBD labeled lipids quenched by dithionite.

lipids was measured by dynamic light scattering (DLS). The DLS analysis revealed that all of the lipids were able to form particles with a diameter around 100 nm (Table 1 and Supporting Information) and with a low polydispersity, indicating the formation of unilamellar vesicles. The formation of a unilamellar bilayer is further supported by the fluorometric procedure described by McIntyre et al.,[32] which was used to study the permeability. Vesicles formed from prodrug **5** was compared to vesicles of 1,2-dipalmitoyl-*sn*-glycero-3-phosphoglycerol (DPPG) and 1-palmitoyl-2-oleoyl-*sn*-glycero-3-phosphoglycerol (POPG). The lipids were formulated with 1,2-dipalmitoyl-*sn*-glycero-3-phosphoethanolamine-*N*-[7-nitro-2-1,3-benzoxadiazol-4-yl] (NBD-DPPE, 0.15 mol %). The fluorescence of the NBD group was monitored over time before and after the addition of dithionite ($S_2O_4^{-2}$), which functions as a quenching agent. At the end of the experiment, the detergent Triton X-100 was added to solubilize the lipid vesicles and cause 100% quenching (see Figure 5). As evident from the figure, the decrease in the fluorescence of the NBD-labeled gel-state DPPG occurs in two distinct steps, an immediate and fast one completed after 20 min followed by much slower decay of fluorescence. We anticipate that the quick drop in fluorescence signal corresponds to quenching of the dye in the outer leaflet and is dependent on the fraction of lipids exposed to the surrounding, i.e., vesicle size and lamellarity. The slower second step is due to quenching of the dye in the inner leaflet, which is controlled by membrane permeability to dithionite. In the case of the fluid POPG vesicles, the quenching of both leaflets occurs simultaneously, resulting effectively in a single exponential-like decay in the NBD fluorescence. A comparable behavior for gel-state and fluid membranes has been reported previously.[32,33] The quenching of the NBD-labeled vesicles for prodrug **5** resembles that of DPPG, demonstrating that **5** forms a bilayer membrane, however seemingly more permeable to dithionite than the vesicles of DPPG.

Differential scanning calorimetry scans (15−65 °C) of the lipid solutions of **3** and **5** displayed no gel-to-liquid crystalline or any other thermotropic phase transition in the tested temperature range (data not shown), indicating that the lipid bilayers are in a fluid state. This was not surprising taking into account the bulky and stiff nature of the substituents in the *sn*-2-position, which hampers well-ordered chain packing.

The ability of $sPLA_2$ to hydrolyze the formulated lipids at 37 °C was investigated with matrix-assisted laser desorption/ionization time-of-flight (MALDI-TOF) MS. MALDI-TOF MS is a fast and sensitive technique which has been shown to be a reliable tool for detection of lipids.[34] In Figure 6, the obtained MS data for the *sn*-1-ether prodrug **3** subjected to purified $sPLA_2$ from snake (*Agkistrodon piscivorus piscivorus*) venom is shown. Gratifyingly, and as evident from the spectra (Figure 6), the prodrug ($M + H^+$) is consumed by the enzyme and the desired constituents, lysolipid **7** ($M + H^+$) and ATRA ester **9** ($M + Na^+$), are released. The MALDI-TOF MS analysis of the *sn*-1-ether prodrugs **3** and **5** and the *sn*-1-ester prodrugs **4** and **6** revealed that all of the prodrugs were degraded by the enzyme (Table 2) and the desired molecules were released (see Supporting Information). The observation that the *sn*-1-ether prodrugs were consumed by $sPLA_2$ to the same extent as the *sn*-1-ester prodrugs illustrate and confirm that *sn*-1-ether phospholipids are excellent substrates for $sPLA_2$. On the basis of the MALDI-TOF MS analysis of the $sPLA_2$ activity on the various prodrugs, we can conclude that the incorporation of an aliphatic C_6-linker between ATRA and the lipid backbone resolved the issue of $sPLA_2$ activity on ATRA-lipid prodrugs. The experimental observations are in agreement with the outcome from the MD simulations, illustrating the power and potential of using MD simulations in the design of $sPLA_2$ degradable lipid prodrugs. To rule out that the degradation of the prodrugs was caused by nonenzymatic hydrolysis, a sample of each prodrug was subjected to the reaction conditions in the absence of $sPLA_2$. As evident from the spectra in Figure 6 (and in Supporting Information), no degradation of the prodrugs was observed within 48 h and none of the release products were detectable. Finally, we compared the enzyme activity of the purified $sPLA_2$ from snake (*Agkistrodon piscivorus piscivorus*) venom with the commercially available $sPLA_2$ from snake (*Naja mossambica mossambica*) venom, and as can be seen in Table 2, the two enzymes perform equally well on all substrates.

Fawzy et al.[35] and Hope et al.[36] have demonstrated two decades ago that ATRA is an inhibitor for $sPLA_2$, reporting IC_{50} values of < 50 and 10 μM respectively. However, we have later shown that DPPG is fully hydrolyzed by $sPLA_2$ in the presence of 0.1 and 1.0 equiv of ATRA,[7b] proving that the lack of hydrolysis for the ATRA-lipid prodrug **1** is not a consequence of inhibition by ATRA. These observations are further supported by the present work, in which it was found that **9** ($IC_{50} = 8\ \mu M$, $K_i = 6\ \mu M$, see Supporting Information) inhibits $sPLA_2$ at the same level as ATRA ($IC_{50} = 15\ \mu M$, $K_i = 11\ \mu M$), and whereas the ATRA-lipid prodrug **1** is not consumed by the enzyme, the prodrugs **3** and **4** are fully degraded. This demonstrates that under the conditions used, the released ATRA ester **9** does not inhibit $sPLA_2$, and the difference in degradation of the prodrugs therefore solely relies on the ability of $sPLA_2$ to hydrolyze the different prodrugs. Additionally, Cunningham et al. have reported K_i values < 100 nM[37] for potent $sPLA_2$ inhibitors, illustrating that ATRA and **9** are weak inhibitors.

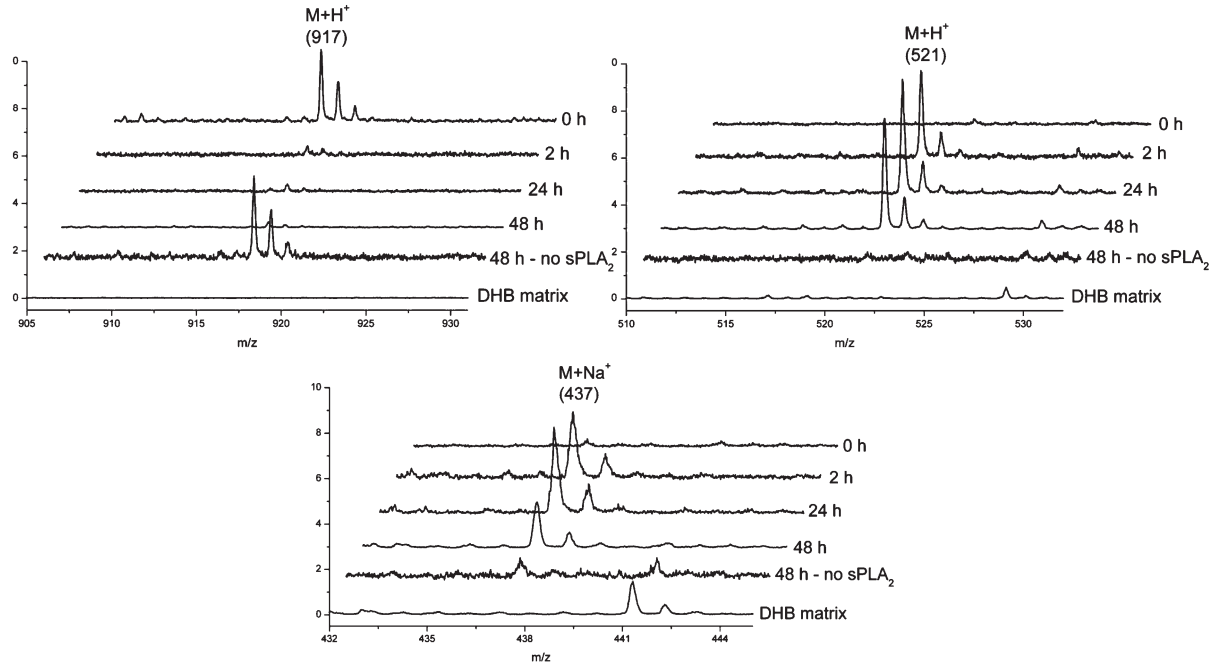

Figure 6. MALDI-TOF MS monitoring of snake (*Agkistrodon piscivorus piscivorus*) venom $sPLA_2$ activity on the *sn*-1-ether prodrug **3**. The spectra demonstrate that the prodrug **3** (top left) is consumed and that the lysolipid **7** (top right) and the ATRA ester **9** (bottom) are released.

Table 2. Measurement of $sPLA_2$ Activity on the Prodrugs by MALDI-TOF MS

	hydrolysis by $sPLA_2$[a]	
prodrug	*Agkistrodon piscivorus piscivorus*	*Naja mossambica mossambica*
3	+	nd
4	+	+
5	+[b]	+[b]
6	+	+

[a] Determined by MALDI-TOF MS after 48 h incubation at 37 °C with purified $sPLA_2$ from snake (*Agkistrodon piscivorus piscivorus* or *Naja mossambica mossambica*) venom. [b] After 48 h, a small signal for prodrug **5** remains; nd = not determined.

Cytotoxicity

The cytotoxicity of ATRA, **2**, **9**, and **10** were evaluated in MT-3 breast carcinoma, HT-29 colon carcinoma, and Colo205 colon adenocarcinoma cell lines (Table 3). Interestingly, the retinoid esters were either more active than ATRA and **2** or equal in potency in the tested cell lines. A possible explanation for the enhanced activity of these molecules is that the derivatization increases the lipophilicity of the drugs, augmenting transport over the cell membrane. RARβ2 agonists **2** and **10** showed very little activity against HT-29 cells, and presumably this is because growth inhibition in this cell line is induced by RARα agonists[38] and **2** has a low affinity for that receptor.[13] The result is also a strong indication that the cytotoxicity of **10** in MT-3 and Colo205 originate from RARβ2 activation.

The cytotoxicity of the prodrugs **3**−**6** was investigated in HT-29 colon carcinoma and Colo205 colon adenocarcinoma cells. HT-29 colon carcinoma cells do not secrete $sPLA_2$, which allowed us to test the activity in the presence and absence of $sPLA_2$. As evident from Table 4 and the dose−response curve for **3** and **5** (Figure 7), none of the prodrugs were able to induce significant cell death in the absence of $sPLA_2$, whereas upon $sPLA_2$ addition, all of the prodrugs displayed IC_{50} values below 10 μM in HT-29 cells and complete cell death was obtained when higher concentrations were applied (see Figure 7). Evidently, the cytotoxicity is induced by $sPLA_2$ triggered breakdown of the prodrugs into **9** or **10** and the lysolipids. Interestingly, we observed that the *sn*-1-ester prodrug **6** in the presence of $sPLA_2$ displayed almost the same cytotoxicity toward HT-29 cells as the corresponding *sn*-1-ether prodrug **5**, and taking the low activity of **10** in HT-29 cells

Table 3. IC_{50} (μM) Values for the Retinoids in Three Cancer Cell Lines[a]

compd	MT-3 IC_{50} (μM)	HT-29 IC_{50} (μM)	Colo205 IC_{50} (μM)
ATRA	30 ± 4	4.3 ± 0.2	37 ± 1
9	17 ± 1	3.6 ± 1.8	17 ± 2
2	51 ± 3	> 200	> 200
10	14 ± 1	> 200	127 ± 18

[a] Cytotoxicity was measured using the MTT assay as cell viability 48 h after incubation with the indicated substances for 24 h and shown by mean ± SD (n = 3).

Table 4. IC_{50} (μM) Values for the Prodrugs **3**−**6**, the Lysolipids **7** and **8**, DSPG, and 1-*O*-DSPG in HT-29 and Colo205 Cancer Cell Lines[a]

compd	HT-29 IC_{50} (μM)	HT-29 + $sPLA_2$[b] IC_{50} (μM)	Colo205 IC_{50} (μM)
3	> 200	7 ± 2	16 ± 4
4	> 200	6 ± 1	12 ± 3
5	> 200	3 ± 1	7 ± 6
6	> 200	8 ± 1	19 ± 4
7	11 ± 6	nd	25 ± 2
8	7 ± 1	nd	22 ± 3
DSPG	> 200	25 ± 11	54 ± 7
1-*O*-DSPG	> 200	9 ± 2	33 ± 4
$C_{17}H_{35}COOH$	> 200	nd	> 200
$sPLA_2$	*c*	*c*	*c*

[a] Cytotoxicity was measured using the MTT assay as cell viability 48 h after incubation with the indicated substances for 24 h and shown by mean ± SD ($n \geq 3$); nd = not determined. [b] Snake (*Agkistrodon piscivorus piscivorus*) venom $sPLA_2$ was added to a final concentration of 5 nM. [c] No change in cell viability was observed after 24 h.

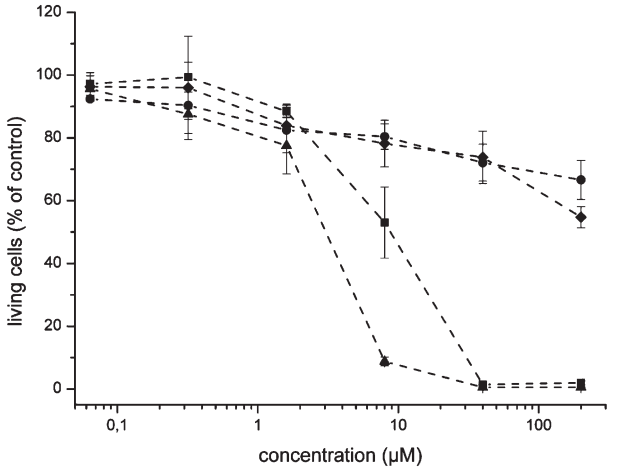

Figure 7. Dose−response curves for the treatment of HT-29 cells with the *sn*-1-ether prodrugs **3** (●), **3** + $sPLA_2$ (■), **5** (◆), and **5** + $sPLA_2$ (▲).

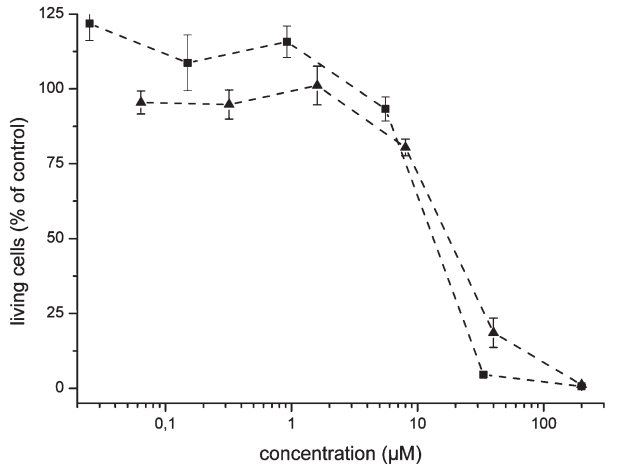

Figure 8. Dose−response curves for the treatment of Colo205 cells with *sn*-1-ester prodrugs **4** (■) and **6** (▲).

(Table 3) into account, these results indicate that *sn*-1-ester lysolipids (**8**) contribute with the same degree of potency as *sn*-1-ether lysolipids (**7**). These findings were verified when the free lysolipids **7** (see Supporting Information) and **8** were tested against HT-29 cells. Both lysolipids displayed IC_{50} values close to 10 μM, and similar results were obtained for DSPG and 1-*O*-stearyl-2-stearoyl-*sn*-glycero-3-phosphoglycerol (1-*O*-DSPG, see Supporting Information) in the presence of $sPLA_2$ (Table 4). We conclude that even though *sn*-1-ester lysolipids generally are rapidly metabolized, under these in vitro conditions, there is no significant metabolism of the lipid backbone and therefore we observe an equal potency of the two lysolipids. With the control experiments in hand, it is possible to determine the origin of the cytotoxicity of the prodrugs in HT-29 cells, and as evident from Tables 3 and 4, the majority of the activity arises from the lysolipids in prodrug **5** and **6** while for the prodrugs **3** and **4** there appear to be an equal contribution from the lysolipids (**7** and **8**) and the ATRA ester **9**. Colo205 cells express $sPLA_2$, and encouragingly, the four prodrugs induce cell death with IC_{50} values below 20 μM (Table 4) and complete cell death was obtained when higher concentrations were applied (see Figure 8), indicating that the secreted $sPLA_2$ in Colo205 cells provides the desired hydrolysis and release of the anticancer agents. Additionally, the prodrugs **3** and **4** displayed IC_{50} values below the free lysolipids but similar to **9**, indicating that the majority of the cytotoxicity can be ascribed to the released ATRA ester **9**. For prodrugs **5** and **6**, the IC_{50} values indicate a cumulative effect because these prodrugs are more potent than both of the released cytotoxic compounds by themselves, demonstrating the advantage of the prodrug formulation.

Conclusion

In the present study we have successfully synthesized lipid prodrugs of retinoids and demonstrated that they can be formulated as liposomes that are degraded by $sPLA_2$. On the basis of MD simulations, we incorporated a C_6-linker between the glycerol backbone of the lipids and the retinoids to overcome the lack of enzymatic activity stemming from the rigid nature of ATRA and **2**. The resulting prodrugs **3**−**6** were hydrolyzed completely by $sPLA_2$ within 24 h and were demonstrated to be cytotoxic to cancer cells in the presence of the enzyme.

The liposomal formulation is very well suited for active substances with low water solubility, and the novel prodrugs present a solution to formulation of retinoids for applications in cancer therapy. Furthermore, our findings underpin the overall strategy of covalently linking cytotoxic compounds to lipids and widen the scope of the approach because even very sterically hindered substrates can now be effectively incorporated into liposomes and released through an enzyme-triggered degradation.

Experimental Section

General. Starting materials, reagents, and solvents were purchased from Sigma-Aldrich and used without further purification. POPG, DPPG, DSPG, 1-stearoyl-2-hydroxy-*sn*-glycero-3-phospho-(1′-*rac*-glycerol) (**8**), and NBD-DPPE were purchased from Avanti Polar Lipids (Alabaster, AL). The purified snake venom $sPLA_2$ from *Agkistrodon piscivorus piscivorus* was donated by Dr. R. L. Biltonen (University of Virginia), and $sPLA_2$ from *Naja mossambica mossambica* was purchased from Sigma-Aldrich. CH_2Cl_2 was dried over 4 Å molecular sieves, and THF was dried over sodium/benzophenone and distilled before use. Evaporation of solvents was done under reduced pressure (in vacuo). TLC was performed on Merck aluminum sheets precoated with silica gel 60 F_{254}. Compounds were visualized by charring after dipping in a solution of Ce(IV) (6.25 g of $(NH_4)_6Mo_7O_{24}$ and 1.5 g of $Ce(SO_4)_2$ in 250 mL of 10% aq H_2SO_4) or an ethanolic solution of phosphomolybdenic acid (48 g/L). Flash column chromatography was performed using Matrex 60 Å silica gel. The purity of all tested compounds was found to be >95% by HPLC (see Supporting Information). HPLC was performed on a Waters Alliance HPLC equipped with a DAD, using a LiChrospher Si 60 column and eluting with water/isopropanol/hexane mixtures.[39] NMR spectra were recorded using a Bruker AC 200 MHz spectrometer, a Varian Mercury 300 MHz spectrometer, or a Varian Unity Inova 500 MHz spectrometer. Chemical shifts were measured in ppm and coupling constants in Hz, and the field is indicated in each case. IR analysis was carried out on a Bruker Alpha FT-IR spectrometer, and optical rotations were measured with a Perkin-Elmer 341 polarimeter. HRMS was recorded on an Ionspec Ultima Fourier transform mass spectrometer.

Molecular Dynamics Simulations. The crystal structures of bee venom (*Apis Mellifera*) phospholipase A_2 complexed with the transition-state analogue, L-1-*O*-octyl-2-heptylphosphonyl-*sn*-glycero-3-phosphoethanolamine (diC8(2Ph)PE),[19] resolved to 2.0 Å, and human phospholipase A_2 IIA complexed with 6-phenyl-4(*R*)-(7-phenyl-heptanoylamino)-hexanoic acid,[40] resolved to 2.1 Å, were obtained from the Protein Data Bank[41] (entry codes: 1poc and 1kqu, respectively). The initial modeling step

involved placing diC8(2Ph)PE into the binding cleft of human phospholipase A_2 IIA, as described previously.[18] A previously assembled $sPLA_2$−substrate complex[18] was used as the template to place lipid prodrugs into the active site. The optimized lipid prodrugs were manually overlapped with the pre-existing substrate, which was subsequently deleted. NAMD software[42] with the Charmm27 all-atom parameter set and TIP3 water model was used for all simulations.[43] The lipid prodrugs were first energy-minimized for 1000 steps before using them in simulations. Missing force field parameters for the prodrug molecules were taken from similar atom types in the CHARMM27 force field. The $sPLA_2$−lipid complexes were solvated using the program SOLVATE.[44] Eighteen water molecules were randomly replaced with chloride ions to neutralize the systems. Ultimately, the system contained ∼4900 water molecules in a simulation cell of dimensions $52.7 \times 51.7 \times 67.3$ Å^3. An initial energy minimization of the complex was carried out for 1000 steps, and the system was further minimized for 100, 200, 300, 400, and 500 steps to generate different starting structures. Periodic boundary conditions were applied in x, y, and z directions. Initial MD simulations were conducted for ∼100 ps in which each system was slowly heated to 300 K. Simulations were carried out for 10 ns in the NPT ensemble, i.e., at constant number of atoms (N), pressure (P), and temperature (T). A time step of 1 fs and an isotropic pressure of 1 atm using the Langevin piston method[45] were employed. Electrostatic forces were calculated using the particle mesh Ewald method with a uniform grid spacing of ∼1 Å.[46] A 12 Å cutoff was used for terminating the van der Waals interactions in combination with a switching function starting at 10 Å. Analysis of the trajectories were performed using the Visualization Molecular Dynamics software suite.[47]

Liposome Preparation and Particle Size Determination. The lipid prodrugs **3**−**6** were dissolved in $CHCl_3$ in a glass tube and dried under vacuum for 15 h to form a thin film. The lipid prodrugs (2 mM) were solubilized by addition of aqueous buffer (0.15 M KCl, 30 μM $CaCl_2$, 10 μM EDTA, 10 mM HEPES, pH 7.5) and vortexed periodically over 1 h at 20 °C. Subsequently, the solutions were extruded through a 100 nm polycarbonate cutoff membrane (20−30 repetitions) using a Hamilton syringe extruder (Avanti Polar Lipids, Birmingham, AL). The particle size distribution of the formulated lipids was measured by DLS. The DLS measurements were obtained using a Zetasizer nano particle analyzer (ZS ZEN3600, Malvern Instrument, Westborough, MA).

Permeability Assay. The permeability of the lipid vesicles was examined using the procedure described by McIntyre et al.[32] The lipid vesicles were labeled with NBD-DPPE (0.15 mol %) and prepared in an aqueous buffer (10 mM HEPES, 1 M sucrose, 150 mM NaCl, pH 7.4) by sonication for 30 min at 45 °C and then extrusion through a 100 nm filter at 45 °C. Sucrose was added to minimize the osmolarity difference between the external solution and the vesicle interior that will arise after the addition of dithionite.[48] The experiments were performed in duplicates or more using FLUOstar Omega microplate reader (BMG LABTECH) in a 96-well microplate at 20 °C (150 μL). The lipid samples (100 μM) were allowed to equilibrate at 20 °C before the addition of sodium dithionite ($Na_2S_2O_4$) solution (33 mM), which was used as a quenching agent. Because of the high instability of dithionite,[49] the dithionite solution was freshly prepared prior to use. The NBD fluorescence was observed at 520 nm (ex 485 nm). After 85 min, Triton X-100 was added to the medium (0.3 wt %).

$sPLA_2$ Activity Measurements Monitored by MALDI-TOF MS. The formulated lipid prodrugs (0.40 mL, 2 mM) were diluted in an aqueous buffer (2.1 mL, 0.15 M KCl, 30 μM $CaCl_2$, 10 μM EDTA, 10 mM HEPES, pH 7.5), and the mixture was stirred at 37 °C in a container protected from light. The catalytic reaction was initiated by addition of snake (*Agkistrodon piscivorus piscivorus* (20 μL, 42 μM) or *Naja mossambica mossambica* (12 μL, 71 μM)) venom $sPLA_2$. Sampling was done after 0, 2, 24, and 48 h by collecting 100 μL of the reaction mixture and rapidly mixing it with a solution of $CHCl_3$/MeOH/H_2O/AcOH 4:8:1:1 (0.5 mL) in order to stop the reaction. The mixture was washed with water (0.5 mL), and the organic phase (80 μL) was isolated by extraction and then concentrated in vacuo. The extract was mixed with 9 μL of 2,5-dihydroxybenzoic acid (DHB) matrix (0.5 M DHB, 2 mM CF_3COONa, 1 mg/mL DPPG in MeOH), and 0.5 μL of this mixture was used for the MS analysis.

Cytotoxicity. Colon cancer HT-29 cells were cultured in McCoy's 5A medium in the presence of 10% fetal calf serum and 1% Pen-Strep (InVitrogen). Breast cancer MT-3 and colon cancer Colo205 cells were cultured in RPMI 1640 supplemented with 10% fetal calf serum and 1% Pen-Strep in a humidified atmosphere containing 5% CO_2. Colo205 cells secrete $sPLA_2$-IIa, however as the cytotoxicity assay was made with low cell density and for a short incubation period, inadequate concentrations were reached in the medium, which is why conditioned medium was used. Conditioned medium was made as follows: Colo205 cells were grown to confluency for 72 h, at which point the cells were pelleted and the medium, which contained approximately 100 ng/mL $sPLA_2$ IIA, was collected and used for the assay. Cells were plated in 96-well plates at a density of 1×10^4 cells per well for HT-29 and MT-3 cells and 2×10^4 cells per well for Colo205 cells, 24 h prior to addition of the tested compound. The retinoids (ATRA, **2**, **9**, **10**, and stearic acid) were solubilized in DMSO and water (final DMSO concentration ≤0.5%). Liposomes were diluted in PBS, and initial lipid concentrations in the liposome solutions were determined by phosphorus analysis.[50] After 24 h of incubation, the substances were removed and the cells were washed and incubated in complete medium for another 48 h. Cytotoxic activity was assessed using a standard 3-(4,5-dimethylthiazolyl)-2,5-diphenyltetrazolium bromide (MTT) assay (Cell Proliferation Kit I, Roche, Germany).[51] Cell viability is expressed as percentage reduction of incorporated MTT.

1-*O*-Octadecyl-2-(6-(all-*trans*-retinoyloxy)-hexanoyl)-*sn*-glycero-3-phospho-(*S*)-glycerol (3). Alcohol **15** (13 mg, 0.014 mmol), ATRA (6 mg, 0.019 mmol), and PPh_3 (9 mg, 0.043 mmol) were dissolved in THF (1.0 mL). DIAD (11 μL, 0.043 mmol) was added, and the reaction mixture was stirred at 20 °C for 1 h and then concentrated in vacuo and purified by flash column chromatography (heptane/EtOAc 2:1 then heptane/EtOAc 1:2) to give 13 mg that was dissolved in CH_2Cl_2 (1.0 mL) and DBU (2 μL, 0.012 mmol) was added. The reaction mixture was stirred for 30 min at 20 °C and then purified directly by flash column chromatography (heptane/EtOAc 1:1 then CH_2Cl_2/MeOH 9:1) to afford 8 mg that was dissolved in MeCN (0.9 mL) and CH_2Cl_2 (0.3 mL) and cooled to 0 °C. Aqueous HF (40%, 30 μL) was added dropwise, and the reaction mixture was allowed to reach 20 °C. After 3.5 h, the reaction was quenched by dropwise addition of $MeOSiMe_3$ (0.3 mL) and the mixture was stirred for 30 min, after which $NaHCO_3$ (6 mg, 0.07 mmol) was added and the mixture was concentrated in vacuo and purified by flash column chromatography (CH_2Cl_2/MeOH 10:1 then CH_2Cl_2/MeOH 4:1) to afford 4 mg (31% over 3 step) of **3** as a yellow amorphous solid. R_f = 0.44 (CH_2Cl_2/MeOH 4:1). ^{1}H NMR (500 MHz, $CDCl_3$/CD_3OD 4:1): δ 7.02 (dd, J = 15.0, 11.4 Hz, 1H), 6.32−6.27 (m, 2H), 6.15 (d, J = 11.4 Hz, 1H), 6.14 (d, J = 16.2 Hz, 1H), 5.77 (s, 1H), 5.18−5.13 (m, 1H), 4.11 (t, J = 6.6 Hz, 2H), 4.03−3.94 (m, 2H), 3.94−3.90 (m, 2H), 3.82−3.77 (m, 1H), 3.62 (t, J = 5.2 Hz, 2H), 3.60−3.57 (m, 2H), 3.49−3.39 (m, 2H), 2.39−2.33 (m, 5H), 2.05−2.00 (m, 5H), 1.72 (s, 3H), 1.71−1.60 (m, 6H), 1.57−1.51 (m, 2H), 1.50−1.45 (m, 2H), 1.45−1.40 (m, 2H), 1.31−1.23 (m, 30H), 1.03 (s, 6H), 0.88 (t, J = 6.9 Hz, 3H). ^{13}C NMR (50 MHz, $CDCl_3$/CD_3OD 4:1): δ 174.0, 168.0, 153.7, 140.0, 138.0, 137.7, 135.3, 131.7, 130.3, 129.8, 129.2, 118.5, 72.2 (2C), 71.2, 69.4, 66.7, 64.5, 64.1, 62.7, 40.0, 34.5 (2C), 33.4, 32.3, 30.1, 29.7 (12C), 29.2 (2C), 28.7, 26.4, 25.9, 24.9, 23.0, 22.0, 19.6, 14.3, 14.1, 13.3. IR (neat) 3325, 2923, 2853, 1733, 1709, 1609, 1584, 1457, 1259, 1064, 798 cm^{-1}; m/z (M + H$^+$) 917.58.

1-Octadecanoyl-2-(6-(all-*trans*-retinoyloxy)-hexanoyl)-*sn*-glycero-3-phospho-(*S*)-glycerol (4). Alcohol **18** (47 mg, 0.052 mmol), ATRA (31 mg, 0.104 mmol), DMAP (13 mg, 0.104 mmol), and Et_3N (72 μL, 0.52 mmol) were dissolved in Et_2O (1.2 mL). DCC (27 mg, 0.13 mmol) was added, and the reaction mixture was stirred at 20 °C for 22 h and then concentrated in vacuo and purified by flash column chromatography (toluene then toluene/EtOAc 5:1) to give 32 mg that was dissolved in CH_2Cl_2 (2.2 mL) and DBU (4.2 μL, 0.028 mmol) was added. The reaction mixture was stirred for 30 min at 20 °C and then purified directly by flash column chromatography (heptane/EtOAc 1:1 then CH_2Cl_2/MeOH 9:1) to afford 21 mg that was dissolved in MeCN (1.5 mL) and CH_2Cl_2 (0.5 mL) and cooled to 0 °C. Aqueous HF (40%, 90 μL) was added dropwise, and the reaction mixture was allowed to reach 20 °C. After 3.5 h, the reaction was quenched by dropwise addition of $MeOSiMe_3$ (0.3 mL) and the mixture was stirred for 30 min, after which $NaHCO_3$ (6 mg, 0.07 mmol) was added and the mixture was concentrated in vacuo and purified by flash column chromatography (CH_2Cl_2/MeOH 10:1 then CH_2Cl_2/MeOH 4:1 then CH_2Cl_2/MeOH/H_2O 65:25:1) to afford 15 mg (31% over 3 step) of **4** as a yellow amorphous solid. R_f = 0.56 (CH_2Cl_2/MeOH 5:1). ^{1}H NMR (500 MHz, $CDCl_3$/CD_3OD 4:1): δ 7.02 (dd, J = 15.0, 11.4 Hz, 1H), 6.32−6.27 (m, 2H), 6.15 (d, J = 11.4 Hz, 1H), 6.15 (d, J = 16.2 Hz, 1H), 5.77 (s, 1H), 5.25−5.20 (m, 1H), 4.39 (dd, J = 12.0, 3.3 Hz, 1H), 4.16 (dd, J = 12.0, 6.6 Hz, 1H), 4.11 (t, J = 6.6 Hz, 2H), 3.99−3.91 (m, 4H), 3.83−3.78 (m, 1H), 3.63 (t, J = 5.1 Hz, 2H), 2.36 (t, J = 7.5 Hz, 2H), 2.34 (s, 3H), 2.31 (t, J = 7.6 Hz, 2H), 2.05−2.00 (m, 5H), 1.71 (s, 3H), 1.71−1.65 (m, 4H), 1.65−1.57 (m, 4H), 1.50−1.45 (m, 2H), 1.45−1.41 (m, 2H), 1.34−1.21 (m, 28H), 1.03 (s, 6H), 0.88 (t, J = 7.0 Hz, 3H). ^{13}C NMR (50 MHz, $CDCl_3$/CD_3OD 4:1): δ 174.2, 173.5, 168.0, 153.6, 140.1, 138.0, 137.6, 135.3, 131.6, 130.3, 129.7, 129.1, 118.5, 71.2, 70.7, 66.8, 64.0 (2C), 62.6 (2C), 39.9, 34.3 (3C), 33.4, 32.2, 29.9 (12C), 29.2 (2C), 28.7, 25.8, 25.1, 24.8, 23.0, 21.9, 19.5, 14.3, 14.1, 13.1. ^{31}P NMR (202 MHz, $CDCl_3$/CD_3OD 4:1): δ −0.08. IR (neat): 3390, 2924, 2853, 1734, 1709, 1661, 1458, 1260, 1237, 1153, 1050, 805 cm^{-1}; m/z (M + H$^+$) 931.57.

1-*O*-Octadecyl-2-(6-(4′-octyl-4-phenylbenzoyloxy)-hexanoyl)-*sn*-glycero-3-phospho-(*S*)-glycerol (5). Alcohol **15** (62 mg, 0.068 mmol), carboxylic acid **2** (43 mg, 0.14 mmol), and DMAP (25 mg, 0.20 mmol) were dissolved in CH_2Cl_2 (4.5 mL). DCC (42 mg, 0.20 mmol) was added, and the reaction mixture was stirred at 20 °C for 18 h. The mixture was concentrated in vacuo and purified by flash column chromatography (toluene then toluene/EtOAc 5:1) to give 65 mg that was dissolved in CH_2Cl_2 (5.0 mL) and DBU (9 μL, 0.06 mmol) was added. The reaction mixture was stirred for 35 min at 20 °C and then purified directly by flash column chromatography (heptane/EtOAc 1:1 then CH_2Cl_2/MeOH 10:1) to afford 58 mg that was dissolved in a mixture of MeCN (4.2 mL) and CH_2Cl_2 (1.4 mL) and cooled to 0 °C. Aqueous HF (40%, 250 μL) was added dropwise, and the reaction mixture was allowed to reach 20 °C. After 3.5 h, the reaction was quenched by dropwise addition of $MeOSiMe_3$ (0.93 mL), and the mixture was stirred for 30 min, after which $NaHCO_3$ (8 mg, 0.095 mmol) was added and the mixture was concentrated in vacuo and purified by flash column chromatography (CH_2Cl_2/MeOH 10:1 then CH_2Cl_2/MeOH 4:1) to afford 24 mg (38% over 3 step) of **5** as a colorless amorphous solid. R_f = 0.23 (CH_2Cl_2/MeOH 4:1). ^{1}H NMR (300 MHz, $CDCl_3$/CD_3OD 4:1): δ 8.08 (d, J = 8.3 Hz, 2H), 7.67 (d, J = 8.3 Hz, 2H), 7.55 (d, J = 8.1 Hz, 2H), 7.29 (d, J = 8.1 Hz, 2H), 5.19−5.14 (m, 1H), 4.34 (t, J = 6.6 Hz, 2H), 4.06−3.93 (m, 4H), 3.85−3.80 (m, 1H), 3.66−3.61 (m, 2H), 3.60−3.56 (m, 2H), 3.48−3.38 (m, 2H), 2.66 (t, J = 7.7 Hz, 2H), 2.40 (t, J = 7.5 Hz, 2H), 1.86−1.79 (m, 2H), 1.76−1.70 (m, 2H), 1.69−1.62 (m, 2H), 1.56−1.49 (m, 4H), 1.39−1.19 (m, 40H), 0.89 (t, J = 6.8 Hz, 3H), 0.88 (t, J = 6.9 Hz, 3H). ^{13}C NMR (50 MHz, $CDCl_3$/CD_3OD 4:1): δ 173.9, 167.3, 146.1, 143.6, 137.5, 130.3 (2C), 129.3 (2C), 128.9, 127.4 (2C), 127.1 (2C), 72.1 (2C), 71.3, 69.3, 66.7, 65.2, 64.6, 62.6, 35.9, 34.5, 32.1 (2C), 31.8, 30.0, 29.7 (15C), 28.8, 26.3, 25.8, 24.9, 23.0 (2C), 14.3 (2C). ^{31}P NMR (202 MHz, $CDCl_3$/CD_3OD 4:1): δ −1.02. IR (neat): 3320, 2920, 2851, 1717, 1276, 1102, 1069 cm^{-1}; m/z (M + H$^+$) 927.58.

1-Octadecanoyl-2-(6-(4′-octyl-4-phenylbenzoyloxy)-hexanoyl)-*sn*-glycero-3-phospho-(*S*)-glycerol (6). The synthesis was performed as for **5**, starting from alcohol **18** (70 mg, 0.077 mmol) and affording 51 mg (70% over 3 step) of **6** as a colorless amorphous solid. R_f = 0.54 (CH_2Cl_2/MeOH 5:1). ^{1}H NMR (500 MHz, $CDCl_3$/CD_3OD 4:1): δ 8.08 (d, J = 8.3 Hz, 2H), 7.67 (d, J = 8.3 Hz, 2H), 7.56 (d, J = 8.1 Hz, 2H), 7.29 (d, J = 8.1 Hz, 2H), 5.27−5.22 (m, 1H), 4.39 (dd, J = 12.0, 3.2 Hz, 1H), 4.34 (d, J = 6.6 Hz, 2H), 4.17 (dd, J = 12.0, 6.6 Hz, 1H), 4.05−4.00 (m, 2H), 3.98−3.91 (m, 2H), 3.85−3.80 (m, 1H), 3.65−3.61 (m, 2H), 2.66 (t, J = 7.7 Hz, 2H), 2.40 (t, J = 7.5 Hz, 2H), 2.31 (t, J = 7.6 Hz, 2H), 1.86−1.78 (m, 2H), 1.76−1.69 (m, 2H), 1.68−1.62 (m, 2H), 1.62−1.56 (m, 2H), 1.55−1.49 (m, 2H), 1.39−1.20 (m, 38H), 0.89 (t, J = 6.7 Hz, 3H), 0.88 (t, J = 6.8 Hz, 3H). ^{13}C NMR (50 MHz, $CDCl_3$/CD_3OD 4:1): δ 174.4, 173.6, 167.4, 146.3, 143.7, 137.6, 130.4 (2C), 129.4 (2C), 129.0, 127.5 (2C), 127.2 (2C), 71.2, 70.8, 67.1, 65.2, 64.4, 62.7 (2C), 36.0, 34.4 (2C), 32.3 (2C), 31.8, 29.9 (15C), 28.8, 25.9, 25.2, 24.9, 23.0 (2C), 14.3 (2C). ^{31}P NMR (202 MHz, $CDCl_3$/CD_3OD 4:1): δ −1.30. IR (neat): 3314, 2921, 2851, 1737, 1467, 1277, 1103 cm^{-1}; m/z (M + H$^+$) 941.55.

Acknowledgment. We would like to acknowledge Prof. Helena Danielson (Department of Biochemistry and Organic Chemistry, Uppsala University) for her assistance with the enzyme inhibition assays. The technical help of Lars Duelund (MEMPHYS, University of Southern Denmark) is much appreciated. We thank the Danish Council for Strategic Research (NABIIT Program) for financial support. MEMPHYS-Center for Biomembrane Physics is supported by the Danish National Research Foundation.

Supporting Information Available: Analytical and spectral data for all synthesized compounds, experimental procedures for the synthesis of **2**, **7**, **9**, **10**, **14**, **15**, **17**, **18**, and 1-*O*-DSPG, Mosher ester analysis data of **17**, DLS analysis, further MALDI-TOF MS data for $sPLA_2$ degradation experiments, experimental procedures for the inhibition experiments and figures from MD simulations. This material is available free of charge via the Internet at http://pubs.acs.org.

References

(1) Barua, A. B.; Furr, H. C. Properties of Retinoids. *Mol. Biotechnol.* **1998**, *10*, 167–182.
(2) Rolewski, S. L. Clinical Review: Topical Retinoids. *Dermatol. Nurs.* **2003**, *15*, 447–465.
(3) (a) Okuno, M.; Kojima, S.; Matsushima-Nishiwaki, R.; Tsurumi, H.; Muto, Y.; Friedman, S. L.; Moriwaki, H. Retinoids in Cancer Chemoprevention. *Curr. Cancer Drug Targets* **2004**, *4*, 285–298. (b) Freementle, S. J.; Spinella, M. J.; Dmitrovsky, E. Retinoids in cancer therapy and chemoprevention: promise meets resistance. *Oncogene* **2003**, *22*, 7305–7315.
(4) (a) Huang, M. E.; Ye, Y. C.; Chen, S. R.; Chai, J.; Lu, J. X.; Zhoa, L.; Gu, L. J.; Wang, Z. Y. Use of all-*trans* retinoic acid in the treatment of acute promyelocytic leukemia. *Blood* **1988**, *72*, 567–572. (b) Castaigne, S.; Chomienne, C.; Daniel, M. T.; Ballerini, P.; Berger, R.; Fenaux, P.; Degos, L. All-trans retinoic acid as a differentiation therapy for acute promyelocytic leukemia. I. Clinical results. *Blood* **1990**, *76*, 1704–1709. (c) Regazzi, M. B.; Iacona, I.; Gervasutti, C.; Lazzarino, M.; Toma, S. Clinical Pharmacokinetics of Tritinoin. *Clin. Pharmacokinet.* **1997**, *32*, 382–402.
(5) Muindi, J. R. F.; Frankel, S. R.; Huselton, C.; DeGrazia, F.; Garland, W. A.; Young, C. W.; Warrell, R. P. Clinical pharmacology of oral all-*trans*-retinoic acid in patients with acute promyelocytic leukemia. *Cancer Res.* **1992**, *52*, 2138–2142.
(6) (a) Shimizu, K.; Tamagawa, K.; Takahashi, N.; Takayama, K.; Maitani, Y. Stability and antitumor effects of all-*trans* retinoic acid-loaded liposomes contained sterylglucoside mixture. *Int. J. Pharm.* **2003**, *258*, 45–53. (b) Kawakami, S.; Opanasopit, P.; Yokoyama, M.; Chansri, N.; Yamamoto, T.; Okano, T.; Yamashita, F.; Hasdida, M.

Biodistribution Characteristics of All-trans Retinoic Acid Incorporated in Liposomes and Polymeric Micelles Following Intravenous Administration. *J. Pharm. Sci.* **2005**, *94*, 2606–2615. (c) Díaz, C.; Vargas, E.; Gätjens-Boniche, O. Cytotoxic effect induced by retinoic acid loaded into galatosyl-sphingosine containing liposomes on human hepatoma cell lines. *Int. J. Pharm.* **2006**, *325*, 208–115. (d) Suzuki, S.; Kawakami, S.; Chansri, N.; Yamashita, F.; Hasdida, M. Inhibition of pulmonary metastasis in mice by all-trans retinoic acid incorporated in cationic liposomes. *J. Controlled Release* **2006**, *116*, 58–63.

(7) (a) Pedersen, P. J.; Christensen, M. S.; Ruysschaert, T.; Linderoth, L.; Andresen, T. L.; Melander, F.; Mouritsen, O. G.; Madsen, R.; Clausen, M. H. Synthesis and Biophysical Characterization of Chlorambucil Anticancer Ether Lipid Prodrugs. *J. Med. Chem.* **2009**, *52*, 3408–3415. (b) Christensen, M. S.; Pedersen, P. J.; Andresen, T. L.; Madsen, R.; Clausen, M. H. Isomerization of all-(E)-Retinoic Acid Mediated by Carbodiimide Activation—Synthesis of ATRA Ether Lipid Conjugates. *Eur. J. Org. Chem.* **2009**, 719–724. (c) Linderoth, L.; Peters, G. H.; Madsen, R.; Andresen, T. L. Drug Delivery by an Enzyme-Mediated Cyclization of a Lipid Prodrug with Unique Bilayer-Formation Properties. *Angew. Chem., Int. Ed.* **2009**, *48*, 1823–1826.

(8) (a) Newton, D. L.; Henderson, W. R.; Sporn, M. B. Structure−Activity Relationships of Retinoids in Hamster Tracheal Organ Culture. *Cancer Res.* **1980**, *40*, 3413–3425. (b) Um, S. J.; Kwon, Y. J.; Han, H. S.; Park, S. H.; Park, M. S.; Rho, Y. S.; Sin, H. S. Synthesis and Biological Activity of Novel Retinamide and Retinoate Derivatives. *Chem. Pharm. Bull.* **2004**, *52*, 501–506. (c) Gediya, L. K.; Khandelwal, A.; Patel, J.; Belosay, A.; Sabnis, G.; Mehta, J.; Purushottamachar, P.; Njar, V. C. O. Design, Synthesis, and Evaluation of Novel Mutual Prodrugs (Hybrid Drugs) of All-trans-Retinoic Acid and Histone Deacetylase Inhibitors with Enhanced Anticancer Activities in Breast and Prostate Cancer Cells in Vitro. *J. Med. Chem.* **2008**, *51*, 3895–3904. (d) Ulukaya, E.; Wood, E. J. Fenretinide and its relation to cancer. *Cancer Treat. Rev.* **1999**, *25*, 229–235.

(9) Linderoth, L.; Andresen, T. L.; Jørgensen, K.; Madsen, R.; Peters, G. H. Molecular Basis of Phospholipase A_2 Activity toward Phospholipids with *sn*-1 Substitutions. *Biophys. J.* **2008**, *94*, 14–26.

(10) Camacho, L. H. Clinical applications of retinoids in cancer medicine. *J. Biol. Regul. Homeostatic Agents* **2003**, *17*, 98–114.

(11) (a) Maden, M. Retinoic Acid in the Development, Regeneration and Maintenance of the Nervous System. *Nat. Rev. Neurosci.* **2007**, *8*, 755–765. (b) Swift, C. B.; Hays, J. L.; Petty, J. W. Distinct Functions of Retinoic Acid Receptor Beta Isoforms: Implications for Targeted Therapy. *Endocr., Metab. Immune Disord.: Drug Targets* **2008**, *8*, 47–50.

(12) Zhuang, Y.; Faria, T. N.; Chambon, P.; Gudas, L. J. Identification and characterization of retinoic acid receptor beta2 target genes in F9 teratocarcinoma cells. *Mol. Cancer Res.* **2003**, *1*, 619–630.

(13) (a) Piu, F.; Gauthier, N. K.; Olsson, R.; Currier, E. A.; Lund, B. W.; Croston, G. E.; Hacksell, U.; Brann, M. R. Identification of novel subtype selective RAR agonists. *Biochem. Pharmacol.* **2005**, *71*, 156–162. (b) Lund, B. W.; Piu, F.; Gauthier, N. K.; Eeg, A.; Currier, E.; Sherbukhin, V.; Brann, M. R.; Hacksell, U.; Olsson, R. Discovery of a Potent, Orally Available and Isoform-Selective Retinoic Acid β2 Receptor Agonist. *J. Med. Chem.* **2005**, *48*, 7517–7519. (c) Lund, B. W.; Knapp, A. E.; Piu, F.; Gauthier, N. K.; Begtrup, M.; Hacksell, U.; Olsson, R. Design, Synthesis, and Structure−Activity Analysis of Isoform-Selective Retinoic Acid Receptor β Ligands. *J. Med. Chem.* **2009**, *52*, 1540–1545.

(14) Bonsen, P. P. M.; de Haas, G. H.; Pieterson, W. A.; van Deenen, L. L. Studies on Phospholipase A and its Zymogen from Porcine Pancreas. IV. The Influence of Chemical Modification of the Lecithin Structure on Substrate Properties. *Biochim. Biophys. Acta* **1972**, *270*, 364–382.

(15) (a) Buckland, A. G.; Wilton, D. C. Anionic phospholipids, interfacial binding and the regulation of cell functions. *Biochim. Biophys. Acta* **2000**, *1483*, 199–216. (b) Canaan, S.; Nielsen, R.; Ghomashchi, F.; Robinson, B. H.; Gelb, M. H. Unusual mode of binding of human group IIA secreted phospholipase A2 to anionic interfaces as studied by continuous wave and time domain electron paramagnetic resonance spectroscopy. *J. Biol. Chem.* **2002**, *277*, 30984–30990. (c) Houlihan, W. J.; Lohmeyer, M.; Workman, P.; Cheon, S. H. Phospholipid antitumor agents. *Med. Res. Rev.* **1995**, *15*, 157–223.

(16) (a) Houlihan, W. J.; Lohmeyer, M.; Workman, P.; Cheon, S. H. Phospholipid antitumor agents. *Med. Res. Rev.* **1995**, *15*, 157–223. (b) Andresen, T. L.; Jensen, S. S.; Madsen, R.; Jørgensen, K. Synthesis and Biological Activity of Anticancer Ether Lipids that are Specifically Released by Phospholipase A_2 in Tumor Tissue. *J. Med. Chem.* **2005**, *48*, 7305–7314.

(17) (a) Hsieh, C. C.; Yen, M. H.; Liu, H. W.; Lau, Y. T. Lysophosphatidylcholine induces apoptotic and non-apoptotic death in vascular smooth muscle cells: in comparison with oxidized LDL. *Atherosclerosis* **2000**, *151*, 481–491. (b) Masamune, A.; Sakai, Y.; Satoh, A.; Fujita, M.; Yoshida, M.; Shimosegawa, T. Lysophosphatidylcholine induces apoptosis in AR42J cells. *Pancreas* **2001**, *22*, 75–83. (c) Kogure, K.; Nakashima, S.; Tsuchie, A.; Tokumura, A.; Fukuzawa, K. Temporary membrane distortion of vascular smooth muscle cells is responsible for their apoptosis induced by platelet-activating factor-like oxidized phospholipids and their degradation product, lysophosphatidylcholine. *Chem. Phys. Lipids* **2003**, *126*, 29–38.

(18) Peters, G. H.; Møller, M. S.; Jørgensen, K.; Rönnholm, P.; Mikkelsen, M.; Andresen, T. L. Secretoty Phospholipase A2 Hydrolysis of Phospholipid Analogues is Dependent on Water Accessibility to the Active Site. *J. Am. Chem. Soc.* **2007**, *129*, 5451–5461.

(19) Scott, D. L.; White, S.; Otwinowski, Z.; Yuan, W.; Gelb, M. H.; Sigler, P. B. Interfacial Catalysis—The Mechanism of Phospholipase-A_2. *Science* **1990**, *250*, 1541–1546.

(20) *tert*-Butyl 6-hydroxyhexanoate (**11**) was synthesized according to the litterature. Larock, R. C.; Leach, D. R. Organopalladium Approaches to Prostaglandins. 3. Synthesis of Bicyclic and Tricyclic 7-Oxaprostaglandin Endoperoxide Analoguesnvia Oxypalladation of Norbornadiene. *J. Org. Chem.* **1984**, *49*, 2144–2148.

(21) Mitsunobu, O. The Use of Diethyl Azodicarboxylate and Triphenylphosphine in Synthesis and Transformation of Natural Products. *Synthesis* **1981**, 1–28.

(22) Kaul, R.; Brouillette, Y.; Sajjadi, Z.; Hansford, K. A.; Lubell, W. D. Selective *tert*-Butyl Ester Deprotection in the Presence of Acid Labile Protection Groups with $ZnBr_2$. *J. Org. Chem.* **2004**, *69*, 6131–6133.

(23) Borgulya, J.; Bernauer, K. Transformation of Carboxylic Acid *t*-Butyl Esters into the Corresponding Trimethylsilyl Esters or Free Acids under Nonacidic Conditions. *Synthesis* **1980**, 545–547.

(24) Compound **2** is commercially available (CAS no. 59662-49-6), but during this work, **2** was synthesized in one step from the corresponding nitrile (CAS no. 52709-84-9) by a NaOH mediated hydrolysis in 98% yield (see Supporting Information).

(25) Neises, B.; Steglich, W. Simple Method for the Esterification of Carboxylic Acids. *Angew. Chem., Int. Ed. Engl.* **1978**, *17*, 522–524.

(26) Gaffney, P. R. J.; Reese, C. B. Synthesis of naturally occurring phosphatidylinositol 3,4,5-triphosphate [PtdIns(3,4,5)P_3] and its diastereoisomers. *J. Chem. Soc., Perkin Trans. 1* **2001**, 192–105.

(27) Burgos, C. E.; Ayer, D. E.; Johnson, R. A. A New, Asymmetric Synthesis of Lipids and Phospolipids. *J. Org. Chem.* **1987**, *52*, 4973–4977.

(28) Batten, R. J.; Dixon, A. J.; Taylor, R. J. K. A New Method for Removing the *t*-Butyldimethylsilyl Protecting Group. *Synthesis* **1980**, 234–236.

(29) Qin, D.; Byun, H. S.; Bittman, R. Synthesis of Plasmalogen via 2,3-Bis-*O*-(4′-methoxybenzyl)-*sn*-glycerol. *J. Am. Chem. Soc.* **1999**, *121*, 662–668.

(30) Dale, J. A.; Mosher, H. S. Nuclear Magnetic Resonance Enantiomer Reagents. Configurational Correlations via Nuclear Magnetic Resonance Chemical Shifts of Diastereomeric Mandelate, *O*-Methylmandelate, and α-Methoxy-α-trifluoromethylphenylacetate (MTPA) Esters. *J. Am. Chem. Soc.* **1973**, *95*, 512–519.

(31) (a) Lichtenberg, D.; Barenholz, Y. Liposomes—Preparation, Characterization and Preservation. *Methods Biochem. Anal.* **1988**, *33*, 337–462. (b) Tirrell, D. A.; Takigawa, D. Y.; Seki, K. Interactions of synthetic polymers with cell-membranes and model membrane systems 7. pH sensitization of phospholipid-vesicles via complexation with synthetic poly(carboxylic acid)s. *Ann. N.Y. Acad. Sci.* **1985**, *446*, 237–248.

(32) McIntyre, J. C.; Sleight, R. G. Fluorescence assay for phospholipid membrane asymmetry. *Biochemistry* **1991**, *30*, 11819–11827.

(33) (a) Huster, D.; Muller, P.; Arnold, K.; Herrmann, A. Dynamics of membrane penetration of the fluorescent 7-nitrobenz-2-oxa-1,3-diazol-4-yl (NBD) group attached to an acyl chain of phosphatidylcholine. *Biophys. J.* **2001**, *80*, 822–831. (b) Langner, M.; Hui, S. W. Dithionite penetration through phospholipid bilayers as a measure of defects in lipid molecular packing. *Chem. Phys. Lipids* **1993**, *65*, 23–30.

(34) (a) Harvey, D. J. Matrix-Assisted Laser Desorption/Ionization Mass Spectrometry of Phospholipids. *J. Mass Spectrom.* **1995**, *30*, 1333–1346. (b) Schiller, J.; Arnhold, J.; Benard, S.; Müller, M.; Reichl, S.; Arnold, K. Lipid Analysis by Matrix-Assisted Laser Desorption and Ionization Mass Spectrometry: A Methodological Approach. *Anal. Biochem.* **1999**, *267*, 46–56. (c) Petković, M.; Muller, J.; Muller, M.; Schiller, J.; Arnold, K.; Arnhold, J. Application of matrix-assisted laser desorption/ionization time-of-flight mass spectrometry for monitoring the digestion of phosphatidylcholine by pancreatic phospholipase A_2. *Anal. Biochem.* **2002**, *308*, 61–70.

(35) Fawzy, A. A.; Wishwanath, B. S.; Franson, R. C. Inhibition of human nonpancreatic phospholipases A_2 by retinoids and flavonoids. Mechanism of action. *Agents Actions* **1988**, *25*, 394–400.

(36) Hope, W. C.; Patel, B. J.; Fiedler-Nagy, C.; Wittreich, B. H. Retinoids inhibit Phospholipase A_2 in human synovial fluid and arachidonic acid release from rat peritoneal macrophages. *Inflammation* **1990**, *14*, 543–559.
(37) Cunningham, T. J.; Maciejewski, J.; Yao, L. Inhibition of secreted phospholipase A2 by neuron survival and anti-inflammatory peptide CHEC-9. *J. Neuroinflammation* **2006**, *3*, 25.
(38) Nicke, B.; Kaiser, A.; Wiedernmann, B.; Riecken, E. O.; Rosewicz, S. Retinoic Acid Receptor α Mediates Growth Inhibition by Retinoids in Human Colon Carcinoma HT29 Cells. *Biochem. Biophys. Res. Commun.* **1999**, *261*, 572–577.
(39) (a) Geurts van Kassel, W. S. M.; Hax, W. M. A.; Demel, R. A.; de Gier, J. High Performance Liquid Chromatographic Separation and Direct Ultraviolet Detection of Phospholipids. *Biochim. Biophys. Acta* **1977**, *486*, 524–530. (b) Rivnay, B. Combined Analysis of Phospholipids by High-Performance Liquid Chromatography and Thin-Layer Chromatography. *J. Chromatogr.* **1984**, *294*, 303–315.
(40) Hansford, K. A.; Reid, R. C.; Clark, C. I.; Tyndall, J. D. A.; Whitehouse, M. W.; Guthrie, T.; McGeary, R. P.; Schafer, K.; Martin, J. L.; Fairlie, D. P. D-Tyrosine as a chiral precusor to potent inhibitors of human nonpancreatic secretory phospholipase A(2) (IIa) with antiinflammatory activity. *ChemBioChem* **2003**, *4*, 181–185.
(41) Bernstein, F. C.; Koetzle, T. F.; Williams, G. J.; Meyer, E. E.; Brice, M. D.; Rodgers, J. R.; Kennard, O.; Shimanouchi, T.; Tasumi, M. Protein Data Bank—Computer-Based Archival File for Macromolecular Structures. *J. Mol. Biol.* **1977**, *112*, 535–542.
(42) Phillips, J. C.; Braun, R.; Wang, W.; Gumbart, J.; Tajkhorshid, E.; Villa, E.; Chipot, C.; Skeel, R. D.; Kale, L.; Schulten, K. Scalable molecular dynamics with NAMD. *J. Comput. Chem.* **2005**, *26*, 1781–1802.
(43) Jorgensen, W. L.; Chandrasekhar, J.; Medura, J. D.; Impey, R. W.; Klein, M. L. Comparison of simple potential models for simulating liquid water. *J. Chem. Phys.* **1983**, *79*, 926–935.
(44) Grubmüller, H. *Solvate: a program to create atomic solvent models*. Electronic publication: http://www.mpibpc.gwdg.de/abteilungen/071/solvate/docu.html; accessed 02/11/2010.
(45) Feller, S. E.; Zhang, Y.; Pastor, R. W.; Brooks., B. R. Constant pressure molecular dynamics simulation: the Langevin piston method. *J. Chem. Phys.* **1995**, *103*, 4613–4621.
(46) (a) Darden, T.; York, D.; Pedersen, L. Particle mesh Ewald an Nlog(n) method for Ewald sums in large systems. *J. Chem. Phys.* **1993**, *98*, 10089–10092. (b) Darden, T.; York, D.; Pedersen, L. Particle mesh Ewald: an N-log(N) method for Ewald sums in large systems. *J. Chem. Phys.* **1995**, *103*, 8577–8593.
(47) Humphrey, W.; Dalke, A.; Schulten, K. VMD—Visual Molecular Dynamics. *J. Mol. Graphics* **1996**, *14*, 33–38.
(48) Mills, J. K.; Needham, D. Lysolipid incorporation in dipalmitoylphosphatidylcholine bilayer membranes enhances the ion permeability and drug release rates at the membrane phase transition. *Biochim. Biophys. Acta* **2005**, *1716*, 77–96.
(49) (a) de Carvalho, L. M.; Schwedt, G. Polarographic determination of dithionite and its decomposition products: kinetic aspects, stabilizers, and analytical application. *Anal. Chim. Acta* **2001**, *436*, 293–300. (b) Stutts, K. J. Liquid chromatographic assay of dithionite and thiosulfate. *Anal. Chem.* **1987**, *59*, 543–544.
(50) Chen, P. S.; Toribara, T. Y.; Warner, H. Microdetermination of phosphorus. *Anal. Chem.* **1956**, *28*, 1756–1758.
(51) Carmichael, J.; DeGraff, W. G.; Gazdar, A. F.; Minna, J. D.; Mitchell, J. B. Evaluation of a tetrazolium-based semiautomated colorimetric assay: assessment of chemosensitivity testing. *Cancer Res.* **1987**, *47*, 936–942.